APTD-1084

PB 210 675

REDUCTION OF ATMOSPHERIC POLLUTION

FINAL REPORT ON RESEARCH ON REDUCING EMISSION OF SULPHUR OXIDES, NITROGEN OXIDES, AND PARTICULATES BY USING FLUIDISED COMBUSTION OF COAL

Appendices: (Vol. 3 of 3)
4 -- Experiments with 12-in. corrosion combustor;
5 -- Experiments with 6-in. corrosion combustor,
6 -- Mathematical model of sulphur retention,
7 -- Coal studies,
8 -- Limestone and Dolomite studies,
9 -- Methods for determination of NO_x.

Environmental Protection Agency,
Office of Air Programs,
Research Triangle Park,
North Carolina 27711

Reproduced by
NATIONAL TECHNICAL
INFORMATION SERVICE
U S Department of Commerce
Springfield VA 22151

EC

535

3 - 123A

BIBLIOGRAPHIC DATA SHEET

1. Report No. APTD-1084

2\.

3. Recipient's Accession No. PB-210 675

4. Title and Subtitle

Reduction of Atmospheric Pollution (Vol. 3 of 3)
Appendices

5. Report Date September 1971

6\.

7. Author(s)

8. Performing Organization Rept. No. DHB 060971

9. Performing Organization Name and Address

NATIONAL COAL BOARD
FLUIDISED COMBUSTION CONTROL GROUP
LONDON, ENGLAND

10. Project/Task/Work Unit No.

11. Contract/Grant No. CPA 70-97

12. Sponsoring Organization Name and Address

ENVIRONMENTAL PROTECTION AGENCY
Office of Air Programs
411 West Chapel Hill Street
Durham, North Carolina 27701

13. Type of Report & Period Covered Final

14\.

15. Supplementary Notes

16. Abstracts

Six appendices (numbers 4 through 9) to the main report on research on reducing emission of sulphur oxides, nitrogen oxides, and particulates by using fluidised combustion of coal are presented. They are: Experiments with 12-in. corrosion combustor; Experiments with 6-in. corrosion combustor; Mathematical model of sulphur retention; Coal studies; Limestone and Dolomite studies; and Methods for determination of NO_x.

17. Key Words and Document Analysis. 17a. Descriptors

Air Pollution
Combustion
Coal
Sulfur Oxides
Nitrogen Oxides
Particles
Limestone
Calcium Inorganic Compounds
Additives
Temperature
Pressure
Flow Rate
Tests
Mathematical Models
Chemical Analyses

17b. Identifiers/Open-Ended Terms

17c. COSATI Field/Group 14.1a

18. Availability Statement Unlimited

19. Security Class (This Report) UNCLASSIFIED

20. Security Class (This Page) UNCLASSIFIED

21. No. of Pages 535

22. Price $12.50

FORM NTIS-35 (REV. 3-72)

USCOMM-DC 14952-P72

NATIONAL COAL BOARD

FINAL REPORT

JUNE 1970 - JUNE 1971

REDUCTION OF ATMOSPHERIC POLLUTION

APPENDIX 4. EXPERIMENTS WITH THE 12 IN CORROSION COMBUSTOR. (TASK IV)

PREPARED FOR

ENVIRONMENTAL PROTECTION AGENCY
OFFICE OF AIR PROGRAMS
411 WEST CHAPEL HILL STREET
DURHAM, NORTH CAROLINA 27701

REFERENCE NO. DHB 060971 A4·ib

SEPTEMBER 1971

FLUIDISED COMBUSTION CONTROL GROUP

NATIONAL COAL BOARD
LONDON, ENGLAND

REDUCTION OF ATMOSPHERIC POLLUTION

Research on reducing emission of sulphur oxides, nitrogen oxides and particulates by using fluidised bed combustion of coal

Appendix 4. Experiments with the 12 in corrosion combustor. (Task IV)

Main objective

To obtain data on corrosion of evaporator, superheater and reheater materials for lower fluidising velocities.

Report prepared by: M.J. Cooke and E.A. Rogers

Report approved by: A.D. Dainton and H.R. Hoy

Preceding page blank

FOREWORD

This Appendix describes experimental work carried out using the 12 in corrosion combustor at CRE., between June 1970 and June 1971, as Task IV of the joint N.C.B./O.A.P. research programme. The objective of Task IV was to obtain data on corrosion of evaporator, superheater and reheater materials for lower fluidising velocities, with or without addition of limestone. Attention is drawn to the main results obtained, but these are not discussed here. A summary of the work is presented in the main report and the results are discussed there, together with results from other pilot plants.

Preceding page blank

Page No.

Foreword

1. Description of Plant A4. 1
- 1.1 Coal feed system A4. 3
- 1.2 Fluidising air preheater A4. 4
- 1.3 Fluidised bed combustor A4. 5
- 1.4 Specimen tube assemblies A4. 6
- 1.5 Coarse ash collection hopper A4. 7
- 1.6 Cyclone gas de-dusting system A4. 7
- 1.7 Auxiliary sample equipment A4. 8
  - 1.7.1 Bed sampling A4. 8
  - 1.7.2 Dust sampling A4. 8
  - 1.7.3 Gas sampling A4. 9
  - 1.7.4 SO_2/SO_3 sampling A4. 9
  - 1.7.5 Volatilised alkali sampling A4.10

2. Operating Procedures A4.12
- 2.1 Coal and limestone preparation A4.12
- 2.2 Plant start-up A4.12
- 2.3 Throughput measurements and sampling A4.13
  - 2.3.1 Coal feed A4.13
  - 2.3.2 Product ash A4.13
  - 2.3.3 Bed samples A4.14
  - 2.3.4 Secondary fines A4.14
  - 2.3.5 Dust A4.14
  - 2.3.6 Offtake gas A4.14
  - 2.3.7 Mass balances-data processing A4.14
- 2.4 Plant shut-down A4.16
- 2.5 Corrosion test specimens A4.16
  - 2.5.1 Preparation before tests A4.18
  - 2.5.2 Procedure during tests A4.19
  - 2.5.3 Procedure after tests A4.19

3. Results A4.20
- 3.1 Test Series 1 A4.20
  - 3.1.1 Description of Test Series 1 A4.20
  - 3.1.2 Results A4.21

Preceding page blank

Page No.

3.1.2.1 Plant data A4.21
3.1.2.2 Visual examination of corrosion test specimens A4.28
3.1.2.3 Chemical analysis of deposits A4.29
3.1.2.4 Specimen weight loss A4.32
3.1.2.5 Metallographic examination A4.32

3.2 Test Series 2 A4.33
3.2.1. Description of Test Series 2 A4.33
3.2.2 Results A4.34
3.2.2.1 Plant data A4.34
3.2.2.2 Visual examination of corrosion test specimens A4.42
3.2.2.3 Chemical analysis of deposits A4.43
3.2.2.4 Specimen weight loss A4.46
3.2.2.5 Metallographic examination A4.46

3.3 Test Series 3 A4.47
3.3.1 Description of Test Series 3 A4.47
3.3.2 Results A4.48
3.3.2.1 Plant data A4.48
3.3.2.2 Visual examination of corrosion test specimens A4.60
3.3.2.3 Chemical analysis of deposits A4.60
3.3.2.4 Specimen weight loss A4.61
3.3.2.5 Metallographic examination A4.64
3.3.2.6 Electron probe microanalysis A4.64

4. References A4.66

5. Acknowledgement A4.67

Figs. A.4.1 - A.4.25

(Note that when referring to Tables and Figures in the text the prefix A4 is omitted).

1. DESCRIPTION OF PLANT

The 12 in combustor (Fig. 1 & 2) at CRE was built specifically to investigate whether fireside corrosion of steam generation, superheater and reheater tubes is likely to be a problem. Corrosion specimen tubes, which are comprised of rings of different alloys clamped together, are installed in the fluidised bed combustor, both within the ash bed itself and in the freeboard section. There are also facilities to mount small plates (coupons) of different alloys in and above the bed.

A gas fired fluidising air pre-heater is used for start-up purposes in order to heat the ash bed to a temperature at which combustion of coal takes over. The coal for a test is kept in a 10 ton storage bunker. It is then transported to the coal feed system where it is metered through a calibrated rotary valve and pneumatically fed to the fluidised bed. There it is burnt and much of the heat generated is removed by the corrosion specimen tubes, the walls of which are air-cooled to the required test temperature. The remaining available heat is removed by other air-cooled tubes immersed within the bed.

A constant bed height is maintained by using an over-flow pipe down which the excess bed ash flows into a sealed coarse ash collection hopper. The fine carbonaceous material, elutriated from the bed before being completely burnt, is returned to the bed by means of an internal cyclone. Solids not collected in the internal cyclone are removed by a higher efficiency secondary cyclone. Any remaining dust is then discharged into the atmosphere with the gas.

Sampling equipment for obtaining both combustion data and information regarding the corrosion environment is used.

Special control by safety devices is incorporated to enable the plant to operate continuously and safely with minimum of staff. Basically, the start-up of the plant, coal storage, handling of ash products and sampling are carried out manually when required. For the normal running of the combustor, fluidising and transport air are metered at constant rates and the bed temperature is controlled by the coal feed rotary valve speed. The air flow through the specimen tubes is controlled to give constant specified tube temperatures and the additional air passed through the control tubes is set such that the desired combustion conditions are obtained. For example, if a lower oxygen content in the exhaust gas is required, the air through the control tubes is increased, causing an automatic increase in the coal feed rate to maintain bed temperature.

If conditions within the combustor vary beyond specified limits, the plant is shut down automatically. The coal feed, fluidising and transport air are stopped while the temperatures of the specimen tubes are kept at or below their specified levels until the plant cools down. Should the main air supply fail, there is a standby diesel compressor operating continuously which is capable of supplying sufficient air during the plant shutdown. In the event of complete failure of air supplies, steam is passed through the specimen tubes in order to keep their wall temperatures below the test settings. In this way the corrosion test is "frozen" until restarted. Automatic plant shutdown is affected by:

(a) Bed temperature, high or low
(b) Fluidising air flow rate, high or low
(c) Transport air flow rate, high or low
(d) Specimen tube temperatures, high
(e) Combustor pressure, high
(f) Main air pressure, low
(g) Power failure

For the following more detailed description, the plant is divided as follows (Fig. 1).

1. Coal feed system
2. Fluidising air pre-heater
3. Fluidised bed combustor
4. Specimen tube assemblies
5. Coarse ash collection hopper
6. Cyclone gas de-dusting system
7. Auxiliary Sampling Equipment

General information regarding instrumentation follows the descriptions of each item of the equipment listed above.

1.1 Coal feed system

Coal required for the tests is stored in a 10 ton bunker. All interior surfaces are coated with bitumen paint ("Hevikote") to prevent scaling and to assist the discharge of coal. Prepared coal is fed pneumatically from solids pumps at the coal preparation plant to the bunker.

Coal is fed pneumatically from the 10 ton coal storage bunker via a 5 in rotary valve and ejector to coal feed cyclones and thence to the coal lock hopper. An alternative emergency method of supply is also available from a drum tippler which feeds coal from drums. The coal is pneumatically fed along 1½ in n.b. lines and enters the coal feed lock hopper via primary and secondary feed cyclones situated above a vibratory screen which removes oversize and tramp material. The air is discharged to the atmosphere. The flow of coal may be diverted to a duplicate set of cyclones for sampling.

The coal feed system first lock hopper has a capacity of approx. 800 lb and is lined with "Hevikote". It is used to supply coal by gravity to a second feed hopper, situated vertically and axially beneath the first. It operates under a positive pressure without disrupting the coal feed to the fluidised bed. The second coal feed hopper has also a capacity of approx. 800 lb and is internally lined with "Hevikote".

Coal is metered from the lower hopper through a small stainless steel rotary valve feeder into a ½ in n.b. pneumatic transport line. The feature of this feeder is ease of access, for maintenance and for changing the rotor if necessary. The pockets in the rotor are shaped and sized to promote their filling and discharge. Two air purges are used to keep the sides of the rotor clear in order to prevent seizure by coal binding.

A balance line system is connected to the transport air supply line so that the feed hopper pressure may be maintained the same as the pressure beneath the rotary valve. The feed transport line to the fluidised bed combustor contains a transparent section for a visual check of coal flow.

Instrumentation

When coal is required to be fed to the combustor feed hopper the 5 in rotary valve is started manually from the main control panel on the rig. At the same time, a magnetic valve opens to supply the transport air to the coal transport line to the coal feed cyclones above the combustor feed hoppers.

The lock hopper system is operated manually with Goring and Kerr high and low level capacitance probe indicators on each hopper. The coal feed rotary valve is driven by a 0 - 10 rpm 240 V d.c. electric motor and gearbox with a speed control. From the drive a revolution counter also operates.

The transport air rate is automatically controlled and the safety shut down system will operate if the flow rate falls below or rises above set limits.

1.2 Fluidising air preheater

The hot gas generator burns town's gas or natural gas in air, with excess air used for keeping the exit gas temperature below the maximum of 1300°F. Gas and air are supplied to the burner, controlled at pressures of 10 $\mathrm{lb/in^2}$ gauge. Before the combustor bed temperature is reached (about 1110°F), the hot gas generator is shut off and separate metered air from a 45 $\mathrm{lb/in^2}$ gauge supply reduced from the 80 - 100 $\mathrm{lb/in^2}$ gauge main is used.

Instrumentation

The air supplies are metered through rotameters while the gas rate is automatically controlled by the exit hot gas temperature. Gas is ignited by a spark ignition system and a safety system shuts off the gas if ignition is not achieved or if there is a flame failure. This safety device will also operate with an outlet gas temperature higher than a preset value and also with low gas or air supply pressures.

1.3 Fluidised bed combustor

The mild steel vessel was protected by lining it with 4 in of Amberex insulating blocks (ex Genefax Monolithics Ltd.), followed by a 3 in lining of Durax 1500 hard castable refractory (ex Genefax Monolithics Ltd.) to protect the former. In the top of the combustor are two 4 in diameter explosion relief discs of ¼ in thick asbestos millboard.

The fluidised combustor has been designed to operate at 2 to 4 ft/s fluidising velocity with bed temperatures up to 1650°F. It contains an internal cyclone, which is described later, for returning the elutriated fine coal and ash back to the bed.

The fluidising air distributor consists of a horizontal base plate with nine vertical tubes spaced on a 4½ in square pitch. Each tube has six ⅛ in holes drilled just below the closed ends, to give operating pressure drops of about 4 in and 10 in w.g. at 2 and 3 ft/s fluidising velocities respectively. The tubes are connected to a manifold which receives the fluidising air. The bed level, emergency and sample ash offtake pipes also pass through the base.

Coal is fed into the reactor 3 in above the holes in the air distributor. In order to achieve uniform coal feed discharge in the combustor, the ½ in pneumatic coal feed transport line terminates at the centre of the combustor. To provide a fluidised bed for start up ash is fed in at the top of the vessel.

The fluidised bed depth is kept constant at 2 ft by an adjustable ¾ in n.b. stainless steel pipe which acts as an overflow weir. Excess bed ash produced is discharged into an ash collection hopper.

The specimen tubes, on which rings of different alloys are tested, are described in more detail later. However four such tubes form part of a 6 in triangular pitch of 2 in o.d. tubes four rows deep (Fig. 2). The remainder of the tubes, which make up the pattern, are used for bed control purposes. They are of bayonet construction and are air cooled. An exhaust duct discharges the cooling air outside the building and at the same time acts as a silencer. Two specimen tubes are also situated in the freeboard 2 ft above the top of a 2 ft bed.

Eight studs are situated within the bed on which specimen 'coupon' plates are attached for corrosion tests. In the freeboard section is an assembly mounted from one of the bursting disc flanges on which six coupons may be attached.

The combustor has a number of 3 in n.b. sockets for thermocouples, pressure probes, gas sample probes etc.

Instrumentation

Pressure probes, purged by air, are used to give manometer readings for pressure drops over the air distributor, a fixed depth of fluidised bed, the total bed, the internal primary cyclone and seondary cyclone. Bed height is obtained from the ratio of the pressure drops across a fixed depth of bed and the total bed. A pressure tapping is used for the safety shut down system if the combustor pressure rises too high.

Thermocouples are situated in and above the fluidised bed. Bed temperature is automatically held constant by the coal feed rotary valve speed. High or low bed temperature will operate the shut down system.

1.4 Specimen tube assemblies

There is provision for six 2 in o.d. specimen tubes, four in the fluidised bed itself and two in the freeboard section (Fig. 2). The specimen tubes consist of seventeen rings ¾" long and 2 in o.d. of different alloys (Fig. 3). The rings are initially turned, then lapped with their neighbours and finally the outside surfaces, which are to be exposed to the bed environment, are ground to give a fine surface finish with a minimum of work hardening. The procedures for handling the rings are described in section 2.5.

The rings are clamped together and spring loaded to allow for expansion. Air is passed through the tubes for cooling and steam is available as a temporary coolant if the air supply fails during a run. The central former is shaped so that wall temperatures are as constant as possible throughout the length.

The four tubes in the bed can be removed together with the door on which they are mounted. Similarly, the two tubes above the bed are mounted on another door. A trolley device is used to carry each door when they are being removed or refitted.

Instrumentation

When corrosion tests are conducted, three of the specimen rings in each tube assembly have holes to accommodate 1/16 in bonded pyrotenax thermocouples. The thermocouples are used for control purposes and to operate the high temperature alarm/shut down system.

1.5 Coarse ash collection hopper

This receives ash from the overflow pipe in the combustor and has an ample capacity of 500 lb so that it can take ash for a 24 h period and may therefore be emptied daily.

1.6 Cyclone gas de-dusting system

This consists of two cyclones in series which separate fine ash and unburnt material from the hot effluent gases. The primary cyclone is mounted internally in the combustor so that the coarser fines may be returned to the bed. The dip leg (2 in o.d.) terminates at a level 1 in above coal feed line and 2 in off centre. It is shielded by a 2 in diameter stainless steel plate fixed 1 in beneath the end of the leg. In this way the returned fines have a greater chance to be burnt and so the overall combustion efficiency is improved. The secondary cyclone, which has a higher efficiency, is used for collecting as much of the escaping fine material as possible before the gases are discharged into the atmosphere. A flow straightener has been installed after the secondary cyclone for reducing the swirl of the gases before the dust sampling is carried out.

The primary and secondary cyclones have been designed according to Perry (1950) and based on inlet gas velocities of 50 and 100 ft/s respectively for a fluidising velocity of 3 ft/s at 1470°F.

The secondary cyclone and the gas line from the primary cyclone are electrically heated by three inconel sheathed heating elements, each of 1000 W.

Instrumentation

The electrical heaters are controlled by Sunvic regulators and thermocouples are used for measuring wall temperatures. Pressure probes permit the measurement of pressure drops over the cyclones.

1.7 Auxiliary sample equipment

1.7.1 Bed sampling

Samples of the ash bed are taken through an adjustable vertical stainless steel pipe mounted through the base of the combustor into the fluidised bed. The other end has a ¾ in Milliken valve and a 1½ in union which takes an 8 lb capacity sample container. A sample is taken by discarding the ash initially in the pipe and then collecting the required quantity in the sample container. Care is taken to keep the ash sample air tight until it has cooled sufficiently to prevent the combustion of any carbon in it.

1.7.2 Dust sampling

The exhaust gases from the secondary cyclones are sampled isokinetically. (See Fig.4). The essential features are a 5/16 in i.d. stainless steel probe and a stainless-steel filter (Gallenkamp) with stainless steel ball and socket joints (Size S19). The dust is separated in the filter on a glass paper disc. The gases are cooled in an acetone/solid carbon dioxide cold trap to remove moisture and finally metered through a rotameter and dry gas meter.

Before operating, the system is tested for leaks and a weighed filter paper is fitted into the holder. Gases are then withdrawn at the isokinetic rate for a set time and the volume of gas sampled is recorded. The dust sample is then taken and weighed with the filter paper.

1.7.3 Gas sampling

(a) Batch sampling

A water cooled gas sample probe situated 56.5 in above the air nozzles is used. When samples are not being taken, the probe is kept clear by an air purge. Samples are taken using evacuated 250 ml glass pipettes after the probe has purged itself by discharging combustion gases into the atmosphere for a few seconds.

The gases are analysed on a Fisher-Hamilton gas partitioner, Model 29, for CO_2, O_2, CO and CH_4.

(b) Continuous gas sampling

At the secondary cyclone outlet a continuous sample is withdrawn through an open-ended probe. A water ejector/separator (Mines Safety Appliances Co. Ltd.) pumps the gas to a Kent oxygen analyser, the output of which is continuously recorded. Some of the carbon dioxide in the gases is absorbed by the water but it is assumed that this is reasonably constant. Thus the continuous record give a good indication of the steadiness of the combustion conditions.

1.7.4 SO_2/SO_3 sampling

The SO_2 and SO_3 content of the exhaust gases leaving the secondary cyclone are determined by the 'Shell Condensation' Method. (Goksøyr,1962: Lisle, 1965). A diagram of the apparatus is given in Fig. 5.

A continuous sample of the exhaust gas is withdrawn through a silica glass probe at 6 ft^3/h for 10 min. The probe is followed by a quartz wool filter to separate the dust and the temperature of the gas at this point should be above the acid dew point, preferably above 480°F. The gas sample passes to the condenser which has water coolant between 140°F - 190°F, so that the SO_3 is condensed as sulphuric acid while the other gas constituents remain in the gas phase. After the condenser is a bubbler containing 100 ml of 3% hydrogen peroxide solution to absorb the sulphur dioxide.

The condenser is washed out with 5% isopropyl alcohol solution at pH 4.6 and sulphur is determined gravimetrically as barium sulphate. The solution from the bubbler is transferred to a separate vessel using 5% isopropyl alcohol as wash liquid and then boiled for 10 min to remove excess hydrogen peroxide. The solution is made up to 250 ml with distilled water, and an aliquot is titrated against N/50 sodium hydroxide to give a rough estimate of sulphur emission while the run is being carried out. The remainder is used to determine sulphur gravimetrically as barium sulphate. Alternatively, the total sulphur content of the flue gas during a run is determined by measuring the volume of flue gas required to decolourise a solution containing a known volume of iodine. This method uses the same sampling train already described but the condenser is omitted. The bubbler contains 2-15 ml (depending on SO_2 concentration in the flue gas) of 0.1 N iodine and 100 ml of 2% potassium iodide solution. Exhaust gas is drawn through the bubbler at 2 ft^3/h. Sulphur emission is then calculated from the volume of gas required to decolourise the iodine solution.

1.7.5 Volatilised alkali sampling

The sampling procedure is based on the postulate that the volatilised alkalis are present in the flue gas as alkali aerosols, which are responsible for the formation of alkali rich deposits on superheater tubes (Ounsted, 1958).

A metered bleed from the flue gas leaving the secondary cyclone is sucked through a stainless steel probe and passes through two electrostatic precipitators in series which remove the aerosols, (Fig. 6). These precipitators are washed out with hot distilled water and the alkali content (Na, K and Ca) of the washings is estimated using standard flame photometry. The probe and precipitators are kept above the acid dew point of the gases (above 300°F) using electrical heaters where necessary.

Chloride in the offgases is determined by totally the chloride collected in the electrostatic precipitators and the remainder absorbed in the hydrogen peroxide bubbler situated after the precipitators.

The measurement of chloride in the offgas appears to be satisfactory but there is doubt about the measurements of volatilised alkali salt concentrations. This is because the temperature of the sampling probe was only about 400°F making it possible for these salts to be deposited before reaching precipitators. It has also been found that, in addition to any condensed alkali salt, small quantities of fine ash (dust) containing Na, K and Ca were collected in the precipitators.

2. OPERATING PROCEDURES

2.1 Coal and limestone preparation

Both the Pittsburgh coal and Limestone 18 were crushed to minus 1680 μm. The coal and limestone were prepared on the Fluostatic dryer/sample house crusher system and the Atritor preparation plant respectively. These are described in Appendix I, sections 1.4.1 and 1.4.2.

2.2 Plant start-up

Hot products of combustion from the fluidising air preheater, to which excess air had been added to give a temperature of 1290°F, were passed through the air distributor into the empty fluidised bed combustor. External heat to the offtake gas lines and secondary cyclone was supplied by electric heaters controlled through three Sunvic regulators.

When the temperature within the bed had reached 480°F, the preheat gas was stopped while sufficient bed ash was introduced through a funnel inserted at the top of the combustor to give a 2 ft bed height. The ash bed was then fluidised with the hot gas from the air preheater in order to increase the bed temperature sufficiently for the combustion reaction to take over. At this time the temperature controllers on each of the six specimen tubes were set to operate on automatic control. The preheat gas flow rates were adjusted regularly in order to maintain 3 ft/s fluidising velocity as the bed temperature rose. When the bed temperature had reached 720°F, the coal feed was started at approximately 25% of the expected final rate. At 1110°F the fluidising air preheater was shut off and the main fluidising air controller was used. The coal feed was then increased to 50% and further increased to the final rate by the time that the desired bed temperature of 1560°F had been reached. The bed temperature controller was then switched to AUTO. Any minor adjustments to the fluidising air and specimen tube temperatures were then made.

The amount of air passed through the remaining control tubes was then set to obtain the desired combustion conditions. When the plant had stabilised on the required operating conditions and all alarms were correct, the safety shutdown system was switched on. The plant then shut itself down automatically and safely as described previously when any operating variable changed beyond preset limits.

Each test was commenced when the plant had reached the required bed temperature of 1560°F. The time taken from cold was about 5 h.

2.3 Throughput measurements and sampling

The coal feed and product rates were determined by the methods described below. The sample procedures are also given. Sections 3.1.1, 3.2.1 and 3.3.1 give details of mass balance periods.

2.3.1 Coal feed

Before and after the tests the coal feed rotary valve was calibrated to find the quantity of coal discharged per revolution. The rate was then calculated from the product of the number of revolutions of the rotary valve in a specified time, and thus, the calibration figure in lb/rev. An incremental coal sample over the mass balance period was obtained by diverting the coal to a sample cyclone for 10s every 10 min when the coal feed hoppers were being filled from the main storage bunker. The resulting 70 lb sample consisting of 20 increments of 3½ lb, was then subdivided using a rotary riffler to provide a sample for analysis.

2.3.2 Product ash

Excess bed ash was discharged via the overflow weir into a hopper. The ash collected over a mass balance period was then subdivided using a rotary riffler.

2.3.3 Bed samples

The samples were taken through a vertical pipe mounted through the base of the combustor into the fluidised bed as already described. Subdivision of the samples was carried out with a rotary riffler. During the 500 h tests bed samples were taken at the start and conclusion of each mass balance period.

2.3.4 Secondary fines

Most of the fine ash, which leaves the internal primary cyclone with the offtake gases, was collected by the secondary cyclone and discharged into a collection hopper. This material was also sampled using a rotary riffler.

2.3.5 Dust

The sampling procedure used has already been described. About ten samples of dust from the exhaust gases leaving the secondary cyclone were obtained for each mass balance period. They were bulked for chemical analysis. The chlorine content was high, probably because of the condensation of HCl from the flue gases. For mass balance purposes the chlorine content of the dust was assumed to be similar to that of the secondary fines.

2.3.6 Offtake gas

Sampling and analysis of the gaseous combustion products has already been described. Batch samples were taken at approximately 4 h intervals through a water cooled probe and analysed for CO_2, O_2, CO and CH_4.

The measurement of SO_2, SO_3, chloride and alkali aerosol (Na, K and Ca) content of the exhaust gases leaving the secondary cyclone has already been described. The frequency of sampling in each test is indicated in sections 3.1.2.1, 3.2.2.1 and 3.3.2.1 where the results are presented.

2.3.7 Mass balances - data processing

The feed rates, measured solids output rates and chemical analyses of the input and output streams were used to calculate mass balances which were carried out by computer.

The major factor in the mass balance, which was not measured was the flow rate of flue gas. It was necessary to estimate this. Since the gas analysis was carried out on a dry volume basis, the dry volume rather than mass flow rate of gas was estimated. This was done by correcting the feed air flow rate for the volume changes due to the reactions which occurred. These were:-

(i) $4H \text{ (coal)} + O_2 \longrightarrow 2H_2O \text{ (liquid)}$
(ii) $2O \text{ (coal)} \longrightarrow O_2$
(iii) $2C + O_2 \longrightarrow 2CO$
(iv) $CaCO_3 \longrightarrow CaO + CO_2$
(v) $CaO + \frac{1}{2}O_2 + SO_2 \longrightarrow CaSO_4$

The volume changes due to (i) and (ii) were calculated assuming that all the hydrogen and oxygen in the coal were released.

The increase due to (iii) was calculated from the measured concentration of CO in the flue gas. The net effect of (iv) and (v) was small and this was neglected. Thus the flue gas flow rate was calculated as

$$\text{Flue gas flow-rate} = \frac{\text{Air} + 379\text{X Coal Feed Rate x(O Content/32- H Content/4)}}{(1 - 0.5 \text{ x CO in Flue Gas})} \text{ SCFH}$$

The following mass balances were carried out:-

(i) Total. In this the mass flow rate of dry flue gas was calculated from the composition and a hydrogen balance was assumed.

(ii) Ash. This was a balance for the inorganic solids, i.e. ash and acceptor. No allowance was made for the weight changes due to calcining of $CaCO_3$ and formation of sulphate.

(iii) Carbon. This was a balance for the organic carbon in the coal and is directly relevant to the combustion process.

(iv) Nitrogen. This balance served as a check on the accuracy of the flue gas analysis.

(v) Oxygen. This is a balance for the oxygen in the air and the organic oxygen in the coal. It is directly relevant to the combustion process.

(vi) Sulphur, calcium, sodium, potassium and chlorine.

The following parameters were calculated from the flow rates in the mass balance:-

(i) Excess air level, defined as

$$\text{Excess air} = \frac{\text{Feed air} - \text{Stoichiometric air for coal feed rate}}{\text{Stoichiometric air for coal feed rate}} \times 100\%.$$

(ii) Carbon loss, defined as

$$\text{Carbon loss} = \frac{\text{Unburnt carbon output rate}}{\text{Total carbon output rate}} \times 100\%.$$

The carbon loss is based on the total measured carbon output rate since this is considered to be a more accurate estimate of the carbon input rate than that based on the coal feed rate and chemical composition.

2.4 Plant shut down

At the completion of each test the coal feed and fluidising air were stopped and the bed was fluidised with nitrogen whilst being discharged. The nitrogen supply was continued until the combustor body had cooled to below 390°F.

Specific operational details of the individual tests are given in sections 3.1.1, 3.2.1 and 3.3.1.

2.5 Corrosion test specimens

Seven steels were tested and their nominal compositions are given in Table 1. They represent the range of steels used in conventional coal and oil fired boilers with the exception of 12% Cr ferritic steel and Nimonic PE 16 which are under consideration for certain applications.

Table A.4.1 Typical Analyses of Alloys Tested

Material			Nominal Composition %											
Type	BSS	AISI No.	Cr	Ni	C max	Mn	P max	S max	Si max	Mo	Ti	Al	Fe	Other
Medium Carbon Steel	3059/5				0.25		0.05	0.05					Bal	
2¼% Cr, 1% Mo Steel	3059/622		2.25		0.15	0.7 max	0.04	0.04	0.5	1.00			Bal	
12% Cr Steel	EN 56 A	410	12		0.15	1.0 max	0.04	0.03	1.0				Bal	
Austenitic 316	EN 58 J	316	17	12	0.09	2.0 max	0.05	0.05	0.2	2.5			Bal	
Austenitic 347	EN 58 G	347	18	11	0.08	2.0 max	0.05	0.03	1.0				Bal	Nb 10 : C min
Esshete 1250			15	10	0.15	6.0	0.04	0.03	1.0	1.0			Bal	Nb 1%
Nimonic PE 16			17	43	0.10			0.02	0.3	3.0	1.2	1.2	Bal	

With the exception of Nimonic PE 16, the steels were obtained as 2 in o.d. cold drawn tube in a fully heat treated condition. The Nimonic PE 16 was supplied as 2 in diam. bar, fully heat treated, for the manufacture of the rings and as 16 s.w.g. sheet for the coupon plates.

2.5.1 Preparation before tests

The rings and coupons were manufactured according to Figs. 7 and 8 with the exception of coupons of Nimonic PE 16 (Fig. 9). All faces of the specimens made to Figs. 7 and 8 were fine turned except those indicated which were ground, with the minimum of work hardening to a surface finish, expressed as centre line average, of less than 10 μ in. The coupons of Nimonic PE 16 were cut from sheet and all burrs removed. The specimens were stored in a dessicator.

Before the outer surface of the rings were ground, they were assembled in the required order into tubes. Each ring was ground in with its neighbour using fine grinding paste in order to minimise leaks between the rings during the corrosion test. At this stage the thermocouple holes were drilled in three rings from each tube.

The identification of position of each specimen (rings and coupons) is given in Fig. 10. Rings f, l and p were fitted with thermocouples at the '9 o'clock' and '3 o'clock' positions for tubes 1, 3, 5 and tubes 2, 4, 6 respectively when viewed from the air inlet end.

After surface grinding the specimens were washed in Teepol solution, rinsed, dipped in acetone, dried and weighed. The rings were then assembled in the correct order and orientation into tubes held together by spring tensioned centre bodies. The assembled tubes were leak tested by sealing off the end of each tube and noting the flow rate of air required to maintain a constant pressure of 5 lb in^2 gauge. An acceptable leak rate was less than 30 s.c.f.h. In this case the air weeped uniformly through the ground joints between the rings. The tubes were next mounted in the combustor with the coupons. The tubes were leak tested again to check that their alignment had not been disturbed by the handling procedure.

2.5.2 Procedure during tests

Each tube was controlled to its required wall temperature using air as coolant. There was no failure of the air supply so emergency steam for cooling was not used at any time.

Tube wall temperatures were measured using thermocouples inserted into three rings on each tube (section 2.5.1).

2.5.3 Procedure after tests

When the combustor had cooled to below 200°F the tubes were withdrawn and photographed. The tubes and coupons were then removed from the doors and examined visually. Deposits and scales were sampled where they could be removed without damaging the metal specimens. Rings and coupons were then selected for more detailed microscopic examination of the fireside surfaces.

The majority of the test specimens were then descaled while some were retained. The descaling was carried out by immersing the specimens for 5 min in a bath of molten sodium hydroxide at 680 - 720°F containing 2% of sodium hydride. They were then water quenched and washed to remove all traces of scale.

The specimens were then re-weighed. A selection of both descaled and undescaled rings and coupons were then sectioned for metallographic examination.

3. RESULTS

3.1 Test Series 1

This preliminary run of 100 h duration was carried out to test the operation of the rig when burning the strongly caking Pittsburgh coal. The data on corrosion may be compared with the similar test of longer duration (Test Series 2: 500 h) in order to determine the effect of time on the steels when exposed to the fluidised combustion environment. No limestone was added with the feed.

3.1.1 Description of Test Series 1

The combustor operated continuously from 5th - 10th October 1970 with the exception of one shut-down lasting 5.83 h caused by a coal feed stoppage.

The initial bed was composed of minus 1680 μm burnt Newdigate shale and the average conditions during the test are given in Table 2.

Table A.4.2 Operating conditions during Test Series 1

Coal	Pittsburg
Coal size (upper limit), μm	1680
Acceptor	None
Fluidising velocity, ft/s	3
Bed temperature ^{o}F	1560
Bed depth, ft.	2
Recycle	Yes
Oxygen in flue gas, %	2

Because the original uncooled coal feed nozzle blocked frequently by coking in the hot section when initially tested with Pittsburg coal, a water cooled coal feed pipe was installed. It operated satisfactorily throughout. However, it was apparent that it caused some ash bed material to be occasionally transported up the dip leg of the internal primary cyclone and be collected in the secondary cyclone. This caused the secondary cyclone solids outlet to block.

For this reason it was not possible to measure the fines and dust output rates accurately. Estimates of these rates have been based on the relatively short periods with no blockages. Minus 1680 μm Newdigate shale was added daily to maintain the required bed height.

In order to allow for the 5.83 h shutdown the test was concluded 105.83 h after the start. The mass balance was commenced immediately after the shutdown at 21 h from the start of the test and continued to the end of the test. The length of the mass balance period was 84.83 h.

3.1.2 Results

3.1.2.1 Plant data

Chemical analysis and size distribution of the coal feed are given in Tables 3 and 4 respectively.

Table 5 gives chemical and size analyses of the bulk sample of secondary cyclone fines for the whole mass balance period. The coarseness of these fines was probably the result of the internal cyclone occasionally transporting ash bed material up the dip leg through the secondary cyclone. This would account for the slightly low carbon content of these fines compared with test Series 2 (Table 18).

Table A.4.3 Chemical Analysis of coal feed in test series 1

Proximate analysis		
Total moisture	% a.r.	1.0
Ash	% a.r.	13.6
Volatile matter	% d.a.f.	41.7
Ultimate analysis		
Carbon	% d.b.	70.5
Hydrogen	% d.b.	4.6
Nitrogen	% d.b.	1.45
Sulphur	% d.b.	2.75
Oxygen + errors	% d.b.	3.7
Chlorine	% d.b.	0.08
Carbon dioxide	% d.b.	0.79
Ash analysis		
CaO	% d.b.	7.4
Na_2O	% d.b.	0.7
K_2O	% d.b.	1.5
Fe_2O_3	% d.b.	18.4
Ash fusion Temp.		
Initial deformation	°F	1886
Hemisphere	°F	2174
Flow	°F	2228
Gross Calorific value	Btu/lb d.a.f.	15,120

Table A.4.4 Size distribution of coal feed in test series 1

Particle size (μm)	% in grade by weight
+ 1680	1.2
+ 500 - 1680	44.1
+ 250 - 500	18.7
+ 125 - 250	13.5
+ 63 - 125	14.3
- 63	8.2
Median dia. (μm)	440
Packed density (lb/ft^3)	65.3

Table A.4.5 Chemical and size analyses of secondary cyclone fines from Test Series 1

Weight percentage, "as received"	
Carbon*	23.4
Hydrogen	0.22
Sulphur	1.15
Chlorine	0.00
Carbon dioxide	0.19
CaO	3.6
Na_2O	0.46
K_2O	1.92
Fe_2O_3	10.7
Particle size (µm)	**% in grade by weight**
+ 1680	0.2
+ 500 - 1680	17.8
+ 250 - 500	15.2
+ 125 - 250	8.8
+ 63 - 125	14.0
- 63	44.0
Median dia. (µm)	88
Packed density (lb/ft^3)	60.4

Chemical analysis of the dust is given in Table 6.

Table A.4.6 Chemical analysis of dust from Test Series 1

Weight percentage, "as received"	
Carbon*	27.3
Hydrogen	0.33
Sulphur	1.55
Chlorine	0.18
Carbon dioxide	0.26
CaO	4.1
Na_2O	0.46
K_2O	1.32
Fe_2O_3	13.3

*Carbon does not include carbon present as carbon dioxide

Table 7 gives the chemical and size analyses of bed material. The initial ash bed was Newdigate shale which was also added daily in order to maintain the required bed height. No product ash was therefore obtained.

Table A.4.7 Chemical and size analyses of bed material from Test Series 1

Weight percentage, "as received"		
	Initial Ash Bed	Final Ash Bed
Carbon*	1.33	0.03
Hydrogen	0.33	0.03
Sulphur	0.30	1.05
Chlorine	0.03	0.01
Carbon dioxide	0.04	0.10
CaO	0.78	4.5
Na_2O	0.57	0.58
K_2O	3.94	3.21
Fe_2O_3	6.3	7.5
Particle size (μm)	% in grade by weight	
+ 1680	0.0	0.3
+ 500 - 1680	60.2	87.5
+ 250 - 500	18.2	9.8
+ 125 - 250	8.1	1.8
+ 63 - 125	4.4	0.4
- 63	8.1	0.2
Median dia. (μm)	750	850
Packed density (lb/ft^3)	93.8	83.3

*Carbon does not include carbon present as carbon dioxide

Figs. 11 and 12 present the off gas analyses taken during the test. No CO_2, O_2 and CO measurements were made from 15 h to 21 h because the plant was shut down. Methane was not found in any of the samples. Only two determinations of chloride were made because the equipment was faulty earlier in the test. Those made have been expressed as HCl (p.p.m.). The SO_2 and SO_3 content of the exhaust gases were determined by the 'Shell Condensation' method.

The mean gas analysis used in the mass balance was:

CO_2 %	15.4
O_2 %	1.9
CO %	0.033
SO_2 p.p.m.	2270
HCl p.p.m.	57

The alkali aerosol content of the exhaust gases leaving the secondary cyclone is given in Table 8. Only two determinations were obtained because a fault associated with the miniature electrostatic precipitators developed early in the run. Repairs were completed only just before the conclusion of the test.

There is some doubt about these results as discussed in section 1.7.5.

Table A.4.8 Concentration of Sodium, potassium and calcium in the flue gas: Test Series 1

Elapsed time from start of Test Series (h)	97.83	98.08
Conc. in flue gas (p.p.m. (wt))		
Na	5.7	7.2
K	3.1	2.8
Ca	74.2	64.0

The mass balance for Test Series 1 is given in Table 9. The method of calculation has been discussed in section 2.3.7. It was not possible to measure the fines and dust output rates accurately because the secondary cyclone solids outlet blocked at frequent intervals. Estimates of these rates have been based on the relatively short periods with no blockages. The negative offtake ash rate accounts for the shale which was added daily to maintain the required bed height.

The pressure drops and temperature distribution through the plant are shown in Tables 10 and 11, respectively. The normal operating ranges, excluding start up and shutdowns, are given.

Bed height, calculated from the pressure drop over the 8½ in of bed and the whole bed, varied from 22 in to 29 in during the test.

Table A.4.9 Mass balance for test series 1

Rate: lb/h	Total	Ash	Carbon	Nitrogen	Oxygen
Coal	20.2	3.0	14.3	0	0.7
Air	214.6	0.0	0.0	165	49.6
Total Input	234.8	3.0	14.3	165	50.3
Acc. in bed	0.0	0.0	0.0	0	0
Offtake Ash	-0.9	-0.9	0.0	0	0
Secondary fines	3.9	3.0	0.92	0	0
Exhaust Dust	1.0	0.7	0.27	0	0
Flue gas	229.6	0.0	13.30	167	47.8
Total Output	233.6	2.8	14.49	167	47.8
Loss (In - Out)	1.2	0.2	-0.19	-2	2.5
Loss Percent	0.51	6.67	-1.32	-1.21	4.97

Rate: lb/h	Sulphur	Ca	Na	K	Chlorine
Coal	0.556	0.147	0.014	0.035	0.016
Air	0.000	0.000	0.000	0.000	0.000
Total Input	0.556	0.147	0.014	0.035	0.016
Acc. in bed	0.008	0.026	0.000	-0.006	0.000
Offtake Ash	-0.003	-0.005	-0.004	-0.029	0.000
Secondary fines	0.044	0.100	0.013	0.059	0.000
Exhaust Dust	0.015	0.029	0.003	0.011	0.000
Flue gas	0.511	0.010	0.001	0.000	0.016
Total output	0.575	0.160	0.013	0.035	0.016
Loss (In - Out)	-0.019	-0.013	0.001	0.000	0.000
Loss Percent	-3.42	-8.8	7.1	0	0

Excess air is 2.5%

Carbon loss is 8.2% (Unburnt)

Table A.4.10 Pressure Drops through Plant in Test Series 1

Pressure drop, (in. water gauge)				
Baseplate	Bed	Density (over 8½ in)	1° cyclone	2° cyclone
10.5-12.5	17-23	7.0-8.0	1.2-1.5	3.5-5.5

$$\text{Bed height} = \frac{\Delta P \text{ (Bed)}}{\Delta P \text{ (density)}} \times 8.5 + 3 \text{ in.}$$

Table A.4.11 Temperature Distribution through Plant in Test Series 1

Position	Probe No.	Height above air nozzles (in)	Probe length (in)	Temperature (°F)
In bed	N1	3	3	1580-1600
In bed	N2	6	9	1580-1600
In bed	N2	11	6	1570-1590
In bed	N3	21	3	1560-1580
In bed	N3	21	9	1580-1600
In bed	N3	21	6	1560-1580
1° cyclone inlet	N9	88	3	1400-1450*
1° cyclone exit	-	-	2	1320-1380*
2° cyclone exit	-	-	2	1180-1220*

* Excluding first 24 h.

3.1.2.2 Visual examination of corrosion test specimens

When the tubes and coupons were removed from the combustor they were examined visually.

Tube 1 (in bed, 750°F)

There was a thin dark brown and slightly blistered scale on the rings of medium carbon and 2¼% Cr steel. The surfaces of the high chromium alloy rings had a thin brown film. However, on the underside of rings g - o there was a dark grey coke-like deposit approximately 0.02 in thick. This was probably the result of the close proximity of the coal feed nozzle.

Tube 2 (in bed, 1110°F)

In general, there was a thin reddish brown film except on the two rings of 2¼% Cr steel which had scaled to a greater extent than the same steel held at 750°F and 930°F.

Tube 3 (in bed, 930°F)

It appeared similar to tube 1 except there was no coke-like deposit on any of the rings.

Tube 4 (in bed, 1290°F)

There was a very reddish brown scale or deposit on the rings.

Tube 5 (above bed, 750°F)

There was a band about 3/4 in wide on the top of the tube which was protected by a layer of ash. On the underside of the tube was a thin layer of buff coloured dust-like deposit. The surfaces not covered by deposits had a thin oxide film which was slightly thicker on rings of medium carbon and 2¼% Cr steel.

Tube 6 (above bed, 1290°F)

It appeared similar to tube 5.

Coupons in the bed (1560°F)

The coupons had a red-brown oxide film.

Coupons above the bed (1440°F - 1560°F)

All coupons were covered with a fine buff deposit.

3.1.2.3 Chemical analysis of deposits

The deposits on the rings were in general very thin and adherent except for the deposits from tubes 5 and 6. As a result in most cases it was not possible to obtain a sample because the metal surface of the rings would have been damaged. Chemical analyses of those deposits and scale samples which were obtained are given in Table 12. Comparison with the analysis of bed ash given in Table 7 shows that the deposits were predominantly ash with little enrichment of potentially corrosive salts.

The chloride content of the deposits was low ($\leq$ 0.1%) except for the deposit from the 750°F tube 1 (1%) which was situated close to the coal feed nozzle. This deposit contained 53% carbon and on an ash basis there was three times more sulphur in the deposit than in the bed ash.

There was only a small enrichment of up to about two times the sulphur, sodium and calcium in the deposits from the tubes situated above the bed when compared with the bed ash.

Table A.4.12 Chemical analyses of deposit and scale samples from Test Series 1

Description of sample	Weight percentage, "as received"							
	C	S	Cl	CaO	MgO	Na_2O	K_2O	Fe_2O_3
Deposit from underside, tube 1 (750°F)	53.3	1.6	1.0	1.03	0.28	0.24	0.39	3.4
Scale from 2¼% Cr steel ring, tube 2 (1110°F)	-	0.3	0.07	1.06	0.13	0.42	1.02	94
Deposit from top, tube 5 (750°F)	-	2.3	0.03	6.2	1.13	0.53	1.9	-
Deposit from underside, tube 5 (750°F)	-	1.1	0.10	3.9	0.96	0.75	1.9	-
Deposit from top, tube 6 (1290°F)	-	2.5	0.02	6.3	1.13	0.51	1.9	-
Deposit from underside, tube 6 (1290°F)	-	1.3	0.08	4.1	1.18	0.85	2.5	-

Table A.4.13 Summary of Corrosion Results: Rings and Coupon Weight Loss - $\mu g/cm^2h$ (Test Series 1)

	Tube No.	Location of Ring	a	b	c	d	e	f	g	h	j	k	l	m	n	o	p	q	
Bed	1	Alloy Weight Loss Temperature (°F)	S **	MCS 74	F2 67	MCS 100	S 1	E 1 680	MCS 90 ± 13	F2 83	MCS ***	F2 ***	E 1 700	MCS 101 ± 30	F2 109	F2 111	S 1 860	E 3 ± 18	S **
	2	Alloy Weight Loss Temperature (°F)	S **	S 6	R 8	E 10	S 10	E 11 1150	F2 696 ± 18	R 7	E ***	S ***	E 9 1050	F2 462 ± 13	R 7	S 9	S 8 †	E 7	S **
	3	Alloy Weight Loss Temperature (°F)	S **	MCS 125	F2 153	MCS 193	S 2	E 3 940	MCS 143 ± 27	F2 154	MCS ***	F2 ***	E 3 940	MCS 190 ± 27	F2 198	F2 210	S 2 900	E 3 ± 18	S **
	4	Alloy Weight Loss Temperature (°F)	S **	S 9	R 10	E 17	S 13	E 21 1300	S 13 ± 27	R 12	E ***	S ***	E 24 1350	E 24 ± 36	R 11	S 11	S 11 1220	E 19 ± 18	S **
Freeboard	5	Alloy Weight Loss Temperature (°F)	S **	MCS 63	F2 86	MCS 66	S 3	E 2 740	MCS 62 ± 9	F2 68	MCS ***	F2 ***	E 1 830	MCS 57 ± 13	F2 65	F2 78	S 1 660	E 2 ± 18	S **
	6	Alloy Weight Loss Temperature (°F)	S **	S 3	R 3	E 7	S 3	E 8 1330	S 3 ± 36	R 5	E ***	S ***	E 10 1350	E 10 ± 36	R 6	S 4	S 5 1260	E 16 ± 36	S **

Coupons	Bed								Freeboard					
Temperature (°F)	1560								1440 - 1560					
Location	1	2	3	4	5	6	7	8	9	10	11	12	13	14
Alloy	S	*	*	E	R	*	*	*	*	E	S	R	*	*
Weight Loss	9			20	12					4	2	3		

* Coupon not fitted

† Thermocouple defective

** Ring used as Spacer

*** Ring not descaled, retained for further examination

MCS	Medium Carbon Steel
F2	Ferritic 2¼% Cr Steel
W	Ferritic 12% Cr Steel
S	Austenitic Type 316
R	Austenitic Type 347
E	Austenitic, Esshete 1250
N	Nimonic PE 16

Table A.4.14 Microscopic Examination of Specimens: Test Series 1

Alloy	Temp. (°F)	Specimen + position	Wt. loss (µg/cm²h)	Surface ** Texture	Pits (µm)	Deposit (D)/ Scale (S) (µm)	Penetration (µm)++	
							Sulphide	Oxide
Medium Carbon Steel	750	1j	*	smooth	0	20:S+50:D	0	3
	750	1m	101	smooth	0	-	0	3
	750	5j	*	smooth	0	8:S+30:D	0	0
	750	5m	57	smooth	0	-	0	0
	930	3j	*	rough	0	30:S	0	0
	930	3m	190	rough	0	-	0	8
2¼% Cr 1% Mo Steel	750	1k	*	smooth	0	15:S+50:D	0	0
	750	1o	111	smooth	0	-	0	2
	750	5k	*	rough	0	6:S+20:D	0	8
	750	5o	78	smooth	0	-	0	4
	930	3k	*	rough	0	20:S	15?	15?
	930	3o	210	rough	0	-	18?	18?
	1110	2g	696	v.rough	0	-	30	-
	1110	2m	462	v.rough	0	-	15	-
AISI 316	750	1p	1	smooth	0	-	0	2
	750	5p	1	smooth	0	-	0	0
	930	3p	2	smooth	0	-	0	0
	1110	2k	*	rough	0	10:S+5:D	0	5
	1290	4k	*	v.rough	0	15:S	20	-
	1290	6k	*	smooth	0	2:S+10:D	0	0
	1560	1	9	smooth	few 10	-	15	-
AISI 347	1110	2h	7	rough	0	-	0	2
	1290	4h	12	rough	0	-	0	6
	1290	6h	5	smooth	0	-	0	0
	1560	5	12	rough	few 15	-	0	8
Esshete 1250	750	11	1	smooth	0	-	0	0
	750	51	1	smooth	0	-	0	0
	930	31	3	smooth	0	-	0	0
	1110	2j	*	rough	few 20	10:S+5:D	0	5
	1290	4j	*	rough	0	18:S+10:D	10	-
	1290	6j	*	smooth	few 8	3:S+10:D	0	0
	1470	10	4	smooth	0	-	0	0
	1560	4	20	rough	few 15	-	0	8
PE 16	1560	2	8	smooth	0	-	0	6

* Specimens not descaled and reweighed at end of test.
+ See Fig. 10.
** See Section 3.1.2.5.
++ Sulphide penetration was accompanied by oxide penetration.

3.1.2.4 Specimen weight loss

Rings and coupons were weighed before the test and re-weighed after descaling at the conclusion of the run. The difference or weight loss results are given in Table 13 and expressed as $\mu g/cm^2$ of exposed surface to the fluidised combustion environment per h.

Rings a and r on each tube were not used for corrosion measurements because they were partly shielded by the combustor walls. A few rings were not descaled. These were sectioned for microscopic examination (section 3.1.2.5).

3.1.2.5 Metallographic examination

Some of the specimen rings and coupons were sectioned, mounted and polished. They were examined under a microscope and the observations are given in table 14.

The surface texture of each specimen is described using three categories (Fig. 13).

a.	Smooth:	surface irregularities of up to 4 μm.
b.	Rough:	surface irregularities of up to 12 μm.
c.	Very Rough:	surface irregularities of greater than 12 μm.

Irregularities of greater magnitude than the average texture have been reported as pits of specified depth. Whilst the surface texture is broadly indicative of the amount of corrosion which has taken place, caution should be applied, because a smooth surface does not necessarily imply that corrosion did not occur.

Where possible the maximum thickness of deposit and scale observed on specimens that had not been descaled, has been reported.

Where penetration was found, the maximum depth of sulphidation or oxidation has been given.

The results in Table 14 show that a small amount of sulphide and oxide penetration occurred with medium carbon and 2¼% Cr steels. There was some oxide penetration of the high chromium steels, but little sulphide penetration.

3.2 Test Series 2

This run of 500 h duration was carried out without limestone addition. The effect of limestone dosage on corrosion may be determined by comparing this test with Test Series 3 in which limestone was added to the feed. Corrosion data from this test may also be compared with the similar test of shorter duration (Test Series 1: 100 h) in order to determine the effect of time on the steels when exposed to the fluidised combustion environment.

3.2.1 Description of Test Series 2

The combustor operated continuously for 500 h from 4th - 25th November 1970 except for one short interruption of a few seconds, which was the result of a power cut.

The initial bed was composed of ash resulting from the combustion of Pittsburg coal in Test Series 1 and the average conditions for the test are given in table 15.

Table A.4.15 Operating conditions during Test Series 2

Coal	Pittsburg
Coal size (upper limit), µm	1680
Acceptor	None
Fluidising velocity, ft/s	3
Bed temperature °F	1560
Bed depth, ft	2
Recycle	Yes
Oxygen in flue gas, %	2

In the previous 100 h test (Test Series 1), the water cooled coal feed pipe caused the internal fines cyclone to function erratically. It was modified for this test so that the coal was discharged away from the cyclone dip-leg. The fines return system operated satisfactorily and bed height was maintained throughout with some offtake ash being produced.

Two mass balances were carried out as follows:

1. 0-115 h.
2. 283-383 h.

The coal feed and product rates were determined and samples taken by the methods already described.

3.2.2 Results

3.2.2.1 Plant data

Chemical analyses and size distributions of the coal feed for both mass balance periods are given in tables 16 and 17 respectively.

Table A.4.16 Chemical analysis of coal feed in Test Series 2

		1st balance period	2nd balance period
Proximate analysis			
Total moisture	% a.r.	0.9	1.5
Ash	% a.r.	12.7	13.1
Volatile matter	% d.a.f.	41.0	41.1
Ultimate analysis			
Carbon	% d.b.	72.7	72.3
Hydrogen	% d.b.	4.5	4.6
Nitrogen	% d.b.	1.45	1.45
Sulphur	% d.b.	2.75	2.75
Oxygen + errors	% d.b.	3.9	4.1
Chlorine	% d.b.	0.10	0.10
Carbon dioxide	% d.b.	0.70	0.70
Ash analysis			
CaO	% d.b.	7.9	7.8
MgO	% d.b.	1.3	1.4
Na_2O	% d.b.	0.7	0.7
K_2O	% d.b.	1.6	1.5
Fe_2O_3	% d.b.	17.2	16.2
Gross calorific value	Btu/lb d.a.f.	15,240	15,160

Table A.4.17 Size distribution of coal feed in Test Series 2

Particle size (μm)	% in grade by weight	
	1st balance Period	2nd balance Period
+ 1680	0.4	1.2
+ 500 - 1680	33.4	38.3
+ 250 - 500	18.9	16.0
+ 125 - 250	16.2	12.9
+ 63 - 125	29.6	22.9
- 63	1.5	8.7
Median dia. (μm)	290	300
Packed density (lb/ft^3)	55.2	54.2

Table 18 gives chemical and size analyses of secondary cyclone fines for both mass balance periods. Chemical analysis of dust is given in table 19.

Table A.4.18 Chemical and size analyses of secondary cyclone fines Test Series 2

	Weight percentage, "as received"	
	1st balance period	2nd balance period
Carbon*	30.7	31.6
Hydrogen	0.30	0.30
Sulphur	1.25	1.55
Chlorine	0.04	0.04
Carbon dioxide	0.26	-
CaO	4.5	4.5
MgO	0.81	0.9
Na_2O	0.47	0.46
K_2O	0.95	0.94
Fe_2O_3	12.0	11.3
Particle size (μm)	% in grade by weight	
+ 1680	0.0	0.0
+ 500 - 1680	1.5	1.4
+ 250 - 500	4.5	4.2
+ 125 - 250	5.9	6.2
+ 63 - 125	13.9	14.7
- 63	74.2	73.5
Median dia. (μm)	16	18
Packed density (lb/ft^3)	39.8	39.4

* Carbon does not include carbon present as carbon dioxide

Table A.4.19 Chemical analysis of dust from Test Series 2

	Weight percentage, "as received"	
	1st balance period	2nd balance period
Carbon*	11.9	17.0
Hydrogen	0.20	0.20
Sulphur	1.40	1.80
Chlorine	0.18	0.40
Carbon dioxide	0.11	-
CaO	4.8	10.9
MgO	1.11	1.56
Na_2O	0.70	0.61
K_2O	1.57	1.94
Fe_2O_3	12.7	8.2

* Carbon does not include carbon present as carbon dioxide

Table 20 gives the chemical and size analyses of bed material, including the initial and final ash bed. At the start and conclusion of both mass balance periods bed samples were taken.

Table A.4.20 Chemical and size analyses of bed material from Test Series 2

	Weight percentage, "as received"							
	Initial ash bed	1st balance period			2nd balance period			Final ash bed
		Bed sample 1	Product ash	Bed sample 2	Bed sample 1	Product ash	Bed sample 2	
Carbon*	0.03	0.01	0.50	0.00	0.00	0.48	0.00	0.2
Hydrogen	0.03	0.06	0.06	0.04	0.03	0.05	0.03	0.02
Sulphur	1.05	1.35	1.70	2.35	2.65	2.80	2.95	2.85
Chlorine	0.01	0.02	0.05	0.01	0.01	0.02	0.02	0.02
Carbon dioxide	0.10	0.15	0.17	-	-	-	-	0.40
CaO	4.5	6.7	8.1	9.2	12.3	4.9	11.1	12.2
MgO	-	1.46	1.43	1.52	1.69	1.05	1.59	1.61
Na_2O	0.58	0.68	0.69	0.62	0.58	0.64	0.60	0.59
K_2O	3.21	2.77	2.40	2.06	1.77	1.39	1.87	1.74
Fe_2O_3	7.5	7.3	7.9	7.71	8.3	11.3	8.3	8.0
Particle size (μm)	% in grade by weight							
+ 1680	0.3	0.0	0.3	0.0	1.0	0.6	1.2	0.0
+ 500 - 1680	87.5	86.6	84.3	84.8	84.4	81.3	82.5	75.6
+ 250 - 500	9.8	12.7	11.1	13.4	13.4	14.5	15.0	19.1
+ 125 - 250	1.8	0.6	2.0	1.1	0.8	2.3	0.8	3.9
+ 63 - 125	0.4	0.1	1.5	0.4	0.3	0.8	0.3	1.0
- 63	0.2	0.0	0.8	0.1	0.1	0.5	0.2	0.4
Median dia. (μm)	850	900	820	750	850	800	850	780
Packed density (lb/ft^3)	83.3	84.7	84.3	84.3	89.4	83.7	84.4	91.8

* Carbon does not include carbon present as carbon dioxide

Figs. 14-17 present the offgas analyses taken during the test. Methane was not found in any of the samples. Chloride results are expressed as HCl (p.p.m.). The SO_2 and SO_3 content of the exhaust gases were determined by the 'Shell Condensation' method. Some measurements of sulphur (SO_2) were also made using the iodine bubbler method.

The mean gas analyses used in the mass balances were:

1st balance period		2nd balance period	
CO_2 %	15.2	CO_2 %	15.6
O_2 %	2.3	O_2 %	2.1
CO %	0.066	CO %	0.09
SO_2 p.p.m.	2090	SO_2 p.p.m.	2050
HCl p.p.m.	64	HCl p.p.m.	63

Table 21 gives results of measurements of the alkali aerosol content of the exhaust gas leaving the secondary cyclone. There is some doubt in these results as has been discussed in section 1.7.5.

Table A.4.21 Concentration of sodium, potassium and calcium in the flue gas: Test Series 2

Elapsed time from start of test series (h)	1st balance period			2nd balance period			
	2.17	47.0	47.4	334.58	335.0	338.70	339.07
Conc. in flue gas p.p.m. (wt)							
Na	1.1	1.4	5.5	4.9	5.0	4.3	4.6
K	0.7	0.9	2.2	1.6	1.7	1.2	1.6
Ca	18.0	17.4	14.0	18.7	22.4	25.0	17.0

Table A.4.22 Mass Balance for test series 2: 1st balance period

Rate: lb/h	Total	Ash	Carbon	Nitrogen	Oxygen
Coal	20.4	2.7	14.8	0	0.8
Air	214.6	0.0	0.0	165	49.6
Total Input	235.0	2.7	14.8	165	50.4
Acc. in bed	0.0	0.0	0.0	0	0.0
Offtake Ash	0.4	0.4	0.0	0	0.0
Secondary fines	2.9	2.0	0.89	0	0.0
Exhaust Dust	0.3	0.2	0.03	0	0.0
Flue Gas	229.9	0.0	13.2	167	48.2
Total Output	233.5	2.6	14.12	167	48.2
Loss (In - Out)	1.5	0.1	0.68	-2	2.2
Loss Percent	0.64	3.70	4.59	-1.21	4.37

Rate: lb/h	Sulphur	Ca	Na	K	Chlorine
Coal	0.561	0.147	0.014	0.036	0.020
Air	0.000	0.000	0.000	0.000	0.000
Total Input	0.561	0.147	0.014	0.036	0.020
Acc. in bed	0.009	0.016	0.000	-0.005	0.000
Offtake Ash	0.007	0.024	0.002	0.008	0.000
Secondary fines	0.036	0.092	0.010	0.023	0.001
Exhaust dust	0.004	0.009	0.001	0.004	0.000
Flue gas	0.470	0.002	0.000	0.000	0.017
Total Output	0.526	0.143	0.013	0.030	0.018
Loss (In - Out)	0.035	0.004	0.001	0.006	0.002
Loss Percent	6.24	2.7	7.1	16.7	10.0

Excess air is 6.3%

Carbon loss is 6.5% (Unburnt)

Table.A.4.23 Mass Balance for test series 2: 2nd balance period

Rate: lb/h	Total	Ash	Carbon	Nitrogen	Oxygen
Coal	20.3	2.7	14.7	0	0.8
Air	214.6	0.0	0.0	165	49.6
Total Inout	234.9	2.7	14.7	165	50.4
Acc. in bed	0.0	0.0	0.0	0	0.0
Offtake Ash	0.4	0.4	0.0	0	0.0
Secondary Fines	3.0	2.1	0.96	0	0.0
Exhaust Dust	0.3	0.3	0.05	0	0.0
Flue Gas	230.9	0.0	13.5	167	48.9
Total Output	234.6	2.8	14.51	167	48.9
Loss (In - Out)	0.3	-0.1	0.19	-2	1.5
Loss Percent	0.13	-3.7	1.3	-1.2	2.98

Rate: lb/h	Sulphur	Ca	Na	K	Chlorine
Coal	0.558	0.151	0.014	0.035	0.020
Air	0.000	0.000	0.000	0.000	0.000
Total Input	0.558	0.151	0.014	0.035	0.020
Acc. in bed	0.003	-0.008	0.000	0.001	0.000
Offtake Ash	0.011	0.014	0.002	0.005	0.000
Secondary fines	0.047	0.097	0.010	0.024	0.001
Exhaust Dust	0.006	0.025	0.001	0.005	0.000
Flue gas	0.459	0.003	0.001	0.000	0.016
Total Output	0.526	0.131	0.014	0.035	0.017
Loss (In - Out)	0.032	0.020	0.000	0.000	0.003
Loss Percent	5.7	13.2	0	0	15

Excess air is 4.2%

Carbon loss is 7.0% (Unburnt)

The mass balances for Test Series 2 are given in tables 22 and 23. The method of calculation has been discussed in section 2.3.7. Both balances are thought to be satisfactory.

The pressure drops and temperature distribution through the plant are shown in tables 24 and 25 respectively. The normal operating ranges, excluding start up and shutdown, are given.

Bed height, calculated from the pressure drops over 8½ in bed and the whole bed, was 21 in to 25 in throughout the test.

Table A.4.24 Pressure drops through plant in Test Series 2

	Pressure drop, (in. water gauge)			
Baseplate	Bed	Density (over 8½ in)	1° cyclone	2° cyclone
7.0-9.0	18-23	8.5-9.0	1.5-2.0	5.0-6.5

$$\text{Bed height} = \frac{\Delta P\ (\text{bed}) \times 8.5}{\Delta P\ (\text{density})} + 3\ \text{in}$$

Table A.4.25 Temperature Distribution through plant in Test Series 2

Position	Probe No	Height above air nozzles (in)	Probe length (in)	Temperature (^{o}F)
In bed	N1	3	3	1540-1560
In bed	N2	6	9	1530-1550
In bed	N2	11	6	1540-1560
In bed	N3	21	3	1540-1560
In bed	N3	21	9	1530-1560
In bed	N3	21	6	1540-1560
1^{o} cyclone inlet	N9	88	3	1450-1500*
1^{o} cyclone exit	-	-	2	1340-1420*
2^{o} cyclone exit	-	-	2	1220-1240*

* Excluding first 24 h.

3.2.2.2 Visual examination of corrosion test specimens

When the tubes and coupons were removed from the combustor they were examined visually.

In general the condition of the surfaces appeared similar to that found at the conclusion of Test Series 1 which was conducted under similar operating conditions. However, on tube 1, there was little deposit on the underside of the rings.

3.2.2.3 Chemical analysis of deposits

The deposits on the rings were in general very thin and adherent except for the deposits from tubes 5 and 6. As a result in most cases it was not possible to obtain a sample because the metal surface of the rings would have been damaged. Chemical analyses of those deposits and scale samples which were obtained are given in table 26. Comparison with the analysis of product ash given in table 20 shows that the deposits were predominantly ash with little enrichment of potentially corrosive salts.

Table A.4.26 Chemical analysis of deposit and scale samples from Test Series 2

Description of Sample	Weight percentage, "as received"							
	C	S	Cl	CaO	MgO	Na_2O	K_2O	Fe_2O_3
Scale from 2¼% Cr steel ring, tube 2 (1110°F)	*	0.1	0.00	1.8	0.25	0.36	0.14	94
Deposit from top, tube 5 (750°F)	-	3.9	0.00	7.6	1.26	0.65	1.7	18
Deposit from underside, tube 5 (750°F)	0.4	*	*	3.5	0.88	0.77	1.3	33
Deposit from top, tube 6 (1290°F)	0.2	3.9	0.00	7.8	1.34	0.57	1.7	16
Deposit from underside, tube 6 (1290°F)	1.4	1.7	0.00	5.2	1.13	0.88	1.8	14

* insufficient sample

Table A.4.27 Summary of Corrosion Results: Rings and Coupon Weight Loss - μg/cm^{2}h (Test Series 2)

	Tube No.	Location of Ring	a	b	c	d	e	f	g	h	j	k	l	m	n	o	p	q	
Bed	1	Alloy Weight Loss Temperature (°F)	S **	MCS 73	F2 34	MCS ***	S 2.3	E 1.5 760	MCS 34.8 ± 9	F2 ***	W 1.1	F2 29.2	E 0.4	MCS 36.4	F2 33.0	W 2.4	S 0.3 700	E 0.5 ± 36	S **
	2	Alloy Weight Loss Temperature (°F)	S **	F2 459	R 3.7	W 4.9	S 4.0	E 4.5 1060	F2 793 ± 36	R 1.8	W 4.3	S 3.2	E 4.6 1110	F2 365 ± 18	R 2.0	W 5.9	S 3.0 1150	E 3.0 ± 18	S **
	3	Alloy Weight Loss Temperature (°F)	S **	MCS 64.7	F2 81.2	MCS ***	S 1.8	E 1.5 890	MCS 67.0 ± 27	F2 ***	W 4.5	F2 63.8	E 1.7 940	MCS 132 ± 45	F2 87.4	W 7.8	S 1.2 940	E 0.7 ± 27	S **
	4	Alloy Weight Loss Temperature (°F)	S **	N 2.6	R 3.1	W 2.2	S 4.7	E 6.3 1280	N 2.7 ± 9	R 3.4	W 2.6	S 3.8	E 9.2 1330	N 4.6 ± 13	R 3.8	W 5.1	S 3.6 1230	E 2.0 ± 13	S **
Freeboard	5	Alloy Weight Loss Temperature (°F)	S **	MCS 36.4	F2 29.4	MCS ***	S 0.2	E 0.2 730	MCS 20.8 ± 18	F2 ***	W 0.1	F2 22.7	E 0.1 790	MCS 18.4 ± 13	F2 23.2	W 1.6	S 0.1 700	E 0.2 ± 9	S **
	6	Alloy Weight Loss Temperature (°F)	S **	N 0.8	R 0.8	W 0.6	S 0.9	E 2.2 1300	N 1.2 ± 9	R 1.1	W 0.7	S 1.3	E 5.2 1330	N 2.1 ± 22	R 1.7	W 3.0	S 1.8 1230	E 6.1 ± 9	S **

Coupons	Bed								Freeboard					
Temperature (°F)	1560								1480 - 1560					
Location	1	2	3	4	5	6	7	8	9	10	11	12	13	14
Alloy	S	N	W	E	R	*	*	*	N	E	S	*	W	*
Weight Loss	5.4	2.9	308	7.3	6.6				1.5	3.4	1.2		3.4	

* Coupon not fitted   ** Ring used as Spacer   *** Ring not descaled, retained for further examination

MCS	Medium Carbon Steel	S	Austenitic Type 316
F2	Ferritic 2¼% Cr Steel	R	Austenitic Type 347
W	Ferritic 12% Cr Steel	E	Austenitic, Esshete 1250
		N	Nimonic PE 16

Table A.4.28 Microsopic Examination of Specimens: Test Series 2

Alloy	Temp. (^oF)	Specimen + position	Wt. loss ($\mu g/cm^2h$)	Surface ** Texture	Pits (μm)	Deposit (D)/ Scale (S) (μm)	Penetration (μm)++	
							Sulphide	Oxide
Medium Carbon Steel	750	1d	*	smooth	0	S:70	0	0
	750	1m	36.4	smooth	0	-	0	0
	750	5d	*	smooth	0	S:16+D:15	0	2
	750	5m	18.4	smooth	0	-	0	3
	930	3d	*	rough	few 15	S:65	12	-
	930	3m	132	rough	0	-	10	-
2¼% Cr, 1% Mo Steel	750	1c	34.0	smooth	0	-	0	0
	750	1h	*	smooth	0	S:24	0	0
	750	5c	29.4	smooth	0	-	0	5
	750	5h	*	rough	0	S:23+D:30	0	10
	930	3c	81.2	rough	0	-	24	-
	930	3h	*	v.rough	0	S:50+D:18	18	-
	1110	2g	793	v.rough	0	-	50	-
	1110	2m	365	v.rough	0	-	40	-
12% Cr Steel	750	1o	2.4	rough	0	-	0	6
	750	5o	1.6	smooth	0	-	0	0
	930	3o	7.8	smooth	0	-	0	3
	1110	2o	5.9	smooth	one 10	-	10	-
	1290	4o	5.1	smooth	few 10	-	0	2
	1290	6o	3.0	smooth	0	-	0	0
	1560	3	308	v.rough	0	-	100	-
AISI 316	750	1p	0.3	smooth	0	-	0	0
	750	5p	0.1	smooth	0	-	0	0
	930	3p	1.2	smooth	0	-	0	0
	1110	2p	3.0	smooth	one 6	-	0	0
	1290	4p	3.6	smooth	few 8	-	0	0
	1290	6p	1.8	smooth	0	-	0	0
	1560	1	5.4	smooth	0	-	0	4
AISI 347	1110	2h	1.8	smooth	0	-	0	0
	1290	4h	3.4	smooth	0	-	0	0
	1290	6h	1.1	smooth	0	-	0	0
	1560	5	6.6	rough	0	-	0	0
Esshete 1250	750	11	0.4	smooth	0	-	0	0
	750	51	0.1	smooth	0	-	0	0
	930	31	1.7	smooth	0	-	0	2
	1110	21	4.6	smooth	0	-	0	5
	1290	41	9.2	smooth	few 5	-	0	0
	1290	61	5.2	smooth	0	-	0	0
	1470	10	3.4	smooth	few 10	-	0	0
	1560	4	7.3	smooth	0	-	0	0
Nimonic PE16	1290	4m	4.6	smooth	0	-	0	3
	1290	6m	2.1	smooth	0	-	0	0
	1560	2	2.9	smooth	0	-	0	15

* Specimens not descaled and reweighed at end of test.
+ See Fig. A.4.10.
** See Section 3.2.2.5.
++ Sulphide penetration accompanied by oxide penetration.

3.2.2.4 Specimen weight loss

Rings and coupons were weighed before the test and re-weighed after descaling at the conclusion of the run. The difference or weight loss results are given in table 27 and expressed as μg/cm^2 of exposed surface to the fluidised combustion environment per hour. The weight loss after 500h was only about double that in 100 h, indicating a marked decrease in the rate of weight loss.

Rings a and r on each tube were not used for corrosion measurements because they were partly shielded by the combustor walls. A few rings were not descaled. These were sectioned for microscopic examination (section 3.2.2.5).

3.2.2.5 Metallographic examination

Some of the specimen rings and coupons were sectioned, mounted and polished. They were examined under a microscope and the observations are given in table 28, using the same categories as for Test Series 1, section 3.1.2.5.

Comparison with table 14 shows that for medium carbon and 2¼% Cr steels the amount of sulphide and oxide penetration in 500 h is slightly higher than after 100 h. There was almost no sulphide or oxide penetration of the high chromium steels during the 500 h test, although this was found in the 100 h test and also in a 1000 h test with Newstead coal (U.K.).

Carburisation, which can occur in steels subjected to strongly reducing conditions at elevated temperatures, was not found.

3.3 Test Series 3

This run of 500 h duration was carried out with limestone addition. The effect of limestone dosage on corrosion may be determined by comparing this test with another of similar duration (Test Series 2)in which no limestone was added to the feed. The long term effect on the level of sulphur dioxide in the exhaust gases when adding a constant proportion of limestone with the coal feed may also be determined.

3.3.1 Description of Test Series 3

The test was carried out on 4th-23rd January 1971. It was terminated at 465 h after a failure of the coal feed controller. However, the run time was sufficient to enable a satisfactory comparison to be made with the results of Test Series 2.

The initial bed was composed of ash resulting from the combustion of Pittsburgh coal in Test Series 2 with which a trial run of approximately 100 h duration with limestone addition was carried out immediately before this test. The average conditions are given in table 29.

Table A.4.29 Operating conditions during Test Series 3

Coal	Pittsburgh
Coal size (upper limit), μm	1680
Acceptor	Limestone 18
Acceptor size (upper limit)μm	1680
Stoichiometric ratio Ca/S	2
Fluidising velocity, ft/s	3
Bed temperature ^{o}F	1560
Bed depth, ft	2
Recycle	Yes
Oxygen in flue gas, %	2

Limestone to give a stoichiometric (Ca/S) mol ratio of two (21 lb of limestone to 100 lb coal) was mixed with the coal in 250 lb batches in a ribbon mixer. The mixture was stored in the 10 ton bunker which supplies the coal feed to the 12 in combustor. The usual method of coal feed was employed.

For three hours before the end of the run, while attempts were being made to rectify the fault in the coal feed control unit, the combustion conditions varied from reducing to oxidising. The total time under reducing combustion conditions was about 1½ h.

Except for this period of unsteady combustion, the plant operated satisfactorily. There were four minor interruptions each of several minutes duration caused by (a) temporary shortage of compressed air, (b) failure of instrument nitrogen supply, (c) false high specimen tube temperature alarm, (d) coal feed control fault. On the first three occasions the bed temperature did not fall below 1470°F. On the other occasion, the bed temperature dropped to between 1440 and 1470°F for 25 min because the coal feed rate was low.

Two mass balances were carried out as follows:

1. 0-100 h,
2. 334-434 h.

The coal feed and product rates were determined and samples taken by the methods already described.

3.3.2 Results

3.3.2.1 Plant data

Chemical analyses and size distributions of the coal plus limestone feed for both mass balance periods are given in tables 30 and 31 respectively. Table 31 shows that the feed for the second mass balance was much finer than in the first mass balance possibly the result of segregation in the 10 ton coal storage bunker.

Table 32 gives the chemical analysis of the limestone 18 used in this test. Six drums of mixed coal and limestone from the ribbon mixer were analysed for calcium in order to determine the consistency of mixing (Table 33). Each drum was subdivided using a rotary riffler. On each day during both mass balance periods, when the coal and limestone mix was being fed to the feed hoppers, a sample was obtained as described in section 2.3.1. For this test each day's sample was split using a rotary riffler to give a daily sample and bulked to give a combined sample for the mass balance period. The calcium analysis of each day's sample is given in table 34. It should be noted that the feed would start to be fed from the feed hopper into the combustor about 30 to 40 h from the time of sampling. This is because the lower feed hopper was always operated nearly full (800 lb capacity).

The calcium analyses of the bulk coal feed samples for the first and second mass balance periods were 9.25% and 7.55% CaO on an "as received" basis. The calculated calcium content of the coal plus limestone mix to give a stoichiometric ratio of two is 8.7% CaO, (as received).

Table A.4.30 Chemical analysis of coal feed + limestone in Test Series 3

		1st balance period	2nd balance period
Proximate analysis			
Total moisture	% a.r.	1.2	1.1
Ash	% a.r.	22.9	20.4
Volatile Matter	% d.a.f.	46.8	45.2
Ultimate analysis			
Carbon	% d.b.	57.8	61.6
Hydrogen	% d.b.	3.7	3.8
Nitrogen	% d.b.	1.15	1.30
Sulphur	% d.b.	1.95	2.05
Oxygen + errors	% d.b.	3.6	3.7
Chlorine	% d.b.	0.07	0.06
Carbon dioxide	% d.b.	6.70	5.10
Ash analysis			
CaO	% d.b.	39.9	36.6
MgO	% d.b.	1.2	1.2
Na_2O	% d.b.	0.6	0.6
K_2O	% d.b.	0.7	0.8
Fe_2O_3	% d.b.	6.5	7.3
Gross calorific value	Btu/lb d.a.f.	14,260	14,540

Table A.4.31 Size distribution of coal + limestone feed in Test Series 3

Particle size (μm)	% in grade by weight	
	1st balance period	2nd balance period
+ 1680	0.6	0.3
+ 500 - 1680	44.9	23.0
+ 250 - 500	19.7	18.1
+ 125 - 250	14.2	17.2
+ 63 - 125	9.2	25.7
- 63	11.4	15.7
Median dia. (μm)	440	180
Packed density (lb/ft^3)	66.1	55.0

Table A.4.32 Chemical analysis of limestone

Weight percentage, "as received"	
CaO	45.5
MgO	0.91
Si O_2	15.0
CO_2	36.7

Table A.4.33 Calcium analysis of coal + limestone feed for Test Series 3 (ex drums)

Weight percentage, "as received"						
Drum	1	2	3	4	5	6
CaO	8.8	9.4	7.85	8.0	7.15	7.55

Table A.4.34 Calcium analysis of coal + limestone feed for Test Series 3 (ex plant)

Weight percentage, "as received"									
Elapsed time from start of test series (h)	1st balance period				2nd balance period				
	1	22	46	70	310	334	358	382	406
CaO	8.55	8.7	7.85	8.55	8.25	7.3	7.15	7.85	8.55

Table A.4.35 Chemical and size analyses of secondary cyclone fines Test Series 3

	weight percentage, "as received"	
	1st balance period	2nd balance period
Carbon *	20.9	5.80
Hydrogen	0.35	0.13
Sulphur	4.05	6.30
Chlorine	0.03	0.06
Carbon dioxide	2.80	3.25
CaO	26.0	27.3
MgO	0.81	0.96
Na_2O	0.47	0.53
K_2O	0.57	0.75
Fe_2O_3	6.6	9.3
Particle size (μm)	% in grade by weight	
+ 1680	0.0	0.0
+ 500 - 1680	1.8	0.4
+ 250 - 500	5.0	1.1
+ 125 - 250	12.0	4.3
+ 63 - 125	16.9	9.8
- 63	64.3	84.4
Median dia. (μm)	38	12
Packed density (lb/ft^3)	60.3	46.3

*Carbon does not include carbon present as carbon dioxide

Table 35 gives chemical and size analysis of secondary cyclone fines for both mass balance periods. Chemical analysis of dust is given in Table 36.

It is noted that the carbon contents of the fines and dust from the second mass balance period were markedly lower than those from the first mass balance period. In addition the ash collected in the secondary cyclone was finer in the second balance period. This indicates that the internal fines return cyclone was probably working more efficiently towards the end of the test.

Table A.4.36 Chemical analysis of dust from Test Series 3

	Weight percentage, "as received"	
	1st balance period	2nd balance period
Carbon*	19.4	6.5
Hydrogen	0.45	0.24
Sulphur	3.60	5.30
Chlorine	1.00	0.60
Carbon dioxide	3.20	3.30
CaO	20.0	22.7
MgO	0.78	0.93
Na_2O	0.54	0.59
K_2O	0.83	0.94
Fe_2O_3	7.1	8.4

* Carbon does not include carbon present as carbon dioxide

Table 37 gives the chemical and size analyses of bed material, including the initial and final ash bed. At the start and conclusion of both mass balance periods bed samples were taken.

Table A.4.37 Chemical and size analyses of bed material from Test Series 3

	weight percentage "as received"							
	Initial ash bed	1st balance period			2nd balance period			Final ash bed
		Bed sample 1	Product ash	Bed sample 2	Bed sample 1	Product ash	Bed sample 2	
Carbon*	0.4	0.30	0.40	0.09	0.15	0.40	0.04	0.50
Hydrogen	0.08	0.06	0.07	0.06	0.07	0.09	0.08	0.05
Sulphur	6.9	6.60	8.05	9.05	9.20	9.40	10.6	9.85
Chlorine	0.02	0.01	0.02	0.02	0.02	0.03	0.02	0.04
Carbon dioxide	2.77	1.25	0.40	0.41	0.29	0.36	0.65	0.60
CaO	31.0	30.0	35.8	38.0	39.0	36.8	39.5	37.2
MgO	1.11	1.30	1.11	1.11	1.13	1.06	1.09	1.10
Na_2O	0.47	0.50	0.46	0.44	0.46	0.46	0.43	0.42
K_2O	0.84	0.90	0.57	0.46	0.39	0.39	0.34	0.43
Fe_2O_3	4.1	4.7	3.7	3.1	2.8	3.4	2.6	3.29
Particle size (μm)	% in grade by weight							
+1680	0.1	0.9	0.6	0.2	0.2	0.1	0.1	1.5
+ 500-1680	40.4	46.5	35.6	41.9	29.8	22.6	37.9	33.7
+ 250- 500	32.1	32.8	38.2	43.8	42.7	29.8	44.5	22.3
+ 125- 250	21.5	18.2	22.3	13.7	22.8	25.2	15.3	18.8
+ 63- 125	4.2	1.3	2.2	0.3	3.6	11.9	1.8	9.8
- 63	1.7	0.3	1.1	0.1	0.9	10.4	0.4	13.9
Median dia. (μm)	490	490	400	455	380	265	420	340
Packed density (lb/ft^3)	98.1	94.7	85.3	91.7	99.5	109	93.4	103

*Carbon does not include carbon present as carbon dioxide

It is noted that there was an increase in calcium and sulphur content of the bed material in the second balance period compared with the first balance period. There was also an increase in the amount of fine material in the ash. This evidence supports the possibility already discussed that the internal cyclone was operating more efficiently in the latter half of the test. Alternatively, the fineness of the product ash may have been the result of the finer feed in the second balance period.

Figures 18-21 present the offgas analyses taken during the test. Methane was not found in any of the samples. Chloride results are expressed as HCl (p.p.m). No measurements of chloride were made in the second balance period because emphasis was being placed on obtaining SO_2 measurements. The SO_2 and SO_3 content of the exhaust gases were determined by the 'Shell Condensation' method. Some measurements of SO_2 were also made using the iodine method. The mean gas analyses used in the mass balances were:

1st balance period		2nd balance period	
CO_2 %	15.6	CO_2 %	15.0
O_2 %	2.1	O_2 %	2.4
CO %	0.06	CO %	0.06
SO_2 p.p.m.	200	SO_2 p.p.m.	52
HCl p.p.m.	55	HCl p.p.m.	-

The SO_2 content in the flue gas averaged about 200 p.p.m. at the start and fell towards 50 p.p.m. at the end of the test which is equivalent to an improvement in SO_2 reduction from 0.90 to 0.97. This improvement in the efficiency of SO_2 removed from the exhaust gas could have been caused by a change in the sulphur or calcium content of the coal plus limestone feed. However, chemical analysis of the feed indicates no marked change in composition that could account for this reduction. This improvement in SO_2 reduction may have been the result of the internal cyclone operating more efficiently or the finer size of feed in the latter part of the test.

Table 38 gives results of measurements of the alkali aerosol content of the exhaust gas leaving the secondary cyclone. There is some doubt in these results as has been discussed in section 1.7.5.

Table A.4.38 Concentration of sodium, potassium and calcium in the flue gas: Test Series 3

Elapsed time from start of Test Series (h)	1st balance period				2nd balance period		
	51.05	51.48	92.67	93.03	361.87	433.35	433.72
Conc. in flue gas (p.p.m. (wt))							
Na	3.9	3.3	5.1	6.0	4.0	3.1	4.2
K	0.7	0.5	0.8	0.9	0.6	0.7	1.2
Ca	100	91	100	100	76	101	231

The mass balances for Test Series 3 are given in tables 39 and 40. The method of calculation has been discussed in section 2.3.7. Both balances seem satisfactory. Chlorine in the flue gas was not determined in the second balance period because the emphasis was being placed on obtaining SO_2 measurements.

The carbon loss dropped from 6.3% in the first balance period to 1.2% in the second balance period, probably due to the increase in efficiency of the internal cyclone in the latter half of the test as already discussed.

Table A.4.39 Mass balance for test series 3: 1st balance period

Rate: lb/h	Total	Ash	Carbon	Nitrogen	Oxygen
Coal + limestone	23.1	5.3	13.4	0	0.8
Air	214.6	0.0	0.0	165	49.6
Total Input	237.7	5.3	13.4	165	50.4
Acc. in bed	0.0	0.0	0.0	0	0.0
Offtake ash	2.6	2.6	0.01	0	0.0
Secondary fines	4.0	3.2	0.84	0	0.0
Exhaust dust	0.3	0.2	0.06	0	0.0
Flue gas	229.9	0.0	13.5	167	48.1
Total Output	236.8	6.0	14.41	167	48.1
Loss (In - Out)	0.9	-0.7	-1.01	-2	2.3
Loss Percent	0.38	-13.2	-7.5	-1.2	4.56

Rate: lb/h	Sulphur	Ca	Na	K	Chlorine
Coal + limestone	0.450	1.523	0.022	0.033	0.016
Air	0.000	0.000	0.000	0.000	0.000
Total Input	0.450	1.523	0.022	0.033	0.016
Acc. in bed	0.024	0.059	0.000	-0.004	0.000
Offtake ash	0.210	0.667	0.009	0.012	0.001
Secondary fines	0.162	0.743	0.014	0.019	0.001
Exhaust dust	0.011	0.044	0.001	0.002	0.000
Flue gas	0.046	0.014	0.001	0.000	0.015
Total Output	0.453	1.527	0.025	0.029	0.017
Loss (In - Out)	-0.003	-0.004	-0.003	0.004	-0.001
Loss Percent	-0.7	-0.26	-13.6	12.1	-6.25

Excess air is 5.5%

Carbon loss is 6.3% (Unburnt)

Table A4.[illegible] Mass balance for test series [illegible] 2nd balance period

Rate: lb/h	Total	Ash	Carbon	Nitrogen	Oxygen
Coal + limestone	21.0	4.3	12.9	0	0.8
Air	214.6	0.0	0.0	165	49.6
Total Input	235.6	4.3	12.9	165	50.4
Acc. in bed	0.0	0.0	0.0	0	0.0
Offtake ash	2.6	2.5	0.01	0	0.0
Secondary fines	1.9	1.8	0.11	0	0.0
Exhaust dust	0.5	0.5	0.03	0	0.0
Flue gas	229.1	0.0	13.0	168	46.9
Total Output	234.1	4.8	13.15	168	46.9
Loss (In - Out)	1.5	-0.5	-0.25	-3	3.5
Loss Percent	0.64	-11.6	-1.94	-1.8	6.94

Rate: lb/h	Sulphur	Ca	Na	K	Chlorine
Coal + limestone	0.431	1.134	0.019	0.030	0.013
Air	0.000	0.000	0.000	0.000	0.000
Total Input	0.431	1.134	0.019	0.030	0.013
Acc. in bed	0.014	0.004	0.000	0.000	0.000
Offtake ash	0.240	0.670	0.009	0.008	0.001
Secondary fines	0.120	0.372	0.008	0.012	0.001
Exhaust dust	0.028	0.085	0.002	0.004	0.000
Flue gas	0.012	0.018	0.001	0.000	-
Total Output	0.414	1.149	0.020	0.024	-
Loss (In - Out)	0.017	-0.015	-0.001	0.006	-
Loss Percent	3.9	-1.3	-5.26	20.0	-

Excess air is 12.0%

Carbon loss is 1.2% (Unburnt)

The pressure drops and temperature distribution through the plant are shown in tables 41 and 42 respectively. The normal operating ranges, excluding start up and shutdowns, are given.

Bed height, calculated from the pressure drop over 8½ in bed and over the whole bed, was 21 in to 24 in throughout the test.

Table A.4.41 Pressure drops through plant in Test Series 3

Pressure drop, (in. water gauge)				
Baseplate	Bed	Density (over 8½ in)	1° cyclone	2° cyclone
10.5-11.0	16-18	7.5-8.5	1.4-1.8	4.0-6.0

$$\text{Bed height} = \frac{\Delta P \text{ (bed)}}{\Delta P \text{ (density)}} \times 8.5 + 3 \text{ in.}$$

Table A.4.42 Temperature distribution through plant in Test Series 3

Position	Probe No.	Height above air nozzles (in)	Probe length (in)	Temperature (°F)
In bed	N1	3	3	1540-1560
In bed	N2	6	9	1530-1540
In bed	N2	11	6	1530-1550
In bed	N3	21	3	1540-1560
In bed	N3	21	9	1530-1550
In bed	N3	21	6	1550-1560
1° cyclone inlet	N9	88	3	1400-1420*
1° cyclone exit	-	-	2	1280-1320*
2° cyclone exit	-	-	2	1170-1180*

* Excluding first 24 h.

3.3.2.2 Visual examination of corrosion test specimens

When the tubes and coupons were removed from the combustor they were examined visually.

In general the fireside surfaces were in a similar condition as those from Test Series 2.

The following differences were noted:-

(a) The surfaces of the tubes in the bed were darker in colour which may have resulted from the relatively short period of substoichiometric combustion at the end of the test.

(b) There was more deposit (about 2 in. deep) on top of the 'above bed' tube 6. A similar deposit of fine particulate material was found on top of the coupons situated above the bed.

3.3.2.3 Chemical analysis of deposits

The deposits on the rings were in general very thin and adherent except for the deposits from tubes 5 and 6. As a result in most cases it was not possible to obtain a sample because the metal surface of the rings would have been damaged. Chemical analysis of those deposit samples which were obtained are given in table 43. Comparison with the analysis of product ash given in table 37 shows that the deposits were predominantly ash with little enrichment of potentially corrosive salts.

There was insufficient sample of deposit from the underside of tube 1 for a complete analysis. However some enrichment of alkali salt is indicated by the sodium content being three times that of the product ash.

Table A.4.43 Chemical analysis of deposit and scale samples from Test Series 3

Description of sample	Weight percentage, "as received"							
	C	S	Cl	CaO	MgO	Na_2O	K_2O	Fe_2O_3
Deposit from underside, tube 1 (750°F)	*	*	*	14	0.93	1.48	1.08	13
Deposit from top, tube 5 (750°F)	1.8	8.5	0.00	37	1.08	0.50	0.45	9.7
Deposit from underside, tube 5 (750°F)	*	*	*	28	0.93	0.54	0.54	-
Deposit from top, tube 6 (1290°F)	1.3	10.3	0.08	39	1.10	0.46	0.35	8.7
Deposit from underside, tube 6 (1290°F)	*	*	*	25	1.00	0.78	0.69	*

* insufficient sample

3.3.2.4 Specimen weight loss

Rings and coupons were weighed before the test and reweighed after descaling at the conclusion of the run. The difference or weight loss results are given in table 44 and expressed as $\mu g/cm^2$ of exposed surface to the fluidised combustion environment per hour.

There is little difference between the rate of weight loss in this test and in the 500 h test without limestone, Table 27, indicating that the addition of limestone to the bed does not effect the rate of weight loss.

Rings a and r on each tube were not used for corrosion measurements because they were partly shielded by the combustor walls. A few rings were not descaled. These were sectioned for microscopic examination (section 3.3.2.5).

Table A.4.44 Summary of Corrosion Results: Rings and Coupon Weight Loss - $\mu g/cm^2h$ (Test Series 3)

	Tube No.	Location of Ring	a	b	c	d	e	f	g	h	j	k	l	m	n	o	p	q	
Bed	1	Alloy Weight Loss Temperature (°F)	S **	MCS 340	F2 40.3	MCS ***	S 1.4	E 1.1 720	MCS 42.8 ± 13	F2 ***	W 1.4	F2 36.2	E 0.9 740	MCS 47.2 ± 9	F2 50.7	W 1.8	S 0.9 750	E 1.2 ± 36	S **
	2	Alloy Weight Loss Temperature (°F)	S **	F2 94.8	R 2.1	W 3.4	S 2.9	E 2.6 1090	F2 286 ± 9	R 2.2	W 3.0	S 1.7	E 2.6 1120	F2 285 ± 9	R 1.8	W 1.6	S 2.5 1100	E 2.4 ± 9	S **
	3	Alloy Weight Loss Temperature (°F)	S **	MCS 60.5	F2 74.6	MCS ***	S 2.2	E 2.1 940	MCS 80.0 ± 9	F2 ***	W 6.7	F2 82.3	E 2.3 920	MCS 112.0 ± 13	F2 136	W 4.2	S 1.6 905	E 1.8 ± 9	S **
	4	Alloy Weight Loss Temperature (°F)	S **	N 3.1	R 5.7	W 4.6	S 5.7	E 8.2 1320	N 4.8 ± 27	R 6.1	W 7.7	S 6.6	E 16.0 1320	N 5.8 ± 27	R 5.7	W 9.1	S 4.8 1250	E 13.8 ± 13	S **
Freeboard	5	Alloy Weight Loss Temperature (°F)	S **	MCS 12.7	F2 16.1	MCS ***	S 0.2	E 0.5 800	MCS 21.4 ± 27	F2 ***	W 1.1	F2 18.0	E 0.6 730	MCS 18.8 ± 18	F2 20.8	W 3.1	S 0.2 700	E 0.5 ± 54	S **
	6	Alloy Weight Loss Temperature (°F)	S **	N 1.1	R 1.4	W 1.7	S 1.2	E 2.6 1300	N 1.8 ± 9	R 1.5	W 2.2	S 1.4	E 5.4 1320	N 2.7 ± 13	R 2.2	W 2.8	S 1.8 1240	E 8.6 ± 9	S **

Coupons	Bed								Freeboard					
Temperature (°F)	1560								1420 - 1560					
Location	1	2	3	4	5	6	7	8	9	10	11	12	13	14
Alloy	S	N	W	E	R	*	*	*	N	E	S	R	W	*
Weight Loss	2.2	2.1	475	3.4	2.8				2.3	11.6	2.8	1.5	1.6	

* Coupon not fitted

** Ring used as Spacer

*** Ring not descaled, retained for further examination

MCS	Medium Carbon Steel
F2	Ferritic 2¼% Cr Steel
W	Ferritic 12% Cr Steel
S	Austenitic Type 316
R	Austenitic Type 347
E	Austenitic, Esshete 1250
N	Nimonic PE 16

Alloy	Temp. (^{o}F)	Specimen + position	Wt. loss (μg/cm^{2}h)	Surface ** Texture	Pits (μm)	Deposit (D)/ Scale (S) (μm)	Penetration (μm)++	
							Sulphide	Oxide
Medium Carbon Steel	750	1d	*	smooth	0	28:S	0	3
	750	1m	47.2	smooth	0	–	0	2
	750	5d	*	smooth	0	10:S+6:D	0	0
	750	5m	18.8	smooth	0	–	0	0
	930	3d	*	rough	few 26	100:S+D	0	0
	930	3m	112	rough	0	–	10	–
2¼% Cr 1% Mo Steel	750	1c	40.3	smooth	0	–	0	4
	750	1h	*	smooth	0	15:S+20:D	0	0
	750	5c	16.1	smooth	0	–	0	0
	750	5h	*	smooth	0	10:S+6:D	0	0
	930	3c	74.6	smooth	0	–	20	–
	930	3h	*	v.rough	0	50:S+30:D	10	–
	1110	2b	94.8	rough	0	–	16	–
	1110	2g	286	v.rough	0	–	26	–
	1110	2m	285	v.rough	0	–	40	–
12% Cr steel	750	1o	1.8	smooth	0	–	0	0
	750	5o	3.1	smooth	0	–	0	0
	930	3o	4.2	rough	0	–	0	10
	1110	2o	1.6	smooth	few 8	–	8	–
	1290	4o	9.1	smooth	0	–	26	–
	1290	6o	2.8	smooth	few 13	–	0	0
	1560	3	475	v.rough	0	–	100	–
AISI 316	750	1p	0.9	smooth	0	–	0	0
	750	5p	0.2	smooth	0	–	0	0
	930	3p	1.6	smooth	0	–	0	6
	1110	2p	2.5	smooth	one 8	–	12	–
	1290	4p	4.8	smooth	0	–	8	–
	1290	6p	1.8	smooth	0	–	0	0
	1560	1	2.2	smooth	few 15	–	40	–
AISI 347	1110	2h	2.2	smooth	0	–	0	0
	1290	4h	6.1	smooth	0	–	16	–
	1290	6h	1.5	smooth	one 13	–	0	0
	1560	5	2.8	smooth	0	–	28	–
Esshete 1250	750	11	0.9	smooth	0	–	0	2
	750	51	0.6	smooth	0	–	0	0
	930	31	2.3	smooth	0	–	0	0
	1110	21	2.6	smooth	0	–	0	2
	1290	41	16.0	smooth	0	–	10	–
	1290	61	5.4	smooth	0	–	0	0
	1470	10	11.6	smooth	few 20	–	0	0
	1560	4	3.4	rough	0	–	20	–
Nimonic PE 16	1290	4m	5.8	smooth	0	–	18	–
	1290	6m	2.7	smooth	0	–	0	0
	1560	2	2.1	rough	0	–	0	20

* Specimens not descaled and reweighed at end of test.

+ See Fig. A.4.10.

** See Section 3.3.2.5.

++ Sulphide penetration accompanied by oxide penetration.

3.3.2.5 Metallographic Examination

Some of the specimen rings and coupons were sectioned, mounted and polished. They were examined under a microscope and the observations are given in table 45, using the same categories as for Test Series 1, Section 3.1.2.5.

Comparison of these results with Test Series 2, table 28, shows that limestone addition did not increase the penetration of medium carbon and 2¼% Cr steels. The apparent increase for high chromium steels is due to the surprisingly low penetration in Test Series 2 and the actual amount of penetration is little different from that obtained using Newstead coal (U.K.) without limestone.

Carburisation, which can occur in steels subjected to strongly reducing conditions at elevated temperatures, was not found.

3.3.2.6 Electron probe microanalysis

Three specimens from this test with limestone addition have been examined at the University of Aston using an electron probe micro-analyser. They were chosen in order to verify the sulphide attack indicated by optical microscopy.

Two specimens from ring 2m (Ferritic 2¼% Cr steel, 1110°F) which had apparently suffered penetration to depths of up to 40μm were examined and this type of attack was confirmed. Figures 22 and 23 show the optical photo-micrograph with corresponding X-ray photographs of two of the areas examined. The lighter regions in the X-ray photographs indicate higher concentrations of the element being determined. Thus manganese and sulphur are associated with the grey rounded particles forming the intergranular attack with, in one case, a higher concentration of chromium. The rest of the localised higher concentrations of manganese and sulphur are inclusions of manganese sulphide present in the original steel. This has been verified by electron probe micro-analysis at the centre of one of the specimens. A line scan at right angles to the metal surface showed a slight decrease in iron and chromium content to a depth of about 50 μm (Fig. 24).

The other specimen examined was of ferritic 12% Cr steel held at 1290°F (4o). Optical examination showed that sulphide attack was apparent to depths of up to 26 μm. Electron probe microanalysis confirmed this type attack (Fig. 25). It is also evident that there was slightly less chromium in this region adjacent to the metal surface.

4. REFERENCES

Goksøyr, H. and Ross, K., J. Inst. Fuel, (1962), 36, 177-179

Lisle, E.S. and Sensenbaugh, J.D., Combustion, (1965), 36, 12-16

Ounsted, D., J. Inst. Fuel, (1958), 31, 474-479.

Perry, J.H., Chemical Engineer's Handbook, McGraw-Hill, (1950), 1024.

5. ACKNOWLEDGMENT

The authors acknowledge the contributions of their colleagues at CRE in carrying out the work described in this report. The work was administered by Dr. A.D. Dainton and Mr. J. McLaren and the overall experimental programme was devised in consultation with Mr. D.C. Davidson. Mr. B.J. Bowles was responsible for the operation of the plant; the chemical analyses were carried out under the supervision of Dr. H.A. Standing by Mr. G.J. Corney, Mr. H.W. Harris and Mr. L. Stanley; metallographic examination of the corrosion test specimens was carried out under the supervision of Dr. G. Pitt by Mr. A. Page; maintenance of the plant was carried out by the CRE engineering and instrumentation sections.

The electron probe microanalysis of corrosion test specimens was carried out by Mr. R. Howell of the Metallurgy Department, University of Aston in Birmingham.

The contribution made by Mr. E.L. Carls, the O.A.P. representative in the U.K. is also acknowledged.

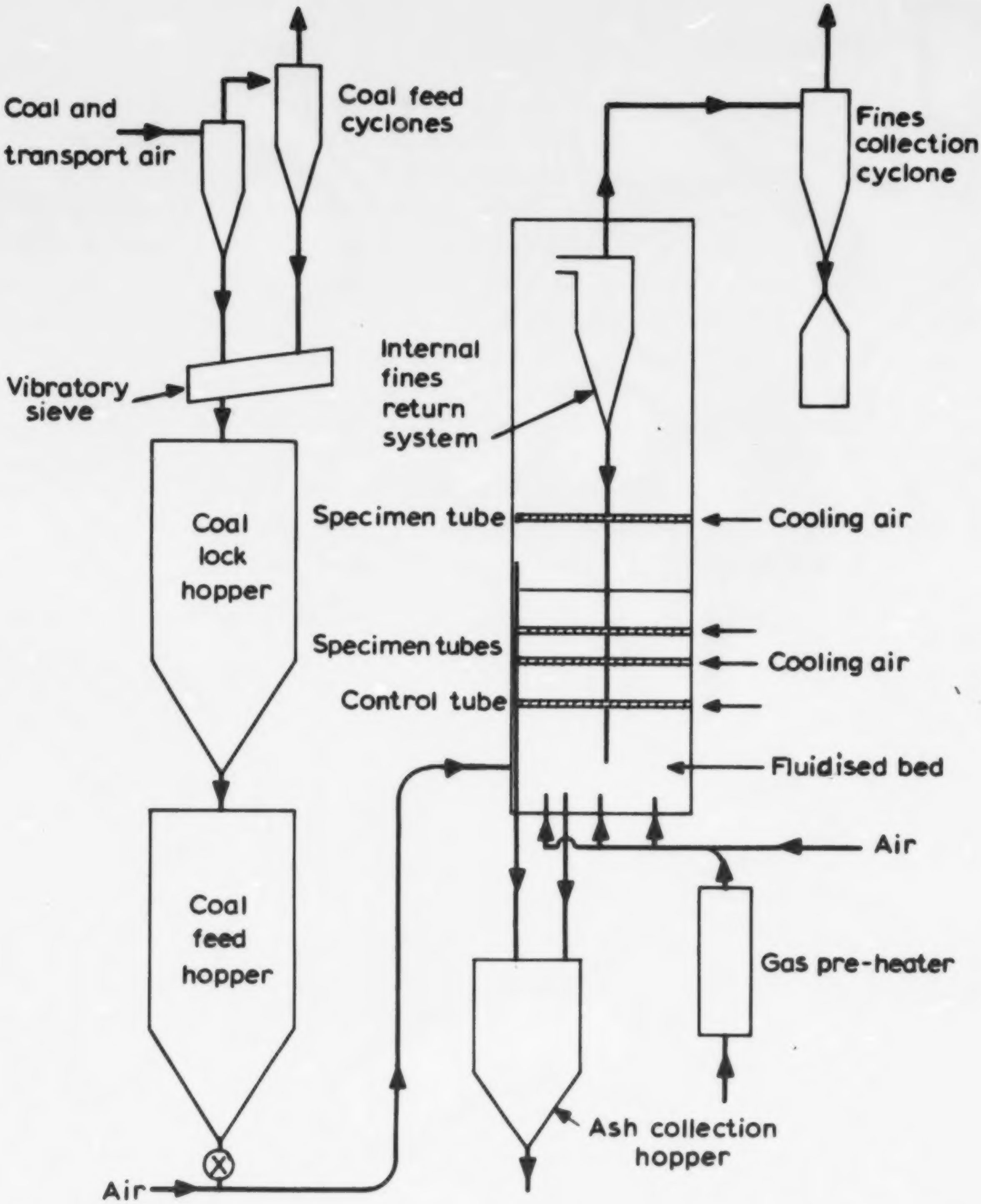
Coal and transport air
Coal feed cyclones
Vibratory sieve
Coal lock hopper
Coal feed hopper
Air
Fines collection cyclone
Internal fines return system
Specimen tube
Cooling air
Specimen tubes
Cooling air
Control tube
Fluidised bed
Air
Gas pre-heater
Ash collection hopper

Fig. A4.1. 12in combustor for corrosion experiments (CRE)

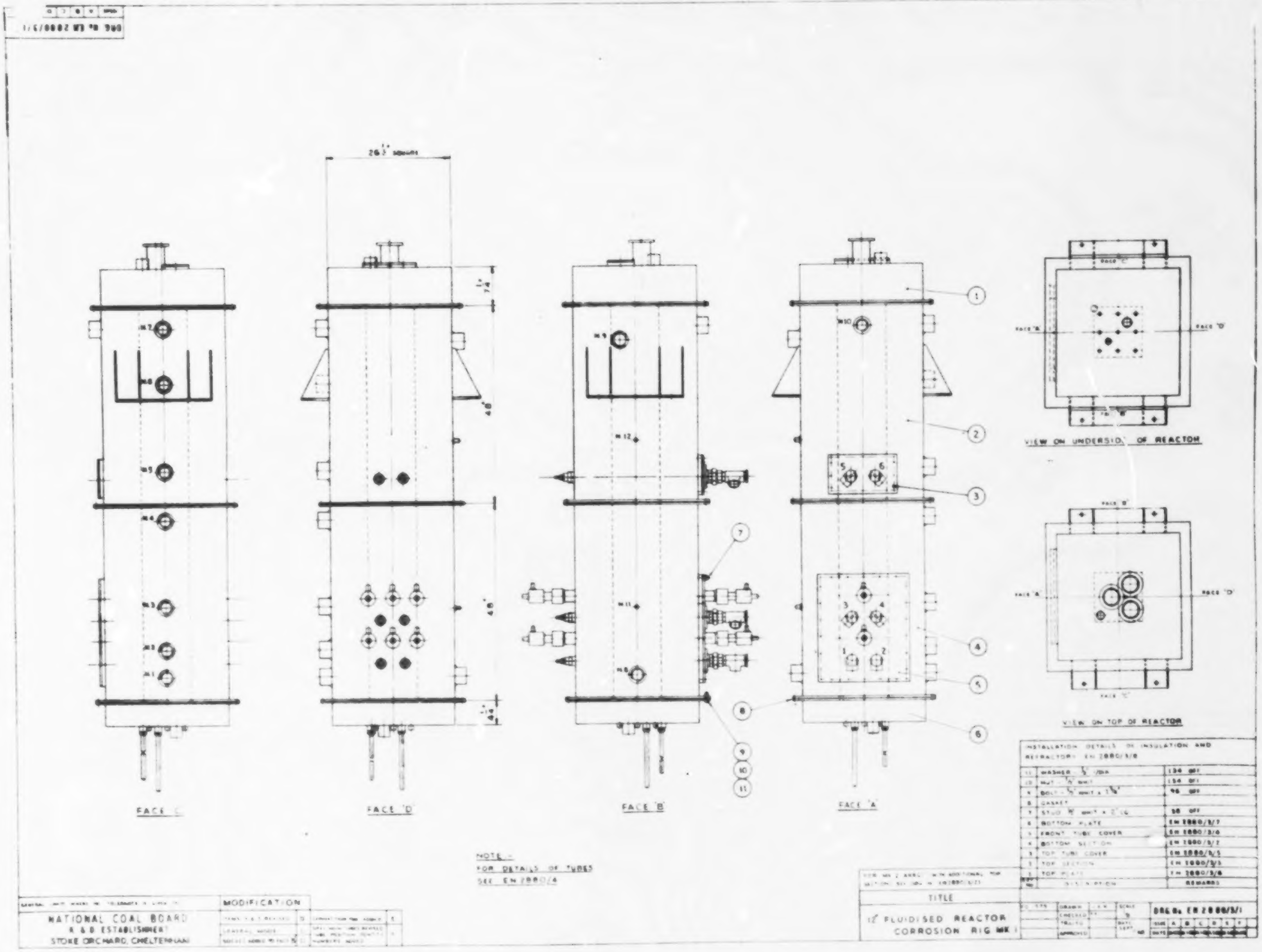
DRG. No. EN 2080/3/1
26 1/2" SQUARE
FACE 'C'
FACE 'D'
FACE 'B'
FACE 'A'
VIEW ON UNDERSIDE OF REACTOR
VIEW ON TOP OF REACTOR
FACE 'A'
FACE 'B'
FACE 'C'
FACE 'D'
1
2
3
4
5
6
7
8
9
10
11
NOTE:-
FOR DETAILS OF TUBES
SEE EN 2080/4
INSTALLATION DETAILS OF INSULATION AND
REFRACTORY EN 2080/3/8
11 WASHER 1/2" DIA 134 OFF
10 NUT 1/2" WHIT 134 OFF
9 BOLT 1/2" WHIT x 1 3/4" 96 OFF
8 GASKET
7 STUD 1/2" WHIT x 2" LG 38 OFF
6 BOTTOM PLATE EN 2080/3/7
5 FRONT TUBE COVER EN 2080/3/6
4 BOTTOM SECTION EN 2080/3/2
3 TOP TUBE COVER EN 2080/3/5
2 TOP SECTION EN 2080/3/3
1 TOP PLATE EN 2080/3/4
DESCRIPTION
REMARKS
TITLE
12" FLUIDISED REACTOR
CORROSION RIG MK I
DRAWN
CHECKED
TRACED
APPROVED
SCALE
DRG. No. EN 2080/3/1
MODIFICATION
NATIONAL COAL BOARD
R & D ESTABLISHMENT
STOKE ORCHARD, CHELTENHAM

Fig. A4. 2. 12in Combustor

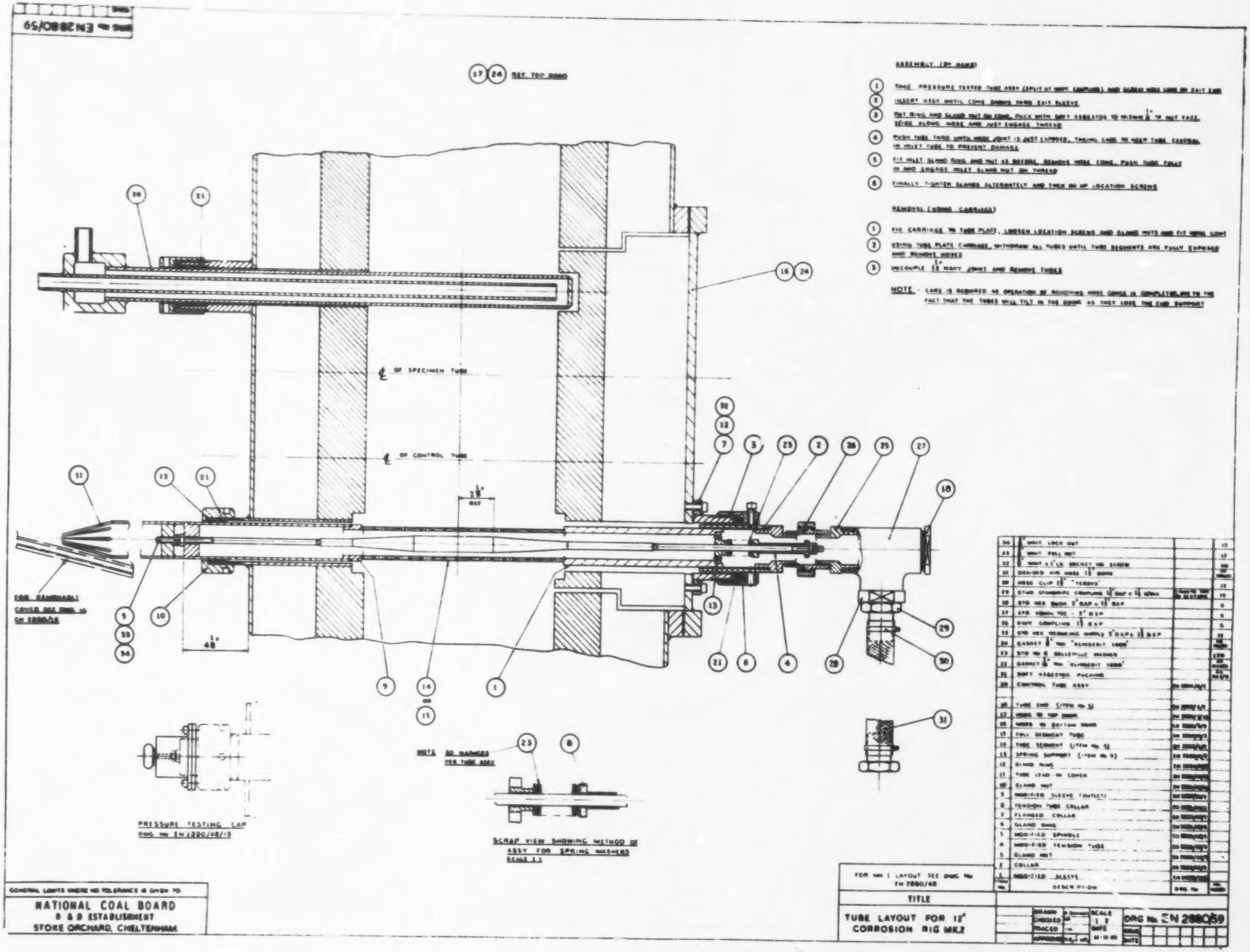
ASSEMBLY (BY HAND)
REMOVAL (USING CARRIAGE)
NOTE
℄ OF SPECIMEN TUBE
℄ OF CONTROL TUBE
PRESSURE TESTING CAP
SCRAP VIEW SHOWING METHOD OF ASSY FOR SPRING WASHERS
CONTROL TUBE ASSY
SOFT ASBESTOS PACKING
FULL SEGMENT TUBE
GLAND NUT
TUBE LEAD-IN COVER
TENSION TUBE COLLAR
FLANGED COLLAR
GLAND RING
MODIFIED SPINDLE
MODIFIED TENSION TUBE
COLLAR
MODIFIED SLEEVE
DESCRIPTION
FOR MK 1 LAYOUT SEE DWG No EN 2880/48
GENERAL LIMITS WHERE NO TOLERANCE IS GIVEN TO
NATIONAL COAL BOARD
R & D ESTABLISHMENT
STOKE ORCHARD, CHELTENHAM
TITLE
TUBE LAYOUT FOR 12" CORROSION RIG MK2
DRAWN
CHECKED
TRACED
SCALE 1:2
DATE
DRG No. EN 2880/59

Fig. A4. 3. 12in Combustor: specimen tube assembly

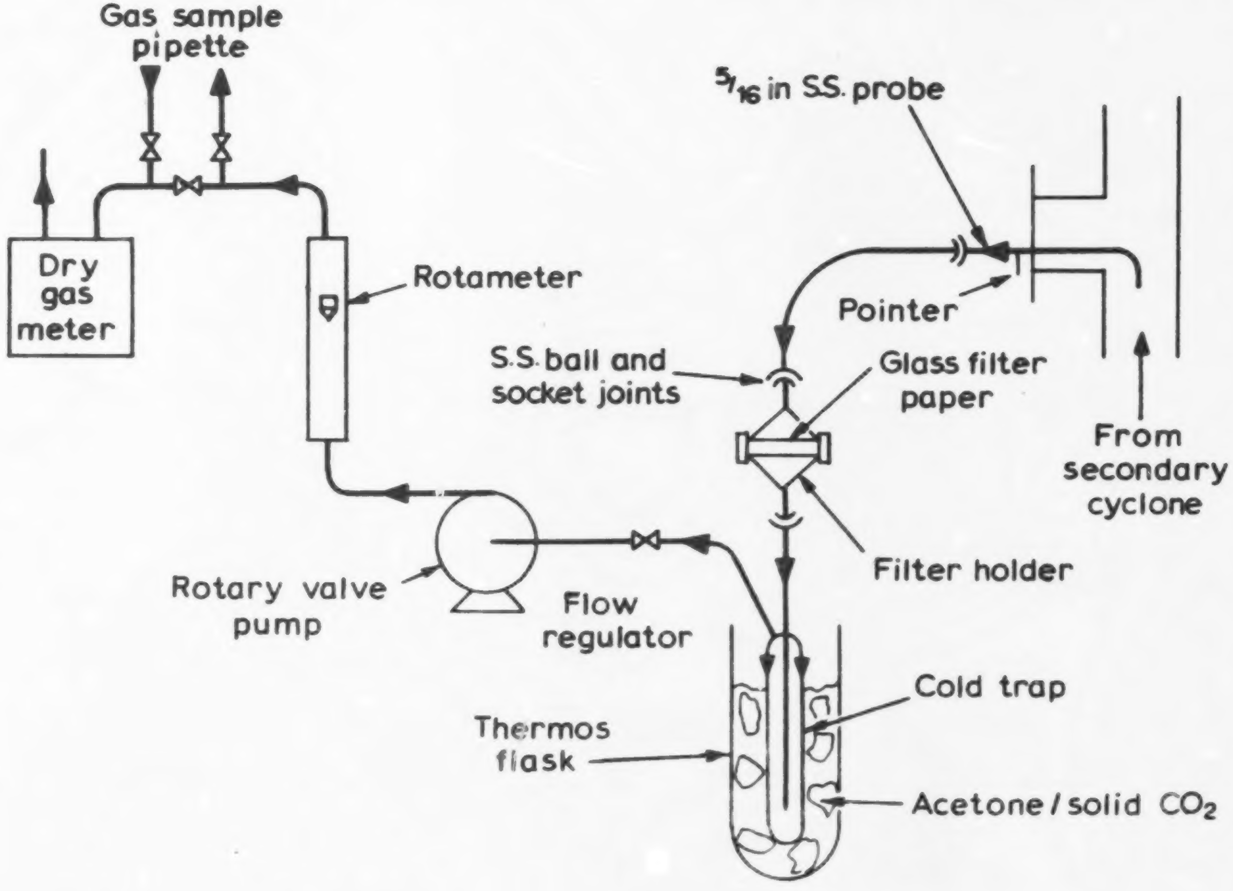
Gas sample pipette
Dry gas meter
Rotameter
Rotary valve pump
Flow regulator
$^5/_{16}$ in S.S. probe
Pointer
S.S. ball and socket joints
Glass filter paper
From secondary cyclone
Filter holder
Cold trap
Thermos flask
Acetone / solid CO_2

Fig. A4.4. Dust sampling equipment

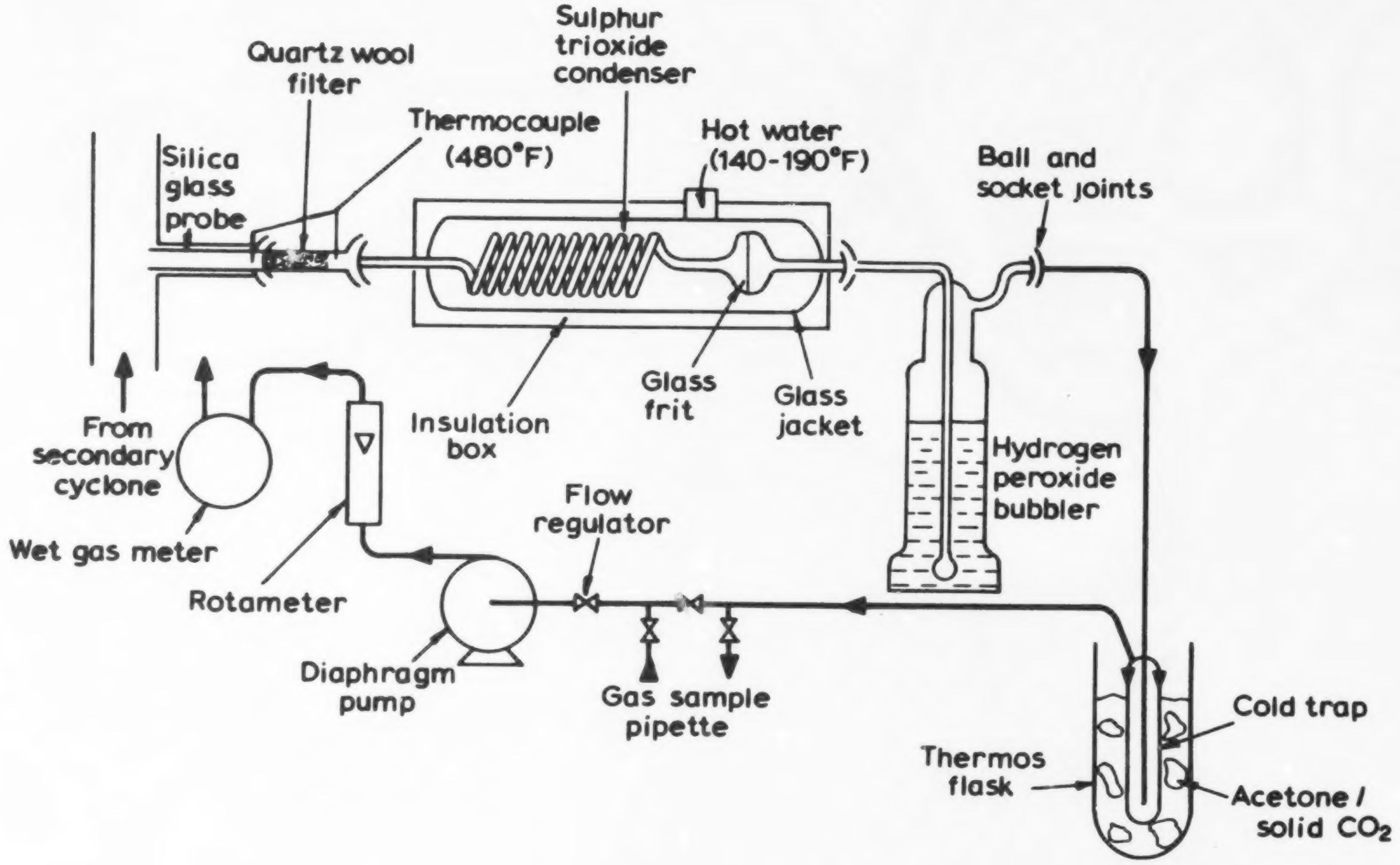
Quartz wool
filter
Sulphur
trioxide
condenser
Thermocouple
(480°F)
Hot water
(140-190°F)
Ball and
socket joints
Silica
glass
probe
Insulation
box
Glass
frit
Glass
jacket
Hydrogen
peroxide
bubbler
From
secondary
cyclone
Wet gas meter
Rotameter
Flow
regulator
Diaphragm
pump
Gas sample
pipette
Cold trap
Thermos
flask
Acetone /
solid CO_2

Fig. A 4. 5. Sampling equipment for sulphur oxides

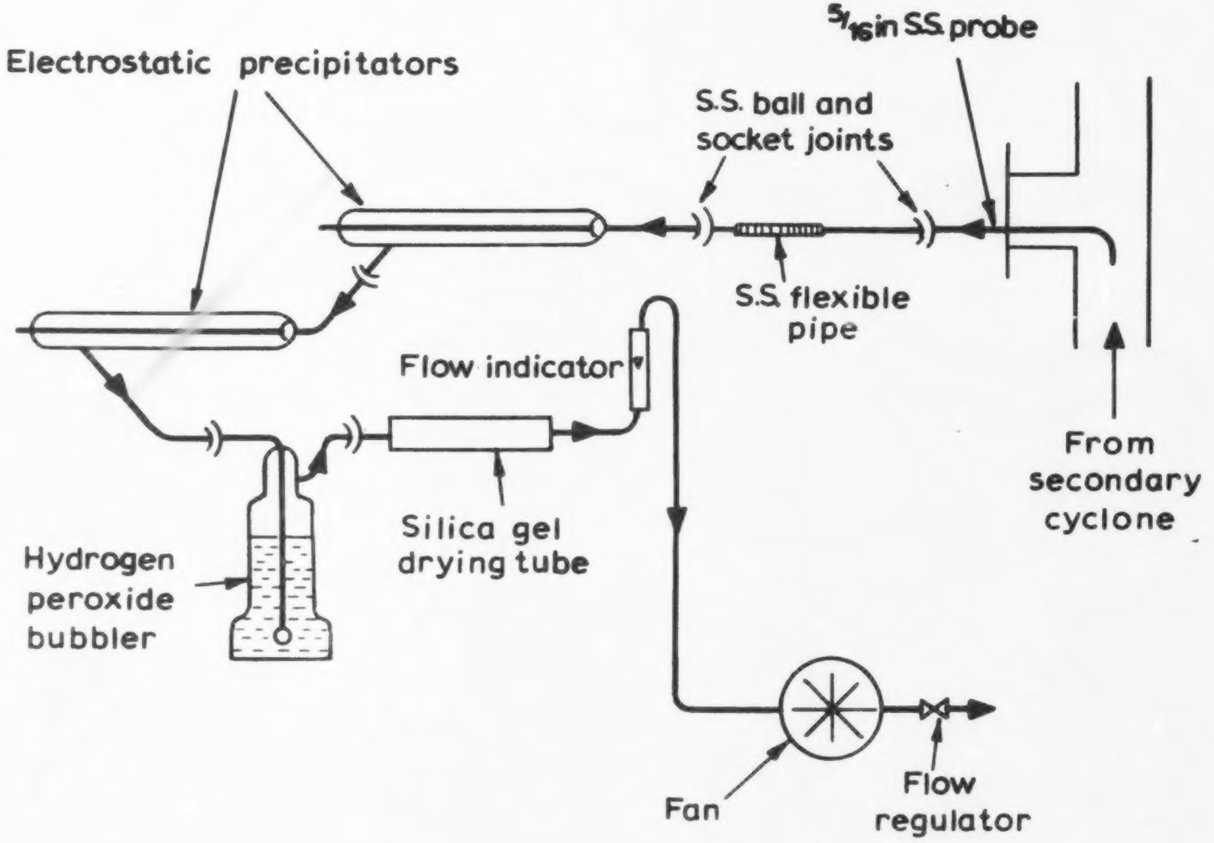
Electrostatic precipitators
S.S. ball and socket joints
5/16 in S.S. probe
S.S. flexible pipe
Flow indicator
From secondary cyclone
Silica gel drying tube
Hydrogen peroxide bubbler
Fan
Flow regulator

Fig. A4. 6. Sampling equipment for volatilised alkali

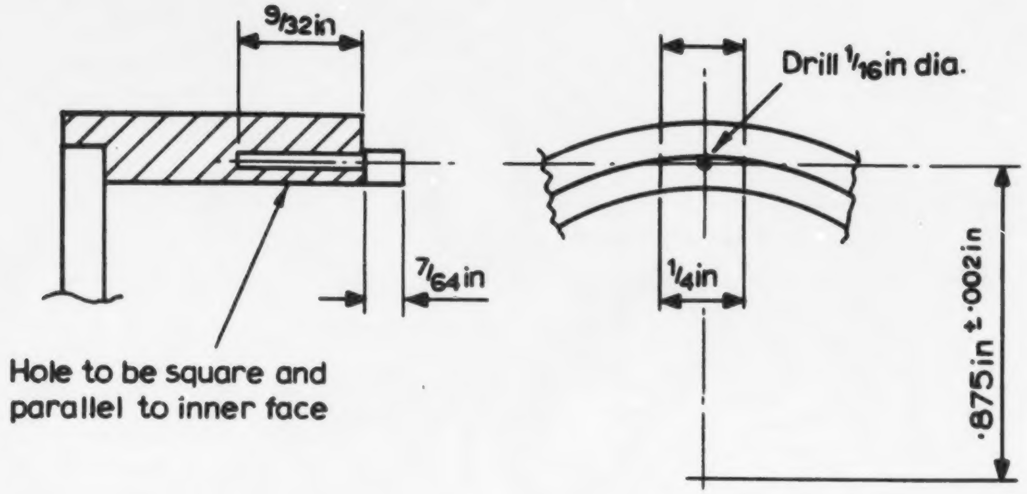
9/32 in
Drill 1/16 in dia.
7/64 in
1/4 in
·875 in ± ·002 in
Hole to be square and
parallel to inner face

Detail of thermocouple socket

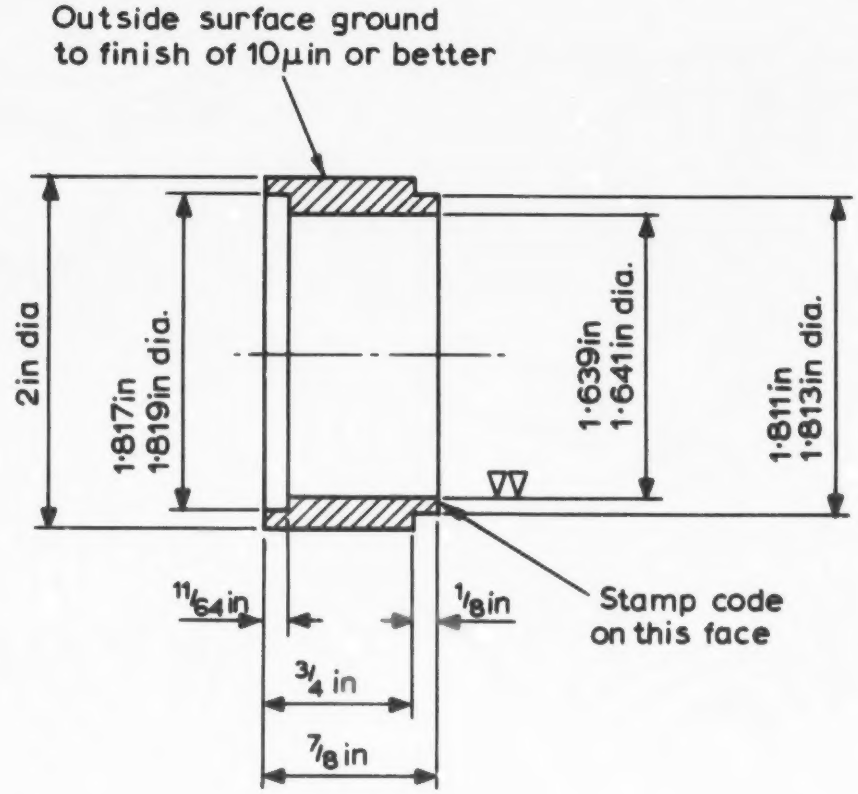
Outside surface ground
to finish of 10μin or better
2in dia
1·817in
1·819in dia.
1·639in
1·641in dia.
1·811in
1·813in dia.
▽▽
11/64 in
1/8 in
Stamp code
on this face
3/4 in
7/8 in

All corners to have 0·005in rad.

Fig. A 4. 7. Test rings

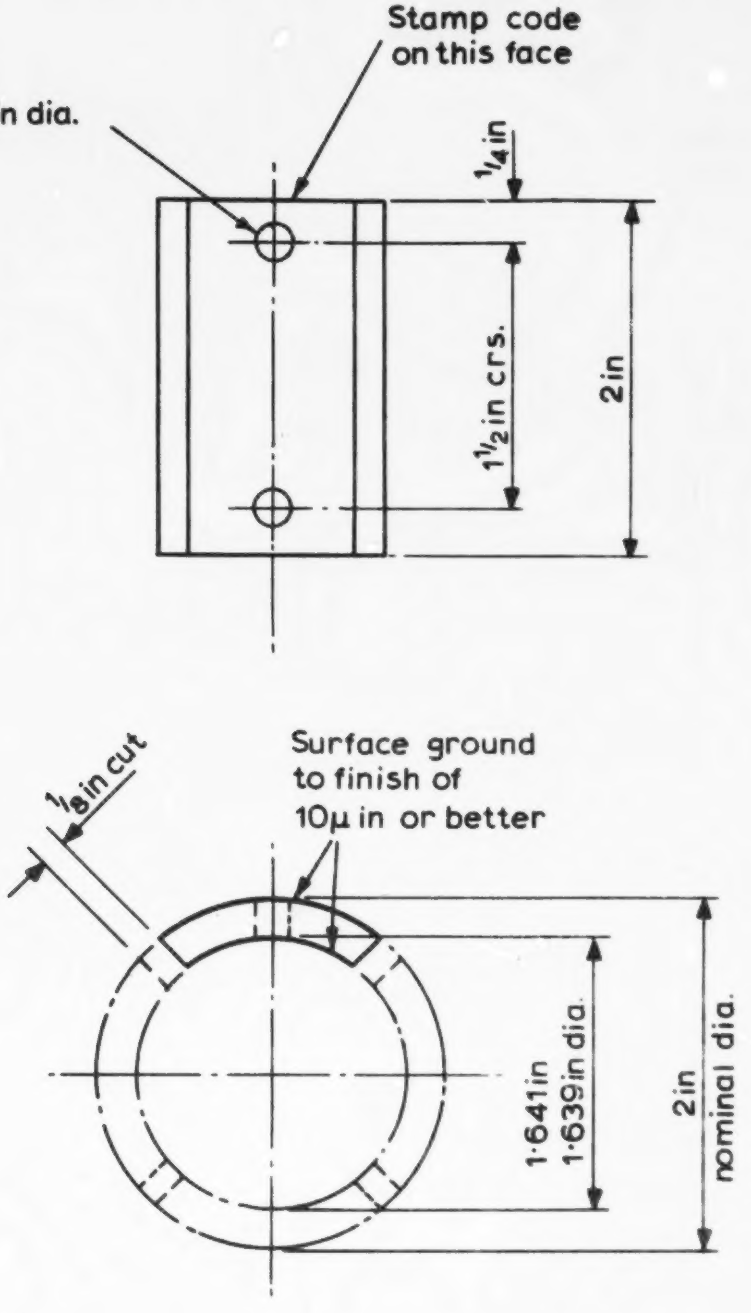
Stamp code on this face
2 holes drill 1/4 in dia.
1/4 in
1 1/2 in crs.
2 in
1/8 in cut
Surface ground to finish of 10μ in or better
1·641 in
1·639 in dia.
2 in nominal dia.

Type 1

Material:- 2 in O/dia. tube x 6 SWG wall

Fig. A4.8. Coupons (not PE16)

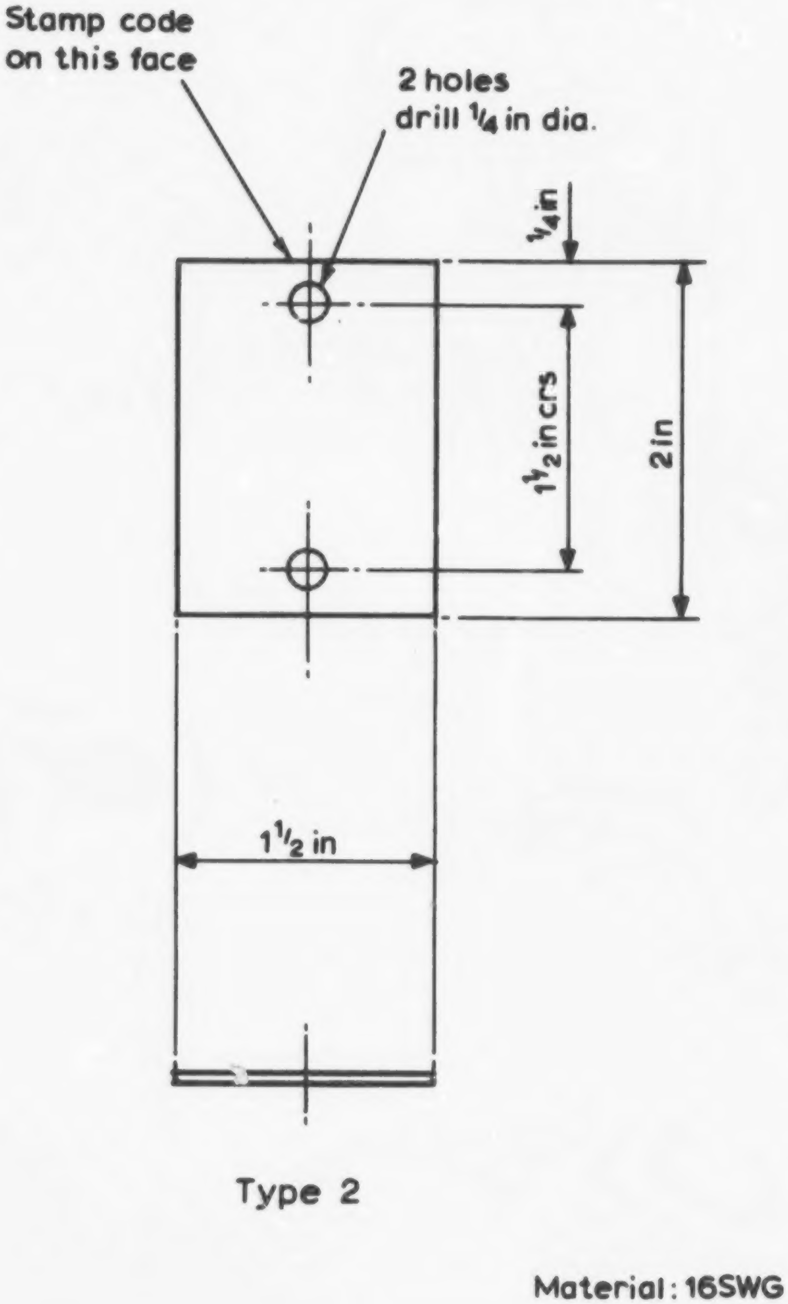
Stamp code on this face
2 holes drill 1/4 in dia.
1/4 in
1 1/2 in crs
2 in
1 1/2 in
Type 2
Material: 16SWG

Fig. A4.9. Coupons of PE16

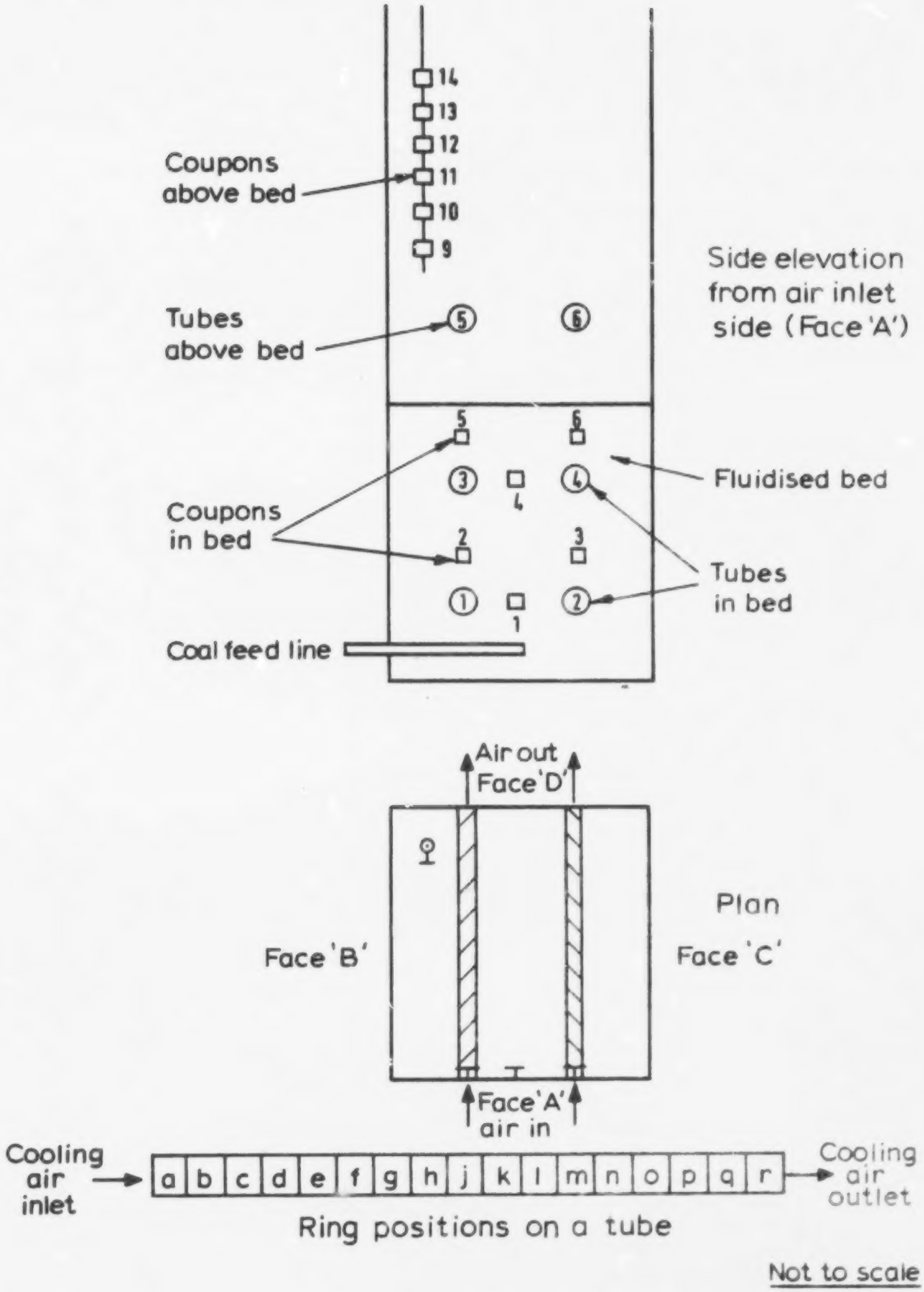
14
13
12
Coupons above bed
11
10
9
Side elevation from air inlet side (Face 'A')
Tubes above bed
5
6
5
6
Fluidised bed
3
4
4
Coupons in bed
2
3
Tubes in bed
1
1
2
Coal feed line
Air out Face 'D'
Plan
Face 'B'
Face 'C'
Face 'A' air in
Cooling air inlet
a b c d e f g h j k l m n o p q r
Cooling air outlet
Ring positions on a tube
Not to scale

Fig. A 4.10. Position of tubes and coupons and position of rings on a tube in 12in combustor

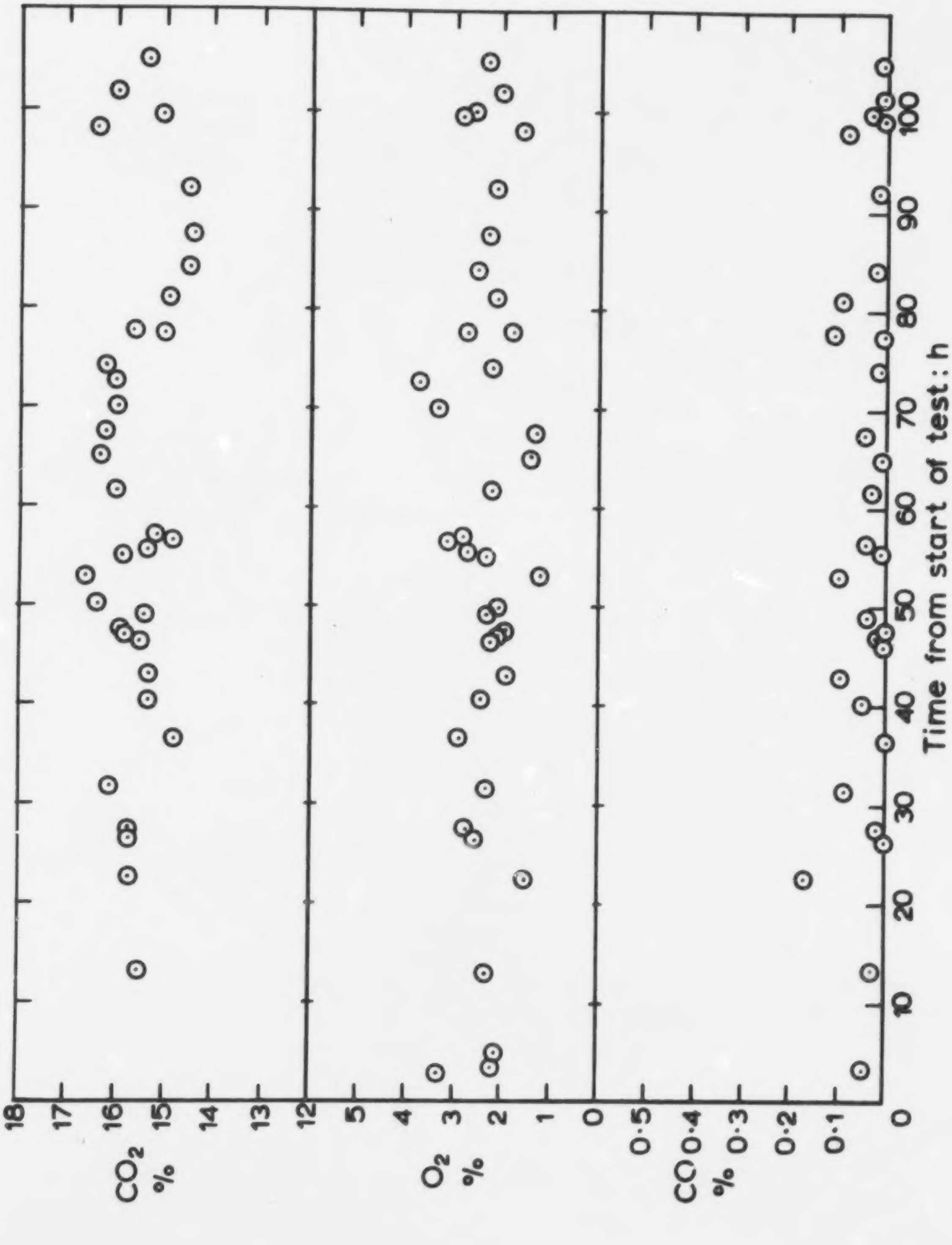

Fig. A 4. 11. Analysis of exhaust gas *vs* time for Test Series 1

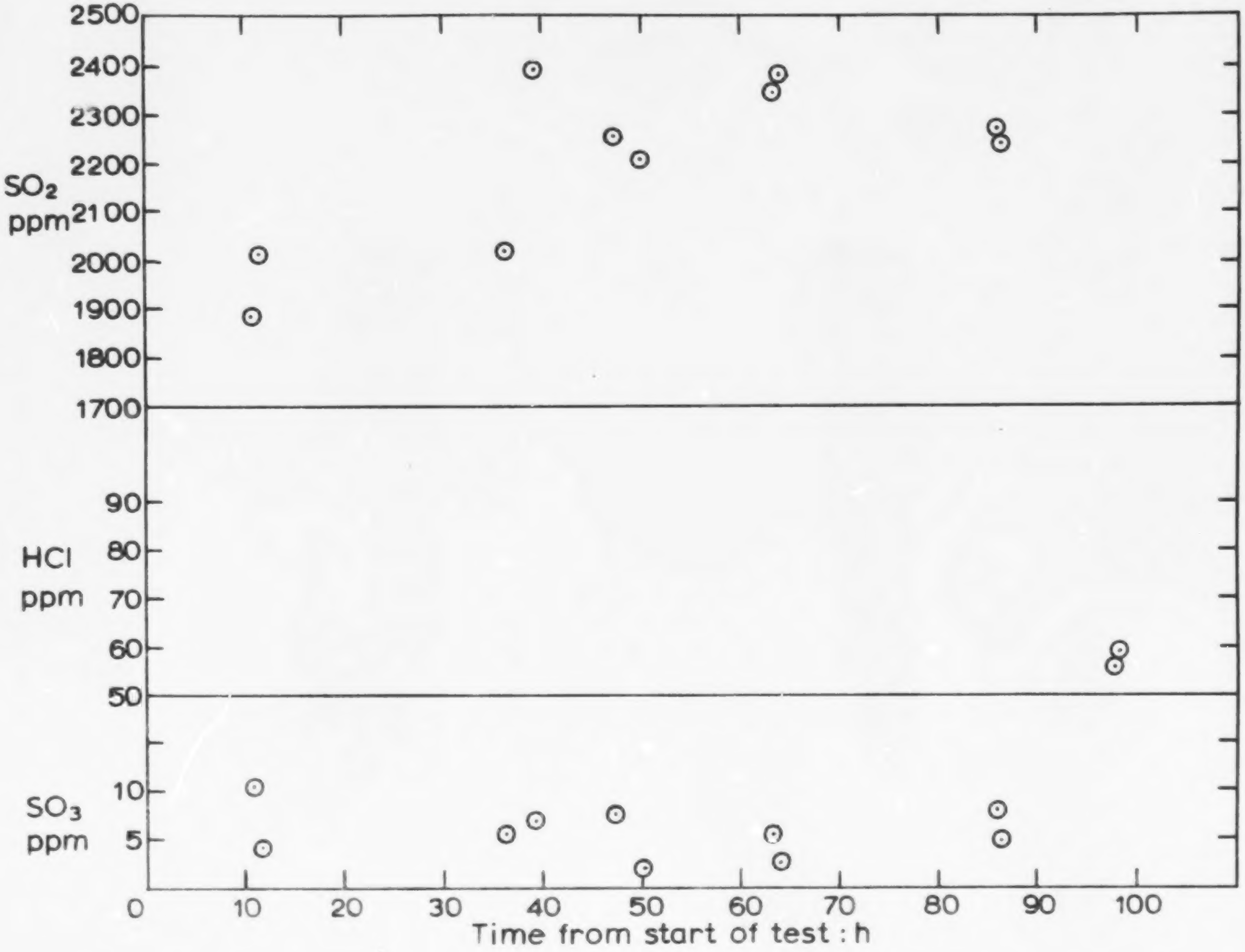

Fig. A4.12. Analysis of exhaust gas *vs* time for Test Series 1

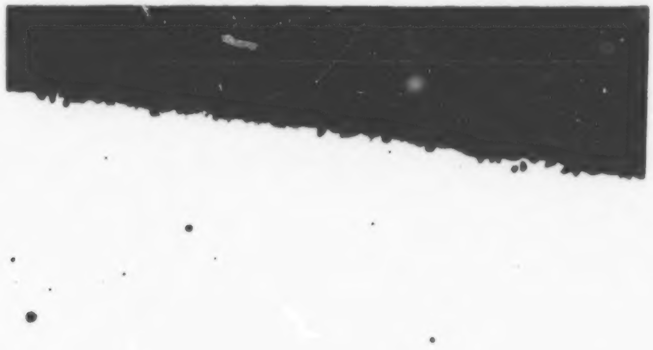

Photomicrograph (x480) of sectioned specimen.
Surface texture: smooth (<4μm)

Photomicrograph (x480) of sectioned specimen.
Surface texture: rough (< 12μm)

Photomicrograph (x480) of sectioned specimen.
Surface texture: very rough (>12μm)

Fig. A4. 13. Surface texture of specimens after test

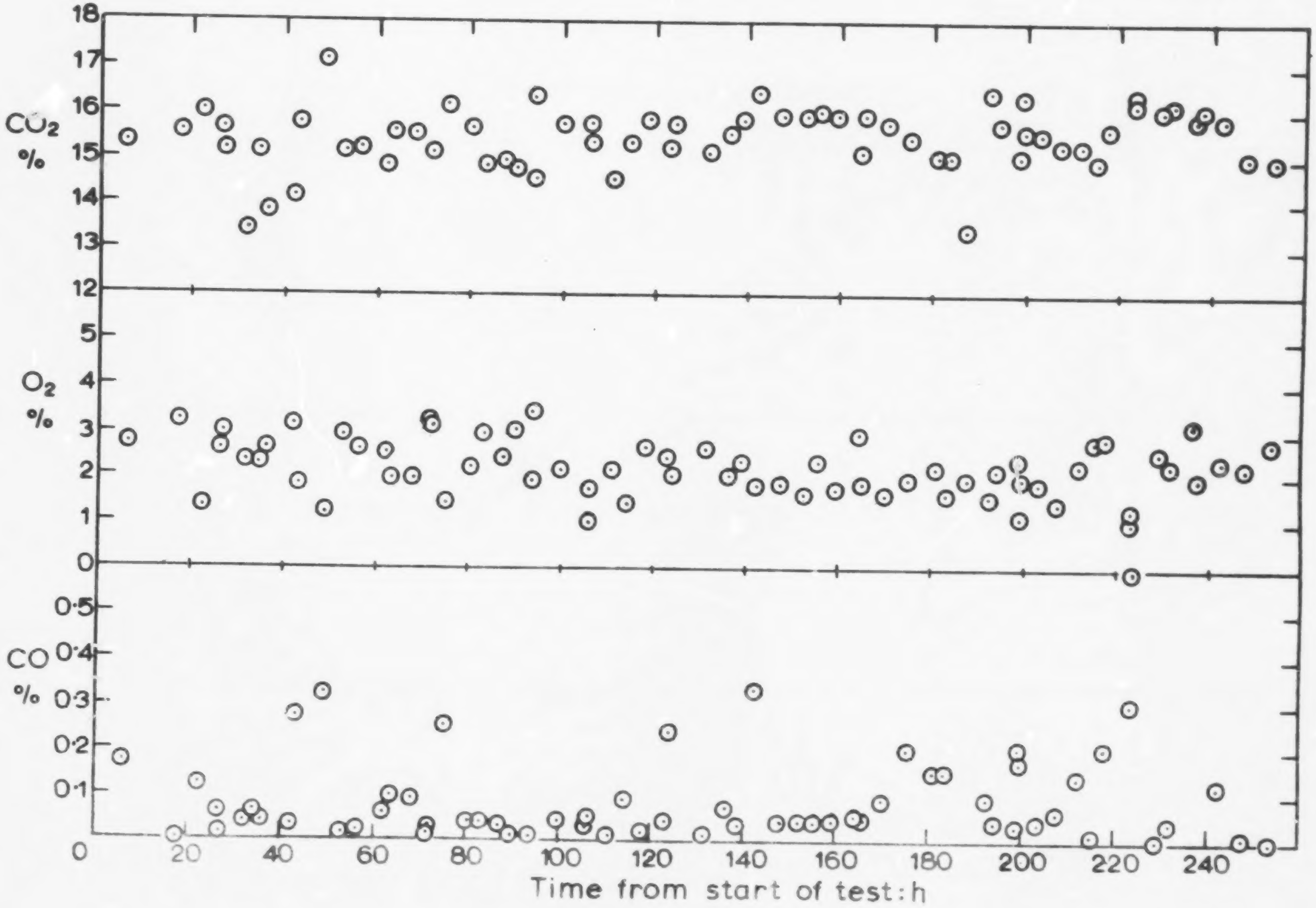

Fig. A 4.14. Analysis of exhaust gas *vs* time for Test Series 2

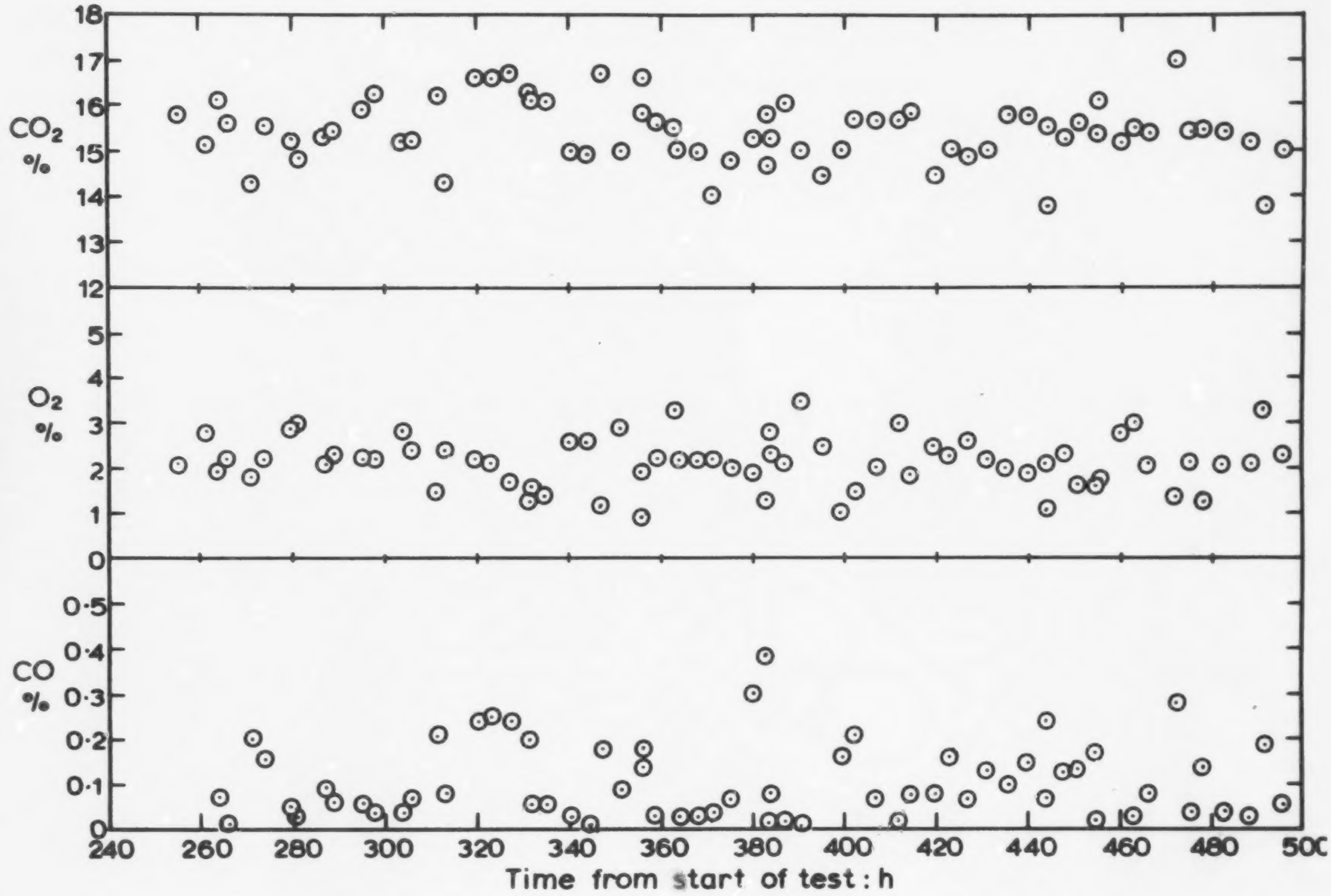

Fig. A 4. 15. Analysis of exhaust gas *vs* time for Test Series 2

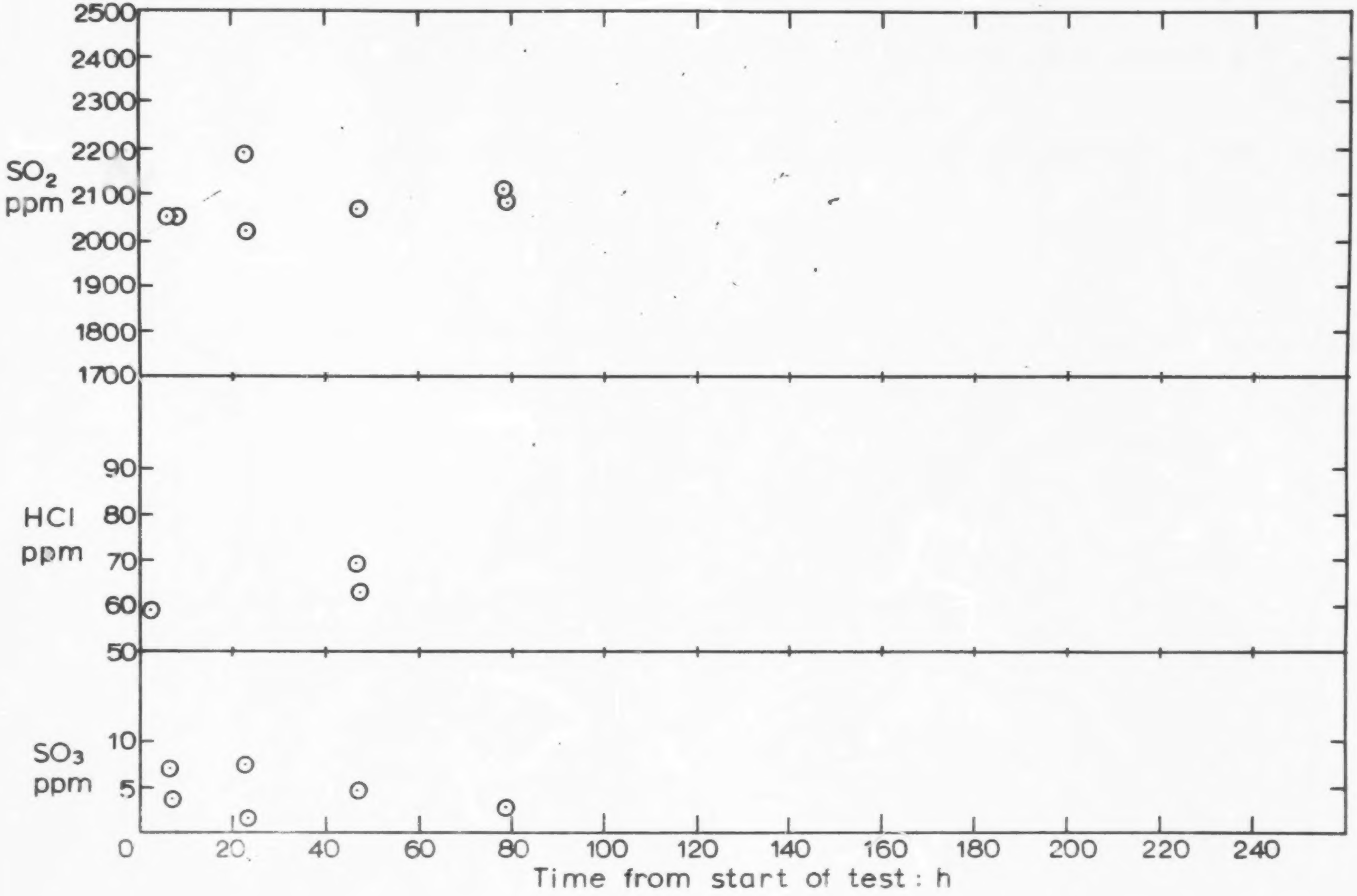

Fig. A4.16. Analysis of exhaust gas *vs* time for Test Series 2

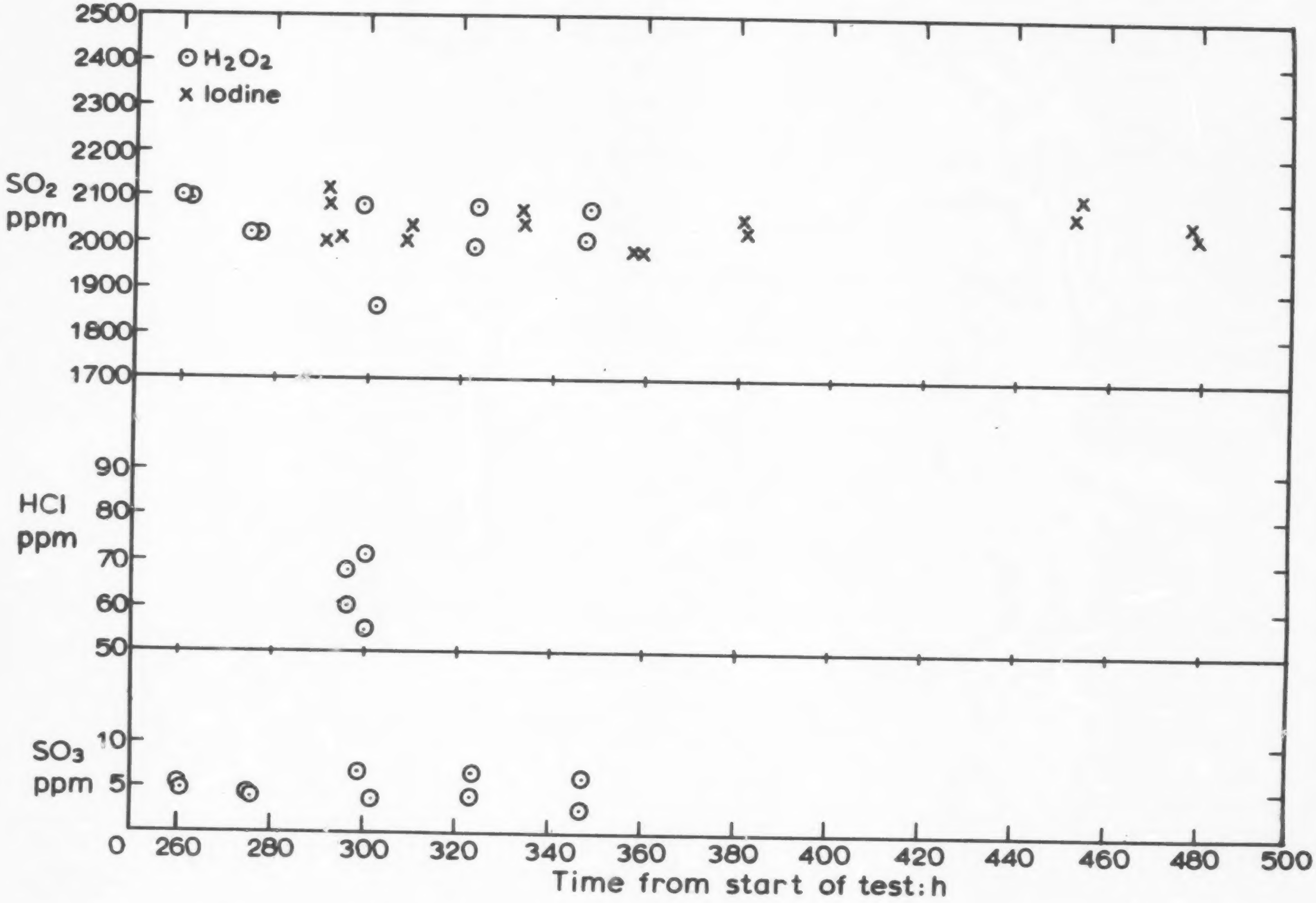

Fig. A 4.17 Analysis of exhaust gas *vs* time for Test Series 2

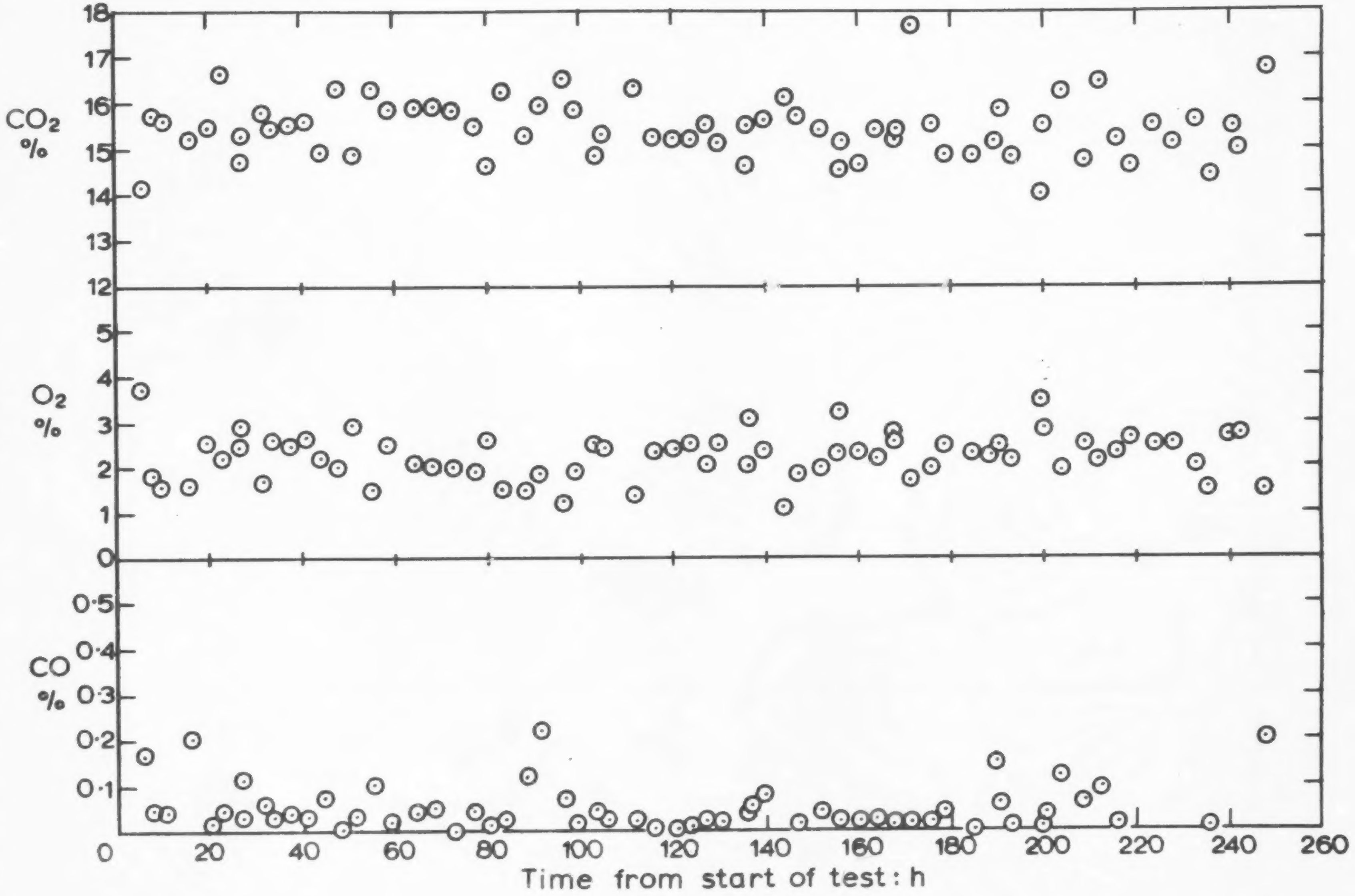

Fig. A 4.18. Analysis of exhaust gas *vs* time for Test Series 3

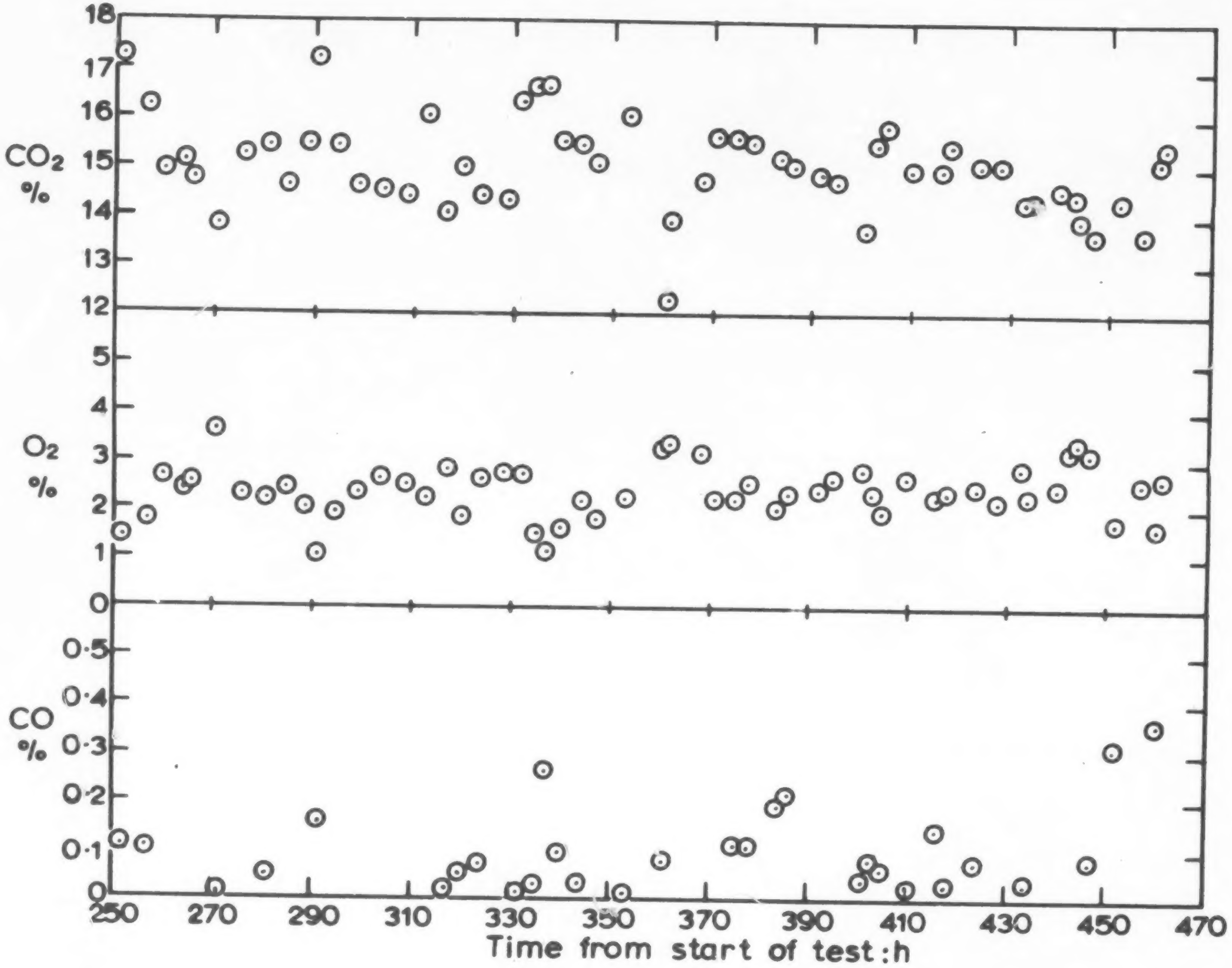

Fig. A4.19. Analysis of exhaust gas *vs* time for Test Series 3

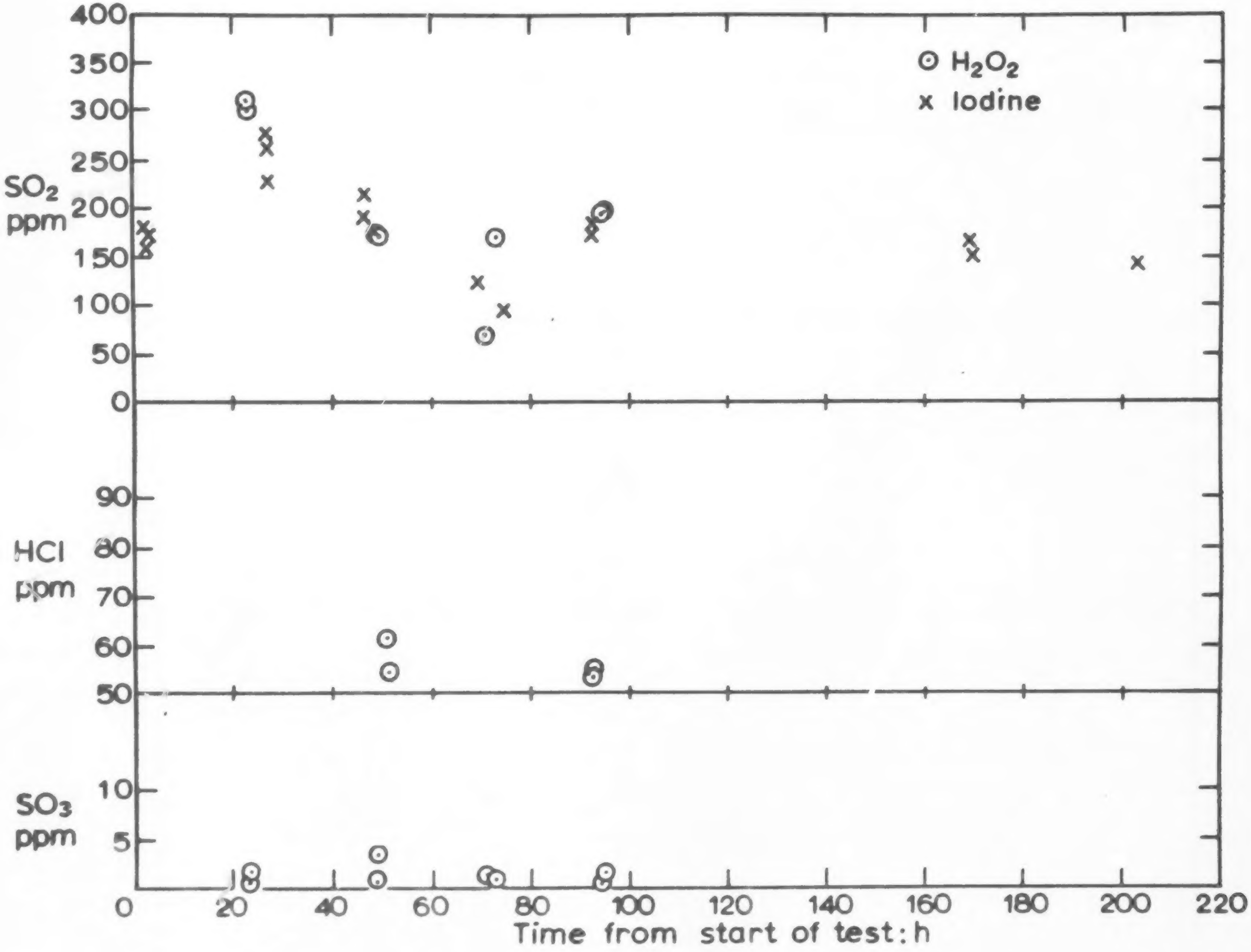

Fig. A 4. 20. Analysis of exhaust gas *vs* time for Test Series 3

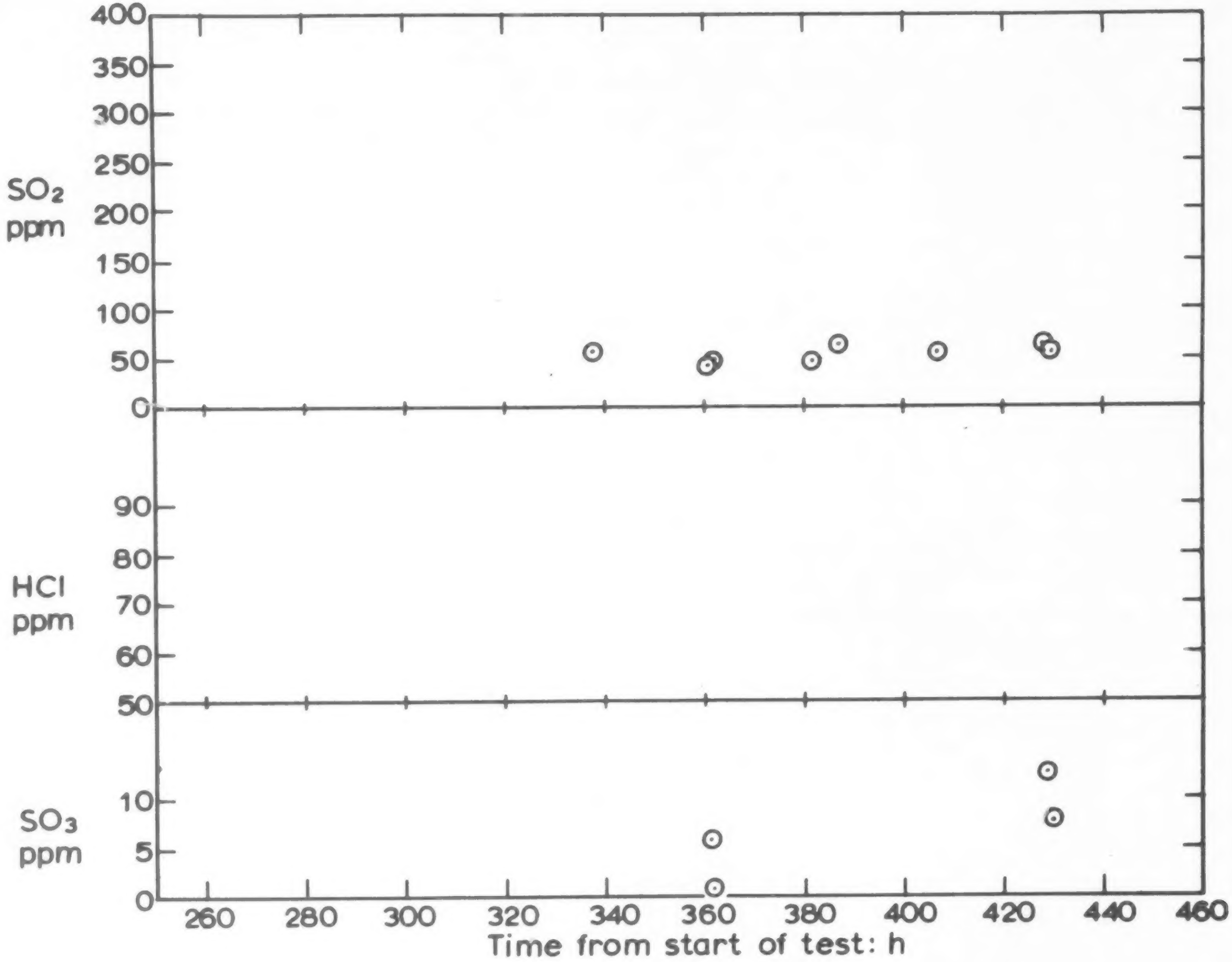

Fig. A4. 21. Analysis of exhaust gas *vs* time for Test Series 3

Ring K2m (Area 1)
(Ferritic 2¼% Cr. 1% Mo. steel)
(Specimen from tube at 600°C after 500h)

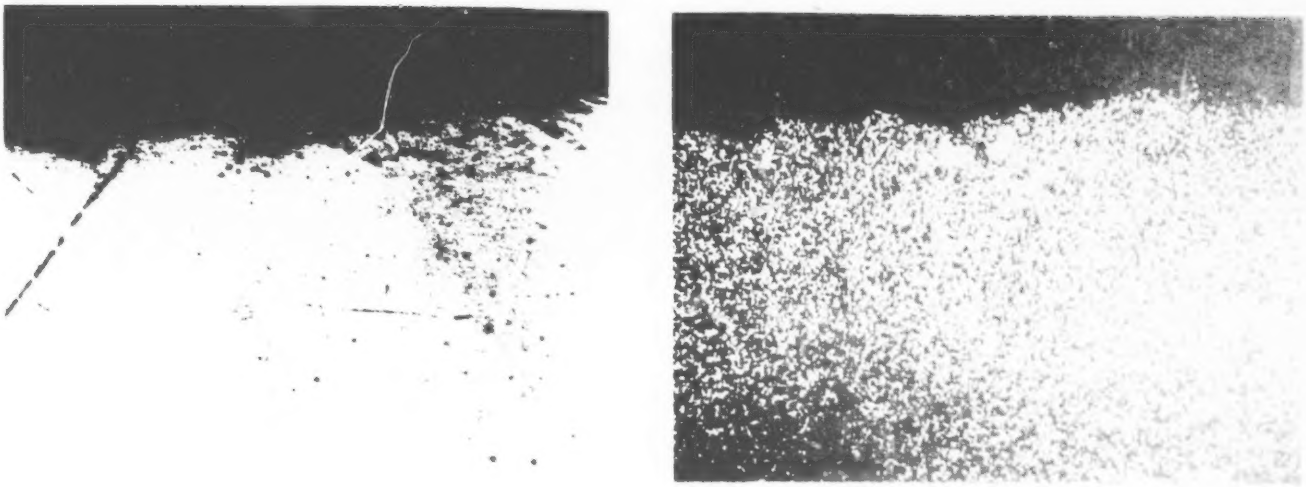

Optical X600

Chromium x-rays X600

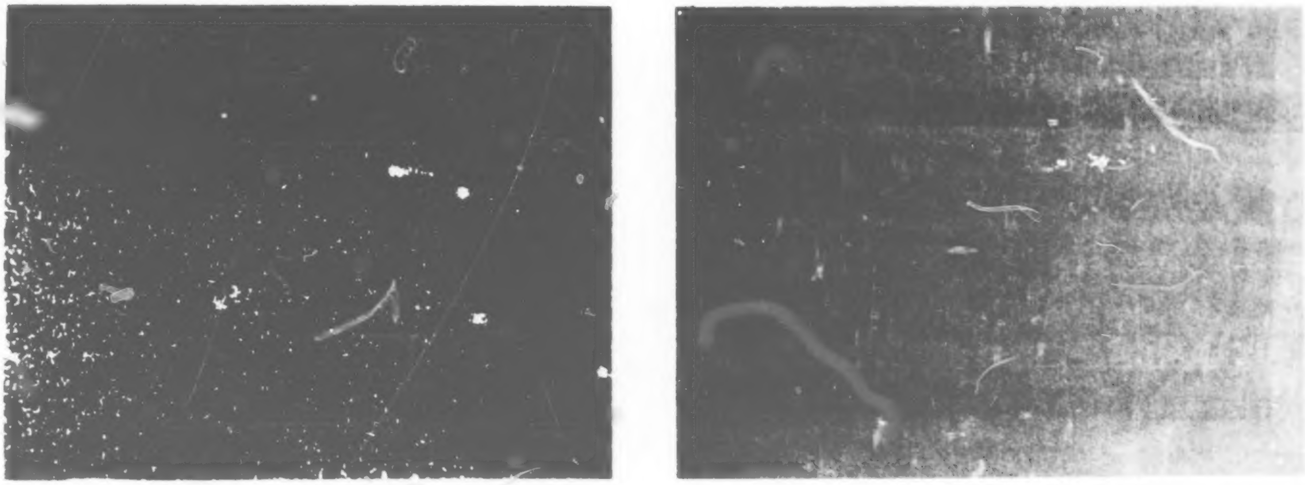

Manganese x-rays X600

Sulphur x-rays X600

Fig. A4. 22. Optical photomicrograph and electron probe micrographs of sectioned tube

Ring K2m (Area 2)
(Ferritic 2¼% Cr. 15% Mo. steel)
(Specimen from tube at 600°C after 500h)

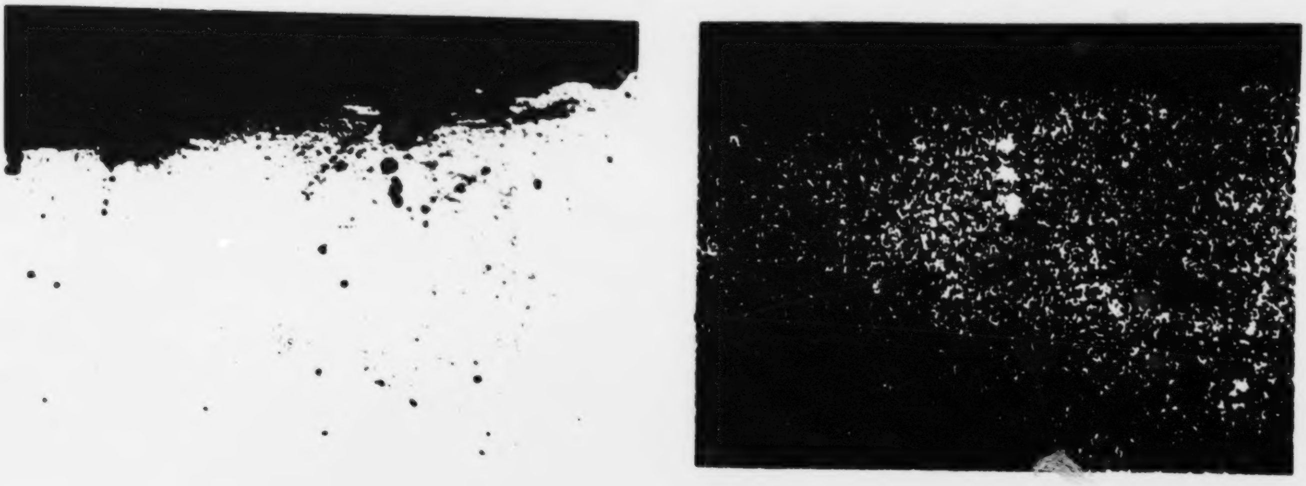

Optical X600

Chromium x-rays X600

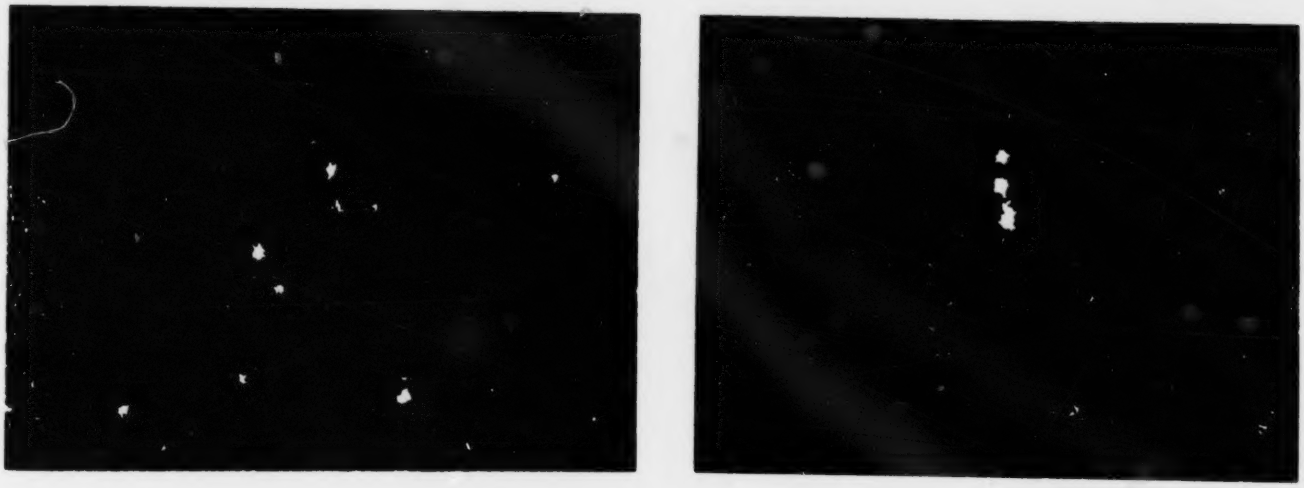

Manganese x-rays X600

Sulphur x-rays X600

Fig. A4.23. Optical photomicrograph and electron probe micrographs of sectioned tube

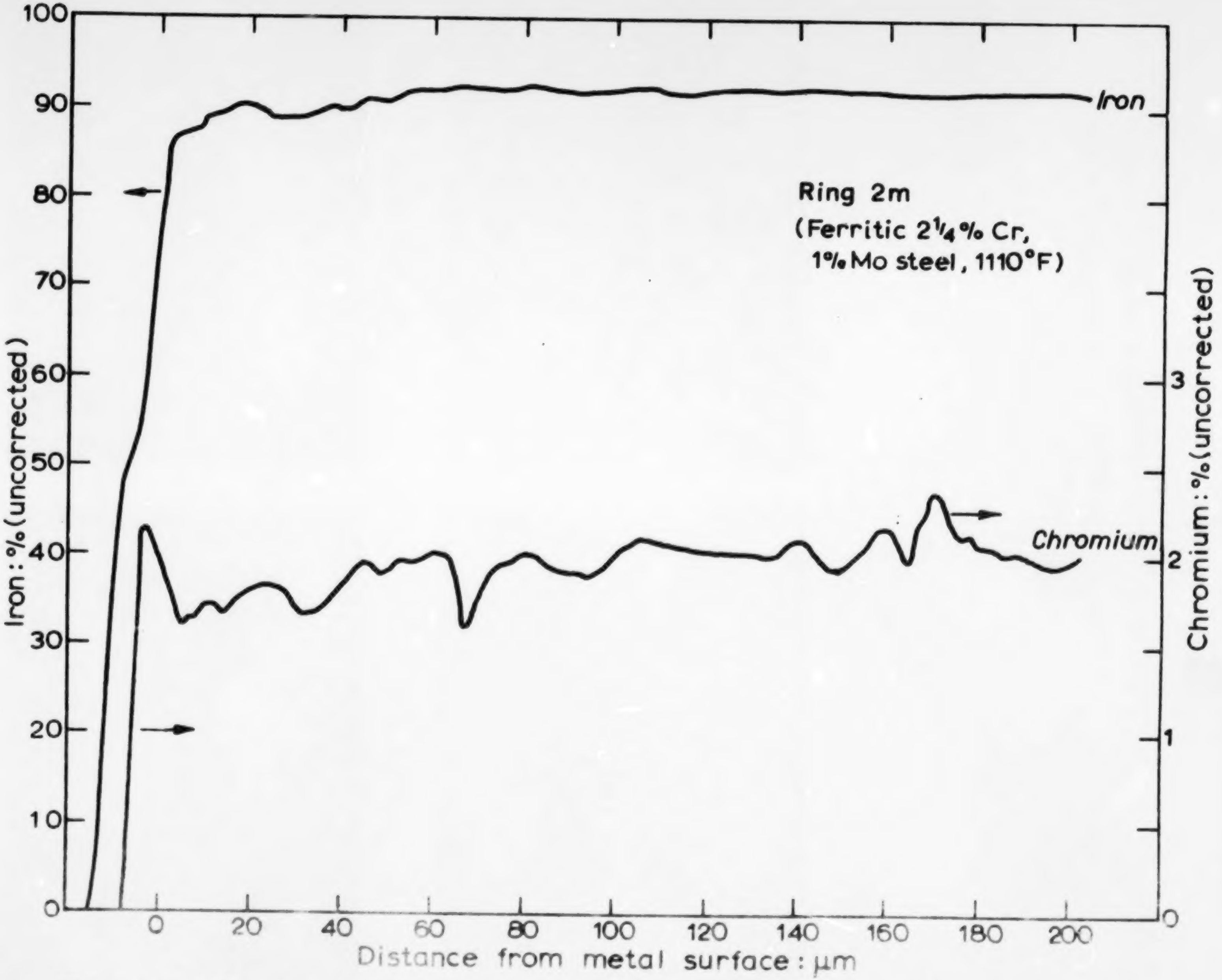

Fig.A4.24. Electron probe microanalysis : elemental line traces

Ring K_{40} (Ferritic 12% Cr.)

(Specimen from tube at 700°C for 500 h

Optical X1000

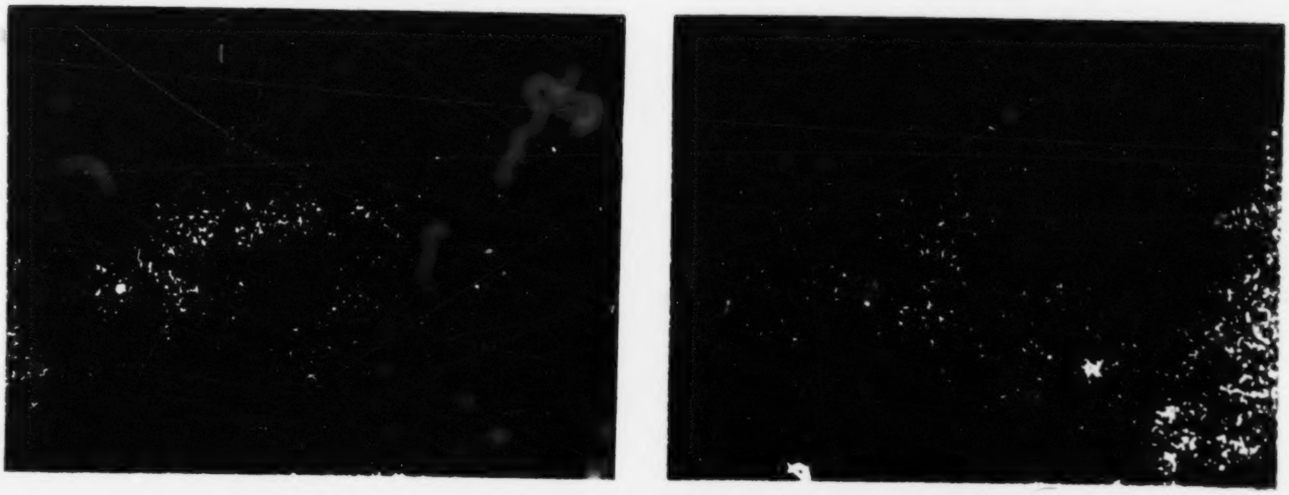

Iron x-rays X1000

Chromium x-rays X1000

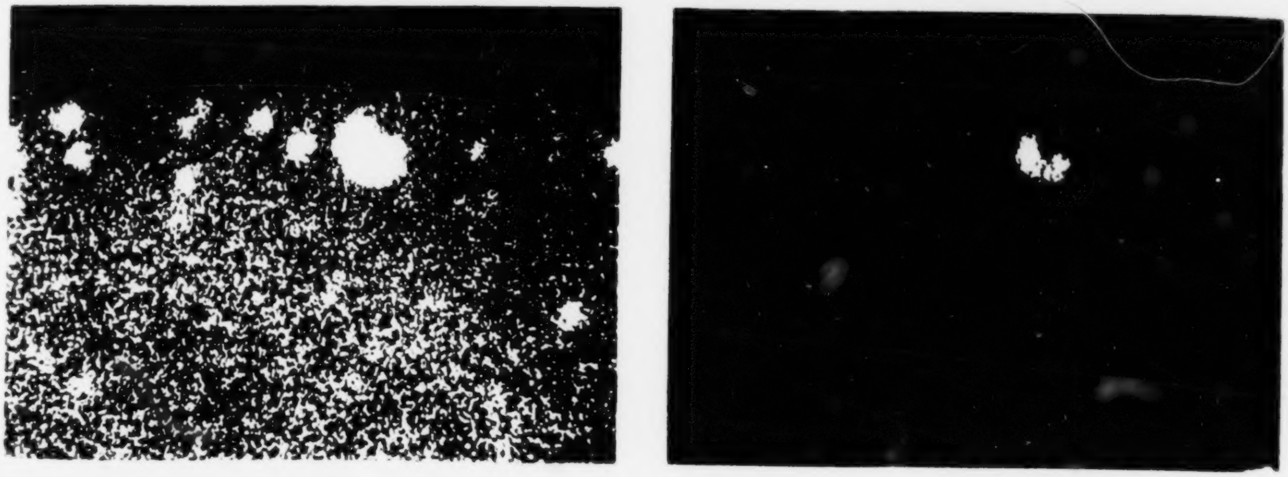

Manganese x-rays X1000

Sulphur x-rays X1000

Fig. A4 25. Optical photomicrograph and electron probe micrographs of sectioned tube

NATIONAL COAL BOARD

FINAL REPORT

JUNE 1970 - JUNE 1971

REDUCTION OF ATMOSPHERIC POLLUTION

APPENDIX 5. EXPERIMENTS WITH THE 6 IN COMBUSTOR. (TASK V)

PREPARED FOR

ENVIRONMENTAL PROTECTION AGENCY
OFFICE OF AIR PROGRAMS
411 WEST CHAPEL HILL STREET
DURHAM, NORTH CAROLINA 27701

REFERENCE NO. DHB 060971

SEPTEMBER 1971

FLUIDISED COMBUSTION
CONTROL GROUP

NATIONAL COAL BOARD
LONDON, ENGLAND

A5.i

REDUCTION OF ATMOSPHERIC POLLUTION

Research on reducing emission of sulphur oxides, nitrogen oxides and particulates by using fluidised bed combustion of coal

Appendix 5. Experiments with the 6 in combustor. (Task V)

Main objective

To obtain data on sulphur retention for a range of coals and limestones, in particular to allow comparison to be made with the 6 in rig at Argonne.

Report prepared by: D.G. Cox
D.C. Davidson
J. Highley
J.C. Holder

Report approved by: A.D. Dainton
H.R. Hoy

Preceding page blank

FOREWORD

This Appendix describes experimental work carried out using the 6 in combustor at CRE, between June 1970 and June 1971, as Task V of the joint NCB/OAP research programme. The main objective of Task V was to obtain data on sulphur retention for a range of coals and limestones, in particular to allow comparison to be made with the 6 in rig at the Argonne National Laboratory (ANL). Attention is drawn to the main results obtained, but, apart from a comparison with the ANL data, the results are not discussed here. A summary of the work is presented in the main report and the results are discussed there, together with results from other pilot plants.

Preceding page blank

Table of Contents

Page No.

Foreword

1. Description of the Combustor A5. 1
   1.1 General A5. 1
   1.2 Air Distributor A5. 1
   1.3 Coal Feeder A5. 1
   1.4 Cooling Circuit A5. 1
   1.5 Bed Height Control A5. 2
   1.6 Flue Gas System A5. 2

2. Experimental Procedures A5. 2
   2.1 Preparation of Feedstock A5. 2
   2.2 Procedure for Start-up A5. 2
   2.3 Test Procedure A5. 3
   2.4 Shut-down Procedure A5. 4
   2.5 Data Processing A5. 4

3. Results A5. 7
   3.1 Test Series 1 A5. 7
      3.1.1 Description of the test series A5. 7
      3.1.2 Results of the test series A5. 8
   3.2 Test Series 2 A5. 9
      3.2.1 Description of the test series A5. 9
      3.2.2 Results of the test series A5.10
   3.3 Test Series 3 A5.12
      3.3.1 Description of the test series A5.12
      3.3.2 Results of the test series A5.12
   3.4 Test Series 4 A5.13
      3.4.1 Description of the test series A5.13
      3.4.2 Results of the test series A5.14
   3.5 Test Series 5 A5.15
      3.5.1 Description of the test series A5.15
      3.5.2 Results of the test series A5.15

Preceding page blank

Page No.

4. Comparison with results from Argonne National Laboratory (ANL) A5.16
  4.1 Illinois coal and Limestone 1359 A5.16
  4.2 Welbeck coal and U.K. limestone A5.17

5 Acknowledgement A5.18

Tables A5.1.1 to A5.1.16 Results of Test Series 1
Tables A5.2.1 to A5.2.23 Results of Test Series 2
Tables A5.3.1 to A5.3.14 Results of Test Series 3
Tables A5.4.1 to A5.4.17 Results of Test Series 4
Tables A5.5.1 to A5.5.10 Results of Test Series 5

Figures A5.1 and A5.2 Details of plant design
Figures A5.3 to A5.9 Reductions of SO_2 emission obtained

(Note that when referring to Tables and Figures in the text the prefix A5 is omitted).

1. DESCRIPTION OF THE COMBUSTOR

1.1 General

The general design of the combustor is shown in Fig. 1. The main reactor was in three sections, all fabricated from stainless steel, (a) a lower cylindrical section 6¼ in diameter and 6 ft long, with the air distributor at the base, (b) a conical expansion section leading to (c) an upper cylindrical section 1 ft 5 in diameter and 4 ft long. This upper section was terminated by a flat plate. The total internal volume of the combustor was 8.18 ft^3, of which the expanded head comprised 6.95 ft^3.

The whole combustor could be heated electrically by external wall heaters embedded in a heat-conducting cement. The heaters were intended to counterbalance heat losses, with the exception of the first 12 inches in length of the 6 in diameter section which had additional windings (bed heaters) to permit more rapid heating of the bed material. A layer of insulation clad the whole exterior of the combustor.

1.2 Air Distributor

Details of the bed section of the combustor are shown in Fig. 2. This shows the air distributor which was a flat plate with forty-five 3/32 in holes covered by three layers of ¼ in diameter alumina balls to prevent ash particles from falling through the holes.

1.3 Coal Feeder

The feed hopper for the coal and coal/limestone mixtures was of stainless steel and terminated in a rotary valve for metering the feed to the combustor. The metered feed was pneumatically injected into the bed tangentially to the combustor diameter through a 5/16 in bore tube ¾ in above the alumina pebbles, i.e. approximately 1½ in above the distributor plate (see Fig. 2). The feed pipe terminated at the inner wall of the combustor.

1.4 Cooling circuit

The heat produced by combustion in the bed could be removed by means of an immersed cooling coil of ¼ in o.d. stainless steel tubing (see Fig. 2) in which water was boiled and superheated. The flow of water was controlled automatically in response to a signal from a thermocouple in the bed. The steam from the coil was condensed and the condensate recirculated.

1.5 Bed height control

The bed height was measured by means of pressure probes in the vessel, and could be automatically maintained constant by emptying surplus ash through a tube in the centre of the base. This was done using a vibrating trough on which the ash in the tube rested.

1.6 Flue gas system

The gases leaving the reactor could be directed through two alternative cyclone systems. Both contained two cyclones of diameter 3 in and 1¾ in respectively, in series. In one system the fines removed from the gas stream by the primary cyclone were returned to the bed through a dip-leg ending 4½ in above the base, and the secondary cyclone fines were collected in a catchpot. In the other, both cyclones were fitted with catchpots, and fines were not recycled to the bed. To ensure satisfactory flow of fines into the catchpots, lines and valves of 1 in bore were used and the catchpots were fitted immediately below the cyclones.

2. EXPERIMENTAL PROCEDURE

2.1 Preparation of Feedstock

The coal feed was normally prepared to -10 B.S. mesh (1680 µm) and screen analyses of the feed coals used in the runs are given in the text. The feed for runs with limestone addition was prepared by weighing and mixing the required quantities of coal and limestone.

2.2 Procedure for Start-up

The feed for a particular run was loaded into the feed hopper which has a maximum capacity of 60 lb of coal. The ash bed was re-used from the previous run, where practicable, but, apart from Test 4.8, a lime-enriched ash was not used for tests at a lower limestone addition than that used to produce the ash. Thus, at the beginning of each run, a fluidised bed was established using either ash from the previous run, or a fresh bed of ash from Welbeck coal, from an earlier run made without limestone addition. The bed temperature was raised initially using the combustor heaters and electrically pre-heated fluidising air at approximately 1200°F. At a bed temperature of 840°F, which was usually reached within 45 minutes, the coal feed was started at approximately half the anticipated final feed rate. The warming-up process then continued for approximately one hour, by which time the bed temperature had reached approximately 1100°F. The coal feed rate was then increased to the anticipated rate for the run. Normally a further one hour was then required for the bed temperature to reach the run condition (usually 1470°F) at which temperature the air preheater was switched off, the bed heaters were turned down, and the cooling water circulated. The bed temperature stabilised within 30 minutes, after which ash was withdrawn to adjust the bed height to the required level. The air flow rate was adjusted to attain the chosen fluidising velocity as calculated for the empty vessel at the temperature of the bed. The coal feed rate was set according to the proportion of excess air at which the run was to be carried out. The electrical supply to the freeboard heaters was adjusted to maintain the freeboard at the same temperature as the bed. Gas samples for chromatographic analysis were taken in evacuated bottles at a gas sampling point downstream of the secondary cyclone to confirm the oxygen analysis on the continuous analyser.

2.3 Test Procedure

Once the experimental conditions had been set, the ash withdrawn from the bed and the cyclone fines were each collected over successive periods of one hour and weighed. Further gas samples were taken to determine the flue gas composition.

The normal test period over which the above procedure was carried out was six hours, and is referred to as the mass balance period. Samples taken during this period, plus samples of feedstock, initial bed and final bed, were analysed for volatile matter, carbon, calcium and sulphur.

Gas samples for sulphur dioxide determinations were taken immediately downstream of the cyclones at one or other of the points shown in Fig. 1, depending upon whether or not fines recycling was being practised.

The sulphur dioxide determinations were made at least four times during a mass balance period using N/10 iodine solution to which 2% potassium iodide had been added to prevent loss of iodine. Each determination was run to complete discolouration of the iodine solution using thiodene as an indicator, and the quantity of iodine initially used was adjusted to give 10 to 20 minutes sampling time at a sampling rate of approximately 2 litres/min. The results sheets for each test show the mean value for SO_2 obtained with iodine.

In addition to iodine tests, samples were also taken by absorption in hydrogen peroxide solution. These solutions were bulked over each half of the mass balance period and subsequently analysed for sulphate, chloride, and ammonium ions.

2.4 Shut-down Procedure

At the end of the run the coal feed was stopped and simultaneously nitrogen was substituted for the fluidising air. To assist in cooling the bed the flow of cooling water was increased. When the bed temperature had fallen to 755°F the ash bed was emptied into tins which were then sealed. Samples of the bed were taken for analysis after cooling down in the sealed tins.

2.5 Data processing

The measured feed rates, solids output rates and chemical analyses of the input and output streams were used to calculate mass balances. These were carried out by computer.

The major factor in the mass balance which was not measured was the flow-rate of flue gas, and it was necessary to estimate this. Since the gas analysis was carried out on a dry volume basis, the dry volume rather than mass flow-rate of gas was estimated. This was done by correcting the total air flow-rate for the volume changes due to the reactions which occurred.

These were:-

(i) $4H\ (\text{coal}) + O_2 \longrightarrow 2H_2O\ (\text{liquid})$

(ii) $2O\ (\text{coal}) \longrightarrow O_2$

(iii) $2C + O_2 \longrightarrow 2\ CO$

(iv) $CaCO_3 \longrightarrow CaO + CO_2$

(v) $CaO + \tfrac{1}{2}O_2 + SO_2 \longrightarrow CaSO_4$

The volume changes due to (i) and (ii) were calculated assuming that all the hydrogen and oxygen in the coal were released. The increase due to (iii) was calculated from the measured concentration of CO in the flue gas. The net effect of (iv) and (v) was small and this was neglected. Thus the flue gas flow rate was calculated as:

$$\text{Flue gas flow-rate} = \frac{\text{Air} + 379 \times \text{Coal Feed Rate} \times (\text{O Content}/32 - \text{H Content}/4)}{(1 - 0.5 \times \text{CO in Flue Gas})}\ \text{SCFH}$$

The following mass balances were carried out:-

(i) Total

In this the mass flow-rate of dry flue gas was calculated from its composition and a hydrogen balance was assumed.

(ii) 'Ash'

This is a balance for the inorganic solids, i.e. ash and acceptor. No allowance was made for the weight changes due to calcination of $CaCO_3$ and formation of sulphate. Because it was not possible to determine directly the bed weight at the beginning and end of the mass balance period, the following procedure was used to find the amount of ash accumulated in the bed. The bed weight at the beginning of the balance was obtained from:- the weight of bed initially fed to the combustor plus the ash in the feed up to the start of the balance minus (ash offtake + ash in fines make) up to the start of the balance. The bed weight at the end of the balance was obtained from:- the weight of the bed from the combustor after shut down plus ash in the fines collected during the shut down procedure. The ash content of the fines produced during start-up and shut-down was taken as 50%.

The bed weight at the end of the balance was then subtracted from the bed weight at the beginning and divided by the period of the mass balance in hours to give the accumulation rate per hour.

(iii) 'Carbon'

This is a balance for the organic carbon in the coal and is directly relevant to the combustion process. No allowance was made for the CO_2 in the flue gas arising from calcination.

(iv) Nitrogen

This balance serves as a check on the accuracy of the flue gas analysis.

(v) 'Oxygen'

This is a balance for the oxygen in the air and the organic oxygen in the coal. It is directly relevant to the combustion process.

(vi) Sulphur

This is a balance for the total sulphur content of the coal, using the mean SO_2 concentration obtained by the iodine method.

(vii) Calcium

This is a balance for the total calcium in the coal and acceptor.

The following parameters were calculated from the flow rates in the mass balance:-

(i) Excess air level, defined as:-

$$\text{Excess air} = \frac{\text{Feed air - stoichiometric air for coal feed rate}}{\text{Stoichiometric air for coal feed rate}} \times 100\%$$

(ii) Carbon loss, defined as:-

$$\text{Carbon loss} = \frac{\text{Unburnt carbon output rate}}{\text{Total carbon output rate}} \times 100\%$$

(iii) Sulphur retention, defined as:-

$$\text{Sulphur retention} = \left(1 - \frac{\text{Sulphur in flue gas}}{\text{Total sulphur input}} \right) \times 100\%$$

(iv) Ca/S mol ratio, defined as:-

$$\text{Ca/S mol ratio} = \frac{\text{mols of Ca in additive}}{\text{mols of S in coal}}$$

3. Results

The programme of work on the 6 in combustor can conveniently be divided into five test series. The actual tests were not carried out in strict chronological order, as delivery of the Illinois coal for Test Series 1 was delayed, and Test Series 2 with U.K. raw materials was therefore completed first. However, all data are presented in serial order, ignoring chronology.

3.1 Test Series 1

To obtain data on sulphur retention for the coal used at Argonne National Laboratories (ANL) to compare with ANL data

3.1.1 Description of the test series

The combustor was operated in the manner described in Section 2. The nominal conditions for the series were as follows:

Coal:	U.S. Illinois (ex ANL), - 1680 μm
Acceptor:	U.S. Limestone 1359, - 1680 μm U.K. Limestone, - 1680 μm
Ca/S mol ratio:	0, 1, 2 & 3
Fluidising velocity:	3 ft/s
Bed temperature:	1470°F
Bed height:	2 ft
Flue gas O_2:	2.5 to 3.5%
Recycle:	None

The Illinois coal was supplied prepared to -¼" by ANL, and it was suggested that the required -1680 μm feedstock could be obtained by scalping off the coarser fraction. As this coarse fraction constituted some 40% of the coal, it was agreed with OAP that the coal would be crushed to give the required top size. This was done using the hammer mill in the "Fluostatic Plant" which is described in Appendix 1, Section 3.1.

The U.S. limestone 1359 was supplied prepared to minus 1/16 in by ANL and it was passed through a 1680 μm sieve before being used for the coal/limestone blends.

Bed ash from Welbeck coal produced in early experiments without limestone addition was used for the first test of the series. Table 1.1 indicates the source of the ash beds for the subsequent tests.

The U.K. limestone was delivered as -½ in + ¼ in graded material and this was processed to pass 1680 μm, using the hammer mill in the "Fluostatic plant".

3.1.2 Results of the test series

Table 1.1 gives the details of the operating conditions for the eight tests carried out in this series. It should be noted that as all tests on the 6 inch combustor occupy the same time scale, running hours are not given in the tables.

Tables 1.2 and 1.3 present the analyses of the coal and limestones used to make up the feed blends. Analyses of the individual blends are given in Table 1.4.

Solid product analyses of cyclone fines and of bed materials are given in Tables 1.5 and 1.6. It should be noted that the primary and secondary cyclone fines were bulked for analytical purposes. The flue gas analyses are given in Table 1.7.

Tables 1.8 to 1.15 give the mass balances and calculated operating parameters for each test in the series.

The carbon balances were good and the excess air levels were within the specified range. The combustion efficiency, without fines recycle, was about 96%. The ash balances here, and in subsequent test series, are not very satisfactory. This is thought to be due to the difficulty in determining the weight of ash accumulated in the bed, which had to be estimated by the indirect method given in Section 2.5. The sulphur balances were satisfactory and the agreement between the two runs without limestone addition was good. In general the SO_2 concentration in the offgas, as measured by the H_2O_2 method was in reasonable agreement with but slightly lower than the value obtained by taking the mean of the results of the iodine method. The values used for comparisons and in compiling graphs are the mean iodine results unless otherwise stated.

The reductions in SO_2 emission, with the addition of limestone 1359 and U.K. limestone, are given in Table 1.16. These results are plotted against the added Ca/S mol ratio in Fig. 3. The graph shows that the U.K. limestone is significantly more effective at reducing SO_2 than is limestone 1359. The same effect was noted at ANL.

3.2 Test Series 2

To substantiate previous sulphur retention data. Also to obtain data for a high-rank U.K. coal and on the effect of substoichiometric operation.

3.2.1 Description of the test series

The combustor was operated in the manner described in Section 2. The nominal conditions for the series were as follows:

Coal:	U.K. (a) Welbeck, and (b) Park Hill, -1680 μm
Acceptor:	U.K. Limestone, -1680 μm
Ca/S mol ratio:	0, 1, 2 and 3.
Fluidising velocity:	2 and 3 ft/s
Bed temp:	1470°F
Bed height:	2 ft
Flue Gas O_2:	2.5% to 3.5% and substoichiometric

Operation both with and without recycle.

The Welbeck coal was supplied processed to -1680 μm by BCURA. It formed part of the batch of Welbeck coal that was used for Task II, and the manner of processing of this material is described in Appendix 2, Section (1.5).

The Park Hill coal was delivered as 1½ in - 0 untreated smalls and was processed in the Fluostatic Plant in a similar manner to the coals used in Task I (see Appendix 1, Section 3.1).

The proposal had been to use a U.K. coal of high rank to contrast with the other U.K. coal (Welbeck-low rank) and to compare with the U.S. Pittsburgh coal (high rank). It was also proposed to use a coal of comparable sulphur content to the Pittsburgh coal. However, the coal received did not possess the expected qualities, in particular the Gray-King coke number, which for the purpose of the comparison should be G4 or higher, was determined as D. It was found on enquiry that the coal supplied was Park Hill, and not Park Mill, and in addition that the Park Mill Colliery was not currently producing a coal of sufficiently high rank to provide the desired comparison. As the sulphur content of the Park Hill coal to hand was satisfactory (2.45%) it was decided to use this for the tests.

Considerable difficulty was experienced with the SO_2 determinations using iodine. during the first tests with Park Hill coal (Tests 2.9,2.10 and 2.11) The subsequent analysis of the hydrogen peroxide solutions from these tests gave better results, but it was felt desirable to carry out further tests, (2.12,2.13 and 2.14). These gave consistent results for SO_2 using iodine solution, and the results were confirmed by the analyses of the hydrogen peroxide solutions.

3.2.2 Results of the test series

Table 2.1 gives the operating conditions for the 15 tests carried out in this series. Tables 2.2 and 2.3 present the analyses of the coal and limestone used to make up the feed blends. Analyses of the individual blends are given in Table 2.4.

Chemical analyses and size distributions of cyclone fines and bed materials are given in Tables 2.5 and 2.6. It should be noted that the primary and secondary cyclone fines were bulked for analytical purposes. The flue gas analyses are given in Table 5.7.

Tables 2.8 to 2.22 give the mass balances and calculated operating parameters for each test in the series.

The carbon balances were good throughout the test series. Without fines recycle, the combustion efficiency for Welbeck coal was about 93%, i.e. 3% lower than with Illinois coal in Test Series 1. With recycle the efficiency increased to about 97%. The change in fluidising velocity from 2 to 3 ft/s did not significantly effect the combustion efficiencies obtained. The run under sub-stoichiometric conditions (run 2.7) gave a carbon loss of 13.5% which is typical for these conditions. In general, for the runs using Park Hill coal, the oxygen concentration in the flue gas was slightly below the nominal condition of 2.5% - 3.5%, with the result that the combustion efficiencies averaged about 90%.

The sulphur balances in this series were generally satisfactory, but there were some exceptions; for example in Tests 2.9 and 2.10 where experimental difficulties were experienced in determining SO_2 using the iodine method. The reduction in SO_2 emission from Welbeck and Park Hill coals using U.K. limestone are given in Table 2.23. A separate SO_2 datum level was calculated for the sub-stoichiometric run, test 2.7, to allow for the increase in coal burnt. Fig. 4 shows the effect of Ca/S mol ratio on SO_2 reduction for U.K. limestone with four different coals, at a fluidising velocity of 3 ft/s. Some results from Test Series 1, 4 and 5 are included in addition to those from the present test series. The graph shows that the SO_2 reduction is about 10% higher with Welbeck coal than with the other three coals. Also, the SO_2 reduction with Pittsburgh coal may be slightly below that with Park Hill and Illinois. Since the Welbeck and Park Hill coals used almost identical properties, apart from sulphur content, (18.2% and 16.5% volatiles, both had a swelling Number of 1, Gray King coke types C and D), the differences between the coals cannot be ascribed to differences in rank. Possible differences for the better SO_2 reduction with Welbeck coal are discussed in the Main Report.

The effect on SO_2 reduction of changing the fluidising velocity is shown by Fig. 5. The results suggest that a decrease in SO_2 reduction of about 10% results from increasing the fluidising velocity from 2 ft/s to 3 ft/s.

Recycle of primary fines and running under sub-stoichiometric conditions, did not significantly effect the SO_2 reductions obtained.

3.3 Test Series 3

To investigate the effect of bed depth and temperature and the effect of fine grinding of limestone

3.3.1 Description of the test series

The combustor was operated in the manner described in Section 2. The nominal conditions for the series were as follows:-

Coal:	U.S. Illinois, -1680 µm
Acceptor:	U.S. Limestone 1359, -1680 µm and -125 µm
Ca/S mol ratio:	1, 2 and 3
Fluidising velocity:	3 ft/s
Bed temperature:	1290° and 1470°F
Bed height:	2 and 3 feet
Flue Gas O_2:	2.5 - 3.5%
Recycle:	None

The coal and limestone for this test series were from the same batches prepared and supplied by Argonne National Laboratory for test series 1. The fine limestone (-125 µm) was prepared on site from the supplied material using a laboratory swing hammer mill, in batches of approx. 1 lb; each batch being hand sieved through a 120 B.S. sieve (125 µm) and the coarse product returned to the mill with some fresh limestone.

3.3.2 Results of the test series

Table 3.1 gives the operating conditions for the six tests carried out in this series. Tables 3.2 and 3.3 present the analyses of the coal and limestone used to make up the feed blends. Analyses of the individual blends are given in Table 3.4.

Chemical analyses and size distributions of cyclone fines and bed materials are given in Tables 3.5 and 3.6. It should be noted that the primary and secondary cyclone fines were bulked for analytical purposes. The flue gas analyses are given in Table 3.7.

Tables 3.8 to 3.13 give the mass balances and calculated operating parameters for each test in the series.

The carbon balances were good, with the exception of Test 3.6. The combustion efficiencies at 1470°F of about 96% confirm the result of Test Series 1. At 1290°F the combustion efficiency was about 93%. The sulphur balances for this series were good. The reductions in SO_2 emission are given in Table 3.14.

The results at 1290°F clearly show that operation at this temperature is unsatisfactory. The chemical analysis of the ash and fines from these tests show that little calcination had taken place. The reductions in SO_2 emission using 2 ft and 3 ft deep beds (taken from Test series 1 and 3) with -1680 μm limestone 1359 and a 2 ft bed with -125 μm limestone 1359 are plotted against the Ca/S mol ratio in Fig. 6. The graph shows a 12-15% improvement in SO_2 reduction with the increase of bed height. The results using -125 μm limestone are not so clear cut, at the low Ca/S mol ratio a marked improvement in SO_2 reduction is shown, but at the higher level of addition the result is close to that obtained with -1680 μm limestone. The latter finding is in agreement with the results in Task 1, where using fine limestone had no significant effect on SO_2 reduction.

3.4 Test Series 4

To obtain sulphur retention data on the U.S. (Pittsburgh) coal using U.S. Limestone No. 18 and U.K. Limestone

3.4.1 Description of the test series

The combustor was operated in the manner described in Section 2. The nominal conditions for the series were as follows:-

Coal:	U.S. Pittsburgh, -1680 μm
Acceptor:	U.S. Limestone 18 and U.K. Limestone, -1680 μm
Ca/S mol ratio:	0, 1 2 and 3
Fluidising velocity:	3 ft/s
Bed temperature:	1470°F
Bed height:	3 ft
Flue Gas O_2:	2.5 - 3.5%
Recycle:	None

The Pittsburgh coal and the limestone 18 used for this test series were part of the batches used for Test Series 1 on the 36 inch combustor (Task I) and the preparation procedures for the two materials are described in Appendix 1, Section 3.1. The U.K. limestone was from the same batch as was used for Test Series 1 and 2 in the present task.

3.4.2 Results of the test series

Table 4.1 gives the operating conditions for the tests carried out in this series. Tables 4.2 and 4.3 present the analyses of the coal and limestone used to make up the feed blends. Analyses of the individual blends are given in Table 4.4.

Chemical analyses and size distributions of cyclone fines and bed materials are given in Tables 4.5 and 4.6. It should be noted that the primary and secondary cyclone fines were bulked for analytical purposes. The flue gas analyses are given in Table 4.7.

Tables 4.8 and 4.16 give the mass balances and calculated operating parameters for each test in the series.

The carbon balances obtained were satisfactory for this series. The combustion efficiency for Pittsburgh coal without fines recycle was about 91%.

The sulphur balances were satisfactory, with two exceptions, Tests 4.8 and 4.9. Both these balances had quite high sulphur losses of 18% and 25% respectively. Examination of these balances and comparison with other tests at similar conditions suggest that the error lies in the underestimation of the sulphur retained in the bed and offtake ash.

The reduction in SO_2 emission with the addition of U.K. limestone and limestone 18 are given in Table 4.17. These results are plotted against the added Ca/S mol ratio in Fig. 7. The graph shows that higher reductions of SO_2 emission are obtained when using limestone 18 as additive. This result in conjunction with the comparison of U.K. stone and U.S. 1359 carried out in Test series 1, shows that limestone 18 was about 15% more effective in reducing the SO_2 emission than was the U.K. stone and the U.K. stone in turn was again about 10% more effective than the U.S. 1359 limestone.

As described in section 2.2, the normal test procedure was to start with either a fresh ash bed or a bed from a previous test which had been carried out at a lower Ca/S ratio than that to be used. In order to demonstrate that an adequate time was being allowed for equilibrium to be reached, Test 4.8 was carried out using a bed from a test in which a higher Ca/S ratio had been used. The SO_2 reduction obtained was not significantly different from those obtained in Tests 4.5 and 4.9 in which beds of fresh coal ash and shale were used, respectively.

3.5 Test Series 5

To check sulphur retention data using a fresh batch of U.K. (Welbeck) coal using U.S. No. 18 and U.K. limestones

3.5.1 Description of the test series

The combustor was operated in the manner described in Section 2. The nominal conditions for the series were as follows:-

Coal: U.K. Welbeck II, -1680 µm
Acceptor: U.S. No. 18 and U.K. Limestones, -1680 µm
Ca/S mol ratio: 2
Fluidising velocity: 3 ft/s
Bed temperature: 1470°F
Bed height: 3 ft
Flue Gas O_2: 2.5 - 3.5%
Recycle: None

3.5.2 Results of the test series

Table 5.1 gives the operating conditions for the tests carried out in this series. Tables 5.2 and 5.3 present the analyses of the coal and limestone used to make up the feed blends. Analyses of the individual blends are given in Table 5.4.

Chemical analyses and size distribution of cyclone fines and bed materials are given in Tables 5.5 and 5.6. It should be noted that the primary and secondary cyclone fines were bulked for analytical purposes. The flue gas analyses are given in Table 5.7.

Tables 5.8 and 5.9 gives the mass balances and calculated operating parameters for each test in the series.

The carbon and sulphur balances were satisfactory in both tests. The combustion efficiencies were similar to those obtained in Test Series 2.

The reductions in SO_2 emission are given in Table 5.10. The result from Test 5.1 using U.K. limestone is plotted in Fig. 5, and agrees well with the results using the same materials from Test series 2, the use of a bed temperature 30° below that desired, did not appear to affect the result.

The SO_2 reduction obtained in test 5.2, using U.S. limestone 18, was the same as in Test series 2, where U.K. limestone was used as additive. This result is a little surprising as the previous tests with Pittsburgh coal had shown the U.S. stone to be the more effective; however, as no other tests were carried out using Welbeck coal and U.S. limestone, the result could not be checked.

4. COMPARISON WITH RESULTS FROM ARGONNE NATIONAL LABORATORY (ANL)

4.1 Illinois coal and Limestone 1359

Preliminary results from Test Series 1 and results from runs at ANL were compared in the ANL monthly progress report, No. 27, Jan. 1971. The materials and operating conditions used were the same at both centres, namely, Illinois coal, limestone 1359, bed temperature 1470°F, fluidising velocity 3 ft/s, and bed height 2 ft. A graph of the results showed the points to fall on a smooth curve and it was concluded that the results from the two centres were the same. Fig. 8 of this report is a re-plot of the same work but using the final results from test series 1. The parameter sulphur retention has been used instead of % SO_2 reduction since the level of SO_2 emission without limestone addition is not known for the ANL work. Sulphur retention is defined as the retained sulphur expressed as a percentage of the total sulphur input.

Fig. 8 confirms the ANL conclusion that there is no significant difference between the results. However, there is a tendency for the ANL results to be above the curve and the CRE results below. This difference corresponds to about 200 p.p.m. of SO_2 in the flue gas, the ANL results being the lower.

4.2 Welbeck coal and U.K. limestone

In a similar manner to Test Series 1, some of the preliminary results from test series 2 had been compared to work at ANL and this was reported in ANL monthly progress reports, Nos. 24 and 25. The conditions and materials used were Welbeck coal, U.K. limestone, 1470°F, 3 ft/s and a 2 ft deep bed. The results were plotted as SO_2 in the flue gas p.p.m. against Ca/S mole ratio (including calcium content of the coal) and showed the SO_2 concentrations from the ANL work to be about 100 - 300 p.p.m. higher than the results from the NCB. This difference is of the same order, but of opposite sign, to that found with the test series 1 results. Since, for Welbeck coal, the SO_2 emission without limestone is only about 1100 p.p.m. there is a significant difference in SO_2 reductions between the two plants, as shown in Fig. 9.

Although there are several design differences between the ANL and NCB 6 in combustors (listed in the Main Report) none of them would account for a difference with one coal and not with another. Thus it must be concluded that at the present time it is not possible to duplicate results on the two plants to an accuracy greater than ± 200 p.p.m. of SO_2.

ACKNOWLEDGEMENT

The authors acknowledge the contributions of their colleagues at CRE in carrying out the work described in this report. The work was administered by Dr. A.D. Dainton and Mr. J. McLaren; the overall experimental programme was devised by Mr. D.C. Davidson and Mr. A.W. Smale, who was also responsible for the operation of the plant; the shift team leaders were Mr. R. Dryburgh, Mr. J.C. Holder, Mr. M. Powell and Mr. L.C. Stephens; the chemical analyses were carried out under the supervision of Dr. H.A. Standing by Mr. G.J. Corney, Mr. H.W. Harris and Mr. L. Stanley; maintenance of the plant was carried out by the CRE Engineering and Instrumentation Sections.

The contribution made by Mr. E.L. Carls, the O.A.P. representative in the U.K., is also acknowledged.

Table A.5.1.1 Operating conditions during Test Series 1

Constant Parameters

Coal: Illinois (ex A.N.L.)
Coal Size: - 1680 μm
Acceptor Size: - 1680 μm
Fluidising Velocity: 3 ft/s
Bed Temperature: 1470°F
Bed Height: 2 ft
Recycle: None

Test No.	1.1	1.2	1.3	1.4	1.5	1.6	1.7	1.8
Date	17/7/70	21/7/70	22/7/70	23/7/70	28/7/70	29/7/70	30/7/70	31/7/70
Acceptor	None	US 1359	US 1359	US 1359	UK LST.	UK LST.	UK LST.	None
Ca/S mol ratio	0	1.5	2.2	3.3	1.1	2.2	3.2	0
Ash Bed	Fresh	ex 1.1	ex 1.2	ex 1.3	Fresh	ex 1.5	ex 1.6	Fresh

Table A.5.1.2 Chemical analyses of coal. Test Series 1

Test Number		1.1 - 1.8
Proximate analysis		
Total moisture	% a.r.	9.8
Ash	% a.r.	11.8
Volatile matter	% d.a.f.	46.6
Ultimate analysis		
Carbon	% d.b.	67.8
Hydrogen	% d.b.	4.45
Nitrogen	% d.b.	1.29
Sulphur	% d.b.	4.38
Oxygen & errors	% d.b.	8.5
Chlorine	% d.b.	0.22
Carbon Dioxide	% d.b.	1.05
Ash analysis		
CaO	% d.b.	10.1
MgO	% d.b.	1.0
Na_2O	% d.b.	1.7
K_2O	% d.b.	1.8
Al_2O_3	% d.b.	12.2
Fe_2O_3	% d.b.	20.6
S_1O_2	% d.b.	40.8
Calorific value (gross)	Btu/lb	14290
Swelling No.		4½
Gray King coke type		D

Table A.5.1.3 Chemical and Size Analyses of Acceptor

Test Series 1

Test No.	1.1-1.4	1.5-1.8
Chemical Analysis	(US 1359)	(UK LST.)
CaO a.r.	55.5	54.9
MgO a.r.	0.3	0.2
CO_2 a.r.	43.3	42.0
SiO_2 a.r.	0.8	1.6
Size Analysis	% in grade by weight	
Particle size (μm)		
+ 1680	0.1	0.5
+ 500 - 1680	36.7	52.1
+ 250 - 500	24.8	19.1
+ 125 - 250	16.6	10.1
+ 63 - 125	8.7	7.2
- 63	13.1	11.0
Median dia. (μm)	353	537

Table A.5.1.4 Chemical and Size Analyses of Feed Blends. Test Series 1

Test No.	1.1	1.2	1.3	1.4	1.5	1.6	1.7	1.8
Moisture a.r.	9.2	7.8	7.2	5.2	8.5	7.2	6.5	8.7
Ash a.r.	11.3	19.4	21.7	26.1	18.6	-	27.2	11.4
Carbon d.b.	67.8	55.5	52.0	45.7	57.0	51.4	43.7	68.0
CaO d.b.	1.15	10.22	13.71	17.5	8.25	13.4	18.47	0.96
Sulphur d.b.	4.6	3.9	3.35	2.85	3.9	3.35	3.15	4.45
CO_2 d.b.	0.72	6.54	10.6	13.65	6.29	10.45	14.12	0.59
Particle size (µm)	% in grade by weight							
+ 1680	0.3	1.2	0.6	0.6	1.7	0.7	0.2	0.1
+ 500 - + 1680	49.2	44.9	51.9	53.1	53.7	53.7	48.1	60.4
+ 250 - + 500	25.1	22.4	19.9	20.0	19.4	18.1	21.3	18.6
+ 125 - + 250	13.9	15.8	12.8	11.8	11.9	12.0	14.4	10.1
+ 63 - + 125	6.1	6.9	7.2	6.4	5.9	7.2	7.6	5.2
- 63	5.4	8.8	7.6	8.1	7.4	8.3	8.4	5.6
Median dia. µm	494	453	543	551	577	566	478	655

Table A.5.1.5 Chemical and Size Analyses of Cyclone Fines

Test Series 1

Test No.	1.1	1.2	1.3	1.4	1.5	1.6	1.7	1.8
Chemical Analysis								
Carbon % a.r.	33.5	21.7	18.1	15.0	24.6	19.4	16.1	24.4
Sulphur % a.r.	1.75	2.75	3.09	3.09	2.86	2.76	2.60	1.90
CO_2 % a.r.	0.82	3.09	5.5	8.54	3.66	6.6	11.80	10.80
CaO % a.r.	3.92	10.63	16.0	21.65	12.6	17.05	23.40	0.56
Size Analysis	% in grade by weight							
Particle size (µm)								
+ 500	0	0	0	0	0	0	0	0.1
+ 250 - 500	0	0	0	0	0	3.0	0.1	0.1
+ 125 - 250	0.3	0.1	1.5	1.7	0.2	1.1	0.3	0.4
+ 63 - 125	11.1	8.8	7.8	7.4	8.8	7.9	5.8	11.2
- 63	88.6	91.1	90.7	90.9	91.0	88.0	93.8	88.2

Table A.5.1.6(a) Chemical and Size Analyses of Bed Material

Test Series 1

Test No.	1.1			1.2			1.3			1.4		
Sample	Initial	Final	Offtake	Initial	Final	Offtake	Initial	Final	Offtake	Initial	Final	Offtake
Chemical Analysis:												
Sulphur % a.r.	0.35	0.95	0.8	2.2	4.15	3.15	4.2	4.95	5.55	6.0	7.9	7.35
CO_2 % a.r.	0.25	0.39	0.23	2.0	4.58	4.32	4.84	6.4	5.9	6.68	7.11	8.68
CaO % a.r.	2.1	3.08	2.66	10.5	21.2	15.4	22.4	31.8	25.6	32.2	49.5	43.0
Size Analysis	% in grade by weight											
Particle size (μm)												
+ 1680	0	0	0	0.1	0.1	0	0	0	0	0	0	0
+ 500 - 1680	52.0	49.5	47.7	48.3	47.8	50.3	41.8	31.7	53.2	38.0	55.2	36.9
+ 250 - 500	35.6	36.4	37.5	37.7	36.0	35.7	39.1	33.7	35.0	32.9	30.6	28.6
+ 125 - 250	10.7	12.1	12.2	10.3	9.8	10.8	14.3	23.4	10.2	18.5	11.7	21.1
+ 63 - 125	1.2	1.8	2.3	3.4	5.4	3.1	4.6	10.6	1.5	9.5	2.4	12.1
- 63	0.5	0.2	0.3	0.2	0.9	0.1	0.2	0.6	0.1	1.1	0.1	1.3
Median diam. (μm)	516	496	483	488	483	502	442	349	526	401	549	378

Table A.5.1.6 (b) Chemical and Size Analyses of Bed Material

Test Series 1 (cont'd).

Test No.	1.5			1.6			1.7			1.8		
Sample	Initial	Final	Offtake	Initial	Final	Offtake	Initial	Final	Offtake	Initial	Final	Offtake
Chemical Analysis:												
Sulphur % a.r.	0.9	4.25	1.25	4.55	6.7	5.6	1.45	3.0	2.0	0.9	0.9*	0.85
CO_2 % a.r.	0.43	1.41	1.72	1.49	1.79	2.33	0.39	0.71	0.55	0.21	0.34	0.41
CaO % a.r.	4.48	18.6	6.85	18.2	31.6	22.4	5.3	11.6	6.6	3.78	3.64*	3.64
Size Analysis	% in grade by weight											
Particle size (μm)												
+ 1680	0	0	0	0.1	0	0	0	0.1	0	0	0	0.1
+ 500 - 1680	49.6	63.6	52.1	50.6	47.2	41.5	44.8	51.5	35.7	57.0	47.6	53.9
+ 250 - 500	43.9	14.6	39.7	37.9	36.5	35.6	38.3	31.9	31.6	38.5	41.7	41.3
+ 125 - 250	5.5	14.6	6.2	7.3	11.7	10.2	10.9	12.0	15.2	3.6	7.5	3.8
+ 63 - 125	0.6	6.3	1.2	3.6	4.3	11.4	5.5	4.3	15.8	0.5	2.7	0.6
- 63	0.4	0.9	0.8	0.5	0.3	1.3	0.5	0.2	1.7	0.4	0.5	0.3
Median diam. (μm)	497	739	515	505	478	434	462	514	379	553	484	528

* Estimated

Table A.5.1.7 Flue Gas Analyses

Test No.	1.1	1.2	1.3	1.4	1.5	1.6	1.7	1.8
Operating Conditions								
Ca/S Mol Ratio	0	1.5	2.2	3.3	1.1	2.2	3.2	0
Fluidising Velocity ft/s	3	3	3	3	3	3	3	3
Bed Temperature ^{o}F	1470	1470	1470	1470	1470	1470	1470	1470
Bed Height ft	2	2	2	2	2	2	2	2
Chromatograph								
Mean CO_2 Vol % Dry	14.5	14.8	15.3	15.4	15.2	15.8	16.0	15.4
Mean O_2 "	2.9	2.8	2.6	2.9	2.6	2.2	2.3	2.6
Mean CO "	0.04	0.05	0.03	0.04	0.06	0.05	0.05	0.08
Mean CH_4 "	0	0	0	0	0	0	0	0
SO_2 by Iodine								
Sample 1. p.p.m. Dry	4016	2045	1431	672	1766	1148	228	4032
Sample 2. "	4057	1910	1494	944	1863	1393	232	4032
Sample 3. "	3997	2504	1417	1163	1733	1376	266	3961
Sample 4. "		1974	1458	845	1783		265	3734
Sample 5. "		2157		831	1781		218	3720
Sample 6. "							219	
Mean SO_2								
By Iodine p.p.m. Dry	4023	2118	1450	870	1785	1306	229	3896
By H_2O_2 p.p.m. Dry	3240	2225	1380	504	1703	751	130	3670
Cl p.p.m. Dry	134	126	150	145	179	182	152	160
NH_3 p.p.m. Dry	20	90	9	23	34	25	17	26

Table A.5.1.8 Mass Balance for Test No. 1.1

Rate lb/h	Total	'Ash'	'Carbon'	Nitrogen	'Oxygen'	Sulphur	Calcium
Coal	4.31	0.56	2.92	0	0.37	0.189	0.041
Acceptor	0	0	0	0	0	0	0
Total Air	45.94	0	0	35.3	10.64	0	0
Bleed Nitrogen	1.9	0	0	1.9	0	0	0
Total Input	52.15	0.56	2.92	37.2	11.01	0.189	0.041
Accumulated in Bed	-0.16	-0.16	0	0	0	0.014	0.017
Offtake Ash	0	0	0	0	0	0	0
Fines	0.54	0.41	0.12	0	0	0.009	0.015
Flue Gas	51.54	0	2.82	37.6	10.74	0.193	0
Total Output	51.92	0.25	2.94	37.6	10.74	0.216	0.032
Unaccounted, input-output	0.23	0.31	-0.02	-0.4	0.27	-0.027	0.009
Unaccounted, % of input	0.44	55.36	-0.68	-1.08	2.45	-14.28	21.4

Excess Air	12.6%	
Carbon Loss	4.2%	(Unburnt)
Sulphur Retention	0%	
Ca/S Mol ratio	0	

Table A.5.1.9 Mass Balance for Test No. 1.2

Rate lb/h	Total	'Ash'	'Carbon'	Nitrogen	'Oxygen'	Sulphur	Calcium
Coal	4.40	0.58	2.98	0	0.37	0.193	0.041
Acceptor	0.89	0.89	0	0	0	0	0.354
Total Air	45.94	0	0	35.3	10.64	0	0
Bleed Nitrogen	1.9	0	0	1.9	0	0	0
Total Input	53.13	1.47	2.98	37.2	11.01	0.193	0.395
Accumulated in Bed	-0.14	-0.14	0	0	0	0.059	0.231
Offtake Ash	0.67	0.67	0	0	0	0.021	0.074
Fines	0.52	0.41	0.11	0	0	0.014	0.040
Flue Gas	51.65	0	2.88	37.5	10.88	0.102	0
Total Output	52.70	0.94	2.99	37.5	10.88	0.196	0.344
Unaccounted, input-output	0.43	0.53	-0.01	-0.3	0.13	-0.003	0.051
Unaccounted, % of input	0.81	36.05	-0.34	-0.81	1.19	-1.7	12.9

Excess Air	12.1%	
Carbon Loss	3.75%	(Unburnt)
Sulphur Retention	47%	
Ca/S Mol ratio	1.5	

Table A.5.1.10 Mass Balance for Test No. 1.3

Rate lb/h	Total	'Ash'	'Carbon'	Nitrogen	'Oxygen'	Sulphur	Calcium
Coal	4.41	0.58	2.99	0	0.38	0.193	0.041
Acceptor	1.32	1.32	0	0	0	0	0.522
Total Air	45.94	0	0	35.3	10.64	0	0
Bleed Nitrogen	1.9	0	0	1.9	0	0	0
Total Input	53.57	1.90	2.99	37.2	11.02	0.193	0.563
Accumulated in Bed	-0.22	-0.22	0	0	0	0.023	0.204
Offtake Ash	1.09	1.09	0	0	0	0.061	0.200
Fines	0.57	0.47	0.10	0	0	0.017	0.063
Flue Gas	51.79	0	2.97	37.4	11.04	0.070	0
Total Output	53.23	1.36	3.07	37.4	11.04	0.171	0.466
Unaccounted, input-output	0.34	0.54	-0.08	-0.2	-0.02	0.022	0.097
Unaccounted, % of input	0.63	28.42	-2.68	-0.54	-0.18	11.8	17.2

Excess Air	11.1%
Carbon loss	3.31% (Unburnt)
Sulphur Retention	64%
Ca/S Mole Ratio	2.2

Table A.5.1.11 Mass Balance for Test No. 1.4

Rate lb/h	Total	'Ash'	'Carbon'	Nitrogen	'Oxygen'	Sulphur	Calcium
Coal	4.40	0.58	2.98	0	0.37	0.193	0.041
Acceptor	1.99	1.99	0	0	0	0	0.789
Total Air	45.94	0	0	35.3	10.64	0	0
Bleed Nitrogen	1.90	0	0	1.9	0	0	0
Total Input	54.23	2.57	2.98	37.2	11.01	0.193	0.831
Accumulated in Bed	0	0	0	0	0	0.049	0.312
Offtake Ash	1.38	1.38	0	0	0	0.101	0.423
Fines	0.69	0.58	0.10	0	0	0.021	0.103
Flue Gas	51.82	0	2.99	37.2	11.24	0.042	0
Total Output	52.03	1.96	3.09	37.2	11.24	0.212	0.838
Unaccounted, input-output	2.2	0.61	-0.11	0	-0.23	-0.019	-0.007
Unaccounted, % of input	4.1	23.7	-3.7	0	-2.1	-10.1	-0.9

Excess Air	12.6%	
Carbon Loss	3.3%	(Unburnt)
Sulphur Retention	78%	
Ca/S Mol ratio	3.3	

Table A.5.1.12 Mass Balance for Test No 1.5

Rate lb/h	Total	'Ash'	'Carbon'	Nitrogen	'Oxygen'	Sulphur	Calcium
Coal	4.37	0.57	2.97	0	0.37	0.192	0.041
Acceptor	0.66	0.66	0	0	0	0	0.257
Total Air	45.94	0	0	35.3	10.64	0	0
Bleed Nitrogen	1.90	0	0	1.9	0	0	0
Total Input	52.87	1.23	2.97	37.2	11.01	0.192	0.298
Accumulated in Bed	0.29	0.29	0	0	0	0.087	0.261
Offtake Ash	0	0	0	0	0	0	0
Fines	0.61	0.47	0.14	0	0	0.017	0.052
Flue Gas	51.72	0	2.96	37.4	10.98	0.087	0
Total Input	52.62	0.76	3.10	37.4	10.98	0.190	0.314
Unaccounted, input-output	0.25	0.47	-0.13	-0.2	0.03	0.002	-0.016
Unaccounted, % of input	0.5	38.2	-4.4	-0.54	0.27	0.7	-5.3

Excess Air	9.8%
Carbon Loss	4.59% (Unburnt)
Sulphur Retention	55%
Ca/S Mole ratio	1.1

Table A.1.5.1.13 Mass Balance for Test No. 1.6

Rate lb/h	Total	'Ash'	'Carbon'	Nitrogen	'Oxygen'	Sulphur	Calcium
Coal	4.25	0.56	2.88	0	0.36	0.186	0.040
Acceptor	1.28	1.28	0	0	0	0	0.501
Total Air	45.94	0	0	35.3	10.64	0	0
Bleed Nitrogen	1.9	0	0	1.9	0	0	0
Total Input	53.37	1.84	2.88	37.2	11.00	0.186	0.541
Accumulated in Bed	-0.07	-0.07	0	0	0	0.066	0.294
Offtake Ash	0.94	0.94	0	0	0	0.053	0.150
Fines	0.57	0.46	0.11	0	0	0.015	0.068
Flue Gas	51.79	0	3.07	37.3	11.04	0.063	0
Total Output	53.23	1.33	3.18	37.3	11.04	0.197	0.513
Unaccounted, input-output	0.14	0.51	-0.30	-0.1	-0.04	-0.011	0.028
Unaccounted, % of input	0.26	27.72	-10.42	-0.27	-0.36	-5.9	5.3

Excess Air	8.5%	
Carbon Loss	3.42%	(Unburnt)
Sulphur Retention	66%	
Ca/S Mole Ratio	2.2	

Table A.5.1.14 Mass Balance for Test No. 1.7

Rate lb/h	Total	'Ash'	'Carbon'	Nitrogen	'Oxygen'	Sulphur	Calcium
Coal	4.47	0.59	3.03	0	0.38	0.196	0.042
Acceptor	2.00	2.00	0	0	0	0	0.784
Total Air	45.94	0	0	35.3	10.64	0	0
Bleed Nitrogen	1.9	0	0	1.9	0	0	0
Total Input	54.31	2.59	3.03	37.2	11.02	0.196	0.826
Accumulated in Bed	-0.29	-0.29	0	0	0	0.050	0.317
Offtake Ash	1.43	1.43	0	0	0	0.111	0.349
Fines	0.75	0.63	0.12	0	0	0.019	0.125
Flue Gas	51.99	0	3.11	37.2	11.27	0.011	0
Total Output	53.88	1.77	3.23	37.2	11.27	0.192	0.791
Unaccounted, input-output	0.43	0.82	-0.20	0	-0.25	0.004	0.035
Unaccounted, % of input	0.79	31.66	-6.60	0	-2.27	2.0	4.2

Excess Air	8.5%
Carbon Loss	3.73% (Unburnt)
Sulphur Retention	94%
Ca/S Mol ratio	3.2

Table A.5.1.15 Mass Balance for Test No. 1.8

Rate lb/h	Total	'Ash'	'Carbon'	Nitrogen	'Oxygen'	Sulphur	Calcium
Coal	4.35	0.57	2.95	0	0.37	0.191	0.041
Acceptor	0	0	0	0	0	0	0
Total Air	45.94	0	0	35.3	10.64	0	0
Bleed Nitrogen	1.9	0	0	1.9	0	0	0
Total Input	52.19	0.57	2.95	37.2	11.01	0.191	0.041
Accumulated in Bed	-0.11	-0.11	0	0	0	0	-0.003
Offtake Ash	0	0	0	0	0	0	0
Fines	0.58	0.44	0.14	0	0	0.011	0.045
Flue Gas	51.77	0	3.00	37.3	11.08	0.188	0
Total Output	52.24	0.33	3.14	37.3	11.08	0.199	0.042
Unaccounted, input-output	-0.05	0.24	-0.19	-0.1	-0.07	-0.008	-0.001
Unaccounted, % of input	-0.09	42.1	-6.44	-0.27	-0.64	-4.5	2.4

Excess Air	9.7%	
Carbon Loss	4.53%	(Unburnt)
Sulphur Retention	1%	
Ca/S Mol ratio	0	

Table A.5.1.16 SO_2 concentrations and % reductions

Test No.	1.1	1.2	1.3	1.4
Limestone Type	-	U.S. 1359	U.S. 1359	U.S. 1359
Fluidising Velocity, ft/s	3	3	3	3
Bed Temperature, °F	1470	1470	1470	1470
Ca/S mol ratio	0	1.5	2.2	3.3
SO_2 concentration, p.p.m.	4023	2118	1450	(680)
SO_2 reduction, %	0	46.5	63.4	83

Test No.	1.5	1.6	1.7	1.8
Limestone Type	U.K.	U.K.	U.K.	-
Fluidising Velocity, ft/s	3	3	3	3
Bed Temperature, °F	1470	1470	1470	1470
Ca/S mol ratio	1.1	2.2	3.2	0
SO_2 concentration, p.p.m.	1785	(1000)	229	3896
SO_2 reduction, %	55	75	94	0

(   ) Mean of iodine and hydrogen peroxide methods.

SO_2 reductions are based on a datum level of 3960 p.p.m.

Table A.5.2.1 Operating Conditions During Test Series 2

Constant Parameters:

Coal size : - 1680 micron
Acceptor : U.K. Limestone
Acceptor size : - 1680 micron
Bed Temperature : 1470°F
Bed Height : 2 ft

Test No.	2.1	2.2	2.3	2.4	2.5	2.6	2.7	2.8
Date	8.6.70	9.6.70	10.6.70	15.6.70	16.6.70	17.6.70	18.6.70	19.6.70
Coal	Welbeck (W)	W	W	W	W	W	W	W
Ca/S mole ratio	0	0.8	0.8	0.8	1.8	2.9	0.8	1.8
Fl. Vel. ft/s	2	2	2	3	3	3	3	2
Ash Bed	Fresh	ex 2.1	ex 2.2	ex 2.3	ex 2.4	ex 2.5	ex 2.6	Fresh
Excess Air %	+10	+10	+10	+10	+10	+10	-10	+10
Recycle	Yes	Yes	No	No	No	No	No	No

Test No.	2.9	2.10	2.11	2.12	2.13	2.14	2.15
Date	23.6.70	24.6.70	25.6.70	3.8.70	4.8.70	5.8.70	22.10.70
Coal	Park Hill (P.H.)	P.H.	P.H.	P.H.	P.H.	P.H.	W
Ca/s mole ratio	0.5	1.3	2.7	0	1.1	2.6	0.8
Fl. Vel. ft/s	3	3	3	3	3	3	3
Ash Bed	Fresh	ex 2.9	ex 2.10	Fresh	ex 2.12	ex 2.13	Fresh
Excess Air %	+10	+10	+10	+10	+10	+10	+10
Recycle	No	No	No	No	No	No	Yes*

* 2.15. Despite repeated attempts it was not possible to sustain recycle in this test.

Table A.5.2.2 Chemical analyses of coal

Test Series 2

Test Number		2.1 - 2.8 & 2.15	2.9 - 2.14
Proximate analysis			
Total moisture	% a.r.	4.2	2.1
Ash	% a.r.	18.2	16.5
Volatile matter	% d.a.f.	38.3	39.2
Ultimate analysis			
Carbon	% d.b.	67.5	68.2
Hydrogen	% d.b.	4.26	4.43
Nitrogen	% d.b.	1.47	1.33
Sulphur	% d.b.	1.3	2.45
Oxygen + errors	% d.b.	5.08	5.3
Chlorine	% d.b.	0.55	0.14
Carbon Dioxide	% d.b.	0.41	0.6
Ash analysis			
CaO	% d.b.	1.77	2.25
MgO	% d.b.	1.39	1.66
Na_2O	% d.b.	1.81	0.75
K_2O	% d.b.	3.21	3.62
Al_2O_3	% d.b.	17.8	21.1
Fe_2O_3	% d.b.	7.28	15.0
S_iO_2	% d.b.	57.5	46.0
Calorific value (gross)	Btu/lb	14600	14750
Swelling No.			1
Gray King coke type			D

Table A.5.2.3 Chemical and Size Analyses of Acceptor Test Series 2

Test No.	2.1 - 2.15
Chemical Analysis	
CaO a.r.	54.9
MgO a.r.	0.2
CO_2 a.r.	42.0
S_iO_2 a.r.	1.6
Size Analysis	% in grade by weight
Particle size (μm)	
+ 1680	0.5
+ 500 - 1680	52.1
+ 250 - 500	19.1
+ 125 - 250	10.1
+ 63 - 125	7.2
- 63	11.0
Median diam. (μm)	537

Table A.5.2.4 (a) Chemical and Size Analyses of Feed Blends

Test Series 2

Test No.	2.1	2.2	2.3	2.4	2.5	2.6	2.7	2.8
Moisture a.r.	4.9	4.4	4.7	5.0	4.7	3.6	5.1	4.4
Ash a.r.	16.3	18.9	19.0	19.5	19.6	22.3	21.8	21.4
Carbon d.b.	67.9	65.6	65.5	63.9	63.2	59.3	61.9	61.5
CaO d.b.	0.38	2.06	2.2	2.07	3.61	6.64	2.14	3.84
Sulphur d.b.	1.26	1.31	1.26	1.26	1.31	1.09	1.27	1.15
CO_2 d.b.	0.37	1.73	1.88	1.82	2.88	5.0	1.79	2.9
Particle size (μm)	% in grade by weight							
+ 1680	0	0.1	0	0	0	0	0	0
+ 500 - 1680	29.4	32.8	30.9	25.0	34.4	31.4	29.8	30.3
+ 250 - 500	37.1	37.2	37.9	37.7	36.9	36.0	38.1	38.1
+ 125 - 250	17.3	15.4	16.0	17.8	15.5	16.0	15.9	16.0
+ 63 - 125	6.4	5.5	5.6	7.5	4.9	5.8	6.5	6.1
- 63	9.8	9.0	9.6	12.0	8.3	10.8	9.7	9.5
Median dia μm	364	376	380	336	386	375	374	377

Table A.5.2.4 (b) Chemical and Size Analyses of Feed Blends Test Series 2 (cont'd)

Test No.	2.9	2.10	2.11	2.12	2.13	2.14	2.15
Moisture a.r.	2.4	2.3	1.9	2.5	2.4	2.0	3.8
Ash a.r.	16.2	20.8	23.6	15.4	21.6	25.0	21.4
Carbon d.b.	64.8	61.5	56.6	69.6	60.1	54.0	62.6
CaO d.b.	2.72	5.81	9.59	0.48	5.19	10.21	2.28
Sulphur d.b.	2.35	2.2	1.95	2.35	2.30	2.10	1.20
CO_2 d.b.	2.35	4.48	7.75	0.44	4.21	8.15	1.80
Particle size (μm)	% in grade by weight						
+ 1680	0	0.1	0.1	0	0.1	0	0
+ 500 - 1680	47.3	50.8	56.6	63.5	53.7	54.7	33.5
+ 250 - 500	22.3	21.4	18.7	16.7	21.5	18.2	35.9
+ 125 - 250	13.2	12.2	10.5	8.9	12.4	12.1	15.3
+ 63 - 125	7.9	7.1	5.9	4.9	6.0	6.6	6.5
- 63	9.3	8.4	8.2	6.0	6.4	8.4	8.8
Median dia. μm	467	512	598	716	549	570	376

Table A.5.2.5 (a) Chemical and Size Analyses of Cyclone Fines

Test Series 2

Test No.	2.1*	2.2*	2.3	2.4	2.5	2.6	2.7	2.8
Chemical Analysis								
Carbon % a.r.	26.9	24.6	40.2	42.6	41.9	33.8	54.2	33.8
Sulphur % a.r.	0.8	1.50	1.1	0.95	1.15	1.41	0.9	1.3
CO_2 % a.r.	0.13	0.19	0.18	0.18	0.62	2.38	0.23	0.43
CaO % a.r.	2.58	5.82	3.33	2.41	5.79	10.6	2.49	5.82
Size Analysis	% in grade by weight							
Particle size (µm)								
+ 500	0.3	0.2	0.3	0.2	0.2	0	0	0
+ 250 - 500	1.4	0.2	0.2	0.2	0	0	0	0
+ 125 - 250	1.7	0.4	1.1	1.4	1.3	0.5	1.7	1.2
+ 63 - 125	3.1	2.1	14.7	13.5	14.9	11.6	19.4	12.5
- 63	93.5	97.1	83.7	84.7	83.6	87.9	78.9	86.3

* Note: Tests 2.1 & 2.2 used recycle. Fines collected in secondary cyclone only.

Table A.5.2.5.(b) Chemical and Size Analyses of Cylone Fines Test Series 2 (cont'd).

Test No.	2.9	2.10	2.11	2.12	2.13	2.14	2.15*
Chemical Analysis							
Carbon % a.r.	37.9	34.8	37.0	42.0	39.7	33.6	-
Sulphur % a.r.	0.95	1.0	1.4	0.82	1.04	1.38	-
CO_2 % a.r.	0.43	1.31	4.0	0.11	1.07	2.96	-
CaO % a.r.	2.5	4.3	6.94	13.1	5.84	9.32	-
Size Analysis	% in grade by weight						
Particle size (μm)							
+ 500	0	0.2	0.1	0	0	0	-
+ 250 - 500	0	0.2	0.4	0.2	0.1	1.1	-
+ 125 - 250	2.0	1.6	1.1	2.0	0.9	1.4	-
+ 63 - 125	22.5	19.0	15.2	24.6	17.9	17.3	-
- 63	75.5	79.0	83.2	73.2	81.1	80.2	-

* Test 2.15 was unsatisfactory - attempted recycle ∴ no representative fines samples.

Table.A.5.2.6 (a) Chemical and Size Analyses of Bed Material

Test Series 2

Test No.	2.1			2.2			2.3			2.4		
Sample	Initial	Final	Offtake	Initial	Final	Offtake	Initial	Final	Offtake	Initial	Final	Offtake
Chemical Analysis												
Sulphur % a.r.	0.55	0.55	0.5	0.55	0.95	0.6	0.8	1.2	0.85	1.0	1.65	1.45
CO_2 % a.r.	0.08	0.31	0.31	0.12	0.18	0.11	0.13	0.23	0.24	0.27	0.17	0.33
CaO % a.r.	1.99	1.99	1.99	2.21	3.54	2.52	3.32	4.45	3.28	4.03	5.48	5.46
Size Analysis	% in grade by weight											
Particle size (μm)												
+ 1680	0	0	0	-*	0	0	0	0	0	0	0	0
+ 500 - 1680	53.2	44.3	47.8	-	40.4	45.7	39.0	44.1	40.1	45.2	33.9	34.9
+ 250 - 500	35.8	36.8	37.9	-	36.8	36.1	39.4	33.7	39.9	35.2	39.4	33.0
+ 125 - 250	9.0	11.3	10.1	-	13.8	12.2	13.4	15.1	13.6	13.8	20.8	15.5
+ 63 - 125	1.4	3.5	2.3	-	5.6	3.7	5.1	6.0	4.6	4.9	5.6	13.4
- 63	0.6	4.1	1.9	-	3.4	2.3	3.1	1.1	1.8	0.9	0.4	3.2
Median diam. (μm)	526	457	484	-	428	467	423	451	431	462	389	377

* Sample lost; Test 2.1 'Final Bed' is similar

Table A.5.2.6 (b) Chemical and Size Analyses of Bed Material

Test Series 2 (cont'd)

Test No.	2.5			2.6			2.7			2.8		
Sample	Initial	Final	Offtake	Initial	Final	Offtake	Initial	Final	Offtake	Initial	Final	Offtake
Chemical Analysis												
Sulphur % a.r.	1.65	2.65	1.85	2.8	3.06	2.65	2.96	2.97	3.10	0.45	1.45	0.55
CO_2 % a.r.	0.24	0.30	0.42	0.75	0.36	0.80	0.46	0.29	0.80	0.21	0.39	0.22
CaO % a.r.	5.42	9.4	6.95	13.6	15.9	11.3	14.7	11.6	13.8	2.56	6.38	2.68
Size Analysis	% in grade by weight											
Particle size (µm) + 1680	0	0	0	0.1	0	0	0	0	0	0	0	0
+ 500 - 1680	43.7	38.9	35.1	38.9	37.3	29.9	37.1	31.0	33.8	69.4	45.3	52.6
+ 250 - 500	37.1	36.7	33.2	37.5	37.0	32.5	36.3	37.4	31.3	38.6	38.9	34.8
+ 125 - 250	13.7	17.8	17.4	16.9	18.8	20.5	18.6	21.8	19.3	10.1	12.4	8.4
+ 63 - 125	4.9	6.4	13.0	6.4	6.7	16.0	7.8	9.4	14.2	1.3	3.1	3.3
- 63	0.6	0.2	1.3	0.2	0.2	1.1	0.2	0.4	1.4	0.6	0.3	0.9
Median diam. (µm)	452	417	379	419	406	336	403	366	361	652	466	521

Table A.5.2.6 (c) Chemical and Size Analyses of Bed Material

Test Series 2 (cont'd).

Test No.	2.9			2.10			2.11			2.12		
Sample	Initial	Final	Offtake	Initial	Final	Offtake	Initial	Final	Offtake	Initial	Final	Offtake
Chemical Analysis												
Sulphur % a.r.	0.7	1.55	0.65	1.25	2.6	1.7	2.15	4.05	3.4	1.55	1.95	1.35
CO_2 % a.r.	0.16	0.27	0.19	0.48	0.85	1.32	0.6	0.9	2.05	0.52	0.02	0.53
CaO % a.r.	3.26	5.92	2.8	5.04	11.8	6.74	9.5	21.6	14.4	5.31	5.73	4.9
Size Analysis	% in grade by weight											
Particle size (μm)	*											
+ 1680	-	0	0	0.1	0.1	0	0	0	0.1	0.1	0	0
+ 500 - 1680	-	47.1	49.0	48.0	45.6	42.5	47.1	46.4	40.4	54.5	50.3	55.9
+ 250 - 500	-	37.8	39.2	38.0	37.1	37.0	37.0	34.8	33.4	38.3	39.6	37.8
+ 125 - 250	-	11.7	10.5	11.4	13.1	13.1	12.1	13.4	15.5	4.7	6.8	4.4
+ 63 - 125	-	3.1	1.2	2.2	3.8	6.3	3.4	5.0	9.3	1.9	3.0	1.4
- 63	-	0.3	0.1	0.3	0.3	1.1	0.4	0.4	1.3	0.5	0.3	0.5
Median diam. (μm)		478	493	486	467	444	478	471	422	535	502	545

* Sample lost : Test 2.1 Initial bed is similar

Table A.5.2.6 (d) Chemical and Size Analyses of Bed Material

Test Series 2 (cont'd)

Test No.	2.13			2.14			2.15		
Sample	Initial	Final	Offtake	Initial	Final	Offtake	Initial	Final	*Offtake
Chemical Analysis									
Sulphur % a.r.	1.45	3.0	2.0	3.2	4.45	4.95	2.85	2.70	-
CO_2 % a.r.	0.39	0.71	0.55	1.89	1.61	2.7	1.33	0.44	-
CaO % a.r.	2.03	4.2	2.8	15.7	23.4	20.4	9.9	9.2	-
Size Analysis	% in grade by weight								
Particle size (μm)									
+ 1680	0	0	0	0	0	0	0	0.1	-
+ 500 - 1680	49.3	46.5	52.0	45.3	50.1	37.4	62.6	75.7	-
+ 250 - 500	41.1	39.4	37.2	39.8	32.6	31.6	27.3	22.1	-
+ 125 - 250	6.5	9.0	6.1	9.6	12.4	15.3	6.9	1.8	-
+ 63 - 125	2.7	4.5	3.9	4.6	4.4	13.6	2.2	0.3	-
- 63	0.4	0.6	0.8	0.7	0.5	2.1	1.0	0	-
Median diam. (μm)	495	475	515	467	501	392	634	828	-

* Test 2.15. Unsatisfactory recycle test - no representative offtake ash sample obtained.

Table A.5.2.7 (a) Flue Gas Analyses

Test No.		2.1	2.2	2.3	2.4	2.5	2.6	2.7	2.8
Operating Conditions									
Ca/s Mol ratio		0	0.8	0.8	0.8	1.8	2.9	0.8	1.8
Fluidising velocity ft/s		2	2	2	3	3	3	3	2
Bed temperature ^oF		1470	1470	1470	1470	1470	1470	1470	1470
Bed height	ft	2	2	2	2	2	2	2	2
Chromatograph									
Mean CO_2	Vol % dry	14.6	14.6	14.2	14.4	15.2	15.7	16.7	15.0
Mean O_2	Vol % dry	3.1	3.1	3.1	3.1	2.3	2.2	0.3	2.6
Mean CO	Vol % dry	0.2	0.2	0.1	0.2	0.12	0.1	0.4	0.1
Mean CH_4	Vol % dry	0	0	0	0	0	0	0	0
SO_2 By Iodine									
Sample 1	p.p.m. dry	1054	422	560	585	219	27	589	160
Sample 2	p.p.m. dry	1088	502	528	591	202	38	623	144
Sample 3	p.p.m. dry	1118	540	472	621	199	34	623	158
Sample 4	p.p.m. dry			492					177
Sample 5	p.p.m. dry								161
Sample 6	p.p.m. dry								149
Mean SO_2									
By Iodine	p.p.m. dry	1087	488	513	599	207	33	612	158
By H_2O_2	p.p.m. dry	1088	564	493	604	223	30	875	146
Cl^-	p.p.m. dry	438	408	456	267	411	289	325	410
NH_3	p.p.m. dry	11	10	6	ND	51	ND	ND	16

ND - Not determined

Table A.5.2.7 (b) Flue Gas Analyses

Test No.		2.9	2.10	2.11	2.12	2.13	2.14	2.15
Operating Conditions								
Ca/s Mol ratio		0.5	1.3	2.7	0	1.1	2.6	0.8
Fluidising Velocity	ft/s	3	3	3	3	3	3	3
Bed temperature	^{o}F	1470	1470	1470	1470	1470	1470	1470
Bed height	ft	2	2	2	2	2	2	2
Chromatograph								
Mean CO_2	Vol % dry	15.5	15.5	15.6	15.4	15.7	15.6	15.4
Mean O_2	Vol % dry	2.0	2.5	2.0	2.3	2.1	2.5	2.0
Mean CO	Vol % dry	0.12	0.11	0.06	0.08	0.1	0.09	0.16
Mean CH_4	Vol % dry	0	0	0	0	0	0	0
SO_2 By Iodine								
Sample 1	p.p.m. dry	2034	1793		2163	1187	340	
Sample 2	p.p.m. dry	2275	1753	452	2145	1200	298	563
Sample 3	p.p.m. dry	2063	1322	554	2055	1230	340	511
Sample 4	p.p.m. dry	2180	1514	422	2002	1220	311	519
Sample 5	p.p.m. dry		1483	443	2094	1210	320	597
Sample 6	p.p.m. dry		1596					
Mean SO_2								
By Iodine	p.p.m. dry	2138	1576	468	2091	1210	322	547
By H_2O_2	p.p.m. dry	1690	1045	237	2045	1024	354	544
Cl^-	p.p.m. dry	136	89	68	175	149	132	337
NH_3	p.p.m. dry	15	25	60	31	36	30	7

Table A.5.2.8 Mass Balance for Test No. 2.1

Rate lb/h	Total	'Ash'	'Carbon'	Nitrogen	'Oxygen'	Sulphur	Calcium
Coal	2.89	0.55	1.95	0	0.15	0.038	0.007
Acceptor	0	0	0	0	0	0	0
Total Air	30.59	0	0	23.5	7.09	0	0
Bleed Nitrogen	1.9	0	0	1.9	0	0	0
Total Input	35.38	0.55	1.95	25.4	7.24	0.038	0.007
Accumulated in Bed	0.15	0.15	0	0	0	0	0
Offtake Ash	1.65	1.65	0	0	0	0.008	0.023
Fines	0.19	0.14	0.05	0	0	0.002	0.004
Flue Gas	34.81	0	1.95	25.4	7.29	0.035	0
Total Output	36.79	1.94	2.00	25.4	7.29	0.045	0.027
Unaccounted, input-output	-1.41	-1.39	-0.05	0	-0.05	-0.007	-0.020
Unaccounted, % of input	-4.0	-252.7	-2.56	0	-0.69	-19.6	-290.5

Excess Air	14.7%
Carbon Loss	2.62% (Unburnt)
Sulphur Retention	7%
Ca/S Mole ratio	0

Table A.5.2.9. Mass Balance for Test No. 2.2

Rate lb/h	Total	'Ash'	'Carbon'	Nitrogen	'Oxygen'	Sulphur	Calcium
Coal	2.88	0.55	1.94	0	0.15	0.037	0.007
Acceptor	0.09	0.09	0	0	0	0	0.035
Total Air	30.59	0	0	23.5	7.09	0	0
Bleed Nitrogen	1.9	0	0	1.9	0	0	0
Total Input	35.46	0.64	1.94	25.4	7.24	0.037	0.042
Accumulated in Bed	-0.27	-0.27	0	0	0	0.012	0.028
Offtake Ash	1.46	1.46	0	0	0	0.009	0.026
Fines	0.21	0.16	0.05	0	0	0.003	0.009
Flue Gas	34.82	0	1.95	25.4	7.29	0.016	0
Total Output	36.22	1.35	2.00	25.4	7.29	0.040	0.063
Unaccounted, input-output	-0.76	-0.71	-0.06	0	-0.05	-0.003	-0.021
Unaccounted, % of input	-2.14	-110.9	-3.09	0	-0.69	-8.11	-50.0

Excess Air	14.7%
Carbon Loss	2.61% (Unburnt)
Sulphur Retention	58%
Ca/S Mole ratio	0.8

Table A.5.2.10 Mass Balance for Test No. 2.3

Rate lb/h	Total	'Ash'	'Carbon'	Nitrogen	'Oxygen'	Sulphur	Calcium
Coal	3.01	0.57	2.03	0	0.15	0.038	0.007
Acceptor	0.09	0.09	0	0	0	0	0.037
Total Air	30.59	0	0	23.5	7.09	0	0
Bleed Nitrogen	1.9	0	0	1.9	0	0	0
Total Input	35.59	0.66	2.03	25.4	7.24	0.038	0.044
Accumulated in Bed	-0.02	-0.02	0	0	0	0.012	0.022
Offtake Ash	0.34	0.34	0	0	0	0.003	0.008
Fines	0.34	0.21	0.14	0	0	0.004	0.008
Flue Gas	34.82	0	1.88	25.6	7.16	0.016	0
Total Output	35.48	0.53	2.02	25.6	7.16	0.035	0.038
Unaccounted, input-output	0.11	0.13	0.01	-0.2	0.08	0.003	0.006
Unaccounted, % of input	0.31	19.70	0.49	-0.79	1.1	7.5	13.4

Excess Air	11.1%
Carbon Loss	6.85% (Unburnt)
Sulphur Retention	56%
Ca/S Mole ratio	0.8

Table A.5.2.11 Mass Balance for Test No 2.4

Rate lb/h	Total	'Ash'	'Carbon'	Nitrogen	'Oxygen'	Sulphur	Calcium
Coal	4.99	0.95	3.37	0	0.25	0.062	0.012
Acceptor	0.16	0.16	0	0	0	0	0.061
Total Air	45.94	0	0	35.3	10.64	0	0
Bleed Nitrogen	1.9	0	0	1.9	0	0	0
Total Input	52.99	1.11	3.37	37.2	10.89	0.062	0.073
Accumulated in Bed	-0.16	-0.16	0	0	0	0.018	0.028
Offtake Ash	0.59	0.59	0	0	0	0.009	0.023
Fines	0.57	0.32	0.24	0	0	0.005	0.010
Flue Gas	51.22	0	2.82	37.3	10.84	0.029	0
Total Output	52.22	0.75	3.06	37.3	10.84	0.060	0.061
Unaccounted, input-output	0.77	0.36	0.31	-0.1	0.05	0.002	0.012
Unaccounted, % of input	1.45	32.4	9.20	-0.27	4.59	3.4	16.6

Excess Air	9.3%
Carbon Loss	7.9% (Unburnt)
Sulphur Retention	54%
Ca/S Mole ratio	0.8

Table A 5.2.12 Mass Balance for Test No 2.5

Rate lb/h	Total	'Ash'	'Carbon'	Nitrogen	'Oxygen'	Sulphur	Calcium
Coal	4.32	0.82	2.92	0	0.22	0.054	0.010
Acceptor	0.31	0.31	0	0	0	0	0.123
Total Air	45.94	0	0	35.3	10.64	0	0
Bleed Nitrogen	1.9	0	0	1.9	0	0	0
Total Input	52.47	1.13	2.92	37.2	10.86	0.054	0.133
Accumulated in Bed	0.11	0.11	0	0	0	0.027	0.076
Offtake Ash	0.79	0.79	0	0	0	0.015	0.039
Fines	0.54	0.31	0.22	0	0	0.006	0.022
Flue Gas	51.34	0	2.97	37.5	10.61	0.010	0
Total Output	52.78	1.21	3.19	37.5	10.61	0.058	0.137
Unaccounted, input-output	-0.31	-0.08	-0.27	-0.3	0.25	-0.004	-0.004
Unaccounted, % of input	-1.22	-7.08	-9.25	-0.81	2.30	-7.41	-3.01

Excess Air	5.6%
Carbon Loss	7.07% (Unburnt)
Sulphur Retention	82%
Ca/S Mole ratio	1.8

Table A.5.2.13. Mass Balance for Test No. 2.6

Rate lb/h	Total	'Ash'	'Carbon'	Nitrogen	'Oxygen'	Sulphur	Calcium
Coal	4.81	0.91	3.25	0	0.25	0.060	0.012
Acceptor	0.55	0.55	0	0	0	0	0.215
Total Air	45.94	0	0	35.3	10.64	0	0
Bleed Nitrogen	1.9	0	0	1.9	0	0	0
Total Input	53.20	1.46	3.25	37.2	10.89	0.060	0.227
Accumulated in Bed	-0.11	-0.11	0	0	0	0.006	0.040
Offtake Ash	0.87	0.87	0	0	0	0.023	0.071
Fines	0.50	0.33	0.17	0	0	0.007	0.038
Flue Gas	51.48	0	3.05	37.2	10.96	0.001	0
Total Output	52.74	1.09	3.22	37.2	10.96	0.037	0.149
Unaccounted, input-output	0.46	0.37	0.03	0	-0.07	0.023	0.078
Unaccounted, % of input	0.86	25.34	0.92	0	-0.64	38.33	34.36

Excess Air	6.5%
Carbon Loss	5.28% (Unburnt)
Sulphur Retention	98%
Ca/S Mole ratio	2.9

Table A 5.2.14 Mass Balance for Test No. 2.7

Rate lb/h	Total	'Ash'	'Carbon'	Nitrogen	'Oxygen'	Sulphur	Calcium
Coal	5.92	1.12	4.00	0	0.30	0.074	0.014
Acceptor	0.19	0.19	0	0	0	0	0.072
Total Air	45.94	0	0	35.3	10.64	0	0
Bleed Nitrogen	1.9	0	0	1.9	0	0	0
Total Input	53.95	1.31	4.00	37.2	10.94	0.074	0.086
Accumulated in Bed	0	0	0	0	0	0	-0.058
Offtake Ash	1.10	1.10	0	0	0	0.034	0.108
Fines	0.94	0.43	0.51	0	0	0.008	0.017
Flue Gas	51.85	0	3.28	37.3	10.92	0.029	0
Total Output	53.89	1.53	3.79	37.3	10.92	0.071	0.067
Unaccounted, input-output	0.06	-0.22	0.21	-0.1	0.02	0.003	0.019
Unaccounted, % of input	0.11	-16.79	5.25	-0.27	0.18	4.0	22.4

Excess Air	-10.9%
Carbon Loss	13.42% (Unburnt)
Sulphur Retention	61
Ca/S Mole ratio	0.8

Table A.5.2.15 Mass Balance for Test No 2.8

Rate lb/h	Total	'Ash'	'Carbon'	Nitrogen	'Oxygen'	Sulphur	Calcium
Coal	2.78	0.53	1.88	0	0.14	0.035	0.007
Acceptor	0.20	0.20	0	0	0	0	0.080
Total Air	30.59	0	0	23.5	7.09	0	0
Bleed Nitrogen	1.9	0	0	1.9	0	0	0
Total Input	35.47	0.73	1.88	25.4	7.23	0.035	0.087
Accumulated in Bed	0.13	0.13	0	0	0	0.029	0.078
Offtake Ash	0.50	0.49	0	0	0	0.003	0.010
Fines	0.31	0.20	0.10	0	0	0.004	0.013
Flue Gas	34.85	0	1.99	25.5	7.20	0.005	0
Total Output	35.79	0.82	2.09	25.5	7.20	0.041	0.101
Unaccounted, input-output	-0.32	-0.09	-0.21	-0.1	0.03	-0.006	-0.014
Unaccounted, % of input	-0.90	-12.3	-11.17	-0.39	0.41	-17.14	-16.09

Excess Air	9.5%
Carbon Loss	5.12% (Unburnt)
Sulphur Retention	86%
Ca/S Mole ratio	1.8

Table A.5.2.16 Mass Balance for Test No. 2.9

Rate lb/h	Total	'Ash'	'Carbon'	Nitrogen	'Oxygen'	Sulphur	Calcium
Coal	4.93	0.83	3.36	0	0.26	0.121	0.013
Acceptor	0.21	0.21	0	0	0	0	0.082
Total Air	45.94	0	0	35.3	10.64	0	0
Bleed Nitrogen	1.9	0	0	1.9	0	0	0
Total Input	52.98	1.04	3.36	37.2	10.90	0.121	0.095
Accumulated in Bed	-0.02	-0.02	0	0	0	0.022	0.050
Offtake Ash	0.30	0.30	0	0	0	0.002	0.006
Fines	0.97	0.60	0.37	0	0	0.009	0.017
Flue Gas	51.54	0	3.01	37.3	10.88	0.102	0
Total Output	52.79	0.88	3.38	37.3	10.88	0.136	0.073
Unaccounted, input-output	0.19	0.16	-0.02	-0.1	0.02	-0.015	0.022
Unaccounted, % of input	0.36	15.38	-0.60	-0.27	0.18	-12.2	23.2

Excess Air	0.2%	
Carbon Loss	10.87%	(Unburnt)
Sulphur Retention	15%	
Ca/S Mol ratio	0.5	

Table A.5.2.17 Mass Balance for Test No. 2.10

Rate lb/h	Total	'Ash'	'Carbon'	Nitrogen	'Oxygen'	Sulphur	Calcium
Coal	4.59	0.77	3.13	0	0.24	0.112	0.012
Acceptor	0.47	0.47	0	0	0	0	0.184
Total Air	45.94	0	0	35.3	10.64	0	0
Bleed Nitrogen	1.9	0	0	1.9	0	0	0
Total Input	52.90	1.24	3.13	37.2	10.88	0.112	0.197
Accumulated in Bed	-0.34	-0.34	0	0	0	0.036	0.134
Offtake Ash	0.58	0.58	0	0	0	0.010	0.028
Fines	0.9	0.58	0.31	0	0	0.009	0.028
Flue Gas	51.56	0	3.02	37.2	11.03	0.078	0
Total Output	52.70	0.82	3.33	37.2	11.03	0.133	0.189
Unaccounted, input-output	0.20	0.42	-0.20	0	-0.15	-0.021	0.008
Unaccounted, % of input	0.38	33.87	-6.39	0	-1.38	-18.7	4.0

Excess Air	4.1%	
Carbon Loss	9.43%	(Unburnt)
Sulphur Retention	30%	
Ca/S Mol ratio	1.3	

Table A 5.2.18 Mass Balance for Test No. 2.11

Rate lb/h	Total	'Ash'	'Carbon'	Nitrogen	'Oxygen'	Sulphur	Calcium
Coal	4.42	0.74	3.02	0	0.23	0.106	0.012
Acceptor	0.9	0.90	0	0	0	0	0.352
Total Air	45.94	0	0	35.3	10.64	0	0
Bleed Nitrogen	1.9	0	0	1.9	0	0	0
Total Input	53.16	1.64	3.02	37.2	10.87	0.106	0.364
Accumulated in Bed	-0.04	-0.04	0	0	0	0.050	0.226
Offtake Ash	0.86	0.86	0	0	0	0.029	0.088
Fines	0.95	0.60	0.35	0	0	0.013	0.047
Flue Gas	51.50	0	3.03	37.4	10.75	0.023	0
Total Output	53.27	1.42	3.38	37.4	10.75	0.104	0.362
Unaccounted, input-output	-0.11	0.22	-0.36	-0.2	0.12	0.002	0.002
Unaccounted, % of input	-0.21	13.41	-11.92	-0.54	1.10	1.9	0.7

Excess Air	0.8%	
Carbon Loss	10.39%	(Unburnt)
Sulphur Retention	79%	
Ca/S Mole ratio	2.7	

Table A.5.2.19 Mass Balance for Test No 2.12

Rate lb/h	Total	'Ash'	'Carbon'	Nitrogen	'Oxygen'	Sulphur	Calcium
Coal	4.66	0.78	3.18	0	0.25	0.114	0.013
Acceptor	0	0	0	0	0	0	0
Total Air	45.94	0	0	35.3	10.64	0	0
Bleed Nitrogen	1.9	0	0	1.9	0	0	0
Total Input	52.51	0.78	3.18	37.2	10.89	0.114	0.013
Accumulated in Bed	-0.07	-0.07	0	0	0	0.010	0.007
Offtake Ash	0.39	0.39	0	0	0	0.005	0.014
Fines	0.82	0.49	0.34	0	0	0.007	0.007
Flue Gas	51.49	0	2.99	37.3	10.89	0.101	0
Total Output	52.63	0.81	3.33	37.3	10.89	0.123	0.028
Unaccounted, input-output	-0.12	-0.03	-0.15	-0.1	0	-0.009	-0.015
Unaccounted, % of input	-0.23	-3.85	-4.72	-0.27	0	-7.6	-127.5

Excess Air	2.6%
Carbon Loss	10.10% (Unburnt)
Sulphur Retention	12%
Ca/S Mole ratio	0

Table A.5.2.20 Mass Balance for Test No. 2.13

Rate lb/h	Total	'Ash'	'Carbon'	Nitrogen	'Oxygen'	Sulphur	Calcium
Coal	4.69	0.79	3.20	0	0.25	0.115	0.013
Acceptor	0.40	0.40	0	0	0	0	0.158
Total Air	45.94	0	0	35.3	10.64	0	0
Bleed Nitrogen	1.9	0	0	1.9	0	0	0
Total Input	52.93	1.19	3.20	37.2	10.89	0.115	0.170
Accumulated in Bed	0.06	0.06	0	0	0	0.046	0.134
Offtake Ash	0.56	0.56	0	0	0	0.011	0.026
Fines	0.91	0.56	0.35	0	0	0.009	0.037
Flue Gas	51.54	0	3.05	37.2	10.96	0.058	0
Total Output	53.07	1.18	3.40	37.2	10.96	0.124	0.197
Unaccounted, input-output	-0.14	0.01	-0.20	0	-0.07	-0.009	-0.027
Unaccounted, % of input	-0.26	0.84	-6.25	0	-0.64	-8.2	-15.4

Excess Air	1.2%
Carbon Loss	10.28% (Unburnt)
Sulphur Retention	49%
Ca/S Mole ratio	1.1

Table A.5.2.21 Mass Balance for Test No. 2.14

Rate lb/h	Total	'Ash'	'Carbon'	Nitrogen	'Oxygen'	Sulphur	Calcium
Coal	4.42	0.74	3.01	0	0.23	0.108	0.012
Acceptor	0.90	0.90	0	0	0	0	0.353
Total Air	45.94	0	0	35.3	10.64	0	0
Bleed Nitrogen	1.9	0	0	1.9	0	0	0
Total Input	53.16	1.64	3.01	37.2	10.87	0.108	0.365
Accumulated in Bed	-0.27	-0.27	0	0	0	0.037	0.164
Offtake Ash	0.96	0.96	0	0	0	0.048	0.140
Fines	0.94	0.63	0.31	0	0	0.013	0.061
Flue Gas	51.56	0	3.03	37.2	11.02	0.015	0
Total Output	53.19	1.32	3.34	37.2	11.02	0.113	0.366
Unaccounted, input-output	-0.03	0.32	-0.33	0	-0.15	−0.005	-0.001
Unaccounted, % of input	-0.06	19.5	-10.96	0	-1.38	-4.4	-0.2

Excess Air	4.3%
Carbon Loss	9.23% (Unburnt)
Sulphur Retention	86%
Ca/S Mole ratio	2.6

Table A.5.2.22 Mass Balance for Test No. 2.15

Rate lb/h	Total	'Ash'	'Carbon'	Nitrogen	'Oxygen'	Sulphur	Calcium
Coal	4.96	0.94	3.35	0	0.25	0.062	0.011
Acceptor	0.16	0.16	0	0	0	0	0.061
Total Air	45.94	0	0	35.3	10.64	0	0
Bleed Nitrogen	1.9	0	0	1.9	0	0	0
Total Input	52.96	1.10	3.35	37.2	10.89	0.062	0.073
Accumulated in Bed	0.26	0.26	0	0	0	-0.004	-0.015
Offtake Ash	0	0	0	0	0	0	0
Fines	1.71	1.43	0.28	0	0	0.033	0.075
Flue Gas	51.43	0	3.00	37.4	10.76	0.029	0
Total Output	53.40	1.69	3.28	37.4	10.76	0.058	0.061
Unaccounted, input-output	-0.44	-0.59	0.07	-0.2	0.13	0.004	0.012
Unaccounted, % of input	-0.83	-53.64	2.09	-0.54	1.19	6.9	16.5

Excess Air	2.2%
Carbon Loss	8.65% (Unburnt)
Sulphur Retention	54%
Ca/S Mole ratio	0.8

Table A.5.2.23 SO_2 concentrations and % reductions

Test No.	2.1	2.2	2.3	2.4	2.5	2.6	2.7	2.8
Coal Type	Welbeck	Welbeck	Welbeck	Welbeck	Welbeck	Welbeck	Welbeck	Welbeck
Fluidising Velocity, ft/s	2	2	2	3	3	3	3	2
Bed Temperature, °F	1470	1470	1470	1470	1470	1470	1470	1470
Ca/S mol ratio	0	0.8	0.8	0.8	1.8	2.9	0.8	1.8
SO_2 concentration, p.p.m.	1087	488	513	599	207	33	612	158
SO_2 reduction, %	0	55	52	45	81	97	48	85

Test No.	2.9	2.10	2.11	2.12	2.13	2.14	2.15
Coal Type	Park Hill	Park Hill	Park Hill	Park Hill	Park Hill	Park Hill	Welbeck
Fluidising Velocity, ft/s	3	3	3	3	3	3	3
Bed Temperature, °F	1470	1470	1470	1470	1470	1470	1470
Ca/S mol ratio	0.5	1.3	2.7	0	1.1	2.6	0.8
SO_2 concentration, p.p.m.	(1690)	(1045)	(237)	2091	1210	322	547
SO_2 reduction, %	19	50	89	0	42	84	50

(   ) Hydrogen peroxide results.

SO_2 reductions for Welbeck runs (except 2.7) are based on a datum level of 1087 p.p.m.

SO_2 reduction for Park Hill runs are based on a datum level of 2090 p.p.m.

SO_2 reduction for Test 2.7 based on calculated datum level of 1190 p.p.m.

Table A 5.3.1 Operating Conditions During Test Series 3

Constant Parameters:

Coal : Illinois (ex A.N.L.)
Coal Size : - 1680 micron
Acceptor : U.S. Limestone 1359
Fluidising Velocity : 3 ft/s
Recycle : None

Test No.	3.1	3.2	3.3	3.4	3.5	3.6
Date	6.8.70	7.8.70	25.8.70	26.8.70	27.8.70	28.8.70
Acceptor Size μm	-1680	-1680	-1680	-1680	-125	-125
Ca/S mole ratio	1.1	2.2	1.1	2.1	1.1	3.6
Bed temp °F	1290	1290	1470	1470	1470	1470
Bed height ft	2	2	3	3	2	2
Ash bed	Fresh	ex 3.1	Fresh	ex 3.3	Fresh	ex 3.5

Table A.5.3.2 Chemical analyses of coal

Test Series 3

Test Number		3.1-3.6
Proximate analysis		
Total moisture	% a.r.	9.8
Ash	% a.r.	11.8
Volatile matter	% d.a.f.	46.6
Ultimate analysis		
Carbon	% d.b.	67.8
Hydrogen	% d.b.	4.45
Nitrogen	% d.b.	1.29
Sulphur	% d.b.	4.38
Oxygen + errors	% d.b.	8.5
Chlorine	% d.b.	0.22
Carbon Dioxide	% d.b.	1.05
Ash analysis		
CaO	% d.b.	10.1
MgO	% d.b.	1.0
Na_2O	% d.b.	1.7
K_2O	% d.b.	1.8
Al_2O_3	% d.b.	12.2
Fe_2O_3	% d.b.	20.6
SiO_2	% d.b.	40.8
Calorific value (gross)	Btu/lb	14,290
Swelling No.		4½
Gray King coke type		D

Table A.5.3.3 Chemical and Size Analyses of Acceptor Test Series 3

Test No.	3.1 - 3.4		3.5 & 3.6
Chemical Analysis			
CaO a.r.	55.5		55.5
MgO a.r.	0.3		0.3
CO_2 a.r.	43.3		43.3
S_iO_2 a.r.	0.8		0.8
Size Analysis	% in grade by weight		
Particle size (µm)		Particle Size(µm)	
+ 1680	0.1	+ 125	8.8
+ 500 - 1680	36.7	+ 90 - 125	9.3
+ 250 - 500	24.8	+ 75 - 90	19.8
+ 125 - 250	16.6	+ 63 - 75	11.8
+ 63 - 125	8.7	+ 45 - 63	30.3
- 63	13.1	- 45	20.0
Median diam. (µm)	353		62

Table A.5.3.4 Chemical and Size Analyses of Feed Blends

Test Series 3

Test No.	3.1	3.2	3.3	3.4	3.5	3.6
Moisture a.r.	5.8	7.1	-	8.1	7.5	5.6
Ash a.r.	19.0	22.7	-	22.3	17.4	27.3
Carbon d.b.	56.4	49.8	-	49.7	58.6	43.9
CaO d.b.	9.09	13.86	-	14.85	7.71	18.25
Sulphur d.b.	3.85	3.30	-	3.40	3.80	2.90
CO_2 d.b.	7.01	11.42	-	12.05	5.96	14.15
Particle size (μm)	% in grade by weight					
+ 1680	1.0	0.5	-	0.8	0.8	0.9
+ 500 - 1680	50.5	50.0	-	54.9	49.7	48.2
+ 250 - 500	22.3	21.4	-	19.1	17.6	18.9
+ 125 - 250	13.6	12.6	-	12.9	9.1	14.7
+ 63 - 125	6.0	7.0	-	5.7	8.4	7.3
- 63	6.6	8.5	-	6.6	14.4	10.0
Median dia. (μm)	519	506		582	508	487

NOTE Test 3.3 Feed Blend sample not taken - operator error.

Table A.5.3.5 Chemical and Size Analyses of Cyclone Fines

Test Series 3

Test No.	3.1	3.2	3.3	3.4	3.5	3.6
Chemical Analysis						
Carbon % a.r.	28.8	23.6	29.0	24.1	16.8	13.3
Sulphur % a.r.	2.05	2.58	2.82	2.84	4.15	3.67
CO_2 % a.r.	5.05	8.21	1.99	4.70	9.41	13.0
CaO % a.r.	10.20	15.6	9.06	13.62	22.38	26.9
Size Analysis	% in grade by weight					
Particle size (μm)						
+ 500	0.1	0	0.2	0	0	0
+ 250 - 500	0.3	0.2	0.2	0	0	0.2
+ 125 - 250	1.0	0.4	2.0	0.4	0.9	0.5
+ 63 - 125	10.7	8.4	16.0	8.4	7.2	5.3
- 63	87.9	91.0	81.6	91.2	91.9	94.0

Table A.5.3.6 (a) Chemical and Size Analyses of Bed Material

Test Series 3

Test No.	3.1			3.2			3.3		
Sample	Initial	Final	Offtake	Initial	Final	Offtake	Initial	Final	Offtake
Chemical Analysis									
Sulphur % a.r.	1.6	2.05	2.05	1.9	1.9	2.5	1.6	3.1	1.75
CO_2 % a.r.	0.33	9.31	2.22	6.95	20.23	13.59	0.35	2.74	0.9
CaO % a.r.	6.15	18.2	9.65	14.41	29.6	23.39	6.1	13.43	7.12
Size Analysis	% in grade by weight								
Particle size (µm)									
+ 1680	0	0.1	0.1	0.1	0	0.1	0	0	0
+ 500 - 1680	41.6	43.5	34.1	41.2	44.5	34.3	50.6	47.0	46.4
+ 250 - 500	41.1	39.0	37.9	40.3	37.6	31.0	37.0	38.1	40.0
+ 125 - 250	14.1	14.4	18.5	15.3	15.0	22.3	10.2	11.9	11.5
+ 63 - 125	2.1	2.8	7.7	2.7	2.8	11.3	1.3	2.7	1.6
- 63	0.1	0.2	1.7	0.4	0.1	1.0	0.9	0.3	0.5
Median diam. (µm)	443	454	387	440	459	356	505	478	474

Table A.5.3.6 (b) Chemical and Size Analyses of Bed Material

Test Series 3 (cont'd)

Test No.	3.4			3.5			3.6		
Sample	Initial	Final	Offtake	Initial	Final	Offtake	Initial	Final	Offtake
Chemical Analysis									
Sulphur % a.r.	2.15	4.45	1.85	1.55	3.5	1.55	3.25	5.0	5.7
CO_2 % a.r.	1.46	5.15	1.0	0.17	0.89	0.36	0.83	2.83	3.02
CaO % a.r.	8.67	23.5	7.26	5.46	10.35	5.46	10.09	29.0	22.82
Size Analysis	% in grade by weight								
Particle size (μm)									
+ 1680	0	0	0	0	0	0	0	0	0
+ 500 - 1680	45.0	46.9	54.0	54.8	51.0	59.2	54.5	48.8	34.4
+ 250 - 500	37.8	36.9	34.1	33.6	32.2	32.3	31.5	34.2	26.8
+ 125 - 250	12.1	12.7	9.6	7.3	9.6	6.7	8.4	10.5	12.9
+ 63 - 125	4.0	3.2	1.8	2.1	6.7	1.2	5.0	6.0	22.3
- 63	1.1	0.3	0.5	2.2	0.5	0.6	0.6	0.5	3.6
Median diam. (μm)	463	476	534	541	509	583	541	490	356

Table A.5.3.7 Flue Gas Analyses

Test No.	3.1	3.2	3.3	3.4	3.5	3.6
Operating Conditions						
Ca/S mol ratio	1.1	2.2	1.1	2.1	1.1	3.6
Fluidising Velocity, ft/s	3	3	3	3	3	3
Bed Temperature, ^{o}F	1290	1290	1470	1470	1470	1470
Bed Height, ft	2	2	3	3	2	2
Chromatograph						
Mean CO_2 Vol % Dry	15.3	15.2	15.4	15.6	15.5	16.0
Mean O_2 Vol % Dry	2.7	2.4	2.7	2.6	2.4	2.5
Mean CO Vol % Dry	0.11	0.12	0.03	0.05	0.07	0.05
Mean CH_4 Vol % Dry	0	0	0	0	0	0
SO_2 by Iodine						
Sample 1. p.p.m. Dry	3438	3126	1693	1082	1418	236
Sample 2. p.p.m. Dry	3409	3121	1853	1117	1328	258
Sample 3. p.p.m. Dry	3326	3379	2041	1120	1362	296
Sample 4. p.p.m. Dry	3375	3347	1984	1160	1527	321
Sample 5. p.p.m. Dry	3335	3337	2004	1190	1708	281
Sample 6. p.p.m. Dry		3162	2007	1146	1689	
Sample 7. p.p.m. Dry					1630	
Mean SO_2						
By Iodine p.p.m. Dry	3376	3245	1930	1136	1523	278
By H_2O_2 p.p.m. Dry	3587	3130	1980	1228	1502	298
Cl^- p.p.m. Dry	141	161	126	125	139	97
NH_3 p.p.m. Dry	34	23	12	11	21	9

Table A.5.3.8 Mass Balance for Test No 3.1

Rate lb/h	Total	'Ash'	'Carbon'	Nitrogen	'Oxygen'	Sulphur	Calcium
Coal	5.11	0.67	3.46	0	0.43	0.224	0.048
Acceptor	0.77	0.77	0	0	0	0	0.304
Total Air	45.94	0	0	35.3	10.64	0	0
Bleed Nitrogen	1.9	0	0	1.9	0	0	0
Total Input	53.72	1.44	3.46	37.2	11.07	0.224	0.352
Accumulated in Bed	-0.23	-0.23	0	0	0	0.013	0.252
Offtake Ash	0.77	0.77	0	0	0	0.016	0.053
Fines	0.83	0.60	0.23	0	0	0.017	0.059
Flue Gas	51.87	0	2.97	37.1	11.36	0.170	0
Total Output	53.24	1.14	3.20	37.1	11.36	0.216	0.364
Unaccounted, input-output	0.48	0.30	0.26	0.1	-0.29	0.008	-0.012
Unaccounted, % of input	0.89	20.83	7.51	0.27	-2.62	3.7	-3.5

Excess Air	7.2%
Carbon Loss	7.29% (Unburnt)
Sulphur Retention	24%
Ca/S Mole ratio	1.1

Table A.5.3.9. Mass Balance for Test No. 3.2

Rate lb/h	Total	'Ash'	'Carbon'	Nitrogen	'Oxygen'	Sulphur	Calcium
Coal	5.05	0.66	3.42	0	0.43	0.221	0.047
Acceptor	1.52	1.52	0	0	0	0	0.602
Total Air	45.94	0	0	35.3	10.64	0	0
Bleed Nitrogen	1.9	0	0	1.9	0	0	0
Total Input	54.41	2.18	3.42	37.2	11.07	0.221	0.649
Accumulated in Bed	-0.13	-0.13	0	0	0	0	0.327
Offtake Ash	1.39	1.39	0	0	0	0.035	0.232
Fines	0.90	0.69	0.21	0	0	0.022	0.097
Flue Gas	51.85	0	2.96	37.3	11.13	0.164	0
Total Output	54.01	1.95	3.17	37.3	11.13	0.221	0.656
Unaccounted, input-output	0.40	0.23	0.25	-0.1	-0.06	0	-0.007
Unaccounted, % of input	0.74	10.55	7.31	-0.27	-0.54	0	-1.1

Excess Air	6.5%
Carbon Loss	6.51% (Unburnt)
Sulphur Retention	26%
Ca/S Mole ratio	2.2%

Table A 5.3.10 Mass Balance for Test No. 3.3

Rate lb/h	Total	'Ash'	'Carbon'	Nitrogen	'Oxygen'	Sulphur	Calcium
Coal	4.37	0.57	2.97	0	0.37	0.192	0.041
Acceptor	0.66	0.66	0	0	0	0	0.260
Total Air	45.94	0	0	35.3	10.64	0	0
Bleed Nitrogen	1.9	0	0	1.9	0	0	0
Total Input	52.87	1.23	2.97	37.2	11.01	0.192	0.301
Accumulated in Bed	0.03	0.03	0	0	0	0.065	0.230
Offtake Ash	0.58	0.58	0	0	0	0.010	0.030
Fines	0.55	0.40	0.16	0	0	0.015	0.035
Flue Gas	51.79	0	2.99	37.3	11.13	0.097	0
Total Output	52.95	1.01	3.15	37.3	11.13	0.188	0.295
Unaccounted, input-output	-0.08	0.22	-0.18	-0.1	-0.12	0.004	0.006
Unaccounted, % of input	-0.15	17.89	-6.06	-0.27	-1.09	2.1	2.0

Excess Air	9.9%
Carbon Loss	4.99% (Unburnt)
Sulphur Retention	49%
Ca/S Mole ratio	1.1

Table A.5.3.11 Mass Balance for Test No. 3.4

Rate lb/h	Total	'Ash'	'Carbon'	Nitrogen	'Oxygen'	Sulphur	Calcium
Coal	4.40	0.58	2.99	0	0.37	0.193	0.041
Acceptor	1.29	1.29	0	0	0	0	0.509
Total Air	45.94	0	0	35.3	10.64	0	0
Bleed Nitrogen	1.9	0	0	1.9	0	0	0
Total input	53.53	1.87	2.99	37.2	11.01	0.193	0.550
Accumulated in Bed	0.01	0.01	0	0	0	0.100	0.461
Offtake Ash	1.02	1.02	0	0	0	0.019	0.053
Fines	0.67	0.51	0.16	0	0	0.018	0.063
Flue Gas	51.80	0	3.03	37.2	11.19	0.057	0
Total output	53.50	1.54	3.19	37.2	11.19	0.195	0.577
Unaccounted, input-output	0.03	0.33	-0.20	0	-0.18	-0.002	-0.027
Unaccounted, % of input	0.06	17.65	-6.69	0	-1.63	-1.0	-4.7

Excess Air	9.2%
Carbon Loss	4.9% (Unburnt)
Sulphur Petention	70%
Ca/S Mole ratio	2.1

Table A.5 3.12 Mass Balance for Test No 3.5

Rate lb/h	Total	'Ash'	'Carbon'	Nitrogen	'Oxygen'	Sulphur	Calcium
Coal	4.42	0.58	3.00	0	0.38	0.194	0.042
Acceptor	0.66	0.66	0	0	0	0	0.263
Total Air	45.94	0	0	35.3	10.64	0	0
Bleed Nitrogen	1.9	0	0	1.9	0	0	0
Total Input	52.92	1.24	3.00	37.2	11.02	0.194	0.305
Accumulated in Bed	-0.36	-0.36	0	0	0	0.059	0.105
Offtake Ash	0.55	0.55	0	0	0	0.009	0.021
Fines	0.76	0.64	0.13	0	0	0.031	0.120
Flue Gas	51.75	0	3.02	37.3	11.05	0.076	0
Total Output	52.70	0.83	3.15	37.3	11.05	0.175	0.247
Unaccounted, input-output	0.22	0.41	-0.15	-0.1	-0.03	0.019	0.058
Unaccounted, % of input	0.42	33.06	5.0	-0.27	-0.27	9.9	18.8

Excess Air	9.0%
Carbon Loss	4.07% (Unburnt)
Sulphur Retention	61%
Cal/S Mole ratio	1.1

Table A.5.3.13 Mass Balance for Test No. 36

Rate lb/h	Total	'Ash'	'Carbon'	Nitrogen	'Oxygen'	Sulphur	Calcium
Coal	3.98	0.52	2.69	0	0.34	0.174	0.037
Acceptor	1.97	1.97	0	0	0	0	0.781
Total Air	45.94	0	0	35.3	10.64	0	0
Bleed Nitrogen	1.9	0	0	1.9	0	0	0
Total Input	53.79	2.49	2.69	37.2	10.98	0.174	0.818
Accumulated in Bed	0.06	0.06	0	0	0	0.058	0.449
Offtake Ash	1.27	1.27	0	0	0	0.073	0.208
Fines	0.88	0.77	0.11	0	0	0.032	0.166
Flue Gas	51.88	0	3.12	37.2	11.20	0.014	0
Total Output	54.09	2.10	3.23	37.2	11.20	0.176	0.822
Unaccounted, input-output	-0.03	0.39	-0.54	0	-0.22	-0.002	-0.004
Unaccounted, % of input	-0.06	15.66	-20.07	0	-2.00	-1.1	-0.5

Excess Air	9.8%
Carbon Loss	3.59% (Unburnt)
Sulphur Retention	92%
Ca/S Mole ratio	3.6

Table A.5.3.14 SO_2 concentrations and % reductions

Test No.	3.1	3.2	3.3	3.4	3.5	3.6
Fluidising Velocity, ft/s	3	3	3	3	3	3
Bed Temperature, ^{o}F	1290	1290	1470	1470	1470	1470
Bed height, ft	2	2	3	3	2	2
Acceptor Size, µm	-1680	-1680	-1680	-1680	-125	-125
Ca/S mol ratio	1.1	2.2	1.1	2.1	1.1	3.6
SO_2 concentration, p.p.m.	3376	3245	1930	1136	1523	278
SO_2 reduction, %	15	18	51	72	61	93

SO_2 reductions are based on a datum level of 3960 p.p.m.

Table A.5.4.1 Operating Conditions During Test Series 4

Constant Parameters:

Coal : Pittsburgh
Coal Size : -1680 micron
Acceptor Size : -1680 micron
Fluidising Velocity : 3 ft/s
Bed Temperature : 1470°F
Bed Height : 2 ft
Recycle : None

Test No.	4.1	4.2	4.3	4.4	4.5	4.6	4.7	4.8	4.9
Date	5.10.70	6.10.70	7.10.70	8.10.70	13.10.70	14.10.70	15.10.70	16.10.70	21.10.70
Acceptor	None	U.K. Lst	U.K. Lst	U.K. Lst	U.S. Lst 18	U.S. Lst 18	U.S. Lst 18	U.S. Lst 18	U.S. Lst 18
Ca/S mole ratio	0	1.0	2.1	3.1	0.9	1.7	2.6	0.9	0.9
Ash bed	Fresh	ex 4.1	ex 4.2	ex 4.3	Fresh	ex 4.5	ex 4.6	ex 4.7*	Newdigate shale

* Run 4.8 : Lime-rich ash bed ex run 4.7 used to provide comparison with run 4.5.

Table A.5.4.2 Chemical analyses of coal

Test Series 4

Test Number		4.1-4.9
Proximate analysis		
Total moisture	% a.r.	1.4
Ash	% a.r.	12.7
Volatile matter	% d.a.f.	41.8
Ultimate analysis		
Carbon	% d.b.	72.9
Hydrogen	% d.b.	4.55
Nitrogen	% d.b.	1.43
Sulphur	% d.b.	2.75
Oxygen + errors	% d.b.	4.3
Chlorine	% d.b.	0.11
Carbon Dioxide	% d.b.	0.64
Ash analysis		
CaO	% d.b.	7.6
MgO	% d.b.	1.3
Na_2O	% d.b.	0.7
K_2O	% d.b.	1.6
Al_2O_3	% d.b.	18.3
Fe_2O_3	% d.b.	17.3
SiO_2	% d.b.	45.8
Calorific value (gross)	Btu/lb	15,320
Swelling No.		8
Gray King coke type		G7

Table A.5.4.3 Chemical and Size Analyses of Acceptor Test Series 4

Test No.	4.1-4.4	4.5-4.9
Chemical Analysis		
CaO a.r.	54.9	45.9
MgO a.r.	0.2	0.9
CO_2 a.r.	42.0	34.7
SiO_2 a.r.	1.6	14.7
Size Analysis	% in grade by weight	
Particle size (μm)		
+ 1680	0.5	0.1
+ 500 - 1680	52.1	21.0
+ 250 - 500	19.1	22.0
+ 125 - 250	10.1	22.5
+ 63 - 125	7.2	12.2
- 63	11.0	22.2
Median diam. (μm)	537	207

Table A.5.4.4 Chemical and Size Analyses of Feed Blends

Test Series 4

Test No.		4.1	4.2	4.3	4.4	4.5	4.6	4.7	4.8	4.9
Moisture	a.r.	1.3	0.9	0.9	1.0	1.2	1.1	1.2	1.1	1.1
Ash	a.r.	12.4	17.3	18.3	23.5	18.0	22.5	25.9	17.3	17.1
Carbon	d.b.	72.9	65.4	62.3	54.7	65.2	59.3	54.0	65.9	66.6
CaO	d.b.	0.90	5.45	9.25	13.44	4.61	7.96	11.08	4.61	4.76
Sulphur	d.b.	2.75	2.45	2.40	2.20	2.60	2.35	2.05	2.50	2.45
CO_2	d.b.	0.6	4.28	7.08	10.41	3.7	5.80	8.75	3.55	3.0
Particle size (μm)		% in grade by weight								
+ 1680		0	0	0.1	0.2	0.7	0.2	0.1	0.2	0.1
+ 500 - 1680		36.6	47.3	43.2	46.6	45.2	45.7	43.2	65.2	50.3
+ 250 - 500		23.5	21.9	22.6	20.0	19.7	21.0	20.3	16.1	20.1
+ 125 - 250		17.0	12.8	14.3	13.0	14.2	14.4	13.2	7.3	11.7
+ 63 - 125		12.8	8.5	8.9	8.5	9.5	8.8	9.8	4.7	7.8
- 63		10.1	9.5	10.9	11.7	10.7	9.9	13.4	6.5	10.0
Median dia. (μm)		340	46[illegible]	420	457	444	447	412	752	505

Table A.5.4.5 (a) Chemical and Size Analyses of Cyclone Fines

Test Series 4

Test No.	4.1	4.2	4.3	4.4	4.5	4.6
Chemical Analysis						
Carbon % a.r.	40.95	40.60	47.9	36.6	40.4	39.0
Sulphur % a.r.	1.45	1.80	2.01	1.95	1.91	1.96
CO_2 % a.r.	0.64	2.59	4.20	6.85	3.09	5.87
CaO % a.r.	3.77	7.05	8.62	14.1	7.79	10.25
Size Analysis	% in grade by weight					
Particle Size (μm)						
+ 500	0	0	0	0	0	0.1
+ 250 - 500	0.1	0	0	0	0	0.1
+ 125 - 250	0.6	1.1	0.2	0.4	0.9	1.0
+ 63 - 125	16.4	12.9	10.1	9.7	13.4	11.0
- 63	82.9	86.0	89.7	89.9	85.7	87.8

Table A.5.4.5 (b) Chemical and Size Analyses of Cyclone Fines

Test Series 4 (Cont'd)

Test No.	4.7	4.8	4.9
Chemical Analysis			
Carbon % a.r.	33.3	40.5	43.4
Sulphur % a.r.	1.88	2.11	2.11
CO_2 % a.r.	9.68	4.67	2.57
CaO % a.r.	16.2	9.78	7.6
Size Analysis	% in grade by weight		
Particle size (μm)			
+ 500	0.1	0	0
+ 250 - 500	0.5	0	0.1
+ 125 - 250	0.3	0.1	0.7
+ 63 - 125	6.7	9.8	14.5
- 63	92.4	90.1	84.7

Table A.5.4.6(a) Chemical and Size Analysis of Bed Material

Test Series 4

Test No.	4.1			4.2			4.3			4.4		
Sample	Initial	Final	Offtake	Initial	Final	Offtake	Initial	Final	Offtake	Initial	Final	Offtake
Chemical Analysis												
Sulphur % a.r.	0.75	1.0	1.0	1.2	2.45	1.55	2.55	3.75	2.85	3.45	4.8	4.5
CO_2 % a.r.	0.26	0.31	0.45	0.39	2.53	0.41	2.13	6.9	2.62	5.82	8.08	9.3
CaO % a.r.	3.64	3.64	3.64	5.45	10.62	5.17	10.22	20.35	12.10	18.95	29.81	24.4
Size Analysis	% in grade by weight											
Particle size (μm)												
+ 1680	0	0.1	0.1	0	0	0	0.1	0.1	0	0	0.1	0.1
+ 500 - 1680	57.4	62.9	56.2	59.1	53.4	59.9	54.5	54.9	50.8	57.2	54.2	60.9
+ 250 - 500	32.6	29.6	31.9	30.0	32.3	30.3	33.6	28.5	32.5	29.2	29.9	24.9
+ 125 - 250	7.5	6.2	8.4	7.3	10.1	6.4	8.9	11.2	9.9	9.7	11.6	7.2
+ 63 - 125	1.5	1.1	2.6	2.4	3.8	2.5	2.5	4.8	5.7	3.5	3.9	5.2
- 63	1.0	0.1	0.8	1.2	0.4	0.9	0.4	0.5	1.1	0.4	0.3	1.7
Median dia. (μm)	566	628	557	588	530	595	539	550	507	571	541	626

Table A.5.4.6(b) Chemical and Size Analyses of Bed Material

Test Series 4 (cont'd)

Test No.	4.5			4.6			4.7			4.8		
Sample	Initial	Final	Offtake	Initial	Final	Offtake	Initial	Final	Offtake	Initial	Final	Offtake
Chemical Analysis												
Sulphur % a.r.	2.0	3.5	2.05	2.85	4.25	4.35	2.95	5.10	5.45	5.3	5.4	5.1
CO_2 % a.r.	0.48	1.23	0.66	1.05	2.61	2.46	3.03	3.96	5.38	4.01	4.92	3.87
CaO % a.r.	7.0	11.51	7.29	10.65	16.12	14.45	11.09	21.75	21.41	21.0	20.7	20.9
Size Analysis	% in grade by weight											
Particle size (μm)												
+ 1680	0.3	0	0.1	0	0	0.1	0.1	0	0	0	0	0
+ 500 - 1680	62.9	57.1	71.5	68.5	48.3	47.4	51.1	52.4	30.1	63.9	51.8	36.3
+ 250 - 500	26.9	30.1	21.7	26.0	33.7	27.7	34.2	30.0	25.3	27.3	30.7	33.3
+ 125 - 250	5.7	9.0	3.6	4.5	13.1	12.4	8.6	13.7	20.3	7.3	12.4	20.8
+ 63 - 125	2.2	3.4	1.6	0.6	4.3	10.2	5.4	3.5	19.6	1.2	4.5	8.3
- 63	2.0	0.4	1.5	0.4	0.6	2.2	0.6	0.4	4.7	0.3	0.6	1.3
Median dia. (μm)	642	568	780	707	486	475	510	523	290	648	517	389

Table A.5.4.6 (c) Chemical and Size Analyses of Bed Material
Test Series 4 (cont'd)

Test No.	4.9		
Sample	Initial	Final	Offtake
Chemical Analysis			
Sulphur % a.r.	0.3	1.25	0.45
CO_2 % a.r.	0.12	0.42	0.37
CaO % a.r.	0.74	5.32	1.96
Size Analysis	% in grade by weight		
Particle size (μm)			
+ 1680	0	0	0
+ 500 - 1680	91.0	82.1	72.9
+ 250 - 500	6.9	11.6	19.0
+ 125 - 250	0.2	4.6	8.1*
+ 63 - 125	0.4	1.7	-
- 63	1.5	0	-
Median diam. (μm)	1184	1042	826

* - 250 μm

Table A.5.4.7 Flue Gas Analyses

Test No.		4.1	4.2	4.3	4.4	4.5	4.6	4.7	4.8	4.9
Operating Conditions										
Ca/S Mol Ratio		0	1.0	2.1	3.1	0.9	1.7	2.6	0.9	0.9
Fluidising Velocity	ft/s	3	3	3	3	3	3	3	3	3
Bed Temperature	^{o}F	1470	1470	1470	1470	1470	1470	1470	1470	1470
Bed Height	ft	2	2	2	2	2	2	2	2	2
Chromatograph										
Mean CO_2	Vol % dry	14.9	15.0	15.2	15.5	14.5	15.3	15.3	14.6	14.8
Mean O_2	Vol % dry	2.3	2.4	2.2	2.4	2.5	2.2	2.3	2.1	2.5
Mean CO	Vol % dry	0.08	0.06	0.06	0.06	0.08	0.06	0.06	0.06	0.08
Mean CH_4	Vol % dry	0	0	0	0	0	0	0	0	0
SO_2 By Iodine										
Sample 1	p.p.m. dry	1941	1395	963	285	1135	566	194	1158	890
Sample 2	p.p.m. dry	1946	1408	928	245	1077	571	223	1250	1014
Sample 3	p.p.m. dry	2052	1307	911	228	1131	598	193	1268	996
Sample 4	p.p.m. dry	1945	1457	960	205	1165	579	170	1276	1028
Sample 5	p.p.m. dry	2013	1292	931		1177	573	175		1089
Sample 6	p.p.m. dry						581 604	159		940
Mean SO_2										
By Iodine	p.p.m. dry	1980	1372	938	241	1137	581	185	1238	990
By H_2O_2	p.p.m. dry	2120	1415	1000	275	1180	640	217	1185	1115
Cl^-	p.p.m. dry	121	75	89	95	83	69	65	69	47
NH_3	p.p.m. dry	ND	ND	ND	ND	0	ND	21	22	24

ND - Not Determined

Table A.5.4.8. Mass Balance for Test No. 4.1

Rate lb/h	Total	'Ash'	'Carbon'	Nitrogen	'Oxygen'	Sulphur	Calcium
Coal	3.82	0.49	2.79	0	0.16	0.105	0.027
Acceptor	0	0	0	0	0	0	0
Total Air	45.94	0	0	35.3	10.64	0	0
Bleed Nitrogen	1.90	0	0	1.9	0	0	0
Total Input	51.66	0.49	2.79	37.2	10.80	0.105	0.027
Accumulated in Bed	-0.96	-0.96	0	0	0	0.005	0
Offtake Ash	0.50	0.50	0.01	0	0	0.005	0.013
Fines	0.49	0.30	0.20	0	0	0.007	0.013
Flue Gas	51.21	0	2.90	37.6	10.41	0.099	0
Total Output	51.24	-0.16	3.11	37.6	10.41	0.116	0.026
Unaccounted, input-output	0.42	0.65	0.32	-0.4	0.39	-0.011	0.001
Unaccounted, % of input	0.8	133	11.1	-1.2	3.6	-10.4	3.9

Excess Air	6.7%
Carbon Loss	6.3% (Unburnt)
Sulphur Retention	5%
Ca/S Mole ratio	0

Table A.5.4.9 Mass Balance for Test No 4.2

Rate lb/h	Total	'Ash'	'Carbon'	Nitrogen	'Oxygen'	Sulphur	Calcium
Coal	4.22	0.54	3.08	0	0.18	0.116	0.030
Acceptor	0.38	0.38	0	0	0	0	0.147
Total Air	45.94	0	0	35.3	10.64	0	0
Bleed Nitrogen	1.90	0	0	1.9	0	0	0
Total Input	52.44	0.92	3.08	37.2	10.82	0.116	0.177
Accumulated in Bed	-0.11	-0.11	0	0	0	0.036	0.105
Offtake Ash	0.36	0.36	0.01	0	0	0.006	0.013
Fines	0.77	0.47	0.31	0	0	0.013	0.038
Flue Gas	51.36	0	2.91	37.5	10.65	0.069	0
Total Output	52.38	0.72	3.23	37.5	10.65	0.124	0.156
Unaccounted, input-output	0.06	0.20	-0.15	-0.3	0.17	-0.008	0.021
Unaccounted % of input	0.1	21.7	-5.0	-0.7	1.6	-6.4	11.6

Excess Air	4.0%
Carbon Loss	9.5% (Unburnt)
Sulphur Retention	41%
Ca/S Mole ratio	1.0

Table A 5.4.10 Mass Balance for Test No 4.3

Rate lb/h	Total	'Ash'	Carbon'	Nitrogen	'Oxygen'	Sulphur	Calcium
Coal	4.04	0.52	2.94	0	0.17	0.111	0.028
Acceptor	0.73	0.73	0	0	0	0	0.285
Total Air	45.94	0	0	35.3	10.64	0	0
Bleed Nitrogen	1.9	0	0	1.9	0	0	0
Total Input	52.61	1.25	2.94	37.2	10.81	0.111	0.313
Accumulated in Bed	-0.06	-0.06	0	0	0	0.034	0.206
Offtake Ash	0.76	0.76	0	0	0	0.022	0.066
Fines	0.76	0.41	0.35	0	0	0.015	0.046
Flue Gas	51.33	0	2.95	37.2	10.58	0.047	0
Total Output	52.79	1.11	3.31	37.2	10.58	0.118	0.317
Unaccounted, input-output	-0.18	0.14	-0.37	0	0.13	-0.007	-0.004
Unaccounted, % of input	-0.34	11.2	-12.59	0	1.20	-6.5	-1.3

Excess Air	1.7%
Carbon Loss	10.74% (Unburnt)
Sulphur Retention	57%
Ca/S Mole ratio	2.1

Table A 5.4.11 Mass Balance for Test No 4.4

Rate lb/h	Total	'Ash'	Carbon'	Nitrogen	'Oxygen'	Sulphur	Calcium
Coal	4.33	0.55	3.15	0	0.19	0.119	0.030
Acceptor	1.16	1.16	0	0	0	0	0.455
Total Air	45.94	0	0	35.3	10.64	0	0
Bleed Nitrogen	1.9	0	0	1.9	0	0	0
Total Input	53.33	1.71	3.15	37.2	10.83	0.119	0.485
Accumulated in Bed	-0.02	-0.02	0	0	0	0.036	0.210
Offtake Ash	0.90	0.90	0	0	0	0.041	0.157
Fines	0.80	0.52	0.29	0	0	0.015	0.079
Flue Gas	51.46	0	3.00	37.2	10.94	0.012	0
Total Output	53.14	1.40	3.29	37.2	10.94	0.105	0.446
Unaccounted, input-output	0.19	0.31	-0.14	0	0.11	0.014	0.039
Unaccounted, % of input	0.36	18.1	-4.4	0	1.02	12.1	8.0

Excess Air	4.4%
Carbon Loss	8.7% (Unburnt)
Sulphur Retention	90%
Ca/S Mole ratio	3.1

Table A.5.4.12 Mass Balance for Test No 4.5

Rate lb/h	Total	'Ash'	'Carbon'	Nitrogen	'Oxygen'	Sulphur	Calcium
Coal	4.11	0.53	3.0	0	0.18	0.113	0.029
Acceptor	0.37	0.37	0	0	0	0	0.121
Total Air	45.94	0	0	35.3	10.64	0	0
Bleed Nitrogen	1.90	0	0	1.9	0	0	0
Total Input	52.32	0.90	3.0	37.2	10.82	0.113	0.150
Accumulated in Bed	0.01	0.01	0	0	0	0.042	0.090
Offtake Ash	0.34	0.34	0.01	0	0	0.007	0.018
Fines	0.67	0.41	0.26	0	0	0.012	0.036
Flue Gas	51.24	0	2.82	37.7	10.41	0.057	0
Total Output	52.26	0.75	3.08	37.7	10.41	0.118	0.144
Unaccounted, input-output	0.06	0.15	-0.08	-0.5	0.41	-0.005	0.006
Unaccounted, % of input	0.1	16.7	-2.7	-1.2	3.8	-4.8	3.7

Excess Air	5.8%	
Carbon Loss	8.6%	(Unburnt)
Sulphur Retention	50%	
Ca/S Mole ratio	0.9	

Table A.5.4.13 Mass Balance for Test No 4.6

Rate lb/h	Total	'Ash'	'Carbon'	Nitrogen	'Oxygen'	Sulphur	Calcium
Coal	4.28	0.55	3.12	0	0.18	0.118	0.030
Acceptor	0.77	0.77	0	0	0	0	0.253
Total Air	45.94	0	0	35.3	10.64	0	0
Bleed Nitrogen	1.90	0	0	1.9	0	0	0
Total Input	52.89	1.32	3.12	37.2	10.82	0.118	0.283
Accumulated in Bed	-0.01	-0.01	0	0	0	0.040	0.112
Offtake Ash	0.76	0.76	0	0	0	0.036	0.085
Fines	0.79	0.49	0.30	0	0	0.015	0.057
Flue Gas	51.41	0	2.97	37.4	10.72	0.029	0
Total Output	52.95	1.24	3.27	37.4	10.72	0.120	0.254
Unaccounted, input-output	-0.06	0.08	-0.15	-0.2	0.10	-0.002	0.029
Unaccounted, % of input	-0.1	6.1	-4.8	-0.5	1.0	-2.2	10.1

Excess Air	3.1%
Carbon Loss	9.2% (Unburnt)
Sulphur Retention	75%
Ca/S Mole ratio	1.7

Table A.5.4.14 Mass Balance for Test No. 4.7

Rate lb/h	Total	'Ash'	'Carbon'	Nitrogen	'Oxygen'	Sulphur	Calcium
Coal	4.36	0.56	3.18	0	0.19	0.120	0.031
Acceptor	1.18	1.18	0	0	0	0	0.386
Total Air	45.94	0	0	35.3	10.64	0	0
Bleed Nitrogen	1.90	0	0	1.9	0	0	0
Total Input	53.38	1.74	3.18	37.2	10.83	0.120	0.417
Accumulated in Bed	-0.19	-0.19	0	0	0	0.063	0.223
Offtake Ash	0.95	0.95	0.01	0	0	0.052	0.146
Fines	0.76	0.51	0.24	0	0	0.014	0.084
Flue Gas	51.37	0	2.96	37.3	10.80	0.009	0
Total Output	52.89	1.27	3.21	37.3	10.80	0.138	0.453
Unaccounted, input-output	0.49	0.47	-0.03	-0.1	0.03	-0.018	-0.036
Unaccounted, % of input	0.92	27.0	-1.0	-0.3	0.3	-14.8	-8.7

Excess Air	5.2%
Carbon Loss	7.6% (Unburnt)
Sulphur Retention	92%
Ca/S Mole ratio	2.6

Table A.5.4.15 Mass Balance for Test No. 4.8

Rate lb/h	Total	'Ash'	'Carbon'	Nitrogen	'Oxygen'	Sulphur	Calcium
Coal	4.27	0.55	3.10	0	0.18	0.117	0.029
Acceptor	0.38	0.38	0	0	0	0	0.125
Total Air	45.94	0	0	35.3	10.6	0	0
Bleed Nitrogen	1.90	0	0	1.9	0	0	0
Total Input	52.49	0.93	3.10	37.2	10.78	0.117	0.154
Accumulated in Bed	-0.06	-0.06	0	0	0	0.003	-0.006
Offtake Ash	0.50	0.50	0	0	0	0.026	0.075
Fines	0.75	0.45	0.30	0	0	0.015	0.051
Flue Gas	51.25	0	2.83	37.8	10.30	0.052	0
Total Output	52.44	0.89	3.13	37.8	10.30	0.097	0.120
Unaccounted, input-output	0.05	0.04	-0.03	-0.6	0.48	0.020	0.034
Unaccounted, % of input	0.1	4.3	1.0	-1.5	4.5	17.8	12.4

Excess Air	2.8%
Carbon Loss	9.4% (Unburnt)
Sulphur Retention	55%
Ca/S Mole ratio	0.9

Table A.5.4.16 Mass Balance for Test No. 4.9

Rate lb/h	Total	'Ash'	'Carbon'	Nitrogen	'Oxygen'	Sulphur	Calcium
Coal	4.57	0.58	3.33	0	0.2	0.126	0.032
Acceptor	0.41	0.41	0	0	0	0	0.134
Total Air	45.94	0	0	35.3	10.64	0	0
Bleed Nitrogen	1.90	0	0	1.9	0	0	0
Total Input	52.82	0.99	3.33	37.2	10.84	0.126	0.166
Accumulated in Bed	-0.69	-0.69	0	0	0	0.026	0.089
Offtake Ash	0.43	0.43	0	0	0	0.002	0.006
Fines	0.85	0.49	0.36	0	0	0.017	0.045
Flue Gas	51.33	0	2.87	37.4	10.72	0.050	0
Total Output	51.92	0.23	3.23	37.4	10.72	0.095	0.140
Unaccounted, input-output	0.90	0.76	0.10	-0.2	0.12	0.031	0.026
Unaccounted, % of input	1.7	76	3.0	-0.6	1.1	24.6	16.1

Excess Air	3.0%
Carbon Loss	11.1% (Unburnt)
Sulphur Retention	60%
Ca/S Mole ratio	0.9

Table A.5.4.17 SO_2 concentrations and % reductions

Test No.	4.1	4.2	4.3	4.4	4.5	4.6	4.7	4.8	4.9
Limestone type	-	U.K.	U.K.	U.K.	U.S. 18	U.S. 18	U.S. 18	U.S. 18	U.S. 18
Fluidising Velocity, ft/s	3	3	3	3	3	3	3	3	3
Bed Temperature, °F	1470	1470	1470	1470	1470	1470	1470	1470	1470
Ca/S mol ratio	0	1.0	2.1	3.1	0.9	1.7	2.6	0.9	0.9
SO_2 concentration, p.p.m.	1980	1372	938	241	1137	581	185	1238	(1115)
SO_2 reduction, %	0	31	52	88	43	71	91	38	43

SO_2 reductions are based on a datum level of 1980 p.p.m.

(   ) Hydrogen peroxide result.

Table A.5.5.1 Operating Conditions During Test Series 5

Constant Parameters:

Coal : Welbeck II (ex Task I)
Coal Size : - 1680 micron
Acceptor Size : - 1680 micron
Fluidising Velocity : 3 ft/s
Bed Height : 2 ft
Recycle : None

Test No	5.1	5.2
Date	31.12.70	1.1.71
Acceptor	U.K. Lst	U.S. Lst 18
Ca/S mole ratio	1.6	1.9
Bed Temp. °F	1440 *	1470
Ash Bed	ex 2.15	ex 5.1

* Test 5.1 Bed temperature accidentally maintained 30°F below test 5.2

Table A.5.5.2 Chemical analyses of coal

Test Series 5

Test Number		5.1 & 5.2
Proximate analysis		
Total moisture	% a.r.	2.8
Ash	% a.r.	25.6
Volatile Matter	% d.a.f.	36.9
Ultimate analysis		
Carbon	% d.b.	60.5
Hydrogen	% d.b.	3.5
Nitrogen	% d.b.	1.27
Sulphur	% d.b.	1.39
Oxygen + errors	% d.b.	3.9
Chlorine	% d.b.	0.58
Carbon Dioxide	% d.b.	1.0
Ash analysis		
CaO	% d.b.	3.1
MgO	% d.b.	2.1
Na_2O	% d.b.	1.67
K_2O	% d.b.	3.3
Al_2O_3	% d.b.	21.4
Fe_2O_3	% d.b.	8.7
SiO_2	% d.b.	54.8
Calorific value (gross)	Btu/lb	14390
Swelling No.		1
Gray King coke type		B

Table A.5.5.3 Chemical and Size Analyses of Acceptor

Test Series 5

Test No.	5.1	5.2
Chemical Analysis		
CaO a.r.	54.9	45.9
MgO a.r.	0.2	0.9
CO_2 a.r.	42.0	34.7
SiO_2 a.r.	1.6	14.7
Size Analysis	% in grade by weight	
Particle size (μm)		
+ 1680	0.5	0.1
+ 500 - 1680	52.1	21.0
+ 250 - 500	19.1	22.0
+ 125 - 250	10.1	22.5
+ 63 - 125	7.2	12.2
- 63	11.0	22.2
Median dia. (μm)	537	207

Table A.5.5.4 Chemical and Size Analyses of Feed Blends

Test Series 5

Test No.	5.1	5.2
Moisture a.r.	3.5	2.7
Ash a.r.	28.1	30.8
Carbon d.b.	55.6	52.7
CaO d.b.	4.48	4.76
Sulphur d.b.	1.35	1.25
CO_2 d.b.	3.75	4.20
Particle size (μm)	% in grade by weight	
+ 1680	0.1	0.1
+ 500 - 1680	39.8	35.3
+ 250 - 500	18.3	18.5
+ 125 - 250	12.7	13.7
+ 63 - 125	10.1	11.5
- 63	19.0	20.9
Median dia. μm	347	292

Table A.5.5.5 Chemical and Size Analyses of Cyclone Fines

Test Series 5

Test No.	5.1	5.2
Chemical Analysis		
Carbon % a.r.	39.95	34.1
Sulphur % a.r.	1.4	1.33
CO_2 % a.r.	0.52	0.53
CaO % a.r.	6.39	7.55
Size Analysis	% in grade by weight	
Particle size (μm)		
+ 500	0	0
+ 250 - 500	0	0.2
+ 125 - 250	0.6	0.5
+ 63 - 125	11.0	9.5
- 63	88.4	89.8

Table A.5.5.6 Chemical and Size Analyses of Bed Material

Test Series 5

Test No.	5.1			5.2		
Sample	Initial	Final	Offtake	Initial	Final	Offtake
Chemical Analysis						
Sulphur % a.r.	2.9	3.15	2.9	2.8	3.1	3.45
CO_2 % a.r.	0.64	1.19	0.69	0.96	0.72	0.43
CaO % a.r.	9.94	11.91	9.8	11.05	12.89	13.04
Size Analysis	% in grade by weight					
Particle size (μm)						
+ 1680	0	0.1	0	0	0	0
+500 - 1680	69.1	66.4	67.1	62.1	47.8	49.4
+ 250 - 500	26.8	25.3	21.6	26.9	32.5	25.4
+ 125 - 250	3.1	5.1	6.7	6.0	11.7	10.3
+ 63 - 125	0.7	2.9	4.1	4.7	7.7	13.5
- 63	0.3	0.2	0.5	0.3	0.3	1.4
Median diam. (μm)	709	689	723	630	481	493

Table A.5.5.7 Flue Gas Analyses

Test No.		5.1	5.2
Operating Conditions			
Ca/S Mol Ratio		1.6	1.9
Fluidising Velocity, ft/s		3	3
Bed Temperature °F		1440	1470
Bed Height, ft		2	2
Chromatograph			
Mean CO_2	Vol % Dry	14.8	15.4
Mean O_2	Vol % Dry	2.8	2.6
Mean CO	Vol % Dry	0.2	0.18
Mean CH_4	Vol % Dry	0	0
SO_2 By Iodine			
Sample 1.	p.p.m. Dry	361	225
Sample 2.	p.p.m. Dry	390	229
Sample 3.	p.p.m. Dry	352	232
Sample 4.	p.p.m. Dry	315	246
Sample 5.	p.p.m. Dry	291	250
Mean SO_2			
By Iodine	p.p.m. Dry	342	236
By H_2O_2	p.p.m. Dry	355	255
Cl^-	p.p.m. Dry	303	363
NH_3	p.p.m. Dry	12	3

Table A.5.5.8 Mass Balance for Test No. 5.1

Rate lb/h	Total	'Ash'	'Carbon'	Nitrogen	'Oxygen'	Sulphur	Calcium
Coal	5.69	1.50	3.44	0	0.22	0.079	0.033
Acceptor	0.41	0.41	0	0	0	0	0.160
Total Air	45.94	0	0	35.3	10.64	0	0
Bleed Nitrogen	1.9	0	0	1.9	0	0	0
Total Input	53.94	1.91	3.44	37.2	10.86	0.079	0.193
Accumulated in Bed	-0.07	-0.07	0	0	0	0.008	0.044
Offtake Ash	1.10	1.10	0.01	0	0	0.032	0.077
Fines	1.22	0.75	0.47	0	0	0.018	0.054
Flue Gas	51.27	0	2.90	37.3	10.79	0.017	0
Total Output	53.52	1.78	3.38	37.3	10.79	0.074	0.175
Unaccounted, input-output	0.42	0.13	0.06	-0.1	0.07	0.005	0.018
Unaccounted, % of input	0.8	6.8	1.7	-0.3	0.6	5.9	9.6

Excess Air	1.3%
Carbon Loss	14.0% (Unburnt)
Sulphur Retention	79%
Ca/S Mole ratio	1.6

Table A.5.5.9 Mass Balance for Test No. 5.2

Rate lb/h	Total	'Ash'	'Carbon'	Nitrogen	'Oxygen'	Sulphur	Calcium
Coal	5.71	1.50	3.45	0	0.22	0.079	0.033
Acceptor	0.56	0.56	0	0	0	0	0.184
Total Air	45.94	0	0	35.3	10.64	0	0
Bleed Nitrogen	1.90	0	0	1.9	0	0	0
Total Input	54.11	2.06	3.45	37.2	10.86	0.079	0.217
Accumulated in Bed	-0.18	-0.18	0	0	0	0.009	0.040
Offtake Ash	1.30	1.30	0.01	0	0	0.045	0.121
Fines	1.21	0.80	0.40	0	0	0.016	0.064
Flue Gas	51.49	0	3.01	37.2	11.00	0.012	0
Total Output	53.82	1.92	3.42	37.2	11.00	0.082	0.225
Unaccounted, input-output	0.29	0.14	0.03	0	-0.14	-0.003	-0.008
Unaccounted, % of input	0.5	6.8	0.9	0	-1.3	-3.8	-3.9

Excess Air	2.0%	
Carbon Loss	11.9%	(Unburnt)
Sulphur Retention	85%	
Ca/S Mole ratio	1.9	

Table A.5.5.10 SO_2 concentrations and % reductions

Test No.	5.1	5.2
Coal Type	Welbeck	Welbeck
Limestone Type	U.K.	U.S. 18
Fluidising Velocity, ft/s	3	3
Bed Temperature °F	1440	1470
Ca/S mol ratio	1.6	1.9
SO_2 concentration, p.p.m.	342	236
SO_2 reduction, %	71	80

SO_2 reductions are based on a datum level of 1170 p.p.m.

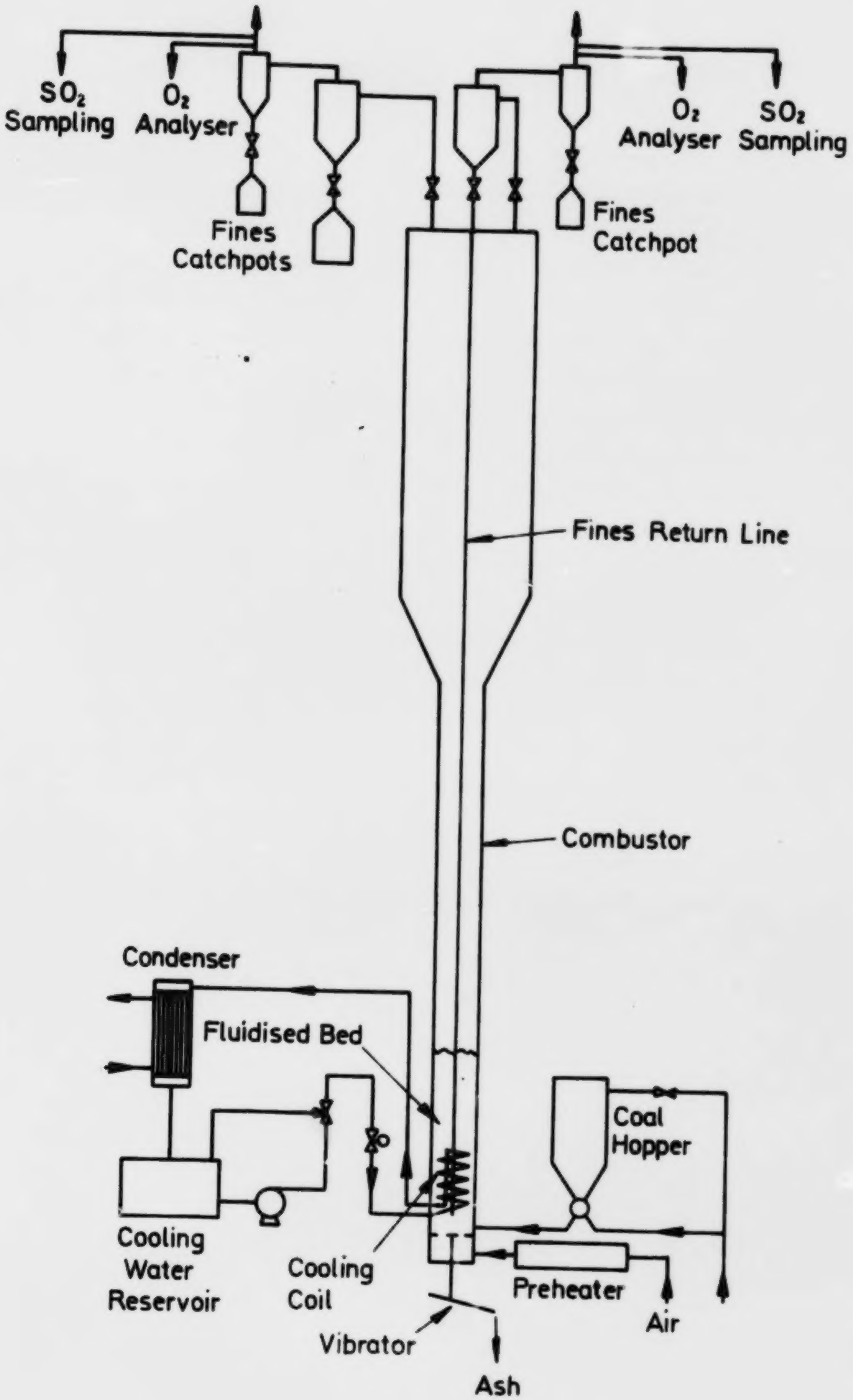
SO2 Sampling
O2 Analyser
Fines Catchpots
Fines Catchpot
O2 Analyser
SO2 Sampling
Fines Return Line
Combustor
Condenser
Fluidised Bed
Coal Hopper
Cooling Water Reservoir
Cooling Coil
Preheater
Air
Vibrator
Ash

Fig. A5.1. General Design Of The 6in Combustor

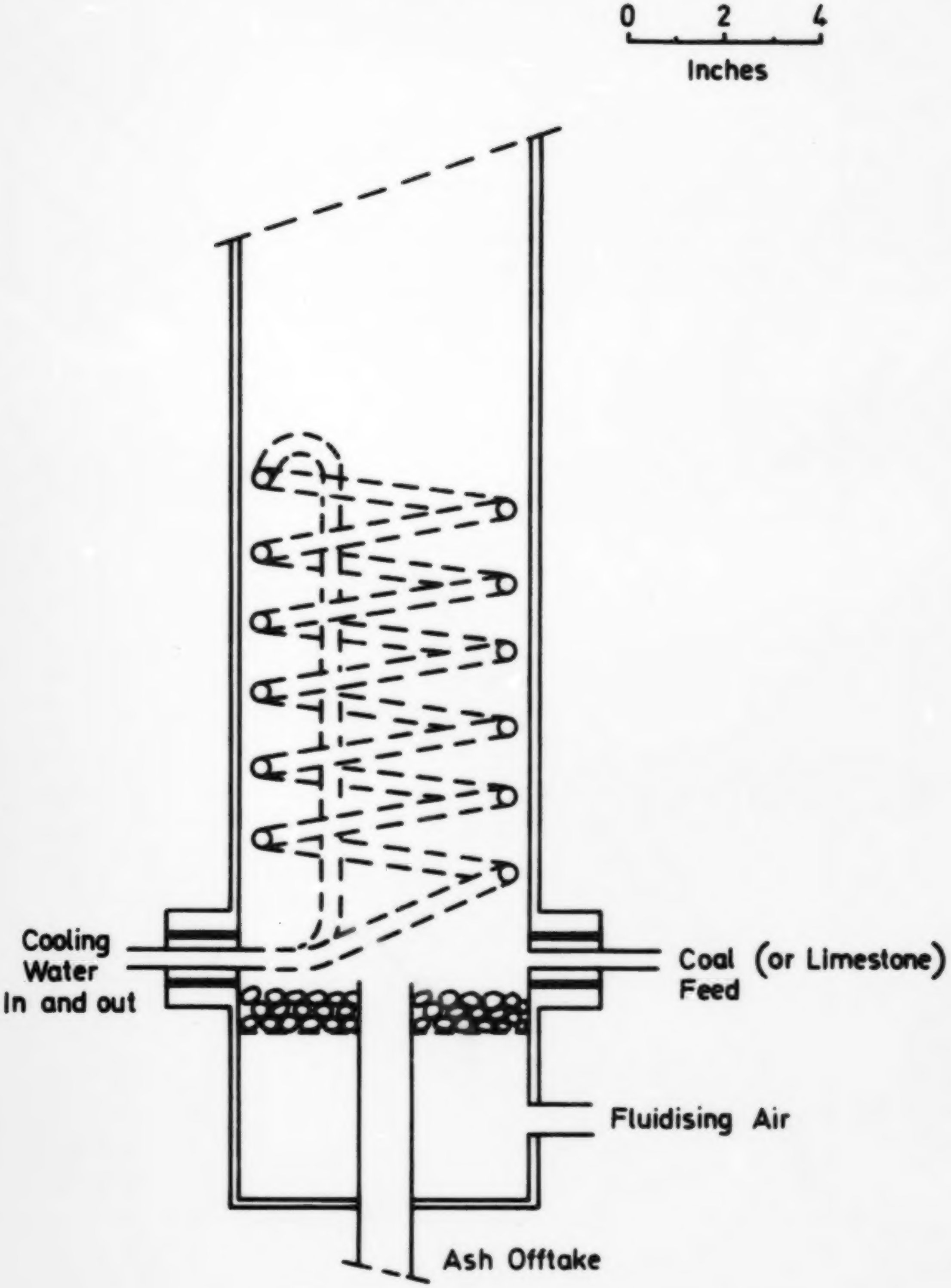
0
2
4
Inches
Cooling
Water
In and out
Coal (or Limestone)
Feed
Fluidising Air
Ash Offtake

Fig. A 5.2. Detail Of Bed Section Of 6in Combustor

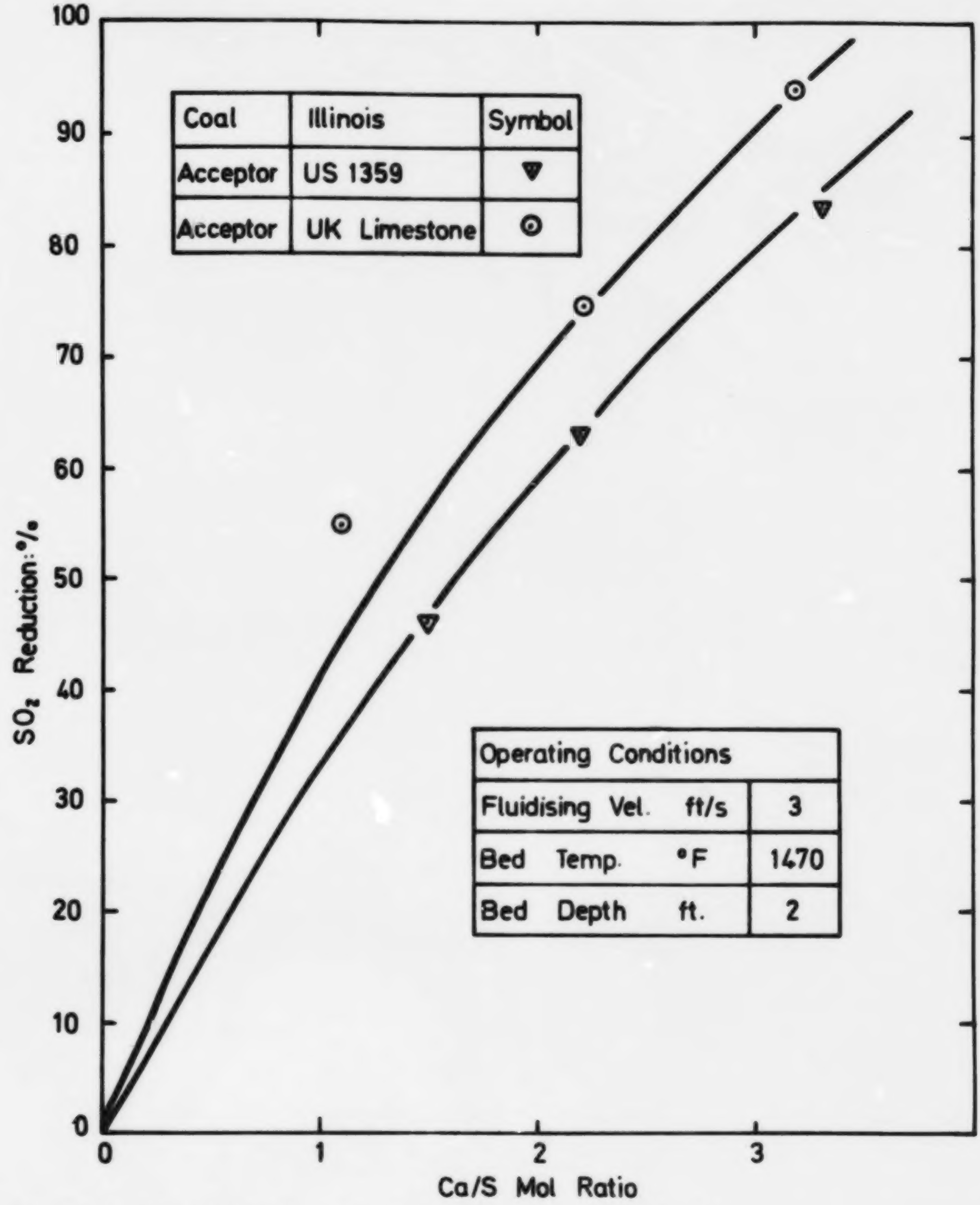

Fig. A5.3. Test Series 1. SO_2 Reduction v Ca/S mol ratio

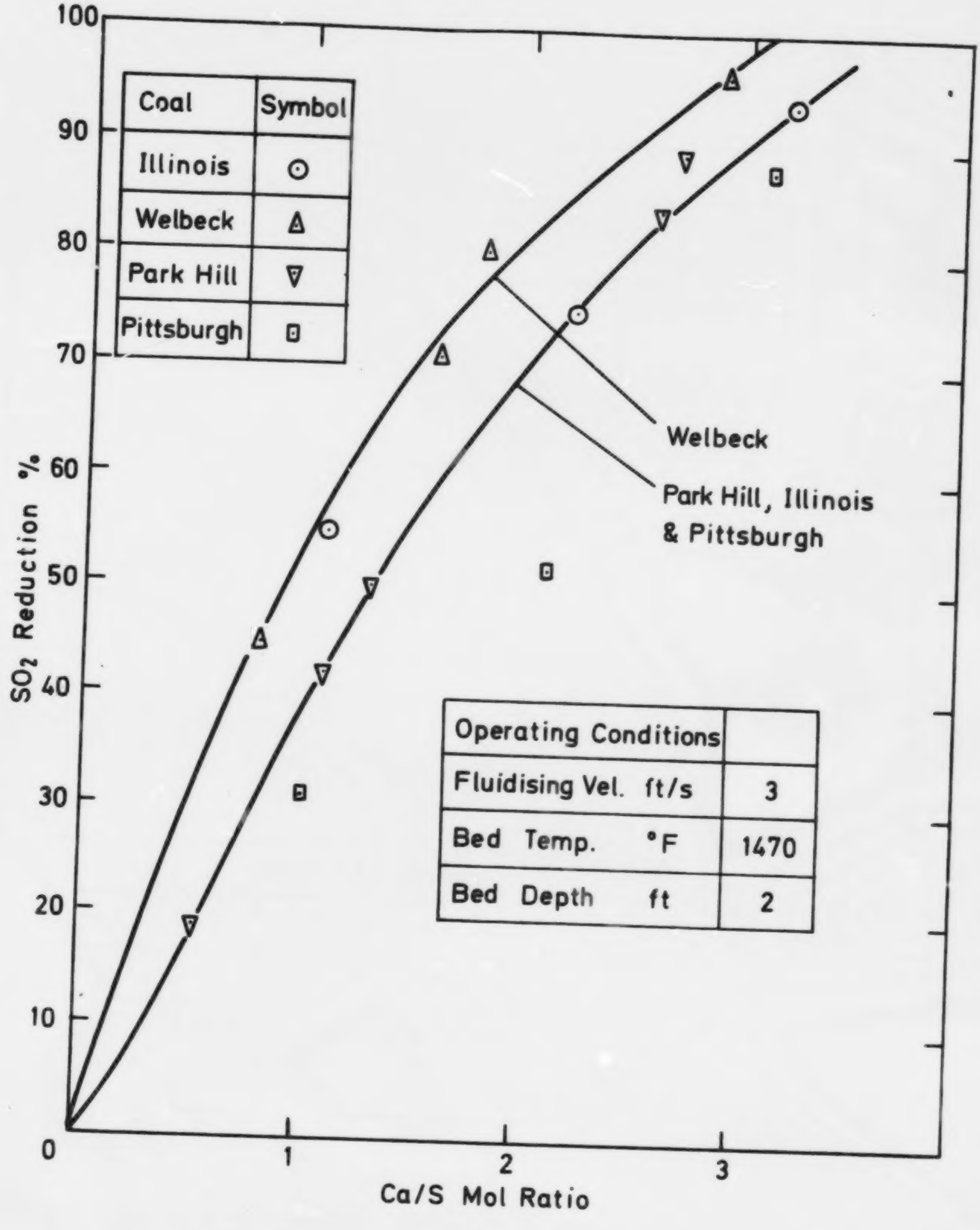

Fig. A5.4. Test Series 1,2,4 &5. SO_2 Reduction vs Ca/S Mol Ratio for Different Coals with U.K. Limestone

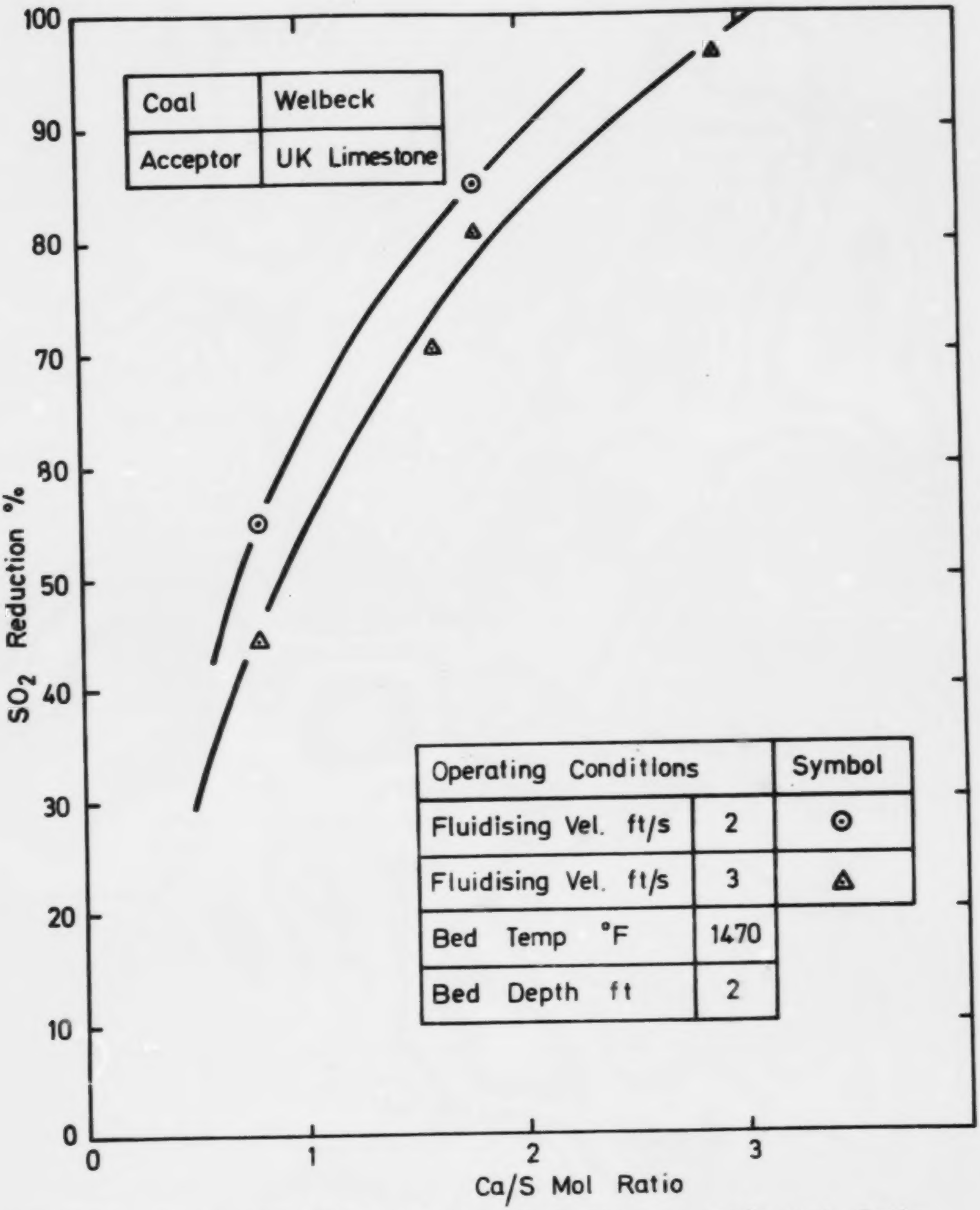

Fig. A5.5 Test Series 2 & 5. Sulphur Reduction vs Ca/S Mol Ratio

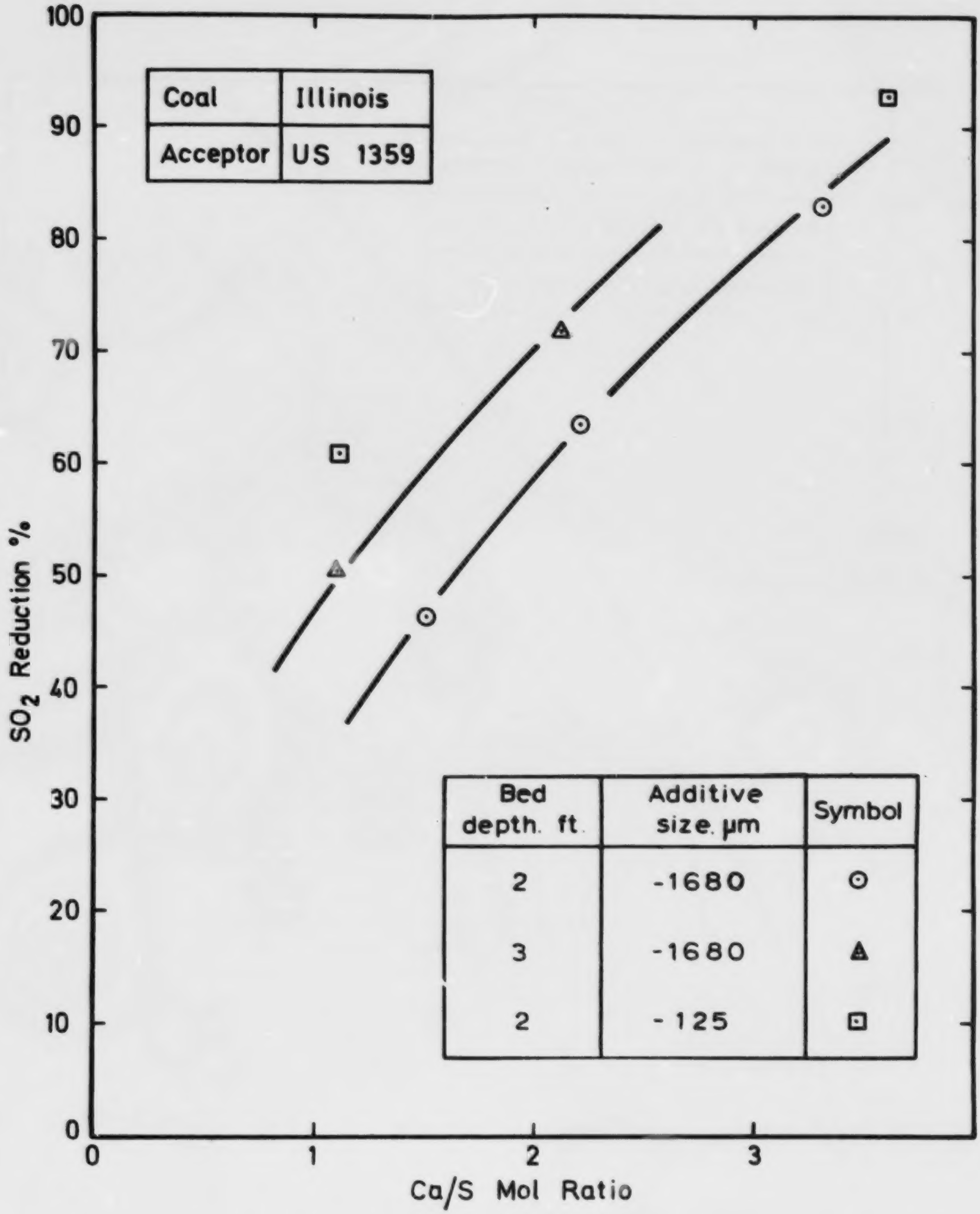

Fig A 5.6 Test Series 1 & 3. SO_2 Reduction vs Ca/S Mol Ratio For Various Bed Depths And Acceptor Sizes.

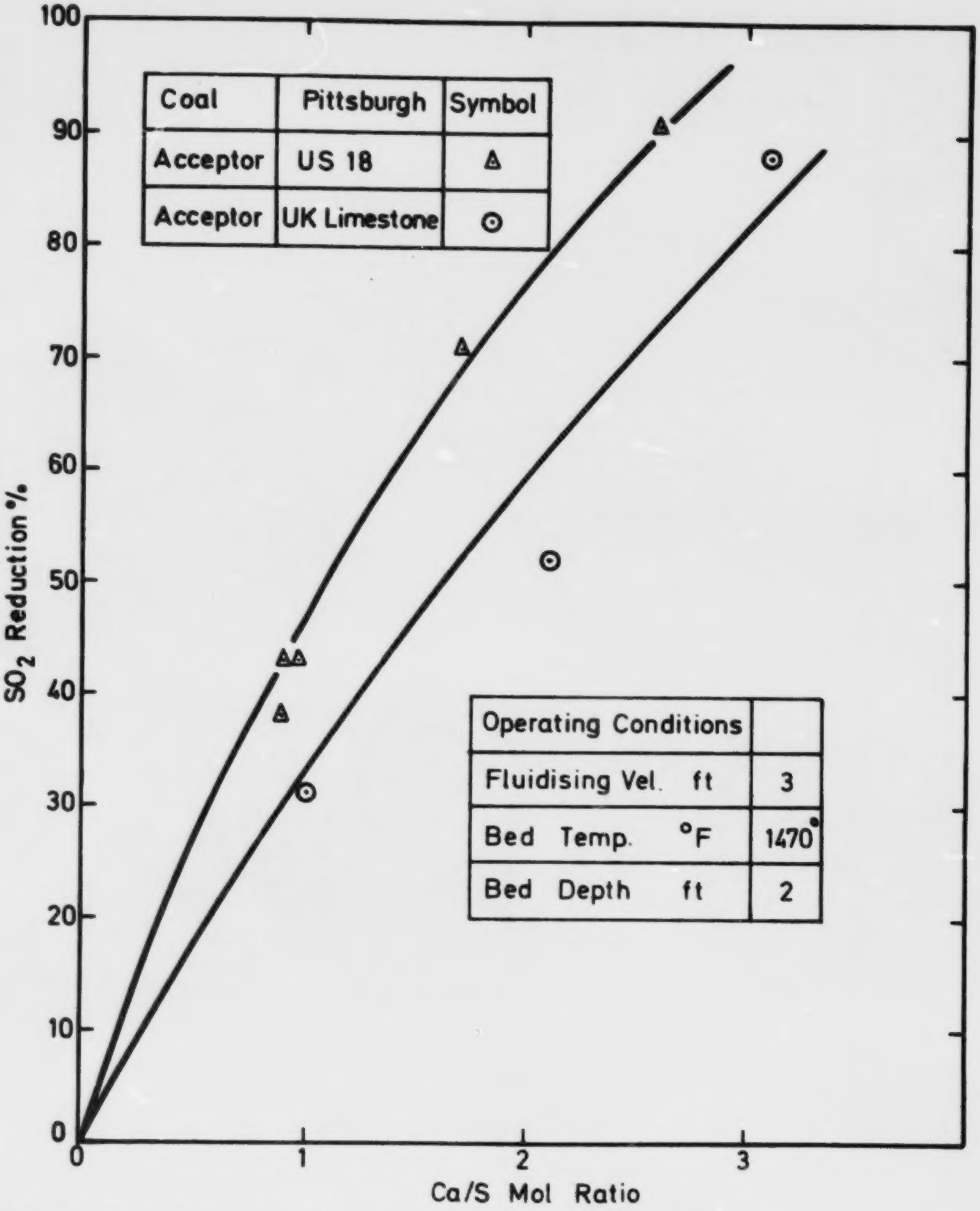

Fig A 5.7 Test Series 4. SO_2 Reduction vs Ca/S Mol Ratio for Two Acceptors

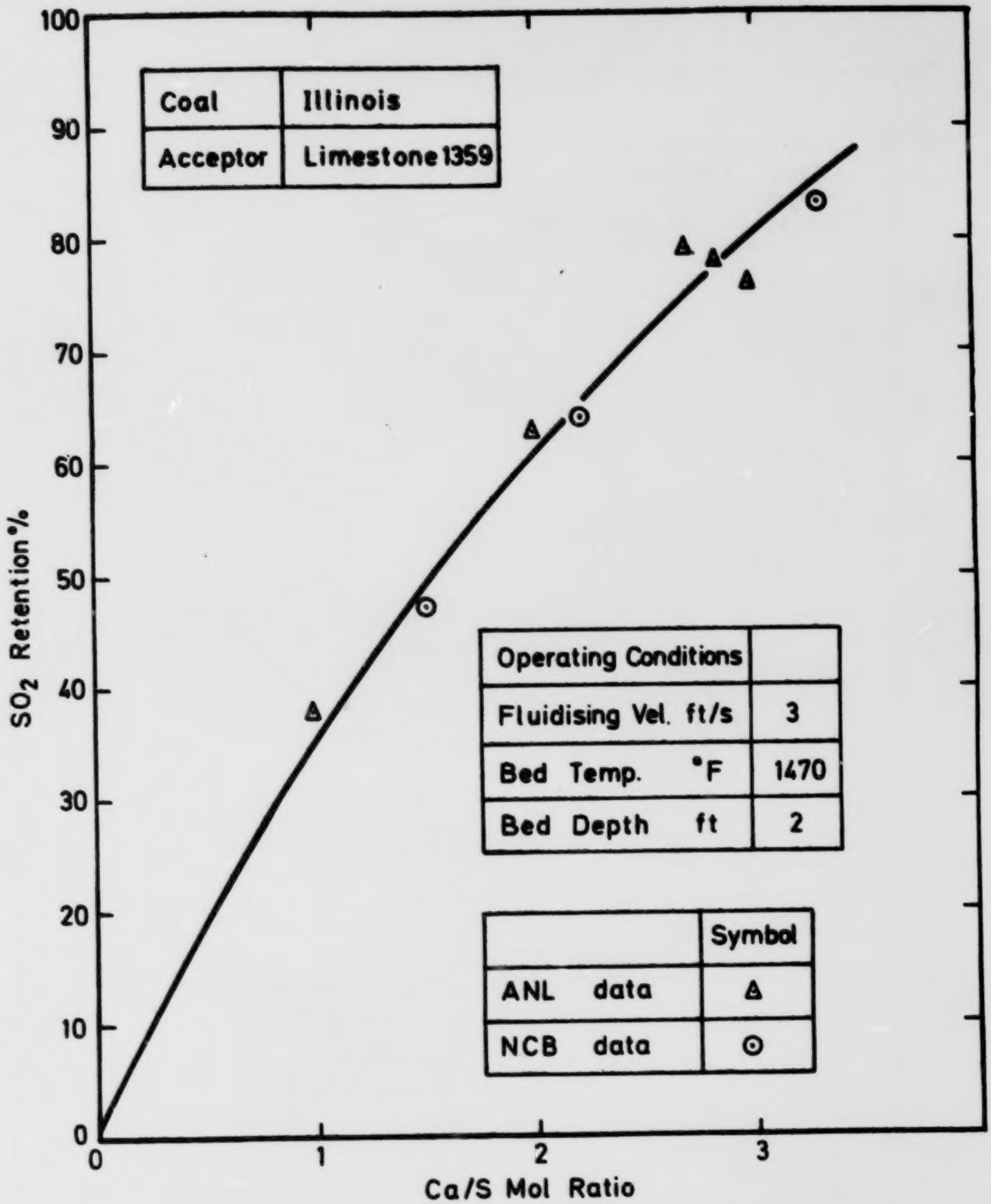

Fig A5.8 SO_2 Retention vs Ca/S Mol Ratio. Comparison of Data from ANL and NCB.

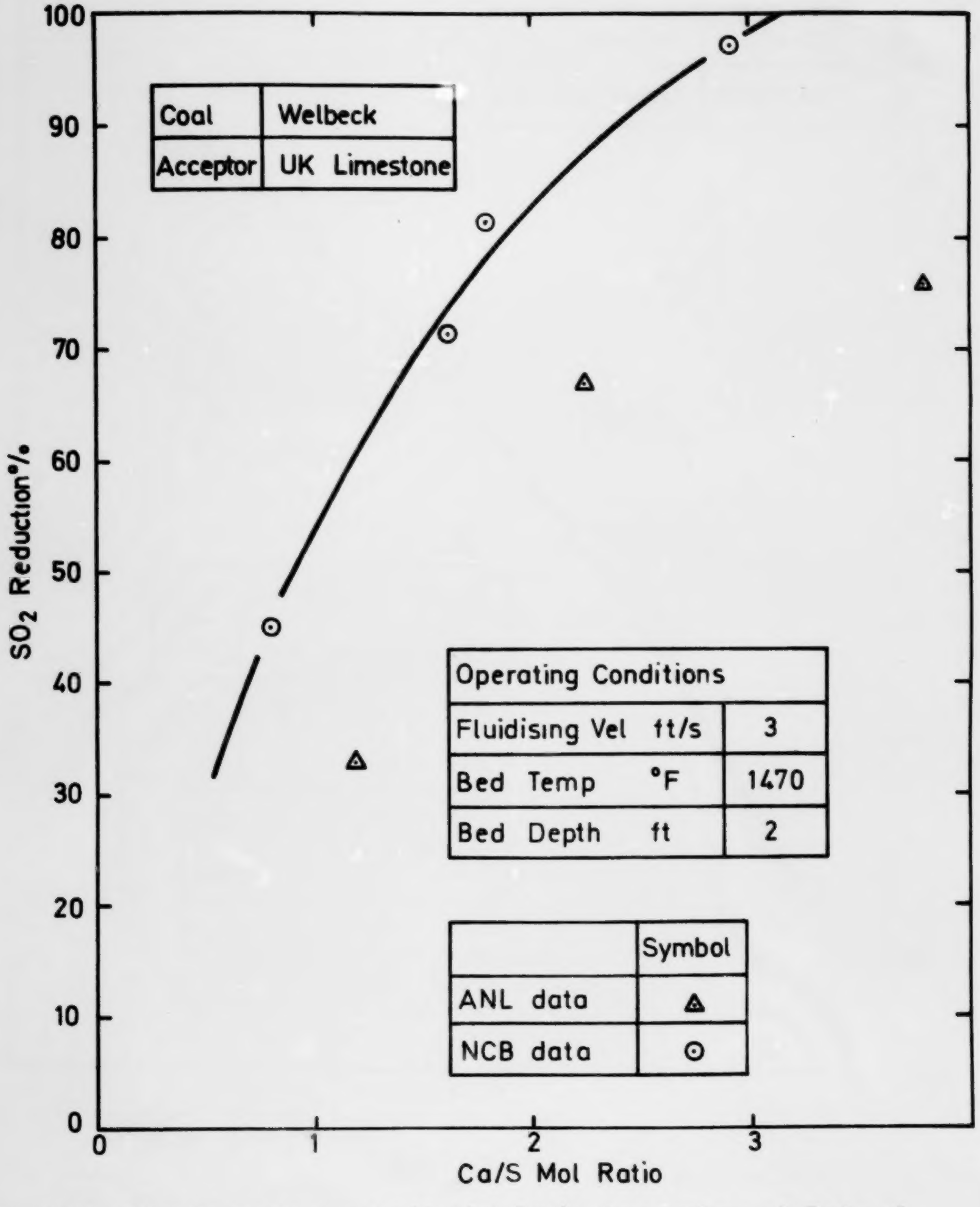

Fig A5.9 SO$_2$ Reduction vs Ca/S Mol Ratio Comparison of Data of from ANL and NCB.

NATIONAL COAL BOARD

FINAL REPORT

JUNE 1970 - JUNE 1971

REDUCTION OF ATMOSPHERIC POLLUTION

APPENDIX 6. MATHEMATICAL MODEL OF SULPHUR RETENTION. (TASK VI)

PREPARED FOR

ENVIRONMENTAL PROTECTION AGENCY
OFFICE OF AIR PROGRAMS
411 WEST CHAPEL HILL STREET
DURHAM, NORTH CAROLINA 27701

REFERENCE NO. DHB 060971

SEPTEMBER 1971

FLUIDISED COMBUSTION
CONTROL GROUP

NATIONAL COAL BOARD
LONDON, ENGLAND

A6.i

REDUCTION OF ATMOSPHERIC POLLUTION

Research on reducing emission of sulphur oxides, nitrogen oxides and particulates by using fluidised bed combustion of coal

Appendix 6. Mathematical model of sulphur retention. (Task V1)

Main objective

To complete the development of a mathematical model of sulphur retention and to compare its predictions with the results of laboratory and rig experiments, and to up-date it as appropriate.

Report prepared by: F.V. Bethell
D.W. Gill
B.B. Morgan

Report approved by: A.D. Dainton
H.R. Hoy

Preceding page blank

Table of Contents

Page No.

SUMMARY AND CONCLUSIONS

1. INTRODUCTION A6. 1

2. DESCRIPTION OF MODEL A6. 2

2.1 Absorption Calculation A6. 8
2.2 Input Data A6. 8
2.3 Initial Calculations A6. 8
2.4 Calculation of Elutriation Constants A6. 9
2.5 Adjustment of mass fractions of ash and limestone A6.11
2.6 Calculation of bed composition A6.11
2.7 Calculation of particle residence times A6.12

3. FORM OF INPUT DATA FOR MODEL A6.12

3.1 Bed voidage A6.12
3.2 Densities of ash and limestone A6.12
3.3 Attrition coefficients A6.13
3.4 Constants in reactivity equation A6.13
3.5 Recirculation cyclone efficiency A6.13

4. GENERAL OBSERVATIONS ON PERFORMANCE OF MODEL A6.13

4.1 Elutriation A6.14
4.2 Attrition A6.14
4.3 SO_2 generation pattern A6.15
4.4 Absorption of SO_2 in the gas space above the bed A6.15

5. COMPARISONS WITH RESULTS FROM THE CURRENT CONTRACT PROGRAMME A6.16

5.1 Task I A6.16
5.2 Task II A6.17
5.3 Task III A6.19
5.4 Task V A6.20
5.5 Pope, Evans and Robbins Data A6.20

6. DISCUSSION A6.21

7. COMPUTER PROGRAMME A6.26

ACKNOWLEDGEMENTS A6.27

ADDENDUM ON ACCURACY OF THE REACTION RATE DATA A6.27

REFERENCES

NOMENCLATURE

TABLES A6.1 - A6.6

FIGURES A6.1 - A6.19

(Note that when referring to Tables and Figures in the text the prefix A6 is omitted).

Preceding page blank

SUMMARY AND CONCLUSIONS

There were two main objectives in developing the model of the sulphur absorption process, firstly, to assist in understanding the performance of the experimental plant and secondly to develop a technique to assist in extrapolating the results to other plants and feed materials.

The model broadly comprises two sections. The first calculates from the input data the terminal velocities of particles in up to ten size groups, and thence the bed composition as regards the weights of ash and limestone particles in the selected size groups. The calculation procedure also gives the mean residence time of each group of particles. The second part calculates the absorption of SO_2 in and above the bed. To do this a mean SO_2 concentration is calculated using an assumed mean reactivity for the bed. This mean SO_2 concentration is used to calculate the utilisation of each size group of particles. The procedure involves solving equations relating reactivity to utilisation and the equation for the sulphur balance over the bed. The utilisation values that result enable an improved estimate to be calculated for the mean reactivity of the bed and thence the calculation procedure is repeated until a satisfactory degree of convergence is obtained.

The model uses semi-empirical constants to compute the rate of reduction of particle size in the bed due to attrition and the residence time of fines in the bed; constants are also applied to express the mode of evolution of SO_2 in the bed. Subsequent to the initial testing of the model a computational procedure was introduced to allow for the exposure of fresh unsulphated lime by abrasion of the sulphated layer i.e. to compensate for 'regeneration' by attrition.

Agreement between the predictions from the model (summarised at the end of Section 6) and plant performance is in general good where the acceptor does not contain a large fraction of material fine enough to be elutriated. In circumstances where it does the predicted retention is lower than that achieved. The general shape

Preceding page blank

of the curves of retention vs Ca/S mole ratio obtained from plant experiments is more consistent with SO_2 evolution occurring throughout the bed rather than solely at the bottom of the bed.

The attainment of closer representation of plant performance where there is a high proportion of elutriable fines would most likely be achieved by rigorous experimental determination of elutriation indices for each rig. The factors that affect elutriation and attrition in plant need to be more fully characterised before general extrapolation of the results beyond the current range of process and design conditions can be attempted with confidence.

Further development of the model should include the effect of bubble growth and its effect on the contact efficiency between gas and solids. Nevertheless, the existing model provides a valuable guide as to the effects of changes in process conditions.

1. INTRODUCTION

The development of a mathematical model had been started before the present contract was negotiated. It seemed appropriate that the work should continue and form a part of the programme of work under the terms of the contract, and it was accordingly written into the contract proposals.

Simultaneously with this development, similar work was in progress at ANL (Argonne National Laboratories)by L B Koppel.[1] It is interesting to compare the approach used in the two models. Both postulate a well-stirred reactor in respect of the solid particles, but the ANL model stipulates that all of the solids are removed by overflow from the bed, whereas the British model assumes that solids removal is partly by overflow and partly by elutriation, depending on particle size. Both models assume plug flow of gas and allow of an SO_2 generation function so that it is possible to simulate the case in which SO_2 is released at the bottom of the bed, or various cases in which the SO_2 is formed in various patterns throughout the bed depth. (The difficulty in testing the models here lies in the absence of reliable information about SO_2 generation patterns). Both models assume a uniform temperature throughout the bed and uniform SO_2 concentration across any horizontal plane, and both make the assumption that the rate of reaction is proportional to the SO_2 concentration in the surrounding gas. The assumption that the reaction rate coefficient is the same in the plants as in the laboratory measurements of reactivity is common to both, but the ANL model is more complete than the British model in that it allows for the presence of two phases, a particulate phase and a bubble phase, with continuous exchange of gas between them. Incorporation of this facility in the model, described in this appendix, is considered to be desirable, if any future work were to be done in development of the model.

The British model is capable of taking into account the actual measured reactivity of limestone particles of different sizes, whereas the American model is believed to apply a mean reaction rate coefficient to all sizes of particle. The measurements of reaction rate coefficients made in Task VIII of the present contract indicate that for stone of zero utilization, the reactivity is about the same for all sizes, but as the degree of utilization increases, the reactivity of the coarser particles drops off more rapidly.

A further assumption of the present model is that gas/solids contact time does not play any part in controlling the reaction rate, which is presumed to be governed by processes taking place within the limestone particle.

Support for this assumption is given by Table 2 of reference 6, which records the results of experiments in which air containing SO_2 was passed through shallow fluidised beds of limestone particles. For gas velocities in the range 0.5 to 5 ft/s and bed depths of about 1 to 2 inches, practically 100% removal of SO_2 was noted with fresh limestone in the majority of cases.

2. DESCRIPTION OF MODEL

The core of the mathematical model lies in the procedure for calculating SO_2 absorption by limestone in the bed. Steady-state operation is assumed and the rate of absorption is calculated by solving, for each of a number of particle size groups, equations relating the rate of sulphur take-up by the limestone to the rate of sulphur removal from the bed due to passage of 'stone through the bed. There are two unknowns, limestone utilization and SO_2 concentration. To solve the equations the relation between these two is also used.

The rate of sulphur take-up is dependent on the mass of stone of the particular size group present in the bed, on its extent of utilization, on the identity of the stone, and on the SO_2 concentration throughout the bed. Since, for a first order gas/solids reaction, the SO_2 concentration decreases exponentially with height above the air distributor, solution of the equations is simplified by using an equivalent mean concentration, which bears a known relation to the concentration at the top of the bed. The model permits the use of an SO_2 generation function so that, either the case in which all the SO_2 is formed very close to the air distributor, or cases in which SO_2 is formed throughout the bed, may be simulated. Details of the sulphur balance and of the SO_2 generation function are given in the next section.

The remaining parts of the model serve the purpose of providing, in suitable form, information required to solve the equations in the SO_2 absorption calculation. This includes rates of flow of limestone of the different size groups into and out of the bed, and weights and residence times in the bed.

All the comparisons described were obtained using the final version of the model.

A flow chart of the mathematical model computer programme is shown in Fig. 6.1, and the programme itself, in ALGOL, is reproduced at the end of this appendix.

Each of the steps will be discussed in detail, starting with the main SO_2 absorption calculation.

2.1 Absorption Calculation

The validity of this calculation is crucial to the whole model. The assumption has to be made that the rate at which SO_2 is taken up by the limestone in the bed is equal to that measured at the same utilization under the conditions of the laboratory experiments performed as part of Task VIII under the contract.

It is apparent on studying the results obtained in this laboratory programme, that the reaction rate falls off in most cases to a negligibly small value well before 100% utilization of the limestone has been achieved. With limestone 1359, in particular, less than 25% utilization is indicated for 180 μm particles at limiting sulphation, and only just over 10% for 55 μm particles.

On comparing this with some of the results from plant experiments using the same limestone it became apparent that, in the plant, a greater degreee of utilization was being achieved than seemed possible on the basis of the laboratory measurements. There seemed to be only one likely explanation of this behaviour*, that is that attrition of the partly-sulphated particles in the bed was exposing fresh surfaces to the SO_2 laden gas.

---

* It has since been learned that ANL have suggested that the higher than expected degree of utilization may be due to exposure of the stone alternately to oxidising and reducing conditions in the bed.

It was therefore considered imperative to take this factor into account in some way in the mathematical model, even though the time available would permit of only a fairly crude treatment. The way this has been done is as follows:-

> It is assumed that the sulphated particles consist of completely unsulphated cores surrounded by shells of completely sulphated material.

The effect of attrition on particle size is taken into account according to the following equation:-

$$\ln \frac{(x\ )}{(x_o)} = - K_d . t_a / 3600 \qquad (1)$$

where x_o is the characteristic size in the feed material

x is the size after attrition of the sulphated layer

K_d is the attrition coefficient, h^{-1}

t_a is the time required to regenerate the particles, s

If the limiting utilization (i.e. the utilization at which the reactivity falls to zero) is denoted by U_c, then the ratio of thickness of the sulphated shell to particle radius, at utilization U_c is $(1 - (1 - U_c)^{1/3}) : 1$. Thus X/X_o in equation 1 may be replaced by $(1 - U_c)^{1/3}$:-

$$t_a = - \frac{3600}{K_d} \ln (1 - U_c)^{1/3} \qquad (2)$$

The rate of 'regeneration' will be proportional to the chances that a particle will stay in the bed for a time t_a, i.e. $\exp(-t_a/\tau)$, where τ is the mean residence time of particles in the bed. It will also depend on the weight of unused limestone, of each size group in the bed i.e. $W_i (1 - U_i)$. The rate of regeneration (F_R) is therefore given by:-

$$F_{R,i} = \exp(- t_a/\tau_i)\ W_i\ (1 - U_i)/t_a \qquad (3)$$

and the mean utilization of the particles remaining in the bed (U_i^1) to be used for calculating the reaction rate is:

$$U_i^1 = F_i U_i / (F_i + F_{R,i}) \tag{4}$$

The regeneration procedure is only applied to non-elutriated particles. Since the abraded stone is sulphated, it is recommended that when applying this calculation procedure the adjustment of input limestone sizes, to allow for attrition (as described in section 2.3) should not be used in calculating F_i; otherwise there will be an error in the absorption calculation. For calculating bed composition and residence times the adjustment of input sizes can still be used.

The relation between reaction rate and utilization is:-

$$\frac{d(SO_2)i}{dt} = k_i\ (a_{o,i} + a_{1,i}\ U_i + a_{2,i}\ U_i^{\ 2} + a_{3,i}\ U_i^{\ 3}).\ c\ .\ W_i \tag{5}$$

where $\frac{d(SO_2)i}{dt}$ is the rate of SO_2 absorption by particles in size group i, kg/s

k_i is a basic rate constant for size group i, m^3/kgs

$a_{b,i}$ are coefficients derived from laboratory experiment.

c is SO_2 concentration, kg/m^3

The priciples of the absorption calculation procedure have been described in detail by Morgan[5]. The outline principles only will be given here. In the method of calculation employed, the reactivity of a limestone size group is assumed to be the same as that of limestone with a utilization equal to the mean utilization of all particles of that size group in the bed. In fact, of course, there is quite a wide spread of utilizations, due to the fact that there is a wide spread of residence times of particles in the bed. Investigation of a few examples indicated that in most cases the error introduced by this simplification was small - a few percent only. Use of a more exact method, in which reaction is integrated over the range of utilization for each size group would have made the total computing time very much longer.

The mass balance of sulphated limestone in the bed at equilibrium is represented by the set of N simultaneous non-linear equations:

$$\left[f\,(\bar{U}^{1}) - \frac{\bar{U}}{\bar{\tau}k\bar{c}} + \frac{\tau\bar{U}_r}{\bar{\tau}k\bar{c}} \right]_i = 0 \qquad (6)$$

where $f(U)_i = (a_{o,i} + a_{1,i}U_i + a_{2,i}U_i^{\,2} + a_{3,i}U_i^{\,3})$

$\bar{U}_r$ = mean utilization of recycled limestone.

In Equation (6), the first term on the left-hand side represents the rate of absorption of SO_2 by group i; the second term represents the rate at which SO_2 is eliminated from the bed by removal of sulphated limestone from the bed, and the third term represents the rate which SO_2 is returned to the bed in the form of recycled stone.

The calculation permits the solution of this equation for assumed values of (a) the mean reactivity of all the limestone in the bed, and (b) the amount of SO_2 absorbed by limestone dust in the gas space above the bed. (a) is necessary, because the value of U depends on the mean SO_2 concentration, which in turn depends on the mean reactivity of the bed. The procedure used is to input a trial value for mean bed reactivity; calculate the mean SO_2 concentration corresponding to this value; solve Equation (6), by the Newton-Raphson method, using an assumed value for SO_2 absorption above the bed (initially assumed to be zero) in order to obtain $\bar{U}_r$, and so obtain a revised estimate for mean bed reactivity. The process is repeated until satisfactory convergence has been obtained. The SO_2 concentration at the top of the bed is then used to calculate a more exact value for absorption above the bed, assuming plug flow in the gas stream (Equation (7)), and the whole process is repeated again and again until satisfactory convergence is obtained.

$$\frac{d\,(\bar{U})_i}{dt} = k \cdot f\,(\bar{U})_i \cdot c \qquad (7)$$

In practice, it was found that absorption above the bed is very small, and only one iteration is normally required.

Some instability of the solution procedure may arise if K_d, (Equation 1), is greater than 0.03. There has not been time to correct this fault, but it only occurs at values of K_d which are appreciably higher than are likely to occur in practice.

In calculating $\bar{c}$, the mean SO_2 concentration in the bed, an SO_2 generation function is input. This is of the form:

$$c = c_o + \int_0^{z'} \phi(z) \, . \, dz \qquad (8)$$

where c_o is the concentration resulting from SO_2 formation at the bottom of the bed, and $\phi(z)$ is a function giving the rate of concentration increase with height (in the absence of absorption) up to a height z' above the air distributor ($\leq$ bed depth), at which SO_2 generation ceases.

The form of function ϕ used is:

$$\phi\ (z) = 2\beta(z' - z)/(z')^2 \qquad (9)$$

β is a constant.

The use of this function means that the rate of SO_2 generation decreases linearly from a maximum value at $z = 0$ to zero at $z = z'$.

When absorption of SO_2 is occurring, the concentration at height z is given by:

$$\frac{dc}{dz} + Kc - \phi(z) = 0 \qquad (10)$$

where K is a constant characterising the absorptive capacity of the bed.

In the solution procedure, K is an initially unknown parameter. A value is guessed and the true value approached by an iterative process. A formal definition of K, however, is:

$$K = \frac{\lambda}{z_e . M} \sum_{i=1}^{N} \left[F + k \int_0^{U_c} p\ (U)\ f\ (U).dU \right]_i \quad \text{...........} (11)$$

where λ is the mass of SO_2 equivalent to unit mass of calcined limestone M is the volume flowrate of gas

p(U) is probability of particle of utilization U (in range of U corresponding to residence time distribution)

Solution of Equation (10) gives for c_e, the concentration at the top of the bed:

$$c_e = c_o \ \exp\ (-Kz_e) + \int_0^{z_e} \exp \left[-K(z_e - z) \right] \phi\ (z)\ dz \ \text{.....} (12)$$

It can also be shown that $\bar{c}$, the mean concentration, averaged over the height of the bed is:

$$\bar{c} = (c_e' - c_e)/Kz_e \quad \text{........................} (13)$$

where c_e' is the concentration that would be found at the top of the bed in the absence of absorption.

2.2 Input Data

A typical set of input data, as used in simulation of Test Series 4 of Task II, is shown in Table 6.1. This is largely self-explanatory, but where appropriate further details are given in discussion of the following steps.

2.3 Initial Calculations

Volume flow-rates are calculated assuming a fixed gas density of 1.236 kg/m^3 at 273 K and 1 atm pressure, and the weight of bed material is calculated from overall bed volume, voidage (input as data) and a mean density of bed material derived from relative input rates of coal ash and limestone. It is assumed that the carbon content of the bed is negligibly small. The effect of particle attrition on size distribution is taken into account by reducing the median and bottom sizes according to the following equation:

$$x = x_o \exp (- K_d . \tau/3600) \text{ .... } (14)$$

A more complete treatment of attrition in the bed has been developed[2], but in order not to complicate the present model unnecessarily during its development stage, this simple treatment has been used. The general principle behind its adoption is that because of the spread of residence times in the bed (well-stirred reactor principle), some particles will be subjected to very little attrition, while others will be subjected to considerable attrition. Thus the actual spread of sizes will be widened. This has been done in the model by altering the median and bottom sizes of the feed mixture, and keeping the top size the same.

The allocation of the ash and limestone into N groups of sizes respectively 4 to 8 μm, 8 to 16 μm ....2^{N+1} to 2^{N+2} ....2048 to 4096 μm is done using the assumption that the distribution fits a relation of the type:-

$$\log (\text{weight \% undersize}) = m \log (\text{size}) + C \text{ .... } (15)$$

2.4 Calculation of Elutriation Constants

The treatment of elutriation from the bed is based on the postulate that the elutriation constant, K_e is a function of the ratio of gas velocity to the terminal velocity of the particles.

K_e is defined as rate of elutriation divided by the mass of particles in the bed, and has units s^{-1}. Experimental work on elutriation from a cold 12 inch bed at CRE yielded a relation[3].

$$K_e = \frac{0.00732}{z_e} \left(\frac{v_f}{v_t} - 1 \right)^{0.7} \text{ .... } (16)$$

where z_e is the bed depth, m

v_f is superficial gas velocity, m/s

v_t is the terminal velocity of the particle, m/s

Work by Field and Littlejohn[3] suggested that K_e may vary widely according to the design of reactor and the manner of feeding the solids. An empirical constant, n, has therefore been introduced into the model to allow for this uncertainty:-

$$K_e' = K_e^n \quad \text{(17)}$$

The significance of K_e in the computations of sulphur retention is that its reciprocal is equal to the mean residence time of the particles in the bed, before they are elutriated. A low value of K_e is therefore associated with better utilization of that particular size group of particles.

Terminal velocity (v_t) is calculated by applying corrections recommended by Davies[4] to the Stokes velocity(v).

$$v_t = v \times [Re]_t \; / \; [Re]_v \quad \text{(18)}$$

where $[Re]_t$ is the Particle Reynolds number for the terminal velocity
and $[Re]_v$ is the Particle Reynolds number for the Stokes velocity.

The corrections differ according to whether the (Stokes velocity) Reynolds number, $[Re]_v$ is greater than or less than about 5.

For $[Re]_v \leqslant 5$:

$$[Re]_t = \gamma_1 B - \gamma_2 B^2 + \gamma_3 B^3 - \gamma_4 B^4 \quad \text{(19)}$$

and for $[Re]_v > 5$:

$$\log [Re]_t = -\gamma_5 + \gamma_6 \log (B) - \gamma_7 (\log B)^2 + \gamma_8 (\log B)^3 \quad \text{(20)}$$

where $B = 24 [Re]_v$

$\gamma_1 = 1/24$	$\gamma_5 = 1.29536$
$\gamma_2 = 2.3363 \times 10^{-4}$	$\gamma_6 = 0.986$
$\gamma_3 = 2.0154 \times 10^{-6}$	$\gamma_7 = 0.046677$
$\gamma_4 = 6.9105 \times 10^{-9}$	$\gamma_8 = 1.1235 \times 10^{-3}$

In calculation of the gas velocity, the volume occupied by the bed particles is ignored, because it is the velocity in the free gas stream above the bed which determines whether or not a particle will be elutriated.

The value of gas viscosity used in calculation of the terminal velocity is taken to be the same as that of air at the same temperature$^{(T)}$, and an approximation is made to a linear relation for temperatures within 100 to 150°C of 800°C:

$$\mu = 10^{-5}(4.33 + 0.0024(T - 1073)) \text{ Ns/m}^2 \quad \ldots\ldots\ldots\ldots\ldots \quad (21)$$

The mean particle size for each size group used in calculations of terminal velocities is $\bar{x} = (x_1 x_2)^{1/2}$ where x_1, x_2 are the lower and upper particle sizes in the group.

2.5 Adjustment of mass factions of ash and limestone

This adjustment was found to be necessary because of the extreme sensitivity of the model to very small changes in gas velocity under some circumstances.

The sensitivity was due to the fact that whether or not a whole size fraction was elutriated (in the model) depended on whether the gas velocity was greater or less than the terminal velocity corresponding to the mean particle size for the group.

The exact value of the critical velocity for elutriation is calculated, and the mass of the size groups in the feed size distribution, on either side of this critical velocity is adjusted in proportion. The effect of the adjustment is that the mass fraction of the two groups can be increased or decreased by as much as 50%, depending on the ratio of the critical size for elutriation to the geometric mean particle size of the groups.

2.6 Calculation of bed composition

(a) Particles small enough to be elutriated:

In the general case, when solids recycling is being practised, at equilibrium the rate of escape of solids through the cyclone is equal to the feed rate. The loss of fines by overflow is ignored, because it is small compared with the elutriation. If α_i is the cyclone efficiency for particles of size group i, then:

$$G_i = F_i + R_{r,i}$$

$$R_{r,i} = \alpha_i G_i$$

$$\text{hence} \quad G_i = F_i/(1 - \alpha_i) \quad \ldots\ldots\ldots\ldots\ldots\ldots\ldots \quad (22)$$

where G_i is the total mass flow of limestone of size i reaching the cyclone, $F_i R_{r,i}$ are the feed rate and recycle rate respectively of limestone in size group i.

The weight, W_i, of particles of group i in the bed is given by the elutriation equation:

$$G_i = K_e \cdot W_i \quad \text{.................................} \quad (23)$$

Summation of W_i for all groups of elutriable size gives the total weight of elutriable particles in the bed.

(b) Particles not elutriated:

Subtraction of the weight of elutriable particles from the total bed weight gives the weight of non-elutriable particles. This is allocated between the various size groups in the same ratio as exists in the feed.

2.7 Calculation of particle residence times

For elutriable particles, this is the reciprocal of the elutriation constant, otherwise it is the same for all size groups, and is the weight of non-elutriable particles in the bed, divided by the feed rate of non-elutriable particles.

3. FORM OF INPUT DATA FOR MODEL

Most of the data required (Table 6.1) can be derived easily from knowledge of the plant construction, limestone analysis and plant operating conditions. Items requiring further explanation are as follows:-

3.1 Bed voidage: Precise information is not available for each test. The value 0.7 has been used throughout, as being a fairly representative figure for fluidised-bed combustors.

3.2 Densities of ash and limestone: The value 2920 kg/m^3 (182 lb/ft^3) has been taken for the particle density of ash throughout, and a constant value 1578 kg/m^3 (98.5 lb/ft^3) for calcined limestone. It might be argued that there is a case for using the density of limestone before calcination (176 lb/ft^3), since the time taken for calcination is not negligible compared with the residence time of fines in the bed. However, some runs using the higher density value did not show a significant difference in the results, so the matter was not pursued.

3.3 Attrition coefficients: There are no reliable data for these, and a range of values have been tried in order to discover the sensitivity of results to this parameter. It had been hoped to obtain some information on values of attrition coefficients by study of the size distribution of sulphated stone leaving the combustors by various routes, but there was insufficient time to do this.

3.4 Constants in reactivity equation: These are listed, together with values of U_c, the limiting utilization, in Table 2. The curves of reaction rate coefficient vs utilization corresponding to the values of these constants used are compared with the experimentally determined curves in Figs. 2 to 5.

3.5 Recirculation cyclone efficiency: The test series for which model simulations were performed, which used solids recycle were: Task II, Test Series 1, 2 and 4, and Task III, Test Series 2.

On the basis of the cyclone design data, the cyclone efficiencies for the various particle size groups were assumed to be as shown in Table 3.

In addition, to show the general effect upon retention, some runs of the model were made for Task I, assuming the same cyclone efficiency for each particle size group, at a range of efficiencies. Results are shown in Fig. 6.

There is no proof in any test that the cyclones were functioning as they were intended. Any failure of the dip-leg system for returning the collected particles to the bed would reduce the efficiency of the cyclones.

4. GENERAL OBSERVATIONS ON PERFORMANCE OF MODEL

Early experience in running a simpler version of the model not incorporating regeneration by attrition, with input data derived from operating conditions and plant geometry appropriate to Tasks I, II, III and V in the current contract, showed that, in most cases, the predicted retention was equal to or less than the measured retention. Closer examination of the results, particularly of the utilization of each size fraction, showed that there were two principal reasons for the low predicted retentions:

(i) When using previously reported values for elutriation constants, the model predicted that the fine particles would be elutriated from the bed so quickly that they would not have time to react to any great extent.

(ii) As mentioned before, the low values determined in the laboratory for the limiting utilization of the limestones, particularly 1359, meant that if there were no attrition of the sulphated layer, the retention measured on the plant could not possibly be attained. An example of this is in the tests in Task V using limestone 1359. The size distribution of this limestone was such that only 70% of it would be retained in the bed, yet the actual sulphur retention measured at a Ca/S mol ratio of 1 was 44%, in spite of the fact that the laboratory experiments indicated zero reactivity at less than 15% utilization for particles of non-elutriable size. It was because of this fact (which was also apparent in other tasks, to a lesser extent) that the procedure for taking into account the exposure of fresh surfaces by attrition was introduced.

4.1 Elutriation

The two items in the input to the mathematical model which might be expected to have a bearing on the residence time of fines in the system, and about which there is some uncertainty regarding the actual figures to be inserted when preparing the input data, are the elutriation constant, K_e, and the grade efficiencies of the recirculation cyclones - especially when these are internal cyclones. The cyclone efficiency is dependent upon effective functioning of the dip-leg for return of the collected solids to the bed, and these have been a frequent source of trouble in the running of fluidized-bed combustors.

Fig. 7 shows the effect of variation in n, (the exponent applied in the calculation of K'_e (Equation (16)), on predicted retention, and Table 4 shows how increase in n causes an increase in the utilization of particles not quite large enough to be retained in the bed.

4.2 Attrition

The effect of attrition of an outer sulphate layer is most striking in those cases where the limestone reactivity falls off rapidly with increase in sulphation, as in Limestone 1359. Fig. 8 shows how increase in K_d from 0 to 0.025 brings the predicted retention up very markedly to values approaching those found on the plant. The shapes of the predicted and measured curves in Fig. 8 are not alike. As mentioned later (Section 4.3) formation of SO_2 above the bottom of the bed, and gas bypassing in bubbles may be responsible for this difference in shape.

With limestone 18, however, the effect of variation in K_d is not nearly so pronounced (Fig. 9). This is because this limestone is more reactive in a partially sulphated state than is Limestone 1359. The way in which attrition allows fuller utilization of the limestone is illustrated in Table 6. The limiting utilization of this limestone, in the absence of attrition, is 57.4%.

4.3 SO_2 generation pattern

In a few runs with the model, it was assumed that the SO_2, instead of being all generated at the bottom of the bed, is all generated between the bottom and the top of the bed, the rate of generation falling linearly from a maximum at the bottom to zero at the top of the bed. The constants in the generation equation were chosen so that all the sulphur in the coal is converted to SO_2.

One set of results, (Fig. 10) shows that the evolution of SO_2 throughout the bed makes little difference to predicted retention at retentions of less than about 80%, but above this it can account for substantial differences in the shape of the retention curve.

It is impossible to guess at the form of the SO_2 generation function occurring in practical combustors; it will probably depend on the chemical reaction mechanism by which SO_2 is formed from the sulphur compounds in the coal and coal ash, on the vertical profile of oxygen concentration in the bed, and possibly also on the physical behaviour of coal in the bed - swelling or breakage. It is probable, however, that the two cases tried, viz. generation only at the bottom of the bed, and generation throughout the bed represent extremes in between which all the practical systems lie.

4.4 Absorption of SO_2 in the gas spaee above the bed

In all cases this was found to be negligibly small, because of the short residence times of particles above the bed compared with the times needed for significant amounts of reaction.

5. COMPARISONS WITH RESULTS FROM THE CURRENT CONTRACT PROGRAMME

The retentions predicted by the mathematical model are expressed as a percentage of sulphur in the coal fired. There is an implicit assumption that all the sulphur would (in the absence of limestone) be converted to SO_2 and appear in the combustion gases. It is therefore more appropriate to compare the predicted retentions with experimental SO_2 reductions rather than with experimental sulphur retentions since any inaccuracies of the model due to the assumptions of complete sulphur release in the absence of limestone will then be eliminated. This course has been adopted in comparisons for all the Tasks.

5.1 Task I

5.1.1 Test Series 1

This test series used Pittsburgh coal, sized -1/16 in to zero, and Limestone 18 similarly sized. The allocation to particle size groups by the mathematical model gave a good agreement with the actual size distribution in the case of the coal, but not quite so good in the case of the limestone (Fig. 11). The input data to the model were: ash top size 1300 μm, ash median size 460 μm; limestone top size 1200 μm, median size 200 μm and bottom size zero.

It was learned shortly before this Appendix was prepared that the actual bed depth in most of the tests in this series was 2.2 ft, whereas the nominal depth of 2 ft had been used in the computations. The result of this input error would be the slight underestimation of retention. Some idea of the magnitude of the error may be gained by comparing curves A and B in Fig. 12.

The measured SO_2 retention on the plant is higher than the model predicts when using values of n close to 1 especially at a Ca/S mol ratio of about 1 (~~Curve A~~, Fig.9 ~~12~~). Reasons for this have been discussed (4.1 and 4.2), but even when using values for n and K_d which are almost outside the probable ranges, the retention is not predicted correctly. There is obviously some factor which is not correctly simulated in the model. Possibilities are, (a) greater sulphation of the fines in the bed than is predicted by the model and (b) inaccuracies in the procedure used by the model for taking into account the effect of particle attrition.

With regard to the first of these possibilities, it was not possible, for practical reasons, to measure in the laboratory the reaction rate coefficients of very fine particles. However, simple calculation shows that the rates would have to be several orders of magnitudes higher to compensate for the much shorter residence time of the fines as compared with the material which is too coarse to be elutriated. Fig. 13 shows how the residence time varies with mean particle diameter, and also illustrates the effect that variation in n has on the residence time of the fines.

Possible reasons for the different shapes of the retention vs Ca/S mol ratio curves in plant and model in Task I have already been discussed. They are, (a) the generation of SO_2 throughout the bed, and (b) gas bypassing in bubbles passing up through the bed.

5.1.2 Test Series 2

This differed from Test Series 1 in that -1/8 inch to 0 coal and limestone were used, and fluidizing velocities of 8 ft/sec and 4 ft/sec. The comparison shown in Fig. 14 is for an 8 ft/sec test.

A reasonably true fit to the measured retentions is obtained by inserting $K_d = 0.02$ and $n = 3$ in the input data.

5.2 Task II

5.2.1 Test Series 1

These tests were unusual in that the limestone used (U.K. dolomite) contained very little -72 mesh material. In fact, using as input data for the limestone size distribution the values 1588 µm for top size, 700 µm for median size and 300 µm for bottom size, only the size groups $i = 7$, 8 and 9 were represented, and of these only group 7 was elutriated. Hence variation in n might be expected to have relatively little effect, and this was found to be so.

Fig. 15 shows that good agreement is obtained with $n = 1$, by putting K_d equal to 0.025. The measured retention at Ca/S ratio 1.07, if correct, suggests an extremely steep slope of the retention curve, and one must therefore allow for the possibility of error in measurement here.

The curves used to represent the reactivity of the stone (Fig. 3) are the least satisfactory fits to the laboratory data of all the stones. The reason for choosing cubic equations to represent reactivity vs utilization, rather than linear onces, as would appear at first sight to be best, is that it is known that dolomites in general can be sulphated to a much greater extent than limestones, even though the reaction rate may fall to a very low level at high utilizations. The equations for calculating reactivity used in running the model will over-estimate retention, because of the positive error they introduce in the 20-40% utilization range.

The effect of CO_2 partial pressure has been ignored because it was shown in earlier work (Ref. 6, p.2) that partial pressures encountered in fluidised combustion, under these conditions of temperature and pressure, did not seriously affect the reaction rate when using dolomite.

5.2.2 Test Series 2

These tests used Pittsburgh coal and dolomite 1337, again without fines, and having a top size 1588 μm, median size 930 μm and bottom size 400 μm. Once again, therefore, the vàlue taken for the elutriation constant n was not particularly critical.

In choosing the constants a_o to a_3 in the reactivity equation, a similar device was used as in the case of U.K. dolomite, and it was assumed that U_c had values approaching unity (Fig. 4).

Results predicted by the model for the two cases in which all the SO_2 is generated at the bottom of the bed, and all is generated between the bottom and the top of the bed are shown in Fig. 10. As in the previous test series, good agreement is obtained without using high values of the exponent n, but as pointed out above, little of the coal feed was of a size small enough to be elutriated (without breakage) from the bed. The experimental measurements show that the case in which SO_2 is evolved throughout the bed gives the best-fitting curve.

5.2.3 Test Series 4

This series again used Pittsburgh coal and dolomite 1337. The dolomite had a wide size distribution -1600 μm to zero - and the procedure used by the model for allocating mass fractions to size groups gave a close agreement with the actual size distribution.

In contrast to the earlier test series in Task II, the model in this case underestimated the retention (Fig. 16). Since the main difference between this test and Test Series 2 is in the size distribution of the limestone, it may reasonably be inferred that the discrepancy lies in the fact that the model predicts that the fines will be elutriated from the bed before they have had time to react to any great extent. Fig. 16 shows how an increase in n brings the predicted retention up towards the measured values.

5.3 Task III

Only one comparison has been made for Task III, namely with Test Series 2, in which a range of Ca/S ratios was used in the course of a run of long duration, using Pittsburgh coal and Limestone 18, both sized 3200 μm to zero. The combustor incorporated an internal recirculation cyclone, designed to collect particles larger than 50 μm in size; and the assumed values of α appropriate to the different size groups are shown in Table 3.

The predicted retentions for two cases are shown, together with measured SO_2 reductions in Fig. 17. The solid line represents the case in which all the SO_2 is formed at the bottom of the bed, and $n = 1$; the broken line represents the case in which the SO_2 is all formed between the bottom and the top of the bed, and $n = 0.6$. It should be noted that it was on this combustor that Field and Littlejohn[3] determined elutration rates using a radioactive labelled tracer in the coal feed. The values they found corresponded to a value for n of only about 0.6, but these values were determined when firing a coarse coal (1/4 in to zero), which required a high velocity in the transport air. It was suspected that this air initiated bubbles which caused the elutriation of a lot of the fines before they mixed in with the bed.

When putting n equal to 0.6 the model predicts very closely the retention that was found in practice. The only two tests which fall appreciably off the line given by the model are 2.16.1 and 2.16.2, neither of which used recycle of fines, so that the input data for the model was not strictly applicable to these two tests.

5.4 Task V

The only comparison made for Task V was with the experiments in Test Series 1 which used 10 mesh to zero coal and limestone (1359) and a fluidizing velocity of 3 ft/s. The comparison is shown in Fig. 8 which well illustrates the importance of attrition when using this limestone.

There is little doubt that the better retention achieved later in tests 3.5 and 3.6 using -120 mesh limestone was due to the higher limiting utilization possible with fine particles, although because the laboratory method for measuring reaction rates could not be used for very fine particles this cannot be confirmed. The model would predict an opposing effect due to increased elutriation of the finer limestone, so once again there seems to be something that requires further clarification, i.e. how the fines are able to pick up so much SO_2 in the limited time available.

5.5 Pope, Evans and Robbins Data

In an attempt to reduce this data[7] to a form more suitable for comparison with the mathematical model, a statistical treatment of the results was carried out.[8] This showed that over the range of experimental conditions, retention data could be fitted (for one size of a particular limestone) by an equation containing only temperature and stoichiometric ratio as variables.

Comparisons were made for the cases in which (a) coarse and (b) fine Limestone 1359 were used with unwashed coal (10.7% ash), and (c) fine Limestone 1359 was used with washed coal (7.2% ash). The top, median and bottom sizes respectively for coarse limestone were estimated to be 1400 μm, 1200 μm and 1000 μm respectively (-14 + 18 U.S. mesh), and for fine limestone 432 μm, 216 μm and 0 μm respectively (-325 U.S. mesh).

Rate data, the same as determined in the present Task VIII experiments, was used; K_d for coal ash and limestone was taken as 0.02, and n as 1.0.

The statistical correlations indicated the following equations for retention:

Case (a):

$$R = \exp(-2.8603 + 1.180 \ln y + 5920/T)$$

Cases (b) and (c):

$$R = \exp(2.4312 + 0.562 \ln y + 0.194 \ln t + 1797/T)$$

where R is percentage retention;

y is Ca/S mol ratio
t is gas residence time (seconds)
T is bed temperature (K)

Retentions predicted by the model ($n = 1$ and $K_d = 0.02$) and as given by the above two equations are plotted in Fig. 18.

There is no similarity at all between the predicted retentions and those derived from the statistical analysis. In particular, whereas the plant gave better retention when using fine limestone, the model predicts very low retention. No explanation can be offered for these differences. Lack of familiarity with the PER plant and experimental techniques prevents any helpful speculation.

6. DISCUSSION

Probably the most outstanding feature that has come to light in application and testing of the model against plant data is that whereas agreement is in general good when the limestone fed to the bed does not have a very large fraction of material fine enough to be elutriated; the predicted retention is lower than measured when there are significant amounts of fines. This is well illustrated by comparing Test Series 2 and 4 of Task II (Figs. 10 and 16) and also by the Pope, Evans and Robbins results.

This indicates a serious lack of knowledge, at present, concerning the mechanism by which fine particles are elutriated from the bed. The procedure used in the model to calculate terminal velocities is well-established, and has been tested independently and shown to give values that agree well with practical experience. Published data on elutriation constants shows a wide scatter[3, 9], but to account for the utilization of the fines in some of the plants, for example the 36 in x 18 in combustor used in Task I, requires the use of elutriation constants well outside the scatter of existing data.

Amongst possible explanations, neither of which can be strongly argued on technical grounds, are (a) that the particles become sticky when in the combustor, so that the fines tend to adhere to larger particles, and (b) that the fines adhere to refractory or metal surfaces above the bed and remain there for long enough to absorb appreciable amounts of SO_2 before breaking away again. More detailed study of the mass balances made in the experimental programmes, and of the distribution of sulphur between the various particle sizes in the effluent might throw more light on this question, but lack of time has not allowed a systematic analysis of the results with this objective.

The other major result of the comparisons made between the model and the plants was the development of a fairly simple procedure for incorporation in the model to allow for the exposure of fresh limestone surfaces by attrition. Inspection of the plant measurements, alongside the laboratory reactivity measurements, shows that a higher degree of utilization is often achieved in the plant than would seem possible from the laboratory experiments.

It has been suggested recently that exposure of the limestone alternately to oxidising and reducing conditions might lead to greater penetration of sulphur than under continuously oxidising conditions. It cannot be said, at present, whether this is the true explanation, or whether attrition by itself, or a combination of the two is the cause. The simple expedient adopted in the model works satisfactorily, however, and any further development of the model should include an attempt to correlate K_d as used in the model with a laboratory index of degradability.

Study of the general shape of the experimental curves of retention against Ca/S ratio, and comparison with the curves predicted by the model for the two extreme cases of SO_2 evolution pattern (i.e. all at the bottom of the bed or all within the bed) shows that the case in which the SO_2 is assumed to be all evolved within the bed gives curves closest in shape to the experimental ones (Figs. 10 and 17).

The curves fitting the experimental results in Figs. 9, 12, 14 and 16 also show a steeper gradient close to the origin and a less steep gradient at high Ca/S ratios than the curves given by the model when assuming SO_2 evolution all at the bottom of the bed. A better fit could probably be obtained by assuming evolution throughout the bed, but there has not been time to do the computing required to verify this.

When the construction of a mathematical model was first undertaken, it was visualized that benefits would result in two directions: firstly, by throwing light on the relative importance of the various mechanisms entering into the process the direction in which further effort might be most profitably employed would be indicated; and secondly, the model could be used, in conjunction with laboratory measurements to predict the performance of a new plant or limestone, e.g. for purposes of an economic assessment.

The first of these aims can be said to have met with a fair measure of success, in that aspects of plant behaviour which have a marked effect upon retention have been shown up. The second aim cannot yet be regarded as having been fully achieved. Whilst the performance of individual plants can be satisfactorily explained by the model, there are differences between one plant and another that can best be explained by differences in the rate of elutriation of fines and in the rate of particle attrition between the various plants. The reasons for these differences, and how to predict them from a knowledge of plant design is not yet clear, and it is recommended that any future work should include attempts to gain a better understanding of these aspects.

The following summarises the general predictions given by the model of the effects of major input variables on retention:

(i) Bed height

Increase in bed height causes an increase in retention for given firing rate and ratio of Ca/S in the feed. (Fig. 12). This increase in retention is due mainly to the increase in residence time of limestone in the bed, allowing greater sulphation of the particles. An alternative way of looking at it is that the gas has a greater opportunity of coming into contact with limestone particles during its passage through the bed, because there is a greater weight of limestone in the bed. The two explanations are not inconsistent, but the mathematical model approach concentrates on the former.

(ii) Calcium: sulphur ratio

The model is not constructed in such a way that the effect of Ca/S ratio can be reduced to a simple analytical equation. The general shape of most of the curves of retention against Ca/S ratio is a progressively diminishing gradient, but whereas in some cases (e.g. curve B in Fig. 12) the gradient is steep up to over 90% retention, in others (e.g. curve C in the same figure) a more gradual decrease in gradient occurs. The model predicts 100% retention, when there is a sufficiently high Ca/S ratio, and when it is assumed that all the SO_2 is formed at the bottom of the bed. When it is assumed that SO_2 is formed throughout the bed however, 100% retention may not be reached at all. This mode of SO_2 release appears the more likely.

The effect of increasing Ca/S ratio, other conditions being unchanged, is to increase the weight of limestone in the bed, and to decrease the utilization of the stone, at the same time decreasing the mean SO_2 concentration in the gas stream. The interrelation of these quantities is determined by the reactivity function, f (U), and solution requires an iterative process as in the model.

(iii) Gas velocity

Alteration of gas velocity is difficult in practice without at the same time altering other variables. For example, when doubling the air flowrate, the coal rate must also be doubled in order to keep combustion conditions comparable. This means that the SO_2 generation pattern may be altered. Also, the limestone addition rate has to be doubled in order to keep the Ca:S ratio the same.

The model predicts two effects, both acting in the same direction. Firstly, because the limestone throughput is doubled for the same bed capacity, its residence time will be halved, and the time available for its sulphation will be halved. Less efficient use of stone will result, and retentions will be lower (compare curves A and C, B and D in Fig. 12). The second effect is that because of the higher velocities a greater proportion of the limestone feed will be elutriated, and the residence time of these particles will be reduced very greatly. The importance of this will depend upon the size distribution of the acceptor.

As stated earlier, the model contains the assumption that gas/solids contact time is not a rate-controlling factor. The reduction in contact time on increasing gas velocity does not therefore have any effect upon retention.

Fig. 12 predicts that the fall-off in retention caused by increasing fluidising velocity can be recovered by increasing the bed depth approximately in proportion to the increase in velocity. This may not be economic with operation at atmospheric pressure, but may be acceptable in pressurized combustors.

(iv) Particle size

Reduction in particle size, other conditions being the same, results in more elutriation of the stone. Indications from laboratory measurements of reaction rate are that the increase in reactivity with decrease in size is not sufficient to compensate for the decreased residence time, and a reduction in retention is predicted, (Fig. 18). It might be expected that with very fine particles a minimum retention might be reached, beyond which increase in specific surface area outweighs decrease in residence time, but laboratory rate data for such fine particles are not available.

(v) Temperature

Temperature can be expected to influence sulphur retention mainly via its effect on the rate of reaction between lime and SO_2. Feeding the data from laboratory measurements of the effect of temperature on reaction rate for limestone 18 into the model led to predictions which showed the correct trends, but under-predicted the magnitude of the effect, Fig. 19.

(vi) Recycle

The model predicts that efficient recycling of elutriated fine particles should improve the sulphur retention (Fig. 6).

Confirmation of this prediction by the plant experimental results is not positive, because the number of comparisons made was not as great as was originally hoped, and there is some uncertainty also as to whether or not the experimental recycle systems were always operating as intended. This may be the reason why two tests showed no improvement in retention when using recycle, while others (Table 7) showed a substantial improvement. For example in Task I, Test Series 4 at 2 ft/s the sulphur retention was increased from 86% at a Ca/S mol ratio of 2.2 to 99% at a ratio of 1.6 by recycling of fines, whereas in Task III, two comparisons showed an improvement in retention after adjusting for Ca/S ratio, one showed little difference, and one showed an adverse effect.

Table A6.7 Effect of recycling fines

Test No.	Test No.	Acceptor size, µm	Velocity ft/s	Ca/S mol ratio	Recycle	SO_2 reduction %
I	4.5	-1680	2.1	2.2	No	86
I	4.6	-1680	2.2	1.6	Yes	99
III	2.9	-150	8.1	1.5*	No	50*
III	2.4	-150	8.1	1.9	Yes	32
III	2.16	-3175	8.1	2.2*	No	60*
III	2.1	-3175	8.1	1.6	Yes	55
III	3.3	-3175	6.6	2.8	No	82
III	3.1	-3175	6.4	2.7	Yes	85
III	3.4	-3175	10.9	2.6	No	77
III	3.2	-3175	10.8	2.7	Yes	77

* Average of results for two tests.

7. COMPUTER PROGRAMME

The following four pages contain a print-out of the programme finally developed, in Elliott-Algol code, for running the mathematical model on an /Elliott 4120 series computer.

```
"FOR"I:=CONSTB"STEP"1"UNTIL"COUNT"DO""BEGIN"
UF:=2↑(2*I+3)/⏨12;VEL(K2,UF,RHOG,MU,UTL);
"IF"LI/UTL<1"THEN""BEGIN"KAPPAL[I]:=0;"GOTO"AVOID2"END";
KAPPAL[I]:=(Y*(LI/UTL-1)↑.7)↑FF;
AVOID2:"IF"KAPPAL[I]>⏨-4"THEN"KL[I]:="TRUE""ELSE"
"BEGIN""IF"KL[I-1]"THEN"IA:=I-1;KL[I]:="FALSE""END";
"IF"KAPPAL[I]>RT"THEN"KAPPAL[I]:=RT;
"END";
FRED: UF:=2↑(2*IA+3)/⏨12*(1+G/10);
"IF"G=31"THEN""GOTO"MILLIE"ELSE"VEL(K2,UF,RHOG,MU,UTL);
"IF"LI/UTL<1"THEN""BEGIN"KAP:=0;"GOTO"AVOID4"END";
KAP:=(Y*(LI/UTL-1)↑.7)↑FF;
AVOID4:"IF"KAP>⏨-4"THEN""BEGIN"G:=G+1;"GOTO"FRED"END";
MILLIE:FRL[IA]:=FRL[IA]/2+.016667*G*(FRL[IA]+FRL[IA+1]);
FRL[IA+1]:=FRL[IA+1]+FRL[IA]/2-.016667*G*(FRL[IA]+FRL[IA+1]);

"COMMENT" CALCULATIONS OF BED COMPOSITION;
BWNE:=BW; WAOF[0]:=WLOF[0]:=0;
"FOR"I:=CONSTA"STEP"1"UNTIL"COUNTA"DO""BEGIN"
"IF"KA[I]"THEN"
"BEGIN"WACO[I]:=FRA[I]*ASHR/(1-CYC[I]); WAB[I]:=WACO[I]/KAPPAA[I];
      WAOF[I]:=0; BWNE:=BWNE-WAB[I] "END" "ELSE"
"BEGIN"WACO[I]:=0; WAOF[I]:=FRA[I]*ASHR "END";
WAOF[0]:=WAOF[0]+WAOF[I];"END";
"FOR"I:=CONSTB"STEP"1"UNTIL"COUNT"DO""BEGIN"
"IF"KL[I]"THEN"
"BEGIN"WLCO[I]:=FRL[I]*VAR[3]/(1-CYC[I]);
      WLB[I]:=WLCO[I]/KAPPAL[I]; WLOF[I]:=0;BWNE:=BWNE-WLB[I]
"END""ELSE""BEGIN"
      WLCO[I]:=0; WLOF[I]:=FRL[I]*VAR[3] "END";
 WLOF[0]:=WLOF[0]+WLOF[I];FR[I]:=FRL[I]*VAR[3]
"END";
OFR:=WAOF[0]+WLOF[0]; TB:=BWNE/OFR; CONST:=COUNT;
"FOR"I:=CONSTA"STEP"1"UNTIL"COUNTA"DO"
"IF""NOT"KA[I]"THEN"WAB[I]:=WAOF[I]*TB;
"FOR"I:=CONSTB"STEP"1"UNTIL"COUNT"DO""IF""NOT"KL[I]"THEN""BEGIN"
WLB[I]:=WLOF[I]*TB;
CONST:=CONST-1 "END";

"IF"KEY(5)"THEN""BEGIN"P(KAPPAA);PL(KAPPAL);P(WAB);PL(WLB);
      P(WACO);PL(WLCO);P(WAOF);PL(WLOF);"PRINT"''L'',FREEPOINT(6),DIGITS(2),
      BW,BWNE,OFR,TB,CONST "END";
 "COMMENT" CALCULATIONS PRELIMINARY TO SOLUTION OF
      ABSORPTION EQUATIONS;
"FOR"I:=CONSTB"STEP"1"UNTIL"COUNT"DO"
TBAR[I]:="IF"KL[I]"THEN"1/KAPPAL[I]"ELSE"TB;
"FOR"I:=CONSTB"STEP"1"UNTIL"CONST"DO"UFAC[I]:=1;
"FOR"I:=(CONST+1)"STEP"1"UNTIL"COUNT"DO""BEGIN"
RE:=(1-UC[I])↑.3333;"IF"KDL>⏨-6"THEN""BEGIN"UFAC[I]:=-LN(RE)/KDL*3600;
UFAC[I]:=FR[I]/(FR[I]+WLB[I]/UFAC[I]*EXP(-UFAC[I]/TBAR[I]));
"IF"KEY(6)"THEN""PRINT"''L'',FREEPOINT(6),UFAC[I]"END""ELSE"UFAC[I]:=1"END";
"FOR"I:=CONSTB"STEP"1"UNTIL"COUNT"DO"
"BEGIN"
"IF""NOT"KL[I]"THEN"CYC[I]:=0; GR[I]:=FR[I]/(1.0-CYC[I]);
XX:=TBAR[I]*KS[I]; BMT:=BMT+WLB[I]; FRT:=FRT+FR[I];
GRT:=GRT+GR[I]; RATIO[I]:=SR*GR[I]/CVR; U[I]:=.2;
QQ[I]:=XX; EPS[I]:=0.0;KG[I]:=GR[I]*XX*SR*RHOG/(MFR*Z);"END";
```

```
"COMMENT" WITH FIXED CORRECTION, SOLVE BY APPROXIMATE METHOD;
DON:"PRINT"''L`TYPE TRIAL VALUE OF KK`;"READ"READER(3),KK;
CYCLE:MEP:=MEZ;
NELLY:EMS(KK);XX:=0.0;"FOR"I:=CONSTB"STEP"1"UNTIL"COUNT"DO"
"BEGIN"UP:=U[I];YY:=1.0/QQ[I]/MBAR;X1:=YY*(1.0-CYC[I]);
X2:=CYC[I]*EPS[I]*YY;UCI:=UC[I];
"COMMENT" FIND UI, USING CURRENT MBAR;
ROOT:RE:=(1-UP*(1-UFAC[I]))/UFAC[I];RE:=1/RE;
UFUN(UP*RE);F0:=FU-UP*X1+X2;F1:=FU1-X1;
"IF"KEY(2)"THEN""PRINT"''L``,FREEPOINT(6),UP,FU,FU1,F0,F1;
UN:="IF"ABS(F1)>₁₀-6"THEN"UP-F0/F1"ELSE"UP;
"IF"UN>1"THEN"UN:=1;"IF"UN<0"THEN"UN:=0;
"IF"ABS(UN-UP)>₁₀-4"THEN""BEGIN"UP:=UN;"GOTO"ROOT"END";
"COMMENT" REVISE ESTIMATE OF K;
U[I]:=UN;"IF"U[I]>1"THEN"U[I]:=UN:=1;UFUN(UN*RE);PORT[I]:=KG[I]*FU;
"IF"UN*RE>UCI"THEN""BEGIN"U[I]:=UCI/RE;PORT[I]:=0.0"END";
XX:=XX+PORT[I]"END";
"COMMENT" TEST CHANGE IN K;"IF"KEY(4)"THEN"
"PRINT"''L``,FREEPOINT(6),ME,MBAR,XX;
"IF"KEY(3)"THEN"WAIT;"IF"KEY(3)"THEN"
"BEGIN""PRINT"''L``,FREEPOINT(6),XX;"GOTO"DON"END";"IF"ABS((MEP-ME)
      /(MEP+ME))>₁₀-4"THEN""BEGIN"
MEP:=ME;KK:=XX; "GOTO"NELLY"END";
"PRINT"FREEPOINT(6),CVR*(MEZ-ME)/SR/FRT,XX;

"COMMENT" NEW ESTIMATE OF ABSORPTION ABOVE BED;
XX:=M:=ME;"FOR"I:=CONSTB"STEP"1"UNTIL"CONST"DO"UL[I]:=U[I];
"FOR"J:=1"STEP"1"UNTIL"NG"DO""BEGIN"
"FOR"I:=CONSTB"STEP"1"UNTIL"CONST"DO""BEGIN"UP:=UL[I];UFUN(UP);
UCI:=UC[I];
DEL:=DT*KS[I]*FU*M;UN:=UP+DEL;
"IF"UN>UCI"THEN""BEGIN"UN:=UCI;DEL:=UCI-UP"END";
XX:=XX-DEL*RATIO[I];UL[I]:=UN"END";M:=XX"END";

"PRINT"''L``,FREEPOINT(6),M,''L2``;

"COMMENT" TEST CHANGE AT CYCLONE;
"IF"ABS(MC-M)/(MC+M)>₁₀-4"THEN""BEGIN"MC:=M;
"FOR"I:=CONSTB"STEP"1"UNTIL"CONST"DO"EPS[I]:=UL[I]-U[I];
"IF"KEY(3)"THEN"WAIT;"IF"KEY(3)"THEN""GOTO"DON"ELSE""GOTO"CYCLE
"END""END";

"COMMENT" OUTPUT RESULTS;
PUNCH(1);"PRINT"''R50L``,FREEPOINT(5),
''L`AIR RATE = `,VAR[1],' KG/S'L`COAL RATE = `,
VAR[2],'KG/S'L`LIME RATE = `,VAR[3],'KG/S'L1``,
''L`MASS FLOW OF SO2 IN ABSENCE OF ABSORPTION = `,
FREEPOINT(6),MFS,' KG/S`,
''L`                    AT EXIT FROM BED           = `,ME*CVR,
''L`                    AT CYCLONE                 = `,M*CVR,
''L`EFFECTIVE RATIO OF FLOWS, CAO/SO2              = `,SR*FRT/MFS,
''L`PERCENTAGE RETENTION OF SO2'S15`= `,(MFS-M*CVR)*100/MFS,
''L2`PARTICLE GROUP     UTILISATION IN BED     UTILISATION AT CYC.`;
"FOR"I:=CONSTB"STEP"1"UNTIL"COUNT"DO""BEGIN"
"PRINT"''LS5``,DIGITS(2),I,''S19``,ALIGNED(1,3),U[I];
"IF"I"LE"CONST"THEN""PRINT"''S15``,ALIGNED(1,3),UL[I]"ELSE"
"PRINT"''S17`-`;"END";"PRINT"''LH``;
VAR[3]:=VAR[3]+ZZZ;"IF"SR*FRT/MFS<3.0"THEN""GOTO"RAT;
"END""END";
```

```
KORANGAR6 DWG EX FVB AND BBM;

"BEGIN""INTEGER"CONST,CONSTA,CONSTB,CONSTG,COUNT,COUNTA,G,IA,
     I,J,JJ,NG;
"REAL"ASH,ASHR,B2,BEDD,BEDR,BETA,BMT,BSA,BSL,BSLR,BW,BWNE,CAO,CFR,CVR,
DB,DEL,DT,DVOL,DZ,F0,F1,FF,FRT,FU,FU1,GRT,INT,K1,K2,KAP,KDA,KDL,KK,LI,
M,M0,MBAR,MC,ME,MEP,MFZ,MFR,MFS,MSA,MSAR,MSL,MSLR,MT,MU,OFR,PA,PN,PP,RE,
RHOA,RHOG,RHOL,RT,RTAB,S,SFR,SR,TB,TSA,TSL,UCI,UF,UN,UP,UTA,UTL,V,VB,
VC,VG,VOID,VOL,WS,X1,X2,XX,Y,YY,Z,ZH,ZZ,ZZZ,BETA1.M1;
"INTEGER""ARRAY"N[1:5];
"REAL""ARRAY"AA[1:10,0:3],CYC,EPS,FR,GR,KAPPAA,KAPPAL,
KG,KS,PORT,QQ,RATIO,TBAR,U,UC,UFAC,UL,WAB,WACO,WLB,WLCO[1:10],E[1:6],
INC,VAR[1:5],FRA,FRL,WAOF,WLOF[0:11];
"BOOLEAN""ARRAY"KA,KL[1:10];   PREFIX(' ');PUNCH(3);
"BEGIN"

"PROCEDURE" P(A); "ARRAY"A;
"BEGIN""PRINT"''L'',DIGITS(2),CONSTA,SAMELINE,' - ',COUNTA,
''L'';"FOR"I:=CONSTA"STEP"1"UNTIL"COUNTA"DO""BEGIN""PRINT"
SAMELINE,SCALED(3),A[I];"IF"I=5"THEN""PRINT"''LS6''"END""END";

"PROCEDURE" PL(A);      "ARRAY"A;
"BEGIN""PRINT"''L'',DIGITS(2),CONSTB,SAMELINE,' - ',COUNT,
''L'';"FOR"I:=CONSTB"STEP"1"UNTIL"COUNT"DO""BEGIN""PRINT"
SAMELINE,SCALED(3),A[I];"IF"I=5"THEN""PRINT"''LS6''"END""END";

"BOOLEAN""PROCEDURE"KEY(N);
"VALUE"N;"INTEGER"N;
"BEGIN""BOOLEAN"BOO:
"CODE"%DECS$N
      %LDK$N
      %CTOM
      %SMRL
      %AND:L$1
      %ST$BOO
;KEY:="NOT"BOO"END";

"PROCEDURE" WEIGHT(A,B,C,D);
"ARRAY"A; "REAL"B,C,D;
"BEGIN""INTEGER"X;"REAL"L;
L:=LN(2);K1:=L/LN(B/C);K2:=-K1*LN(B);X:=4096;
"FOR"I:=0"STEP"1"UNTIL"11"DO"A[I]:=0;I:=11;
TRYT:"IF"B"LE"X"THEN""BEGIN"I:=I-1;X:=X"DIV"2;
      "GOTO"TRYT"END"; X:=4;COUNT:=I;A[I]:=1;I:=I-1;CONSTB:=0;
TRYB:"IF"D"GE"X"THEN""BEGIN"CONSTB:=CONSTB+1;X:=X*2;
      "GOTO"TRYB"END";
"FOR"I:=CONSTB"STEP"1"UNTIL"COUNT-1"DO"A[I]:=EXP(K1*L*(I+2)+K2);
"FOR"I:=COUNT"STEP"-1"UNTIL"CONSTB"DO"A[I]:=A[I]-A[I-1];
"IF"KEY(6)"THEN"PL(A);
"END" OF PROCEDURE FOR ALLOCATING PARTICLE SIZE GROUPS;

"PROCEDURE"VEL(A,B,C,D,E);"REAL"A,B,C,D,E;
"BEGIN"E:=A*B;RE:=C*E*SQRT(B)/D;RE:=24*RE;
"IF"RE<120"THEN"MEP:=RE/24+RE*RE*(-2.3363₁₀-4+RE*
      (2.0154₁₀-6-RE*6.9105₁₀-9))"ELSE"
"BEGIN"XX:=LN(RE)/2.30258;MEP:=EXP(2.30258*(-1.29536+
XX*(.986-XX*(.046677-1.1235₁₀-3*XX))))"END";
E:=E*MEP*24/RE;  "IF"KEY(2)"THEN""PRINT"''L'',FREEPOINT(6),E
"END"OF PROCEDURE FOR TERMINAL VELOCITY;
```

```
 PROCEDURE" UFUN(U);  "VALUE"U; "REAL"U;
"BEGIN"FU:=AA[I,0]+U*(AA[I,1]+U*(AA[I,2]+U*AA[I,3]));
       FU1:=AA[I,1]+U*(2.0*AA[I,2]+U*3.0*AA[I,3]);
"END";

"REAL""PROCEDURE"GEN(ZZ); "VALUE"ZZ; "REAL"ZZ;
GEN:="IF"ZZ<ZH"THEN"B2*(ZH-ZZ)/(ZH*ZH) "ELSE" 0.0;

"PROCEDURE" EMS(KK); "VALUE"KK; "REAL"KK;
"BEGIN"INT:=0.0;PP:=GEN(0.0);X1:=KK*Z;
"FOR"I:=1"STEP"1"UNTIL"JJ"DO""BEGIN"ZZ:=I*DZ;X2:=EXP(-KK*ZZ);
     PN:=GEN(ZZ)/X2;INT:=INT+.5*(PP+PN)*DZ;PP:=PN;
"END";
ME:=(M0+INT)*EXP(-X1); MBAR:=(MEZ-ME)/X1;
"END" OF PROCEDURE FOR ME AND MBAR;


"COMMENT" INPUT DATA AND PERFORM INITIAL CALCULATIONS.
"READ"PA,DB,Z,VOL,VOID,FF,ASH,S,TSA,MSAR,TSL,MSLR,BSLR,RHOA,RHOL,
KDA,KDL,CAO,M1,ZH,BETA1,VAR[1],VAR[2],VAR[3],VAR[4],ZZZ,NG,JJ;
"FOR"I:=1"STEP"1"UNTIL"10"DO"
"READ"UC[I],KS[I],CYC[I],AA[I,0],AA[I,1],AA[I,2],AA[I,3];
RAT:"BEGIN"PREFIX(' ');PUNCH(3);
VC:=.7854*DB*DB*Z;            VG:=VC*VOID;
VB:=VC-VG;                    MFR:=VAR[1]+VAR[2]*(1-ASH/100);
CVR:=MFR*VAR[4]/337.8/PA;        RHOG:=MFR/CVR;
ASHR:=VAR[2]*ASH/100;         SFR:=2*S*VAR[2]/100;
MT:=SFR/CVR;                  BEDR:=ASHR+VAR[3];
BEDD:=BEDR/(ASHR/RHOA+VAR[3]/RHOL);
BW:=VB*BEDD;                  TB:=BW/BEDR;
MSA:=MSAR*EXP(-KDA/3600*TB);
MSL:=MSLR*EXP(-KDL/3600*TB);BSL:=BSLR*EXP(-KDL/3600*TB);
"IF"BSL<4"THEN"BSL:=4;
WS:=CAO/100;                  BSA:=4;

WEIGHT(FRA,TSA,MSA,BSA); CONSTA:=CONSTB;COUNTA:=COUNT;
 WEIGHT(FRL,TSL,MSL,BSL);
SR:=1.14286*WS; M0:=M1*MT; BETA:=BETA1*MT; B2:=2.0*BETA;
MEZ:=M0+BETA; BMT:=FRT:=GRT:=0.0; MFS:=CVR*MEZ;
RTAB:=VOL/CVR; DT:=RTAB/NG; MC:=MEZ; DZ:=Z/JJ;

"COMMENT" CALCULATION OF ELUTRIATION CONSTANTS;
MU:=(4.33+.0024*(VAR[4]-1073))*⏨-5; LI:=CVR*Z/VC;
Y:=.0073/Z;K1:=(RHOA-RHOG)*9.81/18/MU;K2:=(RHOL-RHOG)
   *9.81/18/MU; RT:=CVR/VG;G:=1;
"FOR"I:=CONSTA"STEP"1"UNTIL"COUNTA"DO""BEGIN"
UF:=2↑(2*I+3)/⏨12;VEL(K1,UF,RHOG,MU,UTA);
"IF"LI/UTA<1"THEN""BEGIN"KAPPAA[I]:=0;"GOTO"AVOID1"END";
KAPPAA[I]:=(Y*(LI/UTA-1)↑.7)↑FF;
AVOID1:"IF"KAPPAA[I]>⏨-4"THEN"KA[I]:="TRUE""ELSE"
"BEGIN""IF"KA[I-1]"THEN"IA:=I-1;KA[I]:="FALSE""END";
"IF"KAPPAA[I]>RT"THEN"KAPPAA[I]:=RT;"END";
JOE:UF:=2↑(2*IA+3)/⏨12*(1+G/10);
"IF"G=31"THEN""GOTO"JENNY"ELSE"VEL(K1,UF,RHOG,MU,UTA);
"IF"LI/UTA<1"THEN""BEGIN"KAP:=0;"GOTO"AVOID3"END";
KAP:=(Y*(LI/UTA-1)↑.7)↑FF;
AVOID3:"IF"KAP>⏨-4"THEN""BEGIN"G:=G+1;"GOTO"JOE"END":
JENNY:FRA[IA]:=FRA[IA]/2+.016667*G*(FRA[IA]+FRA[IA+1]);
FRA[IA+1]:=FRA[IA+1]+FRA[IA]/2-.016667*G*(FRA[IA]+FRA[IA+1]);
G:=1;
```

ACKNOWLEDGEMENTS

The authors are grateful to Mr. D. Stockwell for checking the presentation of the mathematics in this report, and for suggestions for its improvement, and to Dr. A.D. Dainton, Mr. H.R. Hoy, Mr. E.L. Carls and Mr. J. Highley for helpful comments on the earlier drafts.

ADDENDUM

Further examination of the results of the reactivity measurements (reported in Appendix 8, section7), has shown that the experimental method used could have led to underestimation of the rate constants for stone of low utilization and fine particle size, especially in the case of Limestone 18.

It is not possible to estimate the magnitude of the error, but it is believed that it could account for the discrepancies between the predictions of the model and the measured values of sulphur retention effected by the small, elutriable particles (e.g. in Task I). A note explaining how this error arises is included in Appendix 8.

REFERENCES

(1) Argonne National Laboratories. Document No. ANL/ES/CEN-F 025, November 1970, Appendix B.

(2) Merrick, D. 'A mathematical model of the behaviour of ash in a fluidized bed combustor and recycle system'. CRE F.C. Section Report 60; August 1970.

(3) M A Field and R F Littlejohn: 'Measurement of the residence time of fine particles in a pilot-scale fluidized-bed combustor', BCURA Report to NCB, Doc.DIB/35, June 1970.

(4) C N Davies: Proc.Phys.Soc., Lond., 57, 259. (1945).

(5) B B Morgan: 'Calculation of Retention of Sulphur Dioxide by Limestone in a Fluidized Bed', BCURA Report to NCB. Doc.No. CT/19, March 1971.

'Addition of Recycling to Calculation of Retention of Sulphur Dioxide by Limestone in a Fluidized Bed', BCURA Mathematics Note No. 112, March 1971.

(6) F V Bethell: 'The Absorption of Sulphur Dioxide by Eleven British Limestones' BCURA Document No. FCP 5, October 1969.

(7) Pope, Evans and Robbins, reports to NAPCA on development work on fluidized bed combustion, Nos. 42, 43, 47-54 inclusive.

(8) F V Bethell: 'Retention of Sulphur in Fluid-Bed Combustion: Analysis of Pope, Evans and Robbins Data'. BCURA Document No. CT/13/1, November, 1970.

(9) D Kunii and O Levenspiel: 'Fluidisation Engineering', J Wiley and Sons Inc., 1968, pp 312-324.

NOMENCLATURE

Note: All limestone weights are expressed as calcined stone.

$a_{b,i}$	Coefficient in reactivity polynomial, f(U), for i th particle size group.		
c	Concentration of SO_2	kg/m^3	lb/ft^3
c_e	Concentration of SO_2 at top of bed		
c'_e	Concentration of SO_2 at top of bed in the absence of absorption		
c_o	Concentration of SO_2 at bottom of bed		
$\bar{c}$	Concentration of SO_2 averaged over height of bed		
C	Constant in equation 15.		
F	Feed rate of limestone	kg/s	ton/h
F_R	Regeneration rate of limestone due to attrition		
G	Flow rate of limestone entering cyclone	kg/s	ton/h
k	Utilization rate constant for particle size group	m^3/kgs	ft^3/lb h
K	Constant characterising the absorptive capacity of the bed	m^{-1}	ft^{-1}
K_d	Coefficient of attrition	h^{-1}	
K_e	Elutriation constant	s^{-1}	
K'_e	Corrected value of Ke		
M	Volume flowrate of gas	m^3/s	ft^3/s
m	Coefficient used in size distribution equation 15		-
n	Empirical exponent in equation 17.		-
R	Percentage retention		
R_r	Recycle rate of limestone	kg/s	ton/h
$[Re]_t$	Particle Reynolds number calculated for the termiminal velocity		-
$[Re]_v$	Particle Reynolds number calculated for the Stokes velocity		-
SO_2	Absorption of SO_2 particles (Eq 5)	kg	lb
t	Gas residence time	s	
t_a	Characteristic time for regeneration (defined by equation 2)		
T	Temperature	K	

NOMENCLATURE (Cont'd.)

U	Fractional utilization of particles	-	
U'	Fractional utilization of particles remaining in the bed after attrition.	-	
U_c	Limiting utilization of particles		
U_r	Fractional utilization of recycled limestone		
v	Stokes velocity of particles	m/s	ft/s
v_f	Superficial gas velocity		
v_t	Terminal velocity of particles		
W	Weight of particles in bed	kg	
x	Particle diameter	μm	B.S.S.
x_o	Characteristic size in the feed material		
x_1	Lower size)		
x_2	Upper size) in the i th size group		
y	Ca/S mol ratio		
z	Height above air distributor	m	ft
z'	Height above air distributor at which SO_2 generation ceases		
z_e	Height above air distributor of bed surface (Bed depth)		
α	Cyclone efficiency		
β	Constant in equation 9		
γ	Constant used with equation 17		
λ	Mass of SO_2 equivalent to unit mass of calcined limestone		
μ	Dynamic viscosity of gas	Ns/m^2	
τ	Mean residence time of solids in the bed	s	
$\phi(z)$	SO_2 generation function	-	

Subscript in general use

i	Referring to property of particle size group i

Table A6.1 Input Data for Test Series 4, Task II

Identifier	Input	Value represented	Units
PA	4.9	Pressure	Atmospheres
DB	0.97	Bed equivalent diameter	m
Z	1.144	Bed depth	m
VOL	1.37	Volume of freeboard	m^3
VOID	0.7	Bed voidage	-
FF	Various	Exponent in elutriation equation (n)	-
ASH	12	Ash content of coal	%
S	2.7	Sulphur content of coal	%
TSA	1588	Top size of ash (coal)	μm
MSAR	300	Median size of ash (coal)	μm
TSL	1588	Top size of limestone	μm
MSLR	400	Median size of limestone	μm
BSLR	0	Bottom size of limestone	μm
RHOA	2920	Density of ash	kg/m^3
RHOL	1578	Density of calcined limestone	kg/m^3
KDA	0	Attrition coefficient of ash	-
KDL	0	Attrition coefficient of limestone	-
CAO	53.0	CaO content of calcined limestone	%
MO	1.0	Fraction of SO_2 released at bottom of bed	-
ZH	1.0	Depth of bed in which SO_2 is released (dummy value)	m
BETA	0	Fraction of SO_2 released above bottom of bed	-
VAR(1)	0.6615	Air feed rate	kg/s
VAR(2)	0.05635	Coal feed rate	kg/s
VAR(3)	0.00345	Feed rate of calcined limestone	kg/s
VAR(4)	1068	Bed temperature	^oK
ZZZ	0.00345	Step increase in VAR(3)	kg/s
NG	10	No. of sections into which freeboard is divided	
JJ	20	No. of sections into which bed is divided.	

continued.......

Table A6.1 (contd.)

Size Fraction I	UC_i	KS_i	CYC_i	$a_{o,i}$	$a_{1,i}$	$a_{2,i}$	$a_{3,i}$
1	1	1	0	0.15	-0.45	0.45	-0.15
2	1	1	0.1	0.15	-0.45	0.45	-0.15
3	1	1	0.3	0.15	-0.45	0.45	-0.15
4	1	1	0.5	0.15	-0.45	0.45	-0.15
5	1	1	0.7	0.15	-0.45	0.45	-0.15
6	1	1	0.8	0.15	-0.45	0.45	-0.15
7	0.9	1	0.9	0.14	-0.466	0.518	-0.192
8	0.8	1	0.95	0.14	-0.525	0.656	-0.2735
9	0.8	1	0.95	0.14	-0.525	0.656	-0.2735
10	0.8	1	0.95	0.14	-0.525	0.656	-0.2735
End of input data							

Notes:

The rate equation used is:

$$\frac{d(SO_2)}{dt} = K_i(a_{o,i} + a_{1,i} U_i + a_{2,i} U_i^2 + a_{3,i} U_i^3).c.W_i$$

where c is SO_2 concentration, kg/m^3

U_i is fractional utilisation of limestone

W_i is mass of limestone of size i in bed

$\frac{d(SO_2)i}{dt}$ is rate of SO_2 absorption by size i, kg/s

UC_i is the limiting utilisation - i.e. the value of U_i at which the rate falls to zero.

Table A6.2 Constants in Reactivity Equation

Stone	Temperature °C	Size range μm	a_o	a_1	a_2	a_3	U_c
Limestone 18	700	4-4096	0.062	0	0	-2.125	0.308
	800	4-4096	0.075	0	-0.228	0	0.574
	900	4-4096	0.0736	-0.03786	0.7575	-5.05	0.29
Limestone 1359	800	4- 64	0.061	-0.001875	-0.261	0	0.48
		64- 128	0.061	-0.00495	-0.973	0	0.24
		128- 256	0.061	-0.0829	-1.624	0	0.17
		256- 512	0.061	-0.004545	-5.0	0	0.11
		512-1024	0.061	-0.03333	-8.05	0	0.085
		1024-4096	0.061	0.1824	-17.25	0	0.065
U.K. Dolomite	800	4- 32	0.117	-0.351	-0.351	0.117	1.0
		32- 64	0.116	-0.348	-0.348	0.116	1.0
		64- 128	0.115	-0.345	-0.345	0.115	1.0
		128- 256	0.1145	-0.3435	-0.3435	0.1145	1.0
		256- 512	0.113	-0.339	-0.339	0.113	1.0
		512-1024	0.1095	-0.3285	-0.3285	0.1095	1.0
		1024-2048	0.108	-0.324	-0.324	0.108	1.0
		2048-4096	0.106	-0.318	-0.318	0.106	1.0
Dolomite 1337	800	4- 256	0.15	-0.45	0.45	-0.15	1
		256- 512	0.14	-0.466	0.518	-0.192	0.9
		512-4096	0.14	-0.525	0.656	-0.2735	0.8

Table A6.3 Tasks II and III - Assumed Recirculation Cyclone Efficiencies

Particle Group No.	Size range μm	Efficiency, α	
		Task II	Task III
1	4- 8	0	0
2	8- 16	0.1	0
3	16- 32	0.3	0
4	32- 64	0.5	0.5
5	64- 128	0.7	0.8
6	128- 256	0.8	0.9
7	256- 512	0.9	0.95
8	512-1024	0.95	0.95
9	1024-2048	0.95	0.95
10	2048-4096	0.95	0.95

Table A6.4 Effect of variation in n

Task I, Test Series 1 - Ca/S mol ratio 1.75

Size group, i	Utilization of particles in size group				
	n = 1.0	n = 1.5	n = 2.0	n = 2.5	n = 3.0
1	0	0	0	0	0
2	0	0	0	0	0
3	0	0	0.001	0.001	0.002
4	0	0.002	0.004	0.012	0.031
5	0.001	0.008	0.037	0.163	0.519
6	0.002	0.060	0.361	0.524	0.519
7	0.006	0.531	0.528	0.524	0.519
8	0.540	0.531	0.528	0.524	0.519
9	0.540	0.531	0.528	0.524	0.519
Retention, %	27.2	46.1	50.7	57.9	64.4

Table A6.5 Effect of variation in α (assumed same for all i)

Task I - Test Series 2 - Ca/S mol ratio 1.84

Size group, i	Utilization of particles in size group				
	α = 0	α = 0.75	α = 0.95	α = 0.98	α = 0.99
1	0	0	0.001	0.003	0.012
2	0	0	0.001	0.004	0.013
3	0	0.001	0.007	0.017	0.049
4	0.005	0.021	0.101	0.229	0.390
5	0.102	0.299	0.499	0.503	0.497
6	0.543	0.538	0.513	0.508	0.501
7	0.543	0.538	0.513	0.508	0.501
8	0.543	0.538	0.513	0.508	0.501
9	0.543	0.538	0.513	0.508	0.501
Retention, %	61.4	63.5	66.4	68.1	70.4

Table A6.6 Effect of Attrition on Utilization of Size Groups (approx. Ca/S mol ratio = 1)

Size Group i	Utilization, %			
	$K_d = 0$	$K_d = 0.0175$	$K_d = 0.02$	$K_d = 0.025$
1	0	0	0	0
2	0	0	0	0
3	0	0	0	0
4	0.001	0.001	0.001	0.001
5	0.002	0.002	0.002	0.002
6	0.006	0.006	0.006	0.006
7	0.553	0.710	0.734	0.774
8	0.553	0.710	0.734	0.774
9	0.553	0.710	0.734	0.774

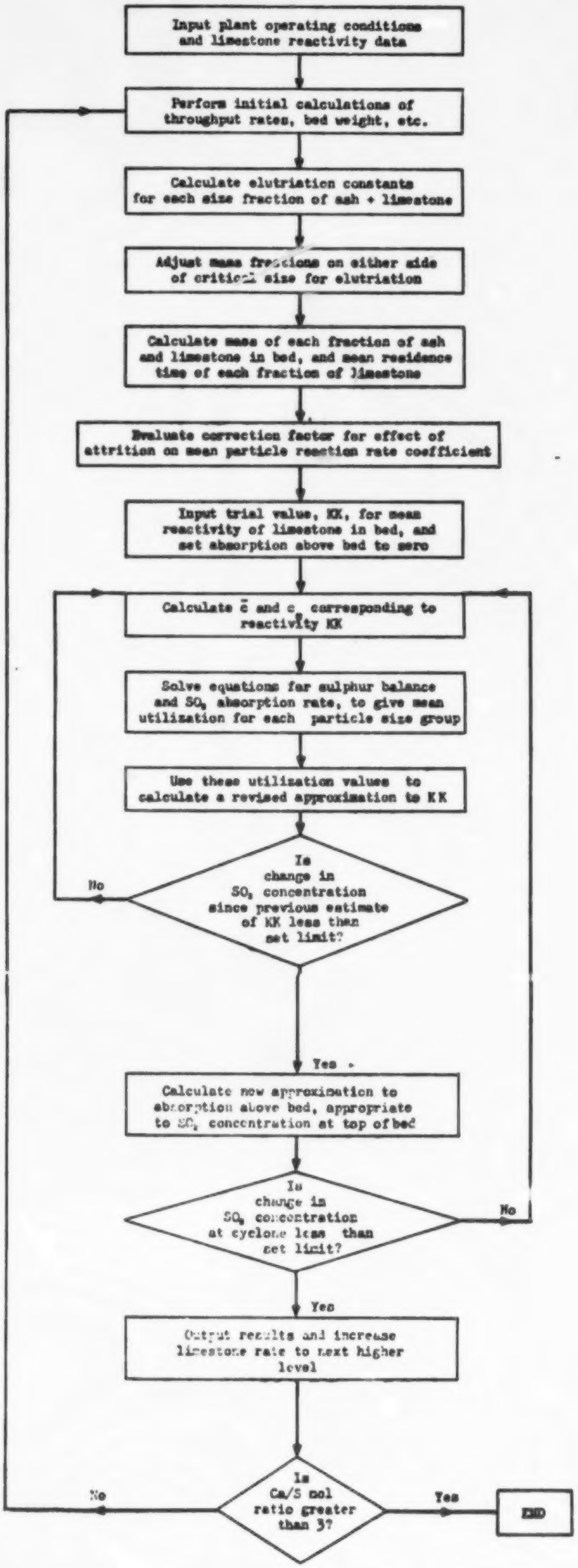
Input plant operating conditions and limestone reactivity data
Perform initial calculations of throughput rates, bed weight, etc.
Calculate elutriation constants for each size fraction of ash + limestone
Adjust mass fractions on either side of critical size for elutriation
Calculate mass of each fraction of ash and limestone in bed, and mean residence time of each fraction of limestone
Evaluate correction factor for effect of attrition on mean particle reaction rate coefficient
Input trial value, KK, for mean reactivity of limestone in bed, and set absorption above bed to zero
Calculate $\bar{c}$ and c_e corresponding to reactivity KK
Solve equations for sulphur balance and SO_2 absorption rate, to give mean utilization for each particle size group
Use these utilization values to calculate a revised approximation to KK
Is change in SO_2 concentration since previous estimate of KK less than set limit?
No
Yes
Calculate new approximation to absorption above bed, appropriate to SO_2 concentration at top of bed
Is change in SO_2 concentration at cyclone less than set limit?
No
Yes
Output results and increase limestone rate to next higher level
Is Ca/S mol ratio greater than 3?
No
Yes
END

Fig. A6.1. Flow chart of mathematical model of sulphur retention

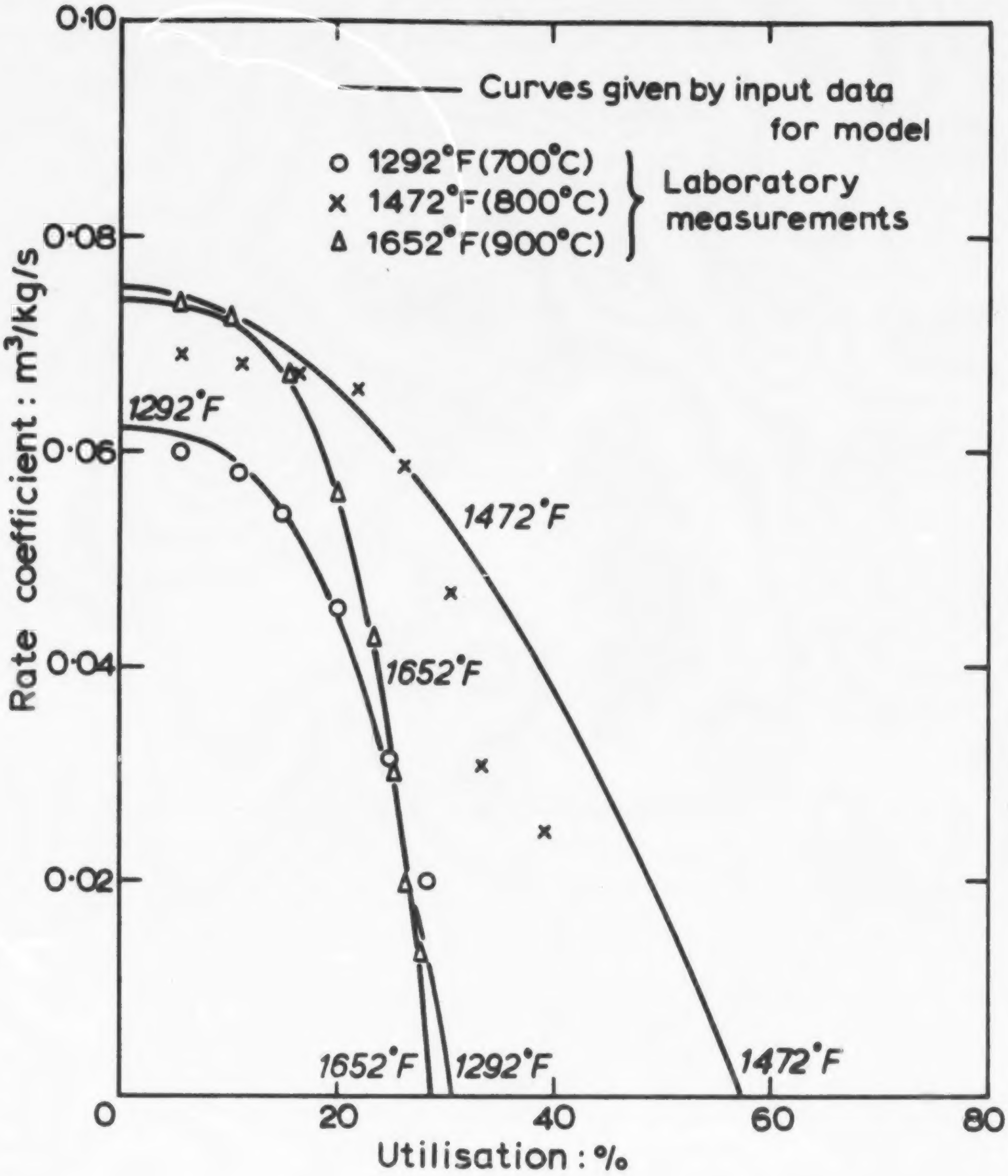

Fig. A6.2. Rate coefficients for Limestone 18

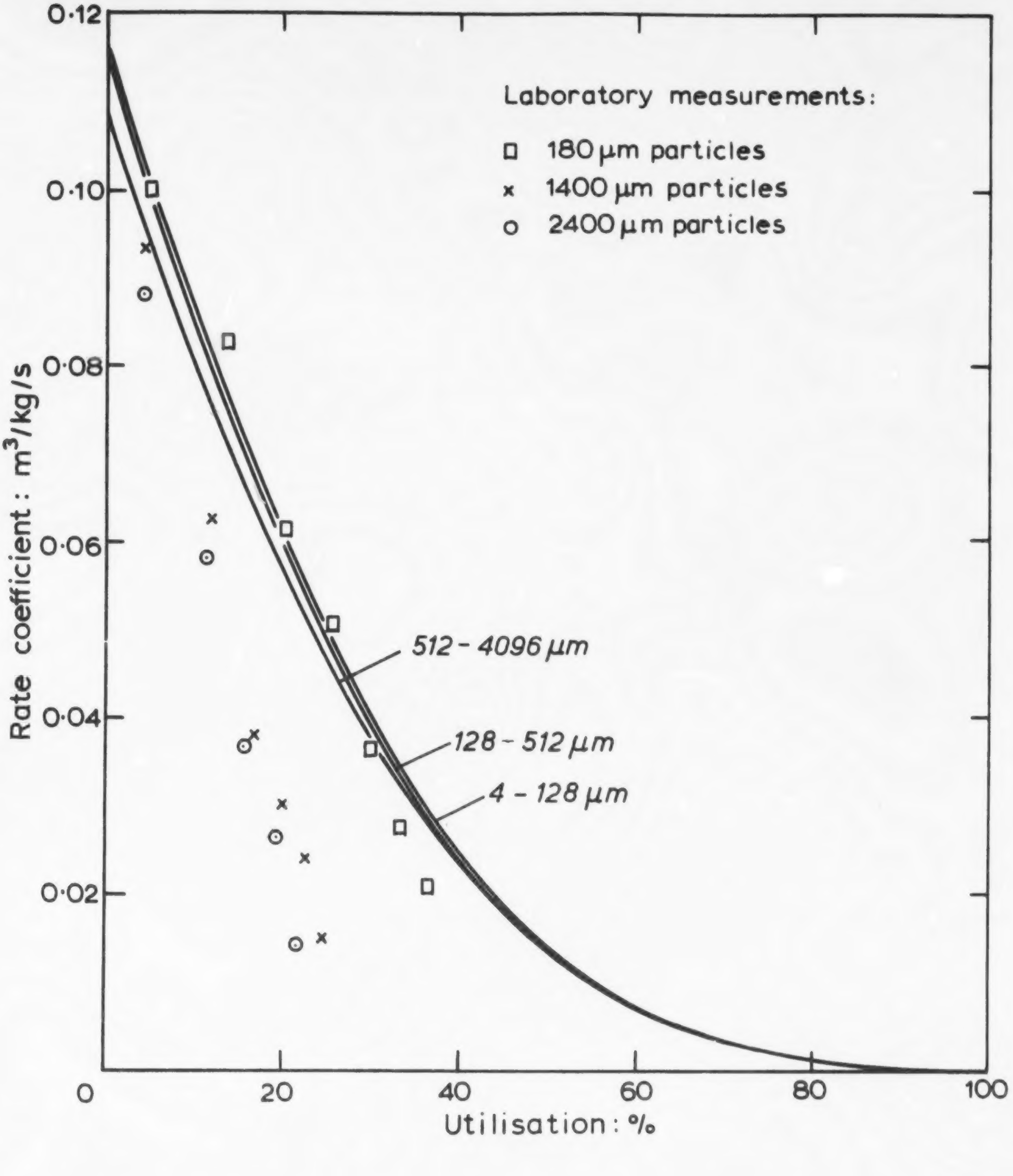

Fig. A6.3. Rate coefficients for U.K. Dolomite

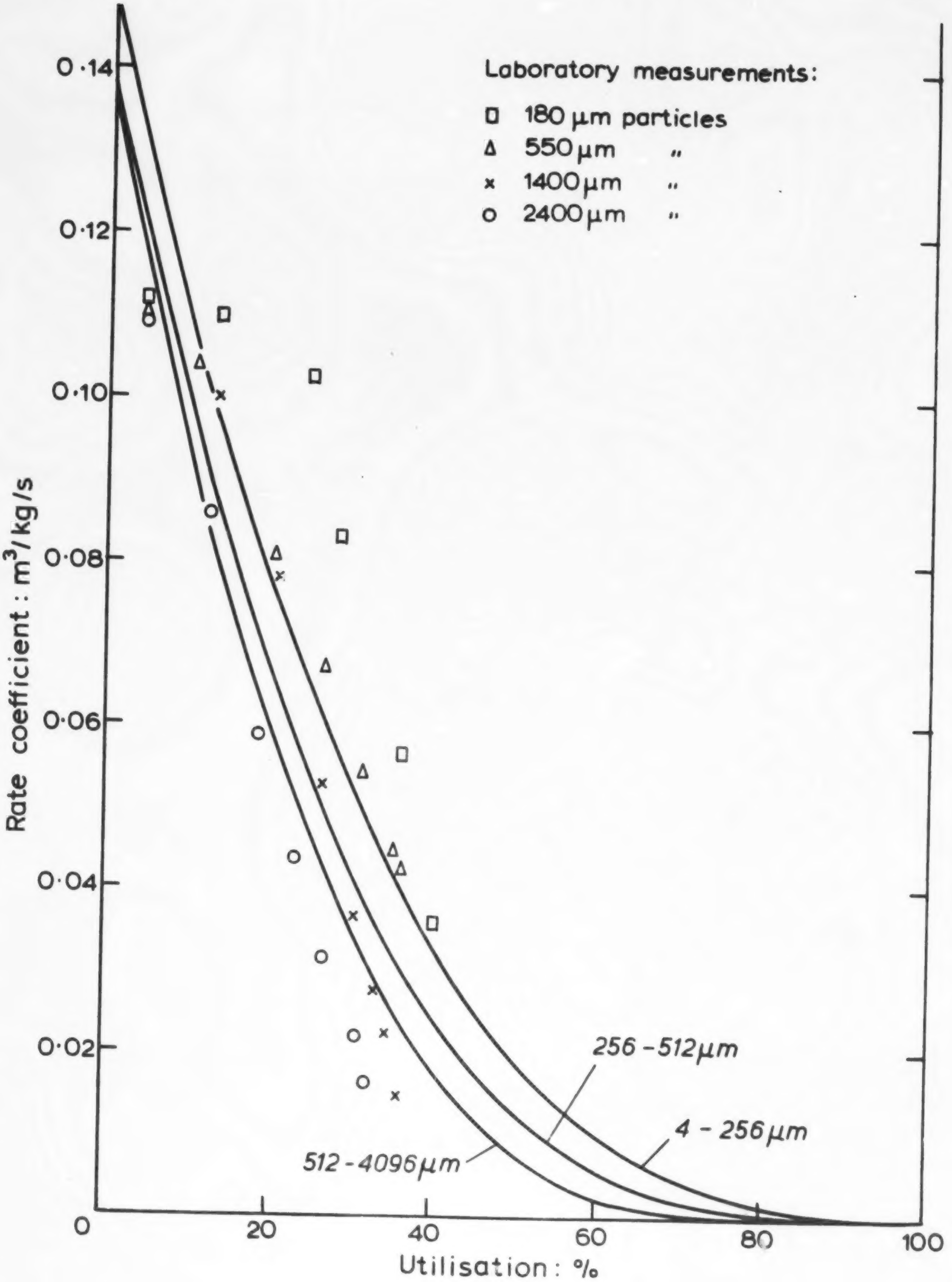

Fig. A6.4. Rate coefficients for Dolomite 1337

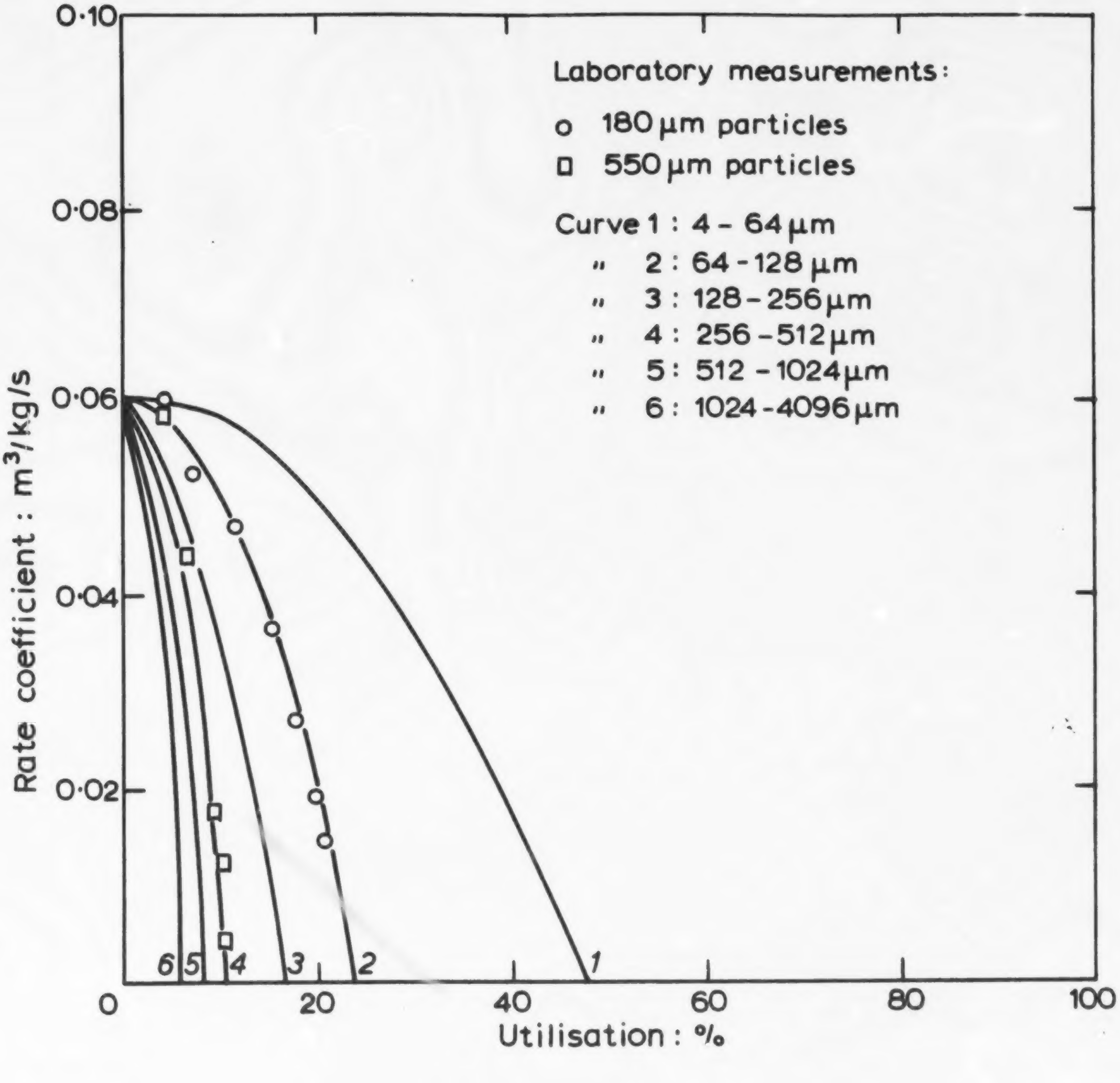

Fig. A6.5. Rate coefficients for Limestone 1359

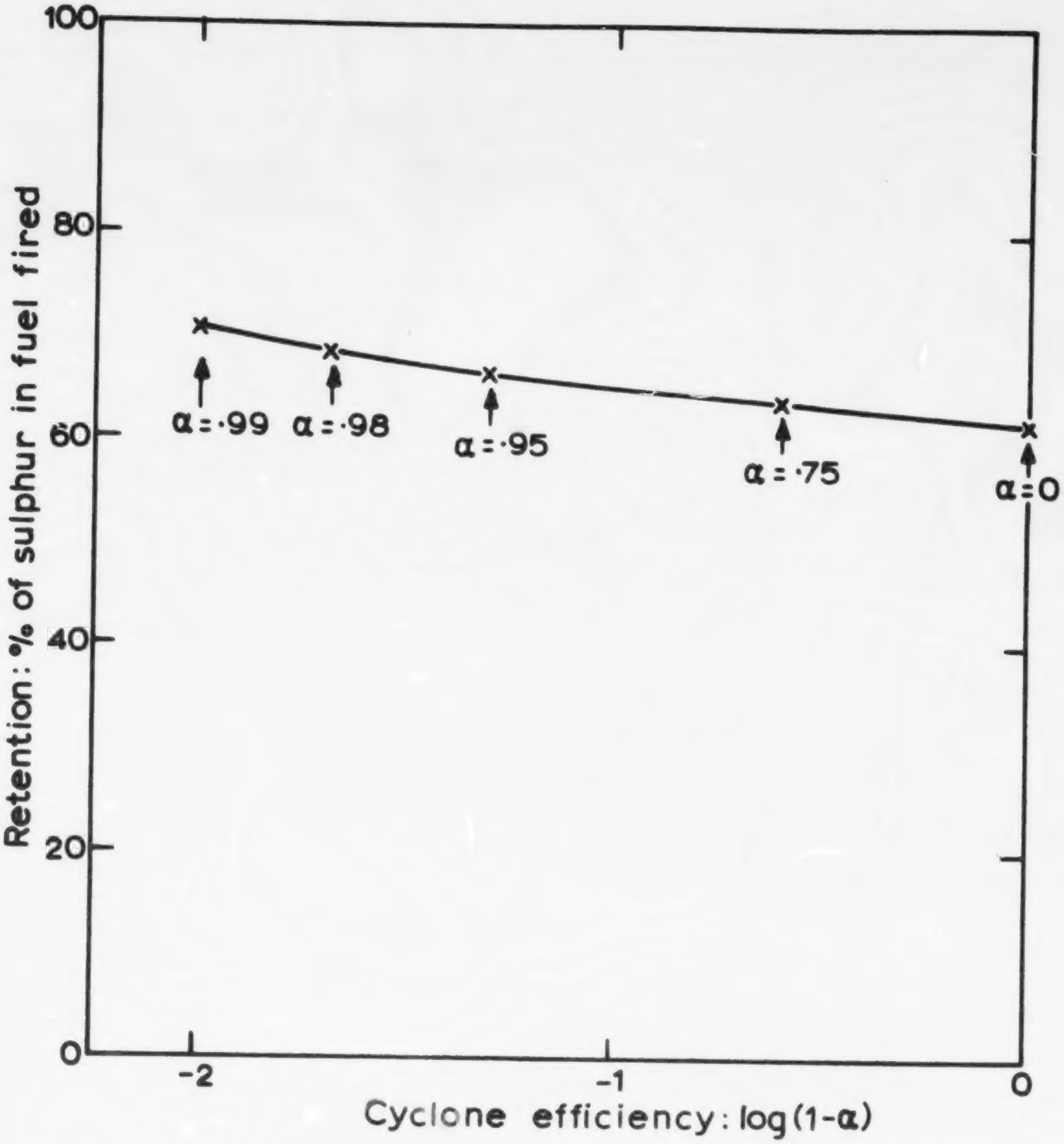

Fig. A6.6. Predicted effect of altering recirculation cyclone efficiency

Note: α assumed the same for all i
n = 3

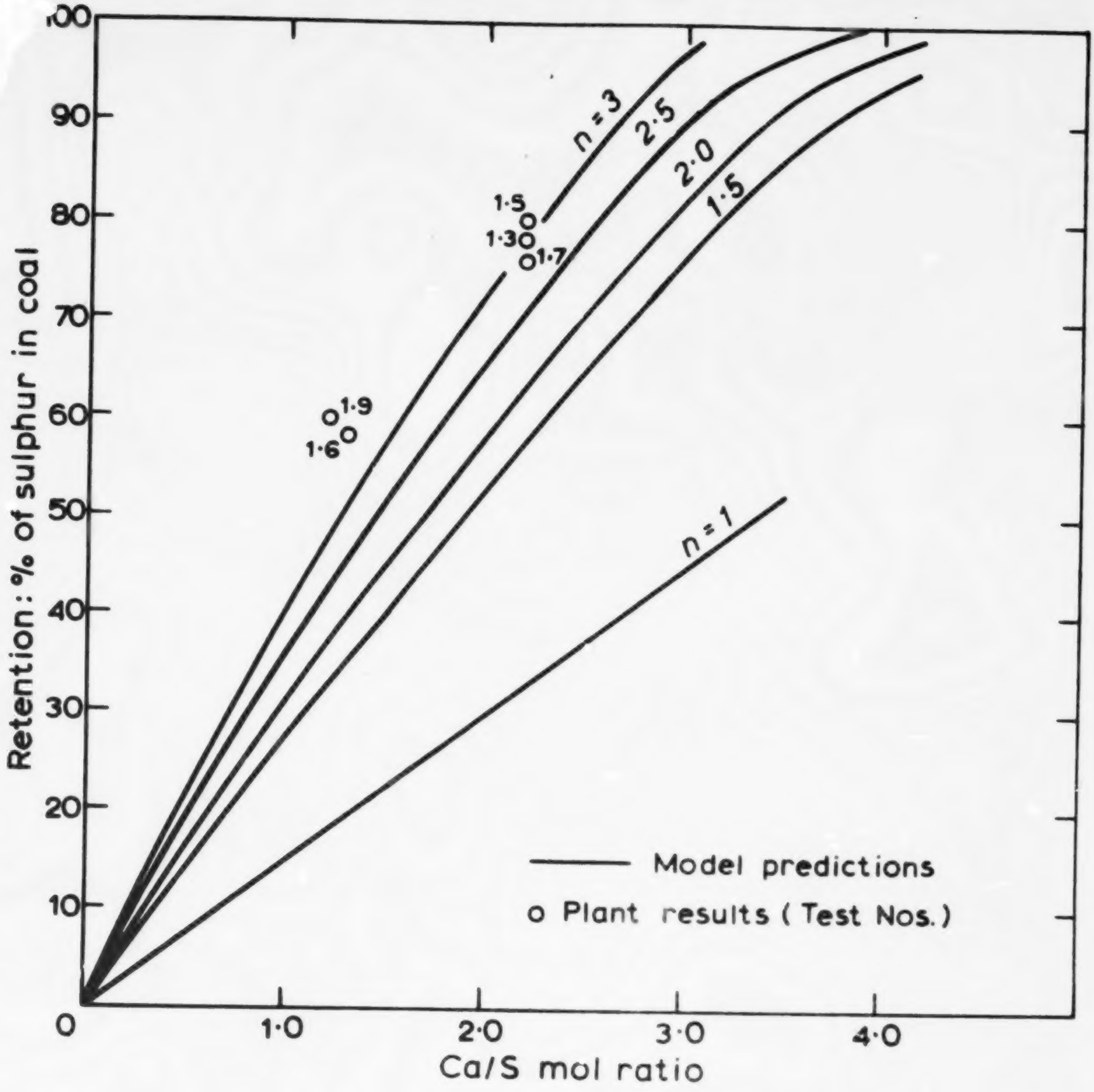

Fig. A6. 7. Task I. Test Series 1. Effect of variation in n (Kd = 0)

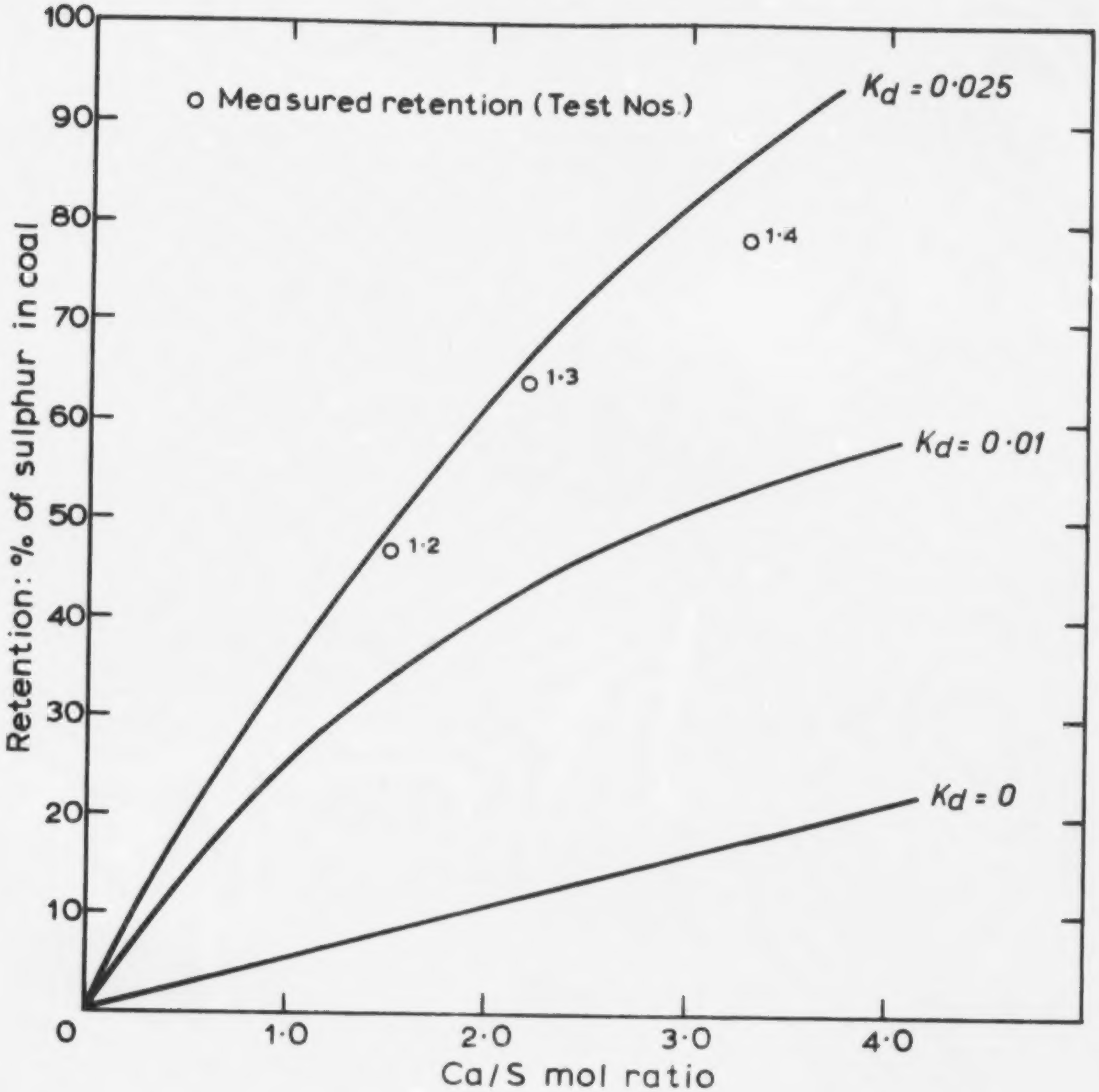

Fig. A6. 8. Task V. Tests 1.2 to 1.4

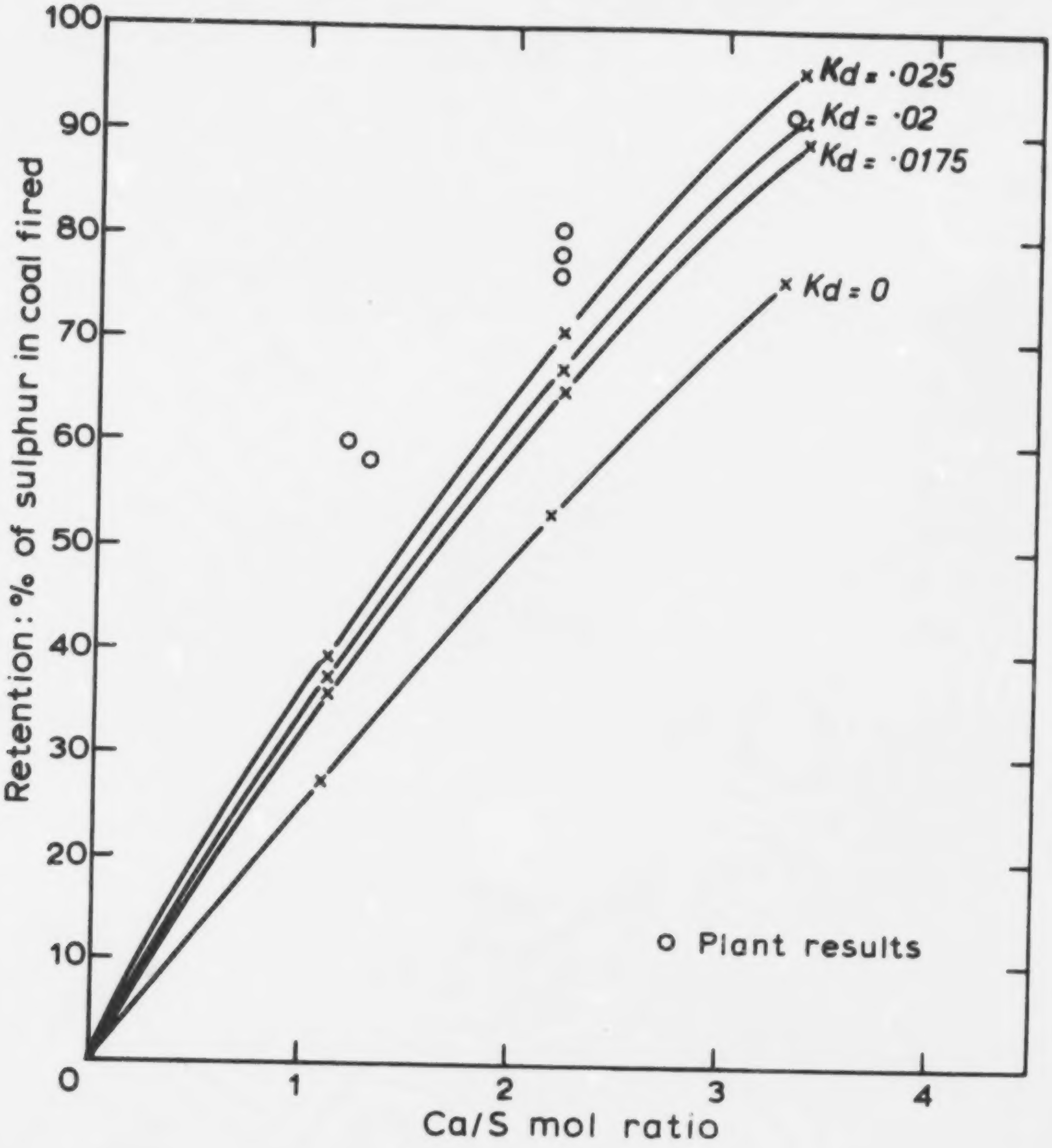

Fig. A6.9. Task I. Test Series 1. Effect of variation in Kd (n = 1)

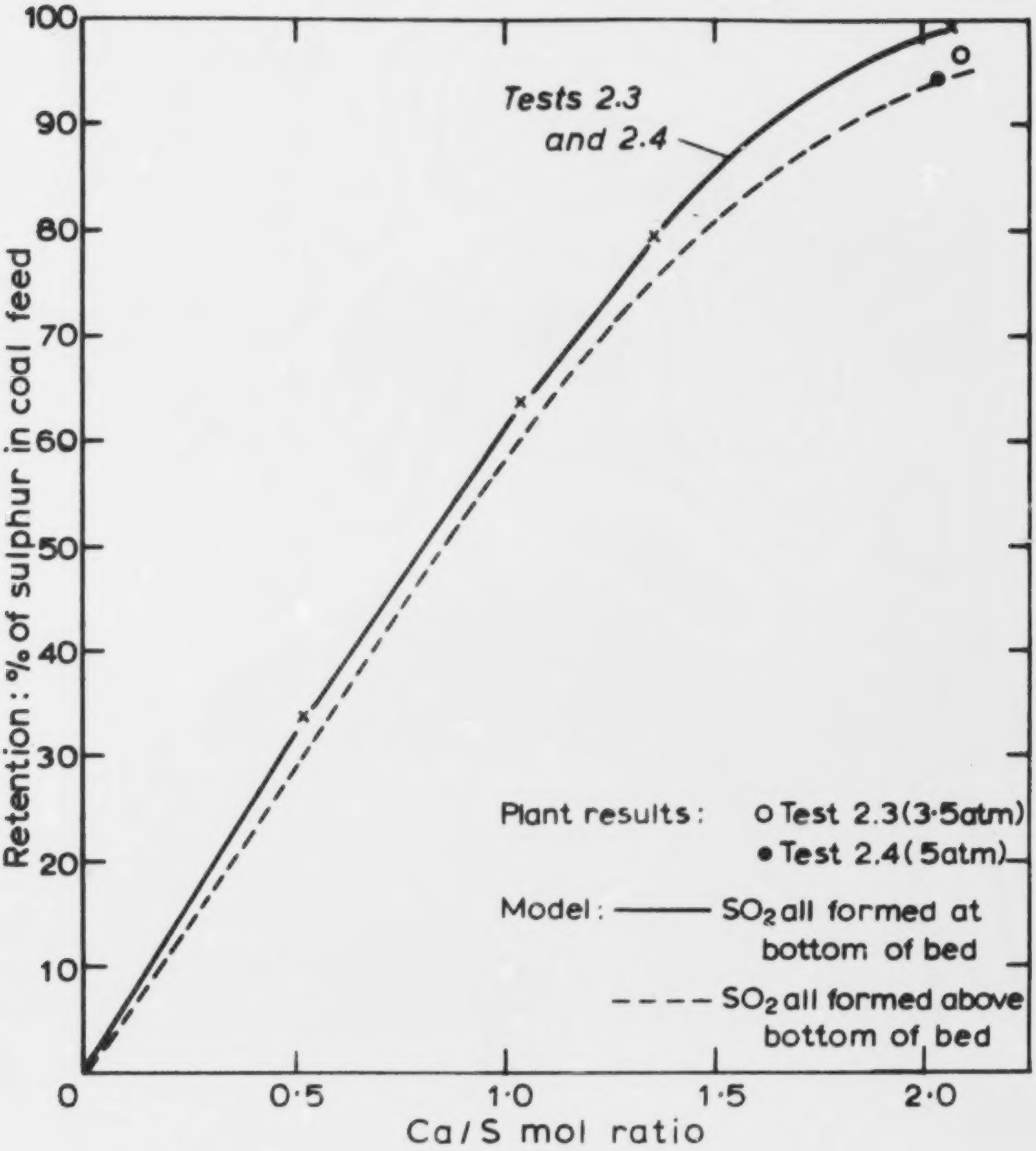

Fig. A6.10. Task II. Test Series 2

$K_d = 0, \; n = 1$

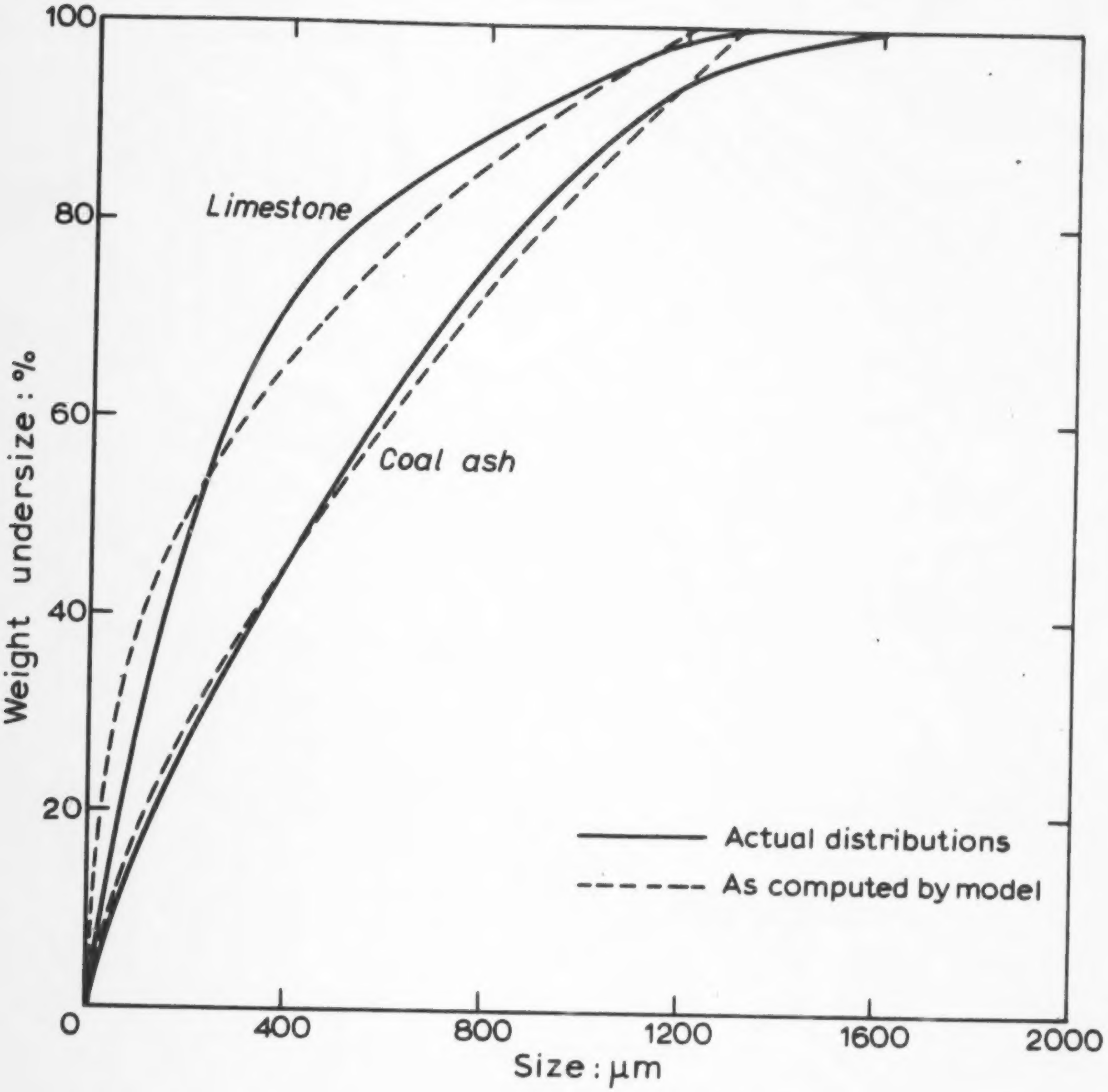

Fig. A6.11. Size distributions. Task I. Test Series 1

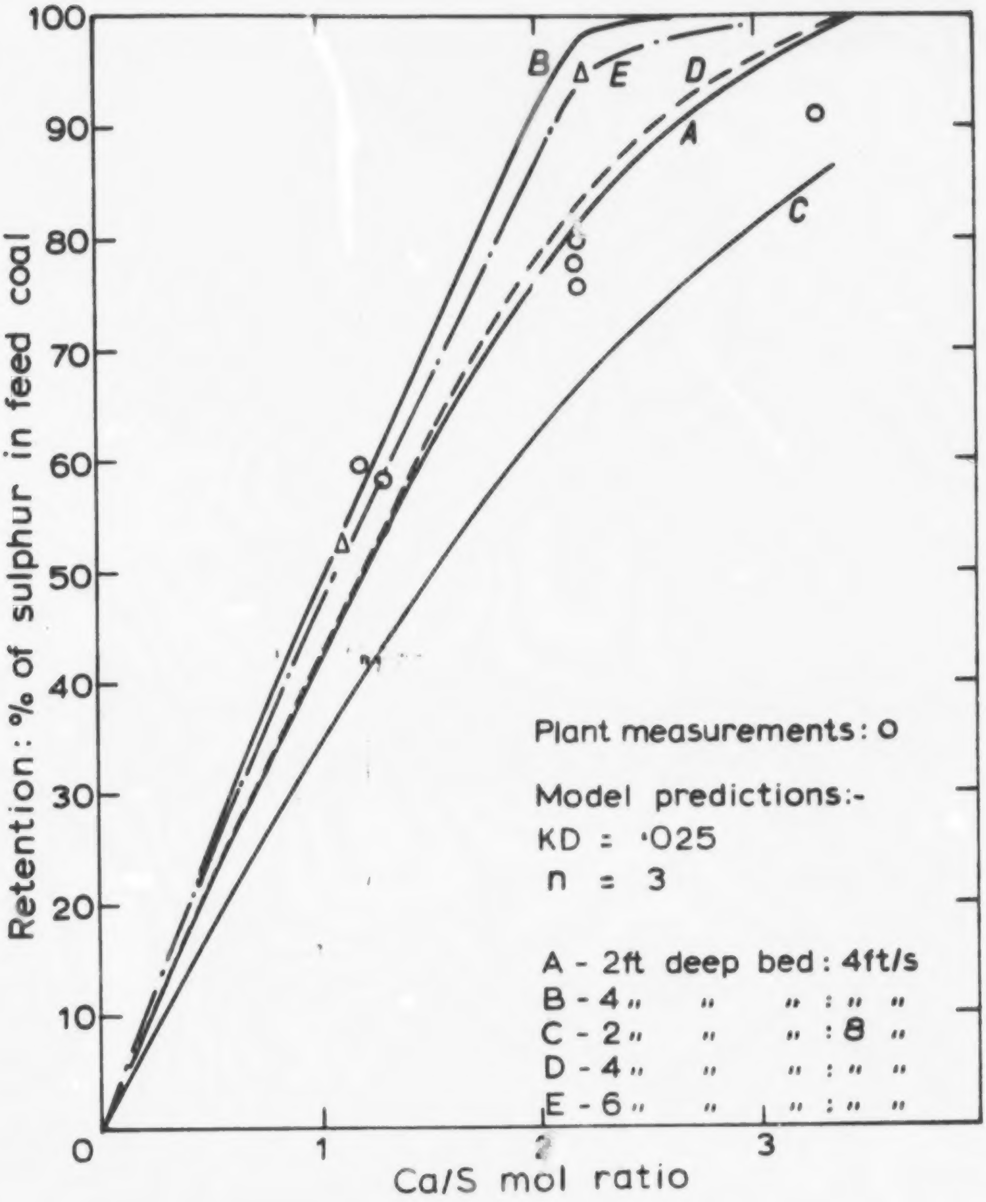

Fig. A6.12. Task I. Test Series 1

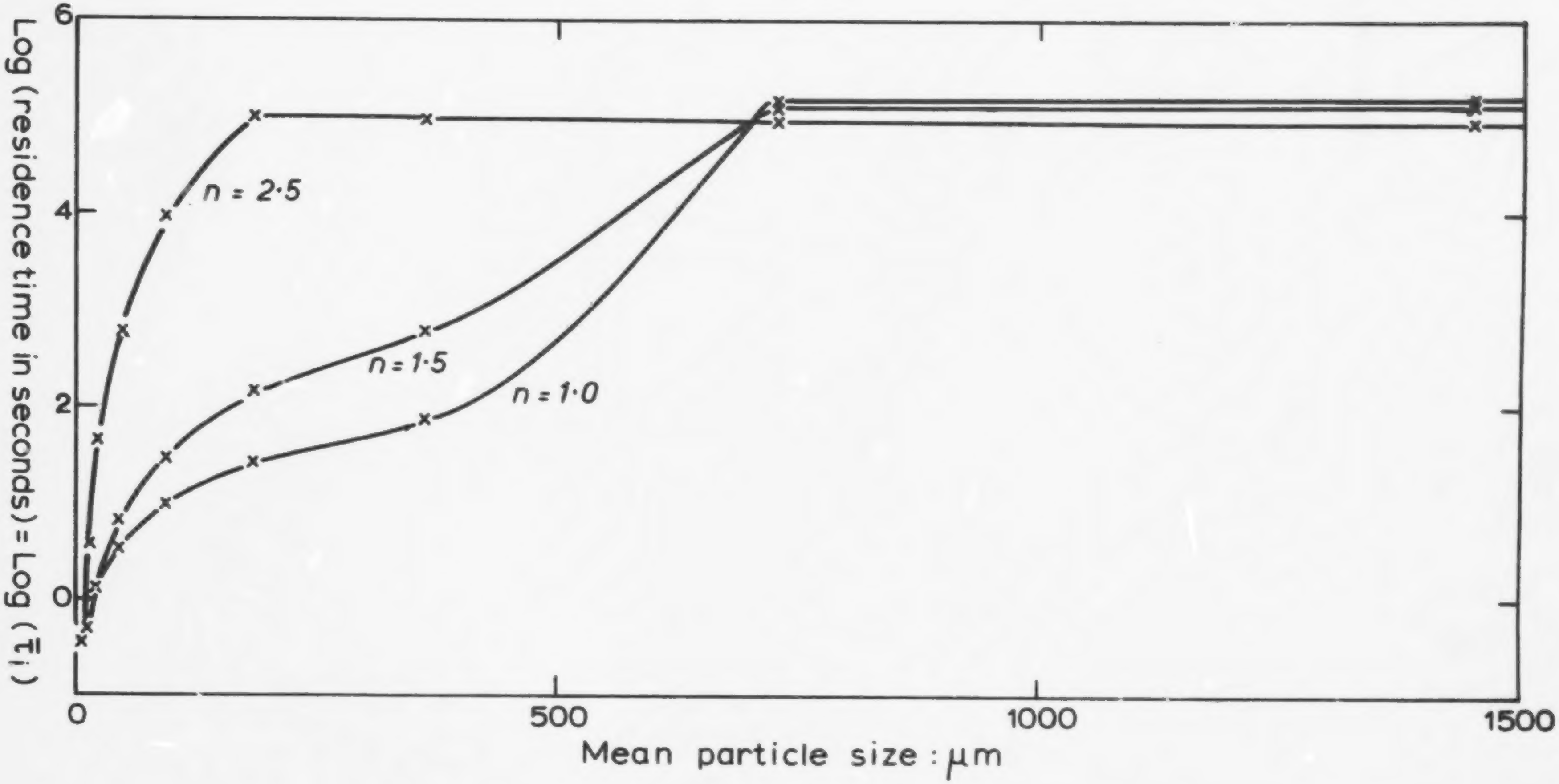

Fig. A6. 13. Task I. Test Series 1. Mean residence time of particles in bed *vs* particle size, for various values of n

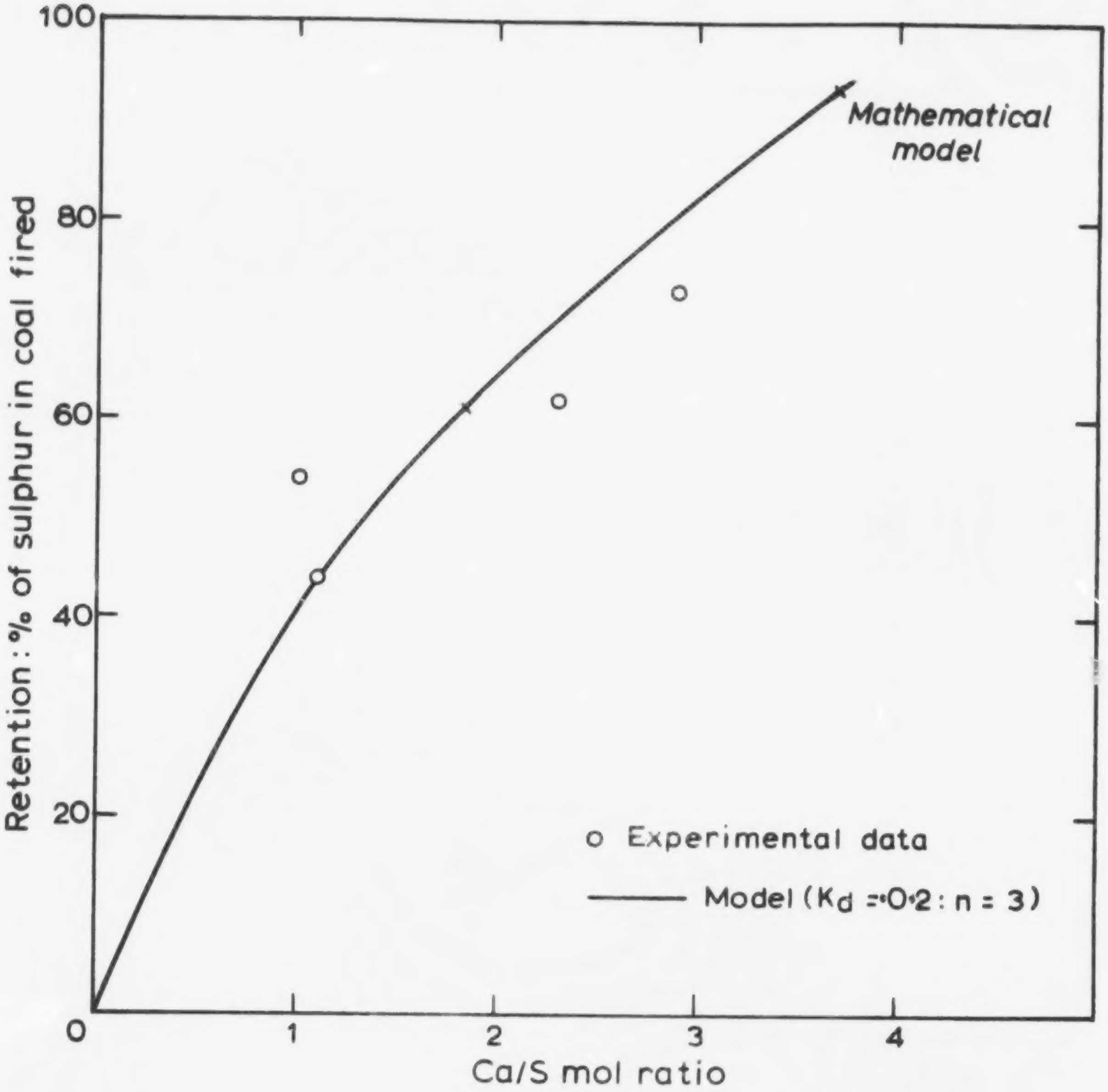

Fig. A6. 14. Task I. Test Series 2

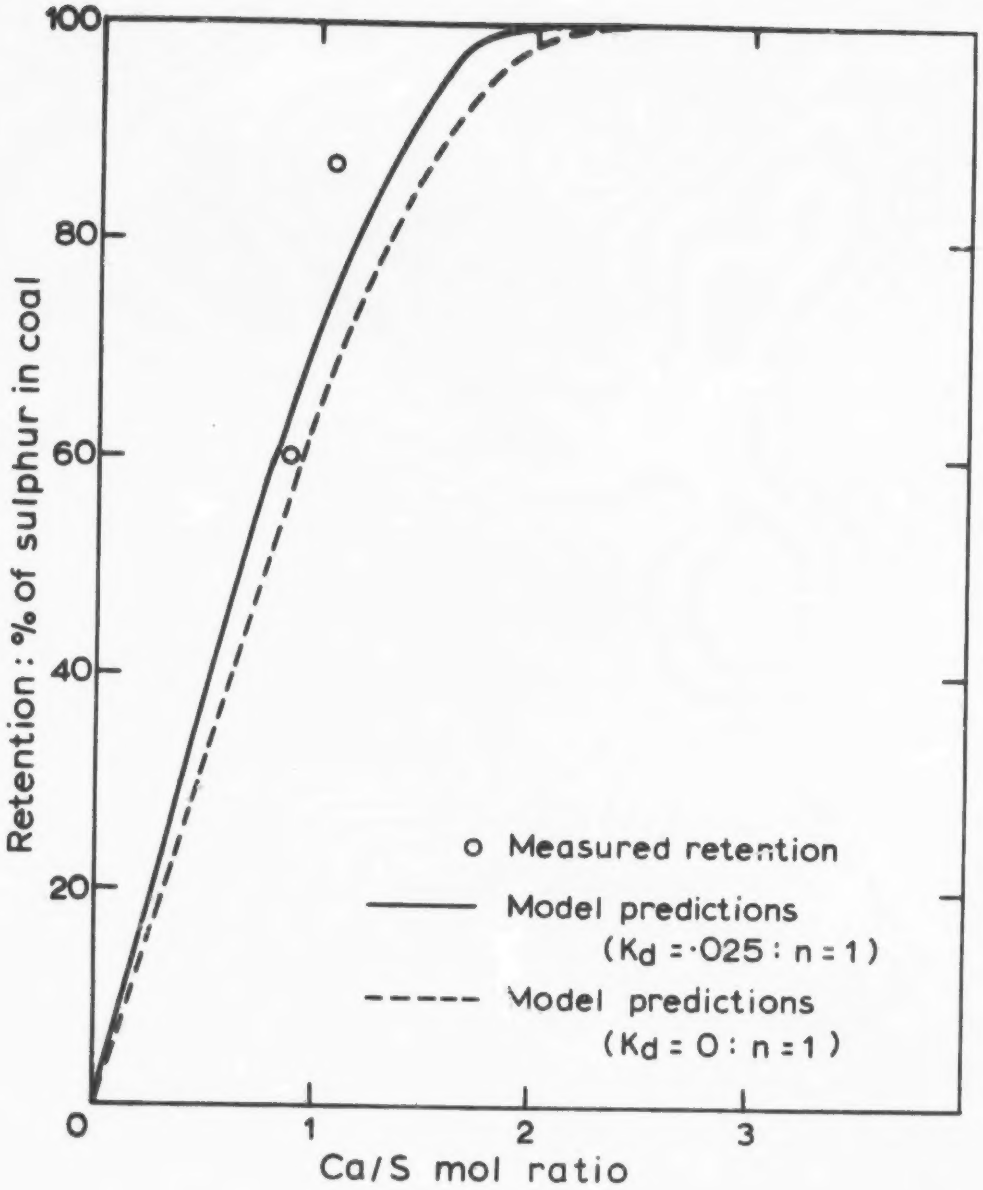

Fig. A6. 15. Task II. Test Series 1

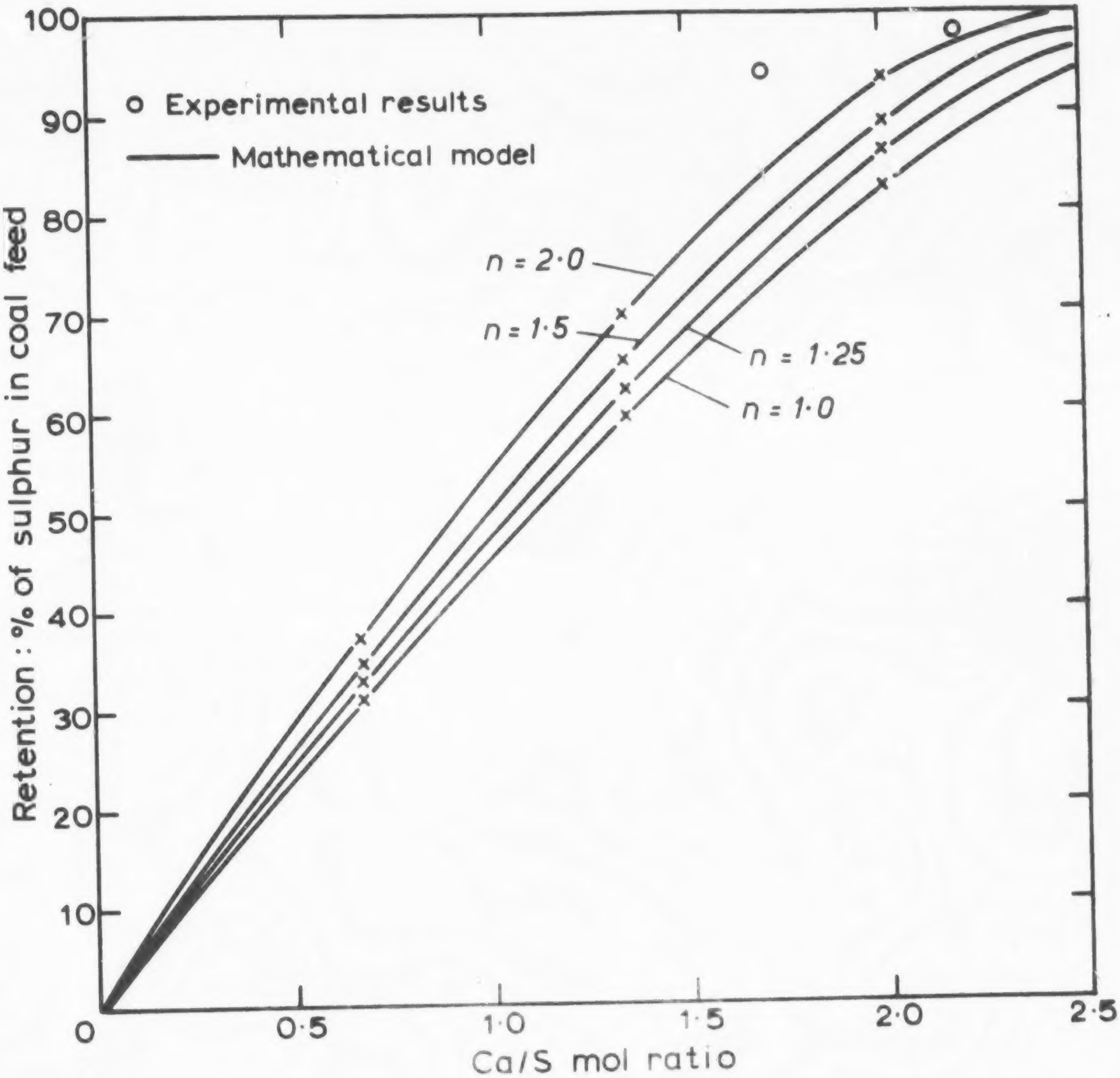

Fig. A6.16. Task II. Test Series 4

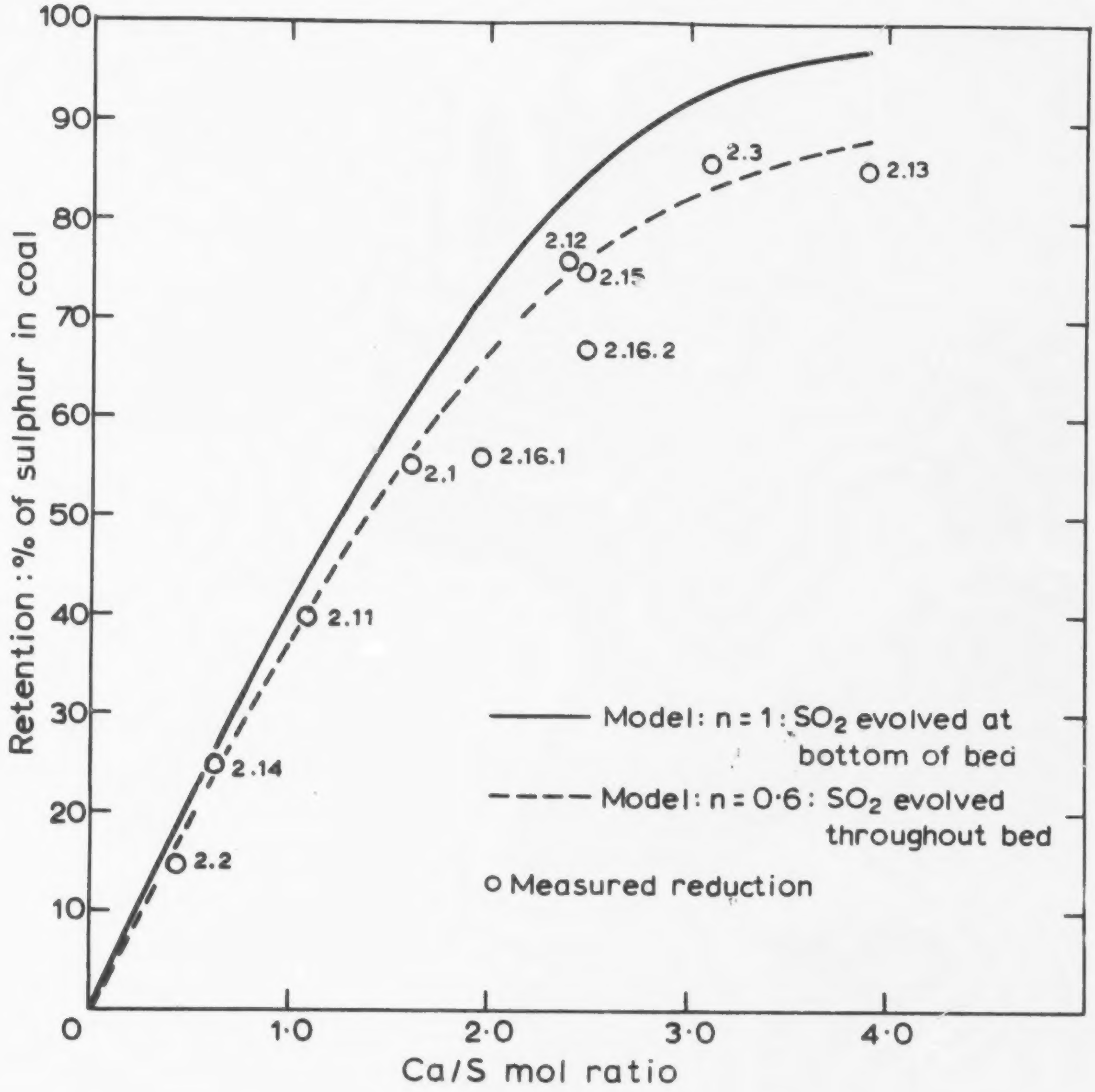

Fig. A6.17. Task III. Test Series 2. Coarse stone

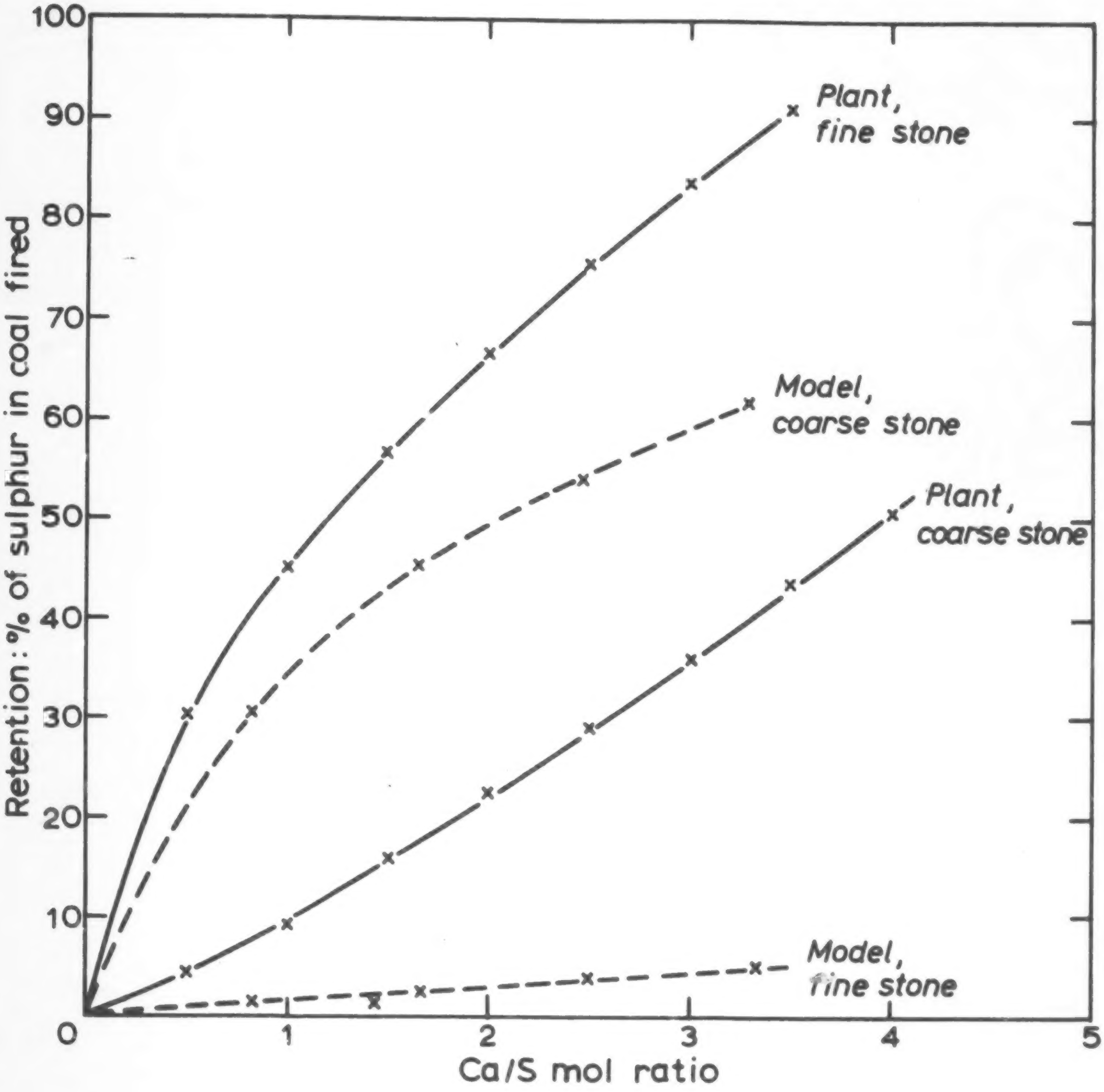

Fig. A6.18. Pope, Evans and Robbins' Fluid Bed Module

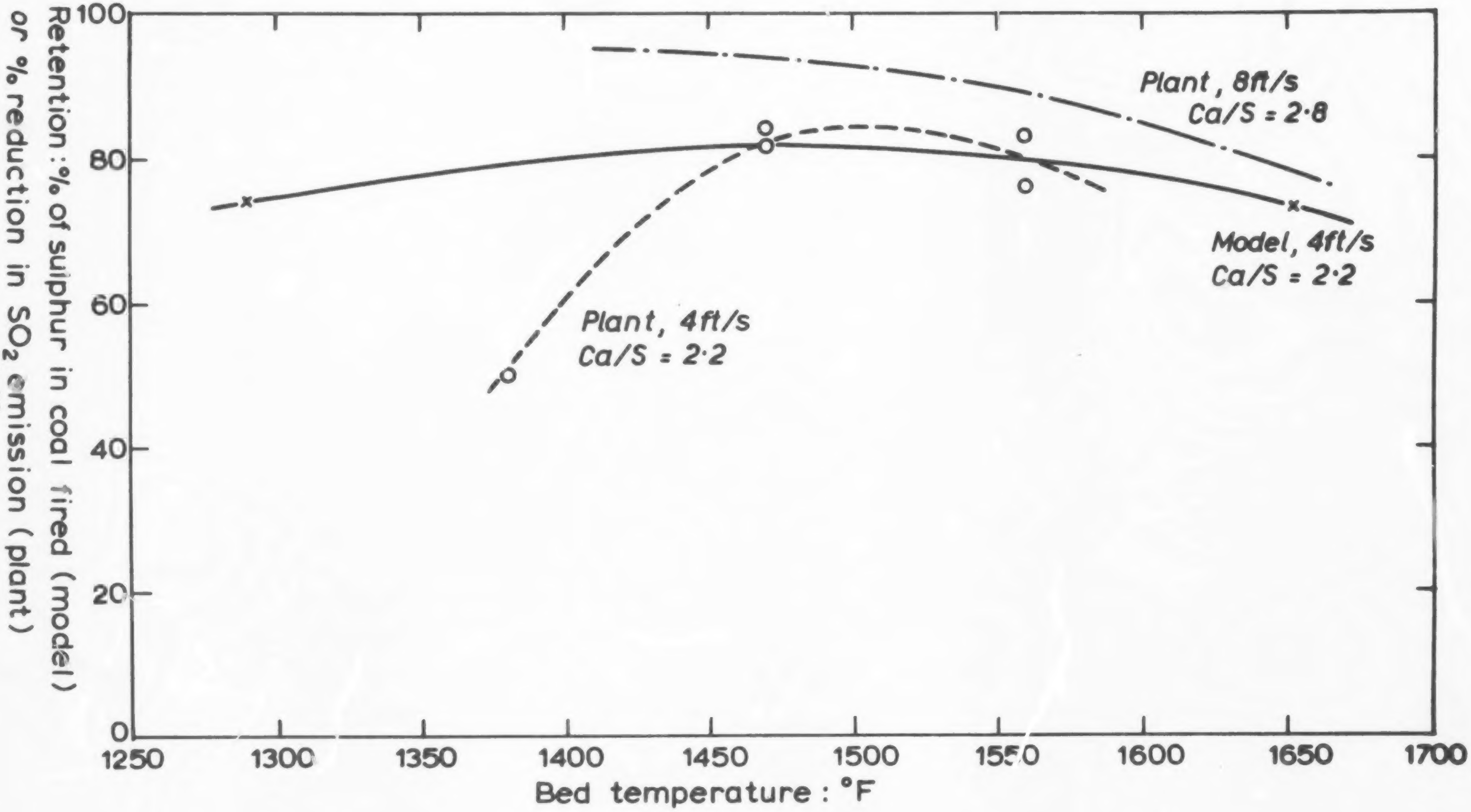

Fig.A6.19. Temperature effect. Task I. Limestone 18

NATIONAL COAL BOARD

FINAL REPORT

JUNE 1970 - JUNE 1971

REDUCTION OF ATMOSPHERIC POLLUTION

APPENDIX 7. COAL STUDIES. (TASK VII)

APPENDIX 8. LIMESTONE AND DOLOMITE STUDIES. (TASK VIII)

PREPARED FOR

ENVIRONMENTAL PROTECTION AGENCY
OFFICE OF AIR PROGRAMS
411 WEST CHAPEL HILL STREET
DURHAM, NORTH CAROLINA 27701

REFERENCE NO. DHB 060971

SEPTEMBER 1971

FLUIDISED COMBUSTION
CONTROL GROUP

NATIONAL COAL BOARD
LONDON, ENGLAND

A7.i

REDUCTION OF ATMOSPHERIC POLLUTION

Research on reducing emission of sulphur oxides, nitrogen oxides and particulates by using fluidised bed combustion of coal

Appendix 7. Coal studies. (Task VII)

Main objectives

To investigate the distribution of sulphur in a range of coals and in the residue from the rigs.

Report prepared by: D.C. Davidson and
J. Highley

Report approved by: A.D. Dainton and
H.R. Hoy

Preceding page blank

Table of Contents

Page No.

1. Introduction A7. 1

2. Background A7. 1

3. Determinations of forms of sulphur A7. 2

4. Sulphur release studies A7. 3
   - 4.1 Objective A7. 3
   - 4.2 The furnace design A7. 3
   - 4.3 The experiments A7. 3
   - 4.4 The results A7. 4

5. Acknowledgement A7. 7

(Note that when referring to Tables and Figures in the text the prefix A.7 is omitted).

Preceding page blank

1. INTRODUCTION

In early work on fluidised combustion, prior to the present contract, it was observed that there were small but significant differences in the sulphur retention obtained with coals of different types when burned under similar operating conditions. It was established that these differences could not be accounted for in terms of the calcium contents of the mineral matter. Consequently, the objective of the present task was to seek further information on the role played by the type of coal and its associated mineral matter on sulphur retention. Because the effects were small compared to those of operating parameters such as Ca/S ratio and fluidising velocity, only a small effort was to be expended in these studies.

2. BACKGROUND

Comparison of results from experimental work at CRE and at the Argonne National Laboratories, before the programme began, had shown differences in the efficiency of sulphur retention under equivalent conditions of particle size, bed temperature, and fluidising velocity. Taken at face value, the differences in design between the two combustors did not appear sufficient to account for the different performance. Further, experiments at CRE on several coals in the same plant revealed differences which appeared to be attributable to the nature of the feed coals themselves, although the property responsible had not been identified.

To explain these differences, two main approaches were followed. On Task V* raw materials were exchanged between CRE and the Argonne laboratory, in order to check on factors arising from differences in plant design. The programme for Task VII provided for measurements on coals to see whether the form in which the sulphur was present was an important factor affecting the efficiency of retention.

In Task V, all four coals used in the programme were burned. It was found that, for any given Ca/S ratio, the SO_2 retention was significantly better with Welbeck coal than with the other three, Illinois, Pittsburgh and Park Hill. Of these last three coals, SO_2 retention with the Pittsburgh was marginally worst.

---

* See Appendix 5.

Welbeck is a low-rank coal with poor caking and swelling properties (See Table 1). In the other three coals, these properties covered a wide range, but in one of the group, Park Hill, they were not significantly different from those of Welbeck. It was therefore possible to discount the swelling properties of coals as a possible factor.

Table A7.1 Caking and Swelling Properties of coals

Coal	Swelling Number	Gray-King Coke Type
Welbeck	1	C
Illinois	4½	D
Park Hill	1	D
Pittsburgh	8	G9

3. DETERMINATIONS OF FORMS OF SULPHUR

The forms of sulphur in the four coals used for the various tasks were determined by standard methods as described in British Standard 1016.11.1939. The results are given in Table 2.

Table A7.2 Forms of sulphur in coals

	Sulphur % as received				Ratio Org./Pyr.
	Total	Organic	Pyritic	Sulphate	
Illinois	3.95	2.45	1.35	0.15	1.8
Pittsburgh	2.75	1.44	1.25	0.06	1.1
Welbeck	1.25	0.73	0.50	0.02	1.4
Park Hill	2.40	1.01	1.35	0.04	0.7

Welbeck coal has the lowest total sulphur content, having about half that of Pittsburgh and Park Hill, and about a third that of Illinois. The relative proportions of organic to pyritic sulphur range from 0.7 in Park Hill to 1.8 in Illinois, with Welbeck having on intermediate value.

4. SULPHUR RELEASE STUDIES

4.1 Objective

In view of the findings described in Section 3, an attempt was made to measure the rate of release of sulphur in laboratory apparatus. The little which could be done in the time available is described below.

4.2 The furnace design

The experiments were carried out using a reaction rate furnace developed at Leatherhead. The furnace was designed originally for studying the devolatilisation and combustion of pulverised coal, and consisted of a vertically mounted silicon carbide tube which could be controlled at any temperature between 1100 and 2700°F. The tube length between the injection and collection points for the reacting particles was isothermal.

The gas with which the particles were to be reacted was pre-mixed in the required concentration with argon as a diluent. This gas was heated to the same temperature as the furnace by a plasma arc and the heated gas flowed downwards through the furnace tube. The flow in the furnace tube was laminar, which ensured that particles were not lost to the walls.

The closely sized graded feed particles were introduced slowly as a dilute stream into the gas along the axis of the furnace through a feeder tube purged with argon. The feeder tube was water cooled to prevent premature reaction of the particles.

4.3 The experiments

The coals chosen for the experiments were U.S. Pittsburgh and U.K. Welbeck.

The feed material was produced by crushing and sieving the coals to give closely graded fractions between 75 and 53 μm particle diameter. This feedstock was analysed for total and pyritic sulphur before use.

The coal was fed to the furnace, using a vibration feeder at approximately 0.1 g/min.

It was intended to measure the sulphur content of the gas and to calculate the sulphur release from the coal from this. An E.E.L. instrument for the measurement of SO_2 in the atmosphere was available and this was used after modification to allow higher SO_2 concentrations to be measured. The instrument gives a photo-electric indication of the extent of de-colourisation of a continuous flow of iodine solution. Since the sulphur was to be determined as SO_2, it was necessary to add oxygen to the argon carrier gas. Unfortunately, it was found that it was not possible to feed the coal steadily at the low rate required. Hence the SO_2 concentration varied widely and unpredictably throughout a test and could not be used to assess the sulphur released from the coal.

The experiments were then repeated without adding oxygen and the solid products were collected and analysed for total and pyritic sulphur. This procedure was successful, but there was insufficient time to make other than a simple comparison between the coals with the furnace maintained at 1470 °F and the collector located to give a solids residence time of approximately 100 ms.

4.4 The results

The experimental results are given in Table 5. In both coals almost all of the pyritic sulphur was released in 100 ms, but less than half of the organic sulphur was released. This confirms the difference in release rates between the forms of sulphur, indicated in Section 3. The amount of organic sulphur released in 100 ms from Welbeck coal is 30% more than from Pittsburgh, i.e. 46% in comparison to 35%. There was a 20% greater release of total sulphur from Welbeck coal during the experiment.

The ratio of organic to pyritic sulphur for the Pittsburgh char in the experiment (13) is in very good agreement with that for the cyclone fines from the combustor when burning this coal (a mean value of 12, see Table 3). However, for Welbeck coal there is a considerable difference between the ratios for the char (17.5) and the cyclone fines (2.5, see Table 4). Although there were oxidising conditions in the combustor and reducing conditions in the experiment, it is surprising that there should be agreement for one coal and not for another.

Selected solids samples from the 36 in combustor (Task I) were also examined for forms of sulphur. These samples were of primary cyclone fines from Test Series 2 (Pittsburgh coal) and Test Series 3 (Welbeck coal). The analyses are given in Tables 3 and 4.

Table A7.3 Forms of sulphur in cyclone Fines : 3 ft combustor: Pittsburgh Coal

	Sulphur % as received				Ratio Org./Pyr.
	Total	Organic	Pyritic	Sulphate	
Test 2.1	2.13	0.4	0.03	1.7	13
Test 2.2	2.50	0.3	0.05	2.15	6
Test 2.3	2.62	0.25	0.02	2.35	12
Test 2.4	2.47	0.30	0.02	2.15	15

Table A7.4 Forms of sulphur in cyclone fines: 3 ft combustor: Welbeck Coal

	Sulphur % as received				Ratio Org./Pyr.
	Total	Organic	Pyritic	Sulphate	
Test 3.4	1.31	0.15	0.06	1.10	2.5
Test 3.5	1.57	0.15	0.07	1.35	2.1

The data in Tables 3 and 4 show that the ratio of organic to pyritic sulphur in the cyclone fines is considerably higher than in the coal, being about 10 for Pittsburgh and about 2.5 for Welbeck. This indicates that in both coals the rate of release of pyritic sulphur was higher than that of organic, the difference in rates being greater for Pittsburgh coal than for Welbeck. The large amount of sulphate in the fines is the sulphur retained as calcium sulphate.

Table A7.5 Results of laboratory furnace experiments

Test conditions:

Carrier gas : Argon
Furnace Tube Temps. °F : 1470°F
Gas temperature : 1470°F
Feed particle size : 53 - 75 μm
Residence time : 100 ms
Coals : (a) Pittsburgh
(b) Welbeck (II) see Tasks I & V

		Pittsburgh	Welbeck
Decomposition:			
Coal feed	g	5.5	5.43
Char yield	g	2.35	2.30
" "	%	42.4	42.5
Total sulphur:			
In coal	%	2.79	1.54
In char	%	2.41	1.12
In char	% of coal	1.02	0.47
Retention	%	37	30.5
Pyritic sulphur:			
In coal	%	1.34	0.70
In char	%	0.17	0.06
In char	% of coal	0.072	0.025
Retention	%	5.4	3.6
Organic sulphur*			
In coal	%	1.45	0.84
In char	%	2.24	1.06
In char	% of coal	0.95	0.45
Retention	%	65	54
Ratio, Organic/Pyritic in char		13	17.5

* Calculated by difference between total and pyritic sulphur.

At the present time it can be concluded that there are differences between the rates of release of the pyritic and organic forms of sulphur, with the pyritic being released more rapidly. However the actual release rates vary from coal to coal and may also be affected by the operating conditions, in particular by whether the surrounding gas is oxidising or reducing.

5. ACKNOWLEDGEMENT

The experimental work described in Section 4 was carried out at BCURA by Mr. R.F. Littlejohn.

REDUCTION OF ATMOSPHERIC POLLUTION

Research on reducing emission of sulphur oxides, nitrogen oxides and particulates by using fluidised bed combustion of coal

Appendix 8. Limestone and dolomite studies. (Task VIII)

Main objectives

To investigate the pore structure and related factors that affect sulphur retention by lime.

Report prepared by: F.V. Bethell
A.A. Herod
G. McDonald
B.A. Napier
D.H.T. Spencer

Report approved by: A.D. Dainton and
H.R. Hoy

A8. i

FOREWORD

This Appendix describes laboratory experimental work carried out at BCURA between June 1970 and June 1971 as Task VIII of the joint NCB/OAP research programme. The objective of Task VIII was to obtain information on the limestones and dolomites selected for the pilot plant work, as follows:

(a) the development of their pore structures on calcination, both with and without sulphation, and

(b) their rates of reaction with SO_2, for use in the Mathematical Model, Task VI.

A summary of the investigations is presented in the Main Report.

Preceding page blan

TABLE OF CONTENTS

Page No

1. INTRODUCTION AND PRESENT POSITION A8.1

2. POROSITY MEASUREMENTS: MERCURY POROSIMETRY AND DISPLACEMENT DENSITY A8.6

  2.1 Introduction A8.6
  2.2 Preparation of Samples A8.6
    2.2.1 Exploratory samples A8.6
    2.2.2 Samples treated in controlled atmospheres A8.7
  2.3 Experimental Techniques Used for Measuring the Porosity A8.8
    2.3.1 Helium density measurement A8.8
    2.3.2 Mercury density measurement A8.9
    2.3.3 Helium and mercury density A8.9
    2.3.4 Mercury injection porosimetry A8.10
  2.4 Results and Discussion A8.13
    2.4.1 Exploratory experiments A8.13
    2.4.2 Controlled atmosphere experiments A8.14
      2.4.2.1 Linear relation between $1/\rho_{Hg}$ and π_{Hg} and between $1/\rho_{He}$ and π_{Hg} A8.16
      2.4.2.2 Evidence that the calcined and calcined-sulphated stones have little or no open porosity behind entrances <0.014 μm in diameter, with possible exceptions A8.17
      2.4.2.3 Increase of pore volume with increase of extent of calcination A8.17
      2.4.2.4 Estimate of porosity development in stone, from mercury density A8.18
      2.4.2.5 Comparison of the distribution of pore volume with respect to entrance diameter for the different stones A8.19
      2.4.2.6 Effect of sintering on pore size A8.20
      2.4.2.7 The effect of sulphation on pore structure A8.21
      2.4.2.8 Sulphur fixation A8.29

  2.5 Conclusions A8.30

3. MERCURY POROSIMETRY ON PARTIALLY SULPHATED PARTICLES BEFORE AND AFTER BREAKAGE A8.34
  3.1 Method and Samples A8.34
  3.2 Results A8.35

4. STUDIES OF POROSITY AT ELEVATED TEMPERATURE A8.38
  4.1 Introduction A8.38
  4.2 Principles A8.38
    4.2.1 Types of pore involved A8.38
    4.2.2 Experimental procedure for measurement A8.38
  4.3 Experimental A8.39
    4.3.1 Description of apparatus A8.39
    4.3.2 Calibration of apparatus A8.40
  4.4 Results A8.42
    4.4.1 Pore closure experiments A8.42
    4.4.2 Pore penetration experiments A8.42
  4.5 Discussion and Conclusions A8.44
    4.5.1 Pore closure A8.44

Preceding page blank

TABLE OF CONTENTS (cont'd)

Page No

4.5.2 Pore penetration A8.44
    4.5.2.1 Helium A8.44
    4.5.2.2 Xenon A8.44
4.5.3 Incidental observations in the pore penetration experiments A8.47

5. THE EFFECT OF THERMAL CYCLING ON SO_2 UPTAKE A8.49

5.1 Introduction A8.49
5.2 Apparatus and Procedure A8.49
5.3 Results and Conclusions A8.50

6. MISCELLANEOUS A8.51
6.1 Optical Microscopical Examination A8.51
6.2 Surface Area A8.51

7. MEASUREMENTS OF SO_2 REACTION RATE CONSTANTS A8.54
7.1 Description of Apparatus and Experimental Procedure A8.54
7.2 Mathematical Procedures A8.57
7.3 Results A8.59
7.4 Discussion A8.60

8. ADDENDUM A8.62

9. GLOSSARY OF TERMS A8.65

10. REFERENCES A8.69

11. ACKNOWLEDGEMENTS A8.71

Tables A8.1 to A8.24

Figures A8.1 to A8.63

Mercury porosimetry data

(Note that when referring to Tables and Figures in the text the prefix A8 is omitted.)

1. INTRODUCTION AND PRESENT POSITION

The removal of sulphur oxides from gaseous combustion products by limestones or dolomites is of the basis of several projected methods for the reduction of atmospheric pollution. The use of such stones is particularly attractive because reaction occurs at elevated temperatures, e.g., 1500°F, and sulphur oxide removal can be effected in the combustion zone. In the stone-injection process for fluidised-bed combustors, with which the present work is concerned, the atmosphere is oxidising and the overall reaction is:

$$CaO + \tfrac{1}{2}O_2 + SO_2 \rightarrow CaSO_4$$

However, it is well known that laboratory studies show that stones differ widely in their capabilities to remove SO_2 at elevated temperatures, and this complicates the choice of a stone for plant use. Reasons for these differences are not well understood, but it is generally accepted that they are ascribable to differences in physical structure rather than in chemical composition[1,2]. Certainly, porosity formation on calcination has been established as an important factor, for example by Potter[1]. However, it is not known why various types of stone calcined under the same conditions should give calcines having markedly different pore structures. Potter's work was aimed at the correlation of the physical properties of eighty six carbonate rock samples with their capacity to remove SO_2 from a simulated flue gas stream. The reactor for sulphation was a 30 mesh screen, preheated to sulphation temperature, on to which the sample was dumped as a static bed. Normally samples were precalcined at 1800°F and then sulphated at that temperature, but supplementary tests were made with two stones, one a limestone and the other a dolomite, as the hydrate and carbonate, as well as the oxide (prepared at 1800°F), with sulphation over a wide temperature range. For each stone the hydrated form showed the best retention characteristics up to 1830°F, whilst the precalcined stone was better than the uncalcined one. A series of calcinations at 2400°F indicated a loss in B.E.T. nitrogen adsorption surface area and (from mercury porosimetry) a loss in total pore volume and an increase in mean pore-entrance diameter, compared with calcination at 1800°F; also the shift in volume of pores with entrances larger than 0.3 μm diameter on calcination for the two temperatures parallelled the shift in SO_2 capacity at 1800°F. In his analysis of data for the samples calcined and then sulphated at 1800°F, Potter calculated correlation coefficients (each correlation coefficient was an index of the probability of there being a valid correlation between SO_2 capacity and some other variable): with the exception of iron content, the chemical composition, e.g., carbonate content, had no significant relevance to SO_2 capacity, and a poor correlation coefficient between B.E.T. nitrogen adsorption surface area and SO_2 capacity was taken to indicate the unimportance of pores with entrances of a few nm diameter; the importance of larger pores was indicated, through mercury porosimetry, by (equally) good correlation between either volume in pores with entrances greater than 0.3 μm diameter, or total pore volume, and the SO_2 capacity.

Classification by Potter of stones according to SO_2 capacity showed that Iceland Spar, comprising large crystallites, was the worst stone - even Magnesite, $MgCO_3$, was better. Chalk and oolitic samples, typically fine grained materials, had the greatest SO_2 capacity; dolomites were better than calcites, which were slightly better than marble samples. In summary, Potter considered that iron content, and mean pore-entrance diameter and total pore volume both measured by mercury porosimetry, are the "most fundamental variables for explaining differences in the SO_2 capacities of samples".

Also, the fact that the SO_2 capacity of a limestone particle may be well below that expected from purely chemical considerations is believed to be due to the formation of a layer ('shell') of sulphate, presumably involving thickening of pore walls, which impedes the further ingress of SO_2 towards the centre of the particle. The presence of such a shell has been observed by optical microscopy[3] and by electron microprobe analysis[3,4]. With dolomites, such a shell is either not formed, or formed to a much less marked extent than with limestone, so that the interior of a dolomite particle is the more readily available for SO_2 sorption. The reason for this difference in behaviour between limestones and dolomites is not clear, but it is probable that the presence of the magnesium oxide in calcined dolomite exerts a modifying influence, particularly as: (a) the pores formed in the decomposition of the magnesium carbonate, which occurs before that of the calcium carbonate, may facilitate the subsequent egress of CO_2 from the latter, resulting in a different final pore structure from that of calcined limestone; (b) MgO remains unchanged during the sulphation, and pores bounded by MgO, as well as CaO, in their surface would seem to be less likely to become blocked by $CaSO_4$ than those bounded by CaO alone.

It is clear therefore that basic studies aimed at obtaining further understanding of the retention of sulphur oxides by stones should include measurements of the pore structures of those stones. Such an investigation is reported in this Appendix, and since in the present work stones were fed into the fluidised combustors in the un-calcined state, particular emphasis has been placed on following the development of pore structure at various stages of calcination and how it is modified during sulphation.

The present studies are limited to the few stones used for the plant tests. The agreed programme of work has been as follows:

1. The first objective was to ascertain whether the accessibility to gases of pores in calcined stones changes with temperature. In the past, the pore structures of stones have been characterised at room temperature or below, and it has been tacitly assumed that those structures do not materially change on increasing the temperature to those of combustors. Changes of pore accessibility to gases are known to occur with some materials, such as synthetic graphites, chars, and glasses, and it was agreed that it would be worthwhile to see whether stones show any such behaviour, using a technique developed by BCURA for work on synthetic graphites under contract to the UKAEA[21a]. This technique concerns penetration of gases only, and discloses whether with temperature change any previously inaccessible pores become accessible or previously accessible pores become inaccessible. The experiments, which were carried out on U.K. Dolomite and Limestone 1359 only (both fully calcined), showed that there is no increase or decrease in pore volume accessible to helium or neon on increasing the temperature of the calcined stones to 1470°F. This means that, with certain reservations, pore structure measurements involving these gases, such as helium displacement density, could justifiably be made at the conventional temperature, i.e., room temperature. There was no decrease of accessibility to either krypton or xenon (which has approximately the same molecular size as SO_2), but there was apparently some increase of accessibility to xenon with certain samples though the results are complicated by an adsorption effect - some attempt at explaining this is made. It is noted that when the temperature of the stone is increased, thermal expansion will cause some modification of the accessible pore structure, so that, for example, mercury injection porosimetry, necessarily carried out at room temperature, may give a pore volume distribution somewhat different from that obtaining at the elevated temperature of interest.

2. When stones are injected into the fluidised-bed combustor they are subjected to rapid heating. In consequence the main body of the present work concerned measurement and application of mercury injection porosimetry (pore-entrance diameters down to 0.014 μm) and mercury and helium displacement

densities, to follow the development of pore structure on rapidly heating stones and then heat soaking them for various times in chosen atmospheres. Exploratory experiments were made in which stone particles were dropped into a furnace at 1470°F and left in the furnace for specified times before removing them for weighing and pore structure examination; the furnace-atmosphere was such that it either initially contained air, no attempt at flushing being made, or it was flushed with nitrogen. The results of these experiments led to a second series of experiments being carried out with the furnace, at 1470°F or 1650°F, flushed with a specified gas mixture - composition by volume, 15% CO_2, 3% O_2, 82% N_2, with and without 2000 ppm of SO_2 being present, - the aim being, when the SO_2 was present, to simulate the behaviour of stone particles in the combustor. The results have enabled a number of conclusions to be drawn regarding changes of pore structure on calcination and sulphation and cause of certain differences in sulphur oxide capacity found among the stones examined. This has led to the specification of a proposed simple test by which stones of unknown sulphur oxide capacities may be placed in order of capacity or 'screened' before carrying out more extensive tests on promising stones.

3. Mercury porosimetry was carried out on calcined-only and sulphated stone particles before and after breakage to obtain further information on the 'sulphate-shell'. Exposure of porosity on breakage occurred with Limestone 1359 sulphated in the laboratory, but not with the stone after sulphation in the combustor; the reason for this difference is not certain. Breakage did not expose further porosity in sulphated dolomites. Electron microprobe analysis[3] also revealed the presence of a 'shell' in laboratory sulphated Limestone 1359 while with sulphated U.K. Dolomite the sulphur was distributed more uniformly throughout.

4. A limited investigation was performed to see whether repeated thermal cycling of stones caused any reduction in their sulphur oxide retention capability. This experiment followed a suggestion that in the recycling of stones in a combustor the alternate heating/cooling process might have such adverse effect. Only U.K. Dolomite and Limestone 1359 were investigated and the results showed no systematic effect of repeated thermal cycling on progressive sulphur oxide uptake.

5. To provide input data for the mathematical model (Appendix 6), quantitative measurements of reaction rate were made using a flowing system in which SO_2 - containing gas was passed through thin beds of stone particles at the required temperature.

Each of the above items of work is described in detail in the following sections of this Appendix.

2. POROSITY MEASUREMENTS: MERCURY POROSIMETRY AND DISPLACEMENT DENSITY

2.1 Introduction

When stones are injected into the fluidised-bed combustor they are subjected to rapid heating. To obtain some information on the development of pore structure under such conditions, exploratory experiments were carried out in which stones were subjected to rapid heating and then heat soaking at 1470°F. The results suggested that pore volume, pore-entrance diameter and the extent and time of calcination were related. Therefore, further experiments were done, to investigate these effects, and those of sulphation, using samples prepared in more closely controlled conditions. These experiments involved calcination only, and calcination and sulphation together, carried out under oxidising conditions using controlled atmospheres (shown in Table 1). The experimental method was arranged to allow rapid heating of the stone from room temperature to 1470° or 1650°F.

2.2 Preparation of Samples

2.2.1 Exploratory samples

Samples of between 2 and 5g of the U.K. Dolomite and Limestone 1359 were rapidly heated by sprinkling them into a vertical furnace closed at the lower end and maintained at 1470°F; the soaking times ranged from 15 min to 115 h. In the first experiments, the atmosphere in the furnace tube was essentially stagnant air with CO_2 escaping by diffusion, causing the partial pressure of CO_2 to increase with time. In later experiments the tube atmosphere was swept by dry nitrogen gas.

The size grades, BS mesh, of the stones used were:

U.K. Dolomite	-6 + 8, -16 + 52, and -300.
Limestone 1359	-16 + 52, and -300.

The extents of calcination (E_c) of the two stones were measured. E_c is defined in this Appendix as:

$$E_c = \frac{100\ W_1}{W_T}\ \% \qquad (1)$$

where W_1 is the mass loss, due to CO_2 loss, undergone by the sample on the partial calcination and W_T is the mass loss the sample would have undergone on complete calcination. In these preliminary experiments, W_1 was obtained by weighing and W_T from chemical analysis data for the uncalcined stone. The calcination histories of individual stones and their designations are shown in Tables 2 and 3. The prefix letter of a stone designation indicates its size grade, as shown in Table 4.

2.2.2 Samples treated in controlled atmospheres

The four stones used during the later part of the contract work, Dolomite 1337, U.K. Dolomite and Limestones 18 and 1359, were prepared under controlled conditions, enabling the development of the porous structure to be assessed in an atmosphere that comprised $CO_2/N_2/O_2$ with and without SO_2.

The apparatus consists of a vertical furnace tube in which the sample is held on a removable perforated tray, in a layer c. 5 mm deep, at the centre of the tube. A feeder is provided which allows samples of material (c. 5g were used) to be fed directly onto the tray thus facilitating rapid heating of the sample to the furnace temperature. An atmosphere of known composition is admitted to the furnace by equipment similar to that used in the thermal cycling experiments (Section 5) and in the reactivity experiments (Section 7).

As noted above, the experimental programme is shown in Table 1, and consists of experiments using one range of particle size(-16 +52 BS mesh), one gas composition with and without SO_2, and two temperatures.

Details of the treatment of individual stones and their designations are shown in Table 5.

Extents of calcination (see Equation 1, Section 2.2.1) for the samples treated in:

(a) The SO_2-free atmosphere, were determined as described in Section 2.2.1.

(b) The SO_2-bearing atmosphere, were determined, as correction was necessary for mass gain due to sulphation, by calculating W_1 (Equation 1) from the chemical analyses of the samples, viz, residual 'CO_3' and 'S' present and taking into account the composition of the original stone.

Sulphation (E_s) of the samples was determined, E_s being defined as:

$$E_s = \frac{100\,\bar{W}_1}{\bar{W}_T} \quad \% \qquad (2)$$

where $\bar{W}_1$ is the mass of sulphur in the sulphated sample and $\bar{W}_T$ is the mass of sulphur that would have been present if all the $CaCO_3$ had been converted to $CaSO_4$. $\bar{W}_1$ was calculated, as with W_1 mentioned under (b) above, from the chemical analysis data.

2.3 Experimental Techniques Used for Measuring the Porosity

Two basic techniques were used to obtain: (i) the total porosity (excepting that in pores with entrances > 14.5 µm and < 0.26 nm in diameter), (ii) the porosity with respect to certain pore-entrance diameter ranges. These techniques were: (i) displacement density in two fluids, helium and mercury, (ii) mercury injection porosimetry. They are described below.

2.3.1 Helium density measurement

The 'helium density' of a solid is the mass of the solid divided by the volume of helium it displaces when immersed in that gas. Helium density, in conjunction with the superficial and solid-matter densities gives, respectively, the pore volume open and closed to helium; it often affords a close approximation to the solid-matter density which is not always determinable.

The helium displacement volume (V_{He}) was measured at 77°F using apparatus in which a known quantity of helium could be transferred to the sample chamber, enabling the volumes the gas occupied in the chamber, empty and with a known mass of the evacuated sample present, to be found using gas-law principles. V_{He} is the difference between those two volumes. The evacuation was at room temperature at 10^{-5} torr. Experimental error was < 1% with the controlled-atmosphere samples, but with the exploratory samples where the quantities available were less, it could be up to 3 or 4%. The error is not considered to have materially affected the general trends that emerged from the use of the density values.

Helium is the nearest to the ideal displacement fluid because:

(i) It has the smallest molecule (kinetic diameter, 0.26 nm) and penetrates all but the finest pores; slow penetration of helium into samples, seen as a slow decrease of V_{He} with lapsed time, would reveal the presence of pores or pore entrances with diameters close to 0.26 nm.

(ii) It is not significantly adsorbed at the measurement temperature of 77°F, except by certain highly microporous materials such as active carbons for which the measurement temperature must be increased: adsorption of helium is expected to be insignificant with the stones.

The justification for applying helium densities measured at 77°F, when the stones are used at elevated temperatures, is discussed in Section 4.

2.3.2 Mercury density measurement

The 'mercury density' of a solid is the mass of the solid divided by the volume of mercury it displaces when immersed in that liquid under a specified pressure (P). Assuming that the mercury does not wet the solid, the fluid will not penetrate pores with entrances smaller than a certain critical level, depending on the value for P – see Section 2.3.4.

Mercury density was measured using a bulb of c. 5 cm^3 volume. The mass and hence volume needed to fill the bulb to a reference mark without and with a known mass of previously evacuated stone present was found. The mercury displacement volume is the difference between those two volumes. The stone samples were evacuated at room temperature at 10^{-5} torr, and mercury was admitted to the bulbs in vacuo from a filling device: the bulbs were placed in a thermostatic bath at 77°F for several hours before the mercury levels were adjusted to the reference marks of the bulbs. The experimental error in the mercury densities is up to c. 0.5%. For pressure P, an average value of 760 torr (1.013 bar) was taken for any particle. In the present work, circular pore-entrances have been assumed (Section 2.3.4) and this pressure has been taken as equivalent to a pore-entrance diameter of 14.5 μm.

2.3.3 Helium and mercury density

Mercury density and helium density together give the volume of pores (V_x) with entrances (assuming them to be circular) of diameter < D and > 0.26 nm, where D is the pore-entrance diameter value corresponding to pressure P, and 0.26 nm is the kinetic diameter of the helium molecule, noted above.

$$V_x = 10^3 \, (1/\rho_{Hg} - 1/\rho_{He}) \; mm^3/g \qquad (3)$$

where ρ_{Hg} and ρ_{He} are the mercury and helium densities, g/cm^3, respectively.

With a lump material, it may be possible for pressure P to be made sufficiently low so that no penetration of pores by mercury occurs, the corresponding mercury density then being equal to the lump density, and V_x in Equation 3 then being equal to the total volume (V_T) of pores with entrances > 0.26 nm in diameter. V_T may also then be expressed as a percentage of the lump volume:

$$V_T = 100\ (1/\rho_{Hg} - 1/\rho_{He})\ \rho_{Hg}\ \% \qquad (4)$$

Mercury density so measured is of valuable application to samples of irregular shape whose lump densities cannot be readily determined by mensuration and weighing.

With particulate materials, the pressure P must be sufficient to ensure that spaces between the particles are filled by mercury, and this may cause some penetration of the particles themselves, so that V_T cannot be calculated in the absence of independent knowledge on the volume of pores with entrances > D in diameter. However, it is often valuable to express V_x as an approximation to the percentage of the particle superficial volume, for example, for comparison among a set of samples, by putting the particle density (mass per unit superficial volume) ρ_P g/cm^3 equal to ρ_{Hg} in the following equation:

$$V_x = 100\ (1/\rho_{Hg} - 1/\rho_{He})\ \rho_P\ \%$$

to give $$V_x = 100(1/\rho_{Hg} - 1/\rho_{He})\ \rho_{Hg}\ \%$$

This approximate calculation of V_x as a percentage is used in the present work.

2.3.4 Mercury injection porosimetry

Mercury injection porosimetry has been reviewed in detail by Rappeneau[5] and Scholten[6] and discussed briefly by Innes[7]; recent papers have been reviewed by Spencer[8].

The method depends on the phenomenon of capillary depression, a certain minimum pressure P being required to force mercury through an entrance whose surface is not wetted by the mercury. In general terms if the entrance has perimeter L and cross-sectional area A:

$$AP = L\ \sigma \cos\ (180 - \theta) \qquad (5a)$$

where σ is the surface tension of the mercury and θ ($> 90^\circ$) is the angle of contact.

In applying this relation to pore structure measurement, it is necessary to make simplifying assumptions on pore-entrance shape: it is normally assumed that the pore entrances are circular, when:

$$P = \frac{4\sigma}{D} \cos (180 - \theta) \tag{5b}$$

Occasionally, when a material is considered to have slot shape pores, then the entrances have been taken to be of rectangular cross-section, with long side nD and small side D, with $n \gg 1$, when:

$$P = \frac{2\sigma}{D} \cos (180 - \theta) \tag{5c}$$

A pore-volume distribution, with respect to D, is obtained by determining the cumulative volumes of mercury that enter the sample as the pressure is increased in steps, the pressures being converted into D values; the curve of cumulative pore volume vs D shows the pore volume lying behind entrances with D values within any chosen limits in the range of D covered. Additionally, the curve may be expressed in the first differential form, or as a histogram. It is important to note that D refers to pore entrances, which may in some instances be narrower than the bodies of the pores themselves.

In almost all mercury porosimeters the previously evacuated sample is immersed in mercury and the penetration into the sample is followed as the loss of mercury from some form of reservoir, usually a uniform-bore tube, connected to the sample chamber. In the particular apparatus that was used in the present work* such a tube is situated vertically above the sample chamber. After evacuation, mercury is admitted to the sample chamber and the tube up to a height (h) above the centre of the sample. The pressure equivalent to h is taken as the starting pressure. The pressure is increased on the mercury surrounding the sample by increasing application of gas pressure above the meniscus in the tube: (1) by admitting air incrementally up to atmospheric pressure; (2) after transfer of the sample chamber unit to a pressure vessel, by admitting nitrogen.

---

*The apparatus was developed at BCURA with permission from original drawings, supplied by Morganite Carbon Ltd., of the apparatus described in Ref 9.

from a compressed gas cylinder to the vessel in steps until the pressure reaches finally c. 8 bar; and (3) by compressing the gas in the vessel up to c. 1035 bar by use of a hydraulic pumping system. The penetration of the mercury is measured as follows: a stretched wire lies along the principal axis of the tube, part of this wire being immersed in the mercury. As the height of the mercury decreases so the length of wire exposed, and hence its electrical resistance, increases. This resistance forms one arm of a Wheatstone bridge. To eliminate the effect, albeit small, of the compression of the mercury, the opposite arm in the bridge is formed of a similar resistance-wire from a dummy sample-chamber unit, which during operation contains a similar amount of mercury to that in the sample unit, but no sample. The progressive change in output from the bridge, measured with a digital voltmeter, is subsequently converted through a previously determined calibration factor to the cumulative quantity of mercury penetrating the sample.

Samples of stones for porosimetry measurements were sieved (+ 52 BS mesh) to remove fines. (These same fines-free samples were used for specific surface measurements - Section 6 - and for the density measurements.) After a preliminary evacuation in a vacuum oven at 200°F, samples were transferred to the sample chamber of the porosimeter and evacuated at room temperature before admission of mercury. A metal gauze was used to prevent the stone particles floating into the capillary measuring-tube.

In the present work, for the conversion of the pressures to D values, it was assumed that the shape of the pore entrances of the stones is circular, viz, Equation 5b above was used, values of 480 dyne/cm and 140° being taken for σ and θ, respectively. The initial height h referred to above was c. 190 mm, equivalent to a D value of c. 58 µm. Any pores with entrances having diameters greater than this value would be filled before the measurements are started and hence be undisclosed. The highest pressure attained, c. 1035 bar, is equivalent to a D value of 0.014 µm.

Calculations were carried out using an Elliot 4120 computer and the distribution curves were plotted by an on-line digital plotter.

The cumulative distribution curves were begun arbitrarily at zero pore-volume at the calculated D value of c. 58 µm corresponding to the initial height h. Because the samples are granular, penetration of mercury into the spaces between the granules will occur in addition to any penetration into the material itself, but earlier work at BCURA on non-porous granular samples shows that the intergranular penetration with the present samples should have been virtually complete at a pressure corresponding to a D value of $\geq$ 10 µm.

2.4 Results and Discussion

Mercury porosimetry measurements were carried out on samples from the exploratory experiments; helium and mercury density measurements were made on U.K. Dolomite samples only.

Mercury porosimetry, helium and mercury density measurements were made on samples from the controlled atmosphere experiments.

The locations of the results used in discussion are given in the following Sections; the 'raw' mercury porosimetry data are collected at the end of this Appendix.

2.4.1 Exploratory experiments

The cumulative pore volume distribution curves, obtained from the mercury porosimetry, are displayed in Figs. 1 to 3, and the corresponding first differential curves are given in Figs. 4 to 6. In Table 6 are listed: the extents of calcination for the stated residence times in the furnace; the total pore volumes reached by mercury, as measured, i.e., the pore volume with entrances between c. 58 µm and 0.014 µm (t.p.v.) - no attempt being made to correct for any contribution due to intergranular volume; and the value for the pore - entrance diameter (Δ) corresponding to the main peak in each of the first differential curves.

Helium and mercury density results for U.K. Dolomite are referred to in the next Section.

As might be expected, it is evident that apart from the early decomposition of the $MgCO_3$ in U.K. Dolomite (see below), the partial pressure of CO_2 in the furnace strongly influenced the rate of calcination, which proceeded much more rapidly in the nitrogen-flushed atmosphere (low partial pressure of CO_2).

An important difference in behaviour between U.K. Dolomite and Limestone 1359 is that the dolomite calcined much more rapidly over an initial 1/4 h period: compare the dramatic development of pore structure in the dolomite after 1/4 h with the small development in the limestone after 1/2 h. This initial calcination of the dolomite appears to be unaffected by the partial pressure of CO_2 in the furnace atmosphere and corresponds to decomposition of $MgCO_3$, which is known to occur at lower temperatures than $CaCO_3$ decomposition. A slow weight loss with elapsed time ensued with both stones at high partial pressures of CO_2; although the corresponding results were not completely obtained at low partial pressures, rate of weight loss was higher as expected.

The results for U.K. Dolomite, Figs. 1, 2, 4 and 5 and Table 6, show that:

(a) the total pore volume (t.p.v.) disclosed increases with the measured extent of calcination, and for the samples calcined to > 99% (samples C5, C7 and C9, Table 6), the t.p.v. appears to increase with the time of calcination.

(b) The peak pore-entrance diameter (Δ) for the samples that have reached approximately the same extent of calcination, viz. samples C2, C6, C8, and samples C5, C7, C9, Table 6, increases with the time of calcination.

In the series of Limestone 1359 samples, the t.p.v. increases with increasing extent of calcination and with time of calcination (Table 6).

In summary, the main differences between the two stones, as revealed by these exploratory experiments, are:

(i) For the same calcination time more pore volume develops in the dolomite than in the limestone, and this difference is most marked for short calcination times, viz. 1/4 or 1/2 h.

(ii) For the limestone, Δ appears to reach a limiting value, whereas for the dolomite no limit in Δ was seen.

(iii) This limit in Δ for the limestone (1.10 μm) is larger than the maximum value for Δ reached with the dolomite (0.46 μm).

(iv) With the dolomite, volume in pores with entrance diameters > Δ <c.58 μm increases with calcination time; with the limestone this effect is either absent or less marked.

2.4.2 Controlled atmosphere experiments

Tables 7 to 10 show, for the four stones: (1) the calcination and sulphation details, (2) the helium and mercury densities, ρ_{He} and ρ_{Hg}, respectively, (3) the helium and mercury displacement volumes, $1/\rho_{He}$ and $1/\rho_{Hg}$, (4) V_x (see Equation 3, p.9) mm^3/g and $V_x\%$ (see p.10), V_x being the volume of pores with entrances < 14.5 μm and > 0.26 nm in diameter; and, from the mercury porosimetry, (5)(a) t.p.v. (as defined above in Section 2.4.1), (b) the volume obtained by interpolation, in pores with entrances <c.58 μm > 14.5 μm diameter, and (c) the volume, τ_{Hg}, obtained by interpolation, in pores with entrances < 14.5 μm and > 0.014 μm diameter, the reason for selecting the value of 14.5 μm here being to coincide with the upper limit of pore-entrance diameter to which V_x refers. The location of other data is indicated within the following text.

In examining the data, attention has been given to seeking possible correlations, and to this end a considerable number of curves have been plotted, and are reproduced in this Appendix. The following Sections include details of:

(i) linear correlations between reciprocal displacement density and π_{Hg} (mm^3/g), which could be useful in estimating the porosity in calcined stones, using simple ρ_{Hg} measurement;

(ii) comparison of V_x with π_{Hg};

(iii) porosity development as a function of (i) time, and (ii) extent of calcination, and the reduction in porosity on sulphation - in particular, development and modification of porosity (including the effect of sintering) behind entrances with diameters in specified ranges, without and with SO_2 being present in the controlled atmosphere;

(iv) the way in which sulphation lags behind CO_2 loss when these processes are carried out together.

Of immediate practical significance, the work shows that:

(a) the development of large(transport) pores is apparently necessary if a stone is to be a good absorber (a condition not met by Limestone 1359), but that much or even most of the sulphur is accommodated in small pores;

(b) the change of reaction temperature of the dolomites from 1470°F to 1650°F did not increase the rate of sulphation to the level expected from chemical kinetics considerations, and a speculative suggestion involving a surface species is put forward that might account for this behaviour and also for the fall-off in sulphur uptake > c. 1560°F in the combustor;

(c) the present type of 'drop-tube' experiment could be used as a simple screening test for placing unknown stones in order of acceptor ability.

2.4.2.1 Linear relation between $1/\rho_{Hg}$ and π_{Hg} and between $1/\rho_{He}$ and π_{Hg}

In the exploratory work it had been found for the U.K. Dolomite that $1/\rho_{Hg}$ and $1/\rho_{He}$ are linearly related to π_{Hg} mm^3/g, and all were functions of weight loss from the stone. (The individual $1/\rho_{Hg}$, $1/\rho_{He}$ results are included in Table 14, together with the π_{Hg} values.)

The corresponding $1/\rho_{Hg}$, $1/\rho_{He}$ vs π_{Hg} graphs for the stones from the controlled atmosphere experiments, calcined only, are shown in Figs. 7 to 10, which are likewise linear.

The intercept value of $1/\rho_{Hg}$ at $\pi_{Hg} = 0$ on the extrapolated line for each stone equals, within experimental error, the value of $1/\rho_{He}$ for the raw stone, this value being (ignoring any pores closed to helium) the volume of the solid matter. The $1/\rho_{He}$ values for the two raw dolomites are the same, c. 355 mm^3/g, while those for the two raw limestones are higher, being c. 370 mm^3/g for Limestone 1359 and c. 375 mm^3/g for Limestone 18. These values are in line with expectations based on listed densities, equivalent to specific volumes of 370 mm^3/g for $CaCO_3$, 330 mm^3/g for $MgCO_3$ (hence c. 350 mm^3/g for dolomite) and 390 to 440 mm^3/g for silica, the main impurity of Limestone 18.

The slopes of the $1/\rho_{Hg}$ (or $1/\rho_{He}$) lines for the dolomites are the same and likewise for the limestones.

Results for the calcined-sulphated samples from the controlled atmosphere experiments are also given in Figs. 7 to 10. In general, the points lie on or below the corresponding lines for calcination only. In Figs. 7 to 9, for Limestone 18 and the two dolomites, broken lines have been drawn through the 1650°F points. The value of π_{Hg} decreases with increasing sulphation (see Tables 7 to 9), and it is seen from the figures that with each stone, the lines meet at $\pi_{Hg} = 0$, and at a lower intercept value than the corresponding $1/\rho_{Hg}$ value for the samples that were calcined only, in accord with the lower specific volume of $CaSO_4$ than that of $CaCO_3$. This difference of intercept value is more marked with the Limestone 18 than with the two dolomites, in line with the fact that the difference in specific volume between $CaSO_4$ and $CaCO_3$ (c. 30 mm^3/g) is larger than that between $CaSO_4 \cdot MgCO_3$ and $CaCO_3 \cdot MgCO_3$ (c. 15 mm^3/g).

The corresponding points for the Dolomite 1337 and Limestone 18 samples calcined-sulphated at 1470°F (Figs. 7 and 9) tend to lie on the appropriate calcination line or between the latter and the broken lines: it is not clear if this is a real effect or due to experimental error.

An application of the above linear relations for the calcined-only samples is discussed in Section 2.4.2.4.

2.4.2.2 Evidence that the calcined and calcined-sulphated stones have little or no open porosity behind entrances < 0.014 μm in diameter, with possible exceptions

In Figs. 11 to 14, V_x mm^3/g is plotted *vs* π_{Hg}. For each stone, the straight line through the points passed through the origin and is of approximately unit slope, viz, for the samples, overall, $V_x \approx \pi_{Hg}$. This means that overall they must contain little or no porosity behind entrances with diameters in the range 0.014 μm to 0.26 nm, but among possible exceptions is the 4 h, 1650°F, calcined-sulphated Limestone 1359 (sample G41, Table 10) - this point is noted in Sections 2.4.2.7 and 3.2.

2.4.2.3 Increase of pore volume with increase of extent of calcination

In Section 2.4.1, on the exploratory experiments, it was shown that t.p.v. increases as the extent of calcination increases. The way in which V_x% and π_{Hg}% (viz, π_{Hg} mm^3/g converted to percentage of assumed particle volume, $1/\rho_{Hg}$, as with V_x mm^3/g) change with extent of calcination is shown in Figs. 15 and 16 for the samples calcined in the controlled atmosphere in the absence of SO_2; the corresponding data for U.K. Dolomite from the exploratory experiments are included. (The variation of both V_x% and π_{Hg}% is given for completeness.) The straight lines were drawn through the points for the samples (excepting the exploratory ones) and show that V_x% or π_{Hg}% is linearly related to the extent of calcination, although the points for Limestone 18 are scattered. In both figures, the stone with the least porosity before calcination, Limestone 1359, has the least porosity over the entire range. The order of increasing initial porosity of the raw stone is maintained at all extents of calcination with the exception of Limestone 18. In this case, however, the porosity is greater than for Limestone 1359 within wide errors at the highest calcination extents. For a particular stone the straight line implies that the amount of porosity formed is directly proportional to the amount of CO_2 lost.

The rate of calcination of all the stones was rapid at 1650 F: the extent of calcination reached after 1/4 h was 85% or more (Tables 7 to 10), and, as might be expected, further calcination occurred when heat-soaking was prolonged up to 4 h. With calcination at 1470°F, however, the situation was quite different. The atmosphere used for the calcination contained 15% CO_2 by volume; the equilibrium dissociation concentration of CO_2 over calcium carbonate at 1470°F is only 26% by volume, hence the atmosphere during the calcination can be expected to retard the rate of calcination. The results, Tables 7 to 10, indicate that this effect is more severe in Limestone 1359, which has the lowest initial porosity: after 1 h at 1470°F, the extent of calcination and porosity (V_x%) have reached, respectively, 4% and 5% compared with 20% and 14% with Limestone 18.

With the dolomites (as was seen with U.K. Dolomite in Section 2.4.1), the calcination follows a two-stage process - calcination to the "halfway" stage, $CaCO_3.MgO$, expected to be unaffected by the CO_2 atmosphere of the furnace, and calcination of the $CaCO_3$ entity, expected to be affected. Thus, at 1470°F, after 1/4 h in the CO_2 atmosphere, both dolomites develop much more porosity than the limestones: with the dolomites the extents of calcination and porosity (V_x%) are, respectively, 34% and 24% for Dolomite 1337 and 57% and 34% for the U.K. Dolomite, which values are much higher than the above mentioned 1 h values (say) for the limestones; for 1 h calcination of the dolomites, the corresponding values are, in the same order: 62% and 38%; and 67% and 38%.

Curves showing the variation of porosity with time of calcination will be seen in Figs. 27 to 35 - these are referred to in a later Section.

It is noted that at 1470°F some difficulty was experienced in this critical region with slight variations in furnace temperature which led to the apparently anomalous situation where the sample of Dolomite 1337 calcined for 1 h reached a greater extent of calcination than the sample calcined for 4 h.

2.4.2.4 Estimate of porosity development in stone, from mercury density

It should in principle be possible to estimate the porosity developed in different stones on calcination in the standardised atmosphere (without SO_2 present) used here, and hence place them in order of porosity development with respect to calcination time, by carrying out simple mercury density (ρ_{Hg}) measurements on the calcined products. Thus, referring to Figs. 7

to 10, as mentioned above the slopes of the $1/\rho_{Hg}$ or the $1/\rho_{He}$ lines are the same for the dolomites, and likewise for the limestones. This means that if a stone is of known composition so that the intercept value of $1/\rho_{Hg}$ (viz, at $\pi_{Hg} = 0$) can be placed, and hence the $1/\rho_{Hg}$ and $1/\rho_{He}$ lines, the experimentally determined $1/\rho_{Hg}$ value for a particular calcined sample will then give π_{Hg} (or $1/\rho_{He}$ to give V_x mm^3/g, and hence π_{Hg}% or V_x%, for that sample.

Such a procedure may be of value to obtain supporting information in assessing the sulphation behaviour of stones discussed in later Sections.

2.4.2.5 Comparison of the distribution of pore volume with respect to entrance diameter for the different stones

To obtain information on the extent to which pores with entrances of a particular diameter are generated during calcination or are reduced in volume during sulphation, the mercury porosimetry data have been analysed in two ways: the first consists of examining the volume in pores with entrances of diameters between 14.5 µm and various smaller values down to 0.014 µm for π_{Hg}; the second involves examining the pore volume for chosen ranges of pore-entrance diameter within the overall range 14.5 µm to 0.014 µm.

The pore volumes, for the various calcined and calcined-sulphated samples, behind entrances of diameters between 14.5 µm and successively*3.15, 0.985, 0.265, 0.105, 0.0305 and 0.0143 µm are shown in Tables 11 and 12; the volumes are expressed as mm^3/g and as percentages of particle volume ($1/\rho_{Hg}$). Incremental pore volumes (%) for the ranges of pore-entrance diameter between the successive values*14.5, 3.15, 0.985, 0.265, 0.105, 0.0305 and 0.0143 µm are shown for the calcined-only stones in Table 13. The diameter values < 14.5 µm are for convenience those corresponding to the measured pressures used in the mercury porosimetry measurements. For simplicity, these diameter values are written throughout as 3, 1, 0.3, 0.1, 0.03, and 0.014 µm.

The pore volumes (%) for the calcined-only stones, for the ranges 14.5 µm down to 0.014, 0.03, 0.1 and 0.3 µm, are plotted vs extent of calcination in Figs. 16 to 19.

The incremental pore volumes % are displayed in histogram form in Figs. 20 to 22.

---

* The third significant figure varies among the determinations.

It is clear from Figs. 16 to 19 that the two dolomites have most of their porosity in the pores with entrance diameters less than 0.1 µm. Also, although most of the relations show smooth curves, the porosity for Limestone 1359 in Fig. 18 shows no simple behaviour, with porosity developing in this range more sharply at the high temperature than the results at the low temperature would suggest. In the range of pore-entrance diameters 14.5 to 0.3 µm, the relations are all reasonably linear, as with the range 14.5 µm to 0.014 µm, but the order of development of porosity is changed, the dolomites lying between the two limestones as far as volume in these large pores is concerned. With Limestone 18 the formation of the latter occurs to a marked extent, but Limestone 1359 remains relatively poor during calcination as regards volume in such pores and this would be expected to militate against ease of access of SO_2 to the interior of the calcined stone, access being facilitated by the presence of wide "transport pores".

The histograms for 1470°F, in Fig. 20, clearly illustrate the lack of pores with the wider entrances in Limestone 1359, discussed above. The way in which the porosity within the overall range 14.5 to 0.03 µm develops in Limestone 18 is seen. The two dolomites show little change in the range 14.5 to 0.1 µm over the 4 h period and the changes in porosity occur in the specific ranges 0.1 to 0.03 µm for Dolomite 1337 and 0.1 to 0.014 µm for U.K. Dolomite. The porosity in U.K. Dolomite in the region 0.03 to 0.014 µm, which develops in the initial 1/4 h of calcination, disappears with time, but this disappearance is accompanied by increase in the 0.1 to 0.03 µm region; this phenomenon presumably involves a form of sintering (crystal growth), causing a shift in entrance diameter from the smaller to the larger of these two ranges.

2.4.2.6 Effect of sintering on pore size

The histograms, for 1650°F, in Fig. 21, show that the stones have more porosity overall than after calcination at 1470°F (Fig. 20), but for the range of smallest entrances, 0.03 to 0.014 µm, the dolomites have less porosity at 1650°F than at 1470°F, and the limestones have little at either temperature. Sintering is evident in all the stones except Dolomite 1337: with Limestone 18 after 4 h calcination there is relatively little porosity with entrances < 0.1 µm diameter, and with Limestone 1359 the progressive decrease with time of porosity with entrances between 0.1 and 0.03 µm diameter and the progressive increase of porosity with entrances between 0.3 and 0.1 µm diameter is most striking. The lesser development of wider pores (viz, having entrances > 0.3 µm in diameter) in Limestone 1359 at 1650° F is seen here.

It is worth noting the extent of sintering in U.K. Dolomite during the very long time of calcination in the exploratory experiments (Section 2.4.1) - Fig. 22: Sintering is much more evident on calcining for 97 h than for the 4 h used in the controlled-atmosphere experiments, and it is worth comparing also the histograms in Fig. 22 for samples C7 and C5, both of which have reached c. 99.5% calcination, although admittedly the atmospheres used in these two experiments were different. It is seen that most of the pores developed in the dolomite lie behind wider entrances in the exploratory experiments than in the controlled-atmosphere ones. The reason for this is not known.

Eventually, sintering could be expected to lead to enlargement of some pore entrances to > 14.5 μm diameter, which would then be penetrated by mercury in the ρ_{Hg} determination causing a decrease in $1/\rho_{Hg}$. A small difference in this direction is apparent between samples C7 and C5 (Table 14), but the observation is equivocal because the expected decrease in V_x is not matched by a decrease in π_{Hg}. With the calcined-only samples from the controlled atmosphere experiments, the only clear evidence of a decrease in $1/\rho_{Hg}$ and in V_x and π_{Hg} is seen with samples N13 and N15, Table 9 - for an increase in time of calcination at 1650°F from 1 h to 4 h, the extent of calcination remaining at 96.0%. However, there may also be an analogous effect with Limestone 1359: see samples G38 and G40, Table 10 (taking into account the small difference in the extents of calcination, since $1/\rho_{Hg}$ and π_{Hg}, expressed as volume per g of calcined sample, are being compared).

2.4.2.7 The effect of sulphation on pore structure

In Fig. 23, the level of sulphation reached by the various stones is plotted vs their residence time in the furnace. It is immediately obvious that Limestone 1359 is a relatively poor acceptor under the present conditions, at either temperature, since the stone has reached its limit of sulphation, c. 3% at 1470° and c. 8% at 1650°F, after only 1 h. These values compare well with the thermal cycling results, Table 22, for Limestone 1359 in the same size grade (-16 + 52 BS mesh), where the sulphur uptakes correspond to sulphations of < 6%. Limestone 18 shows a much better sulphur uptake pattern than Limestone 1359 and shows a significant difference in level of sulphation at the two temperatures. Each dolomite however shows little difference in the level of sulphation at the two temperatures; for the U.K. Dolomite sulphated for 1/4 h, the sample at 1650°F is slightly less sulphated than the sample prepared at 1470°F (10.7% compared with 11.8%

sulphation). If a normal reaction-rate temperature-dependence is expected, then the rate of sulphation should be several times greater at 1650°F than at 1470°F. Since this is not the case with the dolomites it appears that either the reaction has little or no activation energy, probably a result of catalytic mechanism, or that the reaction rate is controlled by other rate determining factors such as a diffusion control mechanism. Since in the pilot plants, the rate passed through a maximum, at c. 1560°F, a catalytic mechanism may be at work, and this point is elaborated, speculatively, in Section 2.4.2.8. It is noted that in Fig. 23, sulphation is the ratio of the quantity of sulphur taken up by the sample to that taken up if all the CaO were converted to $CaSO_4$: this means, for example, that at 1650°F, Limestone 18 would, on a mass or bulk volume of stone basis, be a better acceptor than Dolomite 1337.

Now in the present sulphation experiments the sample was not subjected to complete calcination before the sulphation was carried out, and certainly at 1470°F, CO_2 was being evolved from parts of the decomposing stone at the same time that sulphation was occurring in other parts of the structure. This is more akin to the initial situation in the combustor than would be the case with complete precalcination. As noted previously, the extents of calcination were measured after the particular residence times in the SO_2 bearing atmosphere. The way in which sulphation lags behind calcination is seen from Fig. 24, where sulphation is plotted vs extent of calcination for the same residence time (noting that with the dolomites, initially $MgCO_3$ decomposes to MgO, and that the sulphate is believed to be unstable at the present reaction temperatures).

Given below are the differences ($E_{C1}\%$ - $E_{C2}\%$) between the extents of calcination reached by the stones for the same residence times (t) with ($E_{C1}\%$) and without ($E_{C2}\%$) the SO_2 present: the $E_C\%$ values were taken from Tables 7 to 10

Stone	t, h	Temperature and (E_{C1}% - E_{C2}%)	
		1470°F	1650°F
Dolomite 1337	¼	+28.2	+5.5
	1	+12.6	+1.3
	4	+35.0	+9.0
U.K. Dolomite	¼	+ 4.2	-3.0
	1	+ 4.8	-1.0
	4	+12.4	-1.0
Limestone 18	¼	- 5 (mean)	+0.2
	1	+ 1.5	-2.0
	4	+36.1	+4.0
Limestone 1359	¼	+ 1.7	+3.6
	1	+ 3.7	+9.0
	4	- 9.0	+8.0

In most cases the extent of calcination, for a given time, appears to be greater in the presence of SO_2 than in its absence. It would be tempting to suggest that the presence of SO_2 accelerates the decomposition of the stone, but as the results do not show any self-consistent pattern, such a mechanism is by no means certain, and it has been noted previously (page 18) that at 1470°F, slight variations in furnace temperature led to apparently anomalous calcination-only results for the 1 and 4 h Dolomite 1337 samples. Further, even if some such 'accelerating mechanism' did operate it might be expected to be offset by the tendency of the evolving CO_2 initially to impede the diffusion of SO_2 into the pores. If the decomposition of a stone particle follows a moving front, viz, the front moving inward towards the centre of the particle, then pore formation will move inward and CO_2 from inner portions of the particle will pass through pores already formed, en route to the exterior of the particle; any effect of the inhibition of entry of SO_2 by evolving CO_2 would be expected to be more pronounced in the finer pores, in which there is more restriction to the movement of gas molecules. With dolomites the early decomposition of the $MgCO_3$, and hence attendant early pore-formation, might possibly reduce any such hindrance to SO_2 ingress: it is noted that after this initial decomposition the quantity of CO_2 evolved per particle of stone would be less than that from limestone, so that, overall, if egress of CO_2 hinders ingress of SO_2 that hindrance should be more marked with limestone than with dolomite. These speculations will be taken no further here.

In Section 2.4.2.1, it was noted that π_{Hg} decreases with increasing sulphation. In order to establish in detail the effect of sulphation on the developing and developed pore structure, and in particular which pores accommodate the sulphur, it is necessary to make comparisons among calcined-sulphated samples and also between the latter and calcined-only samples for the same residence times, with the assumption that the calcined-only stone is the correct datum. To some extent this assumption is open to question, as indicated by the results in the table above on page 23. To investigate this problem further, with respect to porosity, the apparent reduction in the porosity V_x% caused by the sulphation has been calculated as: (i) $V_{x2} - V_{x1}$ and (ii) $V_{x3} - V_{x1}$, where V_{x1} is the measured V_x% for the calcined-sulphated stone, V_{x2} is the measured V_x% for the corresponding calcined-only stone, and V_{x3} is the value for V_x% estimated from the extent of calcination of the calcined-sulphated stone using the appropriate line in Fig. 15, on the assumption that this would be the value for the porosity that would be present in the stone if the $CaSO_4$ formed were replaced by CaO, no other change occurring. The results are given in the following tables.

Stone	t,* h	V_x% and differences in V_x%				
		V_{x1}	V_{x2}	V_{x3}	$(V_{x2}-V_{x1})$	$(V_{x3}-V_{x1})$
		Temperature: 1470°F				
Dolomite 1337	¼	32	24	39	-8	7
	1	31	38	46	7	15
	4	23	33	52	10	29
U.K. Dolomite	¼	33	34	36	1	3
	1	31	38	42	7	11
	4	28	41	46	13	18
Limestone 18	¼	14	14(mean)	10	0	-4
	1	15	14	16	-1	1
	4	23	17	37	-6	14
Limestone 1359	¼	3	5	5	2	2
	1	4	5	6	1	2
	4	6	14	7	8	1
		Temperature: 1650°F				
Dolomite 1337	¼	47	52	54	5	7
	1	40	55	56	15	16
	4	29	54	58	25	29
U.K. Dolomite	¼	50	54	53	4	3
	1	48	54	54	6	6
	4	39	56	55	17	16
Limestone 18	¼	43	45	45	2	2
	1	38	50	50	12	12
	4	22	48	52	26	30
Limestone 1359	¼	42	44	46	2	4
	1	43	46	50	3	7
	4	42	46	51	4	9

* residence time

Excepting the 1470°F Dolomite 1337 samples, the values of V_{x2} and V_{x3} for most of the samples agree within 10% relative, which is not unreasonable considering the scatter in Fig. 15. The large discrepancies between V_{x2} and V_{x3} at 1470°F follow those between the extents of calcination referred to above, but no further comment on these can be made, except to note that they may be related to the temperature variation previously mentioned.

In Figs. 25, 25a and 26, $V_{x2}-V_{x1}$, $V_{x3}-V_{x1}$, and $\pi_{Hg2}-\pi_{Hg1}$ are plotted vs sulphation to illustrate the general decrease in porosity on sulphation. π_{Hg1} and π_{Hg2} are π_{Hg}% values, the subscripts 1 and 2 having the same significance as for the V_x% values. It is noted that this porosity reduction for a given value of sulphation (as defined herein) would be expected to be greater with a limestone than with a dolomite because there is more $CaCO_3$ present in the limestone than in the dolomite: this trend is seen in Figs. 25, 25a and 26.

Before proceeding with examination of the porosity for various ranges of pore-entrance diameter it is worth at this stage pointing to the changes in superficial volume that occur on calcination-sulphation compared with those for calcination-only, it being understood that a change in superficial volume in the present context means either a change in the true superficial volume or in the volume of pores with entrances with diameters >14.5 μm, cf. page 21, or in both. The changes (ΔV) are given in Tables 15 and 16 for 1470°F and 1650°F, respectively. They were calculated from:

$$\Delta V = 100(W/\rho_{HgT} - 1/\rho_{HgO})/(1/\rho_{HgO})\%$$

where ρ_{HgO} and ρ_{HgT} are, respectively, the mercury densities, g/cm^3, of the original stone and the treated stone (viz, after calcination-only or calcination-sulphation) and W, g, is the mass of treated stone produced from 1g of the original. As the values stand the following observations may be made. Dolomite 1337 at 1470°F shows slight swelling on calcination-only but shrinkage of up to 5% on sulphation, whilst at 1650°F calcination alone produces a shrinkage that apparently decreases with time - sulphation appears to enhance the shrinkage. The U.K. Dolomite, with calcination alone at 1470°F, shows a slight shrinkage in the controlled atmosphere and a slight swelling in the preliminary experiments, whilst at 1650°F a marked shrinkage of 8% is observed; sulphation seems to retard the shrinkage at either temperature. At 1470°F, Limestone 18 on calcination alone appears to swell slightly after 1/4 h and then it shrinks, whereas at 1650°F, no swelling is apparent and a shrinkage of up to 4% is seen; sulphation at both temperatures interferes with the shrinkage. Limestone 1359 at 1470°F shows a slight swelling on calcination alone and on sulphation, even though the extents of both the calcination and sulphation are small, 19% and 3%, respectively, after 4 h: at 1650°F, calcination alone produces up to 10% shrinkage whilst sulphation appears to enhance the shrinkage still further. That there is ample scope for shrinkage, due to sintering, is evident from the specific volumes of $CaCO_3$, 370 mm^3/g, and CaO, 300 mm^3/g. Thus 1g of $CaCO_3$ of volume 370 mm^3 calcines to 0.56 g CaO which in the close packed fully sintered form would occupy c. 170 mm^3: a shrinkage of 54%.

The variation of porosity in calcined-only and calcined-sulphated samples with residence time is shown in Figs. 27 to 35.

The situation in Figs. 27 to 29 for the results at 1470°F and 1/4 h calcination is clearly anomalous, probably due to a temperature effect noted earlier since (Table 7) Dolomite 1337 sample J6 is calcined-only to 33.6% in 1/4 h, while J9 is 61.8% calcined and partially sulphated in 1/4 h. It is clear that at 1650°F most of the porosity filled, blocked off, or otherwise eliminated on sulphation lies in pores with entrance diameters in the range 0.1 to 0.03 µm and that there is little change in the porosity behind entrance diameters of 0.03 to 0.014 µm. This is to be expected since the amount of porosity behind these finer entrances is relatively small anyway (Fig. 21 and see below also). Porosity in pores with entrances having diameters larger than 0.1 µm is little affected by sulphation. U.K. Dolomite in Fig. 30 follows the trend of Dolomite 1337 (time did not permit mercury porosimetry to be done on any of the sulphated samples prepared at 1470°F).

Of Figs. 31 to 34 for Limestone 18, the first two are practically identical, consistent with the observation of no significant porosity behind the smallest entrances, viz, in the range 0.03 to 0.014 µm diameter (Figs. 20 and 21). It is clear from Fig. 34 that pores with entrances larger than 0.3 µm diameter are active in sulphur uptake with Limestone 18. The equivalent curves for Limestone 1359 (Fig. 35) are unspectacular since little sulphation took place after 1 h. The only point of interest is that for sample G41, the sample sulphated at 1650°F for 4 h, V_{Hg} is appreciably lower than V_x. This may be evidence for a sulphate 'shell' reducing or blocking small pore entrances to mercury penetration (cf. Section 3). Time prevented mercury porosimetry being done on the other Limestone 1359 samples sulphated at 1650°F or on those sulphated at 1470°F.

The mercury porosimetry data for the sulphated samples are presented in an alternative form in Figs. 36 to 38, which show the variation of porosity for various ranges of pore-entrance diameter for the two dolomites and Limestone 18. It is clear that for the two dolomites, the porosity behind the entrances with the largest diameters (i.e., > 0.3 μm) shows little net change on sulphation. This can be interpreted to imply continuing access of gases to the internal structure of the particles via large (viz, 'transport') pores (cf. Section 2.4.2.5). This is true to some extent of the Limestone 18, except that the porosity behind the largest entrances does show some reduction on sulphation; the porosity behind entrances < 0.3 μm diameter is much reduced after 4 h. The above points are exemplified further in Fig. 39, which gives in histogram form the differences in porosity, behind entrances with diameters in particular ranges, between calcined-only and calcined-sulphated stones for the same residence time at 1650°F; the results are listed in Table 17. These differences may be regarded as the changes in the porosities caused by sulphation, the positive values corresponding to decreases. It is helpful to examine Fig. 21 as well as Fig. 39. It is seen that the sulphation is mainly in the smallest pores available (equating these with the smallest entrances), with the exception of Limestone 18 where sulphation occurs over the whole range of pore-entrance diameters. It is thought that the negative porosity changes correspond to either experimental errors or to early sulphation of pores that would in the absence of sulphur sinter and disappear on prolonged calcination, but which are prevented from sintering by partial sulphation.

This apparent effect of sulphation restricting sintering and particle shrinkage was seen earlier in this Section (Tables 15 and 16); it seems to occur with all the stones at 1470°F, except Dolomite 1337 where sulphation appears to enhance shrinkage. At 1650°F, sulphation seems to retard shrinkage in U.K. Dolomite and Limestone 18, but to enhance it in Dolomite 1337 and Limestone 1359. Finally, it is noted that a marked shrinkage of a stone with few transport pores may lead to a situation where the outside of the particle is compacted. Since the small pores tend to block up on sulphation, the initial sulphation may be enough to block off much of the porosity in the outer region of the particle, thus slowing the rate of sulphation. This situation has been described previously by Satterfield and Feakes[10]; such behaviour may have relevance to the poor sulphation behaviour of Limestone 1359 (at 1650°F, Table 16). Thus it does appear that in the assessment of a stone its sintering/shrinkage behaviour should be considered, and indeed Potter[1], Chan et al[11] and Glasson[12] have shown that increasing time of calcination leads to a decreasing surface area and hence sulphation efficacy: although surface areas have not been measured here, it is clear that the same process is going on by the shift of porosity into pores with entrance diameters increasing with time of calcination, referred to in Section 2.4.2.6 as sintering (cf. ref. 16). The role of impurities in the stones - MgO in the dolomites and SiO_2 in Limestone 18-is not entirely clear except that the structures calcine more rapidly and generate more porosity in a given time than the relatively pure Limestone 1359. Chan et al[11] and Glasson[13] consider that silica is liable to form a slag with the CaO and reduce the porosity by enhanced sintering.

2.4.2.8 Sulphur fixation

The mechanism of sulphur fixation is not clear but some points, leading to speculation, arise from the present work:

(a) Since sulphur is found in the smallest pores, the SO_2 probably does not react to sulphate at the point of first contact with the stone, in which case the SO_2 must migrate in some form until a certain favourable site or condition is obtained.

(b) In the elevated-temperature porosity work, it was found that:

(i) (Section 4.5.3) removal of the last traces of water from U.K. Dolomite (presumably held as $Mg(OH)_2$) was very difficult in vacuum at 1470°F, requiring the order of tens of hours of pumping even though that hydroxide is thermochemically unstable in relation to the oxide above 900°F;

(ii) (Section 4.5.2) xenon was strongly adsorbed in some samples of U.K. Dolomite and Limestone 1359 and was even difficult to remove at 1470°F in vacuum: this effect could be associated with the above mentioned difficulty in removing water from the dolomite;

(iii) increasing the temperature from 1470°F to 1650°F does not cause the increase in rate of sulphation with the dolomites that might be expected from chemical kinetics considerations; moreover in the pilot plant work the efficacy of removal of SO_2 passes reversibly through a maximum at c. 1560°F with the dolomites and limestones.

Bearing in mind these observations it can be argued very speculatively (for the dolomites at least) that the sulphur migrates inside the stone perhaps as the sulphite ion which is 'in itself' stable up to 1900°F, but thermochemically unstable with respect to the sulphate under oxidising conditions. The sulphur may thus be able to enter the smallest pores and be oxidised therein. The oxidising agent is not known but may itself be a surface species such as the hydroxide or even a peroxide since calcium peroxide is not much less stable than the hydroxide (Glasson[14]). (The present conditions of controlled atmosphere could have been contaminated with water through the method of injection of the SO_2 into the gas stream.) This mechanism would imply that the important physical factor in uptake of sulphur would be the access of the SO_2 to the stone surface and from there to the interior of the stone - hence the need to generate porosity in transport pores and in small storage pores which have a higher surface/volume ratio - and the chemical step to the sulphate would be dependent on the concentration of hydroxide ions in the stone which, with increasing temperature and instability of the hydroxide, would be expected to decrease at higher temperatures. This mechanism, it is noted, would be in line with the observations mentioned under b(iii) above. The exact role of the gas phase oxygen is not clear. As noted in Section 1, Potter[1] investigated the relative merits as SO_2 acceptor of two stones (a limestone and a dolomite) in their uncalcined, calcined and hydrated (after calcination) forms; for each stone, the hydrated form proved the best acceptor over the temperature range involved here. This may indicate either that the presence of water is beneficial in increasing the uptake of SO_2, or that a more active surface forms, with small pores, on calcination of the hydroxide rather than of the raw stone, as indicated by Glasson[12].

2.5 Conclusions

(i) The development of porosity on calcination is a time and temperature dependent process. The amount of porosity (% v/v) formed is for each stone a linear function of CO_2 loss.

(ii) On calcination, porosity is generated initially much more rapidly in dolomite than in limestone. This difference is most marked in a CO_2 bearing atmosphere at 1470°F. The effect is evidently associated with the decomposition of the $MgCO_3$ in dolomite.

(iii) There is little, if any, porosity behind entrances with diameters in the range 0.014 μm to 0.26 nm, with the calcined-only materials or, with the likely exception of Limestone 1359, with the calcined-sulphated ones.

(iv) Sulphation varies with time, as shown in Fig. 23. It is emphasised that the stones were not precalcined before being exposed to SO_2; it was found that sulphation lagged behind CO_2 evolution.

(v) Sulphation caused a reduction in porosity and it was found that sulphur is accommodated in the smallest pores (as detected by the mercury porosimetry) in the stone: e.g., with Dolomite 1337 at 1650°F most of the porosity filled, blocked off, or otherwise eliminated on sulphation, lay in pores with entrances having diameters between 0.1 μm and 0.03 μm; with Limestone 18, part of the sulphation took place in pores with entrance diameters between 0.3 μm to 0.1 μm.

(vi) As the results in Fig. 23 clearly show, Limestone 1359 is poor compared with the other stones in its ability to absorb SO_2. It is noted that at 1650°F, on a mass or bulk volume of stone basis, Limestone 18 would be a better acceptor than Dolomite 1337 (see (ix) below). The studies of calcination-only showed that, of the stones, Limestone 1359 is poorest in the quantity of relatively large pores (say, with entrance diameters in the range 14.5 μm to 0.3 μm) whose presence would facilitate the more rapid ingress of SO_2 to the interior of the particle and lead to more rapid reaction. On the other hand, Limestone 18 shows a much more pronounced development of pores in this range of pore-entrance diameter; for example, after 4 h at 1650°F, the porosity in these pores in Limestone 18 is 29% compared with only 4% in Limestone 1359. On sulphation, the volume of pores with entrance diameters $>$ 0.3 μm shows relatively little change with the two dolomites, viz, the 'transport pores' tend to retain their identity, but with Limestone 18 reduction in the volume of these pores occurs as the level of sulphation at 1650°F increases.

The level of sulphation reached under the present conditions clearly does not depend solely on the total amount of porosity developed in the stone on calcination alone - a fairly high porosity is developed in Limestone 1359 after 4 h at 1650°F (V_x = 46%). Indeed the porosity (V_x) in the stone after 4 h at 1650°F in the SO_2 bearing atmosphere is as much as 42%, and comparison of the latter with the mercury porosimetry data suggests that the sulphation may have caused narrowing of some pore entrances to $<$ 0.014 μm diameter (see Section 3, and (iii) above).

(vii) It appears that at least two criteria of pore structure have to be met if a stone is to be a good SO_2 absorber:

(a) extensive volume in large, viz, transport, pores for ease of access to the interior of the stone;

(b) extensive volume, for accommodation of the sulphur, in relatively small pores - which have a higher surface/volume ratio than larger pores.

In the case where one factor is missing, as in Limestone 1359 with little porosity in large pores, or in Potter's work[1] with Iceland Spar containing low porosity, then the sulphur uptake is liable to be poor.

With stones not having a very well developed transport pore system, the effect must also be considered of sintering, which could cause contraction at the outer surface and impedance, after initial sulphation, to further sulphation.

(viii) The mechanism of sulphur fixation is not clear, but some points arise from the present work:

(a) Since sulphur is found in the smallest pores the SO_2 probably does not react to sulphate at the point of first contact with the stone, in which case the SO_2 must migrate in some form until a certain favourable site or condition is obtained.

(b) Increasing the temperature from 1470° to 1650°F does not cause the increase in rate of sulphation with the dolomites that might be expected from chemical kinetics considerations. This effect may be related to the observation in the pilot plant work that the efficacy of removal of SO_2 passes reversibly through a maximum at c. 1560°F.

(c) With dolomites, at least, a highly speculative suggestion, based on the observation made during the course of the work (see Section 4.5.3) that the last traces of water were difficult to remove, is that an oxygen-containing species, perhaps hydroxide, localised on the internal surface of the stone, is necessary in the formation of the sulphate; increase of temperature above a certain level could cause such a surface species to become mobile resulting in reduced formation of sulphate. In this case it is possible that subsequent reduction in temperature could reduce the mobility of the species causing an increase in sulphur uptake, in line with the plant observations mentioned under (b) above.

The chemistry of the sulphur retention process, and the possible influence of water on this, and on the formation of the pore structure itself, would seem to be worthy of further study, particularly as such work may lead to an understanding of the mechanism, and hence perhaps elimination, of the fall-off in sulphur retention above c. 1560°F.

(ix) A simple screening test for stones

The most simple and satisfactory laboratory-method of placing unknown stones in order of acceptor ability would seem to be a sulphation experiment wherein stone particles are dropped on to a mesh in a tube, at reactor temperature, through which an appropriate SO_2 bearing gas stream flows, as described in the present work. Subsequent analysis for Ca, CO_2 and SO_2 content would enable curves such as those in Fig. 23 to be constructed showing the variation of the level of sulphur uptake with time. (It is noted that in Fig. 23, sulphation is the ratio of the quantity of sulphur taken up by the sample to that taken up if all the CaO were converted to $CaSO_4$: this means, for example, that at 1650°F, Limestone 18, on a mass or bulk volume of stone basis, would be a better acceptor than Dolomite 1337.)

3. MERCURY POROSIMETRY ON PARTIALLY SULPHATED PARTICLES BEFORE AND AFTER BREAKAGE

3.1 Method and Samples

It has been possible to demonstrate the presence of an 'impermeable' layer or 'shell' within the particles of a sample of Limestone 1359 sulphated in the laboratory using the method described in Section 7, but not within a sample of that stone sulphated in a combustor. It has also been possible to show that such a 'shell' does not exist within sulphated samples of U.K. Dolomite and Dolomite 1337.

The method used was as follows:

(i) Mercury porosimetry curves of the sulphated stones were measured.

(ii) Further samples of the sulphated stones were taken and the particles broken individually using a razor blade; the product was then sieved to remove particles smaller than 52 BS mesh and the porosimetry curves of the +52 BS mesh particles were measured.

The mercury porosimetry method has been discussed in Section 2.3.4. The materials used were:

(i) Limestone 1359, -16 +52 BS mesh, designated sample G7, sulphated during laboratory reactivity tests (Section 7) until 5.8% of the SO_2 stream passing through the bed of limestone was retained. The sulphur content of this stone was 3.6% w/w, a sulphation of c. 7%. The broken fraction was designated G14.

(ii) To confirm that the 'shell' was not an artefact of the calcination, a sample of Limestone 1359 was fully calcined in an O_2/N_2 stream for 3 h but not sulphated. This sample was designated G30. The sample was subdivided and a broken fraction (G31) prepared as before.

(iii) Limestone 1359 sulphated in the 6 inch combustor (Task V, Test Series 1.2). The sulphur content of this stone was 5.2% w/w, a sulphation of c.11 %. The unbroken and broken samples were designated O1 and O2, respectively. Ash was removed with a magnet, as in (v).

(iv) U.K. Dolomite, -6 +8 BS mesh, designated sample B5, sulphated during laboratory reactivity tests until 8.7% of the SO_2 stream was retained. The sulphur content of this sample was 4.9% w/w, c. 17% sulphation. The broken fraction was designated B6.

(v) Dolomite 1337 removed from the bed of the pressure combustor after Task II, Test Series 2; ash was removed from this sample with a magnet. Subsequent analysis showed that the resultant sample contained 1.8% SiO_2 and 0.6% Fe_2O_3, which compounds should form the major component of the ash, indicating that most of the ash was removed. The sulphur content of this stone was 9.3% w/w, c. 35% sulphation. The unbroken sample was designated J2 and the broken one J3.

(vi) U.K. Dolomite removed from the bed of the pressure combustor after Task II, Test Series 1; ash was again removed with a magnet. The sulphur content of this stone was 7.6% w/w, c. 28% sulphation. The unbroken sample was designated M and the broken sample M1.

3.2 Results

The measured porosimetry curves are shown in Figs. 40 to 45 and it can be seen that the curves for the three samples of the two dolomites are virtually unchanged by breakage (Figs. 43 to 45). The differences between the two curves for U.K. Dolomite in Fig. 43 lie in the region of interparticulate penetration and are not significant: the two curves are virtually identical at pore-entrance diameters < 10 µm.

The curves for Limestone 1359 sulphated in the laboratory, Fig. 40, show that there was considerable porosity within the whole sulphated particles that has not been reached by mercury in the porosimeter but that some or all of this porosity has been made accessible by simple cleavage of the particles. The curves in Fig. 42 for the calcined, unsulphated limestone, show that this property is peculiar to the sulphated limestone.

To elaborate: if there were an impermeable shell round the exterior of each unbroken sulphated limestone particle, then once the interparticulate porosity had been filled by mercury little further penetration with the unbroken particles should have been seen. However, this was not the case. Bearing in mind that the pore-entrance diameter range of the porosimeter used is c. 58 µm to 0.014 µm, one, very much simplified, explanation of the observations is that the unbroken particles have a pore structure that consists of:

(a) that disclosed by the porosimetry, consisting of pore entrances at the exteriors of the particles, leading to wider pores (having diameters of < 58 µm), the original pore entrances having been narrowed by sulphation; and

(b) that not disclosed by the porosimetry, comprising pore entrances of diameters < 0.014 µm at the exteriors of the particles (and/or at the surfaces of the pores described under (a)), leading to wider pores with diameters in the range c. 58 µm to 0.014 µm, the original pore entrances having been narrowed by sulphation. (It was noted (Section 2.4.2.2) that most, if not all, of the pore volume of partly or fully calcined, unsulphated stone lies behind entrances > 0.014 µm in diameter, but that Limestone 1359 sulphated for 4 h at 1650°F in the controlled atmosphere appeared to have some volume in pores with entrances < 0.014 µm diameter.) The breakage would now result in mercury penetrating the pores described above under (a) through entrances wider than the original ones: considering the porosimetry curves below the line shown in Fig. 40, such penetration would account for the shift to the left on breakage. Similarly, the part of the porosimetry curve above the line for the broken particles could have resulted from the breakage of pores described above under (b). Such narrowing of pore entrances may be regarded as the forming of a 'shell', which would impede successive sulphation, and is in line with the more constricted structure of the stone, compared with the more open structure of the dolomites which do not show the breakage effect. The presence of a 'shell' in sulphated limestone has been observed by optical microscopy[3] and by electron microprobe analysis for sulphur[4] (including[3] Limestone 1359 - no 'shell' was observed with U.K. Dolomite).

The absence of the breakage effect with the plant-sulphated Limestone 1359 (Fig. 41) could mean that a 'shell' was destroyed, or was prevented from forming, by attrition in the fluidised bed.

The calcined-only limestone was not a true precursor of the sulphated material, and it would not be justified to attempt to compare the corresponding porosimetry curves for the unbroken particles of these two materials - the sensitivity of pore structure of stones to calcination conditions has been discussed in Section 2.4. However, the breakage of the calcined-only limestone resulting in a change in the porosimetry curve (Fig. 42) in the opposite direction from that observed with the laboratory sulphated stone is in line with this sulphation having caused the narrowing of some pore entrances down to diameters beyond the range of the porosimeter, as discussed above.

The change in the porosimetry curve, on breakage of the particular calcined-only limestone, could be accounted for if the unbroken particles contained pores of diameter greater than c. 58 μm but accessible only through entrances indicated by the sharply rising portion of the porosimetry curve. Now breakage would result in some of those pores becoming accessible through entrances >c.58 μm, and hence their volume would not now appear in the porosimetry curve for the broken particles, which would lie below the original curve.

In all the above discussions, any destruction of pore volume due to the breakage has been ignored, as has any interparticulate penetration corresponding to the pore-entrance diameter region c. 58 μm to c. 10 μm.

4. STUDIES OF POROSITY AT ELEVATED TEMPERATURE

4.1 Introduction

When porous solids are used at elevated temperatures in processes involving gases, the geometry and surface properties of the pores at the temperature of operation often play an important or even dominant role. As substantial changes of the accessible porosity of a solid may occur on increasing its temperature - when standard pore structure tests made at room temperature or below would not then accurately reflect the relevant structure of the material - it was considered prudent to carry out some tests of pore-accessibility change on calcined stones.

4.2 Principles

4.2.1 Types of pore involved

There are two types of pore that are affected by temperature in different ways:

Type 1 pores with extremely fine entrances that exclude cold gas but which are penetrated by hot gas either because of its greater kinetic energy (Fig. 46), or because of an increase in the size of the pore entrances owing to thermal expansion of the solid.

Type 2 pores that when cold are open but whose entrances become sealed on increasing the temperature owing to anisotropic thermal expansion of the solid (Fig. 47).

Type 1 pores are fairly common, e.g., they occur in synthetic graphites[21a], coal chars[21b], other carbons[21c], glasses[21d]. Their penetration can result in a large increase of accessible surface; at a given temperature the magnitude of the effect depends on the molecular size of the gas. Type 2 pores are less common but are known to occur in synthetic graphites[21e].

4.2.2 Experimental procedure for measurement

The two counteracting effects of Types 1 and 2 pores can be measured separately using the apparatus described in the next Section. Two procedures are required and are detailed in Figs. 48(a) and 48 (b). The first procedure is named the 'pore penetration' experiment (Figs. 46 and 48(a)) and comprises the following stages: (i) evacuating the heated sample;

(ii) soaking it in a particular gas at elevated temperature T_2 (1470°F); (iii) cooling it to room temperature T_1, the pressure of the ambient gas remaining approximately constant. Now, gas that entered Type 1 pores can no longer pass out through the mouths of those pores, i.e., it has become trapped. In stage (iv), the sample is evacuated at temperature T_1 to remove untrapped gas, and, finally, in stage (v) the sample is reheated to temperature T_2 or above, when the previously trapped gas can now pass out of the pores into a mass spectrometer for measurement.

The second procedure is used to detect Type 2 pores. It is named the 'pore closure' experiment (Figs. 47 and 48(b)) and the thermal cycle used is analogous to that of the first procedure, viz, following initial evacuation of the heated sample, it is cooled (to room temperature) and soaked in a particular gas, after which the temperature is raised (to 1470°F) to effect any trapping; untrapped gas is then removed and the sample again cooled to effect release.

4.3. Experimental

4.3.1. Description of apparatus

The apparatus is shown diagrammatically in Fig. 49. It is basically a sample container connected to an AEI MS 10 mass spectrometer and a Pyrex glass vacuum-system. The vacuum system comprises vacuum pumps, Pirani gauge, 'probe' gas supply and an electric furnace. The sample container is made of recrystallised alumina, impermeable to helium at temperatures up to at least 3000°F. The necessary demountable vacuum-tight joint was made by cementing the alumina tube to Pyrex glass tubing with 'Araldite' resin AY 111. The Pyrex glass tubing is connected to the rest of the apparatus by a B19 ground glass joint sealed with Apiezon T grease.

For easier handling, the sample is packed in a recrystallised alumina tube 75 mm in length. This tube is located in position in the sample container by a length of 4 mm o.d. recrystallised alumina tubing.

A 2 mm bore capillary tube leads from the 4 mm bore stopcock T_4 to the MS 10 to form a slow leak path for the gas sample. This enables gas samples to be taken from the sample container while the gas in the latter is at pressures up to a maximum of 1 torr; in these circumstances the MS 10 reaches its maximum operating pressure of 10^{-4} torr.

The sample is degassed through 10 mm bore tubing, and 10 mm bore stopcocks T_1 and T_2 separated by a cold trap that is cooled by solid carbon dioxide.

Four inert probe-gases were used, of increasing molecular size: helium, neon, krypton and xenon, the last being similar to SO_2 in critical molecular-diameter. They were supplied by the British Oxygen Co. Ltd. in one-litre glass flasks and were of high purity, viz, BOC Grade X. Gas is fed from the flasks through stopcocks T_3 and T_1 to the sample. The pressure of the gas admitted to the sample is measured with a simple mercury manometer.

An advantage of incorporating the spectrometer is that the sample can be soaked in a mixture of the various gases, thus effecting saving in experimental time, the quantity of each gas subsequently released being readily measured. To ensure uniform mixing, the gases are admitted in turn in increments of c. 15 torr until the total pressure of 200 torr is reached. The composition of the mixture is calculated from the measured pressures. The pressure of the ambient gas is not kept constant during the cooling or heating of the trapping process of the pore-penetration and pore-closure experiments, respectively, but it does not change by more than c. 10 torr, which is an insignificant variation in the present work.

During the final stage of either type of experiment all the gas released from the sample is pumped through the MS10 and the partial pressure of the probe gas is monitored. The quantity of the gas released is proportional to the area of chart drawn out by the MS10 chart recorder.

Only one vacuum system is described; there are two others so that three experiments can be done at once. The time scale of the experiments is such that the heated sample is degassed for 24 h. Soaking time was 24 h in either type of experiment. Before the final gas release stage it was not always practicable to reduce to zero the partial pressure of probe gas diffusing from the samples, because unreasonable lengths of evacuation time would have been required, but sufficient time was allowed to reduce this partial pressure to an acceptable level (10^{-10} torr in the MS10).

4.3.2. Calibration of apparatus

The sample container (Fig. 49) is replaced by the Pyrex glass dosing system (Fig. 50) from which known amounts of gas are admitted to the MS10 which is set to record the partial pressure of the particular gas admitted. The calibration factor giving the quantity of gas per unit chart-area is obtained and enables the area of chart drawn out in an experiment to be converted to the quantity of gas released from the sample.

To achieve the low pressure required for gas samples to be admitted to the MS10, two sampling valves are used in series followed by a one litre expansion bulb (Fig. 50). These valves were made from 2 mm bore three-way stopcocks, one side arm of each stopcock being sealed-off. The valves were connected by a short length of glass tubing. The volume of each valve including the sealed-off side arm, and of the connecting tubing, was measured by filling with mercury and weighing. After evacuation of the valves, tubing and one litre bulb, a sample of gas is taken into the first valve T1. The gas pressure is measured with a mercury manometer. On turning the key of valve T1 anti-clockwise (Fig. 50), with valve T2 as shown, the gas is allowed to expand into the connecting tube and valve T2. If the key of valve T2 is then turned clockwise, only the gas in this valve (including that in the sealed-off side arm) is admitted to the one litre bulb and the MS10.

The actual quantity (Q_i) of a particular gas admitted to the MS10 is obtained as follows:

Suppose the volumes of the valves T1 and T2, including their respective sealed-off side arms, are V_I and V_2, respectively, and the volume of the connecting tubing is V_3. If P_1 is the original pressure in valve T1 and P_2 is the pressure of the gas in valve T2 before it is admitted to the one litre bulb, then, since $Q_i = P_2V_2$,

$$Q_i = \frac{P_1 V_1 V_2}{V_1+V_2+V_3} = \text{a constant} \times P_1$$

Now $\frac{Q_i}{A_i}$ should equal k

where A_i is the area drawn out by the recorder pen and k is a constant for the particular gas and is the abovementioned calibration factor. Thus if the area drawn out by the recorder pen in a pore-penetration or pore-closure experiment is A_2, then the corresponding quantity of gas released is kA_2.

The calibrations for helium, neon, krypton and xenon obtained in the present work agreed with those from other work carried out earlier. The latter showed k to be constant for each gas for the experimental range of A_2 values.

4.4. Results

Of the four stones used generally in the present work, only U.K. Dolomite and Limestone 1359 were examined. The results are given in Tables 18, 19 and 20 (cf. Tables 2 and 3) with the exception of certain pore closure results - see Section 4.4.1 below. Those in Table 18 refer to exploratory measurements, those in Table 19 to measurements made on previously uncalcined material, and those in Table 20 to measurements made on the stones subjected to the pretreatment in which they were dropped into a furnace at 1470°F and allowed to heat-soak for various times - see Sections 2.2.1 and 2.4.1. The term 'stagnant' in Table 20 refers to the situation that the pretreatment furnace atmosphere initially contained air, no attempt at flushing being made. The quantities of trapped gas released are expressed in the Tables as the volumes the gas would occupy at the admission pressure (c. 50 torr) at a temperature of 1470°F (or 77°F, in parentheses); each volume refers to unit weight of material on completion of the experiment. It is important to note that irrespective of the pre-treatment history of the stones these results are for the fully calcined materials, since untreated or partially calcined stone would become fully calcined during the initial evacuation of the heated sample.

4.4.1 Pore closure experiments

In addition to the pore closure experiments whose results are given in Table 18, all the samples listed in Table 19 were subsequently examined by this method as were samples B2, E1 and G1 in Table 20, but the results are not included, because in each case the volume of the gas, helium, neon, krypton and xenon, trapped and released was extremely small, i.e., < 0.1 mm^3/g, as with those in Table 18. The Sprotborough 3/4 inch clipping (Table 18) was exposed to helium and krypton only, but there is no reason to suppose that results with neon and xenon would be any different from those obtained for the other stones.

4.4.2 Pore penetration experiments

(i) Helium and neon: There was no measurable effect using helium as probe gas in any of the experiments. The same is true for neon in most of the experiments; the exceptions are seen in Table 18 - samples a and d and sample e (the value for which is relatively insignificant) - but in view of the other results, it is assumed that these high values are spurious, although no definite explanation can be offered to account for this.

(ii) Xenon: Relatively large quantities of xenon were released from some of the U.K. Dolomite and Limestone 1359 samples. Work described below indicated that at least part of this xenon must have originally been adsorbed in open pores at room temperature at the completion of the trapping stage of the experiment and not removed by the evacuation before the heating in the release stage.

Some indication of such residual adsorption was seen with either stone and any of the size grades, in that at room temperature the residual xenon atmosphere over the pumped sample decreased only slowly over 70 h (observed by mass spectrometry), the effect being most marked with the limestone. On the other hand, at the temperature of 1470°F, again with either stone and any of the size grades, the total times taken for the xenon to be released in vacuum were between c. 10 and 100 h; it seems unlikely that all of this released xenon had been merely residually adsorbed, and part of it might be expected to have originated from pores penetrated by the pore penetration mechanism.

As a test of the magnitude of any such residual adsorption of xenon:

(a) U.K. Dolomite sample C11 (Table 20) was exposed at room temperature to a pressure of xenon equal to the partial pressure of that gas in the normal mixture of probe gases (c. 50 torr) and allowed to stand overnight before evacuation at room temperature and subsequent heating to release any residual gas. Although the volume of xenon released (27.6 mm^3/g) was less than that released in the normal experiment (43.5 mm^3/g), it is clear that a large proportion of the xenon released from the samples could have been a result of residual adsorption at room temperature. In addition, an equimolar mixture of xenon, partial pressure c. 50 torr, and SO_2 was admitted to sample C11 at room temperature (Table 20). The volume of xenon released on subsequently heating the evacuated sample to 1470°F was less than 25% of the volume of xenon released in the absence of SO_2. This evidently indicates that at room temperature SO_2 is preferentially adsorbed compared with xenon: SO_2 reached much the same surface sites as xenon alone.

(b) Limestone 1359 sample H1 (Table 20) was given a much shorter pre-release evacuation time at room temperature than H3 and most of the very large quantity of xenon subsequently released must have been residually adsorbed.

(iii) Krypton: The majority of the experiments showed either no measurable, or generally small, effects with krypton. The definite effects that were observed are thought to be probably mainly due to residual adsorption analogous to that mentioned above with xenon. Such residual adsorption of krypton is apparent if the results for samples H3 and H1, Table 20, are compared (cf. above, for xenon). Moreover, krypton is less extensively adsorbed on surfaces in general compared with xenon so that the residual-adsorption effect should be the less with krypton, which is in line with the present results. It is noted that where the xenon effect is not measurable (Tables 18 and 20) neither is that with krypton, which also supports the conclusion that the positive krypton effects arise (at least in part) from residual adsorption.

4.5 Discussion and Conclusions

4.5.1 Pore closure

The absence of any pore closure effects indicates that there is no decrease of accessibility to gas molecules on increasing the temperature to 1470°F.

4.5.2 Pore penetration

4.5.2.1 Helium: The absence of any pore penetration effects with helium indicates that there is no increase of accessibility to that gas on increasing the temperature to 1470°F. This means that the pore volumes at 1470°F can be estimated from helium displacement densities measured at room temperature, as in the present work, in combination with the corresponding mercury displacement densities; it must be assumed that this applies also to the measurements made on the stones prepared at 1650°F, although this assumption is not entirely justified. It is expected that change in pore volume owing to thermal expansion is relatively small: comparable to the present error in the helium density results.

4.5.2.2 Xenon: The pore penetration results for xenon may be summarised as follows:

(a) A large part of the xenon released from the calcined dolomite, and probably from the calcined limestone, is the result of desorption of gas originally adsorbed at room temperature and not pumped away during the pre-release evacuation. However, there is evidence of some "genuine" pore penetration; nonetheless, as the total release-times were relatively long and it is expected that any contribution of xenon due to pore penetration would have been released more slowly than that merely residually adsorbed, it would seem that the penetration of any closed pores at 1470°F is a slow process compared with the rate of sulphur uptake by the stone and is likely to be of only secondary importance, if at all, in the combustor. The situation at 1650°F cannot be guessed at, however.

(b) A number of comparisons may be made between the quoted xenon release values bearing in mind the limited number of samples examined, as follows: (For convenience those samples subjected to pretreatment involving the initial rapid heating in a gaseous atmosphere are termed 'Gas-type', and those calcined entirely in vacuo in the pore-penetration/pore-closure apparatus are designated 'Vac-type')

(i) With the limestone, size grade -16 +52 BS mesh, far more xenon was released from the Vac-type than from the Gas-type samples

(ii) Dolomite, size grades -16 +52 BS mesh and -6 +8 BS mesh, showed the reverse effect, i e , a much enhanced release from Gas-type than from the Vac-type samples.

(iii) However, for the -300 BS mesh material the release from the Gas-type limestone and the Vac-type dolomite was much greater than from the corresponding -16 +52 BS mesh material.

(iv) With the limestone in the -300 BS mesh size grade, the release from the Gas-type material was of the same order as that from the Vac-type material.

(v) With the Gas-type stones in the size grade:

(a) -16 +52 BS mesh, the release from the limestone was low compared with that from the dolomite, which was high.

(b) -300 BS mesh, the release from the limestone was high and of the same order as that from the dolomite

(vi) With the Vac-type stones in the size grade:

(a) -16 +52 BS mesh, there was much more release from the limestone than from the dolomite;

(b) -300 BS mesh, the release from the limestone was about the same as that from the dolomite

Pores in which xenon is residually adsorbed would be expected to be extremely fine; they may even be micropores (having diameters of a few nm or less) in which owing to the overlapping sorption-potential fields xenon would be held more strongly than on an 'open surface' or in wider pores; spaces between adjoining crystallites could form such pores: their volume could be quite small and thus not incompatible with the observations in Section 2.4.2.2 concerning volume in pores with diameters < 0.014 µm. Further, egress of xenon from the structure could be impeded if fine constrictions were present in the pores. Whatever is the true pore structure in question, it does not seem unreasonable to equate its extent with the extent of xenon release. If this structure is called 'fine-pore structure' (fps), then it seems that:

(I) With the −16 +52 BS mesh size grade limestone, the Vac-type material contained a greater extent of fps than the Gas-type material. It may be that the difference in the initial heating rates between the two types contributes to this effect, and the atmosphere in which the calcination was carried out may be critical. Glasson[12] has postulated two sequential processes occurring in the calcination of calcium carbonate: (1) recrystallisation of the cubic oxide-lattice from oxide having a $CaCO_3$ (calcite)-like structure, and (2) sintering of the recrystallised oxide. The first process causes increase in surface area, the second a decrease. Glasson[15] has shown that the presence of CO_2 will (a) inhibit nucleation in the recrystallisation and (b) favour sintering: calcination in vacuo gives a product having a higher surface area than one calcined in an atmosphere containing added CO_2 or in air, the CO_2 forming in the decomposing solid not being eliminated fast enough in the air. Thus a finer pore structure, associated with a smaller average crystallite size is developed by calcination in vacuo. This finding would account for the abovementioned difference in fps: a simple explanation could be that the Vac-type limestone having the smaller average crystallite-size has the larger number of inter-crystallite spaces in which xenon might be held.

(II) With the −16 +52 BS mesh dolomite, the Gas-type material seems to possess a greater extent of fps than the Vac-type one. It is difficult to explain this apparent observation, since the MgO formed should sinter more readily in a gaseous atmosphere than in vacuo[16] as with CaO. However, it is noted that some hydration took place after the pretreatment in the gaseous atmosphere because the samples were allowed to cool in air (see Section 4.5.3): now, it has been found by Girgis and Girgis[16] that calcination of $MgCO_3$ in air followed by hydration to $Mg(OH)_2$ by immersion in water, and then decomposition in vacuo at 450°C, gave a product having a higher surface area than that of the original calcined material. Hence it is possible that in the present work the subsequent calcination, in vacuo, of $Mg(OH)_2$ formed resulted in the enhancement of fps, but the corresponding role of $Ca(OH)_2$ formed after the pretreatment is not clear – the limestone samples were likewise cooled in air.

In conclusion, some qualitative differences in xenon release have been observed between the -16 +52 BS mesh limestone and dolomite: no further comment is made on these differences, attention having been called to them mainly because other differences have been observed between the stones, e.g., in their SO_2 sorption capabilities.

4.5.3 Incidental observations in the pore penetration experiments

Incidental to the pore penetration experiments two further observations were made as follows:

I. All the samples of U.K. Dolomite were observed to release quantities of water during the experiments after the initial heating in vacuo. As noted earlier, the normal experimental method was to evacuate the heated sample of stone for 24 h in vacuo, add the mixture of probe gases, soak, and then cool the sample to room temperature before evacuating. It was on subsequently reheating the sample to release trapped probe gas that water (and carbon dioxide) emission was observed. The quantities of water released were greater with the samples pretreated in the gaseous atmospheres with rapid initial heating than those calcined entirely in vacuo. The most likely explanation of the origin of the larger amounts of water released from the pretreated samples is that some hydroxide was formed on subsequently cooling them in air. On reheating them in vacuo the last traces of water were evidently difficult to remove. Since the effect was not observed in the identically treated Limestone 1359, it is most likely to result from the formation of $Mg(OH)_2$.

The effect of hydration of calcined MgO followed by reheating in vacuo in modifying the pore structure of the oxide has been noted above, and Potter's work[1] on the favourable effect of hydration of calcined limestone and dolomite on sulphur uptake by those stones has been noted in Sections 1 and 2.4.2.8. As suggested in Section 2.5, the possible influence of water on stone sulphation would seem to be worthy of study.

II. Finally, it was noted that during the gas release stage of the pore penetration experiments on the coarse U.K. Dolomite samples, f, g, and h, Table 18, i.e., on reheating to 1470°F, SO_2 was evolved (SO_2 was not monitored during calcination). The partial pressure of the SO_2 increased rapidly on heating from 1470° to 1650°F. The quantity of SO_2 originally present in this coarse material was estimated from this to be < 15 ppm (w/w). Although this is a very small quantity the observation of the evolution may have some significance, possibly in the problem of the reduction in SO_2 uptake on increasing the temperature in the combustor above c. 1560°F. No attempt was made to monitor SO_2 in the corresponding stage of the pore penetration experiments with any of the other samples.

5. THE EFFECT OF THERMAL CYCLING ON SO_2 UPTAKE

5.1 Introduction

Elutriated stone fines are subjected, if recycled, to rapid temperature changes and it has been suggested that such 'thermal cycling' might have an effect on the capability of the recycled fines for absorbing SO_2. The experiments described were designed to test this possibility.

5.2 Apparatus and Procedure

The apparatus comprises a long horizontal tube within which two platinum boats may be manipulated individually, by use of iron attachments and magnets. Part of the tube is heated by a furnace at 1470°F, and thermal cycling is effected by moving one of the boats between the cool and heated regions. This procedure enables two experiments to be done simultaneously: one boat is taken through a thermal cycle experiment, whilst the other is maintained in the hot region at constant temperature. In this way it was intended that the effect of the thermal cycling only should be apparent and possible differences that might have arisen between separate experiments, due for example, to variations in SO_2 flow, avoided. Suitable gas mixtures may be streamed through the furnace tube, the flow rates being measured using GAP flow meters. The small quantity of SO_2 required was displaced from a Toepler pump by liquid paraffin. As the flow-rate of the SO_2 was too small to actuate a standard flow-meter, the flow-rate of the paraffin, and therefore of the SO_2, was measured using a further GAP flow-meter. Initially both boats are inserted in the cool part of the tube and the gas flow, excepting the SO_2 is begun. Both boats are then moved into the 1470°F zone and after a time interval (t_1) the SO_2 is turned on. The SO_2 is allowed to flow for a period of time (t_2), after which it is turned off and the thermal cycling boat removed to the cool zone. After a further period of time (t_3) that boat is replaced in the 1470°F zone, and the cycle is repeated a required number of times. Both boats are removed at the end of the last cycle.

Further details of the experiments, such as the gas composition, the number of cycles and the actual values for t_1, t_2 and t_3, are shown in Tables 21 and 22.

5.3 Results and Conclusions

The results for U.K. Dolomite are shown in Table 21; those for Limestone 1359 are shown in Table 22. There is considerable scatter among the results. The difference between cycled and non-cycled stones is expressed on a fractional basis in column 6: (b - a), the sulphur content of cycled sample (b) less that of non-cycled sample (a), is divided by a. The error of the sulphur determinations is less than 0.1% absolute and it appears therefore that there are real differences within most of the pairs of samples, but as these differences do not show a consistent increase or decrease on thermal cycling it is impossible to conclude that thermal cycling has a systematic effect on either stone.

To enable some comparison to be made between the rows of results in Tables 21 and 22, the percentage sulphur contents of the samples per unit quantity of SO_2, cm^3 (stp), passed over them are shown in columns 3 and 5. Despite the scatter among the results, the following observations can be made:

(i) Change of particle size of either stone from -16 +52 BS mesh to -300 BS mesh results in an increase in SO_2 uptake for any of the gaseous atmospheres used; overall the effect is larger with the limestone.

(ii) With both stones there is no clear-cut effect on SO_2 uptake of increasing the CO_2 concentration to 15% v/v, but a CO_2 concentration of 75% v/v causes a substantial decrease in SO_2 uptake with either particle size: with the -16 +52 BS mesh materials, the decrease with the limestone is much more marked than with the dolomite, but with the -300 BS mesh materials the limestone shows only little more marked decrease than the dolomite.

(iii) Overall, under the conditions of experiment , in the -16 +52 BS mesh size-grade the dolomite is the better SO_2-absorber, as expected, and particularly so in the CO_2 concentration of 75% v/v; changing the particle size to -300 BS mesh appears largely to eliminate the difference in SO_2 uptake between the two stones

6. MISCELLANEOUS

6.1 Optical Microscopical Examination

A brief optical microscopical examination showed that shells had formed on individual particles of U.K. Dolomite removed from the bed of the pressure combustor after completion of Task II, Test Series 1. This material was also used for the breakage studies, Section 3, and as noted in that Section, the major portion of ash was first removed with a magnet and the residue sieved on a 52 BS mesh sieve. The +52 BS mesh particles were examined (un-sectioned) under a stereo-optical microscope and are illustrated in the (non-stereo) photomicrographs in Fig. 51. Generally the particles are covered with a fused brown deposit; some of them are chipped or broken and in others the shell seems to have become detached from the particle. The shell is presumably a slag formed with ash in the combustor. No comment can be made on the role of the shell in the sulphation process. No such shell was observed on the samples prepared in the laboratory.

6.2 Surface Area

During the course of the work, a few measurements of surface area were made at liquid nitrogen temperature. The technique used is outlined as follows. The apparatus is of the volumetric type - an Orr surface-area, pore-volume analyser (Model 2100, Micromeritics Instrument Corporation). In principle, the increasing number of molecules (N) of krypton adsorbed by the sample at 77°K is determined as the pressure (P) is increased in steps. The value for N at which the surface just becomes completely covered with the adsorbed molecules (N_m) is deduced by use of the 'B.E.T.' equation. The area of this surface is then $N_m.A$, where A is the cross-sectional area of each adsorbed krypton molecule in the close-packed monolayer. The value taken for A was $20.2 \times 10^{-20} m^2$; there is some uncertainty as to the value that should be used: McClellan and Harnsberger[17] list a number of values that have been given in the literature and recommended the above value. That suggested in the Orr instruction-manual is $21.0 \times 10^{-20} m^2$, (which value was used previously).[23]

Nitrogen is widely used for high surface areas, but krypton is preferred as an adsorbate at 77°K for samples, such as those considered here, for which the total surface area present in the sample container is low. This is because with krypton, which has a low saturation vapour pressure at 77°K, the quantity of gas in the dead volume of the sample container is low compared with the quantity adsorbed, thus increasing the precision of measurement.

Some further notes on the experiment are as follows:

(i) Duplicate measurements were made using the same portion of sample.

(ii) Before each duplicate determination, the sample was evacuated in the Orr apparatus at 360°F and $<10^{-4}$ torr.

(iii) Dead volumes were determined using helium, also at the low temperature.

(iv) The specific surface values, which are listed below, refer to unit weight of evacuated sample, after heating as in (ii).

Material	B.E.T. specific surface, m^2/g (duplicates)
U.K. Dolomite, -6 +8 BS mesh, sample B	0.39, 0.39
U.K. Dolomite, -16 +52 BS mesh, after 1 h heating at 1470°F in a stagnant atmosphere: 53% calcined, sample C1*.	2.59, 2.70
Limestone 1359, -16 +52 BS mesh, sample G	0.22, 0.23

* cf. Table 2.

It was noted that a slow drift of krypton into the pores occurred on the first addition of krypton to the partly calcined dolomite and the raw limestone; no drift was noted with the raw dolomite. Such drifts normally indicate the presence of micropores with entrance diameters close to that of the particular probe gas molecule; in the present case the absence of drifts in successive additions could merely mean that the micropores in question became completely filled in the first addition. The presence of fine pore structure in fully calcined dolomite was indicated from the pore penetration experiments in Section 4.

The three specific surfaces lie in the same order as the corresponding porosity values (mm^3/g): V_x or t.p.v. or π_{Hg} - Tables 8, 10 and 14 (although the data for U.K. Dolomite sample B is not reported, the specific surface of sample C, sized -16 +52 BS mesh, may be expected if anything to be higher than that of sample B which is of larger particle size). With the dolomite, therefore, increase of pore volume on partial calcination is accompanied, as expected, by increase of surface area.

Finally, the specific surface value for the partly calcined dolomite is at first sight unexpectedly low compared with either the value of 43 m^2/g obtained earlier in other work at BCURA for a fully calcined dolomite[18] or with the values obtained by Chan et al[11] for various fully calcined dolomites. Apart from a factor related solely to the difference in extent of calcination, there are at least four factors that might be involved in this difference: (1) the present sample was prepared with rapid initial heating, whereas all the fully calcined materials were subjected to relatively slow initial heating; (2) the ambient atmosphere with the present sample was 'stagnant', whereas the fully calcined materials were heated in a nitrogen flushed atmosphere; (3) the CaO in the present sample may have retained the crystal structure of the original carbonate (see refs. 12 and 15), but not the CaO in the fully calcined materials; (4) the surface area values may be subject to the difficulties arising in interpreting sorption data for materials containing micropores, e.g., such values may be (a) too high owing to 'micropore filling' which can occur at the same time as normal monolayer formation in wider pores or on open surface[19], or (b) too low owing to the 'activated diffusion effect', whereby molecules require an activation energy to enable them to pass through pore entrances very close in diameter to their own, the extent of penetration being strongly temperature dependent and greatly restricted at 77°K[20]. No attempt has been made in the present work to investigate the possibility of such effects.

7. MEASUREMENTS OF SO_2 REACTION RATE CONSTANTS

The purpose of this work was to provide quantitative values for the reaction rate constants in a form suitable for use in the mathematical model.

7.1 Description of Apparatus and Experimental Procedure

The reaction tube (Fig. 52) consists basically of a 1½ in diameter quartz tube in which the test sample rests on a quartz sinter, the tube being heated by a surrounding furnace. Gas of suitable composition is led in at the bottom and after heating passes through the sinter and sample to the offtake where the SO_2 remaining is absorbed for subsequent titrimetric determination.

If the reaction rate were partly or wholly controlled by the physical transfer of gases to or from the particle surface, the gas velocity relative to the particles would be expected to influence the reaction rate. Argonne National Laboratory have found in previous work[22] that over the range of gas velocities likely to be used in fluidised combustion systems the rate of reaction between SO_2 and limestone is substantially independent of gas velocity. However, in the present work, velocities have been kept as close as possible to those used in the plants, in order to reduce to a minimum any possible errors due to the dependency of reaction rate upon mass transfer to the particle surface.

Referring to Fig. 52: air from a compressed air line was fed through a centrifugal/silica gel drier to a "Flostat' regulator to guard against source pressure variations, and metered by a float type flowmeter regulated and stabilised against back pressure fluctuations by a second 'Flostat'. The arrangements for oxygen and nitrogen were similar, but no drier or entry pressure regulator was used. Since the flowmeter calibrations are pressure-dependent, care was taken to ensure that all gases were supplied at constant pressure, the meters being periodically calibrated at working pressure by use of a soap-film meter connected at the reaction tube outlet.

Because of the low flow rate and corrosive nature of the SO_2, the arrangements for this gas were quite different, the principle being to supply a known mass of gas over a known time.

A vessel C (Fig. 52), of about twice the volume of SO_2 to be delivered, had a fiducial mark half way down its surface. The volume of the vessel between the mark and tap B was determined by filling with mercury and weighing the mercury. The vessel was half filled with liquid paraffin and connected to (a) an SO_2 cylinder, (b) the apparatus, (c) waste and (d) a water supply, as shown in Fig. 52. With the vessel full of paraffin and water, it was connected to the SO_2 supply by tap B and water was allowed to run to waste via tap A until the level of paraffin fell to the fiducial mark. Tap A was turned off and, after a short-interval to ensure a slight positive pressure of SO_2 to build up in C, tap B was also turned off. Venting tap B to atmosphere allowed the pressure in C to fall to atmospheric, so that a known mass of SO_2 (approximately 0.17 g) was enclosed in C.

The SO_2 was displaced at constant rate into the gas manifold by opening tap B to the apparatus and tap A to the water supply. The average rate (and hence the concentration) was determined accurately by measuring the time taken for the paraffin to rise from the mark to the top. The rate and its constancy were adjusted and monitored by a water valve and flow meter.

The liquid paraffin occupied more than half the volume of C, and the walls of the upper part were assumed to remain free of any water film.

The gases were then passed to the reaction tube. In order to ensure thorough gas mixing and to effect heat transfer from furnace to gas it was necessary to pack the tube below the sinter. The top of the tube was also packed in order to constrain the thin layer of stone. This packing material presented a large surface area to the gas and so it was essential that the material should be inert, exert no catalytic effect and absorb no appreciable amount of SO_2 at working temperature. It was found that these requirements could be met by the use of recrystallised alumina, available in convenient form as thermocouple sheathing, and itself kept in place with the minimal quantity of quartz wool.

The tube and gas were heated by a muffle furnace having a long constant temperature zone produced by four separately wound elements. Temperature at the surface of the stone was measured by a thermocouple in a quartz pocket.

The SO_2 in the effluent gases was determined by removal in two impact bubblers filled with 400 ml each of 3 vol H_2O_2, adjusted to neutrality, which generates sulphuric acid quantitatively according to the reaction:

$$H_2O_2 + SO_2 = H_2SO_4$$

The sulphuric acid in the first bubbler was then titrated with N/2 NaOH using bromo-cresyl green as indicator. The second bubbler was used as a guard trap but it was never found to contain more than 5% of the total H_2SO_4. Hence error due to incomplete SO_2 absorption could be neglected.

The stones, Dolomite 1337, U.K. Dolomite and Limestones 18 and 1359, were taken uncrushed as supplied and size fractions were derived from these by sieving:

	BS mesh		approximate particle-size	
(a)	-8	+16	-2000	+1000 µm
(b)	-16	+52	-1000	+300 µm
(c)	-52	+150	-300	+105 µm
(d)	-150	+300	-105	+53 µm
(e)	-300		-53 µm	

In the case of Limestones 18 and 1359, the original sample did not contain enough large particles to permit the preparation of the largest sizes.

The great mass of runs, for stone type and size intercomparison, were made under standard conditions of temperature, an air/SO_2 atmosphere, fixed air rate, and SO_2 content corresponding to concentrations likely to occur in combustion gases in the plants.

The amount of sample taken was initially the subject of some exploration. A portion of the selected sized stone was weighed out, placed in a reaction tube, lightly tamped and shaken to give a level surface, and the top of the tube was then packed. (The bottom of the tube was normally left packed in between experiments.) It was desired, if possible, to use a fairly thick bed to achieve uniform flow of gas across the bed, which might not occur in thin beds of coarse particles. Experiments were carried out in beds of various thicknesses from 1/4 in to 1 in, with the intention of extrapolating the results to zero thickness and possibly deriving a simple expression for bed height. Experimental results showed no simple relation between bed height and SO_2 absorption. Accordingly these experiments were abandoned, although the results are recorded in Table 23.

Instead, thin beds were used for the remaining experiments. To obtain uniform results, a small fixed weight of material was used and to avoid non-uniformities caused by packing problems etc., this was mixed with a fixed amount of recrystallised alumina of size 150 μm to give a bed height of 2 mm. The mixture was poured into place and the reaction tube was gently tapped to give a layer of uniform thickness.

The reaction tube was retained in a vertical position, the quartz wool plug and alumina packing replaced, the tube inserted in the muffle furnace and the flow of carrier gas started. The start of the experiment was delayed for 15 minutes after the apparatus had reached operating temperature to allow calcination to proceed.

With freshly-filled absorption bottles in place the contents of vessel C were passed into the carrier gas stream at constant rate as observed by the water flow meter and controlled by the water valve. The exact time required for passage of the measured amount was determined by the use of a stop-watch. The SO_2 remaining in the system after this operation was chased through with two further volumes of air from vessel C.

The whole process was repeated using fresh absorption bottles until only a small proportion of SO_2 was being removed by the stone.

The actual mass of SO_2 transferred from vessel C was monitored from time to time by passing the gas straight from the reactor inlet pipe to the wash bottles, a procedure itself checked initially by passing SO_2 through the hot, packed tube with no stone in the tube. All runs were duplicated.

7.2 Mathematical Procedures

The input data are symbolised as follows:

C	CaO in fully calcined stone	%
L	100-loss on full calcination of initial stone	%
V_o	volume of N/2 NaOH to titrate blank	mℓ
V_n	volume of N/2 NaOH to titrate H_2O_2 after nth pass	mℓ
t_n	time taken for the nth pass	s
S_m	top size of original stone	μm
S_s	bottom size of original stone	μm
T_s	temperature at start of run	°C
T_f	temperature at finish of run	°C
A	carrier gas rate	ℓ/min

M_ℓ	mass of stone employed	g
H	height of bed	mm
D	diameter of bed	mm (= 40 mm)

The experimental values of these quantities, with the exception of D (given above), are listed for each run undertaken in Table 23.

The quantities evaluated and presented in Table 24 were as follows:

T	average temperature	^oK
S	mean size	µm
M_n	mass SO_2 absorbed up to and including the nth pass	kg
R_n	reactivity averaged over nth pass	(kg SO_2/s) per kg CaO
C_w	concentration SO_2 w/v	mg/m^3
k_w	velocity constant	(m^3/s) per kg
U_n	utilisation of stone after n passes (equal to sulphation E_s - see Section 2.2.2)	-
$\bar{U}_n$	mean utilisation of stone during nth pass	-

These quantities were evaluated as follows:

$$T = (T_f + T_s + 546)/2$$

$$S = (S_m \cdot S_s)^{\frac{1}{2}}$$

$$M_n = M_{n-1} + 1.6\ (V_o - V_n)\ 10^{-5}$$

$$C_w = \frac{16\ V_o \times 60{,}000}{A\ .\ t_n} \cdot \frac{293}{T}$$

$$R_n = (M_n - M_{n-1})/(t_n\ .\ C\ .\ L\ .\ 10^{-7})$$

$$k_w = R/(C_w\ .\ M_\ell)$$

$$U_n = 87.5\ M_n/(C\ .\ L\ .\ M_\ell\ .\ 10^{-7})$$

$$\bar{U}_n = (U_n + U_{n-1})/2$$

7.3 Results

As mentioned above, experiments with thick beds were discontinued but the results are given, together with the results of the thin bed method finally adopted, in Table 23.

The data, recalculated in the form of results required, are presented in Table 24.

Test Series 1 and 2: The experimental results are displayed in Table 23. The results of Test Series 1 showed good repeatability and Test Series 2, in which variation in particle size was introduced, was begun. It was found that a flow rate of 10 ℓ/min of gas (corresponding to a hot gas velocity of c. 2 ft/s) could not be maintained with finer material (Runs 15-18) at the highest gas pressure that it was possible to use and the rate had first to be halved, and reduced further still with the finest size (Run 26).

Test Series 3: The objective of this test series was to determine the velocity constant of U.K. Dolomite as a function of particle size and utilisation at constant temperature (1470°F). The results are recorded in Tables 23 and 24, and plotted in Fig. 53. Velocity constant falls linearly with increasing utilisation and more rapidly the greater the particle size.

Test Series 4, 5 and 6: The objective of the experiments was to repeat the work of Test Series 3 for Dolomite 1337 and Limestones 1359 and 18, respectively. The results are generally similar to those for U.K. Dolomite (Figs. 54-56).

Test Series 7: In this series, temperature was varied from 1290° to 1650°F with the other parameters fixed.

Time allowed measurements to be made only on one stone, and Limestone 18 was chosen as the dolomites from previous work were not expected to be so sensitive to temperature variation (see ref. 18).

The effect of CO_2 upon the reactivity of Limestone 18 was also examined because it was learned that tests with that stone were planned using the high pressure combustor (Task II).

The results show (Figs. 57 and 58) that at zero utilisation the reactivity increases with increasing temperature* as expected from previous laboratory work. As the utilisation increases to values above 25% (i.e., to conditions typical of the average bed limestone composition) the reactivity at first rises with rising temperature and then falls as the temperature rises further. This finding, unforeseen from previous work, discussed in Appendix 6 on other stones is in agreement with certain observations on the pilot plants.

---

* But see Addendum (Section 8)

The effect of CO_2 is in line with previous experience[18], in that the effect of partial pressures of CO_2 above the equilibrium partial pressure for the reaction:

$$CaCO_3 \rightleftharpoons CaO + CO_2$$

in the case of limestone is to reduce the reaction rate (Figs. 59-63). As the temperature rises toward the equilibrium temperature for the partial pressure of CO_2 employed (1607°F at 0.75 atm CO_2) the effect is markedly diminished, but does not apparently quite disappear. With Limestone 18 the suppression of reaction at 1470°F is not so severe as with the limestone used in previous work at BCURA, and this again is in accord with observations on the pressurised rig in which Limestone 18 performed better than was expected - but not so well as the dolomites. It may be noted here that the porosity studies (Section 2 - see, for example, Section 2.5) have disclosed an extensive amount of transport pores in calcined Limestone 18, but not in calcined Limestone 1359.

7.4 Discussion

It is instructive to study the results obtained in measurement of reaction rates of the different stones in conjunction with those in Fig. 23. A difference in procedure must be emphasised between the rate constant determination experiments and the drop-tube experiments (Section 2). In the former, calcination was allowed to proceed for 15 minutes at temperature before SO_2 was introduced, whilst in the latter, no precalcination was carried out.

One of the most notable features in comparing the reactivities of the stones is the poor performance of Limestone 1359 (Fig. 55). At low utilisations the reactivity is about the same as that of Limestone 18 although less than that of the dolomites. As the utilisation increases above about 5%, however, the reactivity of Limestone 1359 falls off very rapidly until it is zero at between 10 and 25% utilisation, depending on particle size. At these utilisations, Limestone 18 is still almost as reactive as the fresh calcined stone, (Fig. 56).

Looking at the results of the controlled atmosphere drop-tube experiments (Section 2) on these two stones, we see (Fig. 23) that −16 +52 BS mesh Limestone 1359 reaches a limiting sulphation value of about 8% (1650°F) or 3% (1470°F) after 1 hour, whereas Limestone 18 continues to absorb SO_2 for at least 4 hours, by which time its utilisation is 46% (1650°F) or 26% (1470°F). It is reasonable therefore to regard these drop-tube experiments as a reliable indicator of the reactivity of the stones, although further work might still be required to make possible the derivation from them of rate constants in a form suitable for input to a mathematical model.

The relation between the measured pore structure of these stones and their reactivity has been mentioned briefly in Section 7.3 and discussed in Section 2. It is noted also that the material from one of the rate constant experiments on Limestone 1359 was used as the subject for porosity measurements before and after particle breakage (Section 2, Fig. 40).

The dolomites both show initial reaction rate constants about 50% higher than the limestones, and the rate constants fall off steadily with increasing utilisation. Of the two, Dolomite 1337 is the better absorber, reaching 37% utilisation for large particles and over 50% for small ones.

The behaviour generally parallels the results of the drop-tube experiments shown in Fig. 23. The geometric mean particle size in the drop-tube experiments was 548 μm, so that the utilisation after 4 hours at 1470°F for Limestone 18 in the drop-tube experiments, i.e., 26%, corresponds to quite a high reaction rate constant (about 0.06 m^3/kg s, from Fig. 56). This is in keeping within the marked gradient of the sulphation curve after 4 hours in the drop-tube experiment.

Comparing the Dolomite 1337 curves in the same way, it is seen that in the drop-tube experiment the utilisation after 4 hours at 1470°F was 32%, which corresponds to a fairly low rate constant (Fig. 54). This is in agreement with the small gradient of this curve in Fig. 23 at 4 hours.

As noted earlier, there was time available to vary the temperature and atmosphere with one stone only, Limestone 18. The results were interesting in that for the first time in laboratory experiments they showed a decrease in reaction rate with increasing temperature above 1470°F, although this decrease occurs only with partially sulphated stone (Fig. 58). In atmospheres containing high partial pressures (0.75 atm) of CO_2 the trends are different, and at all utilisations up to 25% the reaction rate increases with temperature up to 1650°F. This is almost certainly because at lower temperatures calcination of the stone is incomplete in the presence of this partial pressure of CO_2.

8 ADDENDUM

A discussion of errors in interpretation of the rate constant measurements of Section 7

Study of the results, which were evaluated by computer, showed peculiar features, particularly the fact that for any given stone the reaction rate constant at zero utilisation (fresh stone) was almost independent of particle size and temperature, while for partly sulphated stone there were appreciable differences in rate constant for differences in particle size and temperature. Also, the rate constants determined, when fed as input data to the mathematical model (Appendix 6) failed to account adequately for the sulphation undergone by the fine particles of size small enough to be elutriated from the bed.

The purpose of this addendum is to show that the method employed to determine reaction rate constants imposed an artificial upper limit, owing to the fact that SO_2 was not supplied to the stone as quickly as it could have been absorbed, in the case of fresh stone. The error only applies to stone of less than about 10% utilisation for the two dolomites, of less than about 5% utilisation for Limestone 1359, and of less than about 25% utilisation for Limestone 18 (at 1470°F). It is impossible to guess at the magnitude of the error, but it may have been considerable for stones of zero utilisation and small particle size.

Calculation of artificially imposed limit

In each pass, a fixed mass of SO_2, 0.1735 g, was passed through the bed of stone during the specified period. The rate constant was calculated as mass of SO_2 absorbed per second, per unit mass of CaO, per unit SO_2 concentration in the incoming gas (kg/m^3).

Tables 23 and 24 supply all the necessary data for calculating the rate constant limit imposed by the rate at which SO_2 was supplied to the bed:

$$K_L = \frac{M_s}{t} \times \frac{1}{M_L . C} \times \frac{1}{C_w} \quad m^3/kgs$$

where K_L is constraining value of K (all SO_2 absorbed)

M_s is weight of SO_2 per pass (0.1735g)

t is duration of pass, s

M is mass of stone used, g

C is fraction of CaO in fully calcined stone

L is 1- (fractional weight loss on full calcination)

C_w is SO_2 concentration in incoming gas, kg/m^3.

Table 25 lists values calculated for K_L for the first pass of each run included in Table 24.

TABLE 25

Values of K_L

Run No.	Stone	K_L m^3/kgs	Run No.	Stone	K_L m^3/kgs
27	U.K. Dolomite	0.107	67	Limestone 18	0.079
28	"	0.109	68	"	0.080
29	"	0 109	70	"	0.079
30	"	0.109	71	"	0.078
31	"	0.109	74	"	0.077
32	"	0.110	75	"	0.077
49	Dolomite 1337	0 130	79	"	0.067
50	"	0 130	80	"	0.073
51	"	0 131	82	"	0.071
52	"	0 130	83	"	0.069
53	"	0.131	84	"	0.068
56	"	0 132	85	"	0.076
57	"	0.133	86	"	0.077
59	"	0 135	87	"	0.088
61	Limestone 1359	0 074	88	"	0.085
62	"	0.074	89	"	0.079
64	"	0.072			
65	"	0.074			

Discussion

The values for K_L are seen to be in each case only slightly higher than the value for the reaction rate constant determined in the first pass. It is considered that the evidence is overwhelming that in most cases, were it not for the limit imposed by the experimental procedure, considerably higher values would have been found for low utilisations. The conclusions regarding the effect of temperature upon reaction rate at low utilisations (Section 7.3) must also be suspected of being in error, since under these conditions the reactivity was limited by the experimental procedure.

It is recommended that any further work on mathematical modelling of sulphur retention by limestone addition to fluidised beds should be accompanied by a re-determination of reaction rate constants, special attention being paid to the elimination of this source of inaccuracy.

In order to determine the rate constants without error it would be necessary to carry out repeat experiments using much higher SO_2 concentrations in the first (and possibly the second) pass, so that there is a fairly large break-through of SO_2 at the start of the first pass. This would be easier to ensure if a continuous SO_2 analyser were available, as was not the case in the experiments described in this Appendix.

9. GLOSSARY OF TERMS

Most of these terms are defined in the text: they are collected here to facilitate reference.

Atmosphere, controlled The uncalcined stones were sprinkled on to a mesh (at 1470° or 1650°F) contained in a vertical tube, through which flowed a gas mixture of controlled inlet composition. (Section 2.)

Atmosphere, flushed The uncalcined stones were sprinkled into a vertical tube having a closed end (at 1470°F); a second tube through which a stream of dry nitrogen flowed dipped into the first to reach the stone. (Section 2.)

Atmosphere, stagnant The uncalcined stones were sprinkled into a vertical tube having a closed end (at 1470°F). (Section 2.)

Bar Unit of pressure equal to 10^5 N/m^2, 10^6 dyne/cm^2, 0.987 standard atm, 14.5 lbf/in^2, 750 torr.

B.E.T. equation The equation of Brunauer, Emmett and Teller, used for calculating the surface areas of solids from gas adsorption data (see ref. 24). This is a standard method. (Section 6.2.)

c. An abbreviation for circa (approximately)

Calcination, extent of, E_c The amount of CO_2 lost by a stone on calcination, expressed as a percentage of the total amount of CO_2 that would be lost if all the carbonate originally present were converted to oxide

Calcined-only stones Stones calcined in the absence of SO_2.

Calcined-sulphated stones Stones calcined in the presence of SO_2

Dead volume The volume that is not occupied by the sample in the sample container of the helium density or sorption apparatus

Displacement density - helium, ρ_{He} The mass of a solid divided by the volume of helium it displaces when immersed in that gas. Unit: g/cm^3 (Technique, Section 2.3.1.)

Displacement density - mercury, ρ_{Hg} The mass of a solid divided by the volume of mercury it displaces when immersed in that liquid under a specified pressure; in the present work the average pressure on the mercury in contact with each stone particle was taken as 760 torr (1.013 bar). One use of this mercury displacement volume (although it does not include the volume of pores with entrances of diameter 14.5 μm, assuming the entrances to be circular) is as an approximation to the superficial volume of the particles. Unit: g/cm^3. (Technique, Section 2.3.2.)

Drop-tube experiment The calcination or calcination-sulphation experiments in the controlled atmospheres.

Helium density See Displacement density - helium

Helium specific volume, $1/\rho_{He}$ Reciprocal of the helium density. Unit: mm^3/g.

Intergranular volume; interparticulate volume The volume of the spaces between stone particles constrained in the sample chamber of the mercury porosimeter; virtually all this volume can be considered as being behind entrances ≥10 μm diameter and most behind entrances >58 μm

Mercury density See Displacement density - mercury

Mercury specific volume, $1/\rho_{Hg}$ Reciprocal of the mercury density. Unit: mm^3/g.

Mercury injection porosimetry A technique for measuring the volumes of pores behind entrances with diameters between chosen limits within an overall range: c. 58 μm to 0.014 μm in the present work assuming the entrances are circular. Mercury was forced into the stones under stepwise increase of pressure up to c. 1035 bar, the cumulative amount of mercury in the stone being measured at each step. (Technique, Section 2.3.4.)

Particle density, ρ_p The mass of particles in a sample divided by their superficial volume

Peak pore-entrance diameter, Δ The pore-entrance diameter at the main peak in each of the mercury porosimetry differential curves of Figs. 4, 5 and 6.

Pore penetration experiment An experiment to determine the increase in gas penetration on increase of temperature. (Technique, Section 4.)

Pore closure experiment An experiment to determine the decrease in gas penetration on increase of temperature (Technique, Section 4.)

Pore-entrance diameter The diameter of an opening through which access is obtained to a pore. This entrance may be narrower than the pore. When a pore has more than one entrance, it is the larger one that is measured. Where deduced from mercury porosimetry, the symbol is D or p.e.d.; circular entrances are assumed.

Porosity; pore volume The volume of pores behind entrances having a specified range of diameters, expressed on a per gramme (mm^3/g) or percentage of superficial volume of sample basis.

Porosity (helium - mercury density), V_x The pore volume accessible to helium but not to mercury under 760 torr (1.013 bar) calculated from the helium and mercury displacement densities. V_x is taken to be the volume behind entrances with diameters between 14.5 µm and 0.26 nm.

Porosity-mercury porosimetry

(i) Total pore volume, t.p.v. The pore volume behind entrances with diameters between c. 58 µm and 0.014 µm, viz, the whole range covered by the mercury porosimeter.

(ii) π_{Hg} The pore volume behind entrances with diameters between 14.5 µm and 0.014 µm (the value of 14.5 µm being chosen to equal the upper entrance diameter limit of V_x).

Pore volumes with respect to other entrance diameter ranges have also been evaluated.

No correction was attempted for the contribution of intergranular volume, which was small with respect to entrances <14.5 µm diameter.

Rapid heating Heating of uncalcined stones by sprinkling into the hot zone at 1470° or 1650°F in the calcination-only or calcination-sulphation experiments to simulate the rapid heating conditions in the combustor.

Reaction rate constant; velocity constant The mass of SO_2 absorbed per second, by unit mass of CaO in calcined stone, from a gas mixture containing 1 kgSO_2/m^3. The reaction has been taken to be first order. Unit: $m^3/kg.s$. (Technique, Section 7.1.)

Reactivity A general term meaning the magnitude of the reaction rate constant for a given stone under specified conditions, e.g., sulphation, particle size.

'Shell' formation The formation of a sulphated layer that impedes penetration of SO_2 to the internal pores of a particle, as found with Limestone 1359 under laboratory conditions.

Specific surface Surface area per unit mass. Unit: m^2/g

Sulphation, E_s; utilisation, U   The amount of sulphur taken up by a stone, expressed as a percentage of the total amount of sulphur that would be taken up if all the $CaCO_3$ originally present were converted to $CaSO_4$.

Sulphation, limiting   Level of sulphation at which the reaction rate constant falls to a negligibly low value.

Torr   Unit of pressure equal to 1 mm of mercury at 0^oC and standard gravity 980.665 cm/s^2 (750 torr = 1 bar). The torr is often used in vacuum technology to indicate residual gas pressures.

Transport pores   Relatively large pores necessary to facilitate access of SO_2 to the interior of stone particles. In the present work these pores have been considered, for reasons of comparison, as having entrances between 14.5 μm and 0.3 μm.

Utilisation   See Sulphation

Velocity constant   See Reaction rate constant

Volume, superficial, particle or 'lump'   The volume of a stone including that of all the pores it contains.

10. REFERENCES

1. Potter, A.E. Amer Ceramic Soc. Bull., 48(9), 855 (1969).
2. Falkenberry, H.L. and Slack, A.V. Chem. Engng. Prog., 65 (12), 61 (1969).
3. Bethell, F.V. Private Communication, 1970.
4. Coutant, R.W., McNulty, J.S., Barrett, R.E., Carson, J.J., Fischer, R. and Lougher, E.H. 'Investigation of the Reactivity of Limestone and Dolomite for Capturing SO_2 from Flue Gas': Battelle Memorial Institute Report to NAPCA, August 30, 1968.
5. Rappeneau, J. in 'Les Carbones', Vol. II, Ch. 14, Section C.II, pp. 134-140, Masson, Paris, 1965.
6. Scholten, J.J.F. in 'Porous Carbon Solids' (Ed. R.L. Bond), Ch. VI, pp. 225-249, Academic Press, 1967.
7. Innes, W.B. in 'Experimental Methods in Catalytic Research' (Ed. R.B. Anderson), pp. 80-81, Academic Press, 1968.
8. Spencer, D.H.T. BCURA Monthly Bulletin, 33 (No. 10), pp. 228-239, October 1969.
9. Carbon and Its Uses, Issue No. 10, pp. 16-22, Morganite Carbon Ltd., London, 1966.
10. Satterfield, C.N. and Feakes, F. A.I.Ch.E. Journal, 5, 115 (1959).
11. Chan, R.K., Murthi, K.S. and Harrison, D. Canad. J. Chem., 48, 2972 (1970).
12. Glasson, D.R. J. Appl. Chem., 8, 793 (1958).
13. Glasson, D.R. J. Appl. Chem., 17, 91 (1967).
14. Glasson, D.R. J. Appl. Chem., 13, 111 (1963).
15. Glasson, D.R. J. Appl. Chem., 11, 201 (1961).
16. Girgis, B.S. and Girgis, L.G. J. Appl. Chem., 19, 292 (1969).
17. McClellan, A.L. and Harnsberger, H.F. J. Colloid Interface Sci., 23, 577 (1967).
18. Bethell, F.V. BCURA Doc. No. FCP5, 1969.
19. See, for example:
   Lamond, T.G. and Marsh, H. Carbon, 1, 281, 293 (1964).
   Gregg, S.J. and Sing, K.S.W. 'Adsorption, Surface Area and Porosity', Ch. 4, Academic Press, London and New York, 1967.

20. See, for example:
Spencer, D.H.T. *in* 'Porous Carbon Solids' (Ed. R.L. Bond), p.133, *et seq*, Academic Press, London and New York, 1967.

21a. Napier, B.A. and Spencer, D.H.T. *Nature* (Lond.), *218*, 948 (1968).

21b. Napier, B.A. and Spencer, D.H.T. To be published.

21c. Kipling, J.J., Sherwood, J.N., Shooter, P.V., Thompson, N.R. and Young, R.N. *Carbon*, *4*, 5 (1966).

21d. Norton, F.J. *J. Appl. Phys.*, *28*, 34 (1957).
Stern, S.A. *in* 'Argon, Helium and the Rare Gases' Vol.I (Ed. G.A. Cook), pp.217-218, Interscience, New York and London, 1961.

21e. Graham, L.W. Proc. Second Conf. Ind. Carbon Graphite, p.224 (contribution to discussion), Society of Chemical Industry, London, 1966.

22. Jonke, A.A. Argonne National Laboratory: 'Reduction of Atmospheric Pollution by the Application of Fluidized Bed Combustion'. Monthly Progress Report No. 3, p.11, Oct. 1968.

23. NCB Second Three Monthly Progress Report to NAPCA, November, 1970.

24. Gregg, S.J. and Sing, K.S.W. 'Adsorption, Surface Area and Porosity', Academic Press, London and New York, 1967.

11. ACKNOWLEDGEMENTS

The experimental work described in this report was carried out at BCURA Industrial Laboratories Ltd., Leatherhead, Surrey, under the overall direction of Mr. H.R. Hoy.

The work described in:

(a) Sections 2 to 6, was mostly performed in the BCURA Pore Structure Laboratory (Group Leader, D.H.T. Spencer) of the Materials Characterisation Unit (Head, Mr. R.L. Bond). The authors of these Sections - A.A. Herod, B.A. Napier and D.H.T. Spencer - acknowledge the contribution to the experimental work made by their colleagues, Mr. D.J. Ando, Mr. M.A. Hooker, Mr. D.F. Libaert, Mr. N. Peters and Mr. M.E.Turtle. Acknowledgement is also made to Mr. R. Dickinson, of the Mathematics Department, for processing by computer the output from the mercury porosimeter, and to Miss M. Kay, of the Analytical Section of the Materials Characterisation Unit, who carried out most of the sulphur determinations.

(b) Section 7, was carried out by two of the authors - F.V. Bethell and G. McDonald - under the general supervision of Mr. D.W. Gill.

Acknowledgement is made to Mr. Gill for preparing the Addendum in Section 8.

Table A8.1. Scheme followed in the preparation of calcined and calcined-sulphated stones, with rapid heating and using controlled atmospheres

Variables	Levels
Particle-size grade of stone	-16 + 52 BS mesh
Composition of gas passed into furnace tube	(1) 15% CO_2, 3% O_2, balance N_2; (2) 15% CO_2, 3% O_2, 2000 ppm SO_2, balance N_2; all quantities being 'by volume'
Duration of particles in furnace tube	¼, 1 and 4 h
Furnace temperature	1470° and 1650°F

Table A8.2. Calcination details - U.K. dolomite: exploratory experiments and pore-penetration, pore-closure experiments

Sample designation	Particle-size grade, BS mesh	Calcination history at 1470°F	Extent of calcination, %	
			After treatment in atmosphere	After pp-pc*
B1, f	- 6 + 8	in vacuum	-	100.0
B1 (a), g	- 6 + 8	in vacuum	-	100.1
B1 (b), h	- 6 + 8	in vacuum	-	99.5
B2	- 6 + 8	rapidly heated; SA;** 1h	50.5	100.0
C	-16 + 52	in vacuum	-	97.0
C	-16 + 52	slow in air and vacuum	-	97.0
C1	-16 + 52	rapidly heated; SA; 1h	52.8	
C2	-16 + 52	rapidly heated; SA; 23h	69.0	
C3	-16 + 52	rapidly heated; SA; ½h	48.5	
C4	-16 + 52	rapidly heated; SA; ¼h	49.4	
C5	-16 + 52	rapidly heated; SA; 97h	99.5	
C6	-16 + 52	rapidly heated; N_2; 1½h†	67.1	
C7	-16 + 52	rapidly heated; N_2; 16h	99.6	
C8	-16 + 52	rapidly heated; N_2; ½h	69.8	
C9	-16 + 52	rapidly heated; N_2; 3h	99.1	
C10	-16 + 52	rapidly heated; N_2; 1½h	83.4	
C11	-16 + 52	rapidly heated; SA; 3½h	52.9	
E	-300	in vacuum	-	99.0
E1	-300	rapidly heated; SA; 17h	60.7	99.3

* Pore penetration - pore closure experiments (Section 4)

** SA = stagnant atmosphere

† Calcined in slower N_2 flow

Table A8.3. **Calcination details - limestone 1359: exploratory experiments and pore-penetration, pore-closure experiments**

Sample designation	Particle-size grade BS mesh	Calcination history at 1470°F	Extent of calcination, %	
			After treatment	After pp-pc*
Ungraded material		in vacuum	-	99.6
G1	-16 + 52	rapidly heated; SA;**2h	3.4	99.0
G2	-16 + 52	rapidly heated; SA; ¼h	2.3	
G3	-16 + 52	rapidly heated; SA; ½h	2.3	
G4	-16 + 52	rapidly heated; SA; 17h	24.6	
G5	-16 + 52	rapidly heated; SA; 115h	99.1	
G6	-16 + 52	rapidly heated; N_2; 1h†	21.6	
G8	-16 + 52	rapidly heated; N_2; 2h†	45.5	
G9	-16 + 52	rapidly heated; N_2; 1h	15.9	
G10	-16 + 52	in vacuum	-	99.3
H1	-300	rapidly heated; SA; 1h	9.1	
H2	-300	rapidly heated; SA; 5h	9.5	
H3	-300	rapidly heated; SA; 18h	22.5	
H6	-300	in vacuum	-	96.5

* Pore penetration - pore closure experiments (Section 4)

** SA = stagnant atmosphere

† Calcined in slower N_2 flow

Table A8.4. Prefix assigned to sample of a particular stone in a particular particle-size grade

Stone	Particle-size grade, BS mesh, and prefix		
	−6 + 8	−16 + 52	−300
Dolomite 1337	–	J	–
U.K. dolomite	B	C	E
Limestone 18	–	N	–
Limestone 1359	–	G	H

Table A8.5 Designation of samples prepared in controlled atmospheres*

Atmosphere and temperature		SO_2 absent, 1470°F			SO_2 present, 1470°F			SO_2 absent, 1650°F			SO_2 present, 1650°F		
Treatment time, h		¼	1	4	¼	1	4	¼	1	4	¼	1	4
Designation	Dolomite 1337	J6	J4	J5	J9	J8	J10	J14	J15	J16	J13	J12	J17
	U.K. dolomite	C28	C29	C30	C32	C31	C33	C34	C36	C35	C39	C38	C37
	Limestone 18	N3	N2	N4	N6	N7	N8	N14	N13	N15	N11	N12	N16
	Limestone 1359	G32	G33	G34	G36	G35	G37	G39	G38	G40	G43	G42	G41

* 15% CO_2, 3% O_2, 82% N_2, with and without 2000 ppm SO_2, all v/v.

from exploratory experiments

Sample		Calcination		Total pore volume (t.p.v.), mm³/g	Peak pore-entrance diameter (Δ) μm
		Extent, %	Time, h		
U.K. dolomite	C	Nil	-	41	+
	C1	52.8	1	190	0.18
	C2	69.0	23	280	0.30
	C4	49.4	¼	180	0.08
	C5	99.5	~97	510	0.46
	C6	67.1**	1½	260	0.18
	C7	99.6*	16	470	0.30
	C8	69.8*	½	280	0.10
	C9	99.1*	3	440	0.23
	C10	83.4*	1½	340	0.18
Limestone 1359	G	Nil	-	18	+
	G3	2.3	½	33	+
	G4	24.6	17	100	1.10
	G5	99.1	115	360	1.10
	G6	21.6**	1	70	0.30
	G8	45.5**	2	140	0.30

* Calcined in N_2 flow

** Calcined in slower N_2 flow

+ Indeterminate

Table A8.7. Results from controlled-atmosphere experiments: dolomite 1337

Sample designation	Calcination			Sulphation %	ρ_{He}, g/cm^3	$1/\rho_{He}$, (x) mm^3/g	ρ_{Hg}, g/cm^3	$1/\rho_{Hg}$, (y) mm^3/g	Porosity, Vx		Mercury porosimetry porosity, mm^3/g		
	Time, h	Temp., °F	Extent, %						(y − x) mm^3/g	%	t.p.v.	Volume in pores with entrances >14.5μm dia.	πHg
J	Raw stone			0	2.83	354	2.604	384	30	7.8	46.3	9.3	37.
J6	¼	1470	33.6	0	2.88	347	2.196	455	108	23.7	117.6	13.3	104.
J4	1	1470	62.4	0	3.03	330	1.866	536	206	38.4	212.4	12.2	200.
J5	4	1470	52.0	0	2.96	338	1.978	505	167	33.0	186.4	19.8	166.
J9	¼	1470	61.8	9.7	2.94	340	1.991	502	162	32.3	187.3	20.2	167.
J8	1	1470	75.0	28.9	3.01	332	2.092	478	146	30.5	165.4	12.8	152.
J10	4	1470	87.0	53.4	2.99	335	2.292	436	101	23.1	125.7	18.7	107.
J14	¼	1650	85.0	0	3.26	307	1.570	637	330	51.8	351.2	20.0	331.
J15	1	1650	93.0	0	3.39	295	1.534	652	357	54.8	375.2	30.3	344.
J16	4	1650	90.0	0	3.36	298	1.541	649	351	54.1	394.9	26.3	368.
J13	¼	1650	90.5	13.7	3.24	309	1.718	582	273	46.9	296.3	22.2	274.
J12	1	1650	94.3	34.4	3.24	309	1.936	516	207	40.1	221.9	16.8	205.
J17	4	1650	99.0	54.7	3.15	318	2.228	449	131	29.2	152.8	19.0	133.

Table A8.8 Results from controlled-atmosphere experiments: U.K. dolomite

Sample designation	Calcination			Sulphation, %	ρ_{He}, g/cm^3	$1/\rho_{He}$, (x) mm^3/g	ρ_{Hg}, g/cm^3	$1/\rho_{Hg}$, (y) mm^3/g	Porosity, Vx		Mercury porosimetry porosity mm^3/g		
	Time, h	Temp., °F	Extent, %						(y - x) mm^3/g	%	t.p.v.	Volume in pores with entrances >14.5μm dia.	π Hg
C	Raw stone			0	2.83	353	2.696	371	18	4.8	40.8	16.5	24.3
C28	¼	1470	57.3	0	2.98	336	1.976	505	169	33.4	199.1	26.1	173.0
C29	1	1470	67.0	0	3.03	331	1.871	535	204	38.1	225.5	27.0	198.5
C30	4	1470	69.0	0	3.16	317	1.866	536	219	40.8	231.3	22.7	208.6
C32	¼	1470	61.5	11.8	3.01	333	2.025	494	161	32.6			
C31	1	1470	71.8	22.9	2.99	335	2.056	486	151	31.1			
C33	4	1470	81.4	37.4	2.99	335	2.143	467	132	28.2			
C34	¼	1650	96.0	0	3.32	301	1.544	648	347	53.5	395.0	36.6	358.4
C36	1	1650	98.0	0	3.34	300	1.520	658	358	54.4	402.7	33.0	369.7
C35	4	1650	100.0	0	3.39	295	1.509	663	368	55.5	414.1	38.5	375.6
C39	¼	1650	93.0	10.7	3.39	295	1.675	597	302	50.5	328.8	29.0	299.8
C38	1	1650	97.0	22.7	3.33	301	1.745	573	273	47.6	287.9	29.3	258.6
C37	4	1650	99.0	41.5	3.25	308	1.968	508	200	39.4	220.7	21.6	199.1

Table A8.9. Results from controlled-atmosphere experiments: limestone 18

Sample designation	Calcination			Sulphation %	ρ_{He}, g/cm^3	$1/\rho_{He}$, (x) mm^3/g	ρ_{Hg}, g/cm^3	$1/\rho_{Hg}$, (y) mm^3/g	Porosity, Vx		Mercury porosimetry porosity, mm^3/g		
	Time, h	Temp., °F	Extent, %						$(y - x)$ mm^3/g	%	t.p.v.	Volume in pores with entrances >14.5μm dia.	π_{Hg}
N	Raw stone			0	2.67	375	2.471	405	30	7.4	50.1	18.3	31.8
N1	¼	1470	14	0	2.66	375	2.330	429	54	12.6	71.5	11.8	59.7
N3	¼	1470	16	0	2.66	375	2.261	442	67	15.1	92.8	19.3	73.5
N2	1	1470	19.5	0	2.66	375	2.289	437	62	14.2	85.4	14.1	71.3
N4	4	1470	30.5	0	2.68	373	2.221	450	77	17.1	96.5	15.3	81.2
N6	¼	1470	~10	3.9	2.75	364	2.369	422	58	13.7	67.0	15.9	51.1
N7	1	1470	21.0	9.4	2.77	361	2.350	426	65	15.3	77.4	17.2	60.2
N8	4	1470	66.6	26.3	2.89	346	2.210	452	106	23.4	115.4	13.9	101.5
N14	¼	1650	85.0	0	3.12	321	1.706	586	265	45.2	292.7	26.5	266.2
N13	1	1650	96.0	0	3.24	309	1.605	623	314	50.4	323.8	28.0	295.8
N15	4	1650	96.0	0	3.14	319	1.647	607	288	47.5	298.9	26.8	272.
N11	¼	1650	85.2	9.1	3.13	320	1.791	558	238	42.6	246.2	18.7	227.
N12	1	1650	94.0	25.9	3.16	316	1.972	507	191	37.7	209.8	21.0	188.8
N16	4	1650	100.0	46.1	3.03	331	2.360	424	93	22.0	100.7	18.0	82.7

Table A8.10. Results from controlled-atmosphere experiments: limestone 1359

Sample designation	Calcination			Sulphation, %	ρ_{He}, g/cm^3	$1/\rho_{He}$, (x) mm^3/g	ρ_{Hg}, g/cm^3	$1/\rho_{Hg}$, (y) mm^3/g	Porosity, Vx		Mercury porosimetry porosity mm^3/g		
	Time, h	Temp., °F	Extent %						(y − x) mm^3/g	%	[illegible]	Volume in pores with entrances 14.5 µm dia.	[illegible]
G	Raw stone			0	2.72	368	2.669	375	7	1.9	1.0	10.0	8
G 32	¼	1470	4.0	0	2.73	366	2.604	384	18	4.7	2.9	10.1	17
G 33	1	1470	3.6	0	2.72	368	2.583	387	19	4.5	3.3	10.1	21
G 34	4	1470	19.0	0	2.79	358	2.407	415	57	13.7	6.5	9.4	53.
G 36	¼	1470	5.7	1.5	2.70	371	2.606	384	13	3.4			
G 35	1	1470	7.3	3.1	2.71	369	2.594	385	16	4.1			
G 37	4	1470	10.0	3.3	2.72	368	2.566	390	22	5.8			
G 39	¼	1650	86.4	0	3.19	314	1.789	559	245	43.8	5.7	[illegible].3	236.
G 38	1	1650	89.0	0	3.25	308	1.769	565	257	45.[illegible]	18.9	[illegible]	265.
G 40	4	1650	91.0	0	3.29	304	1.775	563	259	46.0	[illegible]9	22.7	252.
G 43	¼	1650	90.0	5.0	3.20	313	1.848	541	228	42.1			
G 42	1 [illegible]	1650	98.0	7.5	3.28	305	1.857	538	233	43.[illegible]			
G 41	4	1650	99.0	8.0	3.26	307	1.900	526	219	[illegible]	[illegible]	[illegible]8	19

Table A8.11. Volume in pores (mm^3/g and percentage of particle volume $1/\rho_{Hg}$) with entrances having diameters between 14.5μm and values shown*

Dolomite 1337 (J samples) and U.K. dolomite (C samples)

Sample designation	3μm		1μm		0.3μm		0.1μm		0.03μm		0.014μm	
	mm^3/g	%	mm^3/g	%	mm^3/g	%	mm^3/g	%	mm^3/g	%	mm^3/g	%
J	5.2	1.3	18.5	4.8	32.0	8.3	36.0	9.4	37.0	9.6	37.0	9.6
J6	11.2	2.4	28.2	6.2	45.5	10.0	50.7	11.2	66.3	14.6	104.3	23.0
J4	9.3	1.7	29.9	5.6	53.6	10.0	64.0	12.0	152.1	28.3	200.2	37.4
J5	11.0	2.2	32.1	6.4	52.2	10.3	58.9	11.7	129.9	25.7	166.6	33.0
J9	15.2	3.1	36.4	7.2	54.4	10.8	57.9	11.5	107.9	21.5	167.1	33.3
J8	11.8	2.5	31.4	6.6	47.4	9.9	51.5	10.8	123.7	25.9	152.6	31.9
J10	12.0	2.7	29.4	6.7	40.6	9.3	43.1	9.9	89.7	20.6	107.0	24.5
J14	16.5	2.6	44.0	6.9	67.1	10.5	76.1	12.0	308.2	48.4	331.2	52.0
J15	19.7	3.0	47.7	7.3	71.5	11.0	80.4	12.3	321.5	49.2	344.9	52.9
J16	22.6	3.5	61.9	9.5	94.1	14.5	104.1	16.1	351.7	54.1	368.6	56.8
J13	16.5	2.8	42.7	7.3	61.4	10.5	68.1	11.7	249.4	42.8	274.1	47.1
J12	19.9	3.9	41.9	8.1	57.2	11.1	61.4	11.9	190.2	36.8	205.1	39.8
J17	13.6	3.0	29.2	6.5	40.8	9.1	44.9	10.0	122.8	27.3	133.8	29.8
C	9.8	2.6	14.8	4.0	19.4	5.2	21.4	5.8	23.9	6.4	24.3	6.5
C28	22.3	4.4	30.8	6.1	42.6	8.4	50.4	10.0	127.9	25.3	173.0	34.3
C29	15.7	2.9	27.1	5.1	39.5	7.4	51.5	9.6	176.9	33.1	198.5	37.2
C30	17.5	3.3	28.7	5.3	43.4	8.1	57.2	10.7	197.0	36.7	208.6	38.9
C34	22.3	3.4	35.9	5.5	53.0	8.2	89.1	13.8	336.3	52.0	358.4	55.4
C36	20.3	3.1	34.1	5.2	52.1	7.9	114.8	17.5	356.2	54.1	369.7	56.1
C35	18.4	2.8	33.1	5.0	51.3	7.7	136.5	20.6	366.1	55.4	375.6	56.8
C39	19.2	3.2	30.9	5.2	45.0	7.5	83.4	14.0	290.8	48.6	299.8	50.1
C38	15.0	2.6	26.8	4.7	35.1	6.2	91.9	16.2	251.9	44.0	258.6	45.1
C37	16.1	3.2	22.8	4.5	29.0	5.7	87.2	17.2	191.4	37.7	199.1	39.3
C1	18.7	3.7	28.8	5.7	50.4	10.0	156.9	31.2	165.9	33.0	167.8	33.3
C5	48.3	6.7	98.8	13.8	406.8	57.0	433.5	60.7	435.8	61.2	439.3	61.5
C10	22.7	3.6	38.5	6.1	87.4	13.8	286.0	45.2	311.4	49.1	313.8	49.4
C9	22.4	3.1	40.0	5.5	115.0	15.7	344.1	47.0	406.1	55.4	410.4	56.1
C7	32.9	4.5	55.9	7.7	249.0	34.3	412.2	56.7	425.5	58.5	424.5	58.4

* Most of these are approximations, for simplicity; see Section 2.4.2.5.

Table A8.12. Volume in pores (mm^3/g and percentage of particle volume $1/\rho_{Hg}$) with entrances having diameters between 14.5μm and values shown*

Limestone 18 (N samples) and limestone 1359 (G samples)

Sample designation	3μm		1μm		0.3μm		0.1μm		0.03μm		0.014μm	
	mm^3/g	%	mm^3/g	%	mm^3/g	%	mm^3/g	%	mm^3/g	%	mm^3/g	%
N	5.3	1.3	14.9	3.7	22.6	5.6	25.9	6.4	30.6	7.5	31.8	7.9
N1	8.6	2.0	24.5	5.7	40.6	9.5	52.4	12.2	57.9	13.5	59.7	13.9
N3	10.0	2.3	30.3	6.8	50.5	11.4	63.2	14.3	71.6	16.2	73.5	16.6
N2	8.6	2.0	27.0	6.2	48.1	11.0	60.9	13.9	70.0	16.0	71.3	16.3
N4	9.0	2.0	28.0	6.2	54.3	12.1	75.1	16.7	80.4	17.8	81.2	18.1
N6	8.3	2.0	21.2	5.0	35.2	8.4	43.8	10.4	49.6	11.7	51.1	12.1
N7	7.5	1.8	20.2	4.8	35.7	8.4	48.9	11.5	58.1	13.7	60.2	14.1
N8	6.6	1.5	25.1	5.5	55.2	12.2	90.8	20.1	99.1	21.9	101.5	22.5
N14	13.9	2.4	69.2	11.8	132.9	22.7	189.3	32.3	264.5	45.1	266.2	45.5
N13	6.5	1.0	76.2	12.2	153.7	24.6	269.1	43.2	292.6	47.0	295.8	47.4
N15	13.0	2.1	71.4	11.8	174.3	28.7	265.5	43.7	269.6	44.4	272.1	44.8
N11	10.2	1.8	52.3	9.4	109.3	19.6	157.7	28.2	224.9	40.4	227.5	40.7
N12	15.9	3.1	58.5	11.5	107.8	21.2	173.9	34.2	186.8	36.8	188.8	37.1
N16	6.1	1.4	24.2	5.7	50.5	11.9	70.5	16.6	78.3	18.5	82.7	19.5
G	2.4	0.6	4.1	1.1	5.9	1.6	6.5	1.7	7.6	2.0	8.0	2.1
G32	2.6	0.7	5.3	1.4	7.5	1.9	10.4	2.7	16.0	4.2	17.8	4.6
G33	3.8	1.0	6.2	1.6	8.4	2.2	12.9	3.3	18.8	4.9	21.2	5.5
G34	3.6	0.9	6.2	1.5	10.7	2.6	35.0	8.4	48.7	11.8	53.1	12.8
G39	7.0	1.2	11.8	2.1	19.7	3.5	35.3	6.3	228.5	41.0	236.9	42.4
G38	8.9	1.6	15.5	2.7	30.7	5.4	134.2	23.8	263.4	46.5	265.5	47.0
G40	5.5	1.0	8.2	1.4	24.4	4.3	223.5	39.7	247.2	43.9	252.2	44.8
G41	6.4	1.2	18.1	3.4	32.6	6.2	169.2	32.2	188.5	35.8	191.3	36.4

* Most of these are approximations, for simplicity; see Section 2.4.2.5.

Table A8.13. Volume in pores (percentage of particle volume $1/\rho_{Hg}$) with entrances having diameters within ranges shown*

(a) Calcination alone at 1470°F

Stone	Sample designation	t,** h	14.5 to 3μm	3 to 1μm	1 to 0.3μm	0.3 to 0.1μm	0.1 to 0.03μm	0.03 to 0.014μm
Dolomite 1337	J6	¼	2.5	3.7	3.8	1.1	3.5	8.3
	J4	1	1.7	3.9	4.4	1.9	16.5	9.1
	J5	4	2.2	4.2	3.9	1.4	14.0	7.3
U.K. dolomite	C28	¼	4.4	1.7	2.3	1.6	15.3	8.9
	C29	1	2.9	2.2	2.3	2.2	23.5	4.0
	C30	4	3.3	2.1	2.7	2.6	26.1	2.1
U.K. dolomite (exploratory experiments)	C1	1+	3.7	2.0	4.3	21.2	1.8	0.3
	C5	97+	6.8	7.0	43.2	3.7	0.4	0.4
	C10	1½++	3.6	2.5	7.7	31.3	4.0	0.3
	C9	3++	3.1	2.4	10.2	31.3	8.4	0.7
	C7	16++	4.5	3.2	26.6	22.4	1.8	0.0
Limestone 18	N3	¼	2.3	4.5	4.6	2.9	1.9	0.4
	N2	1	2.0	4.2	4.8	2.9	2.1	0.3
	N4	4	2.0	4.2	5.9	4.6	1.2	0.1
Limestone 1359	G32	¼	0.7	0.7	0.5	0.8	1.5	0.4
	G33	1	1.0	0.6	0.6	1.1	1.6	0.6
	G34	4	0.9	0.6	1.1	5.8	3.3	1.1

* Most of these entrance diameter values are approximations, for simplicity; See section 2.4.2.5

** Time for calcination

+ In stagnant atmosphere

++ With nitrogen flush

Table A8.13 (contd). Volume in pores (percentage of particle volume $1/\rho_{Hg}$) with entrances having diameters within ranges shown*

(b) Calcination alone at 1650°F

Stone	Sample designation	t,** h	14.5 to 3µm	3 to 1µm	1 to 0.3µm	0.3 to 0.1µm	0.1 to 0.03µm	0.03 to 0.014µm
Dolomite 1337	J14	¼	2.6	4.3	3.6	1.5	36.4	3.6
	J15	1	3.0	4.3	3.7	1.3	37.0	3.6
	J16	4	3.5	6.0	5.0	1.5	38.2	2.6
U.K. dolomite	C34	¼	3.4	2.1	2.7	5.6	38.1	3.4
	C36	1	3.1	2.1	2.7	9.6	36.6	2.1
	C35	4	2.8	2.2	2.7	12.9	34.6	1.5
Limestone 18	N14	¼	2.4	9.4	10.9	9.6	12.8	0.3
	N13	1	1.0	11.2	12.5	18.5	3.8	0.5
	N15	4	2.1	9.7	16.9	15.0	0.7	0.4
Limestone 1359	G39	¼	1.2	0.9	1.4	2.8	34.6	1.5
	G38	1	1.6	1.1	2.7	18.3	22.9	0.4
	G40	4	1.0	0.5	2.8	35.4	4.2	0.9

* Most of these entrance diameter values are approximations, for simplicity; See section 2.4.2.5.

** Time of calcination

Table A8.14 Results from exploratory experiments on U.K. dolomite

Sample designation	Calcination			ρ_{He}, g/cm^3	$1/\rho_{He}$ (x) mm^3/g	ρ_{Hg}, g/cm^3	$1/\rho_{Hg}$ (y), mm^3/g	Porosity, Vx		Mercury porosimetry porosity			
	Time, h	Atmosphere *	Extent, %					y − x, mm^3/g	%	t.p.v., mm^3/g	Volume in pores with entrances >14.5μm dia, mm^3/g	π_{Hg}	
												mm^3/g	%
C	0	-	0	2.83	353	2.696	371	18	4.9	40.8	16.5	24.3	6.5
C1	1	SA	52.8	2.98	335	1.987	503	168	33.3	189.8	22.0	167.8	33.3
C5	97	SA	99.5	3.44	291	1.401	714	423	59.2	510.0	70.7	439.3	61.5
C10	1½	N_2	83.4	3.23	309	1.576	634	325	51.2	342.8	29.0	313.8	49.4
C9	3	N_2	99.1	3.32	301	1.365	732	431	59.0	442.9	32.5	410.4	56.1
C7	16	N_2	99.6	3.40	294	1.376	727	433	59.6	471.5	47.0	424.5	58.4

* SA = stagnant

N_2 = nitrogen flushed

as percentage of 'superficial volume' of original stone*: treatment temperature 1470°F

Stone	t,** h	Calcined-only		Calcined-sulphated	
		Sample designation	Difference, %†	Sample designation	Difference, %†
Dolomite 1337	¼	J6	0.4	J9	-1.6
	1	J4	1.8	J8	-4.2
	4	J5	1.0	J10	-4.7
U.K. dolomite	¼	C28	-0.9	C32	0.9
	1	C29	-2.0	C31	-0.9
	4	C30	-3.4	C33	-2.6
U.K. dolomite (exploratory experiments)	1 x	C1	1.4		
	97 x	C5	1.0		
	1½ xx	C10	3.9		
	3 xx	C9	3.9		
	16 xx	C7	2.7		
Limestone 18	¼	N3	3.1	N6	-
	1	N2	0.5	N7	3.5
	4	N4	-0.9	N8	3.6
Limestone 1359	¼	G32	0.6	G36	1.7
	1	G33	1.6	G35	2.1
	4	G34	1.6	G37	2.0

* 'Superficial volumes' used in the calculation do not include the volume of any pores with entrances >14.5 μm diameter.

** Residence time in furnace.

† A negative sign corresponds to a decrease in 'superficial volume' on treatment.

x In stagnant atmosphere.

xx With nitrogen flush.

A8.87

Table A8.16. Difference in 'superficial volume' between treated and original stone, as percentage of 'superficial volume' of original stone*: treatment temperature 1650°F

Stone	t,** h	Calcined-only		Calcined-sulphated	
		Sample designation	Difference, %†	Sample designation	Difference, %†
Dolomite 1337	¼	J14	-3.9	J13	-3.7
	1	J15	-5.0	J12	-5.3
	4	J16	-3.3	J17	-8.1
U.K. dolomite	¼	C34	-6.1	C39	-2.8
	1	C36	-5.8	C38	-2.7
	4	C35	-8.3	C37	-3.0
Limestone 18	¼	N14	-2.0	N11	3.2
	1	N13	-2.7	N12	3.3
	4	N15	-4.3	N16	-2.0
Limestone 1359	¼	G39	-7.9	G43	-7.2
	1	G38	-8.0	G42	-9.5
	4	G40	-9.9	G41	-11.6

* 'Superficial volumes' used in the calculation do not include the volume of any pores with entrances >14.5 μm diameter.

** Residence time in furnace.

† A negative sign corresponds to a decrease in 'superficial volume' on treatment.

Table A8.17. Difference in pore volume between calcined-only and calcined-sulphated stones for the same residence time in the furnace at 1650°F

Stone	Sample designation		t,* h	Differences in volume in pores (percentage of particle volume $1/\rho_{Hg}$) **with entrances having diameters:											
				Between 14.5 µm and values shown†						Within ranges shown†					
	Calcined-only	Calcined-sulphated		3 µm	1 µm	0.3 µm	0.1 µm	0.03 µm	0.014 µm	14.5 to 3 µm	3 to 1 µm	1 to 0.3 µm	0.3 to 0.1 µm	0.1 to 0.03 µm	0.03 to 0.014 µm
Dolomite	J14	J13	¼	-0.2	-0.4	0	0.3	5.6	4.9	-0.2	-0.2	0.4	0.3	5.3	-0.7
	J15	J12	1	-0.9	-0.8	-0.1	0.4	12.5	13.1	-0.9	0.1	0.7	0.5	12.1	0.7
1337	J16	J17	4	0.5	3.0	5.4	6.1	26.8	27.0	0.5	2.5	2.4	0.7	20.7	0.2
U.K.	C34	C39	¼	0.2	0.3	0.7	-0.2	3.4	5.3	0.2	0.1	0.4	-0.9	3.6	1.9
dolomite	C36	C38	1	0.5	0.5	1.7	1.3	10.1	11.1	0.5	0	1.2	-0.4	8.7	0.9
	C35	C37	4	-0.4	0.5	2.0	3.4	17.7	17.5	-0.4	0.9	1.5	1.4	14.3	-0.2
Limestone 18	N14	N11	¼	0.6	2.4	3.1	4.1	4.6	4.8	0.6	1.8	0.7	1.1	0.5	0.2
	N13	N12	1	-2.1	0.7	3.4	9.0	10.2	10.3	-2.1	2.8	2.7	5.6	1.2	0.1
	N15	N16	4	0.7	6.1	16.8	27.1	25.9	25.3	0.7	5.4	10.7	10.3	-1.2	-0.6
Limestone 1359	G40	G41	4	-0.2	-2.0	-1.9	7.5	8.1	8.4	-0.2	-1.8	0.1	9.4	0.6	0.3

* Residence time in furnace.

** A negative value corresponds to the pore volume in the calcined-sulphated stone being greater than that in the calcined-only one.

† Most of these entrance diameter values are approximations, for simplicity; see Section 2.4.2.5.

Table A8.18. Results of preliminary pore-penetration and pore-closure experiments

Stone	Sample designation	Particle-size grade, BS mesh	Calcination time, h			Type of experiment*	Probe gas and result, mm^3/g**			
			to 1470°F	at 1470°F	at 1650°F		Helium	Neon	Krypton	Xenon
Lotherdale Quarry limestone	a	-16 + 25	23	2	-	p.pen.	<0.1	34.0 (9.4)	<0.1	<0.1
						p.closure	<0.1	<0.1	<0.1	<0.1
Sprotborough ¾ in clipping (dolomite)	b	-16 + 25	92	2	-	p.pen.	<0.1	-	<0.1	-
						p.closure	<0.1	-	<0.1	-
U.K. dolomite	d	-16 + 52	1	16	-	p.pen.	<0.1	27.6 (7.7)	<0.1	<0.1
	c	-16 + 52	144	46	-	p.pen.	<0.1	<0.1	<0.1	<0.1
	e	-16 + 52	144	46	-	p.pen.	<0.1	1.7 (0.5)	3.2 (0.9)	8.7 (2.4)
	f	-6 + 8	1	3	19	p.pen.	<0.1	<0.1	0.4 (0.1)	2.1 (0.6)
						p.closure	<0.1	<0.1	<0.1	<0.1
	g		29	½	2	p.pen.	<0.1	<0.1	<0.1	5.2 (1.4)
						p.closure	<0.1	<0.1	<0.1	<0.1
	h		29	½	2	p.pen.	<0.1	<0.1	<0.1	3.2 (0.9)
						p.closure	<0.1	<0.1	<0.1	<0.1

* p.pen. = pore penetration

p.closure = pore closure

** mm^3 at admission pressure (~50 torr) and 1470°F (or 77°F, in parentheses) per g of calcined sample

Table A8.19. Results of pore penetration experiments: Un-pretreated stones

Stone	Sample designation	Particle-size grade, BS mesh	Probe gas and result, mm^3/g*			
			Helium	Neon	Krypton	Xenon
U.K. dolomite	C	-16 + 52	<0.1	<0.1	0.6 (0.2)	1.7 (0.5)
	C**	-16 + 52	<0.1	<0.1	<0.1	0.6 (0.2)
	E	-300	<0.1	<0.1	<0.1	22.0 (6.1)
Limestone 1359	G10	-16 + 52	<0.1	<0.1	2.2 (0.6)	24.9 (6.9)
	H6	-300	<0.1	<0.1	1.2 (0.3)	27.5 (7.6)
	Ungraded material	-10	<0.1	<0.1	1.9 (0.5)	13.3 (3.7)

* mm^3 at admission pressure (~50 torr) and 1470°F (or 77°F, in parentheses) per g of calcined sample

** Calcined in air at 1470°F before the experiments

Table A8.20. Results of pore penetration experiments on pretreated stones

Stone	Sample designation	Particle-size grade, BS mesh	Pretreatment		Probe gas and result, mm^3/g*				Evacuation time at 77^oF before final release stage, h
			Atmosphere	Time at 1470^oF, h	Helium	Neon	Krypton	Xenon	
U.K. dolomite	B2	-6 + 8	Stagnant	1	<0.1	<0.1	<0.1	26.5 (7.4)	Not recorded
	C3	-16 + 52	Stagnant	½	<0.1	<0.1	3.0 (0.8)	26.7 (7.5)	120
	C8	-16 + 52	Nitrogen flushed	½	<0.1	<0.1	6.6 (1.8)	28.0 (7.6)	100
	C11	-16 + 52	Stagnant	3½	<0.1	<0.1	10.8 (3.0)	43.5 (12.1)	70
	C11	-16 + 52	Stagnant	3½	Xe only, adsorbed at 77^oF			27.6 (7.6)	72
	C11	-16 + 52	Stagnant	3½	Equimolar mixture of Xe and SO_2, adsorbed at 77^oF			6.1 (1.7)	72
	E1	- 300	Stagnant	17	<0.1	<0.1	<0.1	59.3 (16.5)	Not recorded
Limestone 1359	G1	-16 + 52	Stagnant	2	<0.1	<0.1	<0.1	< 0.1	Not recorded
	G9	-16 + 52	Nitrogen flushed	1	<0.1	<0.1	2.5 (0.7)	5.1 (1.4)	120
	H3	- 300	Stagnant	18	<0.1	<0.1	3.8 (1.1)	31.5 (8.8)	120
	H1	- 300	Stagnant	1	<0.1	<0.1	31.5 (8.8)	220 (61)	20

* mm^3 at admission pressure (~50 torr) and 1470^oF (or 77^oF, in parentheses) per g of calcined sample

Table A8.21. Results of thermal cycling experiments: U.K. dolomite

Particle-size grade of sample BS mesh	Sulphur content				$\frac{b-a}{a}$ x 100 %	Quantity of SO_2 passed q, cm^3(stp)	Number of cycles	Times, min			Gas composition, v/v			
	Not cycled		Thermally cycled											
	a, w/w %	a/q x 100	b, w/w %	b/q x 100				t_1	t_2	t_3	SO_2 ppm	N_2 %	O_2 %	CO_2 %
-16 + 52	3.8	1.0	4.7	1.3	24	360	10	2½	4	½	1500	90	10	0
-300	7.4	2.1	8.5	2.4	15	360	10	2½	4	½	1500	90	10	0
-16 + 52	6.6	1.3	6.9	1.4	4	500	5	2½	5	1	4000	98	2	0
-300	11.0	2.2	12.2	2.5	11	500	5	2½	5	1	4000	98	2	0
-300	10.9	2.2	12.7	2.5	20	500	5	2½	5	1	4000	98	2	0
-16 + 52	5.2	1.7	4.2	1.4	-19	300	10	2½	2	½	2500	83	2	15
-300	5.9	2.0	6.9	2.3	17	300	10	2½	2	½	2500	83	2	15
-16 + 52	5.9	1.0	7.2	1.2	20	600	20	½	2	½	2500	83	2	15
-16 + 52	6.1	1.0	5.2	0.9	-15	600	20	½	2	½	2500	83	2	15
-300	7.9	2.4	9.4	2.5	19	375	5	2½	5	1	2500	83	2	15
-16 + 52	6.5	0.5	5.8	0.5	- 9	1200	10	2½	2	½	10000	17	7	75
-16 + 52	5.8	0.5	6.6	0.6	14	1200	10	2½	2	½	10000	14	10	75
-16 + 52	5.3	0.4	6.0	0.5	13	1200	20	½	0*	½	10000	14	10	75
-300	12.5	1.0	12.8	1.1	2	1200	10	2½	2	½	10000	14	10	75

* In this experiment the thermal cycling was completed in a non-SO_2 bearing atmosphere and then the SO_2 bearing stream was passed for 20 min

Table A8.22. Results of thermal cycling experiments: limestone 1359

Particle-size grade of sample BS mesh	Sulphur content				$\frac{b-a}{a} \times 100$ %	Quantity of SO_2 passed q, cm^3 (stp)	Number of cycles	Times, min			Gas composition, v/v			
	Not cycled		Thermally cycled					t_1	t_2	t_3	SO_2 ppm	N_2 %	O_2 %	CO_2 %
	a, w/w %	a/q x 100	b, w/w %	b/q x 100										
−16 + 52	2.8	0.8	3.1	0.9	10	360	10	2½	4	½	1500	90	10	0
−300	7.1	2.0	8.4	2.3	18	360	10	2½	4	½	1500	90	10	0
−16 + 52	2.0	1.1	2.1	1.2	5	180	6	½	2	½	2500	83	2	15
−16 + 52	1.9	1.1	0.7	0.4	−63	180	6	½	2	½	2500	83	2	15
−300	8.2	2.2	6.2	1.7	−25	375	5	2½	5	1	2500	83	2	15
−16 + 52	1.4	0.5	0.7	0.2	−50	300	10	2½	2	½	2500	83	2	15
−300	6.0	2.0	7.1	2.4	18	300	10	2½	2	½	2500	83	2	15
−16 + 52	1.0	0.1	1.0	0.1	0	960	8	2½	2	½	10000	14	10	75
−16 + 52	1.3	0.1	1.1	0.1	−15	1200	10	2½	2	½	10000	14	10	75
−16 + 52	1.2	0.1	1.5	0.1	25	1200	10	½	0*	½	10000	14	10	75
−300	10.0	0.8	9.1	0.8	−8	1200	10	2½	2	½	10000	17	7	75

* In this experiment the thermal cycling was completed in a non-SO_2 bearing atmosphere and then the SO_2 bearing stream was passed for 20 min

Table A8.23 Data record of reaction rate experiments

Series	Run	A ℓ/min	T_s °C	T_f °C	S_m μm	S_s μm	M_ℓ (g)	H (mm)	n	t_n (secs)	Vol_n (mℓ)	Vol_o (mℓ)	Stone	% CaO in stone	Ga Co
1	1	10	800	800	1000	300	8	6.35	1	270	9.2	28.65	U.K. Dolomite	30.7	A
									2	270	21.7				
									3	270	25.9				
	2	10	800	800	1000	300	8	6.35	1	270	6.2	28.65	U.K. Dolomite	30.7	A
									2	270	20.4				
									3	270	25.9				
	3	10	800	800	1000	300	15	12.70	1	270	4.8	28.65	U.K. Dolomite	30.7	A
									2	270	16.2				
									3	270	22.5				
									4	270	25.2				
									5	270	26.1				
	4	10	800	800	1000	300	30	25.40	1	270	0.2	28.65	U.K. Dolomite	30.7	A
									2	270	0.9				
									3	270	9.1				
									4	270	16.3				
									5	270	20.5				
									6	270	23.8				
									7	270	25.6				
	5	10	800	777	1000	300	23	19.05	1	270	0.6	28.65	U.K. Dolomite	30.7	A
									2	270	9.7				
									3	270	20.2				
									4	270	24.1				
									5	270	26.1				
	6	10	810	894	1000	300	23	19.05	1	299	1.9	28.65	U.K. Dolomite	30.7	A
									2	282	10.2				
									3	279	17.7				
									4	278	23.3				
									5	295	25.2				
									6	269	26.2				

Table A8.23 (cont'd) Data record of reaction rate experiments

Series	Run	A ℓ/min	T_s ^oC	T_f ^oC	S_m µm	S_s µm	M_ℓ (g)	H (mm)	n	t_n (secs)	Vol_n (mℓ)	Vol_o (mℓ)	Stone	% CaO in stone	Gas Comp.
1 (contd)	7	10	820	882	1000	300	30	25.40	1	272	0.3	28.65	U.K. Dolomite	30.7	Air
									2	549	5.8				
									3	275	14.4				
									4	275	19.0				
	8	10	812	870	1000	300	30	25.40	1	558	0.1	28.65	U.K. Dolomite	30.7	Air
									2	562	1.3				
									3	570	10.1				
									4	589	20.0				
									5	558	24.3				
									6	564	25.6				
	9	10	800	835	1000	300	15	12.70	1	566	5.4	28.65	U.K. Dolomite	30.7	Air
									2	558	15.9				
									3	553	21.7				
									4	546	24.4				
									5	560	25.5				
									6	544	26.2				
2	10	10	800	850	2800	2000	21	19.05	1	582	3.4	28.65	U.K. Dolomite	30.7	Air
									2	593	15.7				
									3	580	20.8				
									4	610	22.9				
									5	564	23.5				
									6	550	23.8				
	11	10	800	860	2800	2000	21	19.05	1	564	6.1	28.65	U.K. Dolomite	30.7	Air
									2	580	18.6				
									3	626	23.2				
									4	597	24.4				
									5	637	24.6				
									6	593	25.8				
									7	569	25.8				

Table A8.23 (cont'd) **Data record of reaction rate experiments**

Series	Run	A ℓ/min	T_s °C	T_f °C	S_m μm	S_s μm	M_ℓ (g)	H (mm)	n	t_n (secs)	Vol_n (mℓ)	Vol_o (mℓ)	Stone	% CaO in Stone	Gas Comp.
2 (contd)	12	10	790	830	2800	200	21	19.05	1	573	5.3	28.65	U.K. Dolomite	30.7	Air
									2	573	17.6				
									3	540	22.0				
									4	545	24.2				
									5	538	25.2				
									6	589	26.1				
	13	10	800	855	2000	1000	23	19.05	1	565	1.8	28.65	U.K. Dolomite	30.7	Air
									2	561	13.3				
									3	565	20.2				
									4	632	22.5				
									5	543	24.1				
									6	559	24.2				
	14	10	800	850	2000	1000	23	19.05	1	575	2.2	28.65	U.K. Dolomite	30.7	Air
									2	632	14.1				
									3	601	21.4				
									4	597	23.9				
									5	605	24.9				
									6	695	24.7				
	15	5	790	824	300	105	23	19.05	1	1310	0.4	28.65	U.K. Dolomite	30.7	Air
									2	1231	1.0				
									3	1230	6.9				
									4	1260	14.1				
									5	1290	17.1				
	16	5	800	850	300	105	18	12.70	1	1180	1.8	28.65	U.K. Dolomite	30.7	Air
									2	1200	10.2				
									3	1292	14.5				
									4	1298	14.4				

Table A8.23 (cont'd) Data record of reaction rate experiments

Series	Run	A ℓ/min	T_s °C	T_f °C	S_m μm	S_s μm	M_ℓ (g)	H (mm)	n	t_n (secs)	Vol_n (mℓ)	Vol_o (mℓ)	Stone	% CaO in stone	Gas Comp.
2 (contd)	17	5	790	865	300	105	17	12.70	1	1230	7.2	28.65	U.K. Dolomite	30.7	Air
									2	1255	14.9				
									3	1252	17.6				
									4	1241	19.7				
									5	1310	20.7				
									6	1293	21.2				
	18	5	770	810	300	105	17	12.70	1	1309	19.2	28.65	U.K Dolomite	30.7	Air
									2	1280	22.2				
									3	1317	23.0				
									4	1341	23.4				
	19	10	780	835	1000	300	19.5	12.70	1	554	4.6	28.65	1359.	55.7	Air
									2	578	21.0				
									3	595	23.5				
									4	623	26.0				
									5	578	27.1				
	20	10	825	840	1000	300	19.5	12.70	1	614	4.8	28.65	1359	55.7	Air
									2	525	20.3				
									3	556	25.9				
									4	520	26.0				
	21	10	800	830	1000	300	19.5	12.70	1	554	2.9	28.65	1359	55.7	Air
									2	607	17.3				
									3	600	24.8				
									4	535	25.7				
									5	615	26.4				
	22	10	790	810	1000	300	19.5	12.70	1	665	6.4	28.65	1359	55.7	Air
									2	620	18.4				
									3	675	25.2				
									4	547	26.7				
									5	602	27.4				

Table A8.23 (cont'd) Data record of reaction rate experiments

Series	Run	A ℓ/min	T_s °C	T_f °C	S_m μm	S_s μm	M_ℓ (g)	H (mm)	n	t_n (secs)	Vol_n (mℓ)	Vol_o (mℓ)	Stone	% CaO in stone	Gas Comp.	(100-L) %
2 (contd)	23	5	790	824	300	105	17	12.70	1	1260	5.4	28.65	U.K. Dolomite	30.7	Air	
									2	1400	19.0					
									3	1346	23.4					
									4	1338	24.0					
	24	4	824	850	300	105	8	3.56	1	1654	2.4	28.65	U.K. Dolomite	30.7	Air	
									2	1176	17.4					
									3	1145	18.2					
									4	1177	19.0					
									5	1330	21.2					
	25	4	810	340	300	105	8	3.56	1	1152	2.9	28.65	U.K. Dolomite	30.7	Air	
									2	1496	13.5					
									3	1066	16.4					
									4	1218	17.8					
									5	766	20.8					
	26	3.6	800	800	105	53	3	0.75	1	1351	3.7	28.65	U.K. Dolomite	30.7	Air	
									2	1191	16.8					
									3	1036	21.9					
3	27	2.5	790	800	2800	2000	5	0.20	1	286	2.6	10.70	U.K. Dolomite	53.0	Air	45.0
									2	450	5.2					
									3	431	7.0					
									4	431	8.6					
									5	366	9.2					
	28	2.5	810	820	2800	2000	5	0.20	1	465	1.4	10.70	U.K. Dolomite	53.0	Air	45.0
									2	498	4.6					
									3	560	7.0					
									4	524	7.4					
									5	339	9.4					

Table A8.23 (cont'd) Data record of reaction rate experiments

Series	Run	A ℓ/min	T_s ^oC	T_f ^oC	S_m µm	S_s µm	M_ℓ (g)	H (mm)	n	t_n (secs)	Vol_n (mℓ)	Vol_o (mℓ)	Stone	% CaO in stone	Gas Comp.	(100-L) %
3 (contd)	29	2.5	810	820	2000	1000	5	0.20	1	600	1.4	10.70	U.K. Dolomite	53.0	Air	45.0
									2	545	4.8					
									3	589	7.2					
									4	643	8.0					
									5	635	8.4					
									6	695	9.4					
	30	2.5	800	824	2000	1000	5	0.20	1	747	1.6	10.70	U.K. Dolomite	53.0	Air	45.0
									2	610	4.2					
									3	601	6.6					
									4	677	7.4					
									5	666	8.2					
									6	606	9.0					
	31	2.5	790	840	300	105	5	0.20	1	744	0.5	10.70	U.K. Dolomite	53.0	Air	45.0
									2	736	1.8					
									3	678	4.4					
									4	698	5.4					
									5	678	7.1					
									6	740	7.6					
									7	612	8.6					
	32	2.5	790	850	300	105	5	0.20	1	682	1.2	10.70	U.K. Dolomite	53.0	Air	45.0
									2	655	3.2					
									3	633	4.8					
									4	697	5.8					
									5	650	7.2					
									6	624	7.6					
4	49	2.5	810	820	2800	2000	5	0.20	1	692	0.2	9.40	1337	53.0	Air	47.4
									2	609	2.2					
									3	731	4.3					
									4	682	5.9					
									5	523	7.1					
									6	699	7.1					
									7	696	7.5					
									8	576	8.1					

Table A8.23 (cont'd) Data record of reaction rate experiments

Series	Run	A ℓ/min	T_s °C	T_f °C	S_m μm	S_s μm	M_ℓ (g)	H (mm)	n	t_n (secs)	Vol_n (ml)	Vol_∞ (ml)	Stone	% CaO in stone	Gas Comp	(100-I) %
4 (contd)	50	2.5	810	820	2800	2000	5	0.2	1	583	0.5	9.40	1337	53.0	Air	47.4
									2	633	2.8					
									3	607	4.7					
									4	646	5.7					
									5	617	6.6					
									6	614	7.2					
									7	616	7.7					
									8	614	8.0					
	51	2.5	800	825	2000	1000	5	0.2	1	630	0.25	9.35	1337	53.0	Air	47.4
									2	602	1.2					
									3	629	3.1					
									4	625	5.1					
									5	632	6.3					
									6	631	7.0					
									7	623	7.5					
									8	594	8.2					
	52	2.5	800	810	2000	1000	5	0.2	1	679	0.15	9.35	1337	53.0	Air	47.4
									2	657	0.8					
									3	654	2.6					
									4	625	4.8					
									5	620	6.3					
									6	631	7.1					
									7	647	7.7					
									8	642	8.2					
	53	2.5	800	840	1000	300	5	0.2	1	643	0.05	9.30	1337	53.0	Air	47.4
									2	614	0.35					
									3	663	1.3					
									4	633	3.3					
									5	620	5.7					
									6	622	6.5					
									7	618	6.8					
									8	605	7.0					

Table A8.23 (cont'd) Data record of reaction rate experiments

Series	Run	A ℓ/min	T_s °C	T_f °C	S_m µm	S_s µm	M_ℓ (g)	H (mm)	n	t_n (secs)	Vol_n (mℓ)	Vol_0 (mℓ)	Stone	% CaO in stone	Gas Comp	(100-L) %
4 (contd)	56	2.5	820	820	1000	300	5	0.2	1	599	0.1	9.30	1337	53.0	Air	47.4
									2	584	0.1					
									3	615	0.5					
									4	590	1.8					
									5	583	4.0					
									6	604	5.4					
									7	602	6.8					
									8	647	7.3					
	57	2.5	810	810	300	105	5	0.2	1	589	0.2	9.15	1337	53.0	Air	47.4
									2	623	0.8					
									3	614	2.5					
									4	628	3.7					
									5	650	3.9					
									6	632	4.5					
									7	625	5.0					
									8	643	5.4					
	59	2.5	820	830	300	105	5	0.2	1	527	0.1	9.15	1337	53.0	Air	47.4
									2	537	1.6					
									3	612	2.8					
									4	520	3.7					
									5	573	5.8					
									6	545	6.8					
									7	579	5.7					
									8	553	5.9					
5	61	2.5	800	820	1000	300	5	0.2	1	572	0.1	9.40	1359	93.0	Air	43.6
									2	558	2.9					
									3	524	6.8					
									4	540	7.9					
									5	570	8.5					

Table A8.23 (cont'd) Data record of reaction rate experiments

Series	Run	A (l/min)	T [illegible]	T [illegible]	S [illegible]	S [illegible]	M_x (g)	H (mm)	n	t (sec)	[illegible]	V [illegible]	[illegible]	[illegible]	[illegible]	(100-L) %
5 (cont'd)	62	2.5	820	[illegible]	1000	300	5	0.2	1	643	0.2	9.40	1359	93.0	Air	[illegible]
									2	600	2.6					
									3	606	6.6					
									4	586	7.6					
									5	598	8.1					
	64	2.5	[illegible]	81[illegible]	300	105	5	0.2	1	633	0.1	9.55	1359	93.0	Air	[illegible]
									2	617	1.0					
									3	621	2.2					
									4	645	3.7					
									5	622	5.4					
									6	658	7.0					
									7	656	7.8					
	65	2.5	830	840	300	105	5	0.2	1	640	0.05	9.55	1359	93.0	Air	43.6
									2	640	0.6					
									3	670	2.2					
									4	649	3.8					
									5	690	5.1					
									6	665	6.[illegible]					
									7	678	6.7					
									8	661	7.4					
6	67	2.5	82[illegible]	930	2000	1000	5	0.2	1	552	0.02	9.30	18	77.9	Air	36.6
									2	595	0.05					
									3	634	0.1					
									4	623	0.3					
									5	660	1.2					
									6	615	2.6					
									7	619	5.4					
									8	580	6.0					

Table A8.23 (cont'd) **Data record of reaction rate experiments**

Series	Run	A ℓ/min	T_s °C	T_f °C	S_m μm	S_s μm	M_g (g)	H (mm)	n	t_n (secs)	Vol_n (mℓ)	Vol_o (mℓ)	Stone	% CaO in stone	Gas Comp	(100-L) %
6 (contd)	68	2.5	840	840	2000	1000	5	0.2	1	597	0.05	9.30	18	73.9	Air	36.6
									2	540	0.1					
									3	610	0.2					
									4	617	0.4					
									5	597	1.5					
									6	577	3.2					
									7	580	4.9					
	70	2.5	820	880	1000	300	5	0.2	1	673	0.05	9.60	18	73.9	Air	36.6
									2	661	0.05					
									3	697	0.1					
									4	731	0.4					
									5	720	1.1					
									6	790	2.4					
	71	2.5	820	820	1000	300	5	0.2	1	750	0.05	9.40	18	73.9	Air	36.6
									2	715	0.05					
									3	739	0.1					
									4	762	0.4					
									5	730	1.1					
									6	680	2.0					
									7	606	3.0					
									8	802	4.1					
	74	2.5	810	820	300	105	5	0.2	1	608	0.02	9.40	18	73.9	Air	36.6
									2	624	0.05					
									3	640	0.3					
									4	611	1.4					
									5	610	2.5					
									6	700	2.7					
									7	629	3.9					
									8	610	5.0					

Table A8.23 (cont'd) Data record of reaction rate experiments

Series	Run	$\dot{A}$ ℓ/min	T_s ^oC	T_f ^oC	S_m µm	S_s µm	M_ℓ (g)	H (mm)	n	t_n (secs)	Vol_n (mℓ)	Vol_o (mℓ)	Stone	% Cao in stone	Gas Comp.	(100-L) %
6 (contd)	75	2.5	810	820	300	105	5	0.2	1	608	0.05	9.50	18	73.9	Air	36.6
									2	602	0.1					
									3	615	0.5					
									4	645	1.0					
									5	613	2.1					
									6	596	3.0					
									7	654	4.1					
									8	689	4.8					
7	79	2.5	710	710	2000	1000	5	0.2	1	609	0.1	9.80	18	73.9	Air	36.6
									2	629	0.3					
									3	697	1.0					
									4	663	2.8					
									5	695	4.2					
									6	685	6.0					
	80	2.5	700	740	2000	1000	5	0.2	1	567	0.1	9.20	18	73.9	Air	36.6
									2	598	0.2					
									3	592	0.7					
									4	611	2.0					
									5	613	3.2					
									6	563	4.2					
									7	547	5.8					
	82	2.5	690	710	2000	1000	5	0.2	1	600	0.07	9.20	18	73.9	Air	36.6
									2	560	0.4					
									3	565	1.9					
									4	558	3.4					
									5	570	4.7					
									6	626	5.9					
									7	560	6.7					
									8	580	7.0					

Table A8.23 (cont'd) Data record of reaction rate experiments

Series	Run	A ℓ/min	T_s °C	T_f °C	S_m µm	S_s µm	M_ℓ (g)	H (mm)	n	t_n (secs)	Vol_n (mℓ)	Vol_o (mℓ)	Stone	% CaO in stone	Gas Comp.	(100-L) %
7 (contd)	83	2.5	690	695	2000	1000	5	0.2	1	585	0.1	9.45	18	73.9	Air	36.6
									2	615	0.3					
									3	582	0.9					
									4	631	2.1					
									5	599	3.4					
									6	578	4.9					
									7	607	5.9					
									8	616	6.4					
	84	2.5	680	690	2000	1000	5	0.2	1	560	2.7	9.40	18	73.9	CO_2-75% O_2-10% N_2-15%	36.6
									2	607	5.7					
									3	562	7.1					
									4	547	8.0					
	85	2.5	800	820	2000	1000	5	0.2	1	585	0.5	9.50	18	73.9	CO_2-75% O_2-10% N_2-15%	36.6
									2	630	1.8					
									3	570	2.7					
									4	569	5.5					
									5	593	7.2					
									6	579	8.2					
	86	2.5	800	810	2000	1000	5	0.2	1	578	0.6	9.40	18	73.9	CO_2-75% O_2-10% N_2-15%	36.6
									2	565	2.0					
									3	546	2.6					
									4	512	4.8					
									5	540	6.5					
									6	585	8.0					
	87	2.5	940	940	2000	1000	5	0.2	1	594	0.05	9.25	18	73.9	Air	
									2	624	0.2					
									3	658	1.0					
									4	561	2.0					
									5	575	3.3					
									6	608	4.5					

Table A8.23 (cont'd) Data record of reaction rate experiments

Series	Run	A ℓ/min	T_s °C	T_f °C	S_m µm	S_s µm	M_ℓ (g)	H (mm)	n	t_n (secs)	Vol_n (mℓ)	Vol_o (mℓ)	Stone	% CaO in stone	Gas Comp.	(100-L) %
7 (contd)	88	2.5	890	910	2000	1000	5	0.2	1	627	0.02	9.25	18	73.9	Air	36.6
									2	608	0.1					
									3	632	0.7					
									4	640	2.4					
									5	623	4.5					
									6	595	6.3					
									7	607	6.8					
									8	613	7.5					
	89	2.5	900	905	2000	1000	5	0.2	1	527	0.8	9.90	18	73.9	CO_2-75%	
									2	548	1.4				O_2-10%	
									3	558	1.8				N_2 -15%	
									4	510	2.8					
									5	545	5.0					
									6	547	6.8					
									7	555	7.4					

Table A8.24 Reduced experimental results

Test Series	Run	A ℓ/min	T deg. K	S μm	n	M_n (g)	C_w (mg/m^3)	$R_n.10^5$	$K_w.10^2$	U_n	$\overline{U}_n$	Stone	Gas Comp.
3	27	2.5	1068	2366	1	0.13	3870	31.10	8.04	7.8	3.9	U.K. Dolomite	Air
					2	0.22	2460	13.40	5.46	13.1	10.4		
					3	0.28	2570	9.42	3.67	16.6	14.8		
					4	0.31	2570	5.35	2.08	18.6	17.6		
					5	0.33	3020	4.50	1.49	20.1	19.4		
	28	2.5	1088	2366	1	0.15	2340	22.00	9.40	8.9	4.5	U.K Dolomite	Air
					2	0.25	2180	13.40	6.16	14.8	11.9		
					3	0.31	1940	7.25	3.74	18.3	16.6		
					4	0.36	2070	6.91	3.33	21.5	19.9		
					5	0.38	3210	4.21	1.31	22.8	22.1		
	29	2.5	1088	1414	1	0.15	1810	17.00	9.40	8.9	4.5	U.K. Dolomite	Air
					2	0.24	1990	11.90	5.96	14.6	11.8		
					3	0.30	1840	6.52	3.54	18.0	16.3		
					4	0.34	1690	4.61	2.73	20.6	19.3		
					5	0.38	1710	3.98	2.32	22.8	21.7		
					6	0.40	1560	2.05	1.31	24.0	23.4		
	30	2.5	1085	1414	1	0.15	1460	13.40	9.17	8.7	4.4	U.K. Dolomite	Air
					2	0.25	1790	11.70	6.55	15.0	11.9		
					3	0.32	1810	7.49	4.13	18.9	17.0		
					4	0.37	1610	5.35	3.33	22.1	20.5		
					5	0.41	1640	4.12	2.52	24.5	23.3		
					6	0.44	1800	3.08	1.71	26.1	25.3		
	31	2.5	1088	177	1	0.16	1460	15.10	10.30	9.8	4.9	U.K. Dolomite	Air
					2	0.31	1480	13.30	9.00	18.3	14.1		
					3	0.41	1600	10.20	6.37	24.4	21.4		
					4	0.49	1560	8.34	5.35	29.5	26.9		
					5	0.55	1600	5.83	3.64	32.9	31.2		
					6	0.60	1470	4.60	3.13	35.9	34.4		
					7	0.63	1780	3.77	2.12	37.9	36.9		

Table A8.24 (cont'd) Reduced experimental results

Test Series	Run	A ℓ/min	T deg. K	S μm	n	M_n (g)	C_w (mg/m^3)	$R_n.10^5$	$K_w.10^2$	U_n	$\overline{U}_n$	Stone	Gas Comp.
3	32	2.5	1093	177	1	0.15	1590	15.30	9.64	9.1	4.6	U.K. Dolomite	Air
					2	0.27	1650	12.60	7.61	16.3	12.7		
					3	0.37	1710	10.20	5.99	22.0	19.2		
					4	0.45	1550	7.72	4.97	26.7	24.3		
					5	0.50	1660	5.91	3.55	30.1	28.4		
					6	0.55	1730	5.45	3.15	33.0	31.6		
4	49	2.5	1088	2366	1	0.15	1380	15.30	11.10	9.2	4.6	1337	Air
					2	0.26	1570	13.60	8.66	16.5	12.9		
					3	0.34	1310	8.01	6.13	21.6	19.0		
					4	0.40	1400	5.89	4.21	25.1	23.4		
					5	0.44	1830	5.05	2.77	27.4	26.3		
					6	0.47	1370	3.78	2.77	29.7	28.6		
					7	0.50	1370	3.13	2.28	31.6	30.7		
					8	0.52	1660	2.59	1.56	32.9	32.3		
	50	2.5	1088	2366	1	0.14	1640	17.50	10.70	8.9	4.5	1337	Air
					2	0.25	1510	12.00	7.94	15.6	12.3		
					3	0.32	1570	8.89	5.65	20.3	17.9		
					4	0.38	1480	6.57	4.45	24.0	22.1		
					5	0.43	1550	5.21	3.37	26.8	25.4		
					6	0.46	1550	4.11	2.65	29.0	27.9		
					7	0.49	1550	3.17	2.04	30.7	29.9		
					8	0.51	1550	2.62	1.68	32.1	31.4		
	51	2.5	1085	1414	1	0.15	1510	16.60	11.00	9.1	4.6	1337	Air
					2	0.28	1580	15.50	9.83	17.3	13.2		
					3	0.38	1510	11.40	7.54	23.6	20.5		
					4	0.44	1520	7.81	5.13	27.9	25.7		
					5	0.49	1510	5.54	3.68	30.9	29.4		
					6	0.53	1510	4.27	2.83	33.3	32.1		
					7	0.56	1530	3.41	2.23	35.2	34.2		
					8	0.58	1600	2.22	1.39	36.3	35.7		

Table A8.24 (cont'd) Reduced experimental results

Test Series	Run	A ℓ/min	T deg. K	S μm	n	M_n (g)	C_w (mg/m^3)	$R_n.10^5$	$K_w.10^2$	U_n	$\overline{U}_n$	Stone	Gas Comp.
4	52	2.5	1078	1414	1	0.15	1410	15.60	11.00	9.2	4.6	1337	Air
					2	0.28	1460	14.90	10.20	17.8	13.5		
					3	0.39	1460	11.80	8.09	24.6	21.2		
					4	0.46	1530	8.36	5.45	29.2	26.9		
					5	0.51	1550	5.65	3.65	32.2	30.7		
					6	0.55	1520	4.09	2.70	34.5	33.4		
					7	0.58	1480	2.93	1.98	36.2	35.3		
					8	0.59	1490	2.06	1.38	37.3	36.7		
	53	2.5	1093	548	1	0.15	1480	16.70	11.30	9.3	4.6	1337	Air
					2	0.29	1530	16.70	10.90	18.3	13.8		
					3	0.42	1420	13.90	9.77	26.3	22.3		
					4	0.52	1490	10.90	7.33	32.3	29.3		
					5	0.57	1520	6.66	4.40	36.0	34.1		
					6	0.62	1510	5.17	3.42	38.8	37.4		
					7	0.66	1520	4.64	3.05	41.3	40.0		
					8	0.69	1550	4.36	2.81	43.6	42.4		
	56	2.5	1093	548	1	0.15	1570	17.60	11.20	9.2	4.6	1337	Air
					2	0.29	1610	18.10	11.20	18.5	13.9		
					3	0.44	1530	16.40	10.70	27.3	22.9		
					4	0.56	1590	14.60	9.16	34.9	31.1		
					5	0.64	1610	10.40	6.47	40.2	37.5		
					6	0.70	1560	7.41	4.76	44.1	42.1		
					7	0.74	1560	4.77	3.05	46.6	45.3		
					8	0.77	1450	3.55	2.44	48.6	47.6		
	57	2.5	1083	177	1	0.14	1580	17.40	11.00	9.0	4.5	1337	Air
					2	0.28	1500	15.40	10.30	17.4	13.2		
					3	0.38	1520	12.40	8.18	24.1	20.7		
					4	0.47	1490	9.96	6.70	29.5	26.8		
					5	0.55	1440	9.27	6.46	34.8	32.2		
					6	0.63	1480	8.45	5.72	39.5	37.1		
					7	0.70	1490	7.62	5.10	43.6	41.6		
					8	0.76	1450	6.69	4.61	47.4	45.5		

Table A8.24 (cont'd)   Reduced experimental results

Test Series	Run	A ℓ/min	T deg. K	S μm	n	M_n (g)	C_w (mg/m^3)	$R_n.10^5$	$K_w.10^2$	U_n	$\overline{U}_n$	Stone	Gas Comp.
4	59	2.5	1098	177	1	0.14	1750	19.70	11.30	9.1	4.5	1337	Air
					2	0.27	1710	16.10	9.41	16.7	12.9		
					3	0.37	1500	11.90	7.92	23.1	19.9		
					4	0.45	1770	12.00	6.79	28.5	25.8		
					5	0.51	1610	6.71	4.18	31.9	30.2		
					6	0.55	1690	4.95	2.93	34.2	33.1		
					7	0.60	1590	6.84	4.30	37.7	36.0		
					8	0.65	1670	6.75	4.05	41.0	39.3		
5	61	2.5	1083	548	1	0.15	1680	9.92	5.92	5.0	2.5	1359	Air
					2	0.25	1720	7.11	4.14	8.4	6.7		
					3	0.29	1830	3.03	1.65	9.8	9.1		
					4	0.32	1780	1.69	0.95	10.6	10.2		
					5	0.33	1680	0.96	0.57	11.1	10.9		
	62	2.5	1093	548	1	0.15	1480	8.73	5.91	4.9	2.5	1359	Air
					2	0.26	1580	6.91	4.37	8.5	6.7		
					3	0.30	1570	2.82	1.80	10.0	9.3		
					4	0.33	1620	1.87	1.16	11.0	10.5		
					5	0.35	1590	1.33	0.84	11.7	11.3		
	64	2.5	1075	177	1	0.15	1550	9.11	5.88	5.0	2.5	1359	Air
					2	0.29	1590	8.45	5.32	9.6	7.3		
					3	0.41	1580	7.22	4.57	13.5	11.6		
					4	0.50	1520	5.53	3.64	16.7	15.1		
					5	0.57	1580	4.07	2.58	18.9	17.8		
					6	0.61	1490	2.36	1.59	20.2	19.6		
					7	0.63	1500	1.63	1.09	21.2	20.7		
	65	2.5	1108	177	1	0.15	1490	9.06	6.08	5.1	2.5	1359	Air
					2	0.29	1490	8.53	5.73	9.8	7.5		
					3	0.41	1420	6.69	4.71	13.8	11.8		
					4	0.50	1470	5.41	3.68	16.8	15.3		
					5	0.58	1380	3.93	2.85	19.2	18.0		
					6	0.63	1430	3.17	2.21	21.1	20.1		
					7	0.68	1400	2.56	1.83	22.6	21.8		
					8	0.71	1440	1.98	1.38	23.7	23.2		

Table A8.24 (cont'd) Reduced experimental results

Test Series	Run	A ℓ/min	T deg. K	S um	n	M_n (g)	C_w (mg/m^3)	$R_n.10^5$	$K_w.10^2$	U_n	$\overline{U}_n$	Stone	Gas Comp.
6	67	2.5	1100	1414	1	0.15	1690	11.50	6.79	5.6	2.8	18	Air
					2	0.30	1570	10.60	6.77	11.[illegible]	8.3		
					3	0.44	1470	9.91	6.73	16.6	13.8		
					4	0.59	1500	9.87	6.58	22.0	19.3		
					5	0.72	1410	8.38	5.92	26.8	24.4		
					6	0.82	1520	7.44	4.90	30.8	28.8		
					7	0.89	1510	4.30	2.85	33.1	32.0		
					8	0.94	1610	3.89	2.41	35.1	34.1		
	68	2.5	1113	1414	1	0.15	1550	10.60	6.84	5.5	2.8	18	Air
					2	0.29	1710	11.60	6.80	11.0	8.3		
					3	0.44	1510	10.20	6.73	16.5	13.7		
					4	0.58	1500	9.85	6.58	21.8	19.1		
					5	0.71	1550	8.92	5.77	26.4	24.1		
					6	0.81	1600	7.22	4.51	30.1	28.3		
					7	0.88	1590	5.18	3.25	32.7	31.4		
	70	2.5	1123	548	1	0.15	1400	9.69	6.90	5.7	2.8	18	Air
					2	0.31	1430	9.87	6.90	11.4	8.6		
					3	0.46	1360	9.31	6.87	17.1	14.3		
					4	0.60	1290	8.60	6.65	22.6	19.8		
					5	0.74	1310	8.06	6.14	27.7	25.1		
					6	0.86	1200	6.22	5.20	32.0	29.8		
	71	2.5	1093	548	1	0.15	1270	8.51	6.72	5.6	2.8	18	Air
					2	0.30	1330	8.93	6.72	11.2	8.4		
					3	0.45	1290	8.60	6.68	16.7	14.0		
					4	0.59	1250	8.07	6.47	22.1	19.4		
					5	0.72	1300	7.77	5.97	27.1	24.6		
					6	0.84	1400	7.43	5.32	31.5	29.3		
					7	0.95	1570	7.21	4.60	35.3	33.4		
					8	1.03	1180	4.51	3.81	38.5	36.9		

Table A8.24 (cont'd) Reduced experimental results

Test Series	Run	A ℓ/min	T deg. K	S μm	n	M_n (g)	C_w (mg/m^3)	$R_n.10^5$	$K_w.10^2$	U_n	$\overline{U}_n$	Stone	Gas Comp.
6	74	2.5	1088	177	1	0.15	1570	10.50	6.71	5.6	2.8	18	Air
					2	0.30	1530	10.20	6.69	11.2	8.4		
					3	0.44	1490	9.71	6.51	16.6	13.9		
					4	0.57	1560	8.94	5.72	21.4	19.0		
					5	0.68	1560	7.73	4.94	25.5	23.5		
					6	0.79	1360	6.54	4.79	29.5	27.5		
					7	0.88	1520	5.97	3.94	32.8	31.2		
					8	0.95	1560	4.93	3.15	35.5	34.1		
	75	2.5	1088	177	1	0.15	1590	10.60	6.69	5.6	2.8	18	Air
					2	0.30	1600	10.70	6.66	11.3	8.5		
					3	0.45	1570	10.00	6.37	16.6	14.0		
					4	0.58	1500	9.00	6.02	21.7	19.2		
					5	0.70	1570	8.24	5.24	26.1	23.9		
					6	0.80	1620	7.45	4.60	30.0	28.1		
					7	0.89	1480	5.64	3.82	33.3	31.6		
					8	0.97	1400	4.66	3.33	36.1	34.7		
7	79	2.5	983	1414	1	0.16	1810	10.90	6.03	5.8	2.9	18	Air
					2	0.31	1750	10.30	5.90	11.5	8.6		
					3	0.45	1580	8.62	5.47	16.7	14.1		
					4	0.56	1660	7.21	4.35	20.9	18.8		
					5	0.65	1580	5.50	3.48	24.3	22.6		
					6	0.71	1600	3.79	2.36	26.5	25.4		
	80	2.5	993	1414	1	0.15	1800	11.00	6.08	5.4	2.7	18	Air
					2	0.29	1710	10.30	6.02	10.8	8.1		
					3	0.43	1730	9.81	5.68	15.9	13.4		
					4	0.54	1670	8.05	4.81	20.2	18.0		
					5	0.64	1670	6.69	4.01	23.8	22.0		
					6	0.72	1810	6.07	3.34	26.8	25.3		
					7	0.77	1870	4.25	2.27	28.8	27.8		

Table A8.24 (cont'd) Reduced experimental results

Test Series	Run	A ℓ/min	T deg. K	S μm	n	M_n (g)	C_w (mg/m^3)	R_n.10^5	K_w.10^2	U_n	$\overline{U}_n$	Stone	Gas Comp.
7	82	2.5	973	1414	1	0.15	1740	10.40	6.00	5.5	2.7	18	Air
					2	0.29	1860	10.70	5.77	10.7	8.1		
					3	0.40	1840	8.82	4.78	15.1	12.9		
					4	0.50	1870	7.10	3.80	18.6	16.8		
					5	0.57	1830	5.39	2.95	21.2	19.9		
					6	0.62	1670	3.60	2.16	23.2	22.2		
					7	0.66	1860	3.05	1.64	24.7	24.0		
					8	0.70	1800	2.59	1.44	26.0	25.4		
	83	2.5	965	1414	1	0.15	1840	10.90	5.92	5.6	2.8	18	Air
					2	0.30	1750	10.20	5.79	11.1	8.3		
					3	0.43	1850	10.00	5.41	16.2	13.6		
					4	0.55	1710	7.96	4.65	20.6	18.4		
					5	0.65	1800	6.90	3.83	24.2	22.4		
					6	0.72	1870	5.38	2.88	26.9	25.5		
					7	0.78	1780	3.99	2.25	29.0	28.0		
					8	0.83	1750	3.38	1.93	30.8	29.9		
	84	2.5	958	1414	1	0.11	1930	8.17	4.23	4.0	2.0	18	CO_2-75% O_2-10% N_2 -15%
					2	0.17	1280	4.16	2.34	6.2	5.1		
					3	0.20	1920	2.80	1.45	7.6	6.9		
					4	0.23	1980	1.75	0.88	8.4	8.0		
	85	2.5	1083	1414	1	0.14	1660	10.50	6.34	5.4	2.7	18	CO_2-75% O_2-10% N_2 -15%
					2	0.27	1540	8.35	5.43	10.0	7.7		
					3	0.38	1700	8.15	4.79	14.0	12.0		
					4	0.44	1700	4.80	2.82	16.4	15.2		
					5	0.48	1630	2.65	1.62	17.8	17.1		
					6	0.50	1670	1.53	0.92	18.6	18.2		
	86	2.5	1078	1414	1	0.14	1670	10.40	6.24	5.3	2.6	18	CO_2-75% O_2-10% N_2 -15%
					2	0.26	1700	8.95	5.25	9.7	7.5		
					3	0.37	1760	8.51	4.82	13.7	11.7		
					4	0.44	1880	6.14	3.26	16.5	15.1		
					5	0.49	1780	3.67	2.06	18.2	17.4		
					6	0.51	1650	1.63	0.99	19.1	18.6		

Table A8.24 (cont'd) Reduced experimental results

Test Series	Run	A ℓ/min	T deg. K	S μm	n	M_n (g)	C_w (mg/m^3)	$R_n.10^5$	$K_w.10^2$	U_n	$\overline{U}_n$	Stone	Gas Comp.
7	87	2.5	1213	1414	1	0.15	1420	10.60	7.44	5.5	2.8	18	Air
					2	0.29	1350	9.91	7.32	10.9	8.2		
					3	0.42	1280	8.56	6.68	15.8	13.4		
					4	0.54	1500	8.83	5.87	20.2	18.0		
					5	0.64	1470	7.07	4.81	23.7	21.9		
					6	0.71	1390	5.34	3.84	26.6	25.1		
	88	2.5	1173	1414	1	0.15	1390	10.10	7.23	5.5	2.8	18	Air
					2	0.29	1430	10.30	7.16	11.0	8.2		
					3	0.43	1380	9.24	6.69	16.1	13.5		
					4	0.54	1360	7.31	5.36	20.2	18.1		
					5	0.62	1400	5.21	3.72	23.0	21.6		
					6	0.66	1470	3.39	2.31	24.8	23.9		
					7	0.70	1440	2.76	1.92	26.3	25.5		
					8	0.73	1420	1.95	1.37	27.3	26.8		
	89	2.5	1175	1414	1	0.15	1770	11.80	6.67	5.4	2.7	18	CO_2-75% O_2-10% N_2 -15%
					2	0.28	1700	10.60	6.23	10.5	8.0		
					3	0.41	1670	9.91	5.94	15.4	12.9		
					4	0.52	1830	9.51	5.20	19.6	17.5		
					5	0.60	1710	6.14	3.59	22.5	21.1		
					6	0.65	1700	3.87	2.27	24.4	23.5		
					7	0.69	1680	3.08	1.83	25.9	25.1		

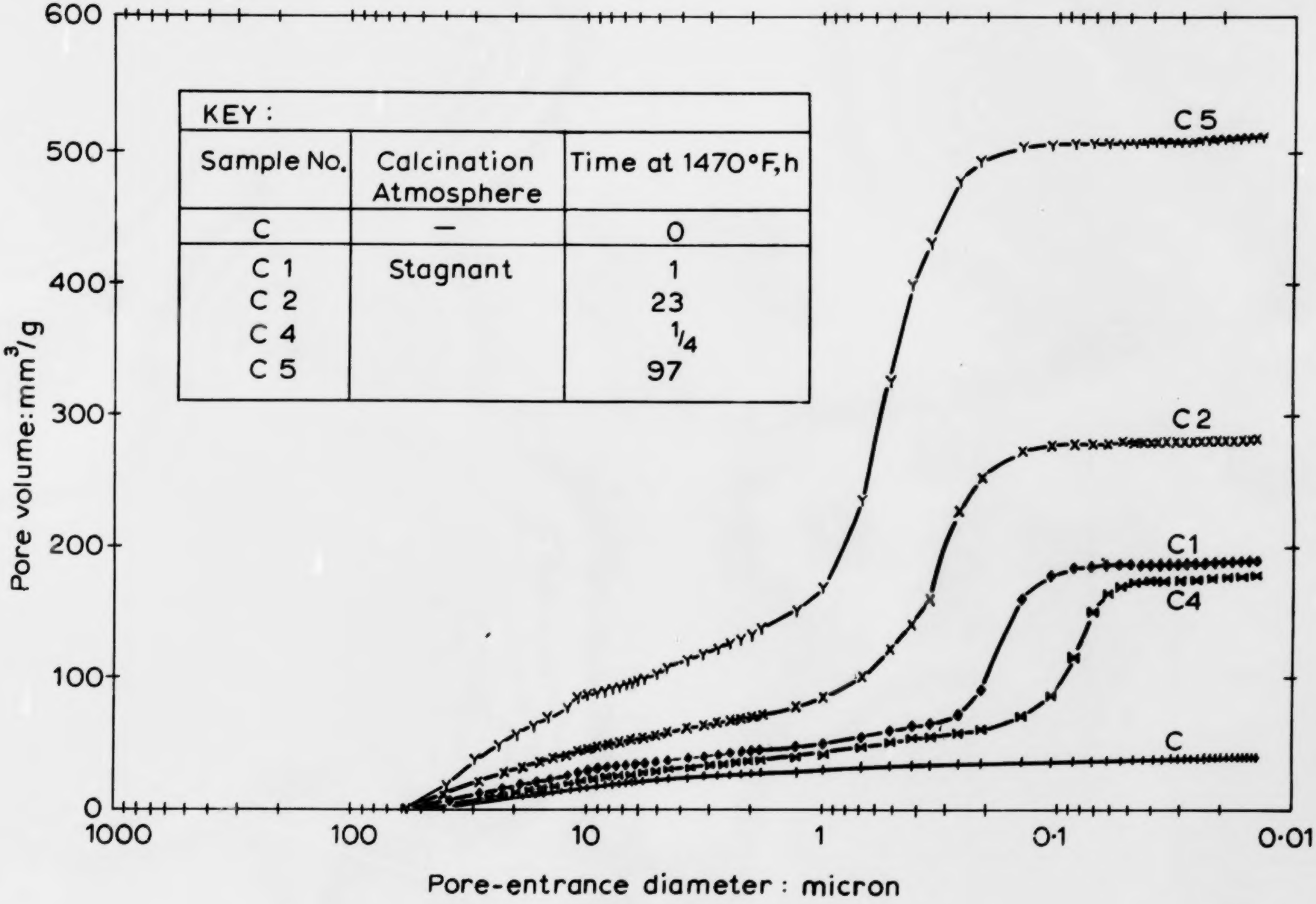

U.K. Dolomite Sample C (-16+52 B S)

Fig. A8. 1. Assessment of pore structure

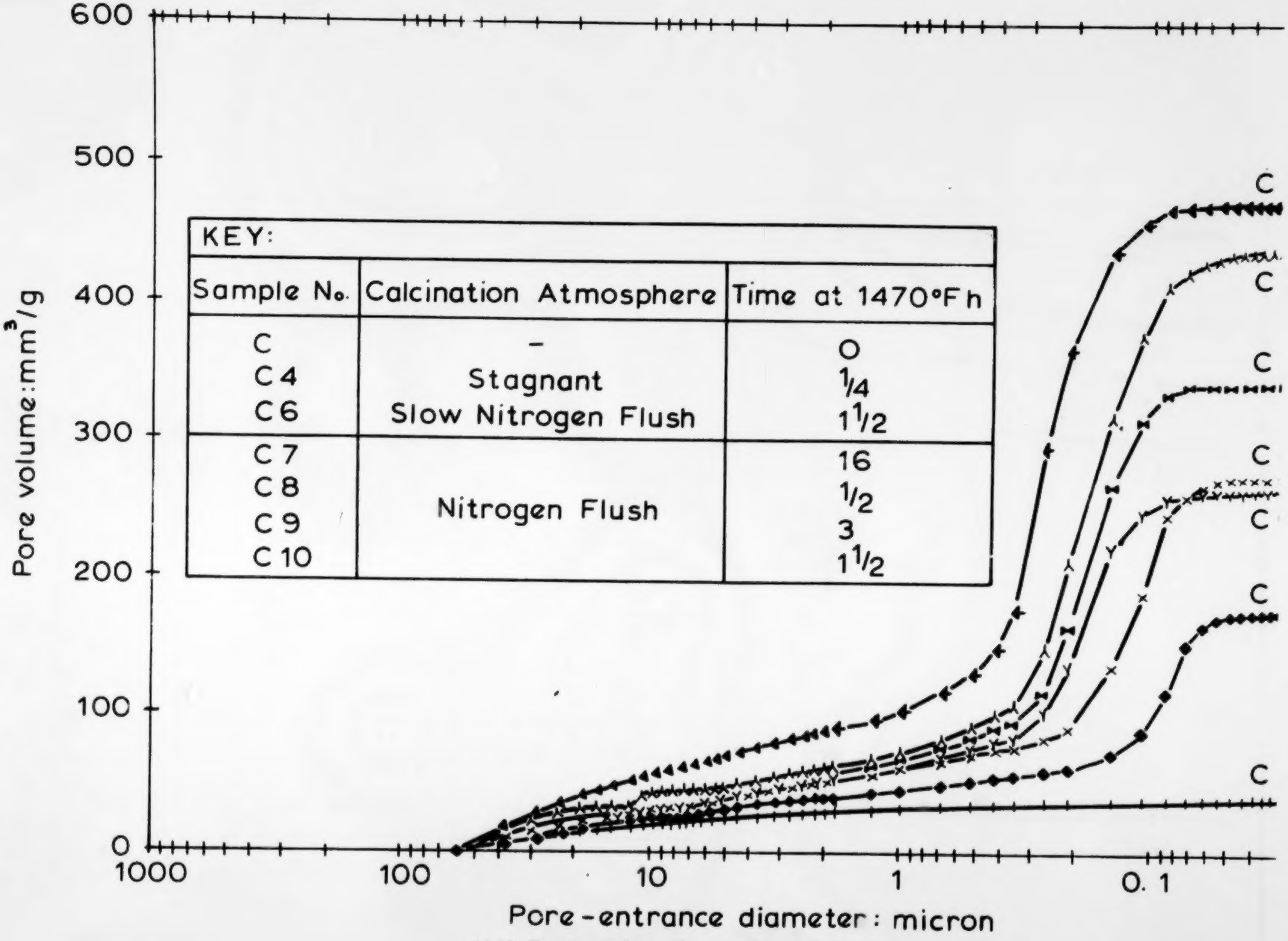

U.K. Dolomite Sample C (-16+52 BS)

Fig. A8.2. Assessment of pore structure

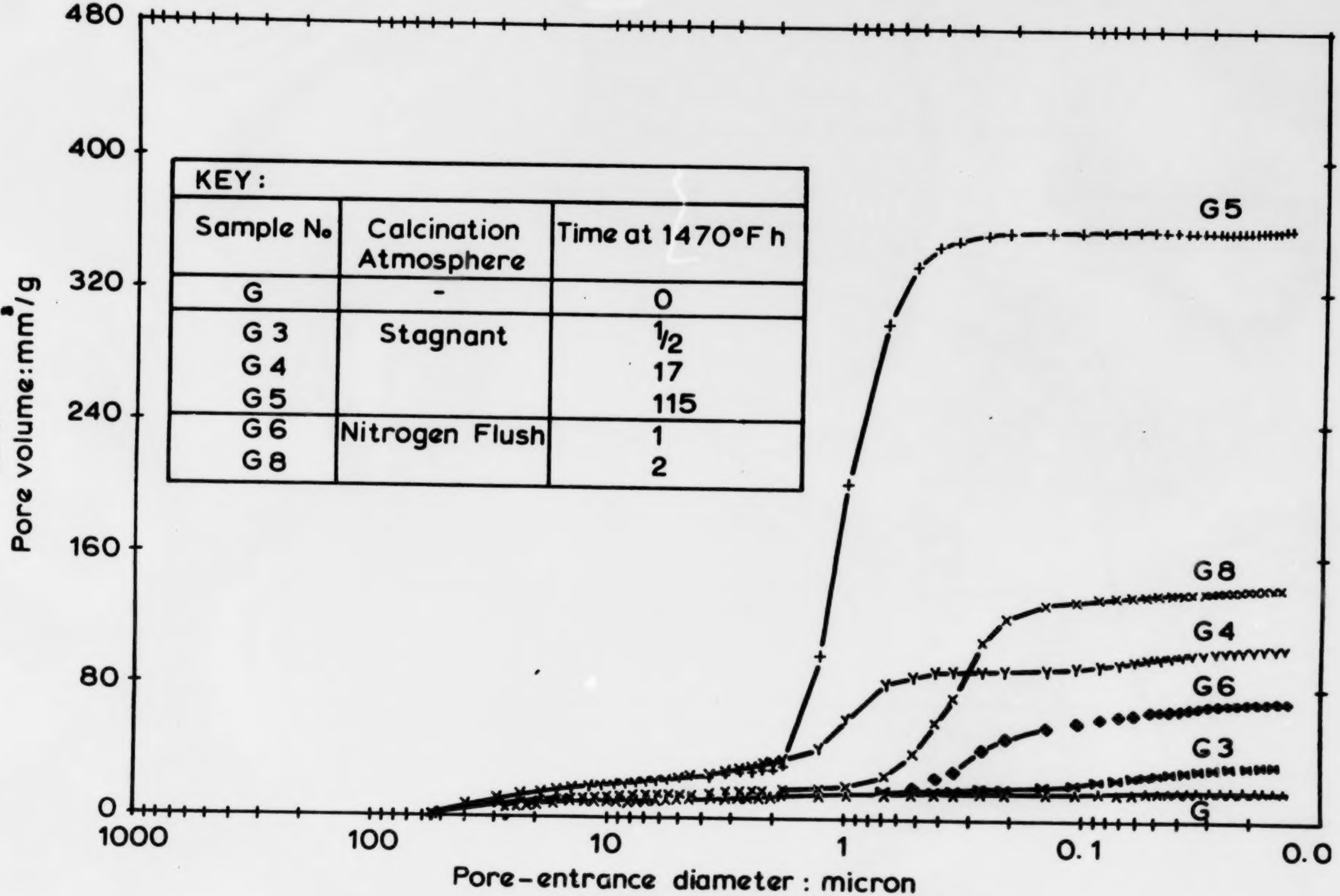

KEY:		
Sample No	Calcination Atmosphere	Time at 1470°F h
G	-	0
G 3	Stagnant	½
G 4		17
G 5		115
G 6	Nitrogen Flush	1
G 8		2

Limestone 1359 Sample G (-16+52 BS)

Fig. A8.3. Assessment of pore structure

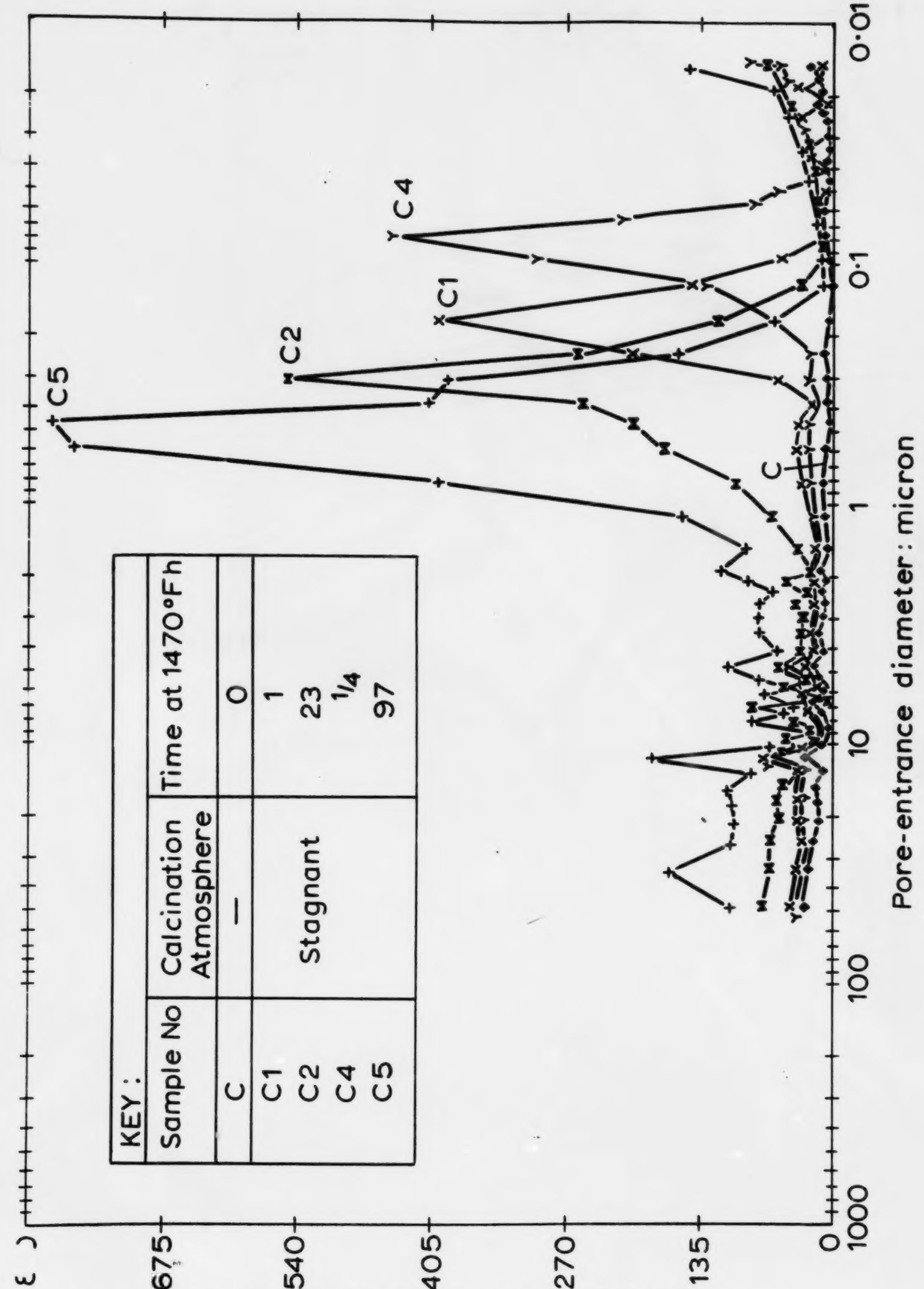

U.K.Dolomite Sample C (-16+52 BS)

Fig. A8.4. Assessment of pore structure

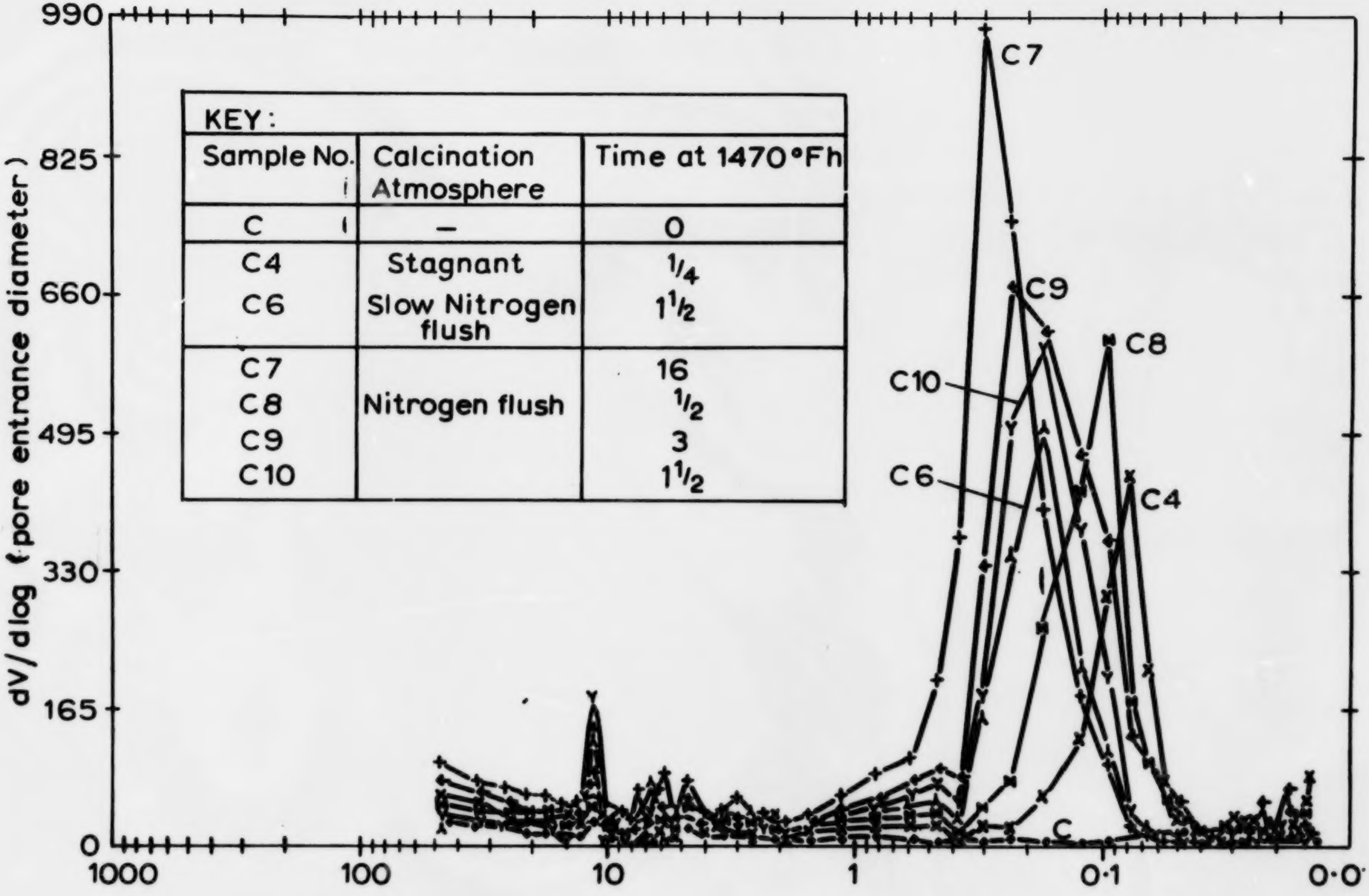

KEY:

Sample No.	Calcination Atmosphere	Time at 1470°Fh
C	–	0
C4	Stagnant	1/4
C6	Slow Nitrogen flush	1 1/2
C7	Nitrogen flush	16
C8		1/2
C9		3
C10		1 1/2

U.K.Dolomite sample C (-16 + 52 BS)

Fig. A8.5. Assessment of pore structure

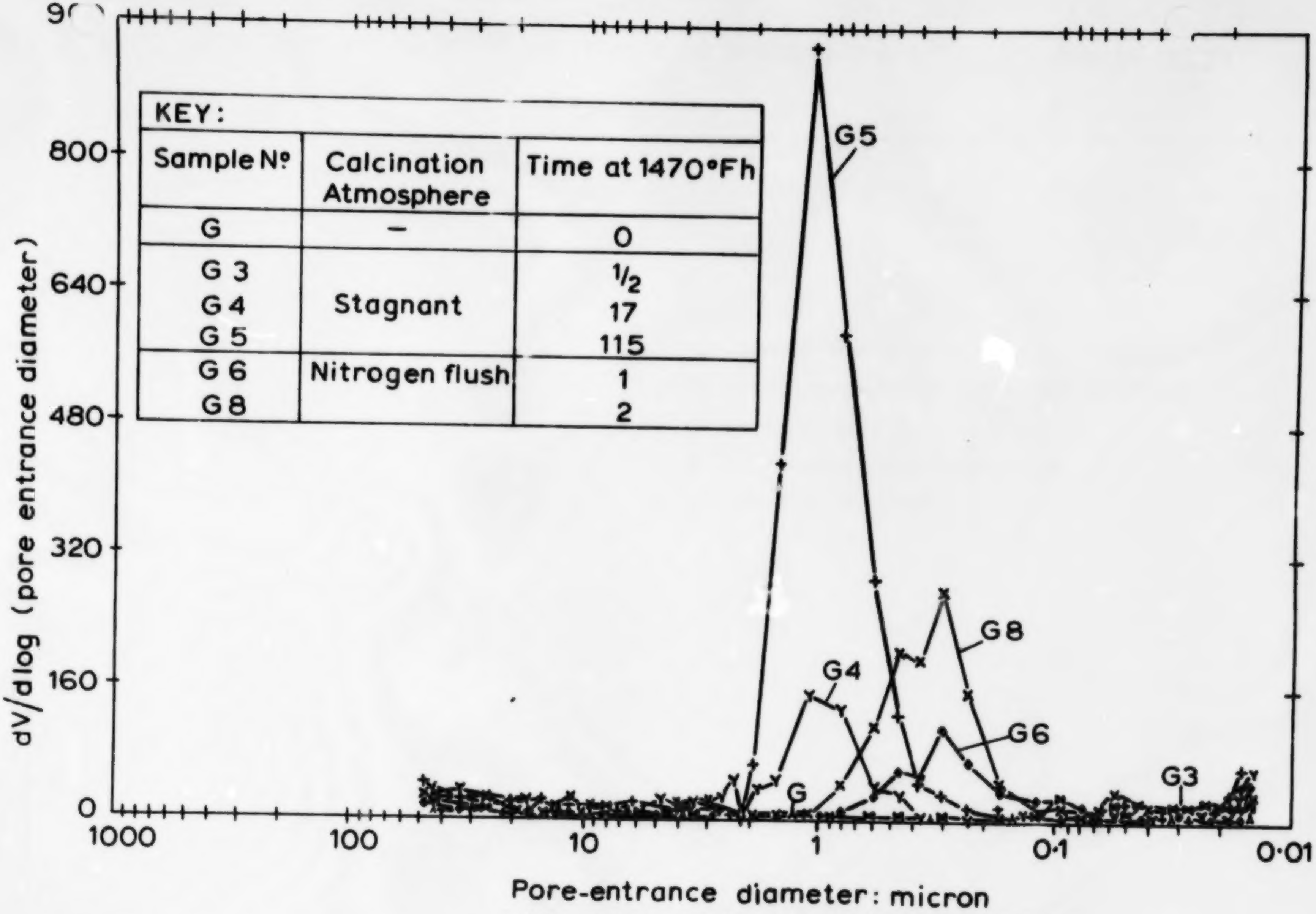

Limestone 1359 Sample G (-16+52 BS)

Fig. A8.6. Assessment of pore structure

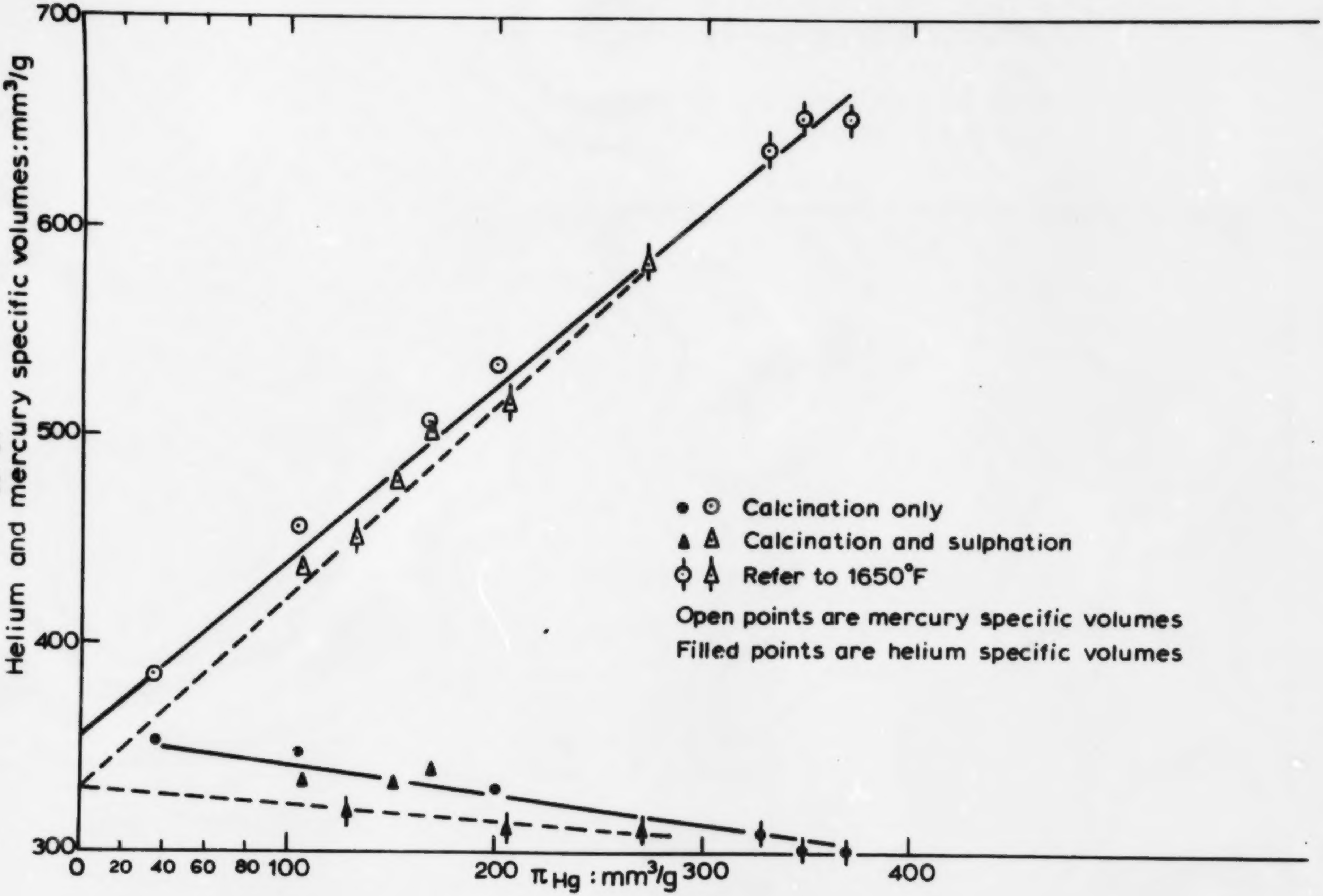

Fig. A8.7. Specific volumes in helium and mercury *vs* π_{Hg} · Dolomite 1337

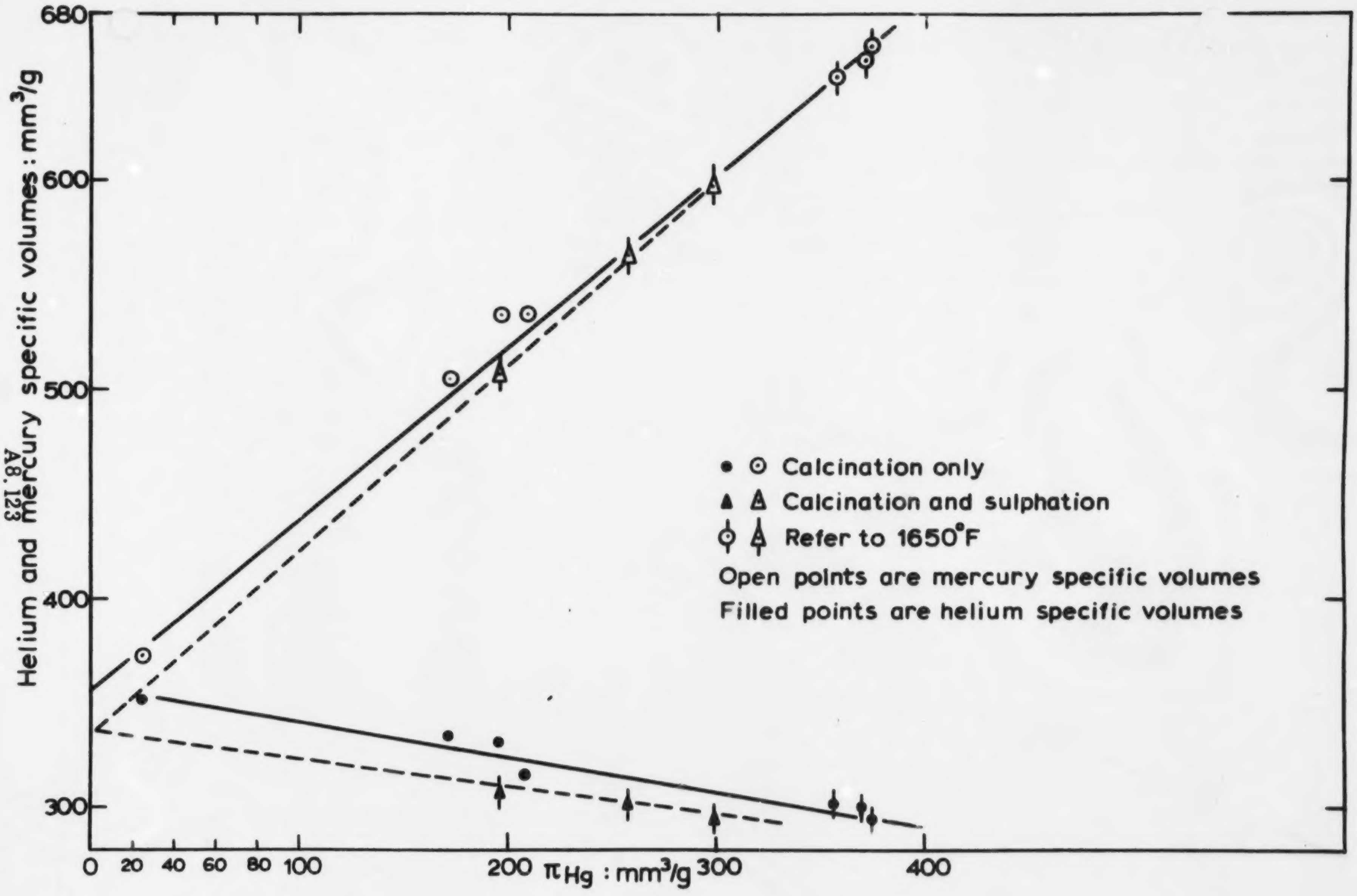

Fig. A8.8. Specific volumes in helium and mercury *vs* π_{Hg}. U.K. Dolomite

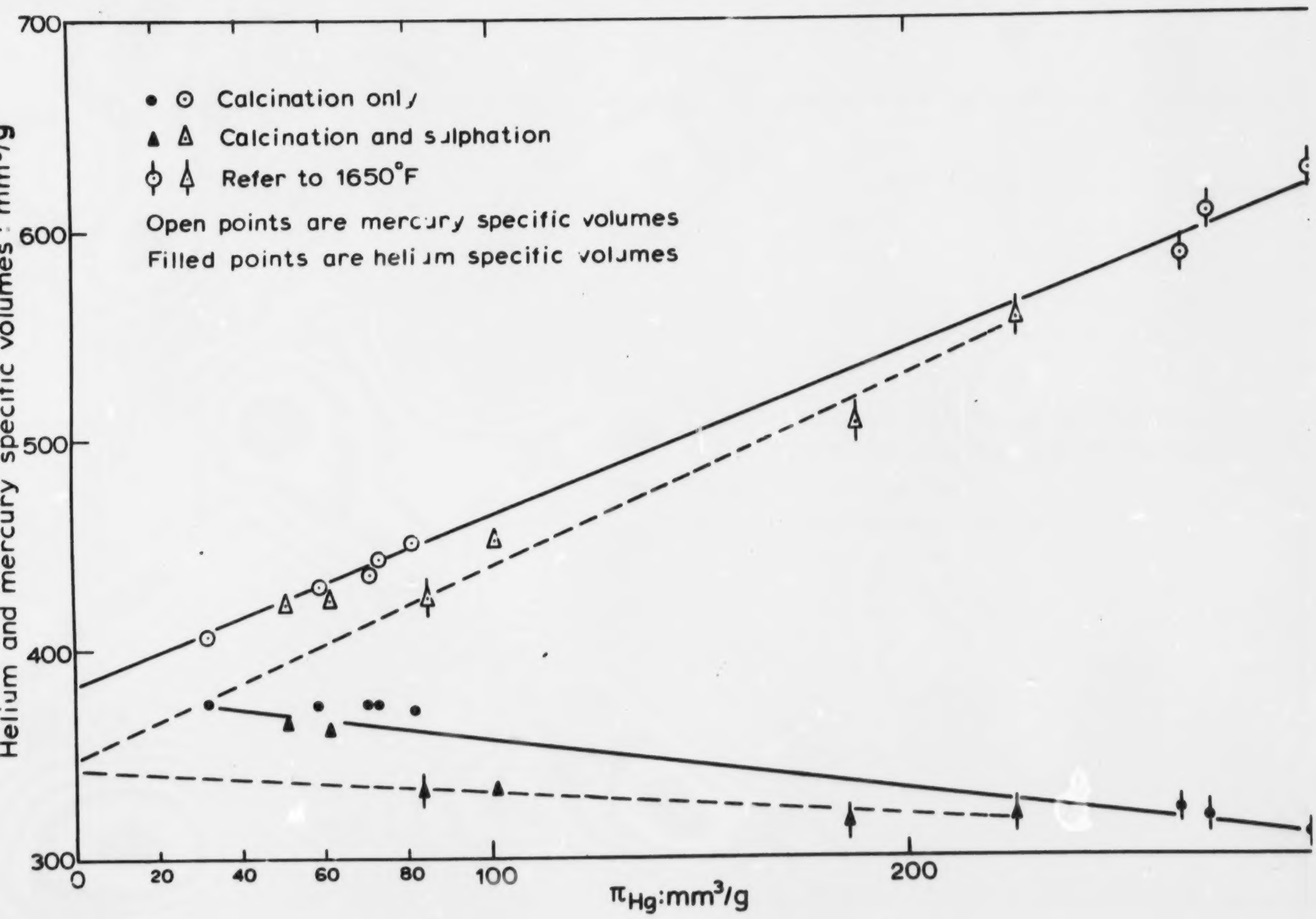

Fig. A8. 9. Specific volumes in helium and mercury *vs* π_{Hg}. Limestone 18

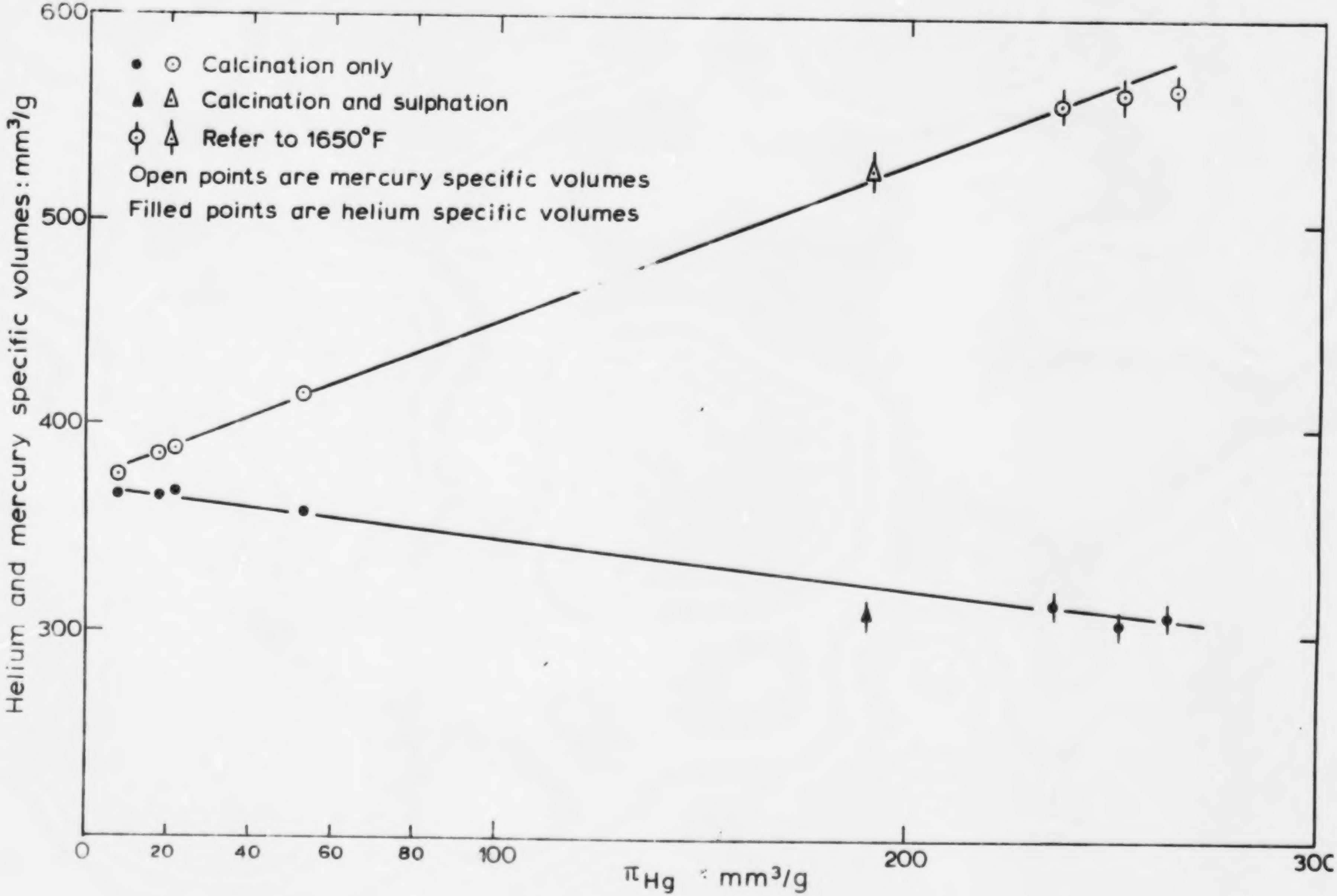

Fig. A8.10. Specific volumes in helium and mercury *vs* π_{Hg}. Limestone 1359

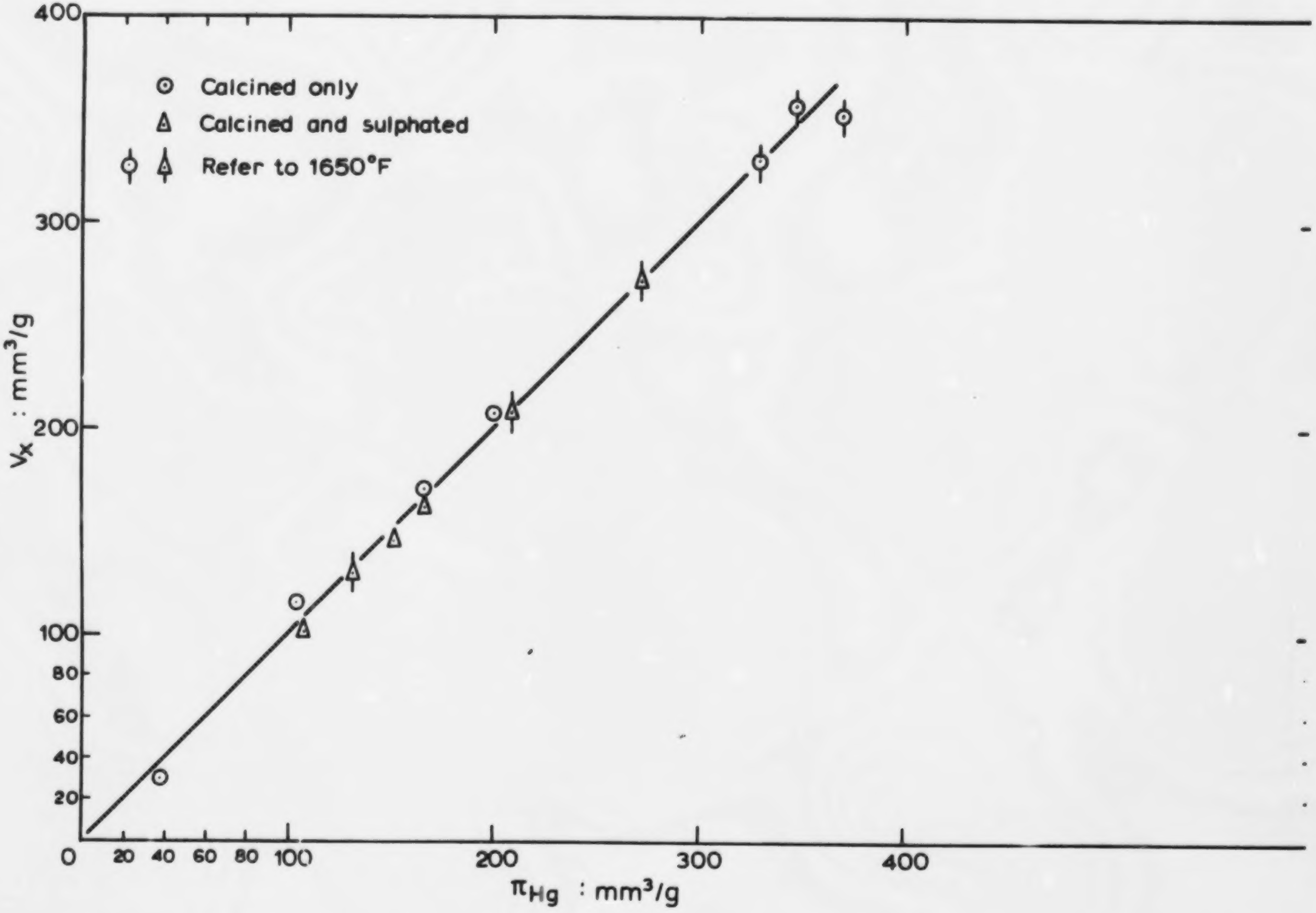

Fig. A 8.11. Porosity V_x vs π_{Hg}. Dolomite 1337

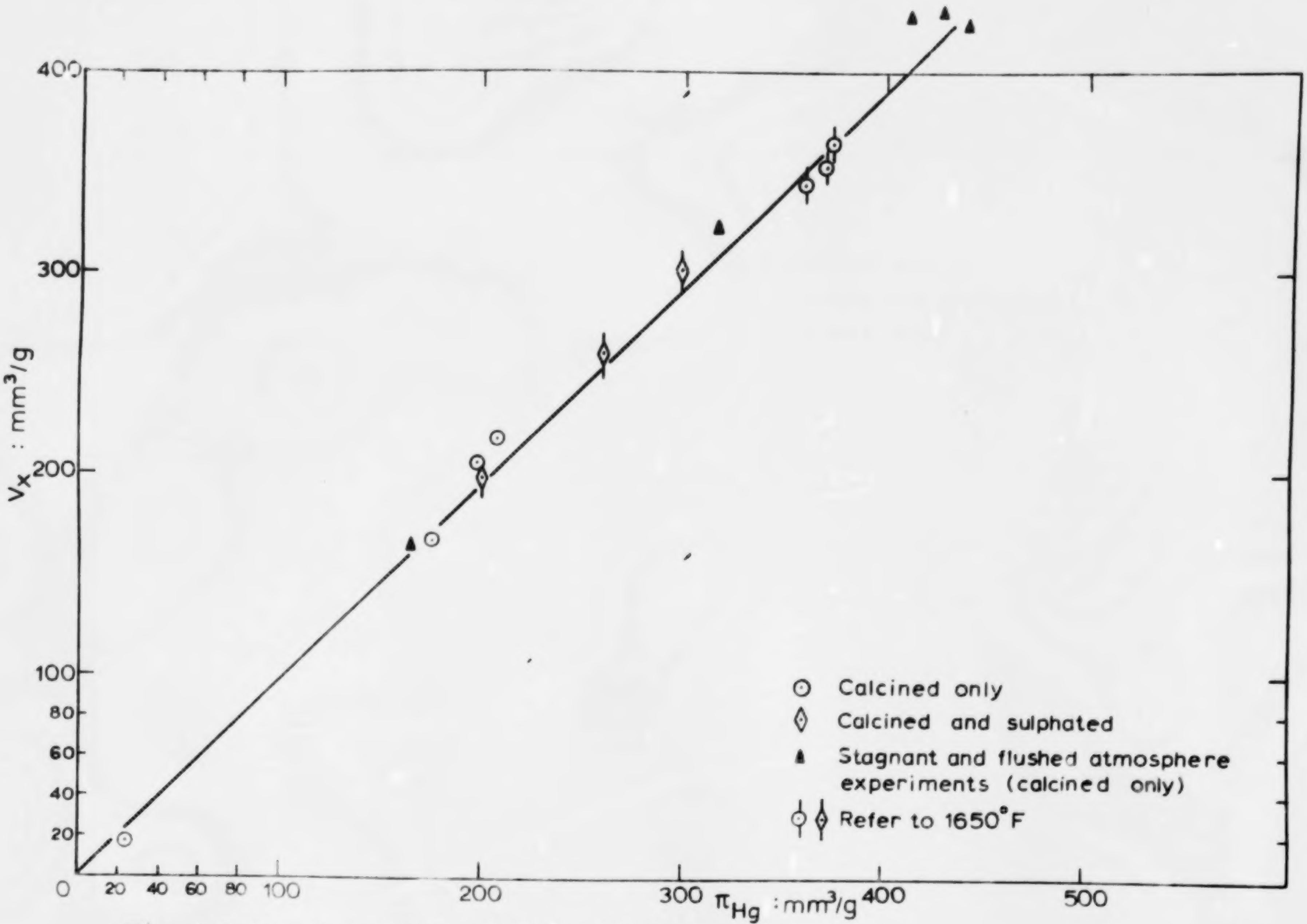

Fig. A8.12. Porosity V_x vs π_{Hg}. U.K. Dolomite

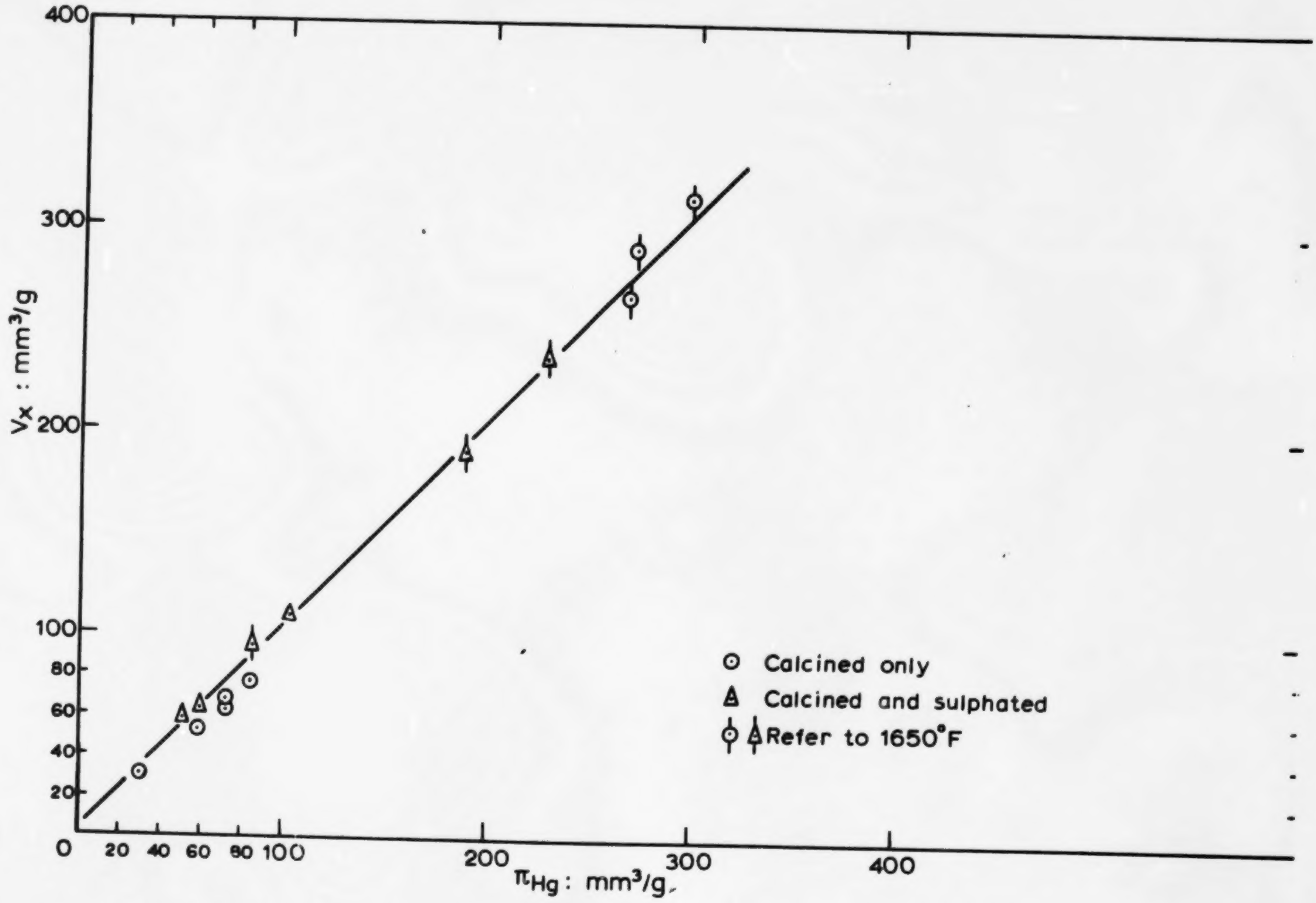

Fig. A 8.13. Porosity V_x vs π_{Hg}. Limestone 18

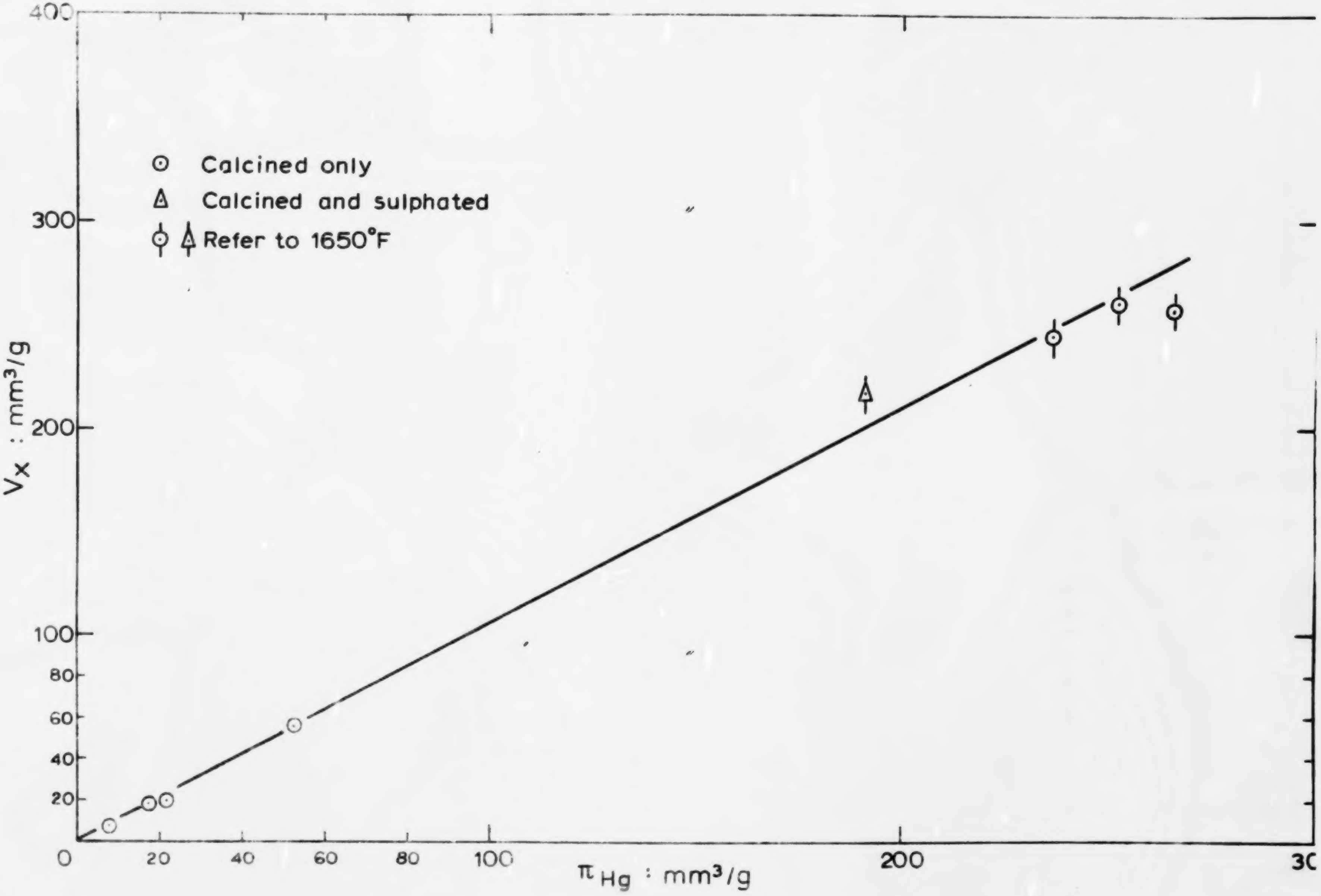

Fig. A8.14. Porosity V_x *vs* π_{Hg}. Limestone 1359

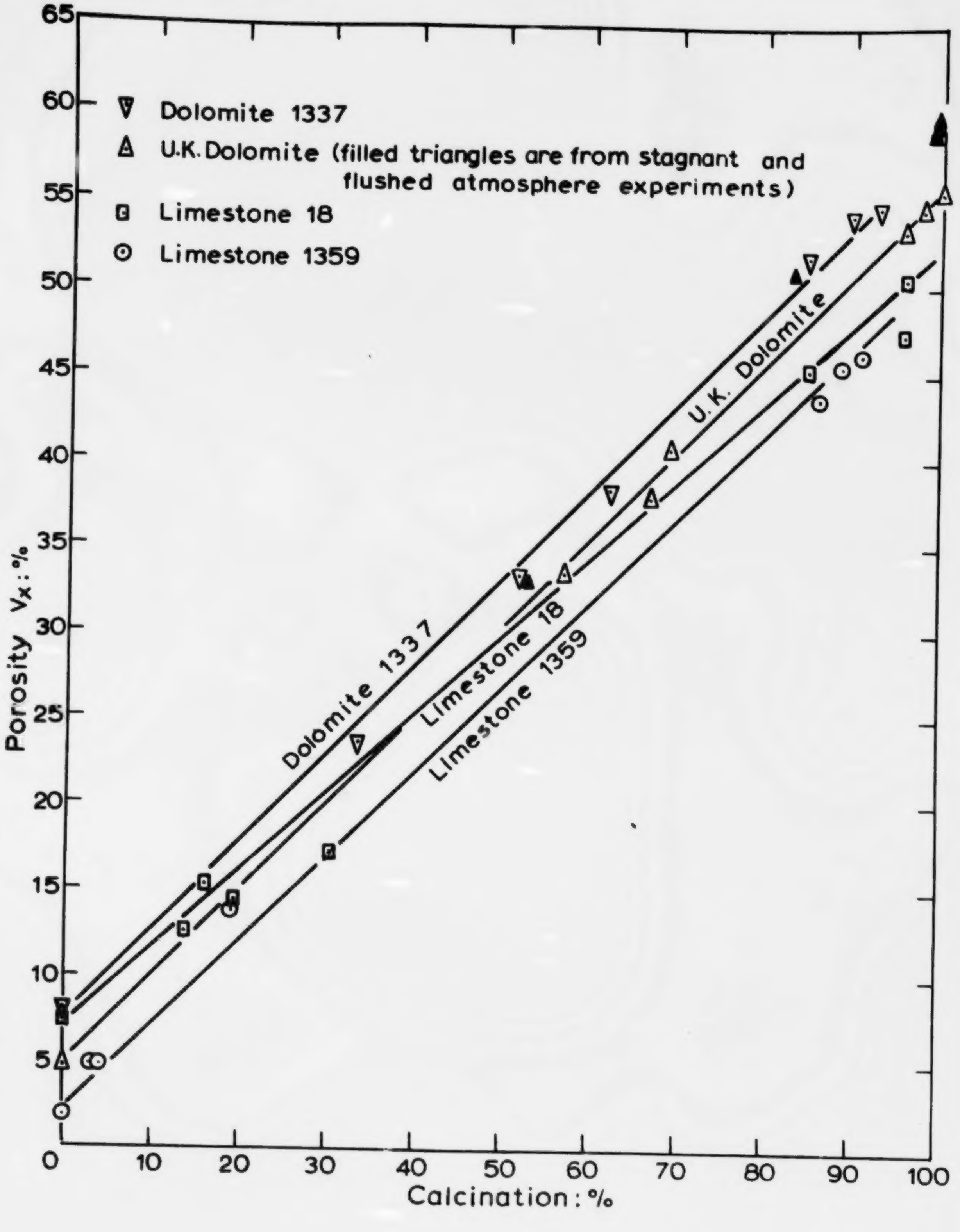

Fig. A8. 15. Porosity (helium-mercury densities) *vs* extent of calcination

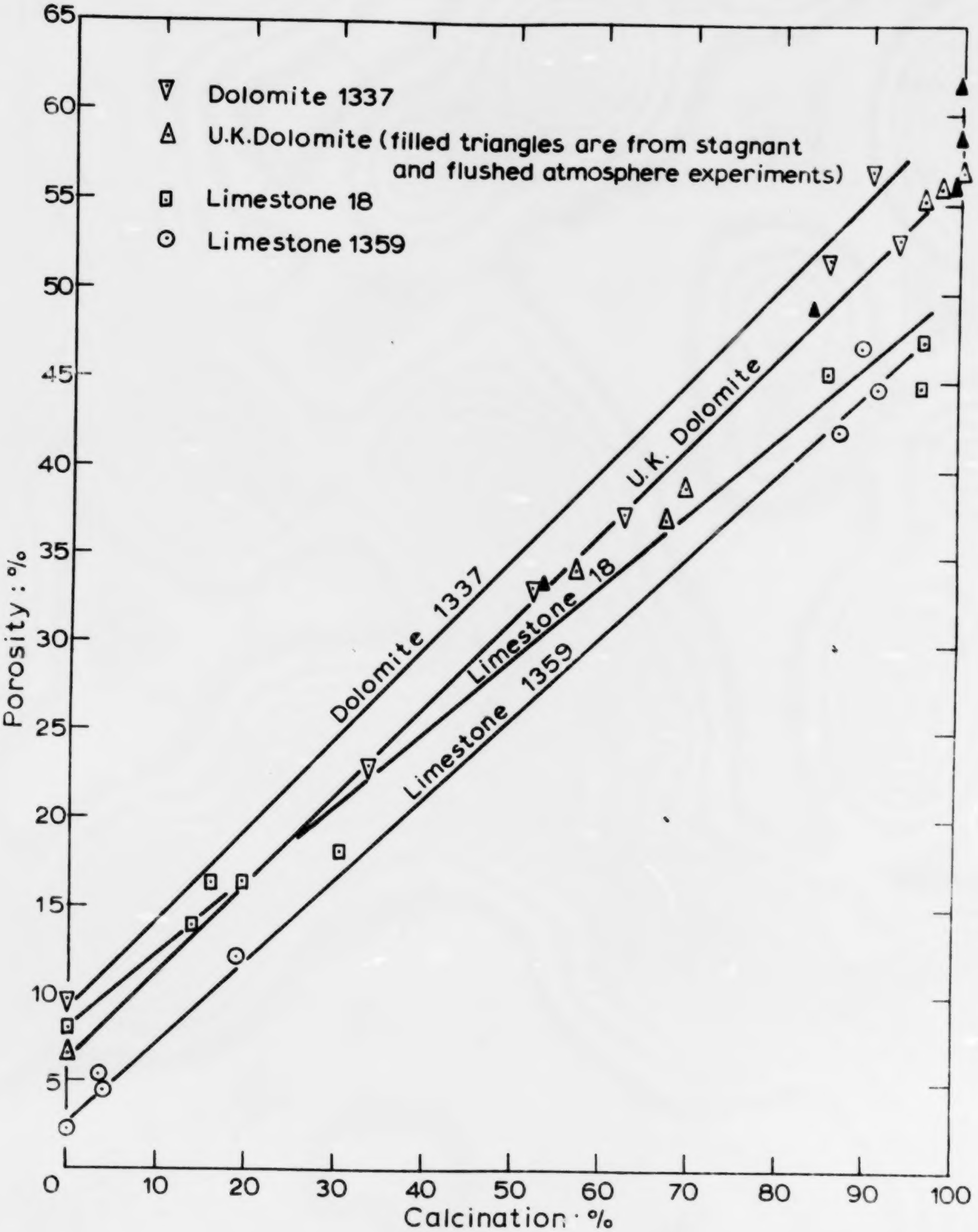

Fig. A8.16. Porosimetry porosity as percentage of 'lump' volume *vs* extent of calcination

(i) volume in the range of pore-entrance diameters 14·5 to 0·014 μm

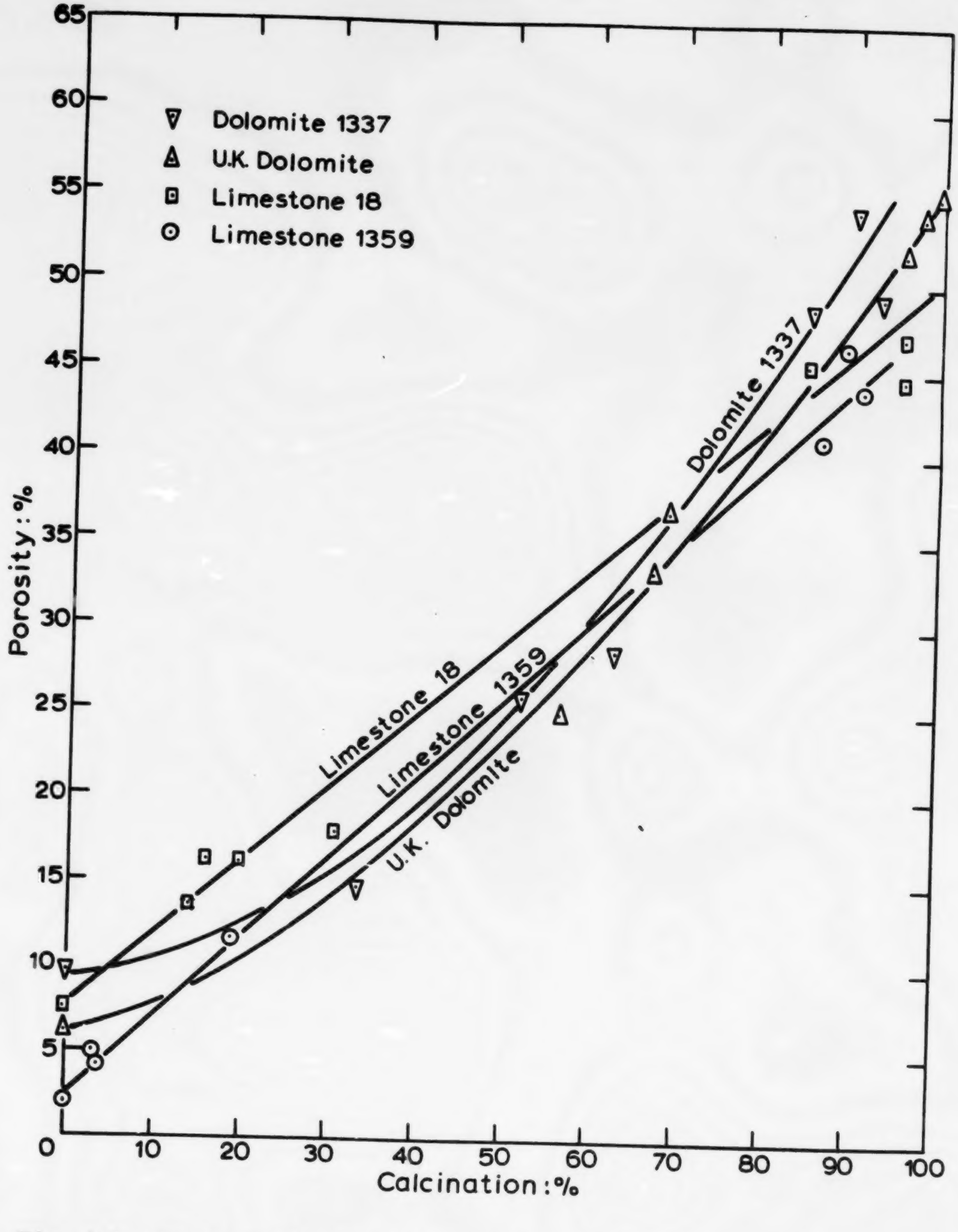

Fig. A8. 17. Porosimetry porosity as percentage of 'lump' volume *vs* extent of calcination

(ii) volume in the range of pore-entrance diameters 14·5 to 0·03 μm

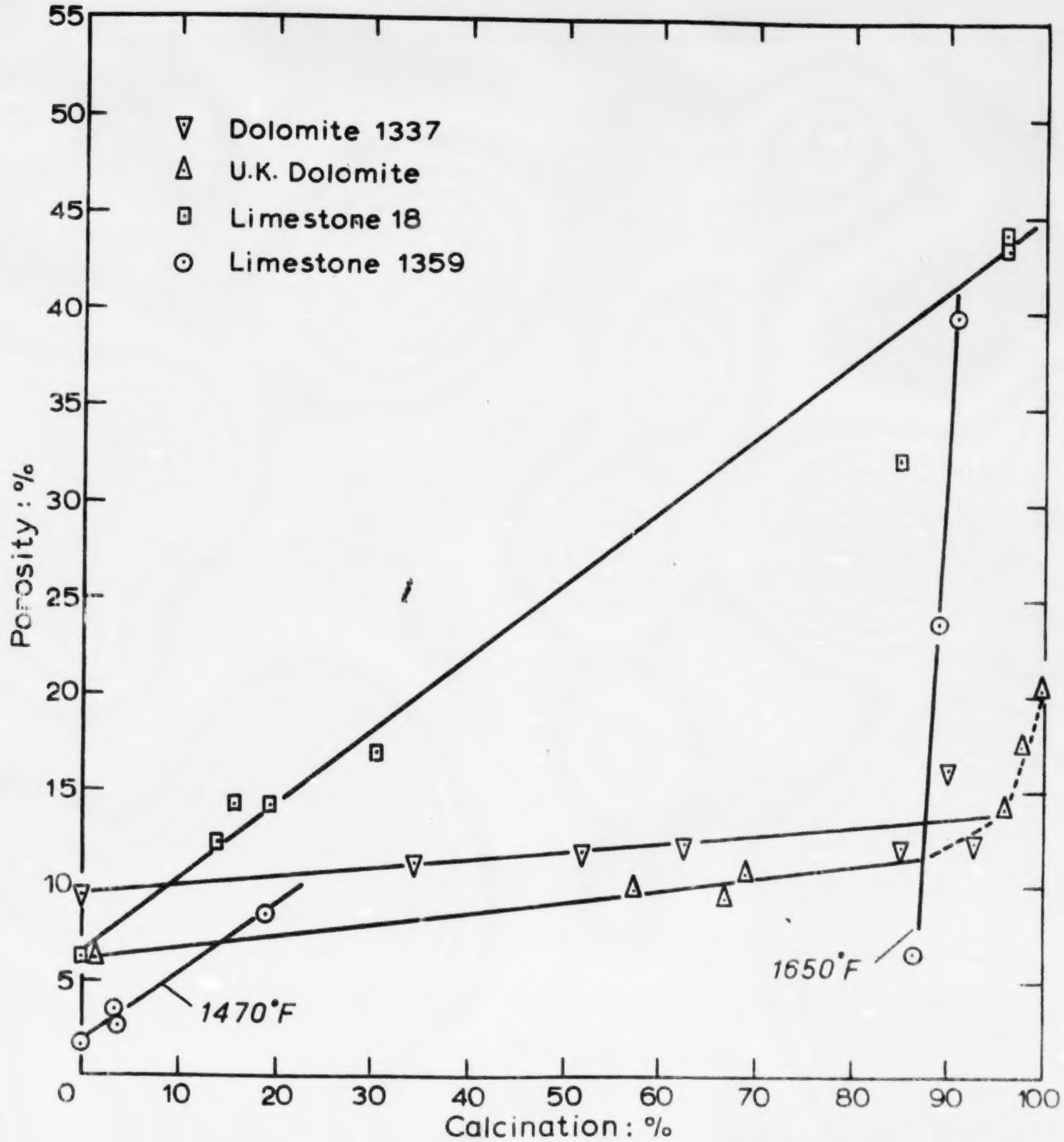

Fig. A8.18. Porosimetry porosity as percentage of 'lump' volume *vs* extent of calcination

(iii) volume in the range of pore-entrance diameters 14·5 to 0·1 μm

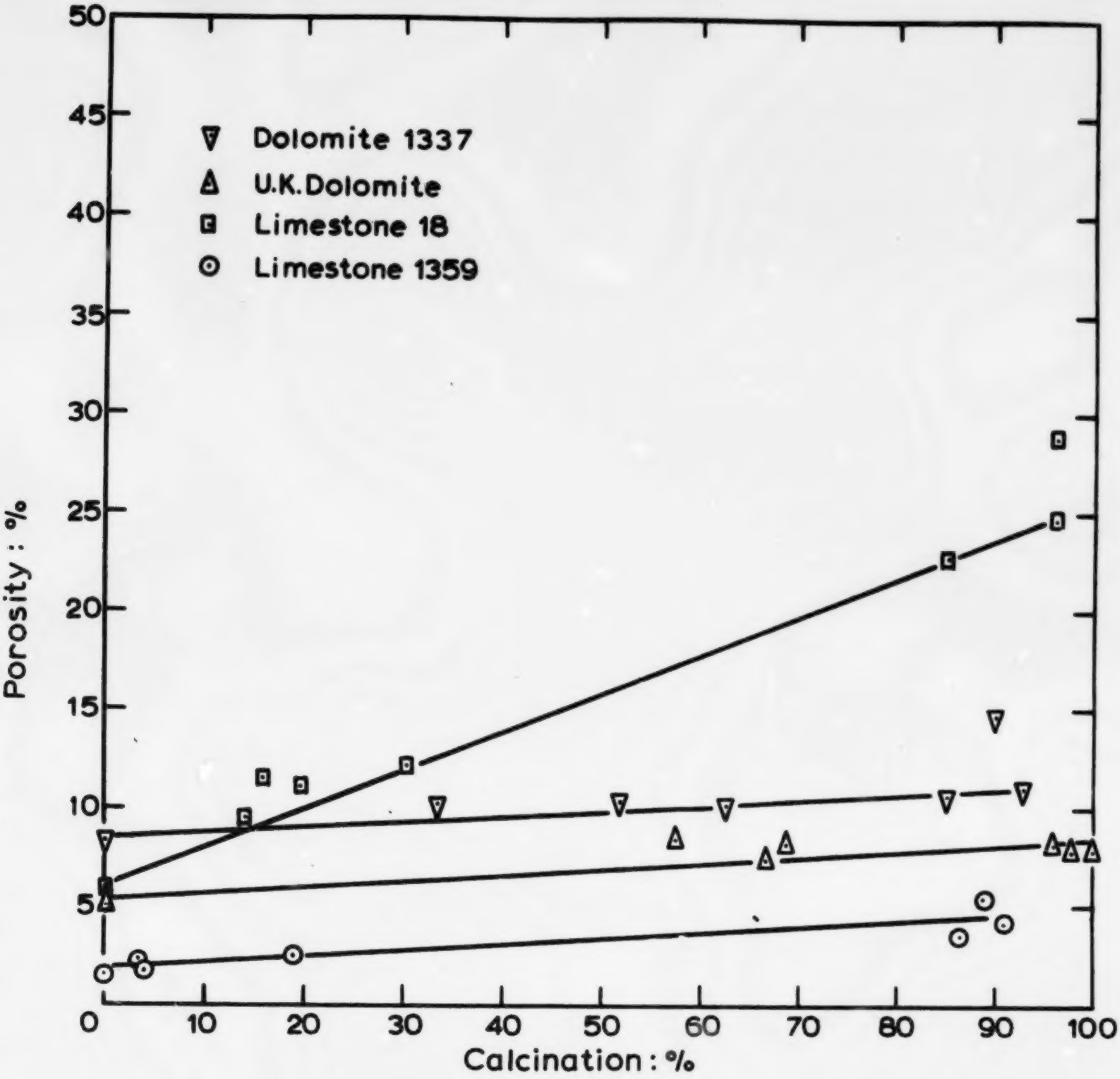

Fig. A8.19. Porosimetry porosity as percentage of 'lump' volume *vs* extent of calcination

(iv) volume in the range of pore-entrance diameters 14·5 to 0·3 μm

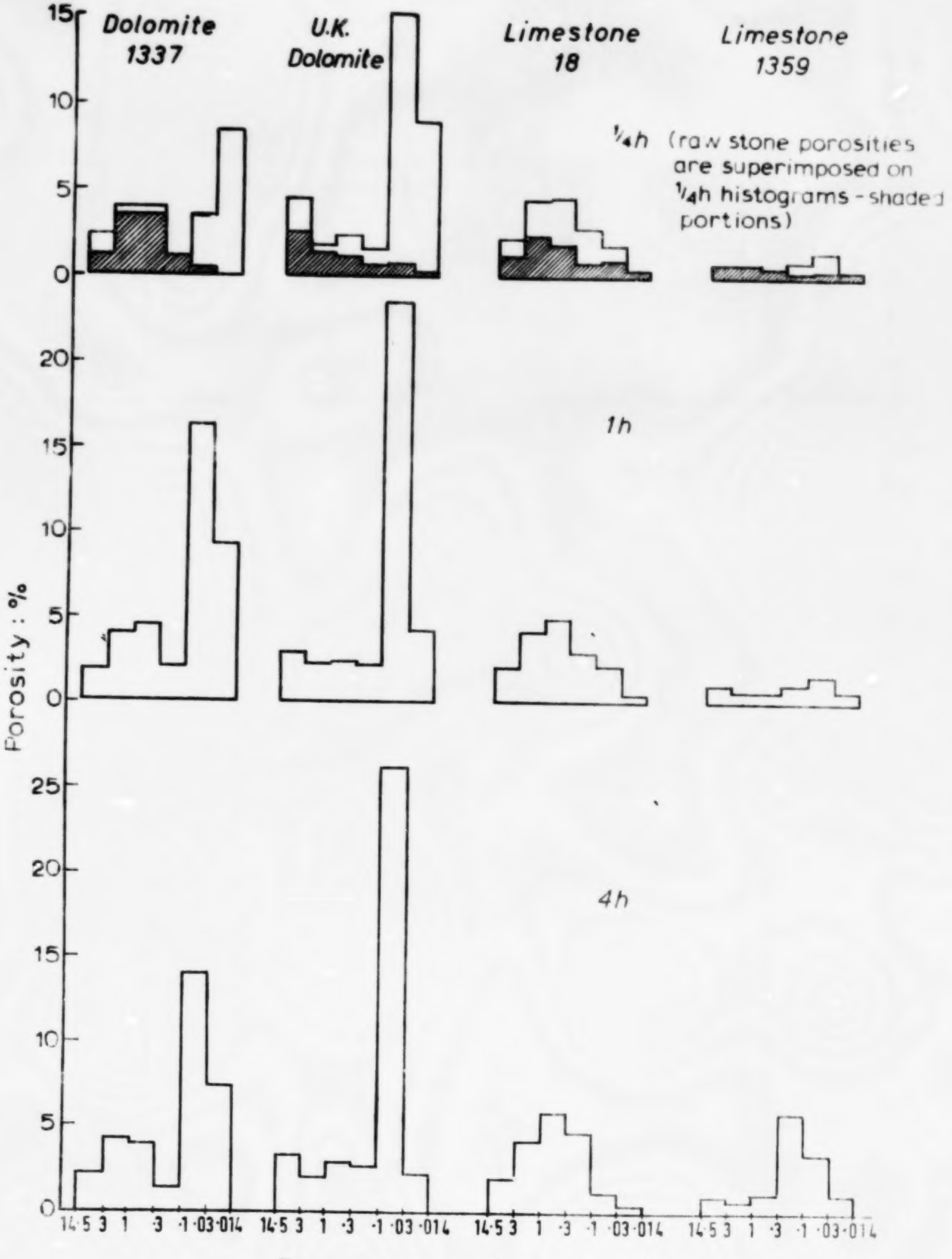

Fig. A 8.20. Porosity of stones calcined at 1470°F - pore volumes as percentages of 'lump' volumes in various ranges of pore-entrance diameter

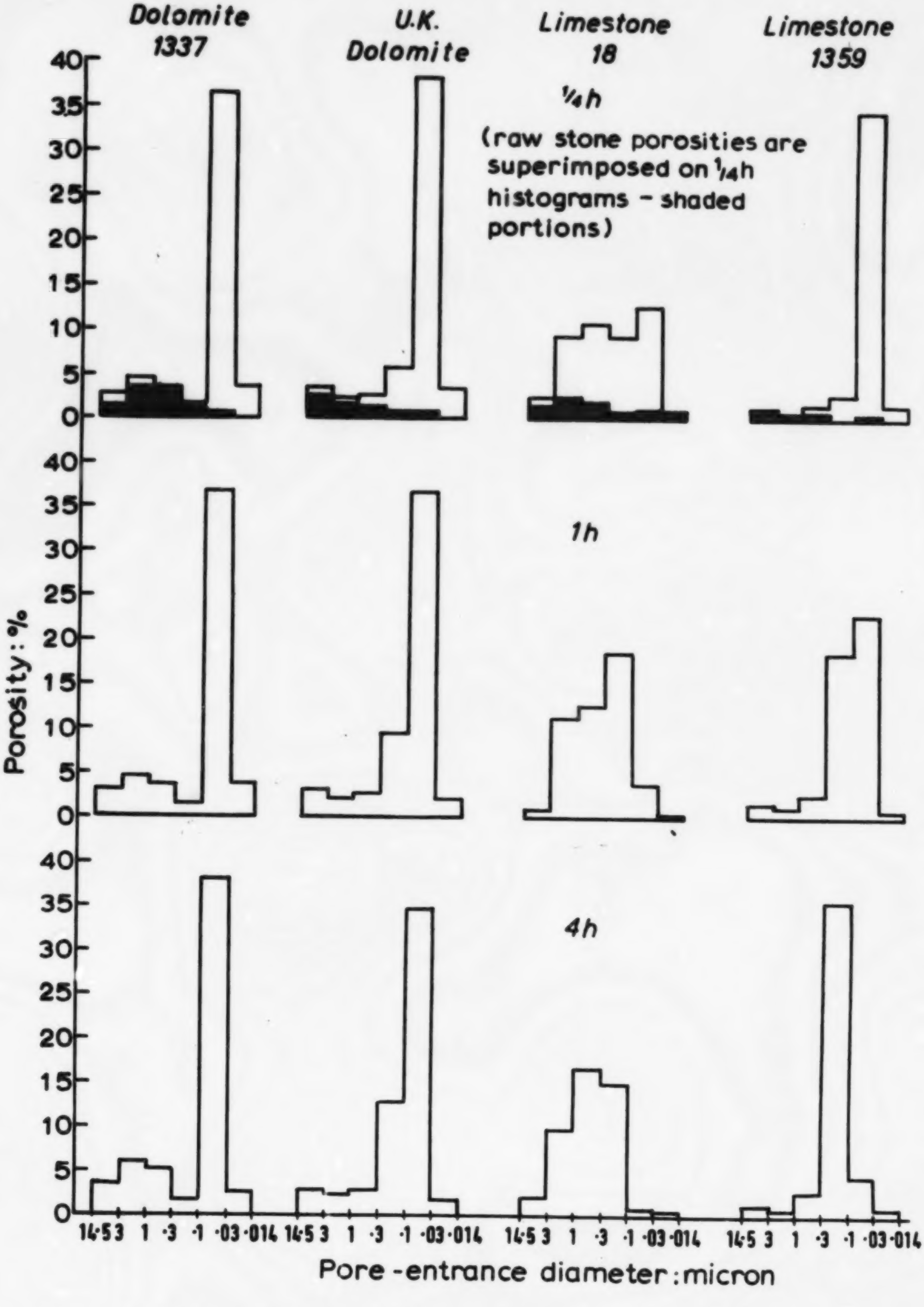

Fig. A8. 21. Porosity of stones calcined at 1650°F – pore volumes as percentages of 'lump' volumes in various ranges of pore-entrance diameter

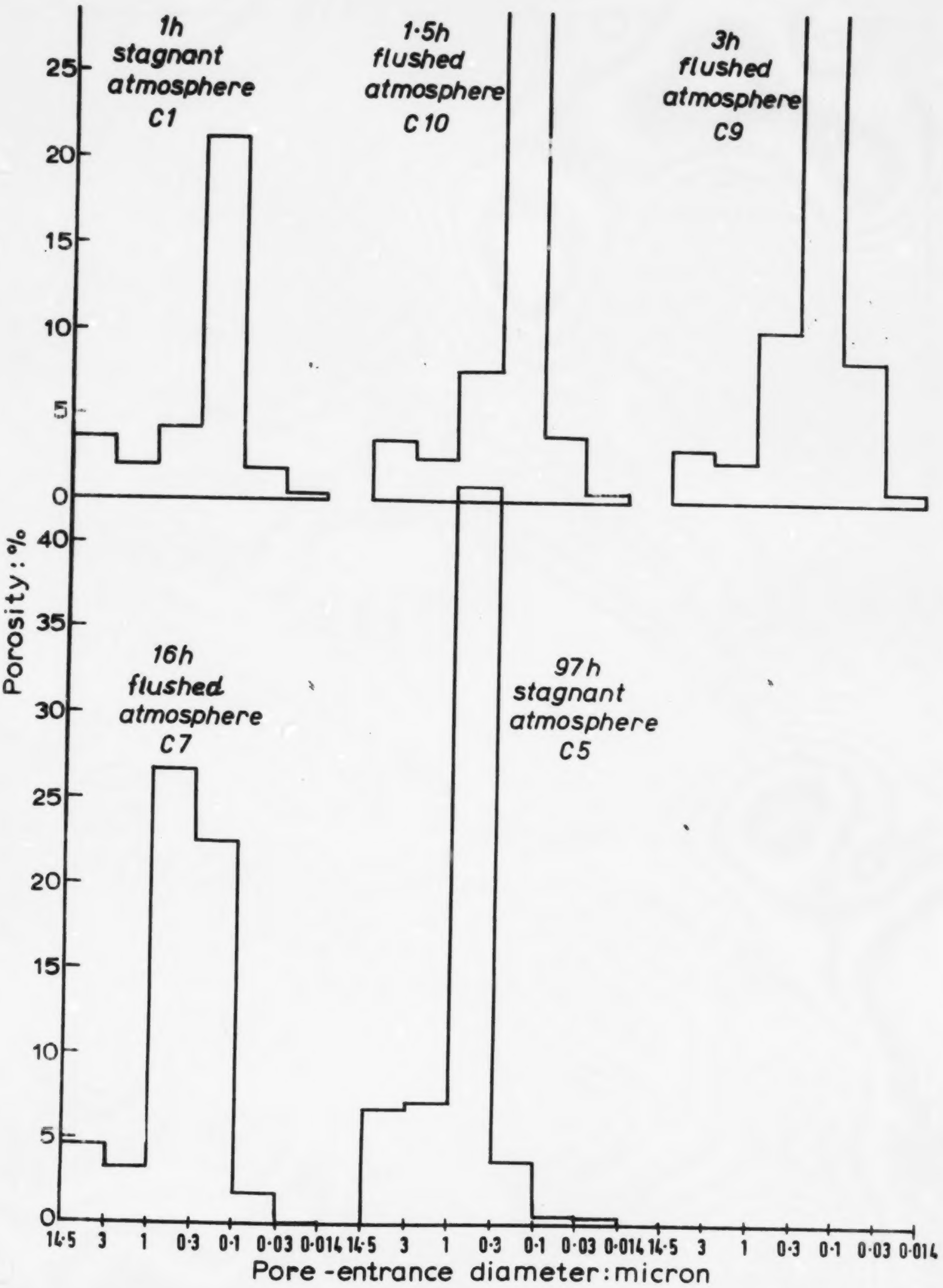

Fig. A8. 22. Porosity of U.K. Dolomite calcined at 1470°F in stagnant and flushed atmospheres. (Porosity is pore volume as percentage of 'lump' volume in various ranges of pore-entrance diameter) A8. 137

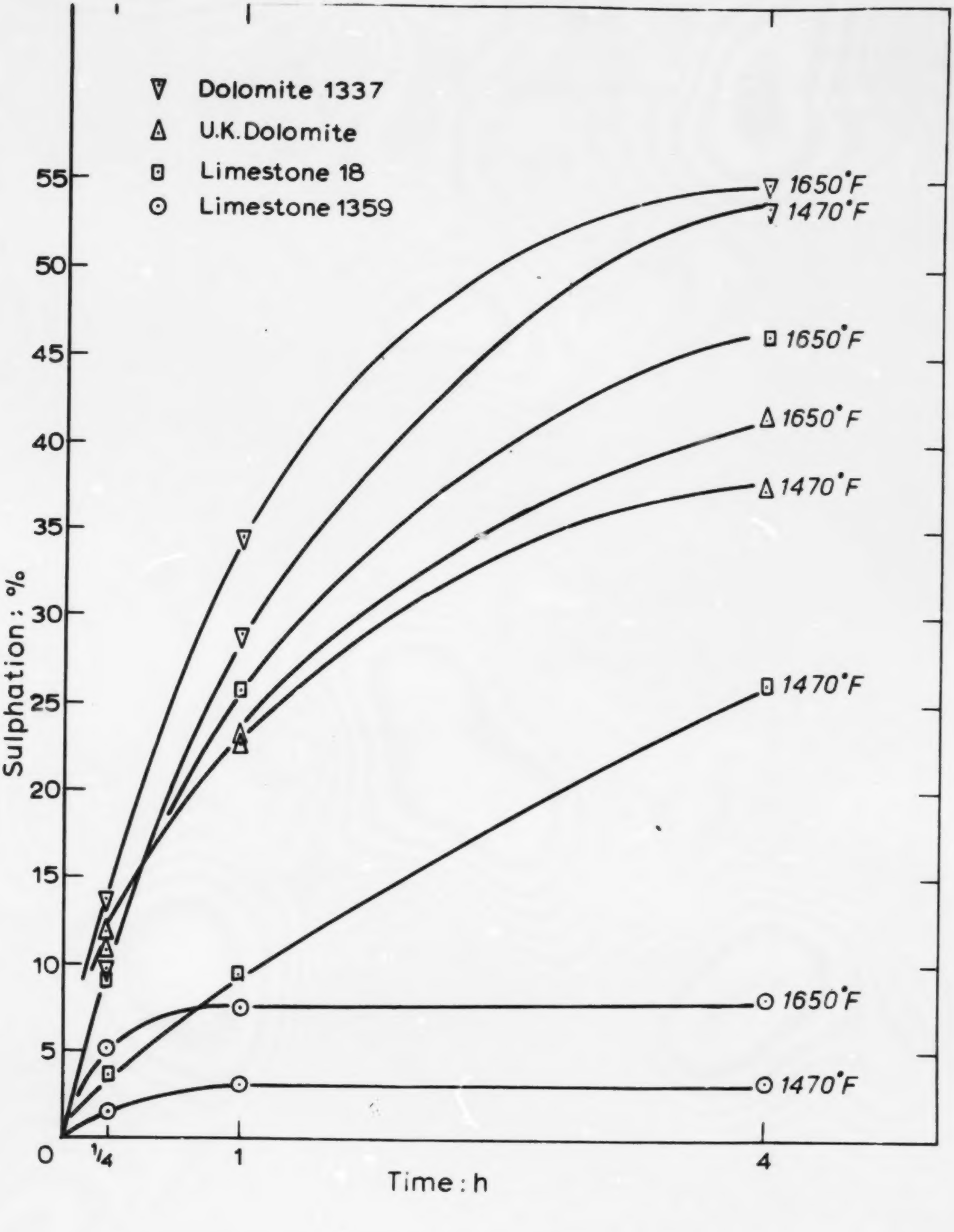

Fig. A8.23. Variation of level of sulphation with time and temperature

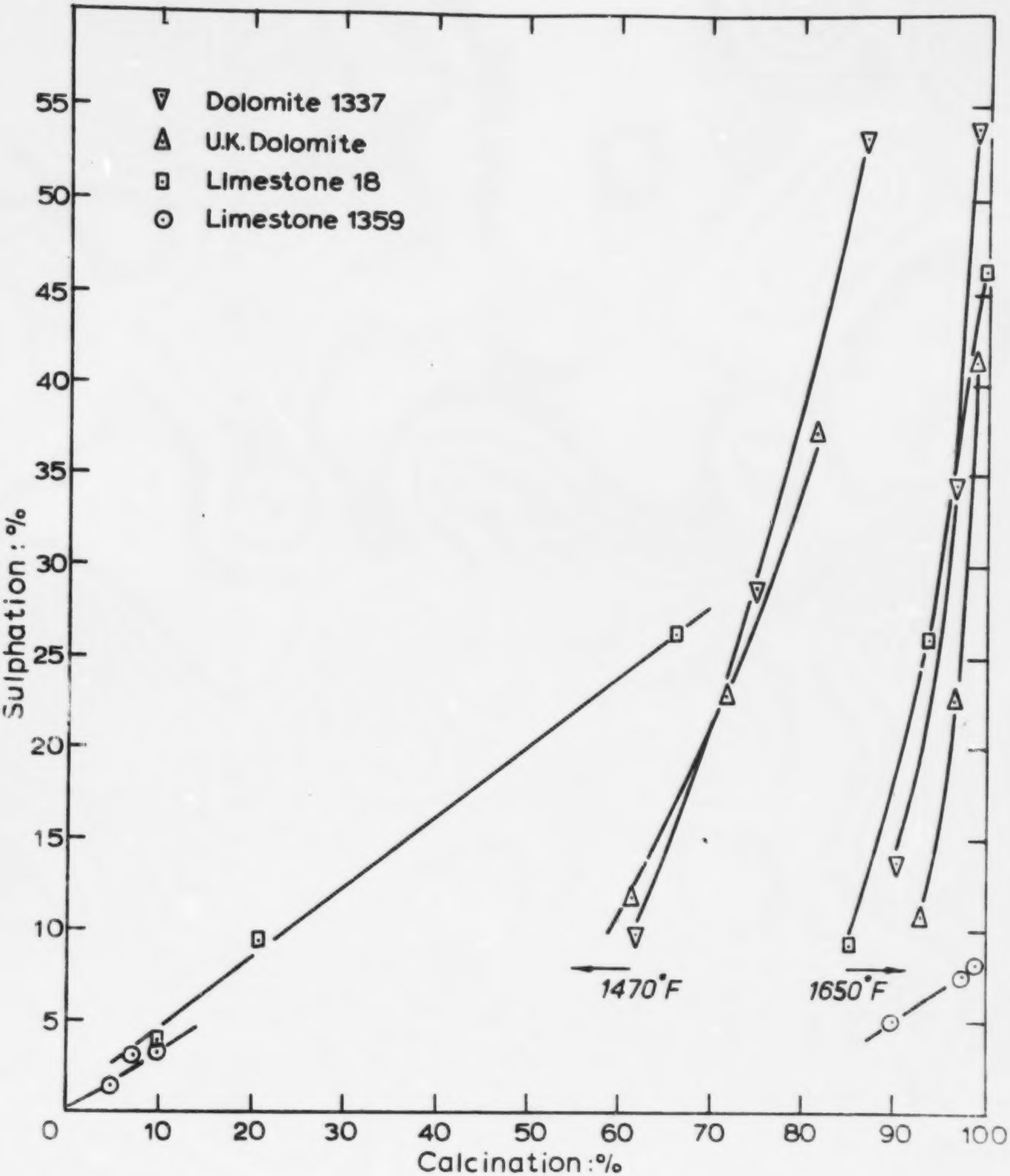

Fig. A 8. 24. Variation of sulphation level with extent of calcination

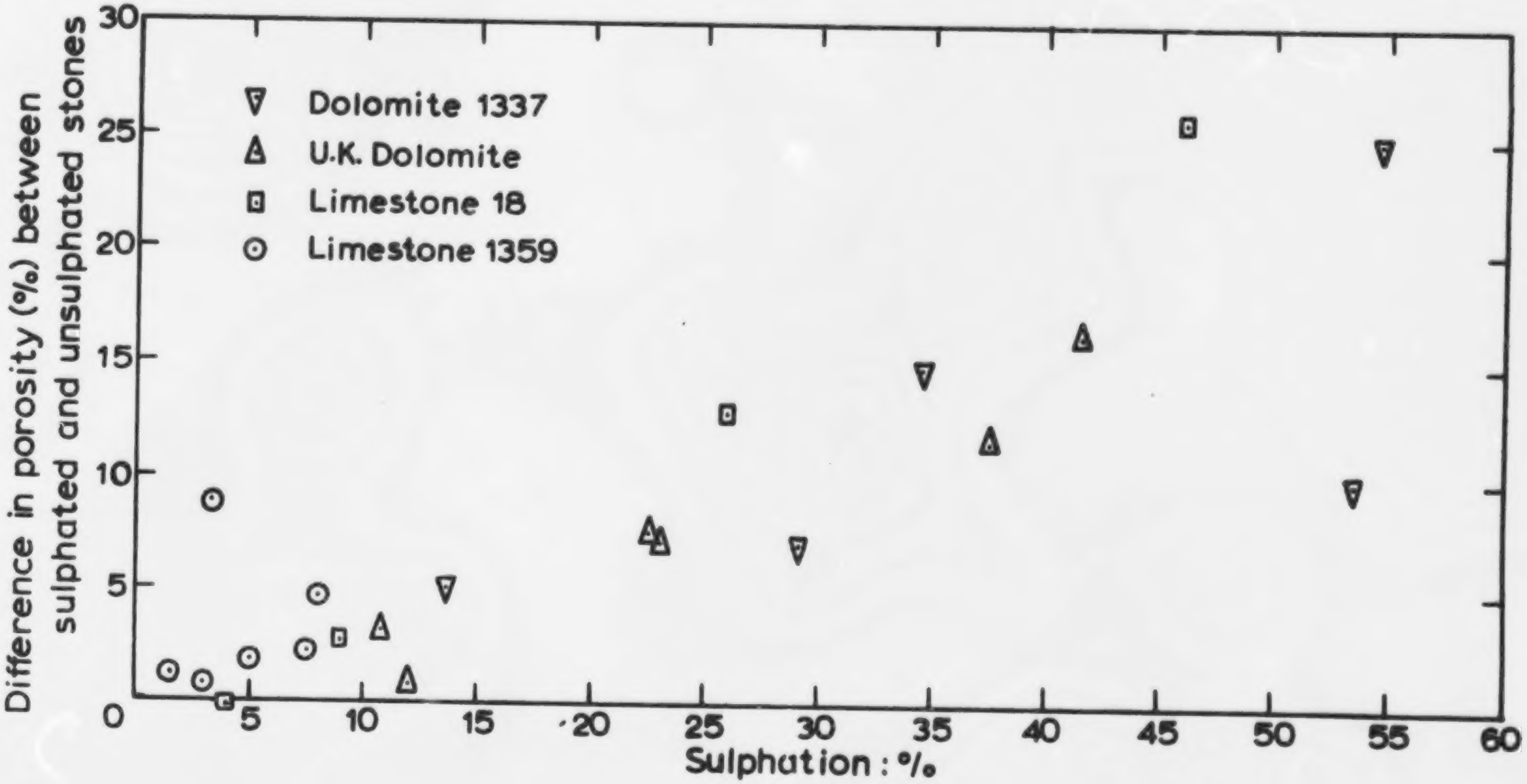

Fig. A 8. 25. Change of porosity (helium-mercury densities) on sulphation with level of sulphation

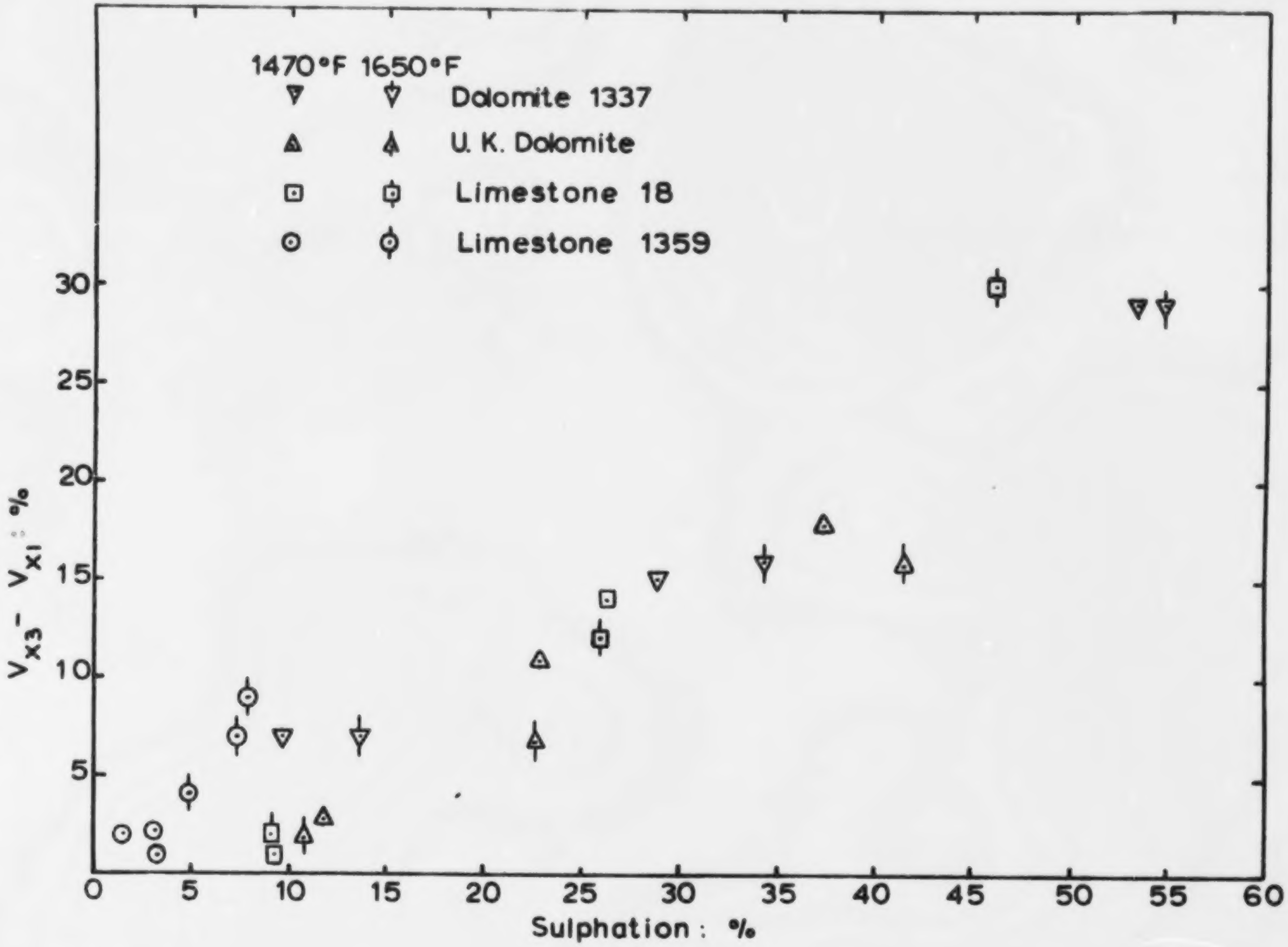

Fig. A8. 25a. Sulphated samples: differences between estimated porosity V_{x3} and measured porosity V_{x1}

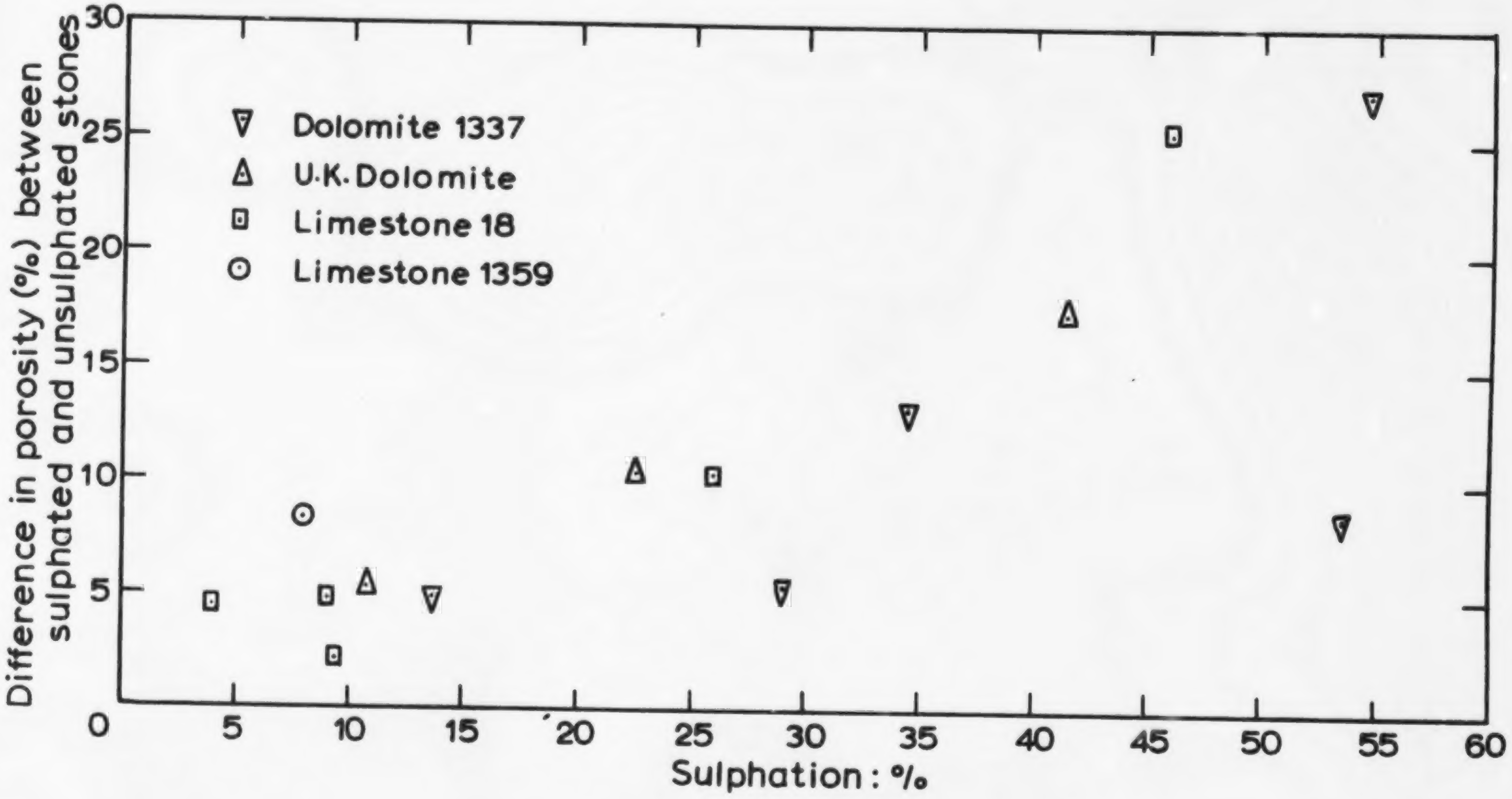

Fig. A8. 26. Change of porosity (porosimetry π_{Hg}) on sulphation with level of sulphation

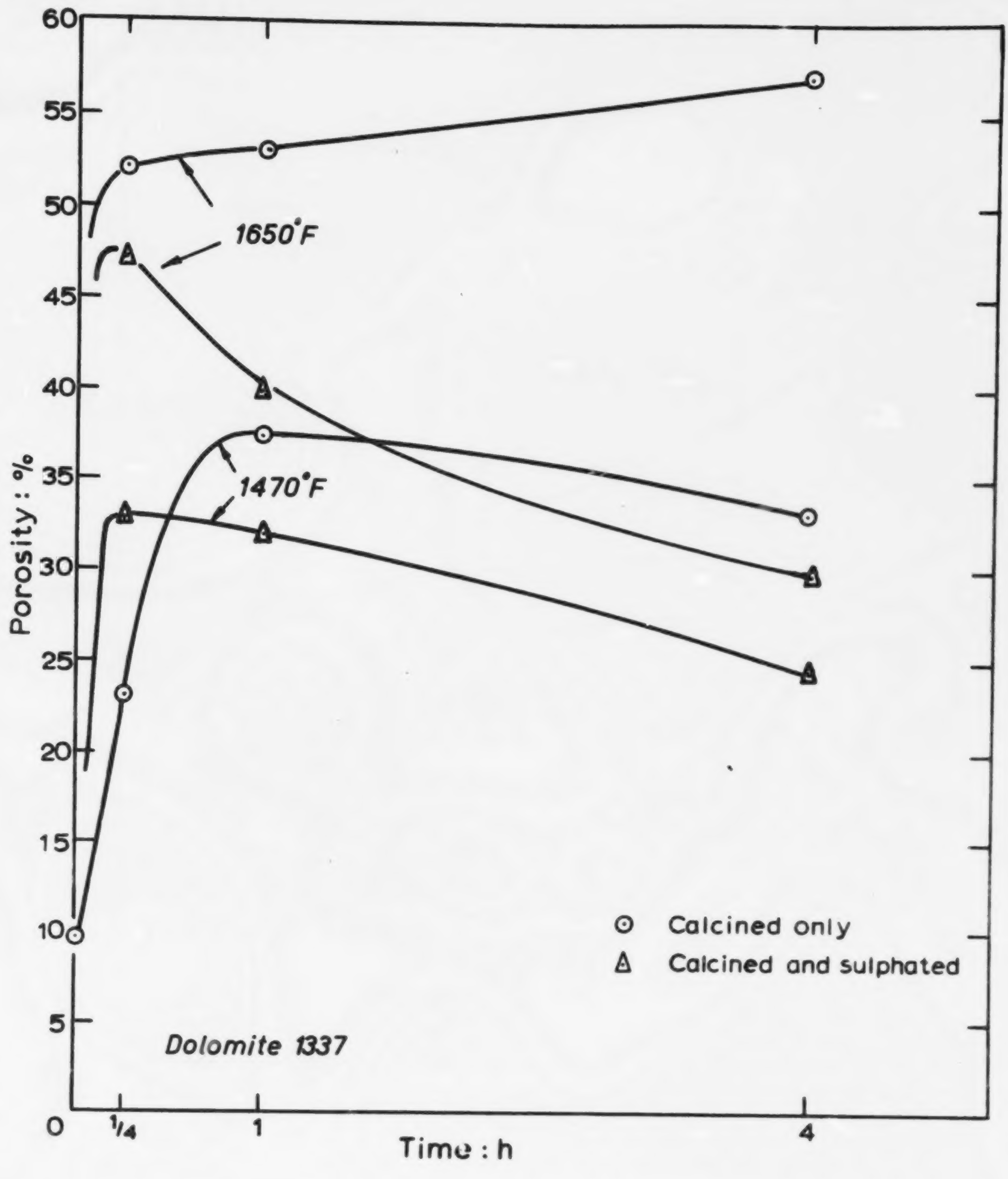

ig. A8. 27. Variation of porosity (14·5 to 0·014μm) with time of calcination and sulphation

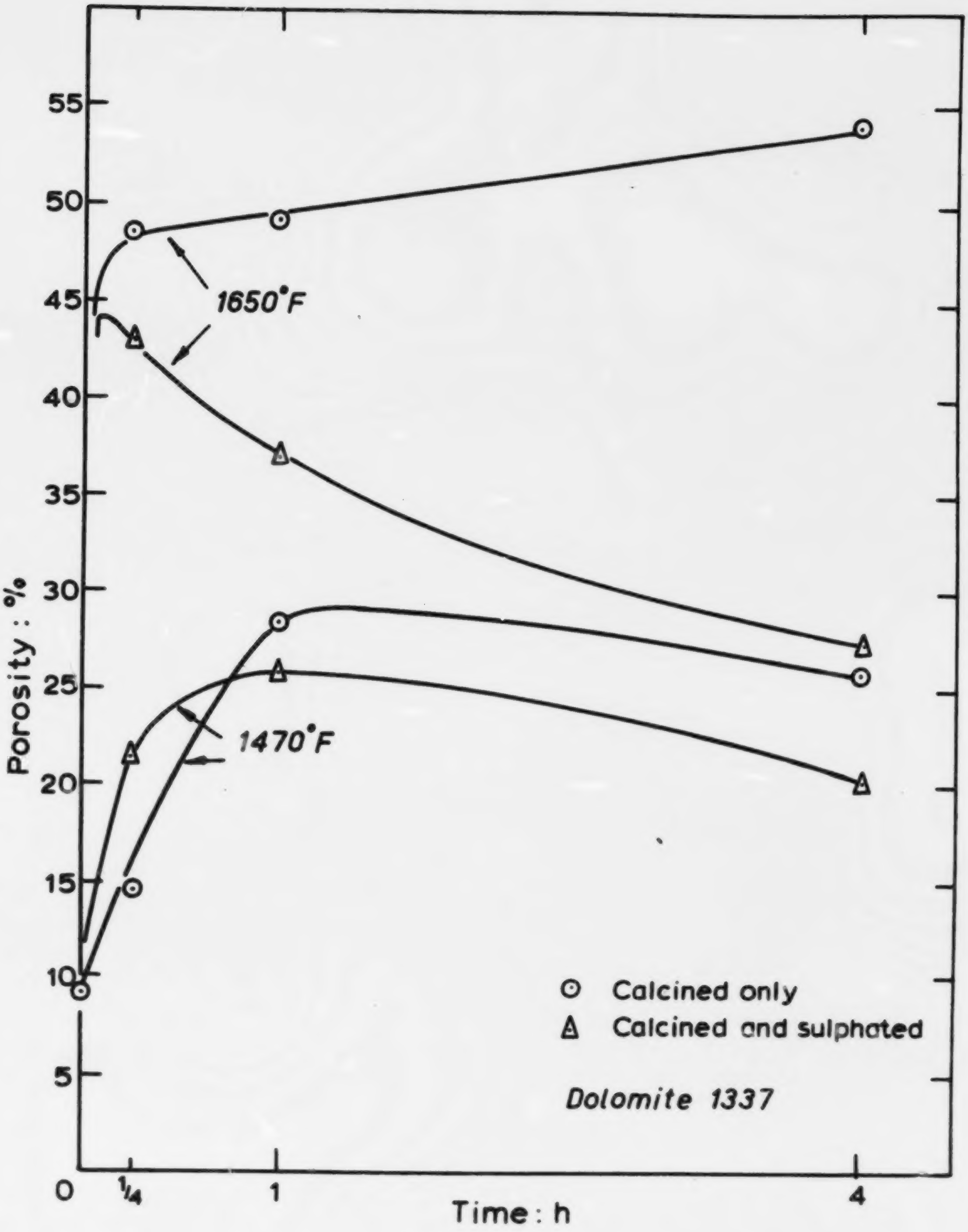

Fig. A 8. 28. Variation of porosity (14·5 to 0·03 μm) with time of calcination and sulphation

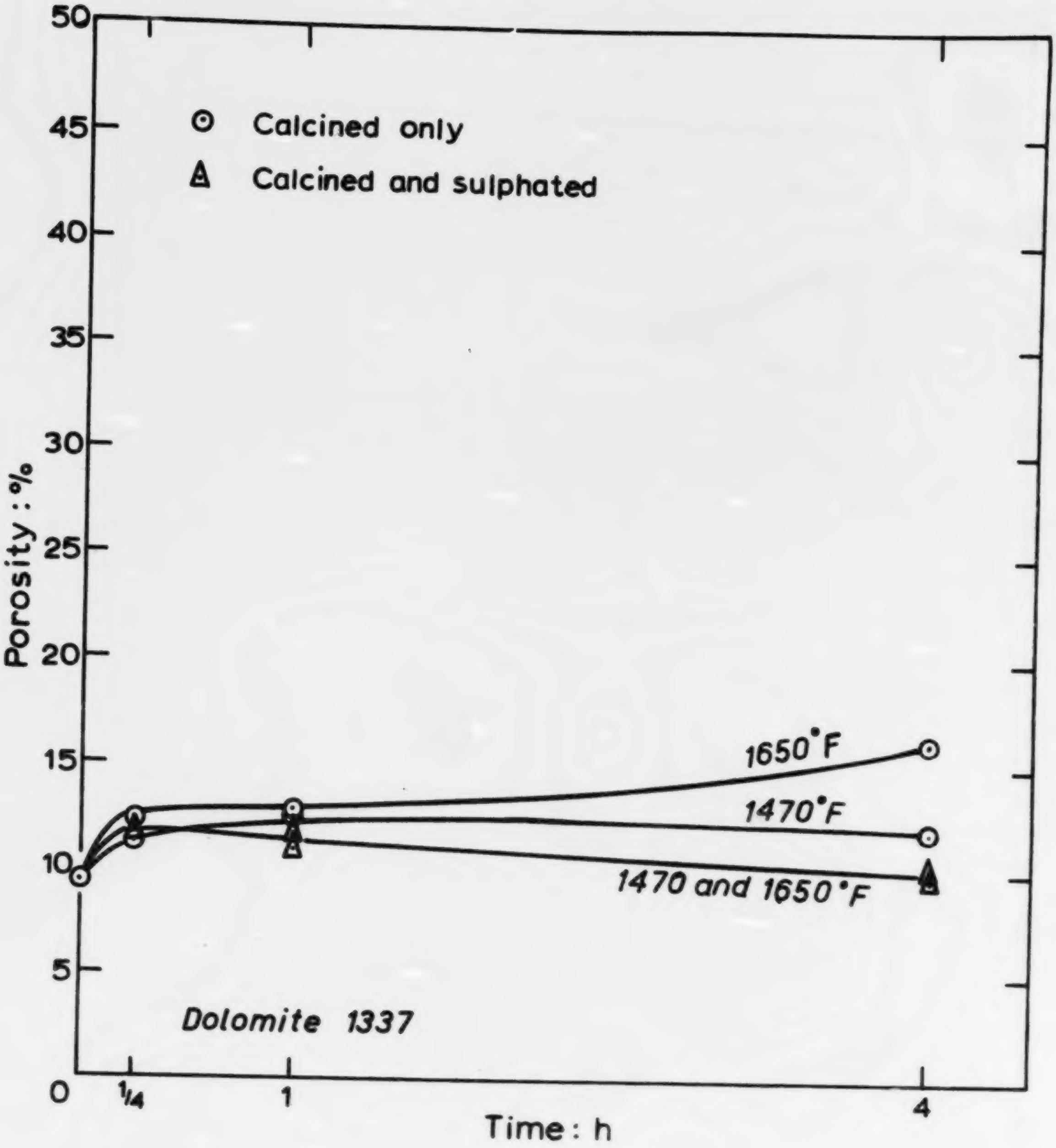

Fig A 8.29. Variation of porosity (14·5 to 0·1 μm) with time of calcination and sulphation

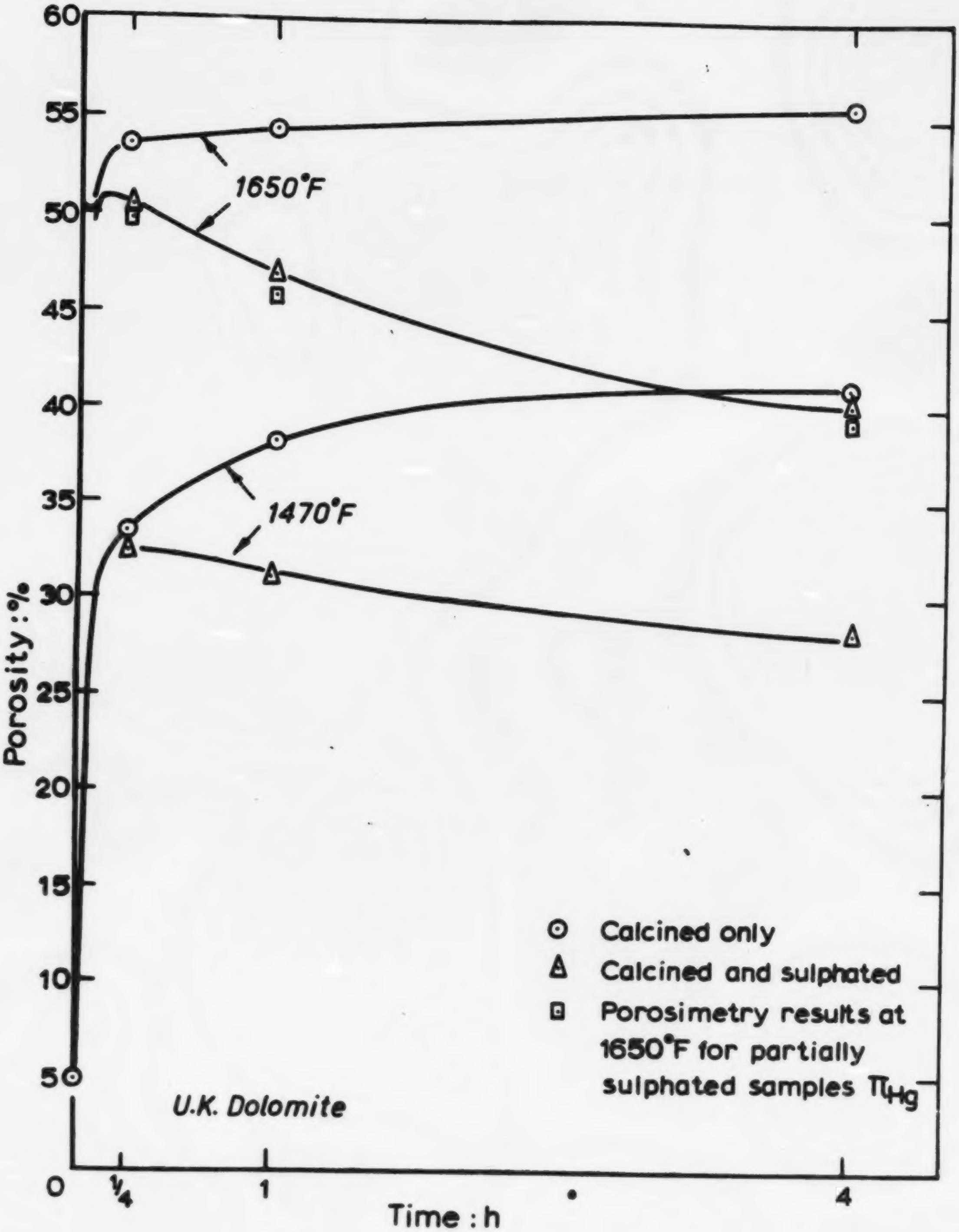

Fig. A 8.30. Variation of porosity (helium-mercury density) with time of calcination and sulphation

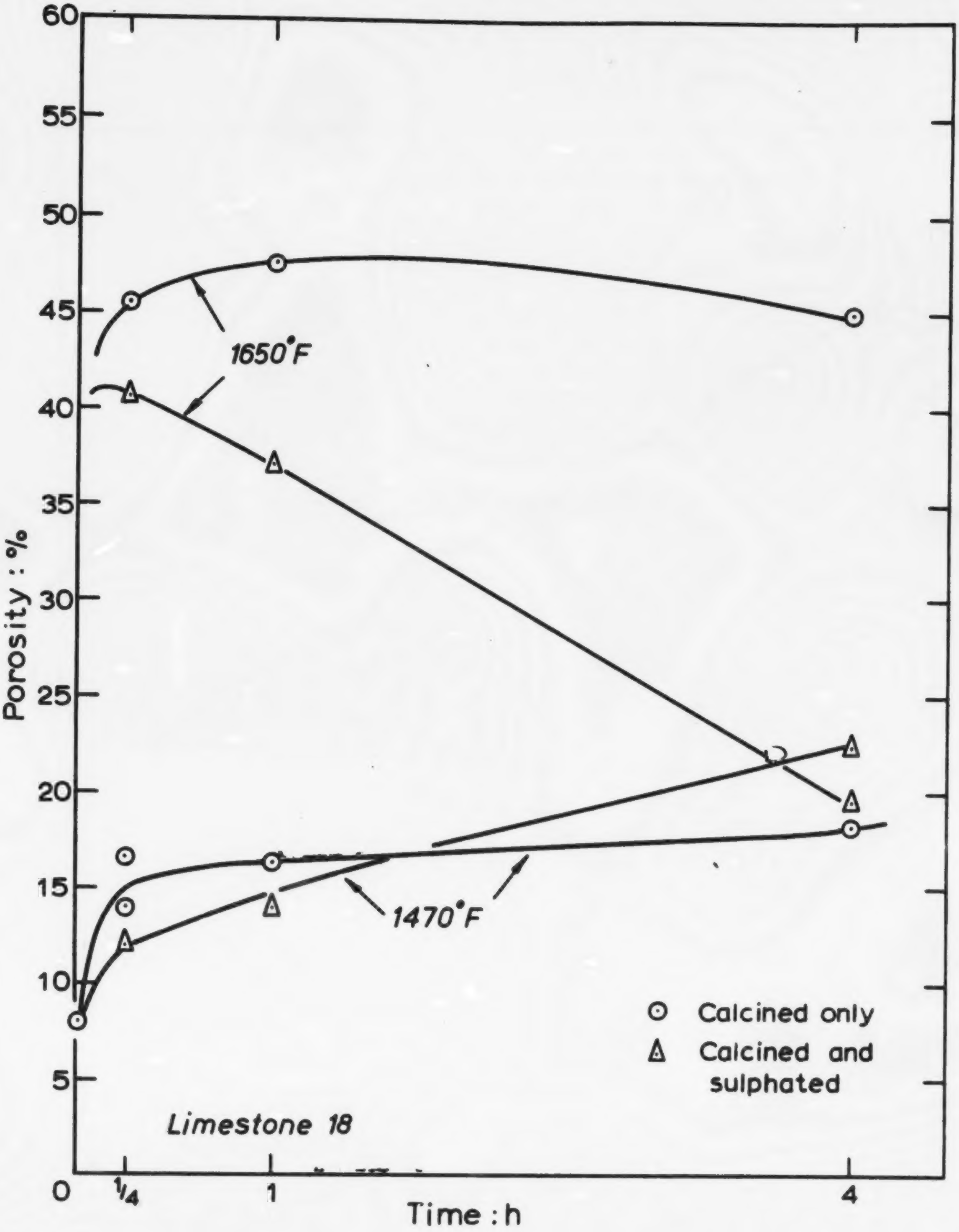

Fig. A 8. 31. Variation of porosity (14·5 to 0·014 μm) with time of calcination and sulphation

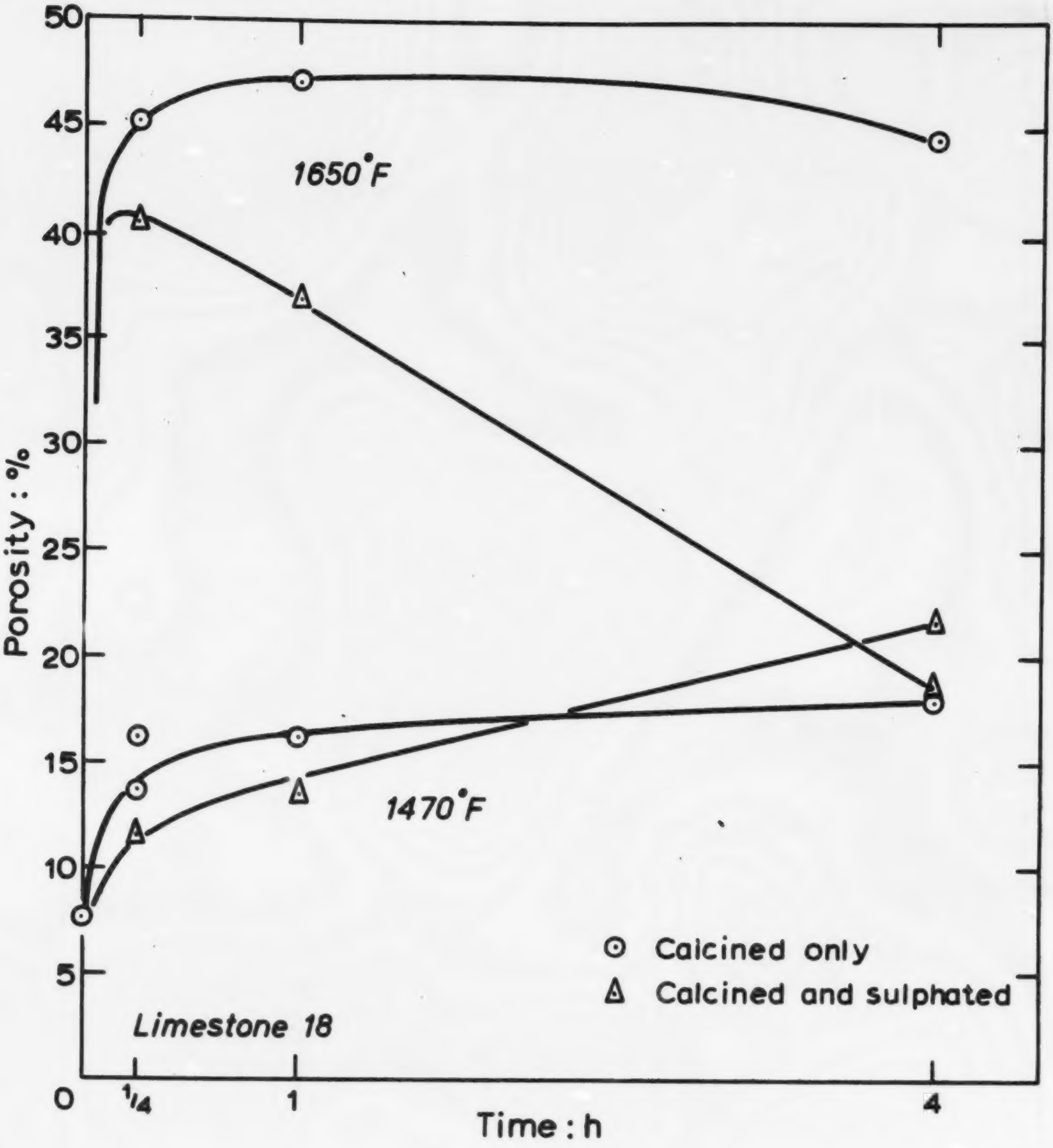

Fig. A 8.32. Variation of porosity (14·5 to 0·03 μm) with time of calcination and sulphation

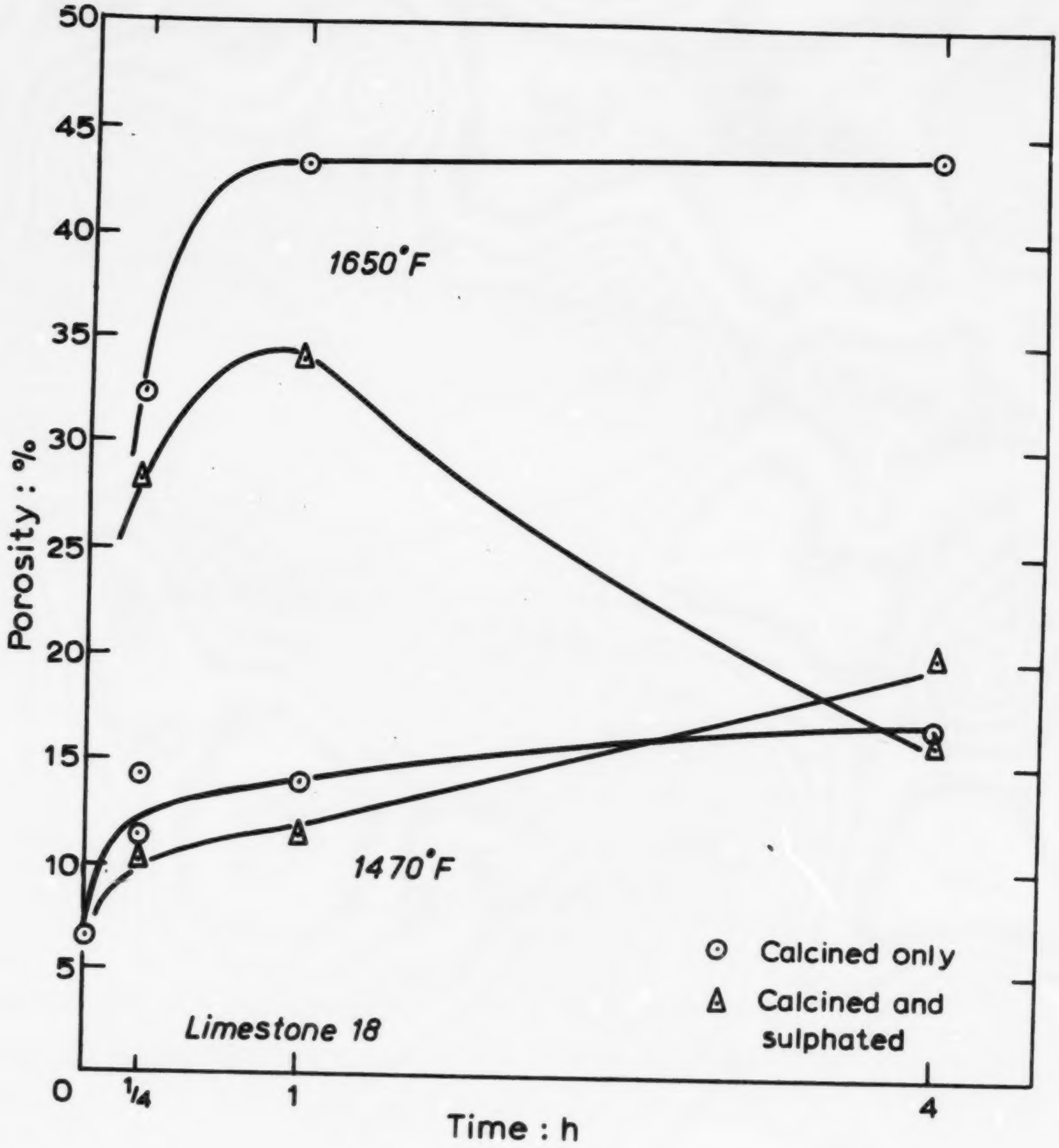

Fig. A 8.33. Variation of porosity (14·5 to 0·1 μm) with time of calcination and sulphation

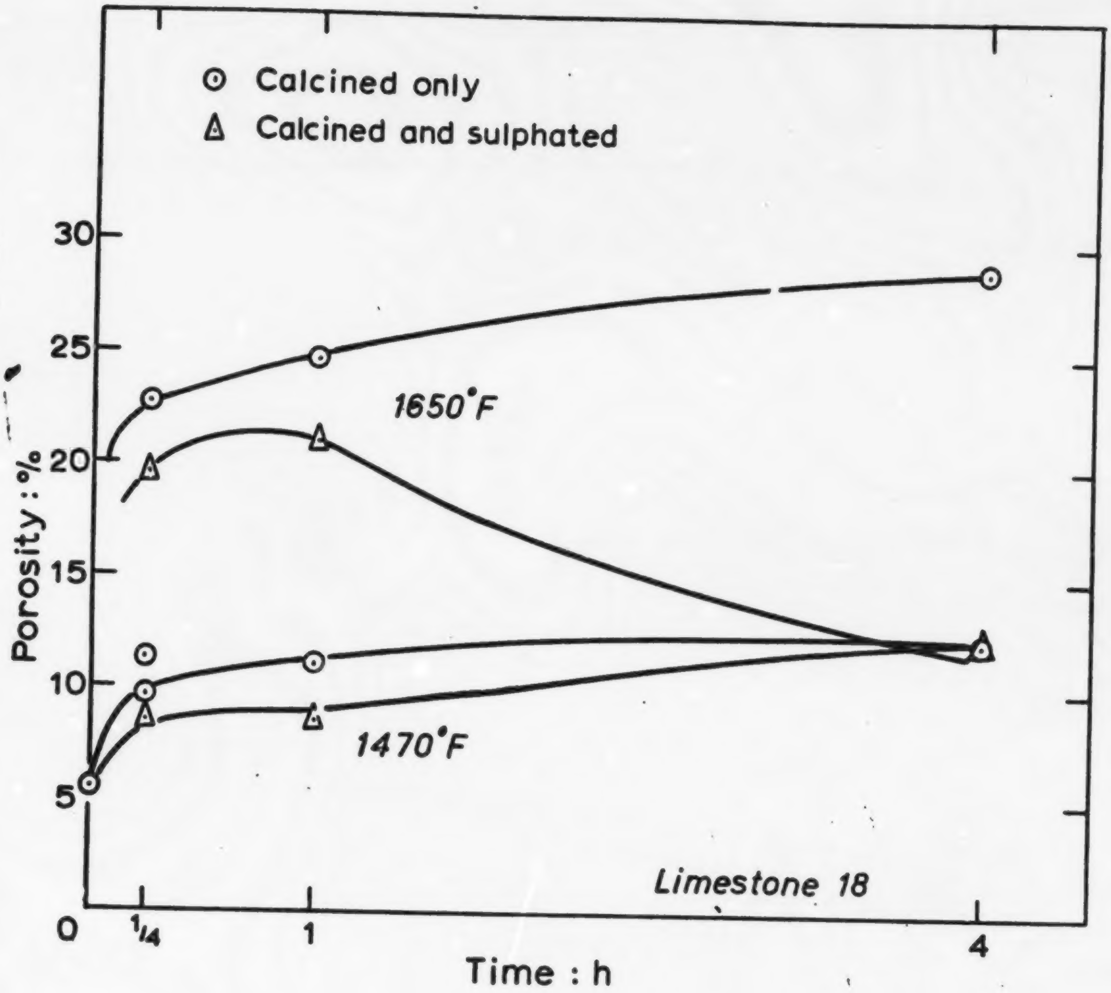

Fig. A 8.34. Variation of porosity (14·5 to 0·3 μm) with time of calcination and sulphation

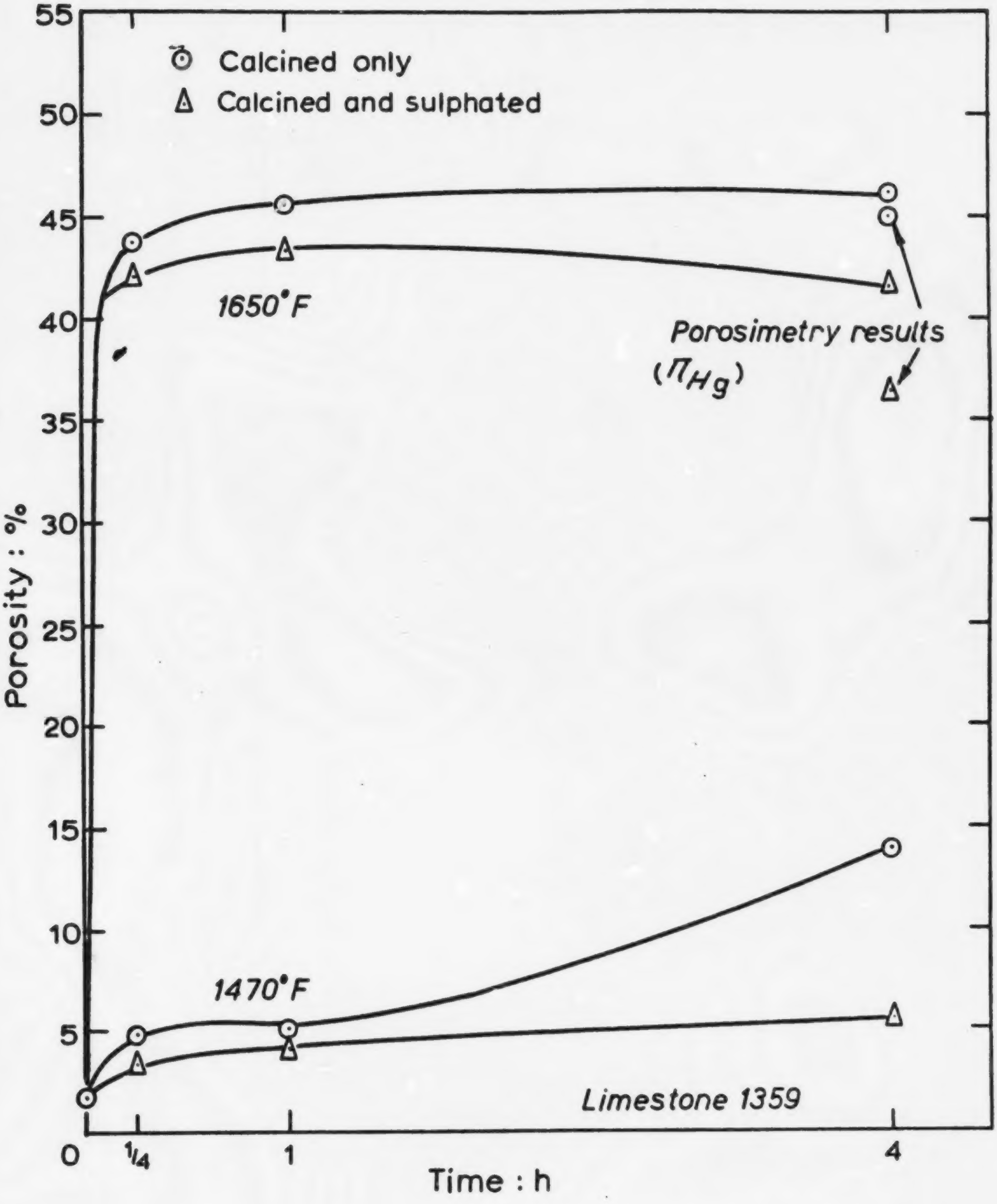

Fig. A 8. 35. Variation of porosity (helium-mercury density) with time of calcination and sulphation

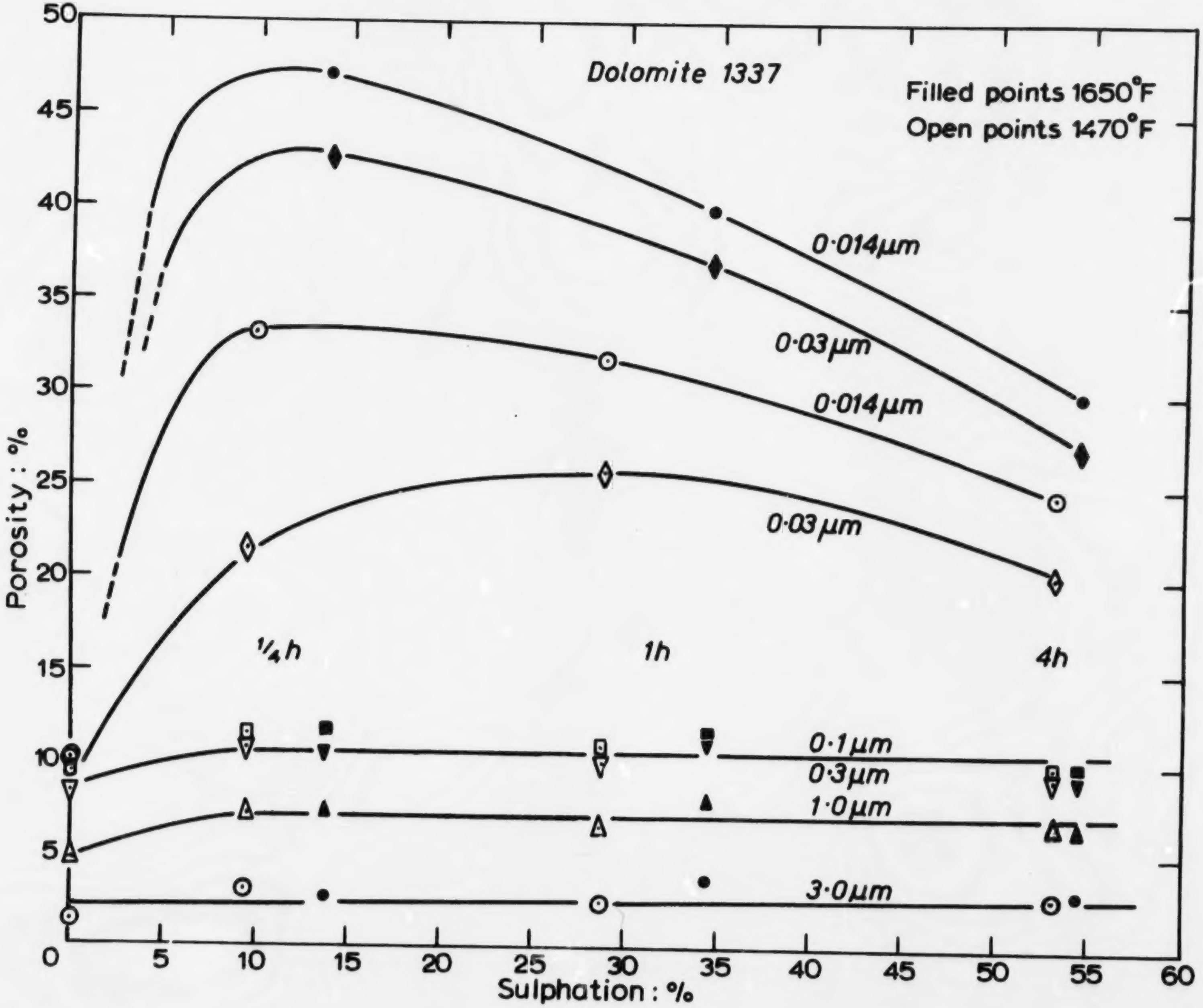

Fig. A 8.36. Variation of porosity (between 14·5µm and pore-entrance dia. shown) with level c sulphation

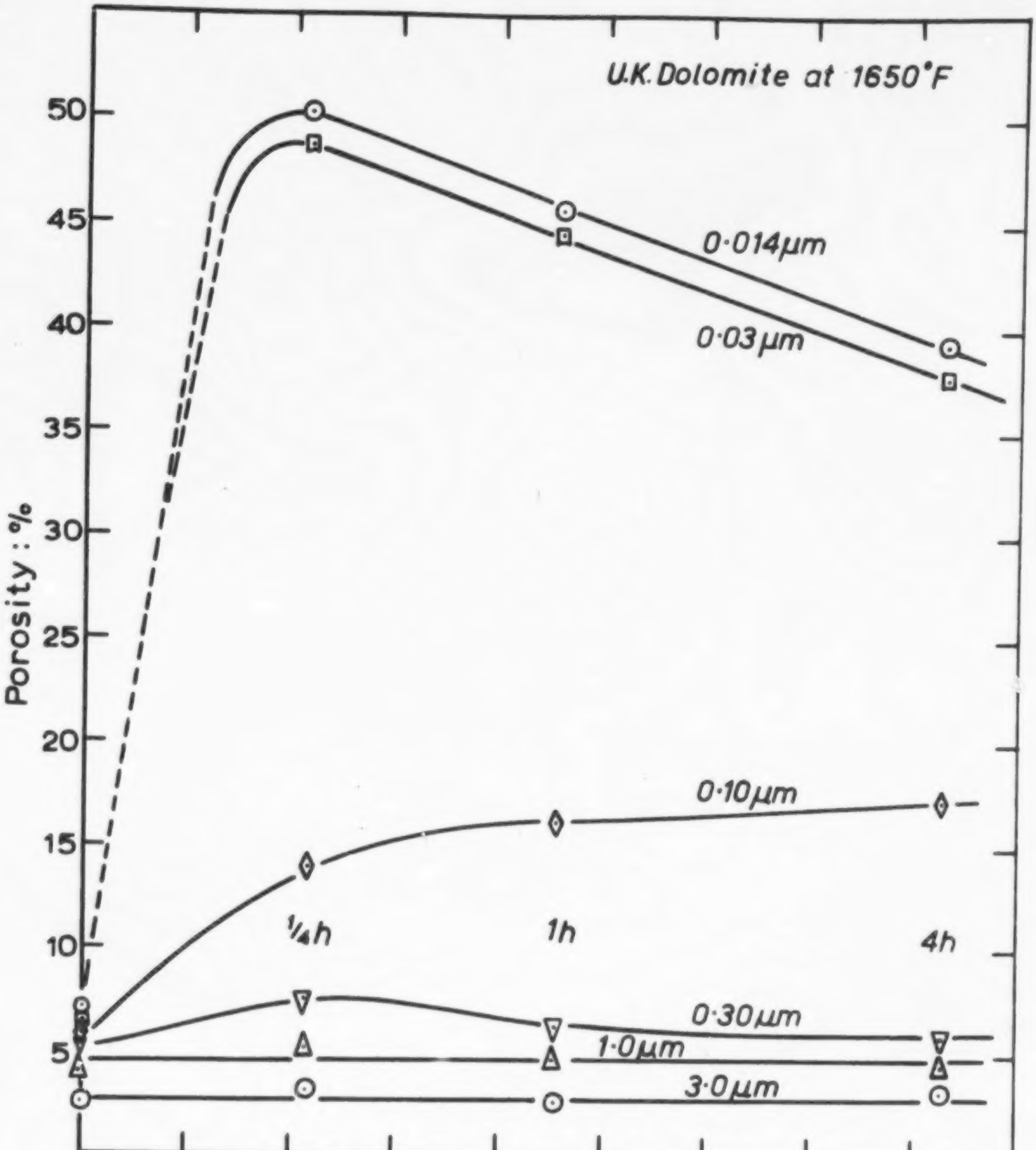

Fig. A 8.37. Variation of porosity (between 14·5μm and pore-entrance dia. shown) with level of sulphation

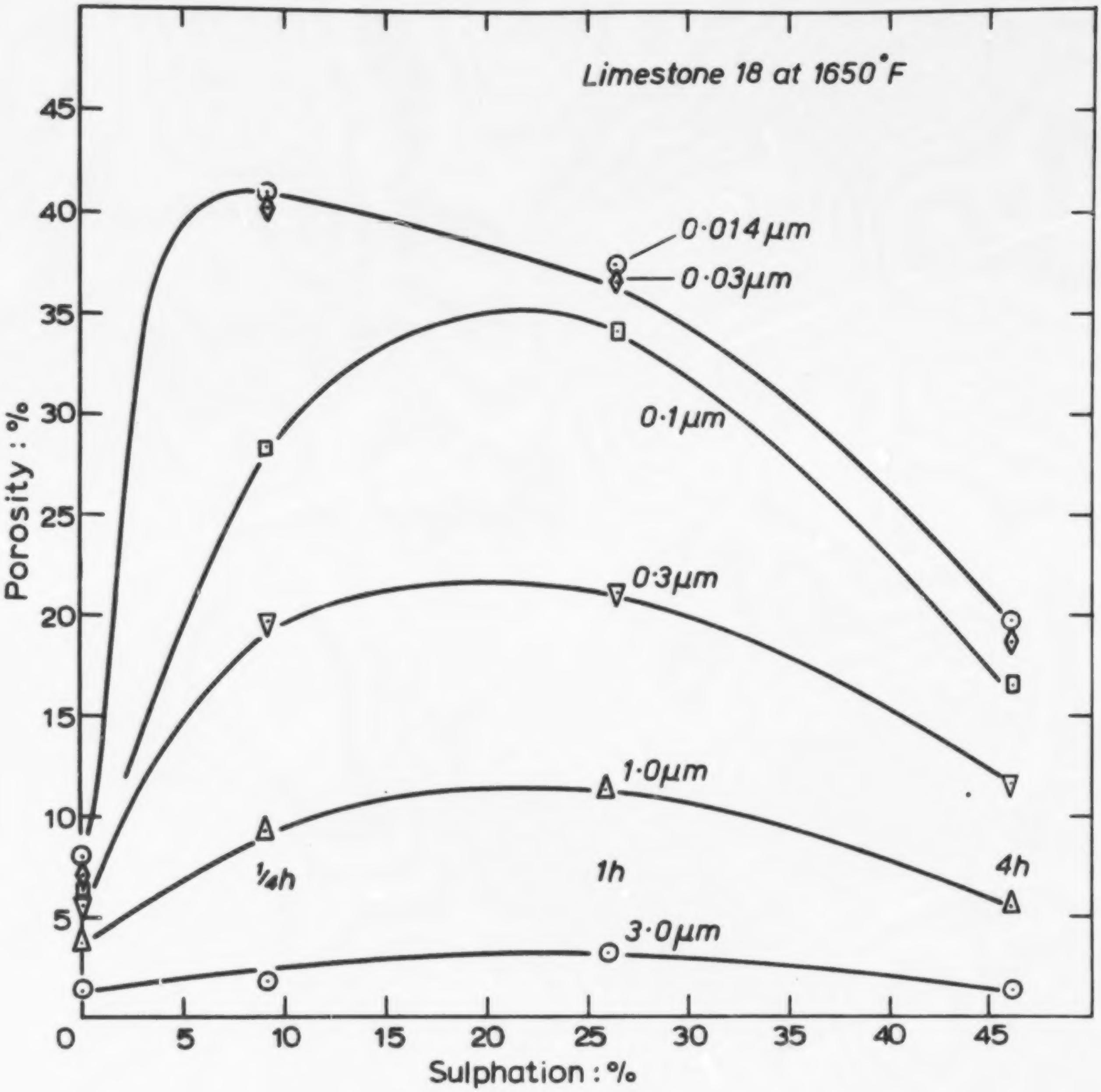

Fig A8. 38. Variation of porosity (between 14·5µm and pore-entrance dia. shown) with level of sulphation

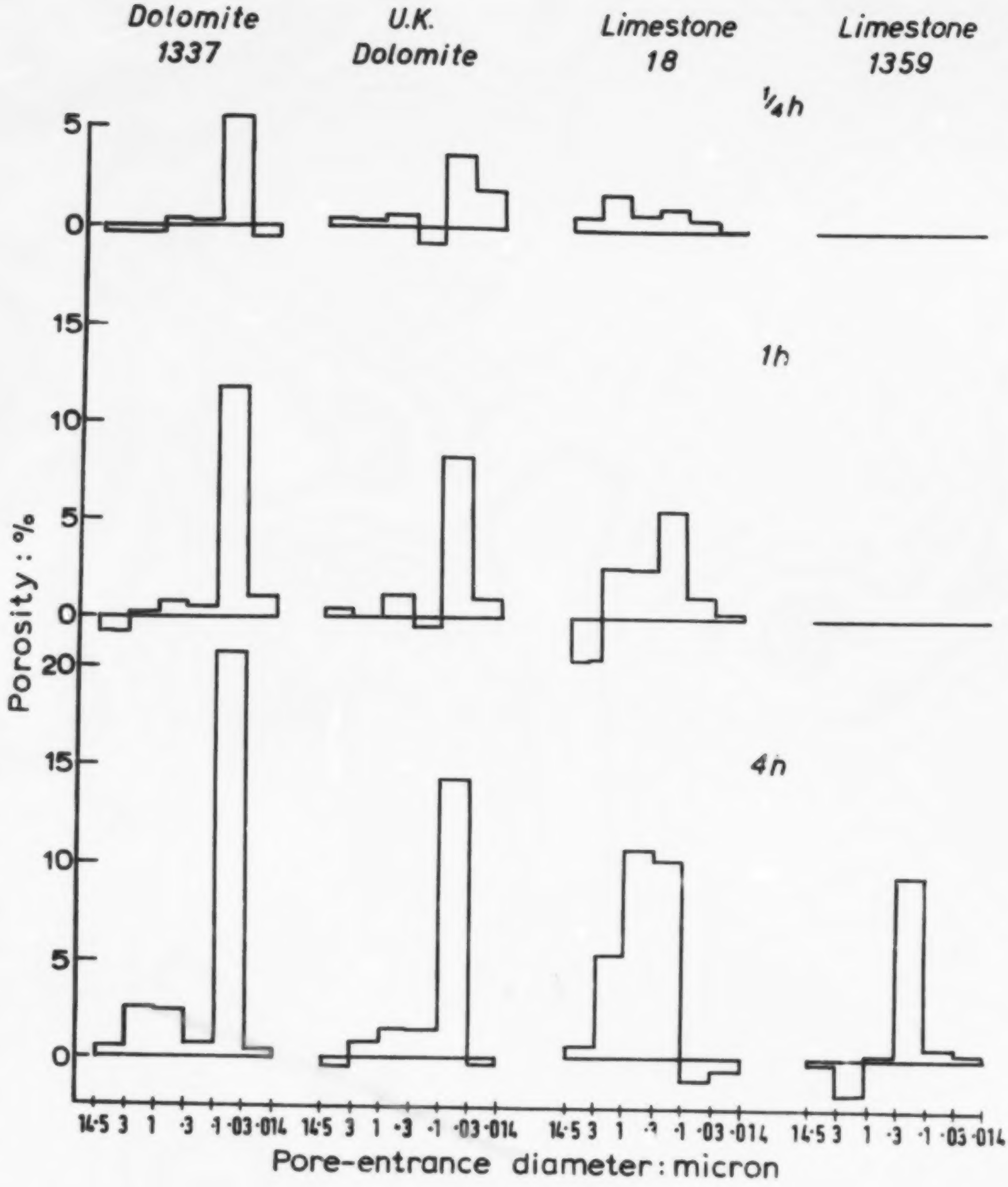

Fig A 8.39. Changes in porosity (% of 'lump' volume) of calcined stones (1650°F), in the ranges of pore-entrance diameter 14·5–3 μm, 3–1 μm, 1–0·3 μm, 0·3–0·1 μm, 0·1–0·03 μm and 0·03–0·014 μm, on sulphation at 1650 °F

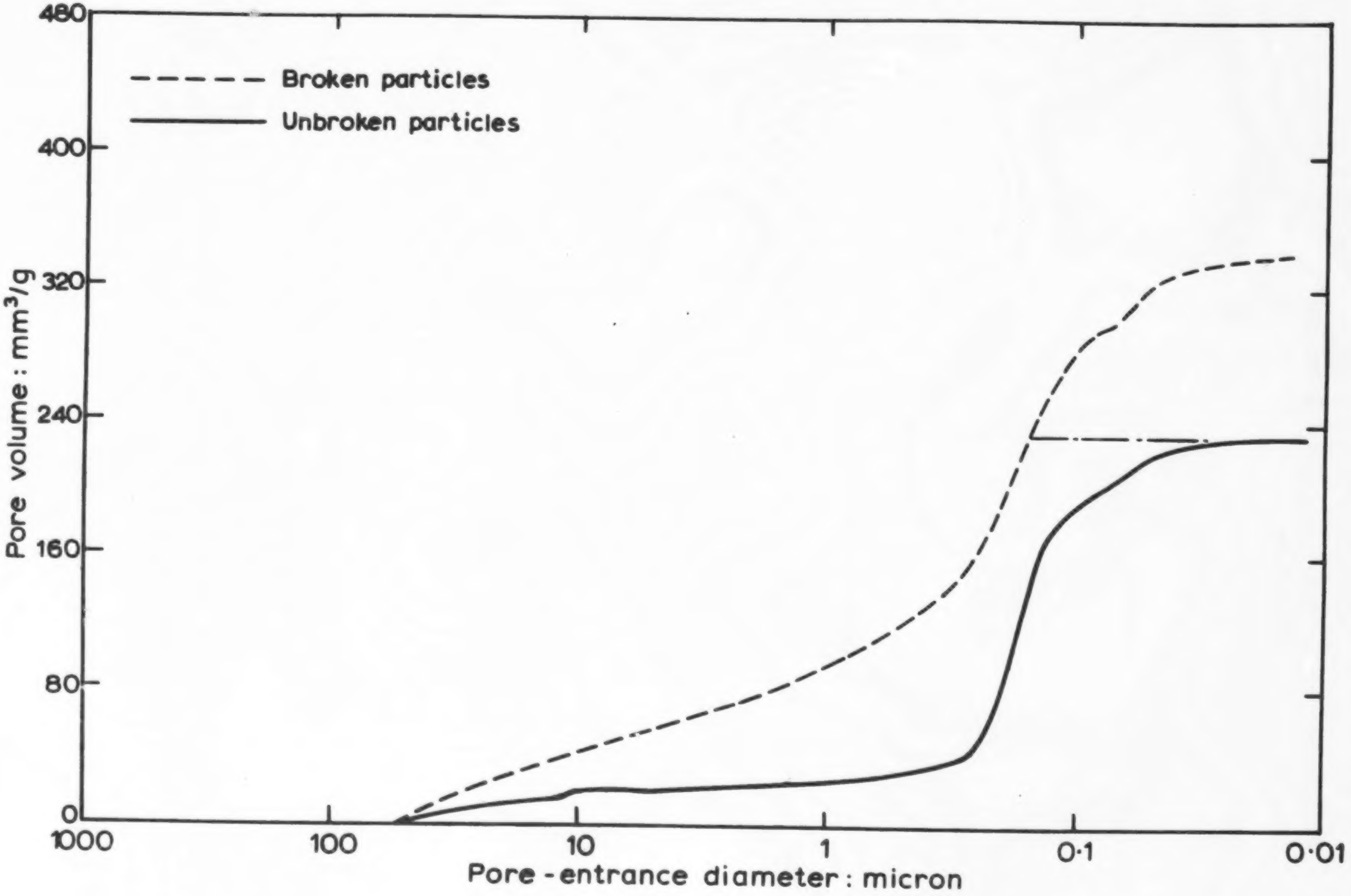

Fig. A8. 40. Effect of breaking Limestone 1359 particles (3·6% w/wS)

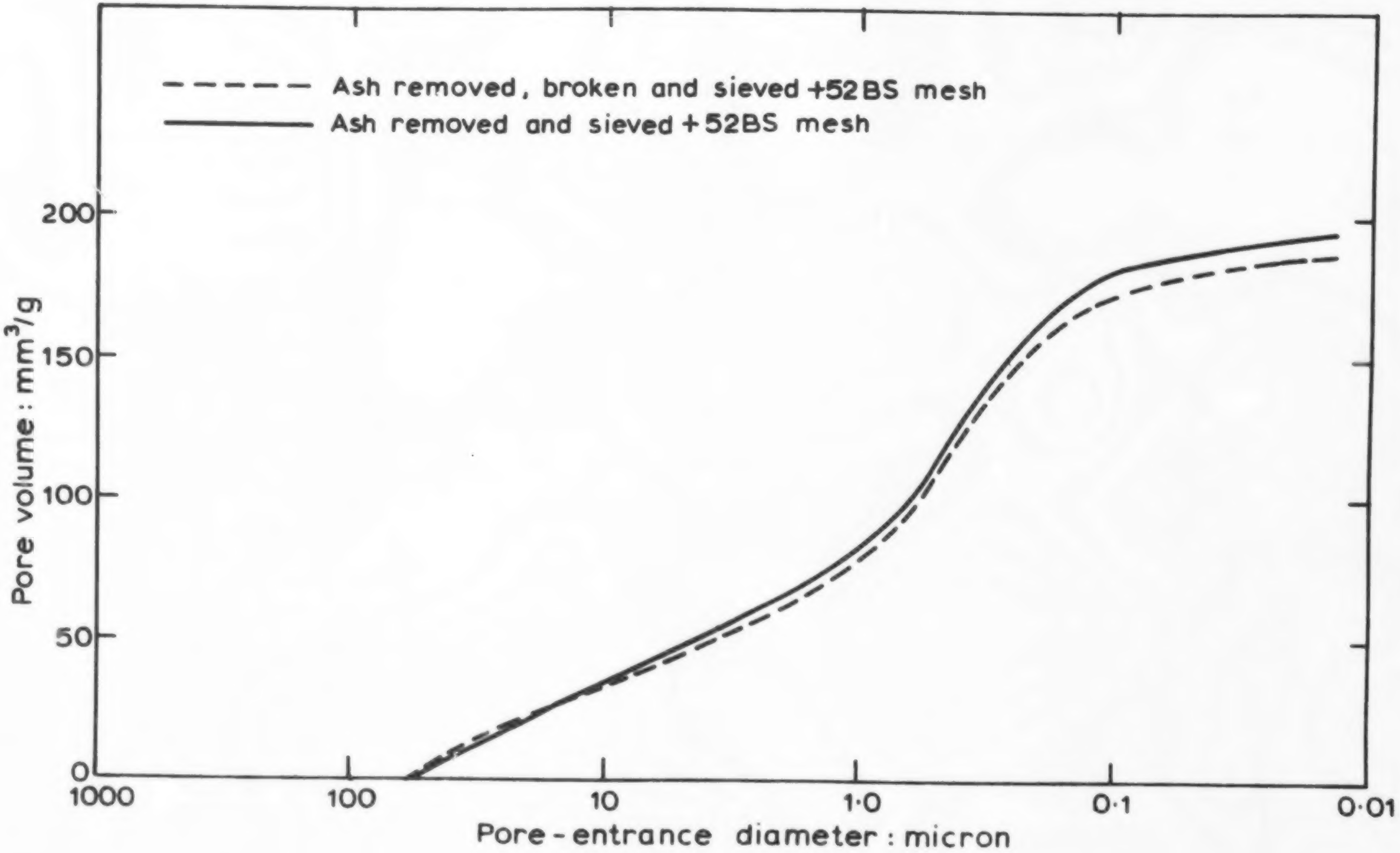

Fig. A8. 41. Task V. Test 1.2. Effect of breaking Limestone 1359 particles from the bed (5·2% w/ws)

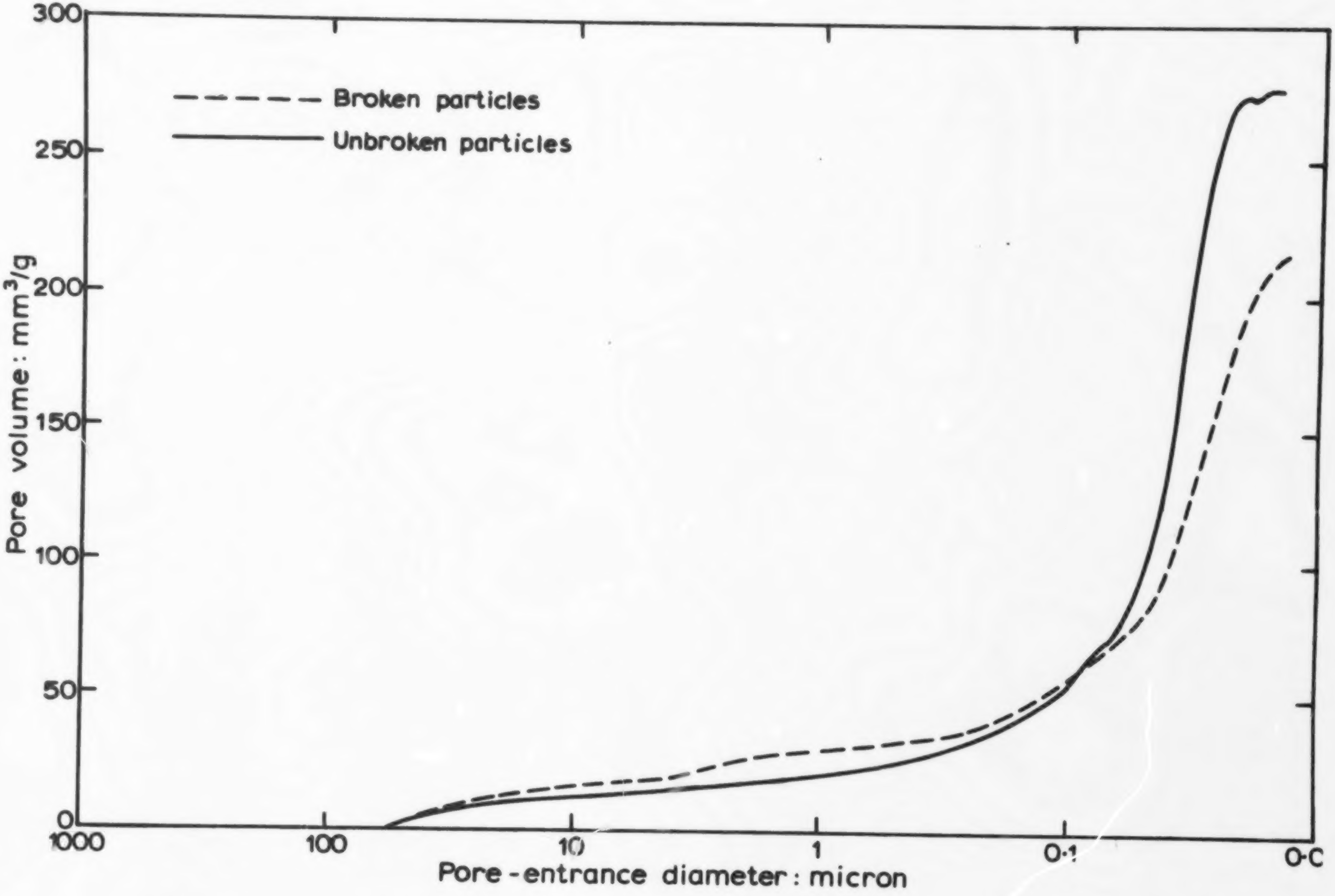

Fig. A8.42. Effect of breaking Limestone 1359 particles (100% calcined)

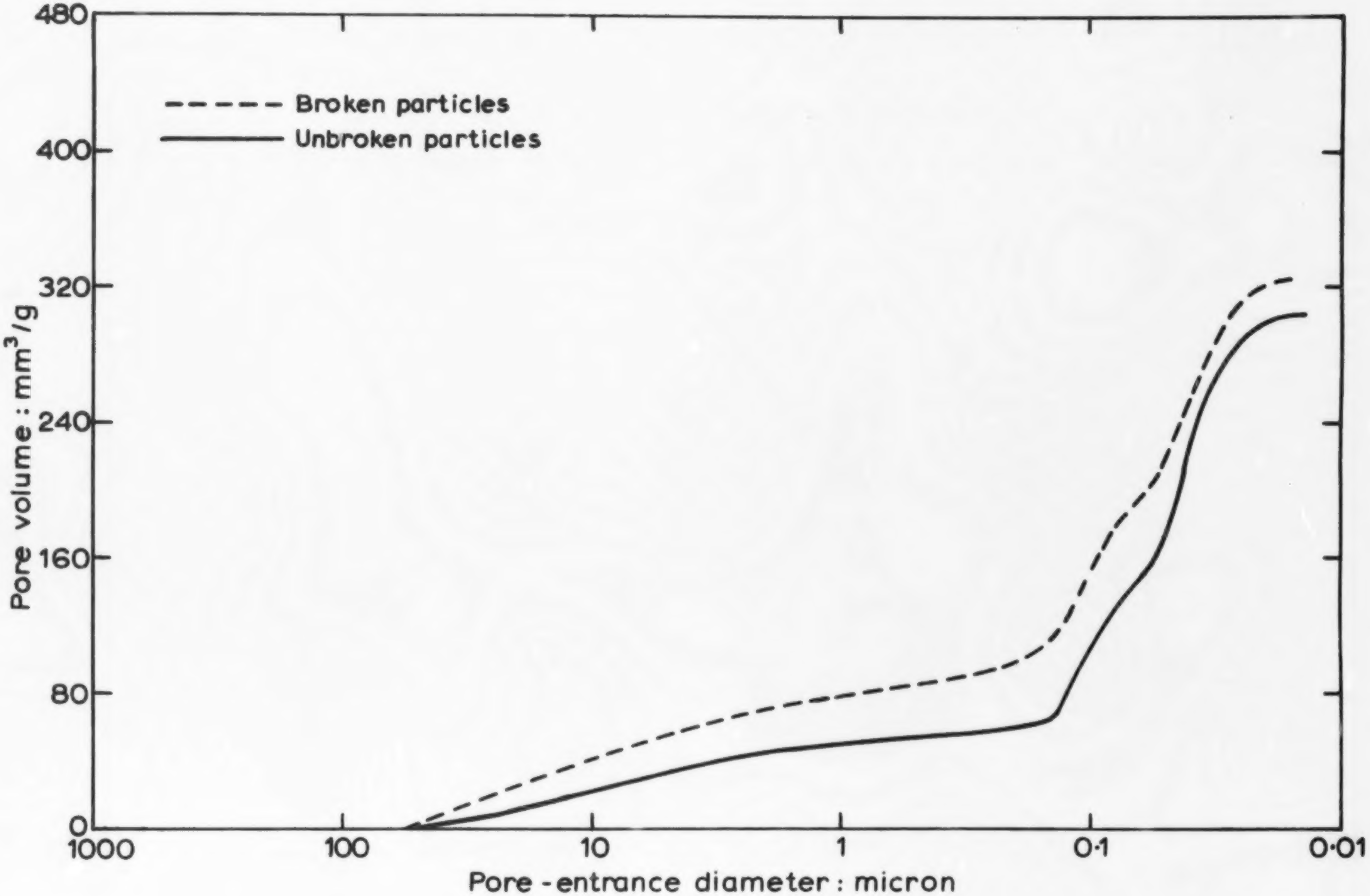

Fig. A 8.43. Effect of breaking U.K. dolomite particles (4·9% w/wS)

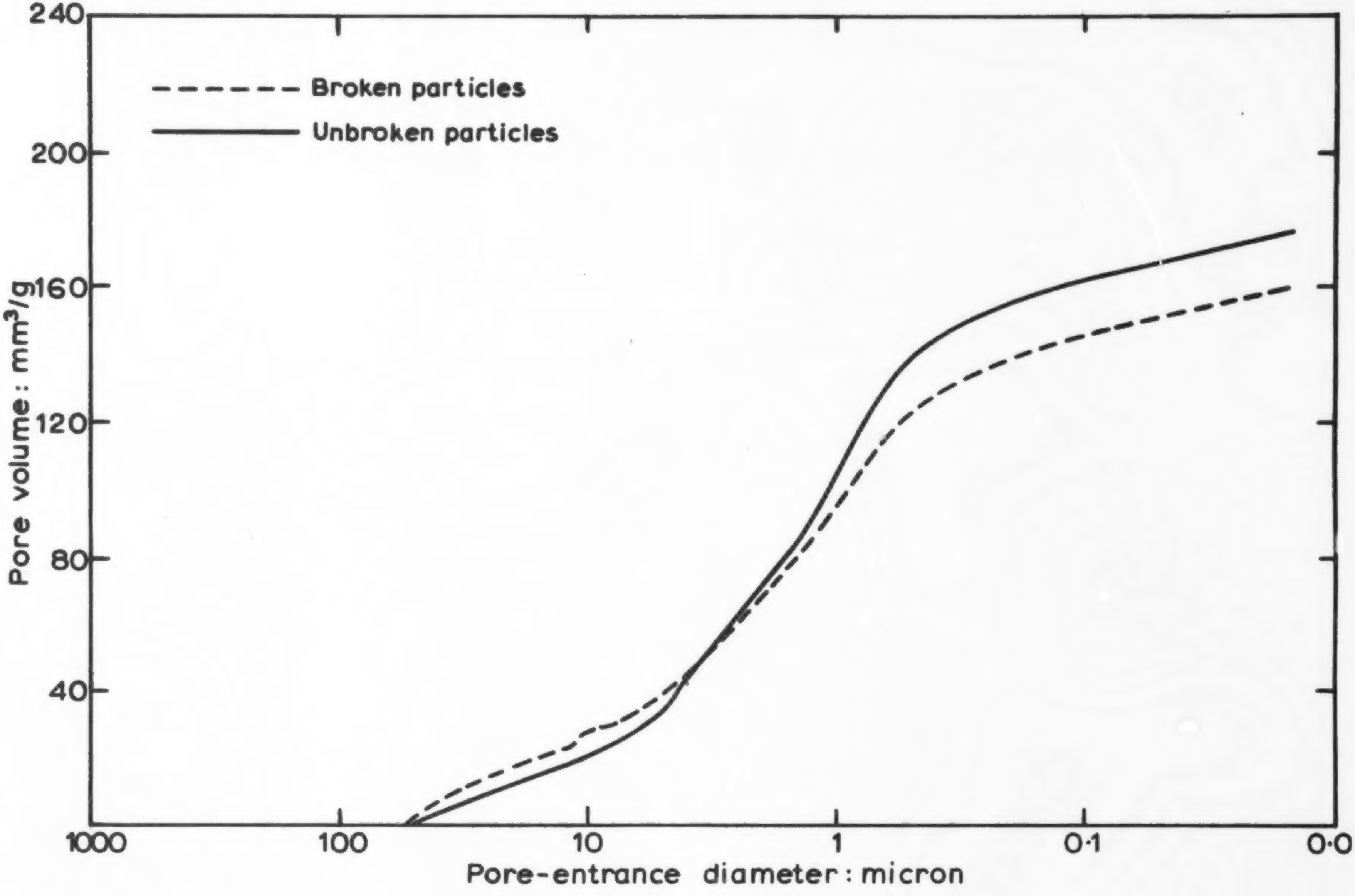

Fig. A8.44 Effect of breaking U.K. dolomite particles (7·6% w/wS)

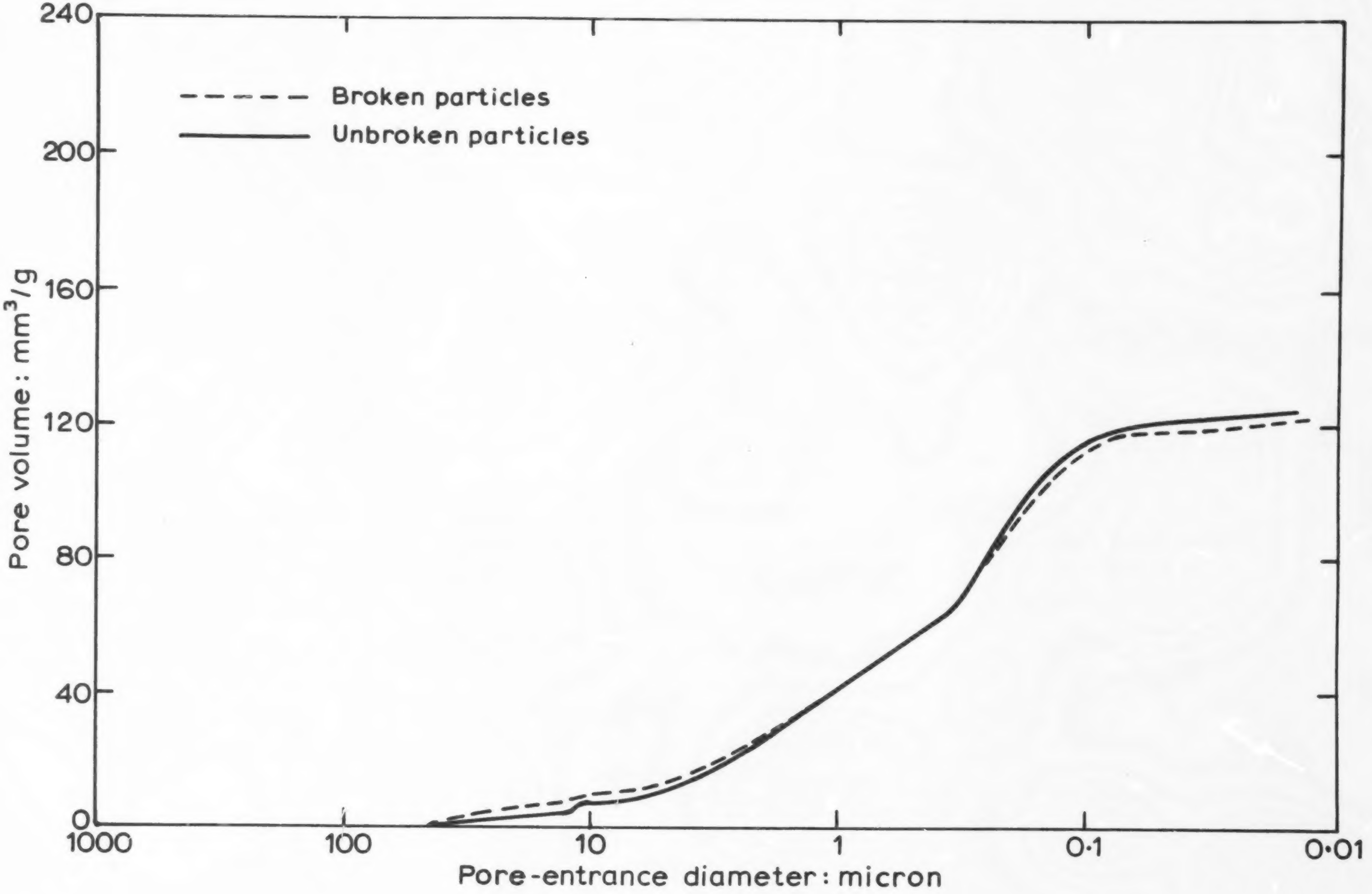

Fig. A 8.45. Effect of breaking Dolomite 1337 particles (9·3% w/wS)

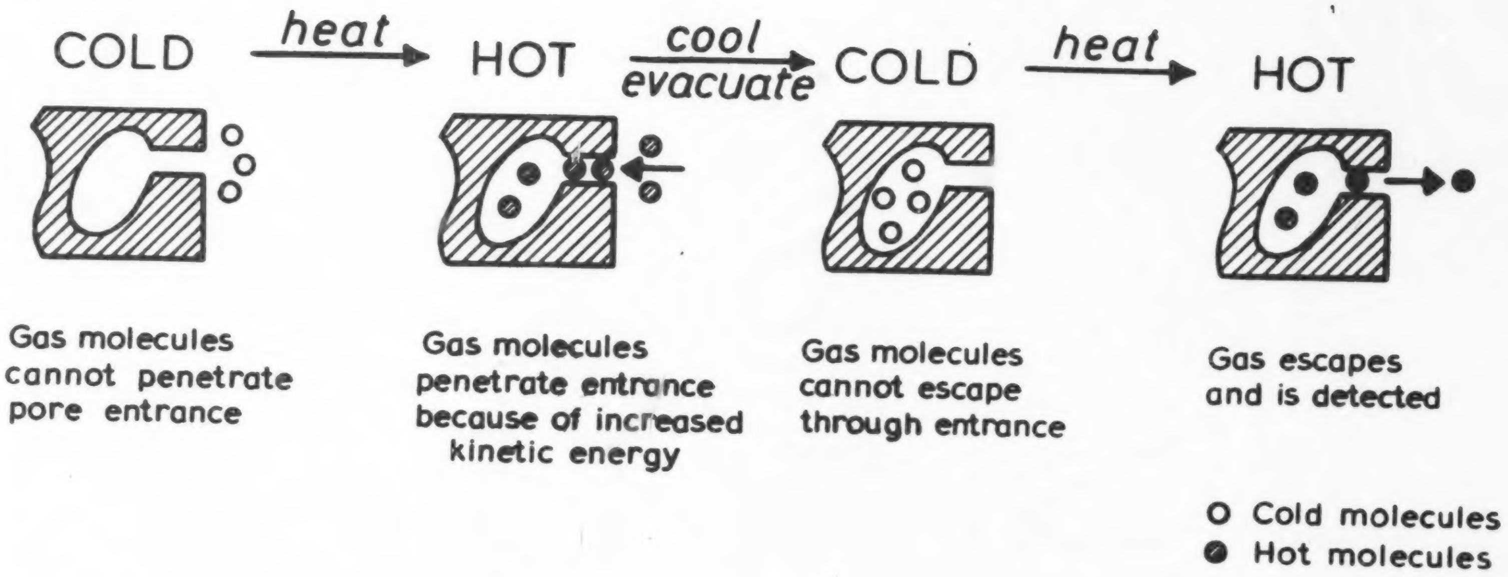
COLD
heat
HOT
cool
evacuate
COLD
heat
HOT
Gas molecules cannot penetrate pore entrance
Gas molecules penetrate entrance because of increased kinetic energy
Gas molecules cannot escape through entrance
Gas escapes and is detected
○ Cold molecules
● Hot molecules

Fig. A8.46. How an increase in accessible porosity may occur on heating, and how it is detected

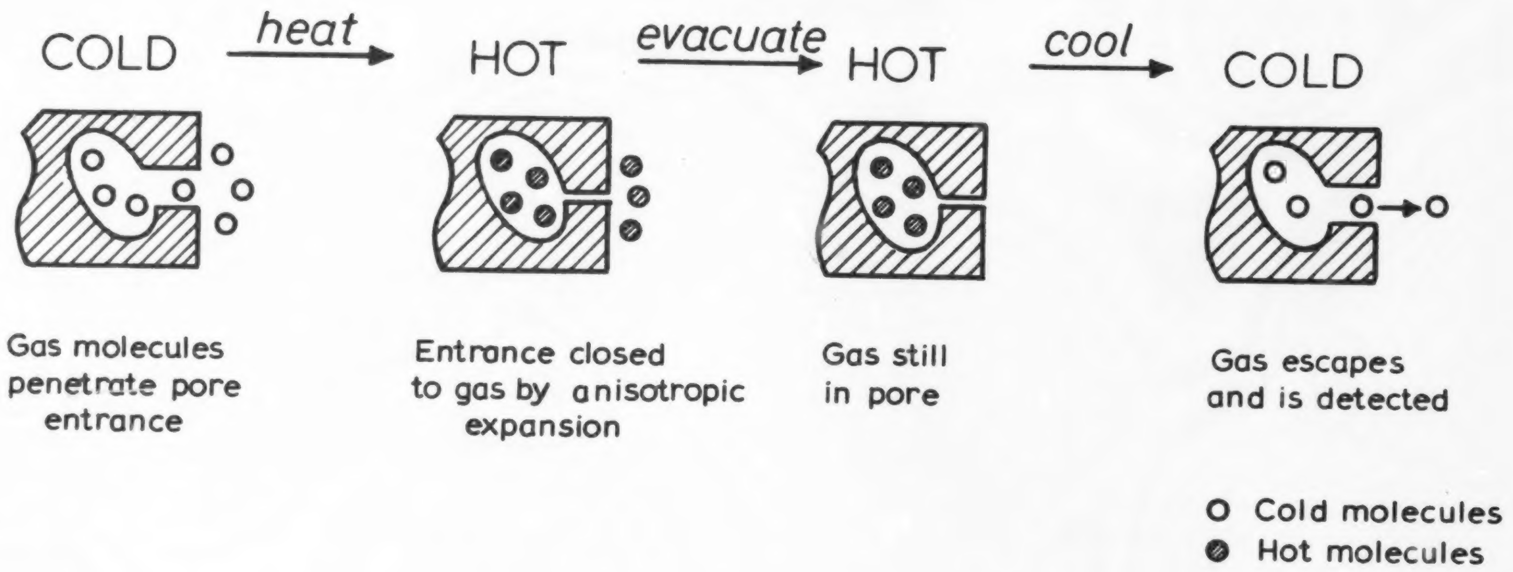
COLD
heat
HOT
evacuate
HOT
cool
COLD
Gas molecules penetrate pore entrance
Entrance closed to gas by anisotropic expansion
Gas still in pore
Gas escapes and is detected
○ Cold molecules
● Hot molecules

Fig. A 8. 47. How a decrease in accessible porosity may occur on heating, and how it is detected

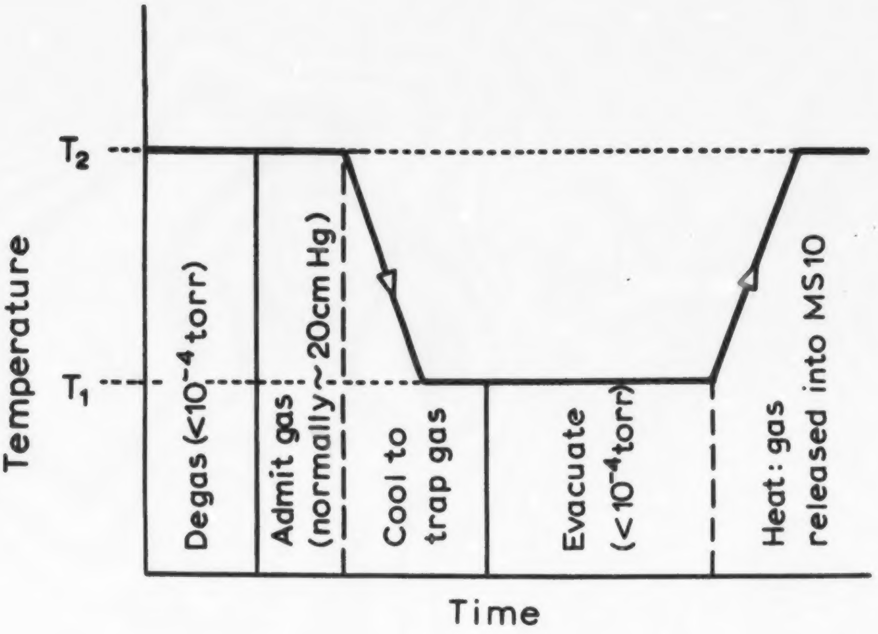
T2
T1
Temperature
Time
Degas (<10^{-4} torr)
Admit gas (normally ~ 20cm Hg)
Cool to trap gas
Evacuate (<10^{-4} torr)
Heat: gas released into MS10

Fig. A8. 48(a). Pore penetration: outline of experiment

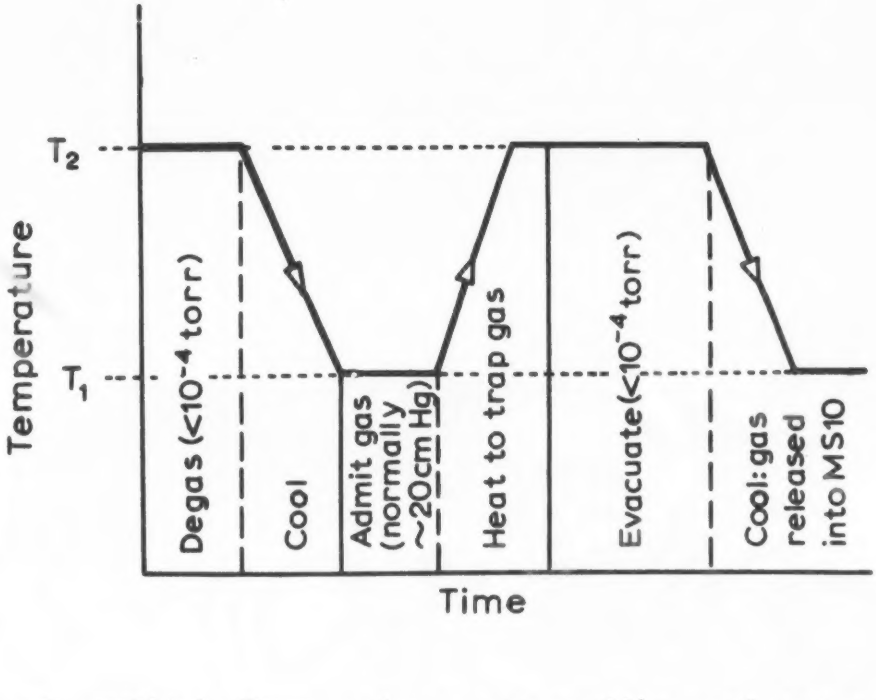
T2
T1
Temperature
Time
Degas (<10^{-4} torr)
Cool
Admit gas (normally ~20cm Hg)
Heat to trap gas
Evacuate (<10^{-4} torr)
Cool: gas released into MS10

Fig. A8. 48(b). Pore closure: outline of experiment

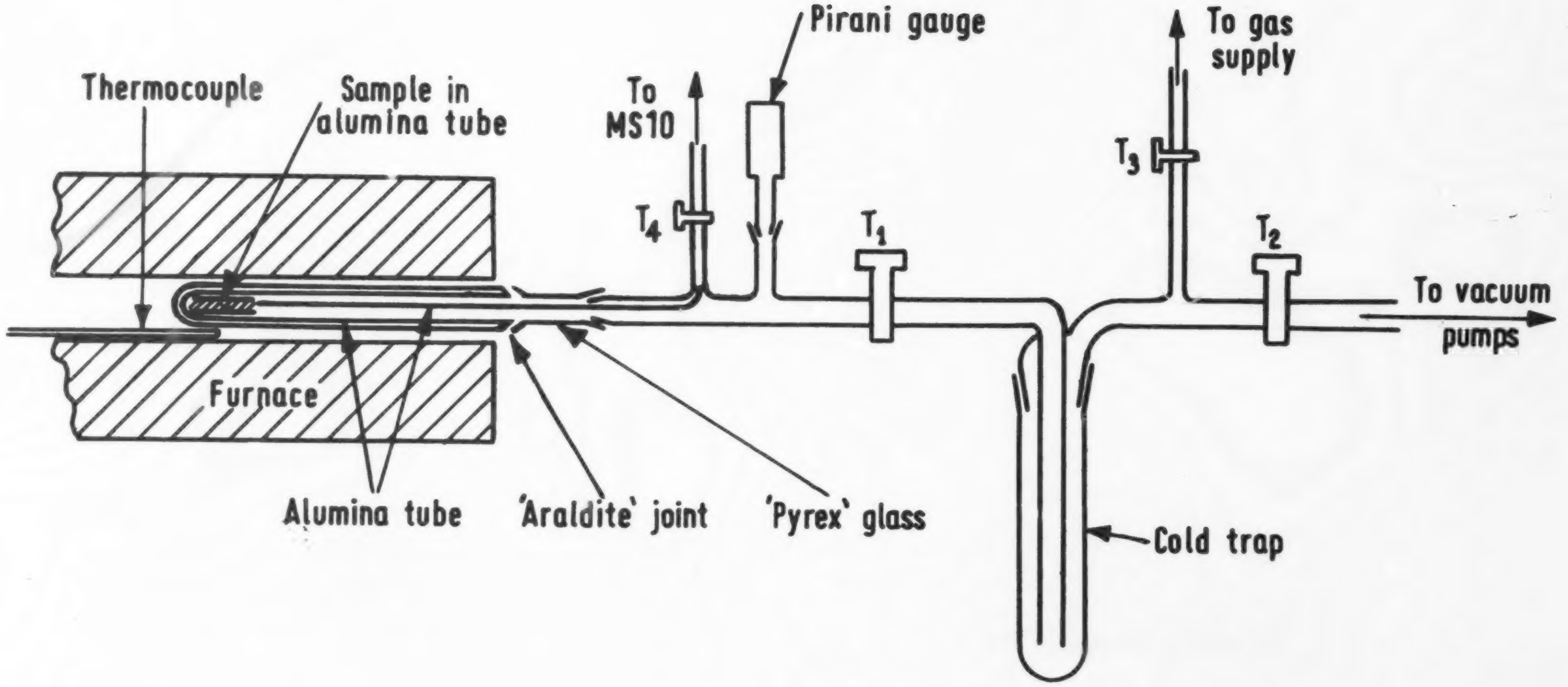
Thermocouple
Sample in alumina tube
To MS10
T4
Pirani gauge
T1
T3
To gas supply
T2
To vacuum pumps
Furnace
Alumina tube
'Araldite' joint
'Pyrex' glass
Cold trap

Fig. A8. 49. Pore-penetration, pore-closure apparatus

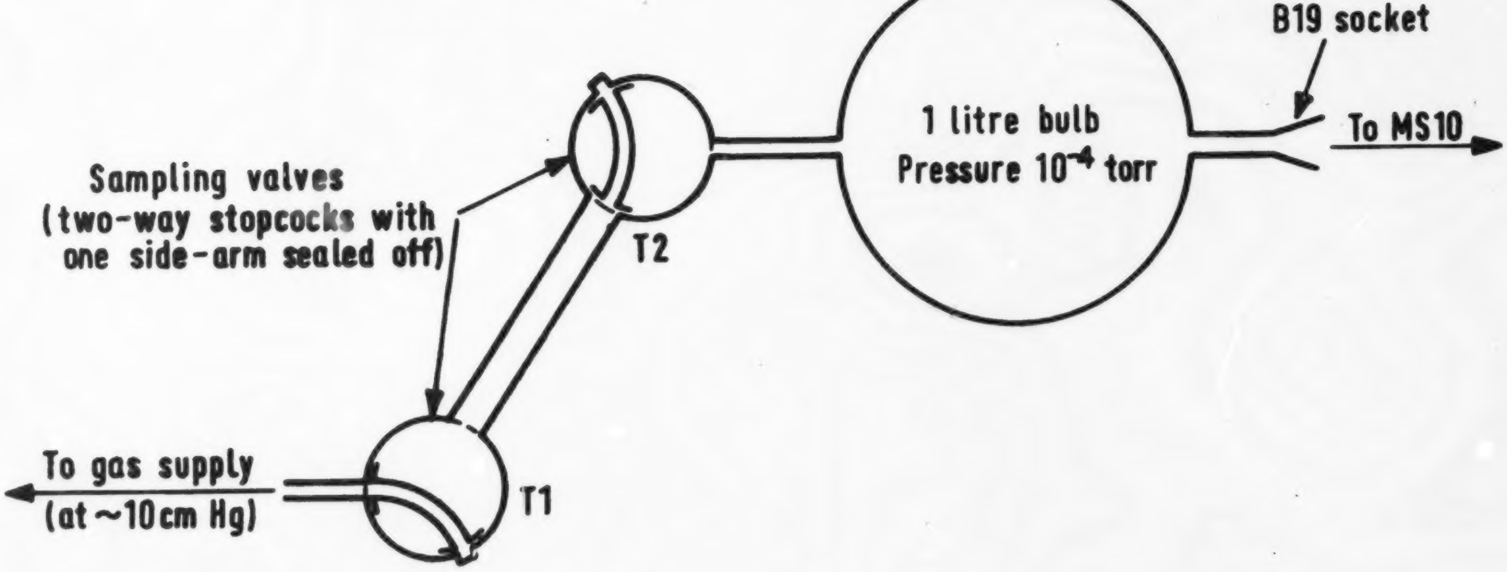
B19 socket
To MS10
1 litre bulb
Pressure 10^{-4} torr
Sampling valves
(two-way stopcocks with
one side-arm sealed off)
T2
T1
To gas supply
(at ~10cm Hg)

Fig. A8.50. Calibration system

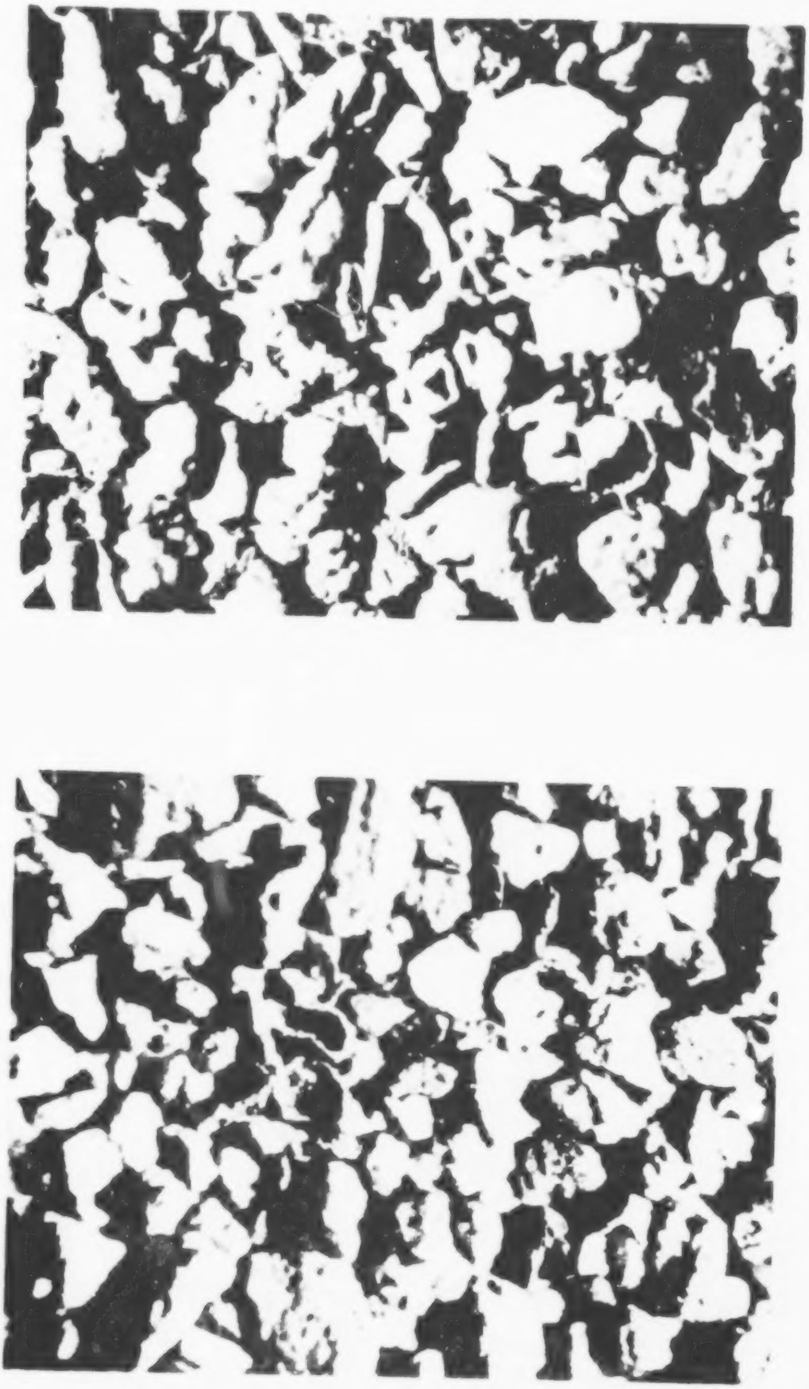

Fig. A8. 51. Shells formed during Task II, Test Series 2. U.K. Dolomite particles x10 magnification

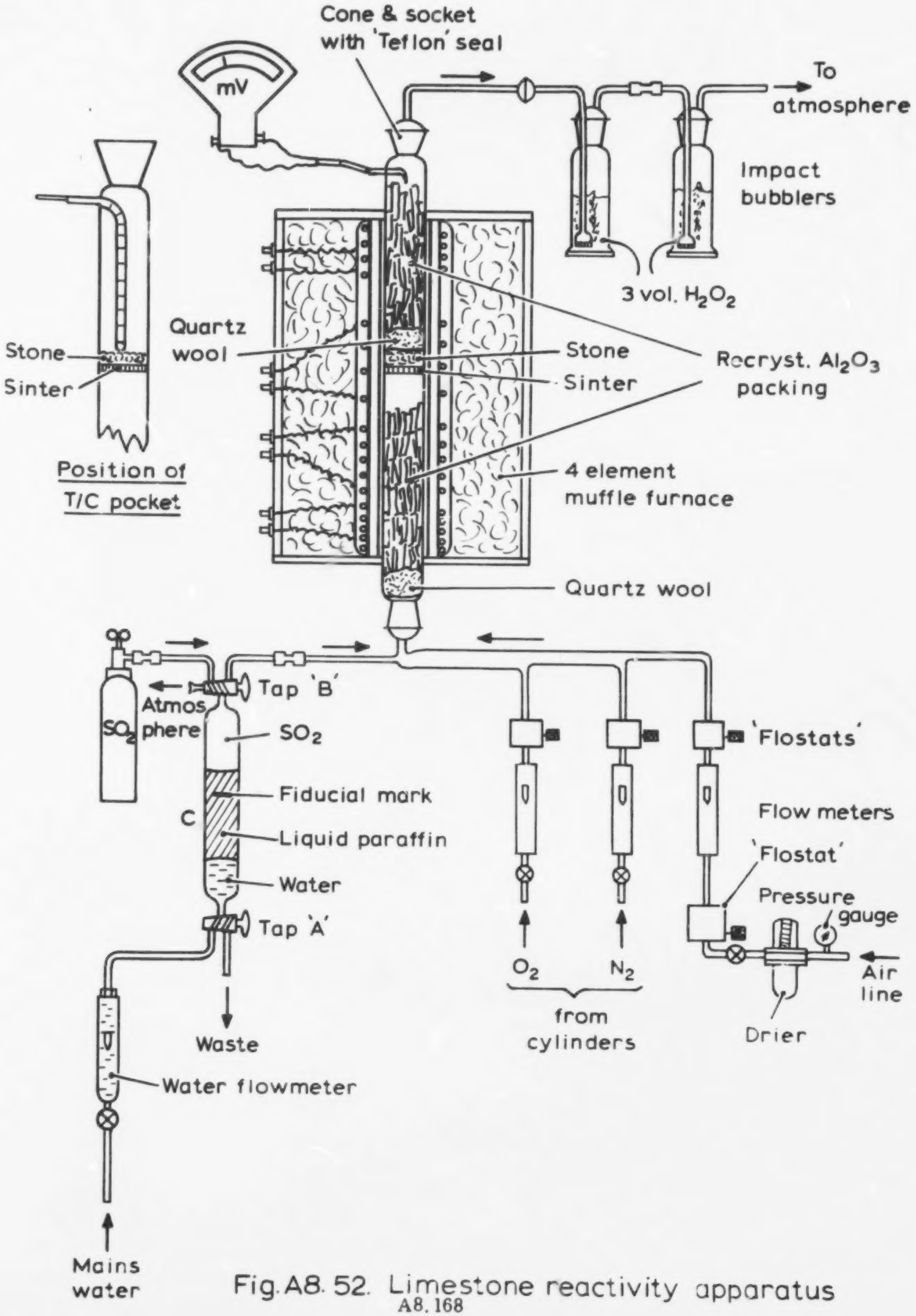
Cone & socket with 'Teflon' seal
mV
To atmosphere
Impact bubblers
3 vol. H_2O_2
Stone
Sinter
Position of T/C pocket
Quartz wool
Stone
Sinter
Recryst. Al_2O_3 packing
4 element muffle furnace
Quartz wool
Tap 'B'
Atmos phere
SO_2
SO_2
Fiducial mark
C
Liquid paraffin
Water
Tap 'A'
Waste
Water flowmeter
Mains water
'Flostats'
Flow meters
'Flostat'
Pressure gauge
O_2
N_2
from cylinders
Air line
Drier

Fig. A8. 52. Limestone reactivity apparatus

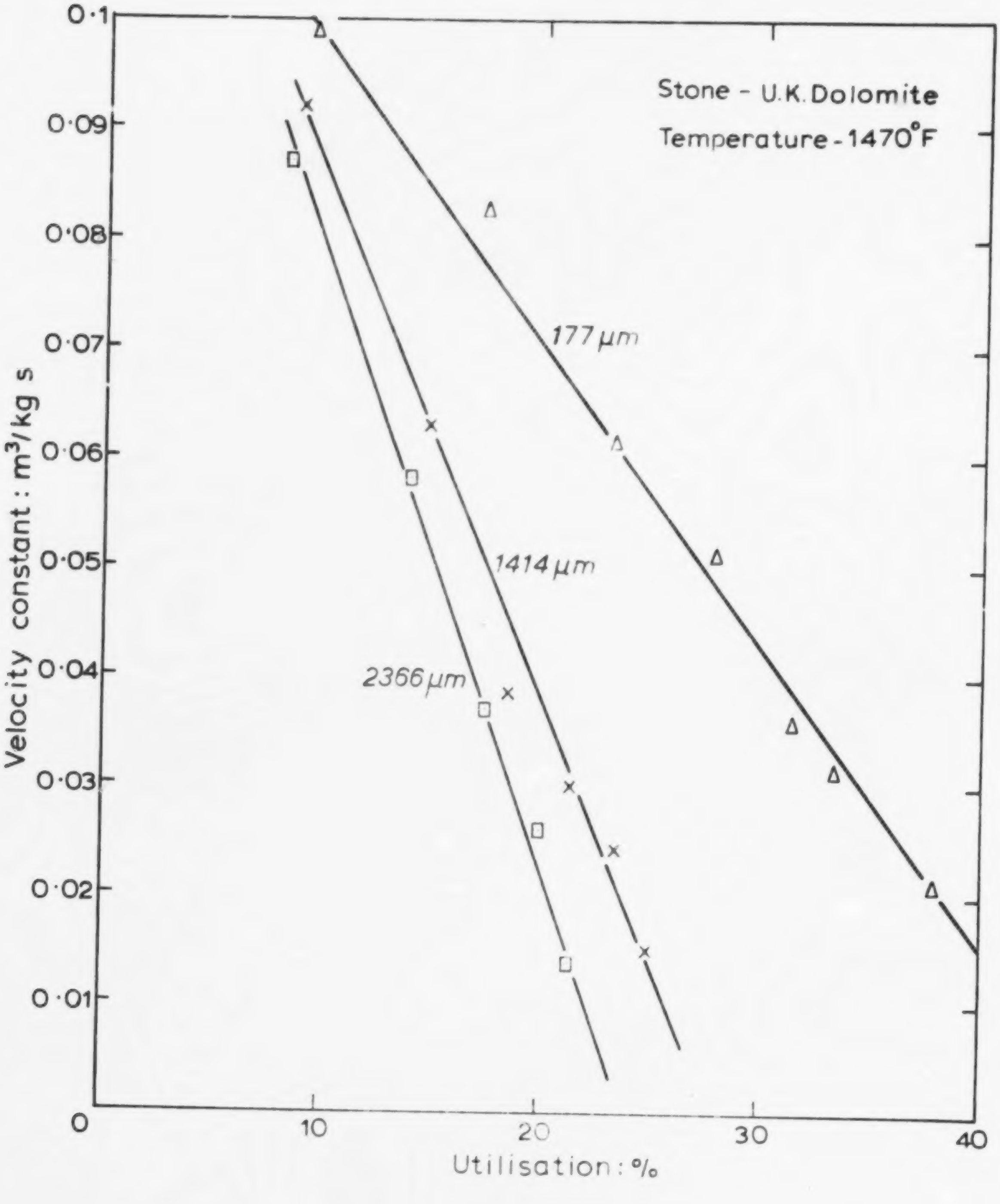

Fig.A8.53. Velocity constant as a function of size and utilisation

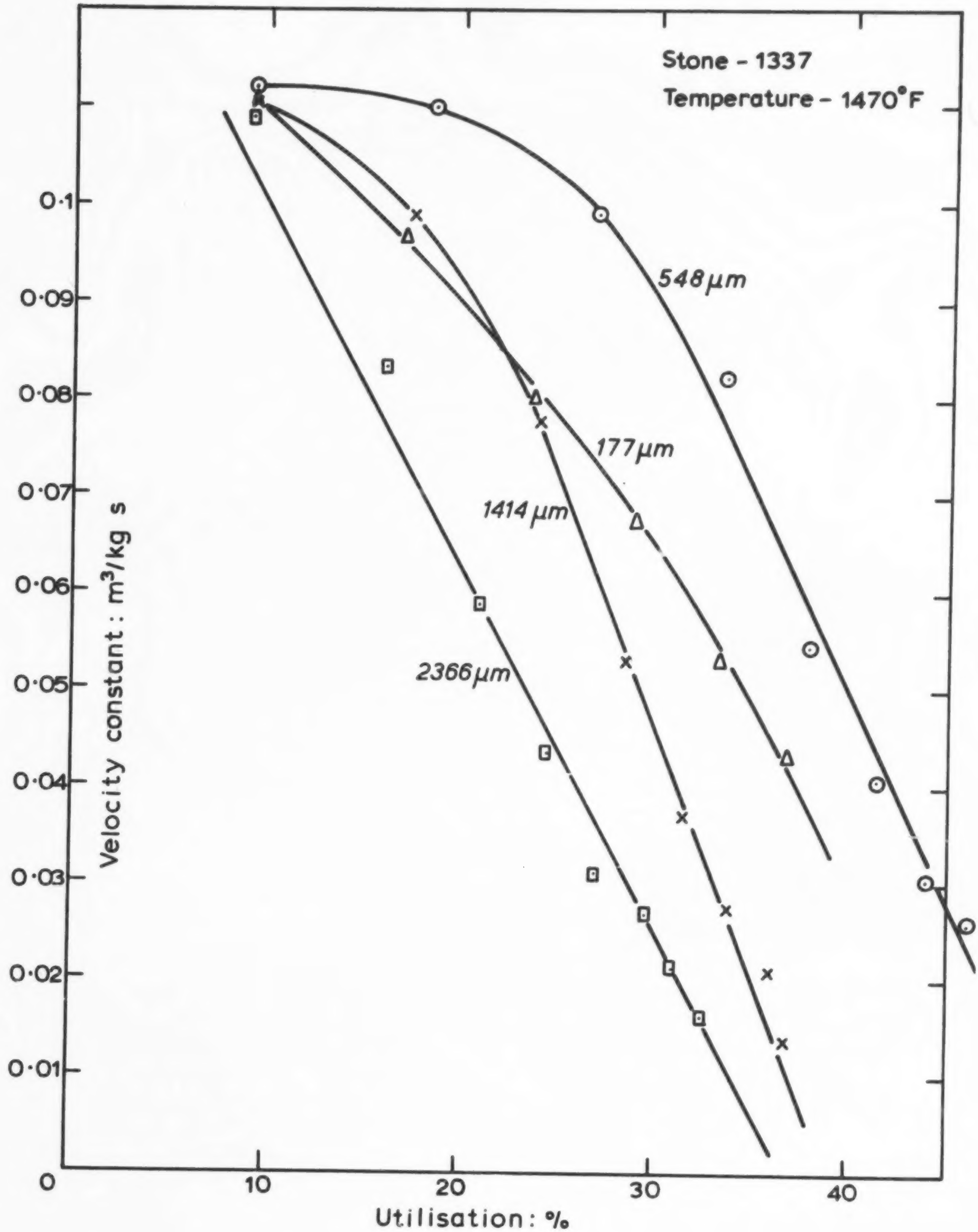

Fig. A8. 54. Velocity constant as a function of size and utilisation

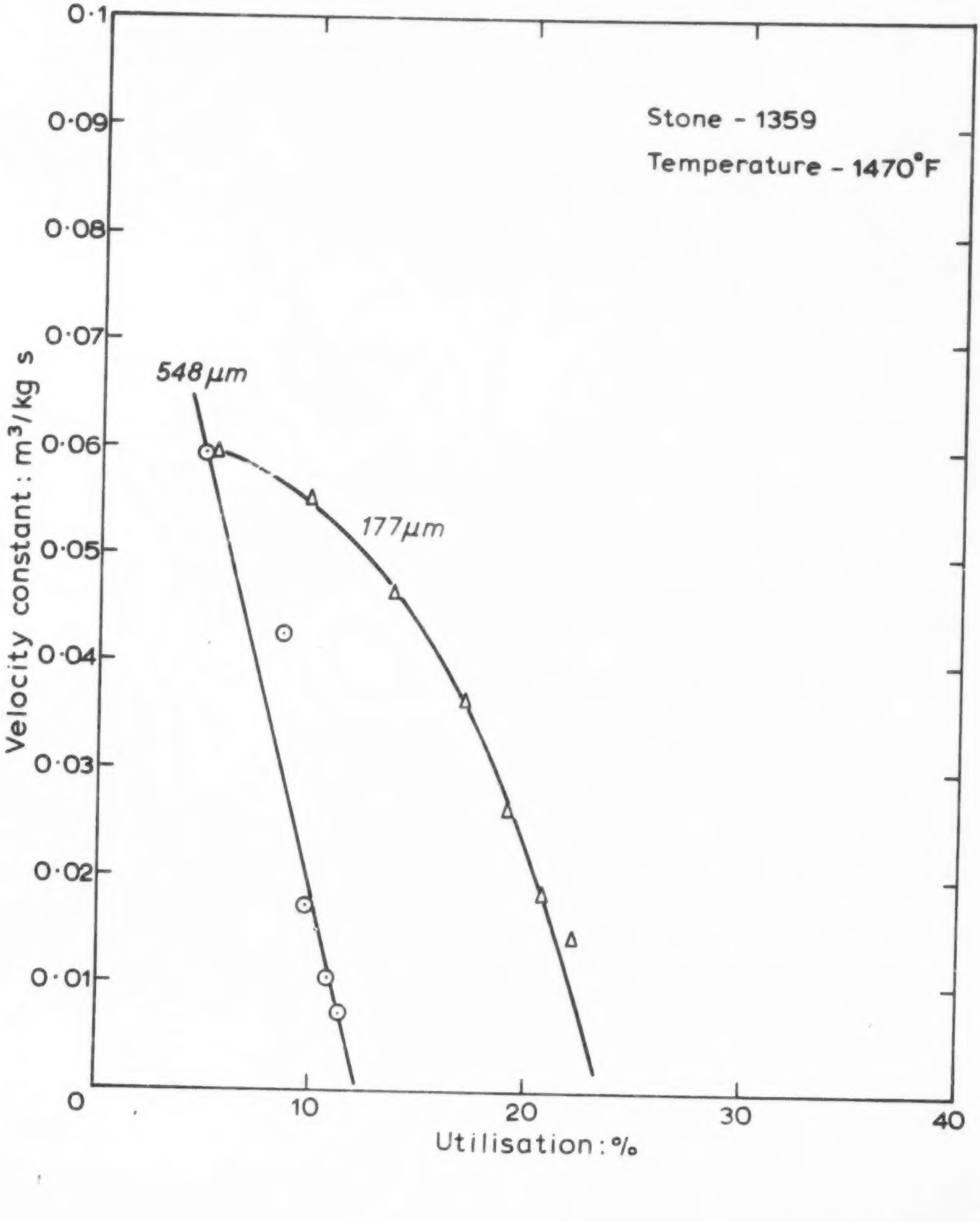

Fig.A8.55. Velocity constant as a function of size and utilisation

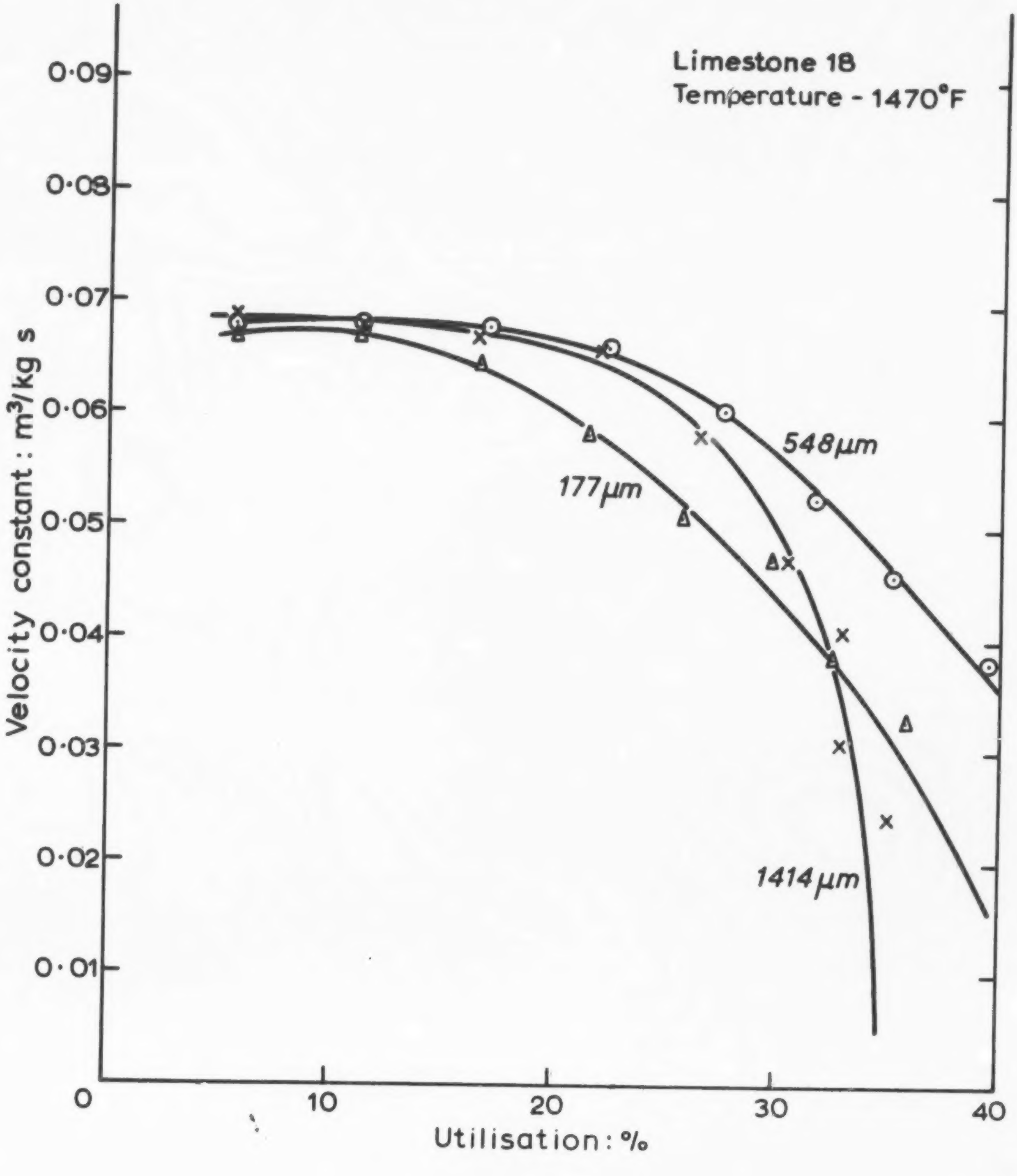

Fig. A8.56. Velocity constant as a function of size and utilisation

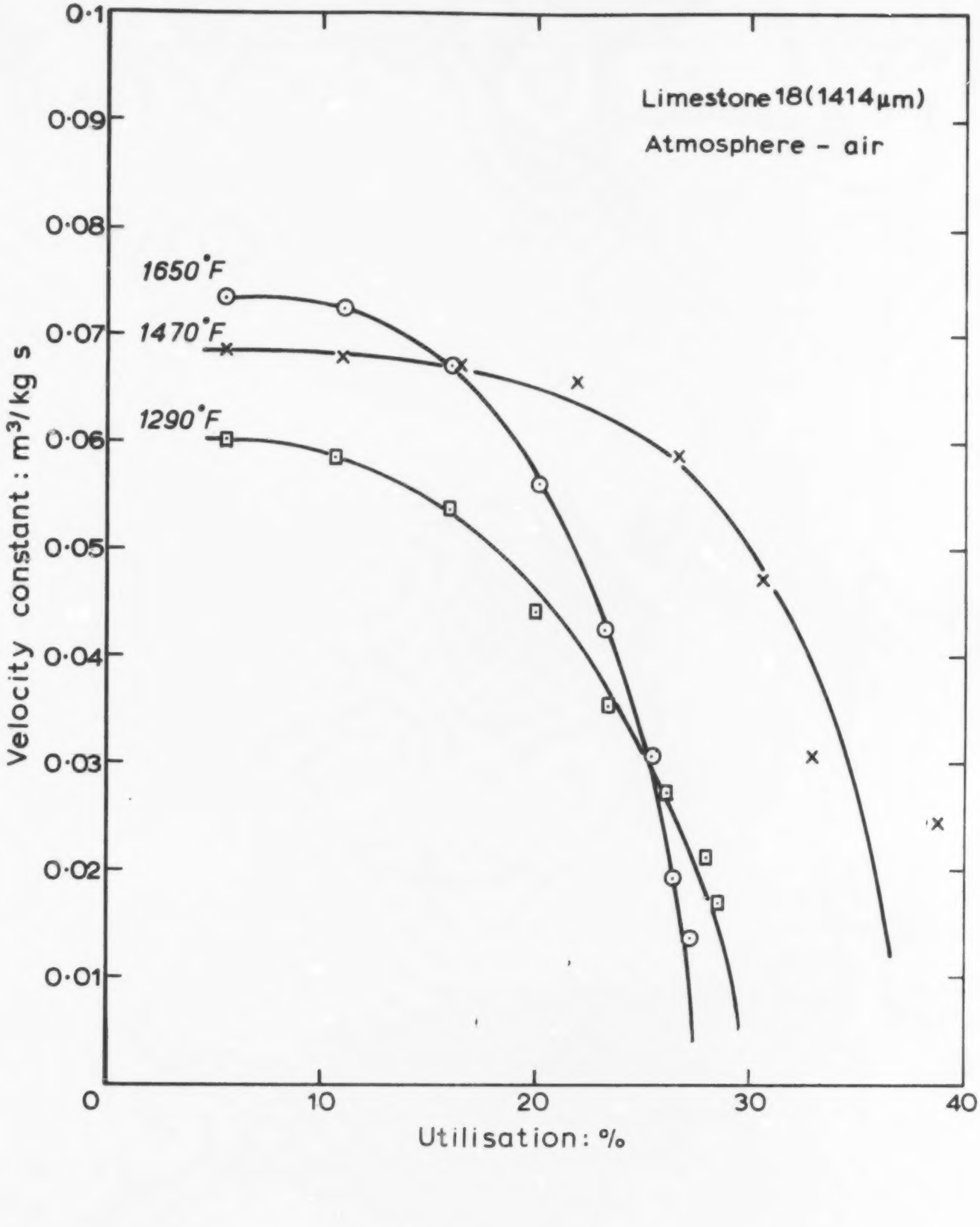

Fig. A8.57. Velocity constant as a function of temperature and utilisation

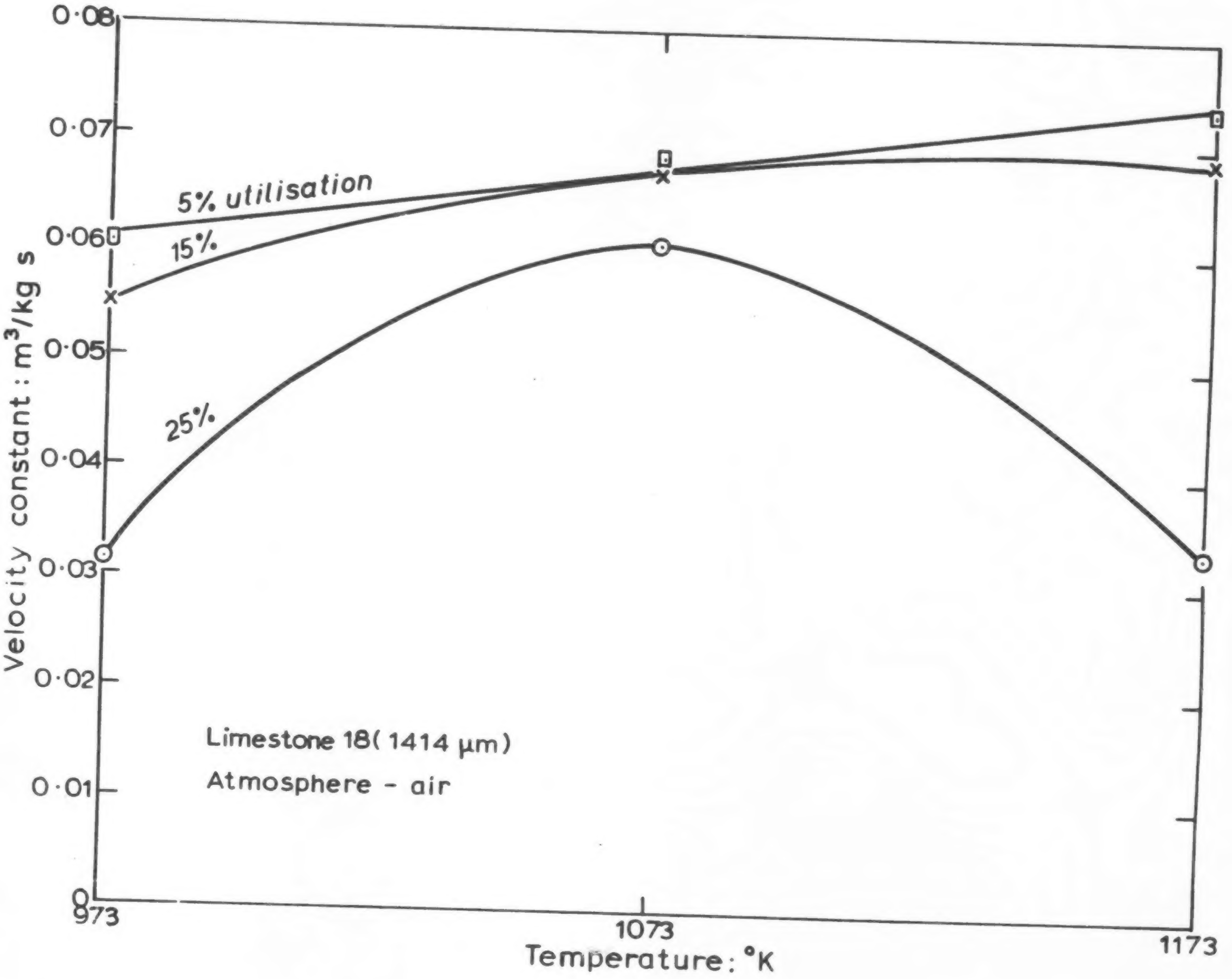

Fig.A8.58. Velocity constant as a function of utilisation and temperature

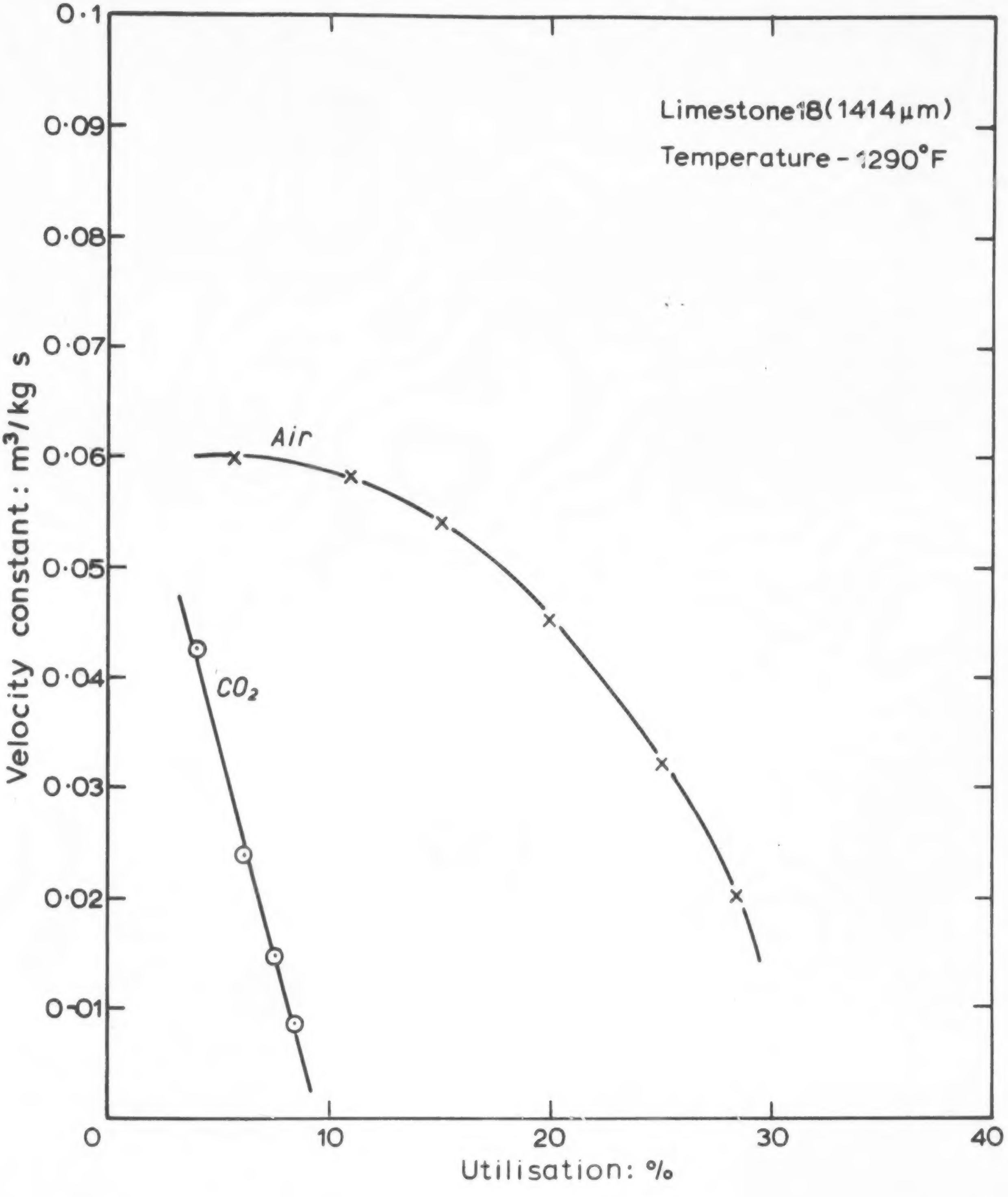

Fig.A8.59. Velocity constant as a function of atmosphere and utilisation

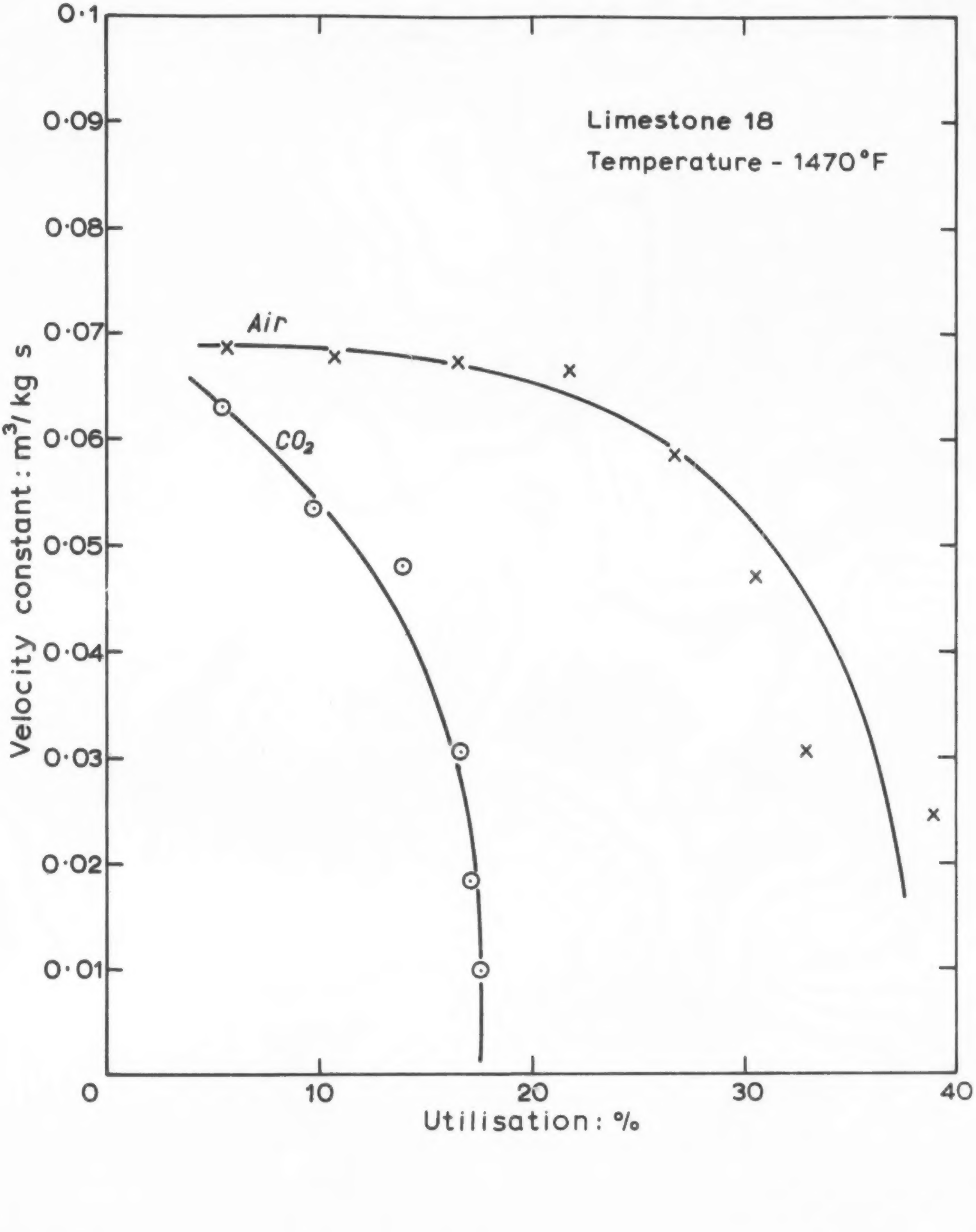

Fig. A8.60. Velocity constant as a function of atmosphere and utilisation

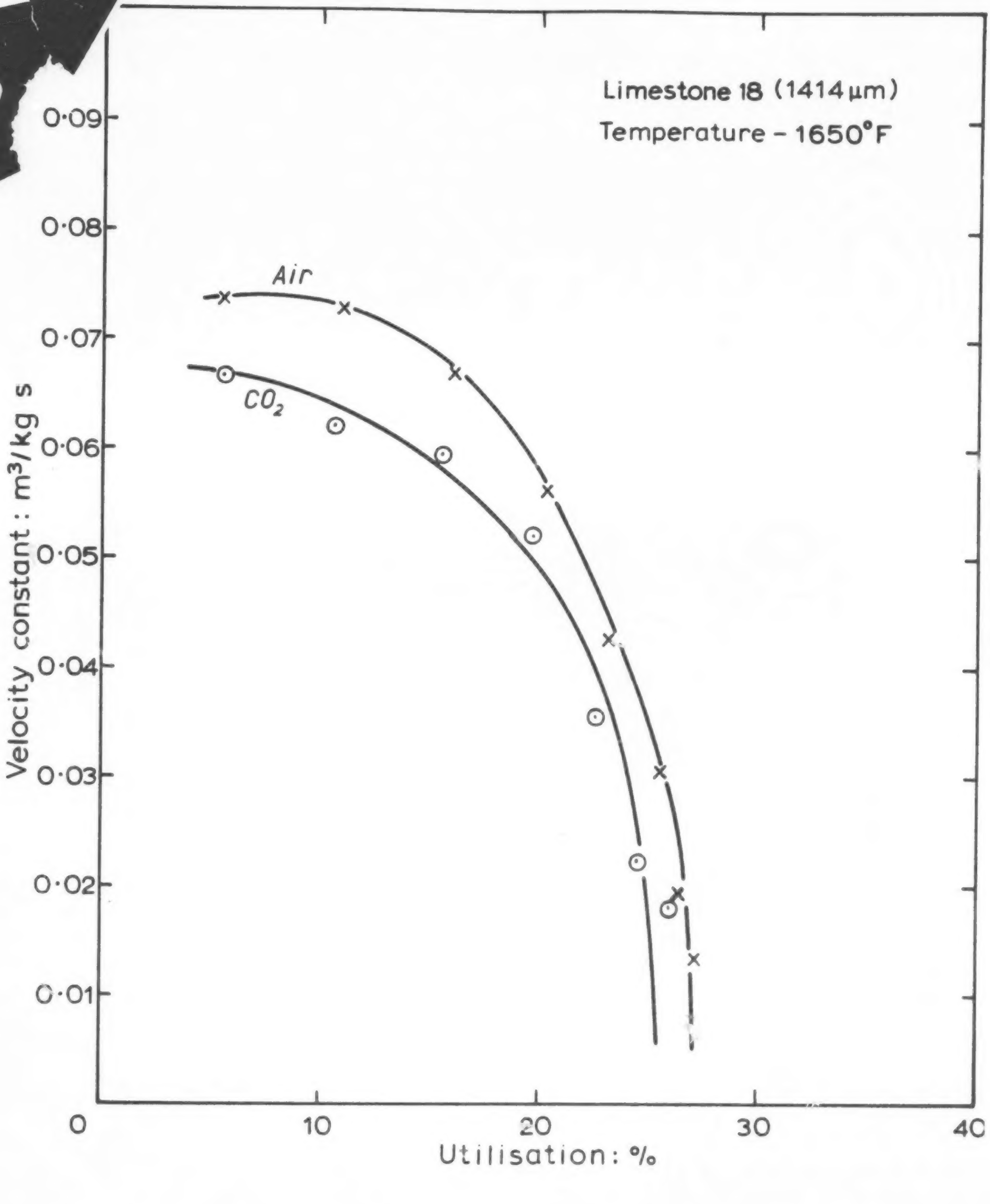

Fig. A8. 61. Velocity constant as a function of atmosphere and utilisation

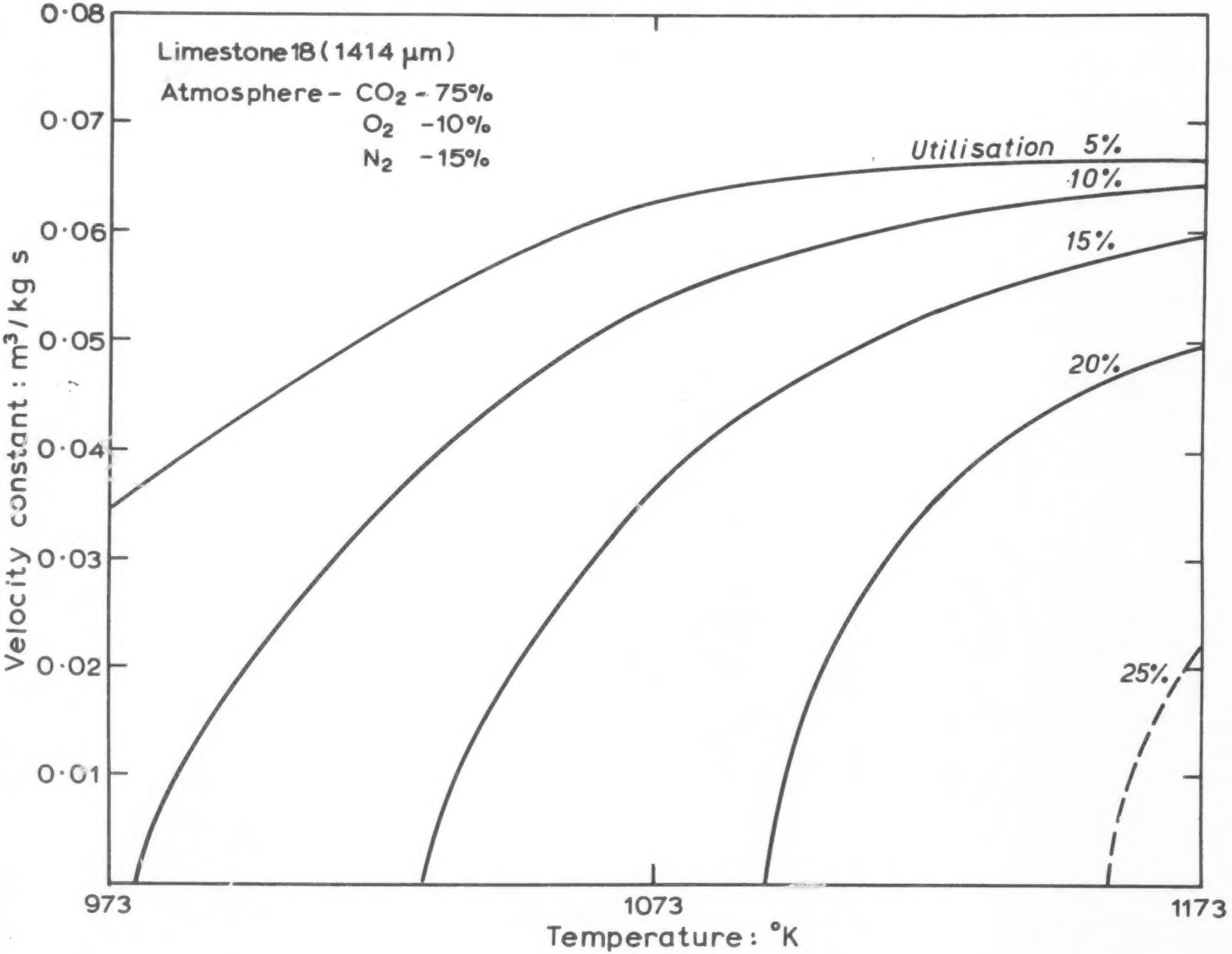

Fig. A8.62. Velocity constant as a function of utilisation and temperature

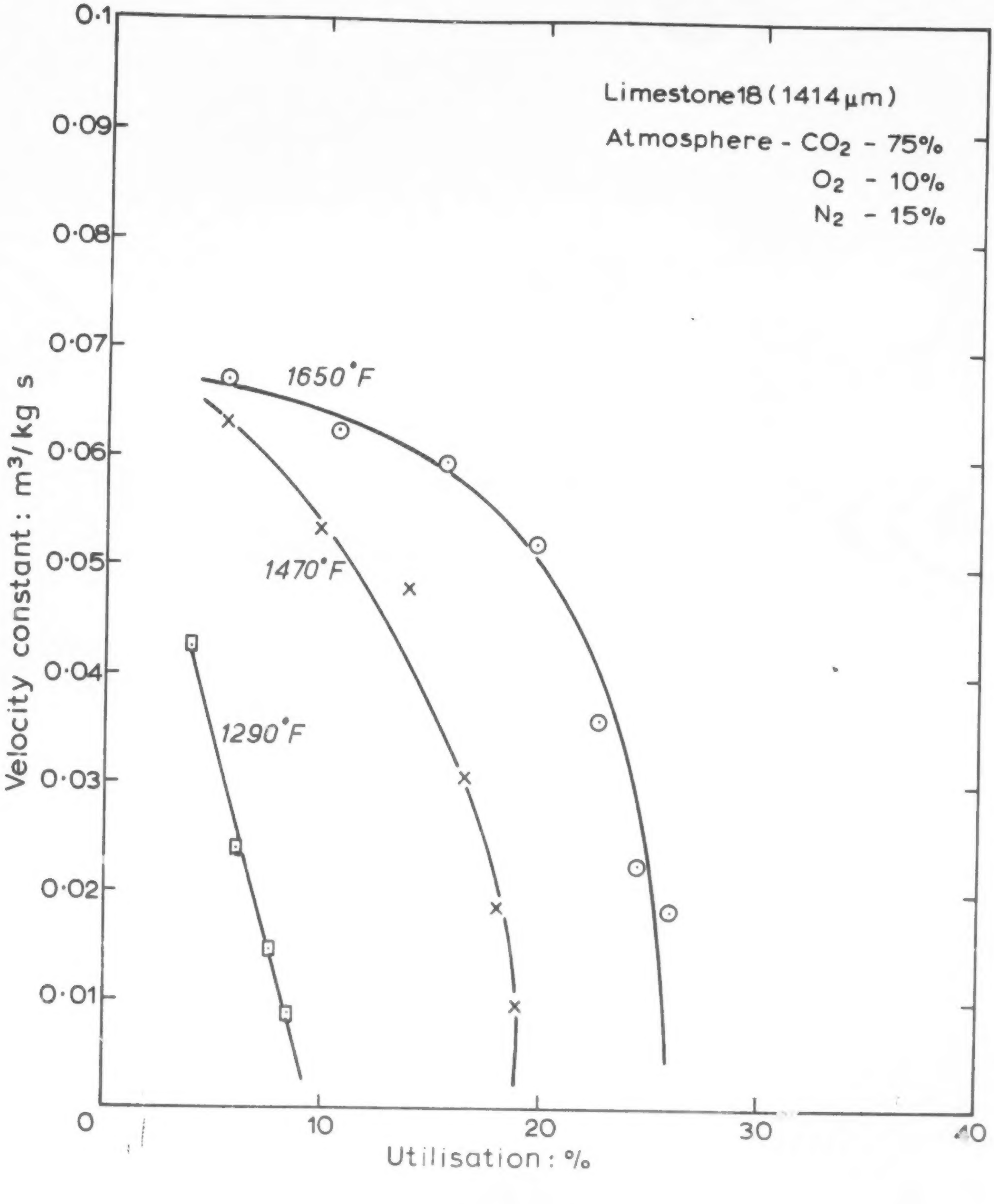

Fig. A8.63. Velocity constant as a function of temperature and utilisation

MERCURY POROSIMETRY DATA

POTENTIAL WIDE-INTEREST REPORT

WARNING TO EVALUATORS FROM INPUT

DOCUMENT WILL REPRODUCE POORLY

Pages
A150.6-

half tones
A4.89
A4.90
A4.92
A4.80

DECISION BY EVALUATORS:

1. Accepted as wide-interest report ____________________
Signature

2. Accepted as regular report ____________________
Signature

3. Return to source ____________________
Signature

Poor-Copy Warning NTIS-182 (2/72)

Sample B 5

PORE-ENTRANCE DIAMETER, MICRONS	CUMULATIVE PORE-VOLUME, CU MM/G
58.5831	0.00
38.2530	3.43
29.0364	6.23
22.1939	9.24
18.9238	12.04
16.2040	14.33
14.0393	16.82
11.8998	19.73
10.7217	22.32
9.7506	22.84
8.9411	23.46
8.2557	24.09
7.6688	25.33
7.1600	26.68
6.7144	27.93
6.3213	29.48
5.9708	30.11
5.6577	31.35
5.0013	33.53
4.4816	36.13
3.7093	38.20
3.1641	40.49
2.7585	41.84
2.4451	43.50
2.1955	44.54
1.9922	45.89
1.8233	46.51
1.2805	48.59
0.9867	51.08
0.6764	53.47
0.5145	54.92
0.4152	55.65
0.3480	56.27
0.2629	57.62
0.2112	58.45
0.1417	63.95
0.1066	99.77
0.0854	125.83
0.0713	140.36
0.0611	149.19
0.0535	163.10
0.0476	185.83
0 0429	209.81
0.0390	231.62
0.0357	247.19
0.0330	261.72
0.0306	271.07
0.0286	278.33
0.0268	284.56
0.0252	288.72
0.0238	292.87
0.0226	290.79
0.0215	295.98
0.0204	297.02
0.0195	299.10
0.0187	297.02
0.0179	300.13
0.0172	299.10
0.0165	302.21
0.0159	303.25
0.0153	302.21
0.0148	304.29
0.0143	304.29

A8.1806

Sample B 6

PORE-ENTRANCE DIAMETER, MICRONS	CUMULATIVE PORE-VOLUME, CU MM/G
58.5831	0.00
38.7573	9.31
28.3398	16.53
22.8555	21.76
18.9777	26.67
16.2325	30.65
14.2335	34.10
11.9184	37.24
10.7422	41.63
9.7627	42.99
8.9576	43.83
8.2706	44.98
7.6816	46.13
7.1737	47.18
6.7232	48.54
6.3098	50.11
5.9783	51.15
5.6645	51.99
5.3371	55.02
4.4866	58.16
3.7128	60.46
3.1667	62.76
2.7627	65.33
2.4463	67.58
2.1973	68.83
1.9935	70.40
1.8244	71.66
1.2311	75.11
0.9871	78.24
0.6766	82.43
0.5146	84.84
0.4153	87.33
0.3483	88.52
0.2623	90.68
0.2113	96.55
0.1417	110.25
0.1066	143.22
0.0854	173.33
0.0713	187.04
0.0611	198.44
0.0535	210.78
0.0476	226.79
0.0429	245.20
0.0390	261.51
0.0357	273.54
0.0330	282.33
0.0306	293.21
0.0286	299.59
0.0268	305.97
0.0252	310.99
0.0238	313.82
0.0226	316.56
0.0215	318.42
0.0204	319.89
0.0195	320.72
0.0187	321.77
0.0179	322.40
0.0172	322.92
0.0165	323.65
0.0159	324.59
0.0153	324.38
0.0148	324.59
0.0143	324.70

Sample C

PORE-ENTRANCE DIAMETER, MICRONS	CUMULATIVE PORE-VOLUME, CU MM/G
58.5831	0.00
38.2226	7.40
28.9940	10.76
23.1801	13.05
18.9048	14.46
16.2476	15.61
14.1796	16.75
11.7974	17.69
10.6370	19.04
9.6813	19.57
8.8825	19.91
8.2050	20.05
7.6244	20.58
7.1203	20.99
6.6792	21.66
6.2885	21.66
5.9419	22.33
5.6308	22.40
4.9797	23.27
4.4637	24.35
3.6968	25.22
3.1549	26.30
2.7514	27.04
2.4394	27.58
2.1909	28.18
1.9884	28.59
1.8201	29.13
1.2769	30.07
0.9856	31.28
0.6759	33.43
0.5143	34.37
0.4156	34.64
0.3479	35.25
0.2628	35.85
0.2112	36.79
0.1416	37.00
0.1065	37.87
0.0854	38.34
0.0712	38.61
0.0611	39.15
0.0535	38.54
0.0476	39.49
0.0428	39.65
0.0390	39.69
0.0357	40.16
0.0330	40.29
0.0306	40.43
0.0286	40.56
0.0268	40.09
0.0252	40.29
0.0238	40.56
0.0226	40.16
0.0215	40.63
0.0204	40.63
0.0195	40.56
0.0187	40.76
0.0179	40.70
0.0172	40.43
0.0165	40.76
0.0159	40.56
0.0153	40.43
0.0148	40.83
0.0143	40.83

Sample C 1

PORE-ENTRANCE DIAMETER, MICRONS	CUMULATIVE PORE-VOLUME, CU MM/G
55.5831	0.00
33.9514	7.70
28.1975	13.04
22.6667	16.03
19.1153	18.75
16.2707	20.83
14.1623	22.74
11.8039	25.36
10.6460	28.26
9.6395	29.26
8.8908	30.25
8.2135	31.16
7.6308	31.34
7.1263	32.16
6.6844	32.97
6.2937	33.51
5.9465	34.33
5.6352	34.78
4.9835	36.32
4.4667	37.59
3.6990	39.31
3.1565	40.67
2.7527	41.94
2.4404	43.03
2.1918	43.75
1.9891	44.57
1.8208	45.47
1.2793	48.10
0.9860	50.82
0.6761	55.98
0.5144	60.60
0.4151	63.95
0.3479	65.58
0.2629	72.37
0.2112	91.67
0.1417	161.05
0.1066	178.90
0.0854	184.06
0.0713	184.96
0.0611	186.05
0.0535	186.78
0.0476	187.23
0.0429	187.41
0.0390	187.68
0.0357	187.14
0.0330	188.23
0.0306	187.95
0.0286	188.23
0.0268	188.41
0.0252	188.41
0.0238	188.41
0.0226	188.68
0.0215	188.77
0.0204	188.59
0.0195	188.95
0.0187	188.41
0.0179	189.13
0.0172	189.40
0.0165	189.40
0.0159	189.40
0.0153	189.67
0.0148	189.86
0.0143	189.67

PORE-ENTRANCE DIAMETER; MICRONS	CUMULATIVE PORE-VOLUME, CU MM/G	PORE-ENTRANCE DIAMETER, MICRONS	CUMULATIVE PORE-VOLUME, CU MM/G
58.5831	0.00	58.5831	0.00
38.3718	13.30	37.8068	6.12
28.2027	21.90	28.0371	10.15
22.2902	28.45	22.0751	12.83
18.5815	32.75	18.2213	15.68
15.7544	36.84	15.6453	18.11
13.9060	39.61	13.3901	19.71
12.0792	41.65	11.8344	21.63
10.8694	44.93	10.6699	24.07
9.8759	46.67	9.7088	24.82
9.0490	48.51	8.9057	25.24
8.3470	48.82	8.2258	25.91
7.7477	50.15	7.6424	26.58
7.2280	50.97	7.1366	27.42
6.7756	53.32	6.6933	28.09
6.3740	53.53	6.3017	28.68
6.0175	53.73	5.9532	29.01
5.6996	54.96	5.6411	29.35
5.0336	56.49	4.9879	30.52
4.5076	59.26	4.4739	32.70
3.7274	62.12	3.7020	34.38
3.1773	64.48	3.1587	35.97
2.7686	66.32	2.7543	36.98
2.4531	68.37	2.4417	37.65
2.2020	69.70	2.1929	38.91
1.9977	71.74	1.9930	39.49
1.8279	72.66	1.8214	39.75
1.2829	78.39	1.2796	42.76
0.9883	85.56	0.9862	45.20
0.6773	101.93	0.6762	49.22
0.5152	122.40	0.5144	52.24
0.4157	141.34	0.4151	54.67
0.3484	160.78	0.3479	55.76
0.2632	227.92	0.2629	58.78
0.2115	252.48	0.2112	60.96
0.1418	272.95	0.1417	71.53
0.1066	277.04	0.1066	87.54
0.0854	278.07	0.0854	116.39
0.0713	278.07	0.0713	151.35
0.0611	279.09	0.0611	165.52
0.0535	280.11	0.0535	170.14
0.0476	279.09	0.0476	173.07
0.0429	279.09	0.0429	173.91
0.0390	279.09	0.0390	174.75
0.0357	280.11	0.0357	174.75
0.0330	280.11	0.0330	174.33
0.0306	280.11	0.0306	175.17
0.0286	280.11	0.0286	174.75
0.0268	280.11	0.0268	175.59
0.0252	280.11	0.0252	175.59
0.0238	280.11	0.0238	176.42
0.0226	281.14	0.0226	176.01
0.0215	281.14	0.0215	176.42
0.0204	281.14	0.0204	176.42
0.0195	281.14	0.0195	176.42
0.0187	281.14	0.0187	176.84
0.0179	281.14	0.0179	176.84
0.0172	281.14	0.0172	177.68
0.0165	281.14	0.0165	177.68
0.0159	281.14	0.0159	177.26
0.0153	281.14	0.0153	176.84
0.0148	282.16	0.0148	177.68
0.0143	282.16	0.0143	178.94

PORE-ENTRANCE DIAMETER, MICRONS	CUMULATIVE PORE-VOLUME, CU MM/G	PORE-ENTRANCE DIAMETER, MICRONS	CUMULATIVE PORE-VOLUME, CU MM/G
58.5831	0.00	58.5831	0.00
38.7797	18.81	37.3325	9.39
29.3268	39.01	27.4709	15.96
23.3733	49.34	22.5606	18.51
19.5831	57.12	18.6588	21.16
16.5379	64.66	15.9988	23.34
14.5274	70.70	14.1003	24.99
11.9487	77.78	11.9537	26.81
10.7761	86.02	10.7783	32.74
9.8004	88.69	9.7966	32.92
8.9831	89.51	8.9791	33.19
8.2919	90.43	8.2880	33.74
7.7018	93.10	7.6954	34.10
7.1888	94.61	7.1821	34.56
6.7394	95.78	6.7333	35.29
6.3434	97.40	6.3387	37.20
5.9914	99.14	5.9861	37.48
5.6757	99.95	5.6708	37.93
5.0164	104.02	5.0114	39.67
4.4947	109.13	4.4895	41.67
3.7191	113.77	3.7149	43.95
3.1719	118.99	3.1685	46.96
2.7649	123.52	2.7618	48.24
2.4504	127.47	2.4477	49.70
2.2000	130.37	2.1977	51.25
1.9962	134.09	1.9940	51.89
1.8269	138.50	1.8248	52.61
1.2827	152.08	1.2813	56.35
0.9884	169.49	0.9873	61.28
0.6778	234.85	0.6767	69.48
0.5159	325.40	0.5148	74.86
0.4164	398.54	0.4153	79.88
0.3489	429.88	0.3481	82.25
0.2635	477.48	0.2630	101.58
0.2116	492.57	0.2113	134.96
0.1418	503.02	0.1418	220.85
0.1067	504.18	0.1066	247.48
0.0855	505.34	0.0854	258.06
0.0713	505.34	0.0713	260.25
0.0612	505.34	0.0611	261.80
0.0535	505.34	0.0535	262.34
0.0476	505.34	0.0476	262.07
0.0429	506.51	0.0429	262.71
0.0390	506.51	0.0390	262.80
0.0357	505.34	0.0357	262.89
0.0330	506.51	0.0330	263.07
0.0306	506.51	0.0306	262.89
0.0286	506.51	0.0286	263.53
0.0268	506.51	0.0268	263.53
0.0252	507.67	0.0252	263.90
0.0238	508.83	0.0238	263.80
0.0226	508.83	0.0226	264.35
0.0215	508.83	0.0215	264.17
0.0204	508.83	0.0204	264.81
0.0195	508.83	0.0195	264.53
0.0187	509.99	0.0187	264.35
0.0179	509.99	0.0179	264.53
0.0172	509.99	0.0172	265.08
0.0165	509.99	0.0165	264.72
0.0159	508.83	0.0159	265.08
0.0153	511.15	0.0153	265.17
0.0148	509.99	0.0148	265.26
0.0143	509.99	0.0143	265.17

PORE-ENTRANCE DIAMETER, MICRONS	CUMULATIVE PORE-VOLUME, CU MM/G	PORE-ENTRANCE DIAMETER, MICRONS	CUMULATIVE PORE-VOLUME, CU MM/G
58.5831	0.00	58.5831	0.00
38.9614	17.90	37.5664	10.64
28.8373	28.18	27.9517	16.51
23.1898	34.88	22.5424	21.06
19.1713	40.07	18.5979	24.27
16.3215	44.35	15.8854	27.26
14.2503	47.35	13.9635	28.59
11.9666	51.39	11.8433	31.14
10.7782	55.09	10.6758	33.91
9.7984	56.13	9.7132	34.69
8.9828	57.63	8.9094	35.24
8.2925	59.13	8.2286	35.91
7.7001	60.17	7.6445	36.57
7.1880	62.25	7.1376	37.02
6.7378	62.59	6.6943	38.01
6.3419	64.10	6.3027	38.90
5.9901	65.83	5.9541	39.45
5.6755	67.91	5.6423	40.23
5.0149	69.75	4.9890	42.23
4.4929	73.57	4.4714	44.33
3.7174	76.80	3.7023	46.44
3.1701	79.92	3.1589	48.21
2.7634	83.50	2.7545	49.76
2.4490	85.69	2.4420	51.76
2.1988	87.54	2.1930	52.64
1.9949	89.04	1.9901	53.53
1.8256	90.20	1.8216	54.31
1.2818	95.85	1.2797	58.30
0.9876	102.90	0.9863	61.84
0.6769	117.22	0.6762	67.05
0.5149	129.81	0.5144	71.15
0.4155	148.52	0.4151	74.92
0.3483	176.93	0.3479	76.25
0.2633	295.99	0.2629	82.12
0.2115	367.02	0.2112	89.55
0.1418	436.89	0.1417	135.10
0.1067	459.18	0.1066	187.85
0.0855	468.53	0.0854	246.37
0.0713	470.38	0.0713	260.11
0.0612	471.30	0.0611	266.98
0.0535	471.88	0.0535	271.30
0.0476	471.76	0.0476	273.08
0.0429	471.76	0.0429	273.63
0.0390	471.88	0.0390	273.96
0.0357	472.23	0.0357	274.30
0.0330	472.00	0.0330	274.30
0.0306	472.46	0.0306	274.30
0.0286	473.15	0.0286	274.74
0.0268	472.57	0.0268	275.29
0.0252	473.03	0.0252	275.63
0.0238	473.38	0.0238	275.18
0.0226	473.61	0.0226	275.41
0.0215	473.61	0.0215	275.41
0.0204	474.07	0.0204	275.96
0.0195	474.31	0.0195	275.96
0.0187	473.96	0.0187	275.96
0.0179	473.50	0.0179	275.63
0.0172	471.19	0.0172	275.85
0.0165	471.07	0.0165	275.74
0.0159	471.42	0.0159	275.52
0.0153	471.19	0.0153	275.63
0.0148	471.53	0.0148	276.29
0.0143	471.30	0.0143	276.29

PORE-ENTRANCE DIAMETER, MICRONS	CUMULATIVE PORE-VOLUME, CU MM/G	DIAMETER, MICRONS	PORE-VOLUME, CU MM/G
58.5831	0.00	58.5831	0.00
38.3754	14.69	38.5329	11.32
28.4637	23.19	28.7251	17.87
22.8485	28.35	22.5522	21.86
18.8125	30.80	18.9323	25.08
16.3108	32.34	15.9631	28.41
14.0245	32.60	13.8840	30.85
11.9108	32.47	11.8618	32.74
10.7332	36.72	10.7050	40.51
9.7601	37.37	9.7376	41.40
8.9491	38.14	8.9310	42.51
8.2623	38.79	8.2469	43.06
7.6731	39.17	7.6600	43.51
7.1633	40.46	7.1506	43.62
6.7168	41.49	6.7046	43.62
6.3226	42.52	6.3111	43.73
5.9723	43.68	5.9616	44.28
5.6585	44.46	5.6488	44.84
5.0017	46.78	4.9933	45.39
4.4817	49.35	4.4749	47.61
3.7094	52.19	3.7046	49.39
3.1642	54.89	3.1606	51.72
2.7586	57.08	2.7559	53.61
2.4451	58.37	2.4430	55.16
2.1956	60.05	2.1939	56.05
1.9923	61.47	1.9909	57.71
1.8234	62.75	1.8222	58.60
1.2806	67.91	1.2800	63.04
0.9868	72.55	0.9865	67.48
0.6765	81.83	0.6763	75.58
0.5146	91.23	0.5145	83.13
0.4153	99.99	0.4152	90.34
0.3481	106.44	0.3480	94.34
0.2630	147.54	0.2629	116.42
0.2114	211.33	0.2113	164.37
0.1418	318.54	0.1417	268.03
0.1066	376.65	0.1066	314.98
0.0854	412.09	0.0854	334.51
0.0713	422.66	0.0713	337.73
0.0611	428.97	0.0611	338.95
0.0535	432.32	0.0535	339.17
0.0476	435.03	0.0476	340.06
0.0429	436.32	0.0429	340.28
0.0390	437.22	0.0390	340.17
0.0357	437.73	0.0357	340.50
0.0330	437.99	0.0330	340.72
0.0306	438.64	0.0306	340.39
0.0286	439.02	0.0286	341.50
0.0268	439.02	0.0268	341.17
0.0252	439.54	0.0252	341.28
0.0238	439.80	0.0238	341.28
0.0226	441.08	0.0226	341.94
0.0215	440.96	0.0215	341.83
0.0204	441.21	0.0204	342.17
0.0195	441.21	0.0195	342.17
0.0187	440.57	0.0187	343.05
0.0179	441.86	0.0179	342.83
0.0172	441.34	0.0172	342.50
0.0165	441.73	0.0165	342.83
0.0159	442.37	0.0159	342.50
0.0153	442.12	0.0153	342.61
0.0148	442.89	0.0148	342.72
0.0143	443.15	0.0143	342.39

PORE-ENTRANCE DIAMETER, MICRONS	CUMULATIVE PORE-VOLUME, CU MM/G	PORE-ENTRANCE DIAMETER, MICRONS	CUMULATIVE PORE-VOLUME, CU MM/G
58.5831	0.00	58.5831	0.00
37.0153	9.41	38.8697	10.33
28.0101	15.02	29.3038	16.16
22.6505	19.45	23.3808	20.28
19.1038	21.79	19.1089	23.46
16.2827	24.43	16.5272	25.09
14.3801	26.14	14.2451	27.19
11.8278	29.26	11.8932	29.21
10.6811	35.64	10.7170	31.31
9.7158	35.64	9.7463	31.54
8.9150	37.27	8.9389	32.55
8.2338	37.89	8.2546	33.33
7.6509	39.29	7.6684	34.49
7.1426	39.29	7.1592	35.27
6.6983	39.76	6.7132	35.89
6.3067	40.69	6.3195	36.51
5.9580	41.32	5.9695	37.21
5.6463	42.33	5.6560	37.76
4.9919	43.42	4.9991	38.38
4.4740	45.28	4.4802	40.79
3.7040	46.68	3.7082	42.03
3.1603	48.40	3.1629	42.73
2.7554	48.86	2.7576	43.97
2.4426	49.95	2.4444	45.37
2.1935	50.57	2.1951	46.38
1.9905	51.12	1.9919	47.47
1.8219	51.59	1.8230	48.01
1.2799	54.54	1.2804	50.73
0.9864	56.88	0.9867	54.07
0.6762	60.92	0.6764	58.50
0.5145	63.26	0.5146	61.37
0.4151	65.05	0.4152	63.39
0.3480	66.37	0.3480	64.09
0.2629	68.70	0.2629	66.50
0.2112	70.34	0.2112	68.99
0.1416	73.68	0.1417	72.79
0.1066	76.56	0.1066	78.54
0.0854	82.94	0.0854	92.92
0.0712	88.39	0.0713	103.40
0.0611	94.54	0.0611	113.58
0.0535	101.62	0.0535	129.04
0.0476	110.80	0.0476	143.65
0.0429	120.37	0.0429	162.99
0.0390	132.58	0.0390	177.13
0.0357	139.59	0.0357	185.83
0.0330	146.43	0.0330	197.17
0.0306	153.98	0.0306	203.86
0.0286	159.89	0.0286	208.75
0.0268	166.58	0.0268	211.86
0.0252	172.58	0.0252	215.74
0.0238	179.50	0.0238	218.46
0.0226	183.86	0.0226	220.40
0.0215	187.59	0.0215	221.34
0.0204	190.78	0.0204	222.58
0.0195	192.81	0.0195	223.28
0.0187	194.91	0.0187	224.13
0.0179	196.00	0.0179	224.13
0.0172	197.63	0.0172	224.68
0.0165	198.02	0.0165	224.99
0.0159	198.80	0.0159	225.45
0.0153	199.11	0.0153	225.30
0.0148	198.25	0.0148	225.92
0.0143	199.11	0.0143	225.53

PORE-ENTRANCE DIAMETER, MICRONS	CUMULATIVE PORE-VOLUME, CU MM/G	PORE-ENTRANCE DIAMETER, MICRONS	CUMULATIVE PORE-VOLUME, CU MM/G
58.5831	0.00	58.5831	0.00
38.3912	8.18	39.2412	14.65
26.7251	13.04	29.3391	22.02
22.7233	16.20	23.1859	26.51
18.7728	18.79	19.2002	31.11
16.0522	21.38	16.3607	34.10
14.1232	22.84	14.2986	36.78
11.8284	25.11	11.8527	39.88
10.6631	26.97	10.6838	42.66
9.7037	27.86	9.7183	42.76
8.9012	28.18	8.9156	44.26
8.2233	29.40	8.2337	44.79
7.6402	30.05	7.6494	45.76
7.1351	31.10	7.1427	46.82
6.6923	31.99	6.6989	47.89
6.3014	32.96	6.3069	48.86
5.9535	33.77	5.9581	49.60
5.6420	34.66	5.6459	50.46
4.9886	35.88	4.9919	52.38
4.4710	37.26	4.4738	54.63
3.7021	38.96	3.7040	56.87
3.1587	40.17	3.1602	58.91
2.7544	41.55	2.7555	60.29
2.4418	42.68	2.4427	61.68
2.1930	43.73	2.1936	62.75
1.9901	44.54	1.9996	64.04
1.8216	45.44	1.8220	64.89
1.2797	48.43	1.2799	68.85
0.9863	51.43	0.9864	72.48
0.6762	56.69	0.6762	77.61
0.5144	59.77	0.5145	81.89
0.4151	61.80	0.4151	84.88
0.3480	62.85	0.3480	85.85
0.2629	66.09	0.2629	89.59
0.2112	68.44	0.2112	92.93
0.1416	72.57	0.1417	101.45
0.1066	79.94	0.1066	125.72
0.0854	100.43	0.0854	166.13
0.0713	113.71	0.0713	181.53
0.0611	125.70	0.0611	197.88
0.0535	145.54	0.0535	220.01
0.0476	170.73	0.0476	252.83
0.0429	184.90	0.0429	288.43
0.0390	199.48	0.0390	324.78
0.0357	209.76	0.0357	350.12
0.0330	215.92	0.0330	363.80
0.0306	219.73	0.0306	372.89
0.0286	223.05	0.0286	378.55
0.0268	225.23	0.0268	383.15
0.0252	226.69	0.0252	385.72
0.0238	227.99	0.0238	387.64
0.0226	228.47	0.0226	389.35
0.0215	229.04	0.0215	390.96
0.0204	229.61	0.0204	391.28
0.0195	229.93	0.0195	392.35
0.0187	230.58	0.0187	393.09
0.0179	230.66	0.0179	393.63
0.0172	231.23	0.0172	393.63
0.0165	231.31	0.0165	393.73
0.0159	231.63	0.0159	394.38
0.0153	231.39	0.0153	394.16
0.0148	231.79	0.0148	394.38
0.0143	231.31	0.0143	395.02

PORE-ENTRANCE DIAMETER, MICRONS	CUMULATIVE PORE-VOLUME, CU MM/G
58.5831	0.00
38.5219	16.73
28.7463	24.66
22.9133	29.56
19.0551	33.36
16.3293	36.48
14.2146	38.60
11.8504	40.94
10.6731	40.72
9.7123	42.06
8.9093	42.95
8.2295	44.18
7.6459	45.29
7.1392	46.08
6.6955	46.97
6.3037	47.75
5.9553	48.64
5.6434	49.42
4.9897	51.10
4.4718	52.88
3.7025	55.00
3.1591	56.90
2.7546	58.24
2.4420	59.80
2.1930	60.80
1.9902	62.03
1.8216	63.14
1.2797	67.38
0.9863	71.62
0.6762	77.65
0.5144	82.11
0.4151	87.02
0.3480	89.25
0.2629	89.81
0.2112	93.49
0.1417	129.52
0.1066	175.04
0.0854	204.27
0.0713	224.24
0.0611	246.55
0.0535	276.23
0.0476	316.39
0.0429	350.64
0.0390	378.64
0.0357	393.93
0.0330	401.07
0.0306	404.64
0.0286	407.54
0.0268	408.54
0.0252	409.55
0.0238	410.44
0.0226	410.77
0.0215	411.00
0.0204	411.22
0.0195	410.89
0.0187	412.00
0.0179	412.00
0.0172	412.23
0.0165	413.23
0.0159	413.45
0.0153	413.56
0.0148	413.56
0.0143	414.12

PORE-ENTRANCE DIAMETER, MICRONS	CUMULATIVE PORE-VOLUME, CU MM/G
58.5831	0.00
38.5211	12.76
28.7797	20.36
22.8057	24.65
18.8641	28.39
16.1989	31.14
14.1430	33.12
11.8361	36.31
10.6678	38.29
9.7058	38.73
8.9045	39.94
8.2254	41.15
7.6422	42.15
7.1365	43.36
6.6932	44.24
5.9535	45.89
5.6413	46.22
4.9878	47.43
4.4704	49.52
3.7013	50.51
3.1583	53.26
2.7541	54.69
2.4415	56.01
2.1927	56.89
1.9898	57.66
1.8213	58.65
1.2796	63.05
0.9862	67.12
0.6762	72.96
0.5144	76.26
0.4151	79.45
0.3479	80.55
0.2629	85.06
0.2112	88.91
0.1417	105.64
0.1066	147.78
0.0854	180.14
0.0713	197.85
0.0611	216.89
0.0535	243.41
0.0476	283.02
0.0429	322.42
0.0390	354.88
0.0357	374.47
0.0330	384.04
0.0306	389.21
0.0286	392.95
0.0268	394.05
0.0252	395.26
0.0238	395.48
0.0226	396.36
0.0215	397.68
0.0204	398.34
0.0195	398.89
0.0187	399.23
0.0179	400.11
0.0172	400.33
0.0165	400.55
0.0159	401.10
0.0153	401.98
0.0148	402.20
0.0143	402.75

Sample C 37		**Sample C 38**	
PORE-ENTRANCE DIAMETER, MICRONS	CUMULATIVE PORE-VOLUME, CU MM/G	PORE-ENTRANCE DIAMETER, MICRONS	CUMULATIVE PORE-VOLUME, CU MM/G
58.5831	0.00	58.5831	0.00
38.0547	5.76	37.6096	11.76
28.5054	12.53	28.2897	17.64
22.8896	15.32	22.6405	21.44
18.9843	17.86	19.1276	24.00
16.2368	19.80	16.0516	26.56
14.1003	21.75	14.1108	29.41
11.8437	23.87	11.8485	34.34
10.6805	27.17	10.6778	36.05
9.7153	27.17	9.7084	34.34
8.9111	27.59	8.9047	34.53
8.2309	28.44	8.2248	35.19
7.6473	29.37	7.6409	35.57
7.1406	30.13	7.1349	36.33
6.6970	30.89	6.6917	37.00
6.3051	31.57	6.3002	37.57
5.9566	32.25	5.9522	38.33
5.6446	32.92	5.6403	38.70
4.9905	34.11	4.9869	39.56
4.4722	35.12	4.4695	41.08
3.7028	36.56	3.7014	43.92
3.1592	37.75	3.1579	44.30
2.7547	38.68	2.7539	46.10
2.4420	39.61	2.4417	48.95
2.1930	40.29	2.1928	49.71
1.9901	40.79	1.9899	50.47
1.8215	41.22	1.8214	51.04
1.2796	43.33	1.2796	53.88
0.9862	44.43	0.9862	56.07
0.6761	46.21	0.6761	58.82
0.5144	47.06	0.5144	59.67
0.4151	47.82	0.4151	60.43
0.3479	48.16	0.3479	60.71
0.2628	50.61	0.2628	64.41
0.2112	53.32	0.2112	66.03
0.1417	86.24	0.1417	92.11
0.1066	108.84	0.1066	121.24
0.0854	125.17	0.0854	146.19
0.0713	134.23	0.0713	159.94
0.0611	143.79	0.0611	174.17
0.0535	158.35	0.0535	195.52
0.0476	177.56	0.0476	229.38
0.0429	196.09	0.0429	254.81
0.0390	205.91	0.0390	268.37
0.0357	209.89	0.0357	275.68
0.0330	211.41	0.0330	279.38
0.0306	213.02	0.0306	281.18
0.0286	214.29	0.0286	282.41
0.0268	215.05	0.0268	283.84
0.0252	215.64	0.0252	284.78
0.0238	216.24	0.0238	285.16
0.0226	216.83	0.0226	285.26
0.0215	217.51	0.0215	286.21
0.0204	218.44	0.0204	286.02
0.0195	218.78	0.0195	286.30
0.0187	218.86	0.0187	286.30
0.0179	219.03	0.0179	286.59
0.0172	219.11	0.0172	286.49
0.0165	219.20	0.0165	286.40
0.0159	219.28	0.0159	286.30
0.0153	220.05	0.0153	287.16
0.0148	220.47	0.0148	287.25
0.0143	220.72	0.0143	287.92

Sample C 39

PORE-ENTRANCE DIAMETER, MICRONS	CUMULATIVE PORE-VOLUME, CU MM/G
58.5831	0.00
38.2301	10.47
28.6145	17.32
22.6905	21.48
18.7928	24.84
16.1043	27.12
14.0595	29.00
11.8065	31.69
10.6472	35.58
9.6895	36.52
8.8894	37.19
8.2107	37.32
7.6287	37.86
7.1243	38.94
6.6824	39.87
6.2920	40.81
5.9445	41.35
5.6334	41.89
4.9816	43.37
4.4649	44.57
3.6976	46.32
3.1554	48.20
2.7517	49.14
2.4396	50.35
2.1911	51.42
1.9886	52.50
1.8203	53.44
1.2790	57.06
0.9858	59.88
0.6760	63.77
0.5143	67.13
0.4150	69.14
0.3479	70.22
0.2628	73.90
0.2112	75.99
0.1416	82.84
0.1065	112.37
0.0854	145.94
0.0712	169.57
0.0611	176.22
0.0535	201.66
0.0476	240.73
0.0429	277.92
0.0390	299.53
0.0357	312.15
0.0330	317.12
0.0306	319.80
0.0286	321.82
0.0268	323.30
0.0252	324.37
0.0238	325.58
0.0226	325.98
0.0215	326.79
0.0204	326.79
0.0195	326.65
0.0187	327.05
0.0179	327.32
0.0172	327.32
0.0165	327.73
0.0159	328.13
0.0153	328.26
0.0148	328.80
0.0143	328.80

Sample G

PORE-ENTRANCE DIAMETER, MICRONS	CUMULATIVE PORE-VOLUME, CU MM/G
58.5831	0.00
38.3305	4.63
27.7585	7.71
21.8222	8.89
18.2449	9.65
15.6364	10.02
13.6866	10.13
11.9048	10.94
10.7182	10.99
9.7467	11.05
8.9380	11.42
8.2525	11.59
7.6640	11.53
7.1548	11.86
6.7086	11.96
6.3144	11.91
5.9642	11.96
5.6507	12.02
4.9946	12.18
4.4749	12.23
3.7040	12.29
3.1597	12.39
2.7550	12.77
2.4422	13.04
2.1931	13.20
1.9901	13.31
1.8215	13.31
1.2795	13.74
0.9861	14.12
0.6761	14.87
0.5143	15.25
0.4151	15.52
0.3479	15.57
0.2628	15.90
0.2112	15.95
0.1416	16.06
0.1065	16.49
0.0854	16.76
0.0712	16.49
0.0611	16.54
0.0535	16.76
0.0476	16.71
0.0428	16.81
0.0390	17.19
0.0357	17.14
0.0330	17.57
0.0306	17.57
0.0286	17.41
0.0268	17.46
0.0252	17.51
0.0238	17.30
0.0226	17.68
0.0215	17.41
0.0204	17.46
0.0195	17.68
0.0187	17.62
0.0179	17.89
0.0172	17.73
0.0165	17.84
0.0159	17.62
0.0153	18.00
0.0148	18.05
0.0143	17.73

Sample [illegible] 3		Sample [illegible] 4	
PORE-ENTRANCE DIAMETER, MICRONS	CUMULATIVE PORE-VOLUME, CU MM/G	PORE-ENTRANCE DIAMETER, MICRONS	CUMULATIVE PORE-VOLUME, CU MM/G
58.5831	0.00	58.5831	0.00
37.8620	4.92	39.9391	6.61
28.5630	6.96	28.9229	11.23
22.8650	8.32	23.2376	13.71
19.0067	9.40	19.0616	15.23
16.1205	9.85	16.3794	16.74
14.0302	10.13	14.1763	17.91
11.9363	10.30	11.9733	19.01
10.7462	10.81	10.7788	20.19
9.7704	10.98	9.7978	20.53
8.9564	10.98	8.9814	21.15
8.2680	11.09	8.2898	21.49
7.6780	11.26	7.6976	22.05
7.1670	11.60	7.1841	22.46
6.7194	11.77	6.7345	22.67
6.3245	12.00	6.3379	22.94
5.9731	12.30	5.9852	23.08
5.6591	12.23	5.6701	23.49
5.0013	12.51	5.0104	24.39
4.4808	13.19	4.4885	25.56
3.7084	13.70	3.7141	27.08
3.1631	14.21	3.1676	28.59
2.7575	14.49	2.7613	29.90
2.4441	14.66	2.4473	31.28
2.1946	14.77	2.1976	33.55
1.9914	14.89	1.9939	34.03
1.8226	14.89	1.8249	35.41
1.2801	15.23	1.2816	42.65
0.9864	15.68	0.9880	59.87
0.6762	16.87	0.6773	82.05
0.5144	17.15	0.5151	86.53
0.4151	17.49	0.4156	89.56
0.3479	17.77	0.3483	89.91
0.2629	18.62	0.2630	89.98
0.2112	18.96	0.2113	90.60
0.1416	19.98	0.1417	91.22
0.1065	21.17	0.1066	92.32
0.0854	24.06	0.0854	94.18
0.0712	24.79	0.0713	95.35
0.0611	25.58	0.0611	96.45
0.0535	26.89	0.0535	98.59
0.0476	27.51	0.0476	99.83
0.0428	28.58	0.0429	100.24
0.0390	28.98	0.0390	101.00
0.0357	29.43	0.0357	101.27
0.0330	29.83	0.0330	101.14
0.0306	30.45	0.0306	101.69
0.0286	30.68	0.0286	101.89
0.0268	31.19	0.0268	102.03
0.0252	31.24	0.0252	102.03
0.0238	31.47	0.0238	102.24
0.0226	31.98	0.0226	102.45
0.0215	32.09	0.0215	102.86
0.0204	32.43	0.0204	102.86
0.0195	32.49	0.0195	102.65
0.0187	32.60	0.0187	103.07
0.0179	32.77	0.0179	103.07
0.0172	33.00	0.0172	103.13
0.0165	32.94	0.0165	103.34
0.0159	33.00	0.0159	103.62
0.0153	33.05	0.0153	103.62
0.0148	33.22	0.0148	103.55
0.0143	33.34	0.0143	103.48

Sample G 5

PORE-ENTRANCE DIAMETER, MICRONS	CUMULATIVE PORE-VOLUME, CU MM/G
58.5831	0.00
38.6341	8.04
28.1233	11.64
22.5308	13.86
18.4046	15.76
15.8575	16.40
14.0426	17.77
11.9149	18.83
10.7286	19.67
9.7550	19.67
8.9439	19.89
8.2575	20.20
7.6691	20.63
7.1587	20.84
6.7122	21.26
6.3181	21.58
5.9679	22.11
5.6543	22.53
4.9978	23.48
4.4779	24.33
3.7064	25.39
3.1618	26.97
2.7566	27.93
2.4435	28.88
2.1942	29.30
1.9911	30.04
1.8225	32.69
1.2828	98.69
0.9907	203.62
0.6794	300.30
0.5165	335.10
0.4165	347.16
0.3489	352.65
0.2634	354.56
0.2116	356.05
0.1418	356.15
0.1066	356.26
0.0854	357.10
0.0713	357.53
0.0611	357.42
0.0535	357.31
0.0476	357.31
0.0429	357.31
0.0390	357.31
0.0357	357.42
0.0330	357.42
0.0306	357.63
0.0286	357.63
0.0268	357.84
0.0252	357.84
0.0238	358.27
0.0226	357.84
0.0215	358.06
0.0204	358.06
0.0195	357.84
0.0187	357.84
0.0179	358.48
0.0172	358.06
0.0165	358.58
0.0159	359.64
0.0153	360.06
0.0148	358.69
0.0143	358.90

Sample G 6

PORE-ENTRANCE DIAMETER, MICRONS	CUMULATIVE PORE-VOLUME, CU MM/G
58.5831	0.00
37.8967	3.88
28.5224	5.51
22.5668	6.64
18.9062	7.20
16.0855	7.82
13.9951	8.20
11.8533	8.64
10.6762	8.64
9.7127	8.89
8.9087	9.14
8.2271	9.20
7.6424	9.26
7.1355	9.39
6.6914	9.45
6.2997	9.64
5.9512	9.83
5.6392	9.95
4.9857	10.27
4.4681	10.70
3.6995	11.02
3.1566	11.39
2.7526	11.83
2.4403	12.14
2.1916	12.33
1.9889	12.64
1.8205	12.77
1.2791	13.52
0.9858	14.15
0.6760	15.96
0.5143	19.53
0.4151	25.10
0.3479	29.23
0.2629	42.75
0.2112	49.51
0.1417	56.21
0.1066	59.40
0.0854	62.35
0.0712	63.85
0.0611	64.54
0.0535	65.41
0.0476	66.67
0.0428	67.23
0.0390	67.35
0.0357	67.86
0.0330	68.48
0.0306	68.79
0.0286	69.17
0.0268	69.48
0.0252	69.73
0.0238	69.92
0.0226	70.36
0.0215	70.11
0.0204	70.48
0.0195	70.55
0.0187	70.55
0.0179	70.61
0.0172	70.36
0.0165	70.92
0.0159	71.11
0.0153	71.05
0.0148	71.74
0.0143	71.80

Sample G 7		Sample G 8	
PORE-ENTRANCE DIAMETER, MICRONS	CUMULATIVE PORE-VOLUME, CU MM/G	PORE-ENTRANCE DIAMETER, MICRONS	CUMULATIVE PORE-VOLUME, CU MM/G
58.5831	0.00	58.5831	0.00
38.2506	7.60	39.1600	5.24
29.0030	11.17	28.8380	7.85
22.9283	13.23	22.8893	9.16
18.9655	14.59	18.8986	9.85
16.3646	15.66	16.1890	10.47
14.0866	16.34	14.1289	10.85
11.7692	16.95	11.8712	11.47
10.6165	19.08	10.6969	12.72
9.6641	19.61	9.7299	12.97
8.8676	19.84	8.9227	13.09
8.1920	19.92	8.2391	13.15
7.6123	20.07	7.6527	13.21
7.1095	20.37	7.1449	13.53
6.6686	20.45	6.6998	13.65
6.2791	20.45	6.3071	13.84
5.9326	20.52	5.9577	13.90
5.6225	20.68	5.6448	13.90
4.9724	20.75	4.9899	14.03
4.4573	21.13	4.4712	14.15
3.6923	21.97	3.7018	14.84
3.1513	22.42	3.1583	15.27
2.7486	22.88	2.7539	15.65
2.4371	23.34	2.4413	16.14
2.1891	23.87	2.1934	16.39
1.9869	24.25	1.9896	16.77
1.8188	24.48	1.8211	17.02
1.2782	25.46	1.2794	18.08
0.9854	26.98	0.9861	19.07
0.6757	30.18	0.6762	26.18
0.5142	32.84	0.5145	39.64
0.4159	35.35	0.4153	58.78
0.3478	36.87	0.3482	73.74
0.2628	42.34	0.2631	107.59
0.2112	67.27	0.2114	122.24
0.1417	163.73	0.1417	130.22
0.1066	187.37	0.1066	132.46
0.0854	198.77	0.0854	134.14
0.0713	203.33	0.0713	134.95
0.0611	210.17	0.0611	136.01
0.0535	217.01	0.0535	136.57
0.0476	223.86	0.0476	137.63
0.0429	226.14	0.0429	138.19
0.0390	227.66	0.0390	138.63
0.0357	228.42	0.0357	139.13
0.0330	228.42	0.0330	139.00
0.0306	228.42	0.0306	139.44
0.0286	229.18	0.0286	139.38
0.0268	229.18	0.0268	139.63
0.0252	229.94	0.0252	139.82
0.0238	229.94	0.0238	139.88
0.0226	229.94	0.0226	140.44
0.0215	229.94	0.0215	140.87
0.0204	229.94	0.0204	140.69
0.0195	229.94	0.0195	140.63
0.0187	230.70	0.0187	140.81
0.0179	230.70	0.0179	140.94
0.0172	231.46	0.0172	140.94
0.0165	230.70	0.0165	141.00
0.0159	230.70	0.0159	141.44
0.0153	230.70	0.0153	141.37
0.0148	230.70	0.0148	141.06
0.0143	231.46	0.0143	141.69

Sample G 14

PORE-ENTRANCE DIAMETER, MICRONS	CUMULATIVE PORE-VOLUME, CU MM/G
58.5831	0.00
39.2111	12.05
28.9416	20.04
22.7038	25.27
18.3601	30.60
15.7828	33.80
13.8289	34.76
11.9207	38.60
10.7409	42.01
9.7702	44.03
8.9593	45.53
8.2729	47.13
7.6834	48.19
7.1730	49.79
6.7257	50.97
6.3304	51.71
5.9796	53.10
5.6651	53.74
5.0073	56.30
4.4871	60.35
3.7133	63.12
3.1673	66.53
2.7612	69.30
2.4475	72.72
2.1975	74.53
1.9940	76.98
1.8249	78.69
1.2815	86.79
0.9875	94.15
0.6769	108.65
0.5149	118.67
0.4154	129.12
0.3482	135.94
0.2630	156.73
0.2114	181.36
0.1417	248.00
0.1066	275.83
0.0854	293.85
0.0713	299.93
0.0611	307.82
0.0535	316.03
0.0476	324.77
0.0429	329.68
0.0390	331.38
0.0357	333.30
0.0330	334.58
0.0306	334.79
0.0286	335.22
0.0268	335.86
0.0252	336.39
0.0238	337.35
0.0226	337.35
0.0215	338.52
0.0204	338.74
0.0195	338.95
0.0187	339.16
0.0179	339.38
0.0172	339.70
0.0165	339.59
0.0159	340.02
0.0153	340.66
0.0148	339.59
0.0143	341.19

Sample G 30

PORE-ENTRANCE DIAMETER, MICRONS	CUMULATIVE PORE-VOLUME, CU MM/G
58.5831	0.00
38.0862	5.06
28.5468	7.03
22.8146	8.14
18.7164	9.08
16.0537	9.77
13.9166	10.28
11.6308	10.80
10.4953	10.80
9.5625	11.05
8.7824	11.48
8.1195	11.65
7.5496	11.82
7.0545	12.00
6.6202	12.08
6.2364	12.34
5.8948	12.59
5.5884	12.68
4.9459	12.94
4.4360	13.45
3.6776	14.14
3.1406	14.82
2.7405	15.34
2.4308	15.94
2.1839	16.36
1.9826	16.88
1.8153	17.39
1.2765	19.19
0.9844	20.99
0.6753	23.99
0.5139	26.05
0.4148	27.93
0.3477	29.05
0.2627	32.56
0.2111	35.90
0.1416	43.61
0.1065	50.81
0.0854	62.20
0.0712	68.89
0.0611	77.97
0.0535	87.22
0.0476	105.39
0.0428	123.46
0.0390	145.74
0.0357	168.02
0.0330	195.52
0.0306	214.11
0.0286	230.05
0.0268	244.87
0.0252	255.15
0.0238	265.35
0.0226	269.55
0.0215	273.32
0.0204	275.54
0.0195	276.31
0.0187	274.34
0.0179	275.12
0.0172	276.49
0.0165	276.66
0.0159	277.17
0.0153	277.34
0.0148	277.26
0.0143	277.69

Sample G 31		Sample G 32	
PORE-ENTRANCE DIAMETER, MICRONS	CUMULATIVE PORE-VOLUME, CU MM/G	PORE-ENTRANCE DIAMETER, MICRONS	CUMULATIVE PORE-VOLUME, CU MM/G
58.5831	0.00	58.5831	0.00
37.7561	6.53	38.3669	4.98
28.5005	9.50	29.7319	6.97
22.9409	11.19	23.6875	8.28
19.0512	12.13	19.0992	9.12
16.0680	12.80	16.5888	9.70
14.1305	13.57	14.4427	10.07
11.7001	14.92	12.1462	10.54
10.5597	17.13	10.9144	10.75
9.6165	17.55	9.9090	10.85
8.8268	17.55	9.0731	10.96
8.1571	17.55	8.3670	10.96
7.5819	17.64	7.7643	11.43
7.0824	17.64	7.2417	11.59
6.6445	17.55	6.7841	11.38
6.2584	18.06	6.3820	11.64
5.9144	18.32	6.0249	11.95
5.6057	18.06	5.7050	11.85
4.9594	18.40	5.0374	12.32
4.4470	19.08	4.5094	12.53
3.6858	21.28	3.7278	12.90
3.1472	23.83	3.1769	12.74
2.7455	24.51	2.7680	13.00
2.4347	24.67	2.4525	13.58
2.1871	25.18	2.2014	13.68
1.9854	27.39	1.9970	13.95
1.8176	27.13	1.8273	13.95
1.2776	28.15	1.2824	14.57
0.9850	29.25	0.9878	15.36
0.6756	32.56	0.6769	16.15
0.5141	34.34	0.5148	16.57
0.4149	34.60	0.4154	16.88
0.3478	35.36	0.3481	16.93
0.2628	38.07	0.2630	17.62
0.2112	41.04	0.2113	17.93
0.1416	49.60	0.1417	19.61
0.1065	56.56	0.1066	20.55
0.0854	63.59	0.0854	21.50
0.0712	68.43	0.0712	22.02
0.0611	73.26	0.0611	22.49
0.0535	79.45	0.0535	23.07
0.0476	85.98	0.0476	23.64
0.0428	91.07	0.0428	24.33
0.0390	101.67	0.0390	24.80
0.0357	110.57	0.0357	25.32
0.0330	122.10	0.0330	25.48
0.0306	132.70	0.0306	26.11
0.0286	144.32	0.0286	26.16
0.0268	155.76	0.0268	26.69
0.0252	164.33	0.0252	26.58
0.0238	173.57	0.0238	26.95
0.0226	179.93	0.0226	26.95
0.0215	187.99	0.0215	27.21
0.0204	193.75	0.0204	27.26
0.0195	199.18	0.0195	27.52
0.0187	204.69	0.0187	27.58
0.0179	208.42	0.0179	27.42
0.0172	209.52	0.0172	27.68
0.0165	208.85	0.0165	27.58
0.0159	210.80	0.0159	27.64
0.0153	214.10	0.0153	27.73
0.0148	215.46	0.0148	28.15
0.0143	215.63	0.0143	27.89

Sample G 33		**Sample G 34**	
PORE-ENTRANCE DIAMETER, MICRONS	CUMULATIVE PORE-VOLUME, CU MM/G	PORE-ENTRANCE DIAMETER, MICRONS	CUMULATIVE PORE-VOLUME, CU MM/G
58.5831	0.00	58.5831	0.00
38.2546	5.42	38.6588	4.57
29.7297	8.00	28.3197	7.35
23.6693	9.66	22.4950	8.69
19.2990	10.84	19.1101	9.36
16.5484	11.59	16.1262	10.14
14.3645	12.02	14.0453	10.58
12.1394	12.61	12.0164	11.08
10.9099	12.99	10.8092	11.25
9.9066	13.37	9.8235	11.64
9.0718	13.63	9.0019	11.86
8.3664	13.79	8.3069	12.03
7.7626	13.90	7.7110	12.03
7.2401	14.01	7.1952	12.14
6.7833	14.01	6.7440	12.20
6.3810	14.17	6.3463	12.42
6.0237	14.28	5.9927	12.53
5.7043	14.44	5.6766	12.70
5.0365	14.65	5.0148	12.92
4.5089	15.08	4.4915	13.31
3.7276	15.57	3.7156	13.70
3.1770	15.89	3.1682	14.03
2.7680	16.10	2.7614	14.26
2.4524	16.37	2.4471	14.37
2.2014	16.64	2.1972	14.81
1.9970	16.91	1.9935	15.09
1.8273	17.18	1.8244	15.20
1.2824	17.82	1.2810	16.04
0.9878	18.30	0.9870	16.60
0.6769	19.00	0.6765	17.32
0.5148	19.32	0.5146	17.99
0.4154	19.70	0.4152	18.49
0.3481	19.86	0.3480	19.05
0.2630	20.50	0.2629	21.11
0.2113	21.58	0.2112	23.89
0.1417	23.46	0.1417	34.37
0.1065	24.96	0.1066	45.45
0.0854	26.68	0.0854	53.52
0.0713	28.72	0.0713	54.86
0.0611	29.04	0.0611	55.69
0.0535	29.47	0.0535	56.25
0.0476	29.68	0.0476	56.81
0.0426	29.79	0.0429	57.42
0.0390	30.22	0.0390	57.87
0.0357	30.59	0.0357	58.25
0.0330	30.65	0.0330	58.70
0.0306	30.92	0.0306	59.09
0.0286	31.29	0.0286	59.59
0.0268	31.40	0.0268	60.20
0.0252	31.56	0.0252	60.48
0.0238	31.56	0.0238	60.71
0.0226	31.72	0.0226	61.10
0.0215	31.88	0.0215	61.21
0.0204	32.21	0.0204	61.37
0.0195	32.21	0.0195	61.71
0.0187	32.58	0.0187	62.10
0.0179	32.63	0.0179	62.15
0.0172	32.63	0.0172	62.49
0.0165	32.69	0.0165	62.77
0.0159	32.85	0.0159	62.99
0.0153	33.12	0.0153	63.27
0.0148	33.17	0.0148	63.32
0.0143	33.33	0.0143	63.49

Sample G 38

PORE-ENTRANCE DIAMETER, MICRONS	CUMULATIVE PORE-VOLUME, CU MM/G
58.58	0.0
39.23	8.25
30.24	12.62
23.94	15.98
20.13	18.33
17.45	19.45
15.29	20.57
11.76	22.60
10.61	23.62
9.65	24.44
8.86	24.84
8.19	25.45
7.61	25.66
7.11	25.96
6.66	26.47
6.28	26.57
5.93	26.98
5.62	27.90
4.97	28.30
4.46	28.71
3.69	29.53
3.15	30.34
2.75	31.36
2.44	31.56
2.19	32.07
1.99	32.89
1.82	33.40
1.28	35.23
0.985	36.86
0.676	41.74
0.514	42.15
0.430	43.88
0.358	44.80
0.269	52.13
0.215	57.53
0.143	90.92
0.108	155.58
0.086	250.98
0.072	271.85
0.0614	278.37
0.0537	280.20
0.0478	281.73
0.0430	282.65
0.0391	282.95
0.0358	284.17
0.0331	284.38
0.0307	284.78
0.0287	285.09
0.0269	285.70
0.0253	285.09
0.0239	285.39
0.0226	285.50
0.0215	285.50
0.0204	286.01
0.0195	285.80
0.0186	286.41
0.0179	286.31
0.0172	286.31
0.0165	287.33
0.0159	286.82
0.0154	286.82
0.0148	286.92
0.0143	286.72

Sample G 39

PORE-ENTRANCE DIAMETER, MICRONS	CUMULATIVE PORE-VOLUME, CU MM/G
58.58	0.0
38.74	8.17
29.21	11.71
22.90	14.02
18.78	15.67
16.08	16.58
14.14	16.91
11.79	17.82
10.63	19.06
9.67	19.22
8.88	19.55
8.20	19.96
7.62	20.38
7.12	20.79
6.67	20.95
6.28	21.20
5.94	21.53
5.63	21.70
4.98	22.19
4.46	22.77
3.69	23.26
3.15	23.84
2.75	24.25
2.63	24.83
2.19	25.24
1.99	25.57
1.82	25.99
1.28	27.22
0.985	28.63
0.676	30.36
0.514	32.09
0.430	33.33
0.358	33.82
0.269	36.46
0.215	38.36
0.143	43.39
0.108	52.14
0.086	78.04
0.072	112.28
0.0614	156.25
0.0537	188.42
0.0478	212.68
0.0430	227.53
0.0391	234.87
0.0358	238.91
0.0331	242.62
0.0307	245.26
0.0287	246.50
0.0269	248.07
0.0253	249.06
0.0239	249.47
0.0226	250.13
0.0215	250.62
0.0204	250.87
0.0195	250.87
0.0186	251.04
0.0179	251.53
0.0172	252.19
0.0165	252.27
0.0159	252.60
0.0154	253.02
0.0.148	253.26
0.0143	253.68

Sample G 40

PORE-ENTRANCE DIAMETER, MICRONS	CUMULATIVE PORE-VOLUME, CU MM/G
58.58	0.0
38.53	16.43
29.05	21.03
23.19	21.66
19.21	22.60
16.42	22.81
14.44	22.71
11.80	23.13
10.63	25.32
9.68	26.16
8.88	26.37
8.21	26.58
7.62	26.68
7.12	26.89
6.68	26.89
6.29	27.21
5.94	27.73
5.63	27.83
4.98	27.94
4.46	28.04
3.69	28.15
3.15	28.25
2.75	28.36
2.44	28.67
2.19	28.67
1.99	28.78
1.82	28.99
1.28	30.24
0.985	30.97
0.676	33.90
0.514	37.57
0.430	42.27
0.358	42.69
0.269	47.09
0.215	70.84
0.143	173.38
0.108	246.22
0.086	266.32
0.072	268.30
0.0614	267.68
0.0537	268.83
0.0478	269.56
0.0430	270.40
0.0391	270.82
0.0358	270.19
0.0331	269.87
0.0307	269.87
0.0287	270.82
0.0269	271.34
0.0253	271.76
0.0239	272.07
0.0226	272.07
0.0215	272.07
0.0204	272.07
0.0195	272.18
0.0186	272.28
0.0179	271.86
0.0172	272.38
0.0165	272.91
0.0159	273.54
0.0154	274.90
0.0148	274.90
0.0143	274.58

Sample G 41

PORE-ENTRANCE DIAMETER, MICRONS	CUMULATIVE PORE-VOLUME, CU MM/G
58.58	0.0
36.94	7.49
28.55	10.06
22.58	12.20
18.78	13.44
16.02	14.47
14.13	14.91
11.81	15.94
10.64	17.12
9.68	17.12
8.88	17.41
8.21	18.00
7.63	18.07
7.12	18.22
6.68	18.44
6.29	18.59
5.94	18.81
5.63	19.25
4.98	19.54
4.46	20.20
3.70	20.57
3.15	21.16
2.75	21.75
2.44	22.04
2.19	22.11
1.99	22.19
1.82	22.33
1.28	24.46
0.99	32.91
0.68	33.06
0.51	33.50
0.430	38.50
0.358	41.58
0.269	47.38
0.215	79.49
0.143	150.75
0.108	183.96
0.086	196.30
0.072	200.41
0.0614	200.85
0.0537	201.59
0.0478	202.62
0.0430	202.62
0.0391	202.98
0.0358	203.50
0.0331	202.76
0.0307	203.28
0.0287	203.94
0.0269	204.45
0.0253	204.31
0.0239	204.67
0.0226	204.38
0.0215	205.19
0.0204	205.11
0.0195	205.85
0.0186	205.63
0.0179	205.33
0.0172	205.41
0.0165	205.48
0.0159	206.14
0.0154	206.07
0.0148	205.48
0.0143	206.00

Sample J

PORE-ENTRANCE DIAMETER, MICRONS	CUMULATIVE PORE-VOLUME, CU MM/G
58.5831	0.00
37.4924	3.51
28.9469	4.21
22.9448	4.91
18.9670	6.37
16.0292	8.60
14.1870	9.42
11.6975	9.88
10.5606	11.99
9.6165	12.11
8.8268	12.11
8.1571	12.11
7.5818	12.11
7.0823	12.11
6.6445	12.11
6.2577	12.11
5.9148	12.92
5.6065	13.04
4.9605	13.63
4.4478	14.04
3.6855	14.21
3.1463	14.50
2.7449	15.03
2.4344	16.02
2.1869	16.38
1.9850	16.55
1.8174	17.55
1.2779	22.81
0.9853	27.78
0.6759	36.38
0.5142	38.31
0.4150	40.30
0.3479	40.47
0.2628	41.29
0.2112	41.64
0.1416	43.04
0.1065	45.33
0.0854	46.14
0.0712	46.79
0.0611	47.43
0.0535	48.37
0.0476	48.42
0.0428	48.25
0.0390	48.07
0.0357	48.54
0.0330	48.42
0.0306	48.48
0.0286	48.42
0.0268	48.48
0.0252	48.37
0.0238	48.25
0.0226	47.90
0.0215	47.55
0.0204	46.85
0.0195	46.26
0.0187	46.20
0.0179	45.73
0.0172	45.62
0.0165	45.56
0.0159	45.62
0.0153	45.85
0.0148	46.20
0.0143	46.32

Sample J 2

PORE-ENTRANCE DIAMETER, MICRONS	CUMULATIVE PORE-VOLUME, CU MM/G
58.5831	0.00
38.3933	1.23
28.7686	2.03
22.6361	2.68
18.7882	3.26
16.0091	3.70
13.9187	4.06
11.7469	4.57
10.6015	7.32
9.6506	7.54
8.8564	7.83
8.1829	8.05
7.6042	8.12
7.1023	8.34
6.6629	8.77
6.2743	8.99
5.9287	9.28
5.6193	9.64
4.9707	10.59
4.4575	13.05
3.6931	15.15
3.1529	18.34
2.7503	20.45
2.4389	22.55
2.1907	24.14
1.9884	25.96
1.8204	28.42
1.2793	35.02
0.9862	41.62
0.6762	49.45
0.5145	55.54
0.4152	60.32
0.3480	64.17
0.2629	76.71
0.2113	90.78
0.1417	107.09
0.1066	114.41
0.0854	117.89
0.0713	118.55
0.0611	120.21
0.0535	120.50
0.0476	120.65
0.0429	121.16
0.0390	121.52
0.0357	121.81
0.0330	121.81
0.0306	121.88
0.0286	121.95
0.0268	122.32
0.0252	122.75
0.0238	122.61
0.0226	122.61
0.0215	122.68
0.0204	122.75
0.0195	122.39
0.0187	122.75
0.0179	122.75
0.0172	123.62
0.0165	123.84
0.0159	123.62
0.0153	124.06
0.0148	123.77
0.0143	124.13

Sample J 3

PORE-ENTRANCE DIAMETER, MICRONS	CUMULATIVE PORE-VOLUME, CU MM/G
58.5831	0.00
38.7933	3.07
28.0818	4.83
22.4419	5.48
18.6905	6.26
15.9070	7.05
13.8540	7.83
11.8123	8.68
10.6501	10.18
9.6906	10.31
8.8901	10.57
8.2116	10.76
7.6294	10.96
7.1242	11.16
6.6820	11.48
6.2914	11.74
5.9442	12.13
5.6331	12.40
4.9817	13.44
4.4664	15.79
3.6993	17.74
3.1573	20.16
2.7538	22.70
2.4418	25.31
2.1930	26.62
1.9903	28.38
1.8220	30.66
1.2802	37.51
0.9868	43.38
0.6765	50.43
0.5146	55.84
0.4153	60.28
0.3481	63.80
0.2630	76.20
0.2113	87.29
0.1417	104.51
0.1066	111.17
0.0854	115.99
0.0713	117.49
0.0611	118.28
0.0535	118.54
0.0476	118.73
0.0429	118.80
0.0390	119.26
0.0357	119.26
0.0330	119.45
0.0306	119.84
0.0286	120.04
0.0268	120.43
0.0252	120.43
0.0238	121.02
0.0226	121.02
0.0215	121.08
0.0204	121.60
0.0195	121.67
0.0187	121.86
0.0179	122.13
0.0172	122.45
0.0165	122.45
0.0159	122.39
0.0153	122.52
0.0148	122.58
0.0143	122.97

Sample J 4

PORE-ENTRANCE DIAMETER, MICRONS	CUMULATIVE PORE-VOLUME, CU MM/G
58.5831	0.00
38.7119	6.08
28.5648	7.01
22.7777	8.03
18.7050	9.97
15.8967	11.22
14.1201	12.31
11.6736	13.48
10.5374	15.35
9.5975	15.58
8.8117	15.90
8.1449	16.21
7.5720	16.60
7.0743	16.91
6.6376	17.06
6.2522	17.38
5.9081	17.06
5.6007	17.38
4.9558	17.92
4.4443	18.93
3.6837	20.42
3.1453	21.51
2.7442	22.83
2.4339	24.23
2.1867	25.87
1.9856	27.43
1.8175	29.38
1.2778	34.91
0.9853	42.08
0.6758	51.74
0.5142	56.57
0.4156	60.08
0.3479	61.40
0.2626	65.76
0.2112	68.73
0.1416	73.17
0.1065	76.21
0.0854	80.10
0.0712	83.22
0.0611	86.49
0.0535	92.72
0.0476	105.27
0.0428	119.22
0.0390	134.26
0.0357	146.49
0.0330	155.53
0.0306	164.26
0.0286	172.75
0.0268	181.48
0.0252	188.80
0.0238	193.71
0.0226	197.56
0.0215	200.80
0.0204	202.90
0.0195	205.63
0.0187	206.88
0.0179	208.36
0.0172	209.53
0.0165	210.54
0.0159	210.85
0.0153	211.63
0.0148	212.25
0.0143	212.41

Sample J 5		**Sample J 6**	
PORE-ENTRANCE DIAMETER, MICRONS	CUMULATIVE PORE-VOLUME, CU MM/G	PORE-ENTRANCE DIAMETER, MICRONS	CUMULATIVE PORE-VOLUME, CU MM/G
58.5831	0.00	58.5831	0.00
39.1604	7.60	39.2900	4.59
28.8749	11.97	28.7222	7.82
22.9602	14.76	23.1678	9.69
19.1144	16.79	19.1461	10.98
16.2701	18.52	16.3148	12.35
14.2354	19.95	14.2490	13.49
11.7045	21.76	11.9727	14.86
10.5556	21.83	10.7825	17.01
9.6141	22.51	9.8009	17.37
8.8257	22.81	8.9829	17.66
8.1568	23.11	8.2913	18.09
7.5825	23.57	7.6979	18.23
7.0839	24.09	7.1845	18.73
6.6470	24.77	6.7352	19.16
6.2606	25.22	6.3391	19.81
5.9168	25.82	5.9869	20.38
5.6084	26.05	5.6713	20.60
4.9621	26.95	5.0110	21.10
4.4497	28.31	4.4890	22.47
3.6873	29.51	3.7142	23.54
3.1480	30.79	3.1675	24.55
2.7463	32.15	2.7610	25.34
2.4356	33.66	2.4470	26.56
2.1880	34.94	2.1972	27.92
1.9860	36.21	1.9936	28.78
1.8183	37.49	1.8246	29.93
1.2783	44.80	1.2814	35.17
0.9856	51.88	0.9874	41.49
0.6760	60.84	0.6768	48.95
0.5143	65.50	0.5148	53.19
0.4151	67.91	0.4154	55.05
0.3479	69.19	0.3481	56.56
0.2628	72.05	0.2630	58.79
0.2112	73.71	0.2113	60.15
0.1416	76.72	0.1417	62.23
0.1065	78.75	0.1066	64.03
0.0854	81.92	0.0854	65.96
0.0712	84.70	0.0713	67.04
0.0611	89.22	0.0611	68.40
0.0535	95.32	0.0535	69.84
0.0476	104.81	0.0476	71.56
0.0428	114.14	0.0429	73.36
0.0390	121.97	0.0390	75.29
0.0357	133.34	0.0357	76.66
0.0330	141.85	0.0330	78.02
0.0306	149.68	0.0306	79.60
0.0286	156.91	0.0286	80.89
0.0268	163.31	0.0268	82.83
0.0252	169.93	0.0252	85.27
0.0238	173.70	0.0238	87.93
0.0226	176.33	0.0226	90.80
0.0215	178.97	0.0215	94.31
0.0204	180.92	0.0204	96.40
0.0195	182.35	0.0195	99.12
0.0187	183.26	0.0187	103.14
0.0179	184.24	0.0179	105.30
0.0172	184.61	0.0172	108.02
0.0165	185.22	0.0165	110.46
0.0159	185.44	0.0159	112.12
0.0153	185.52	0.0153	114.63
0.0148	186.12	0.0148	116.28
0.0143	186.42	0.0143	117.97

Sample J 8		Sample J 9	
PORE-ENTRANCE DIAMETER, MICRONS	CUMULATIVE PORE-VOLUME, CU MM/G	PORE-ENTRANCE DIAMETER, MICRONS	CUMULATIVE PORE-VOLUME, CU MM/G
58.5831	0.00	58.5831	0.00
39.4980	4.12	38.7453	7.19
29.8187	6.71	28.2152	11.80
23.1898	8.83	23.2702	14.25
19.2175	10.36	19.0468	16.76
16.2836	11.95	16.3116	18.79
14.3469	12.82	14.2588	20.25
11.8983	14.61	12.0218	21.93
10.7249	17.20	10.8197	23.47
9.7523	17.27	9.8340	24.44
8.9422	17.60	9.0111	24.86
8.2557	17.66	8.3153	25.28
7.6676	17.93	7.7206	26.26
7.1581	18.39	7.2043	26.75
6.7116	18.59	6.7527	27.24
6.3174	18.73	6.3550	28.14
5.9675	19.26	6.0008	28.49
5.6543	19.72	5.6837	28.63
4.9979	20.39	5.0211	29.54
4.4781	21.12	4.4972	31.01
3.7070	22.64	3.7204	33.10
3.1626	24.57	3.1725	35.41
2.7576	26.16	2.7649	36.39
2.4445	27.69	2.4503	38.27
2.1953	29.75	2.2003	41.83
1.9921	30.95	1.9962	43.16
1.8234	32.07	1.8268	44.56
1.2808	38.38	1.2806	51.75
0.9871	44.23	0.9881	56.57
0.6767	51.53	0.6771	63.90
0.5147	54.98	0.5150	68.30
0.4153	57.57	0.4155	71.65
0.3481	57.71	0.3482	72.70
0.2629	60.16	0.2630	74.59
0.2113	61.36	0.2113	75.49
0.1417	63.48	0.1417	78.01
0.1066	64.35	0.1066	78.08
0.0854	67.27	0.0854	81.15
0.0712	69.79	0.0713	82.55
0.0611	72.91	0.0611	85.06
0.0535	79.82	0.0535	87.93
0.0476	95.09	0.0476	92.33
0.0429	104.26	0.0429	97.91
0.0390	115.08	0.0390	105.94
0.0357	123.65	0.0357	114.60
0.0330	130.95	0.0330	122.91.
0.0306	136.53	0.0306	128.08
0.0286	142.18	0.0286	132.62
0.0268	147.69	0.0268	138.77
0.0252	151.41	0.0252	145.12
0.0238	154.39	0.0238	152.25
0.0226	157.05	0.0226	159.23
0.0215	157.78	0.0215	164.47
0.0204	159.64	0.0204	169.01
0.0195	160.97	0.0195	174.32
0.0187	161.37	0.0187	178.09
0.0179	162.69	0.0179	180.60
0.0172	163.23	0.0172	182.49
0.0165	164.42	0.0165	183.53
0.0159	164.95	0.0159	184.37
0.0153	165.28	0.0153	185.98
0.0148	165.55	0.0148	186.68
0.0143	165.42	0.0143	187.31

Sample J 10		**Sample J 12**	
PORE-ENTRANCE DIAMETER, MICRONS	CUMULATIVE PORE-VOLUME, CU MM/G	PORE-ENTRANCE DIAMETER, MICRONS	CUMULATIVE PORE-VOLUME, CU MM/G
58.5831	0.00	58.5831	0.00
39.2666	9.02	38.8718	6.00
27.7254	12.29	28.6947	9.80
22.9938	14.88	22.8446	12.13
19.1468	17.15	18.7905	14.09
16.2377	18.03	16.2334	15.68
14.3287	18.66	14.1649	16.91
11.8017	19.42	11.8265	18.74
10.6454	21.69	10.6644	22.66
9.6862	21.69	9.7037	23.52
8.8876	22.26	8.9023	24.62
8.2106	22.82	8.2226	25.36
7.6288	23.14	7.6393	26.09
7.1241	23.52	7.1333	26.83
6.6827	24.21	6.6904	27.81
6.2921	24.53	6.2988	28.30
5.9449	24.97	5.9507	28.91
5.6342	25.60	5.6391	29.65
4.9824	26.42	4.9861	30.99
4.4661	27.68	4.4688	32.83
3.6989	29.32	3.7004	34.79
3.1566	30.70	3.1575	36.75
2.7529	32.09	2.7534	38.47
2.4409	33.67	2.4411	40.67
2.1921	34.23	2.1924	42.27
1.9896	36.19	1.9897	44.23
1.8213	37.89	1.8213	45.82
1.2798	43.69	1.2797	52.92
0.9865	48.10	0.9863	58.68
0.6763	54.28	0.6762	65.54
0.5145	56.30	0.5144	68.60
0.4152	57.31	0.4151	70.44
0.3480	58.07	0.3479	71.42
0.2629	59.33	0.2629	73.01
0.2112	59.64	0.2112	74.36
0.1416	60.84	0.1416	76.69
0.1066	61.79	0.1065	78.16
0.0854	63.55	0.0854	82.20
0.0712	65.82	0.0712	85.39
0.0611	70.55	0.0611	88.33
0.0535	78.49	0.0535	94.58
0.0476	84.48	0.0476	112.71
0.0428	90.22	0.0428	144.56
0.0390	95.71	0.0392	174.21
0.0357	101.32	0.0357	192.58
0.0330	105.35	0.0330	201.89
0.0306	108.38	0.0306	207.04
0.0286	111.28	0.0286	210.35
0.0268	114.05	0.0268	212.92
0.0252	115.94	0.0252	215.25
0.0238	118.09	0.0238	216.47
0.0226	119.28	0.0226	217.57
0.0215	120.17	0.0215	218.31
0.0204	120.67	0.0204	218.43
0.0195	121.43	0.0195	220.39
0.0187	122.25	0.0187	220.15
0.0179	123.00	0.0179	219.90
0.0172	123.89	0.0172	220.51
0.0165	124.27	0.0165	220.64
0.0159	124.64	0.0159	221.74
0.0153	124.77	0.0153	221.86
0.0148	125.46	0.0148	221.98
0.0143	125.72	0.0143	221.49

Sample J 13

PORE-ENTRANCE DIAMETER, MICRONS	CUMULATIVE PORE-VOLUME, CU MM/G
58.5831	0.00
38.2707	9.29
28.7161	13.90
22.9731	16.64
19.0556	19.03
16.2991	20.80
14.2005	22.39
11.8725	24.08
10.6967	25.49
9.7316	26.47
8.9261	27.44
8.2429	27.97
7.6573	28.77
7.1493	29.48
6.7047	30.36
6.3119	30.98
5.9627	31.78
5.6498	32.22
4.9948	33.64
4.4761	35.41
3.7055	37.18
3.1612	38.68
2.7564	40.36
2.4436	42.40
2.1944	43.99
1.9915	46.20
1.8228	47.71
1.2806	57.27
0.9870	64.98
0.6766	73.82
0.5147	77.27
0.4153	79.93
0.3480	81.17
0.2629	83.65
0.2113	84.62
0.1417	87.63
0.1066	90.29
0.0854	94.45
0.0712	97.28
0.0611	100.55
0.0535	105.69
0.0476	117.11
0.0429	143.13
0.0390	182.08
0.0357	227.93
0.0330	257.05
0.0306	271.65
0.0286	278.73
0.0268	283.51
0.0252	287.05
0.0238	289.00
0.0226	290.59
0.0215	291.48
0.0204	292.54
0.0195	293.34
0.0187	293.43
0.0179	293.96
0.0172	294.22
0.0165	294.05
0.0159	294.75
0.0153	294.93
0.0148	295.73
0.0143	296.26

Sample J 14

PORE-ENTRANCE DIAMETER, MICRONS	CUMULATIVE PORE-VOLUME, CU MM/G
58.5831	0.00
39.2188	7.44
29.0327	11.57
22.8080	14.51
19.1062	16.62
16.2742	18.46
14.1729	20.20
11.8667	22.04
9.7313	25.81
8.9248	26.36
8.2416	26.82
7.6555	27.27
7.1474	27.83
6.7027	28.47
6.3100	29.02
5.9606	29.48
5.6480	30.03
4.9933	31.41
4.4750	33.34
3.7046	34.71
3.1606	36.55
2.7560	38.39
2.4432	40.22
2.1941	41.78
1.9912	44.26
1.8226	46.28
1.2805	55.56
0.9869	64.31
0.6766	74.66
0.5147	80.17
0.4153	82.93
0.3481	84.21
0.2629	87.15
0.2113	89.54
0.1417	93.49
0.1066	96.06
0.0854	100.83
0.0712	105.70
0.0611	112.13
0.0535	125.17
0.0476	153.27
0.0429	199.56
0.0390	247.95
0.0357	289.64
0.0330	313.61
0.0306	328.21
0.0286	335.54
0.0268	340.34
0.0252	343.64
0.0238	345.76
0.0226	346.95
0.0215	348.05
0.0204	348.42
0.0195	349.34
0.0187	348.79
0.0179	350.44
0.0172	349.89
0.0165	350.93
0.0159	350.25
0.0153	350.99
0.0148	351.27
0.0143	351.17

Sample J 15

PORE-ENTRANCE DIAMETER, MICRONS	CUMULATIVE PORE-VOLUME, CU MM/G
58.5831	0.00
38.5256	12.54
28.2288	19.56
23.3329	23.02
19.0908	26.58
16.3205	29.48
14.2695	30.51
11.7790	32.75
10.6245	35.37
9.6696	35.66
8.8736	36.50
8.1986	37.34
7.6196	38.46
7.1164	39.21
6.6757	40.15
6.2862	40.80
5.9397	41.55
5.6296	42.58
4.9791	44.27
4.4636	46.23
3.6968	47.73
3.1551	49.97
2.7517	51.85
2.4399	54.19
2.1915	55.78
1.9890	57.93
1.8208	60.08
1.2796	69.35
0.9864	77.96
0.6763	88.81
0.5145	94.61
0.4152	97.23
0.3480	98.45
0.2629	101.82
0.2112	104.16
0.1417	107.53
0.1066	110.71
0.0854	116.14
0.0712	121.19
0.0611	126.43
0.0535	137.29
0.0476	163.40
0.0429	214.03
0.0390	267.84
0.0357	311.26
0.0330	338.31
0.0306	351.78
0.0286	359.55
0.0268	364.70
0.0252	367.88
0.0238	369.56
0.0226	371.06
0.0215	371.34
0.0204	372.28
0.0195	372.75
0.0187	373.87
0.0179	373.59
0.0172	374.06
0.0165	374.15
0.0159	374.80
0.0153	374.71
0.0148	375.27
0.0143	375.08

Sample J 16

PORE-ENTRANCE DIAMETER, MICRONS	CUMULATIVE PORE-VOLUME, CU MM/G
58.5831	0.00
38.3228	10.81
28.3000	14.99
22.7004	17.88
19.0883	21.09
16.2418	23.98
14.0585	26.55
11.7515	29.76
10.6006	32.22
9.6499	32.54
8.8576	33.83
8.1863	35.54
7.6079	36.18
7.1062	37.04
6.6664	37.79
6.2774	38.00
5.9317	38.75
5.6223	39.72
4.9734	41.54
4.4589	43.68
3.6939	46.35
3.1530	48.92
2.7502	51.28
2.4388	54.71
2.1907	57.49
1.9884	60.16
1.8203	63.06
1.2795	76.12
0.9864	88.21
0.6763	101.06
0.5145	108.98
0.4152	114.33
0.3480	118.40
0.2629	120.44
0.2112	122.90
0.1417	128.47
0.1066	130.39
0.0854	137.03
0.0712	144.20
0.0611	153.20
0.0535	170.75
0.0476	204.69
0.0429	263.25
0.0390	310.46
0.0357	349.00
0.0330	369.23
0.0306	378.01
0.0286	383.47
0.0268	386.90
0.0252	388.29
0.0238	389.89
0.0226	390.43
0.0215	391.50
0.0204	391.93
0.0195	392.89
0.0187	393.53
0.0179	393.64
0.0172	394.39
0.0165	394.39
0.0159	394.60
0.0153	394.82
0.0148	394.71
0.0143	394.93

Sample J 17

PORE-ENTRANCE DIAMETER, MICRONS	CUMULATIVE PORE-VOLUME, CU MM/G
58.5831	0.00
38.7412	7.61
29.3360	11.49
23.1009	14.25
19.1635	16.49
16.3882	17.76
14.2581	19.03
11.7583	20.82
10.6083	23.05
9.6578	23.73
8.8642	24.62
8.1907	25.29
7.6109	25.37
7.1088	25.96
6.6689	26.56
6.2798	26.86
5.9336	27.23
5.6238	27.68
4.9743	28.73
4.4592	29.70
3.6940	31.19
3.1529	32.61
2.7501	34.02
2.4385	35.29
2.1902	36.26
1.9880	37.83
1.8198	38.80
1.2790	44.17
0.9859	48.20
0.6760	53.50
0.5143	56.11
0.4151	57.53
0.3479	58.20
0.2628	59.76
0.2112	60.64
0.1416	62.60
0.1065	63.94
0.0854	66.11
0.0712	68.34
0.0611	71.33
0.0535	77.22
0.0476	90.65
0.0428	107.74
0.0390	122.51
0.0357	132.73
0.0330	138.03
0.0306	141.76
0.0286	144.75
0.0268	146.16
0.0252	147.51
0.0238	148.77
0.0226	149.15
0.0215	150.04
0.0204	150.27
0.0195	150.04
0.0187	150.34
0.0179	150.49
0.0172	151.39
0.0165	150.71
0.0159	150.71
0.0153	151.76
0.0148	152.36
0.0143	152.80

Sample M

PORE-ENTRANCE DIAMETER, MICRONS	CUMULATIVE PORE-VOLUME, CU MM/G
58.5831	0.00
38.4184	4.79
28.1686	8.16
21.8623	10.76
17.7289	13.20
15.3649	15.22
13.4817	17.41
11.6332	18.25
10.5015	19.43
9.5697	20.35
8.7893	21.11
8.1270	22.03
7.5583	23.38
7.0644	24.98
6.6304	26.07
6.2468	27.33
5.9049	28.34
5.5982	29.10
4.9561	32.55
4.4482	39.27
3.6886	45.83
3.1503	51.38
2.7494	58.36
2.4389	64.50
2.1910	68.20
1.9888	71.57
1.8207	74.60
1.2799	89.14
0.9868	104.70
0.6767	126.65
0.5148	137.92
0.4154	143.98
0.3481	146.33
0.2630	150.79
0.2113	153.65
0.1417	158.27
0.1066	160.29
0.0854	162.14
0.0713	163.82
0.0611	164.83
0.0535	165.76
0.0476	166.60
0.0429	167.27
0.0390	167.69
0.0357	168.70
0.0330	169.46
0.0306	169.71
0.0286	170.81
0.0268	171.06
0.0252	170.89
0.0238	171.48
0.0226	171.65
0.0215	172.40
0.0204	172.15
0.0195	172.91
0.0187	172.74
0.0179	173.33
0.0172	173.24
0.0165	173.33
0.0159	174.08
0.0153	174.08
0.0148	174.67
0.0143	174.34

Sample N 1		Sample N	
PORE-ENTRANCE DIAMETER, MICRONS	CUMULATIVE PORE-VOLUME, CU MM/G	PORE-ENTRANCE DIAMETER, MICRONS	CUMULATIVE PORE-VOLUME, CU MM/G
58.5831	0.00	58.5831	0.00
37.5396	8.63	39.2586	8.85
28.0118	13.03	29.2035	13.05
22.5396	15.31	23.2693	15.18
18.4469	18.57	19.2335	16.24
15.6140	20.69	16.2472	17.70
13.7182	21.66	14.1749	18.20
11.6712	23.21	11.7369	19.10
10.5419	26.88	10.5841	19.55
9.6048	28.26	9.6362	19.72
8.8187	28.91	8.8443	19.94
8.1518	29.65	8.1726	20.11
7.5783	30.22	7.5956	20.28
7.0808	31.11	7.0948	20.44
6.6454	32.58	6.6561	20.72
6.2598	33.55	6.2686	21.00
5.9176	35.43	5.9235	21.17
5.6105	37.06	5.6145	21.40
4.9645	38.93	4.9666	21.84
4.4532	42.68	4.4529	22.46
3.6915	47.97	3.6894	23.13
3.1523	53.02	3.1492	23.64
2.7503	57.25	2.7472	24.59
2.4393	62.14	2.4361	25.15
2.1913	65.40	2.1884	26.16
1.9892	69.63	1.9864	26.83
1.8210	71.83	1.8185	27.50
1.2798	82.58	1.2783	30.58
0.9867	95.37	0.9855	33.16
0.6766	112.96	0.6758	36.18
0.5147	122.41	0.5142	37.75
0.4153	126.81	0.4150	38.98
0.3481	129.49	0.3478	39.43
0.2630	133.89	0.2628	40.89
0.2113	137.39	0.2112	41.78
0.1417	141.71	0.1416	43.35
0.1066	143.83	0.1065	44.19
0.0854	146.43	0.0854	45.54
0.0713	147.57	0.0712	46.15
0.0611	148.96	0.0611	46.82
0.0535	150.26	0.0535	46.99
0.0476	150.67	0.0476	47.33
0.0429	151.65	0.0428	47.61
0.0390	152.46	0.0390	48.00
0.0357	153.19	0.0357	48.45
0.0330	153.44	0.0330	48.50
0.0306	153.60	0.0306	48.95
0.0286	153.52	0.0286	48.95
0.0268	154.82	0.0268	49.51
0.0252	155.31	0.0252	49.23
0.0238	155.56	0.0238	49.57
0.0226	155.31	0.0226	49.79
0.0215	155.47	0.0215	49.68
0.0204	156.53	0.0204	49.57
0.0195	156.53	0.0195	49.57
0.0187	156.78	0.0187	49.74
0.0179	158.08	0.0179	49.62
0.0172	157.76	0.0172	50.02
0.0165	158.33	0.0165	49.79
0.0159	158.81	0.0159	49.85
0.0153	158.73	0.0153	49.51
0.0148	159.22	0.0148	49.74
0.0143	159.79	0.0143	50.13

Sample N 2		**Sample N 3**	
PORE-ENTRANCE DIAMETER, MICRONS	CUMULATIVE PORE-VOLUME, CU MM/G	PORE-ENTRANCE DIAMETER, MICRONS	CUMULATIVE PORE-VOLUME, CU MM/G
58.5831	0.00	58.5831	0.00
38.1070	6.69	38.4729	9.24
28.9915	9.69	29.5644	13.33
22.7824	10.72	23.7544	15.74
18.9891	12.42	19.2729	17.48
16.1377	13.51	16.6194	18.49
14.0099	14.26	14.5280	19.36
11.6402	14.95	11.7429	20.50
10.4972	13.65	10.5889	21.03
9.5651	14.13	9.6420	21.70
8.7846	14.47	8.8501	22.24
8.1217	14.74	8.1775	22.44
7.5522	15.15	7.6000	22.71
7.0573	15.56	7.0989	23.04
6.6227	15.70	6.6599	23.44
6.2388	15.97	6.2720	23.85
5.8974	16.52	5.9268	24.25
5.5910	16.79	5.6174	24.45
4.9486	17.66	4.9692	25.32
4.4387	18.77	4.4556	26.73
3.6801	20.48	3.6913	27.66
3.1431	22.66	3.1511	29.34
2.7427	24.30	2.7487	30.81
2.4329	26.48	2.4376	32.82
2.1859	28.05	2.1898	34.63
1.9844	29.55	1.9876	36.37
1.8170	31.33	1.8197	38.31
1.2776	36.58	1.2790	44.28
0.9851	41.09	0.9860	49.57
0.6757	46.82	0.6761	56.00
0.5142	50.92	0.5144	59.82
0.4150	54.60	0.4151	63.10
0.3478	56.51	0.3479	64.57
0.2628	62.18	0.2629	69.80
0.2112	66.34	0.2112	73.08
0.1416	72.55	0.1417	79.18
0.1065	75.97	0.1066	82.52
0.0854	78.70	0.0854	85.61
0.0712	80.40	0.0712	86.74
0.0611	81.36	0.0611	87.82
0.0535	82.04	0.0535	88.75
0.0476	82.52	0.0476	89.42
0.0428	82.93	0.0428	89.83
0.0390	83.34	0.0390	90.09
0.0357	83.34	0.0357	90.50
0.0330	83.41	0.0330	90.56
0.0306	84.09	0.0306	90.90
0.0286	83.88	0.0286	91.10
0.0268	84.22	0.0268	91.30
0.0252	84.29	0.0252	91.43
0.0238	84.57	0.0238	91.50
0.0226	84.09	0.0226	91.57
0.0215	84.22	0.0215	91.70
0.0204	84.70	0.0204	91.90
0.0195	84.50	0.0195	91.90
0.0187	84.70	0.0187	92.24
0.0179	85.04	0.0179	92.10
0.0172	85.52	0.0172	92.10
0.0165	84.91	0.0165	92.17
0.0159	85.11	0.0159	92.10
0.0153	85.32	0.0153	92.37
0.0148	85.79	0.0148	92.71
0.0143	85.45	0.0143	92.77

Sample N 4		**Sample N 6**	
PORE-ENTRANCE DIAMETER, MICRONS	CUMULATIVE PORE-VOLUME, CU MM/G	PORE-ENTRANCE DIAMETER, MICRONS	CUMULATIVE PORE-VOLUME, CU MM/G
58.5831	0.00	58.5831	0.00
39.3419	7.21	37.9648	7.01
28.7727	10.82	28.6848	10.98
23.0485	12.39	22.7135	13.02
19.1675	13.64	18.8406	14.51
16.3764	14.56	16.0184	15.50
14.1444	15.48	13.9651	16.19
11.7526	16.20	11.8663	16.93
10.5968	16.72	10.6917	17.92
9.6462	16.79	9.7256	18.17
8.8534	17.25	8.9194	18.36
8.1816	17.90	8.2375	18.85
7.6036	18.17	7.6523	19.29
7.1015	18.23	7.1442	19.47
6.6618	18.43	6.6999	19.91
6.2732	18.56	6.3070	20.03
5.9277	18.82	5.9576	20.09
5.6182	19.02	5.6450	20.22
4.9695	19.54	4.9909	21.15
4.4557	20.79	4.4722	21.52
3.6918	22.49	3.7029	22.82
3.1515	24.33	3.1595	24.25
2.7491	25.90	2.7551	25.55
2.4379	27.74	2.4426	27.10
2.1900	29.64	2.1936	28.15
1.9878	31.28	1.9907	29.08
1.8199	33.12	1.8221	30.08
1.2791	38.50	1.2801	33.55
0.9860	43.28	0.9866	37.15
0.6761	49.32	0.6764	41.80
0.5144	54.04	0.5145	43.53
0.4151	58.37	0.4152	45.70
0.3480	61.19	0.3480	47.13
0.2629	69.58	0.2629	51.16
0.2112	75.62	0.2112	53.39
0.1417	86.31	0.1417	58.17
0.1066	90.44	0.1066	59.72
0.0854	91.68	0.0854	61.70
0.0712	92.41	0.0712	62.88
0.0611	93.19	0.0611	63.44
0.0535	93.65	0.0535	64.06
0.0476	94.37	0.0476	64.31
0.0428	94.57	0.0428	64.68
0.0390	94.83	0.0390	64.68
0.0357	95.09	0.0357	65.30
0.0330	95.49	0.0330	65.24
0.0306	95.75	0.0306	65.55
0.0286	96.14	0.0286	65.55
0.0268	96.60	0.0268	65.86
0.0252	96.41	0.0252	65.80
0.0238	96.67	0.0238	66.23
0.0226	96.86	0.0226	66.60
0.0215	96.93	0.0215	66.17
0.0204	96.86	0.0204	66.04
0.0195	96.80	0.0195	66.42
0.0187	96.60	0.0187	66.17
0.0179	96.01	0.0179	66.60
0.0172	96.08	0.0172	66.91
0.0165	96.14	0.0165	66.54
0.0159	96.21	0.0159	66.79
0.0153	96.27	0.0153	67.04
0.0148	96.47	0.0148	66.66
0.0143	96.47	0.0143	67.04

Sample N 7

PORE-ENTRANCE DIAMETER, MICRONS	CUMULATIVE PORE-VOLUME, CU MM/G
58.5831	0.00
38.0204	8.50
28.6174	12.12
22.5037	14.26
18.7391	15.46
15.9464	16.67
14.1193	17.27
11.8652	18.08
10.6895	18.88
9.7230	18.95
8.9176	19.28
8.2353	19.55
7.6499	19.82
7.1425	20.22
6.6979	20.42
6.3053	20.55
5.9567	21.09
5.6442	21.22
4.9898	21.69
4.4717	22.56
3.7024	23.70
3.1589	24.70
2.7546	25.84
2.4420	26.98
2.1932	28.32
1.9904	29.39
1.8219	30.53
1.2799	34.21
0.9865	37.36
0.6763	41.71
0.5145	45.26
0.4152	47.33
0.3480	48.80
0.2629	52.95
0.2112	56.57
0.1417	62.26
0.1066	66.14
0.0854	69.89
0.0712	71.23
0.0611	72.17
0.0535	72.44
0.0476	73.24
0.0428	73.57
0.0390	74.24
0.0357	74.44
0.0330	74.64
0.0306	75.31
0.0286	75.38
0.0268	75.52
0.0252	75.72
0.0238	75.78
0.0226	75.92
0.0215	76.32
0.0204	76.25
0.0195	76.32
0.0187	76.25
0.0179	76.45
0.0172	76.72
0.0165	76.85
0.0159	76.72
0.0153	76.85
0.0148	76.79
0.0143	77.39

Sample N 8

PORE-ENTRANCE DIAMETER, MICRONS	CUMULATIVE PORE-VOLUME, CU MM/G
58.5831	0.00
38.7532	5.53
29.3854	8.86
22.9039	10.94
19.0248	12.63
16.1849	13.39
14.3730	13.95
11.8252	14.71
10.6536	14.77
9.6948	15.21
8.8941	15.59
8.2154	15.90
7.6328	16.15
7.1271	16.28
6.6843	16.47
6.2934	16.72
5.9460	17.16
5.6346	17.28
4.9824	17.85
4.4658	18.73
3.6983	19.61
3.1559	20.55
2.7524	21.93
2.4405	23.82
2.1920	25.01
1.9895	26.58
1.8212	28.22
1.2798	34.13
0.9865	38.97
0.6764	46.95
0.5146	51.41
0.4152	56.12
0.3480	58.20
0.2629	69.07
0.2113	77.05
0.1417	97.10
0.1066	104.70
0.0854	108.04
0.0713	109.29
0.0611	109.42
0.0535	110.49
0.0476	110.99
0.0429	111.37
0.0390	111.93
0.0357	112.25
0.0330	112.50
0.0306	113.00
0.0286	113.19
0.0268	113.25
0.0252	113.69
0.0238	113.88
0.0226	113.88
0.0215	113.88
0.0204	114.01
0.0195	114.19
0.0187	114.26
0.0179	114.63
0.0172	114.95
0.0165	114.76
0.0159	115.45
0.0153	115.51
0.0148	115.39
0.0143	115.39

Sample N 11

PORE-ENTRANCE DIAMETER, MICRONS	CUMULATIVE PORE-VOLUME, CU MM/G
58.5831	0.00
39.0434	8.30
29.4354	12.57
23.2170	15.67
19.1685	16.22
16.3648	18.62
14.2703	18.85
11.8367	19.16
10.6633	19.32
9.7041	20.25
8.9009	20.33
8.2200	20.25
7.6365	20.41
7.1310	20.95
6.6875	21.03
6.2961	21.26
5.9480	21.41
5.6366	21.80
4.9844	23.04
4.4685	25.68
3.7004	27.31
3.1576	28.86
2.7539	31.19
2.4417	33.60
2.1930	35.38
1.9905	38.87
1.8221	41.51
1.2807	56.72
0.9873	70.99
0.6770	95.28
0.5150	104.20
0.4155	115.07
0.3482	118.71
0.2631	128.02
0.2114	136.79
0.1417	155.88
0.1066	176.36
0.0854	207.94
0.0713	221.36
0.0611	231.06
0.0535	236.03
0.0476	239.83
0.0429	241.54
0.0390	242.24
0.0357	242.78
0.0330	243.40
0.0306	243.56
0.0286	243.79
0.0268	244.10
0.0252	244.33
0.0238	244.56
0.0226	244.72
0.0215	244.95
0.0204	245.26
0.0195	245.57
0.0187	245.88
0.0179	245.96
0.0172	246.04
0.0165	246.27
0.0159	246.50
0.0153	246.27
0.0148	246.35
0.0143	246.19

Sample N 12

PORE-ENTRANCE DIAMETER, MICRONS	CUMULATIVE PORE-VOLUME, CU MM/G
58.5831	0.00
38.7627	10.03
29.1564	13.95
23.2173	16.79
19.0867	18.71
16.3576	19.99
14.3102	21.13
11.8703	22.56
10.7009	25.05
9.7327	25.19
8.9264	25.76
8.2437	26.40
7.6577	26.90
7.1496	27.47
6.7045	27.89
6.3119	28.53
5.9624	28.96
5.6495	29.32
4.9946	30.45
4.4757	31.66
3.7057	33.87
3.1621	36.86
2.7574	39.28
2.4446	42.19
2.1954	44.33
1.9925	47.82
1.8241	52.23
1.2818	67.67
0.9879	79.48
0.6772	95.85
0.5151	107.09
0.4156	114.20
0.3483	117.05
0.2631	128.79
0.2114	142.10
0.1417	177.18
0.1066	194.89
0.0854	203.50
0.0713	205.21
0.0611	206.14
0.0535	206.06
0.0476	206.42
0.0429	206.85
0.0390	207.27
0.0357	207.63
0.0330	207.70
0.0306	207.77
0.0286	207.99
0.0268	208.27
0.0252	208.48
0.0238	208.84
0.0226	208.77
0.0215	209.05
0.0204	208.98
0.0195	209.27
0.0187	209.27
0.0179	209.05
0.0172	208.91
0.0165	209.34
0.0159	209.34
0.0153	209.41
0.0148	209.55
0.0143	209.76

Sample N 13		Sample N 14	
PORE-ENTRANCE DIAMETER, MICRONS	CUMULATIVE PORE-VOLUME, CU MM/G	PORE-ENTRANCE DIAMETER, MICRONS	CUMULATIVE PORE-VOLUME, CU MM/G
58.5831	0.00	58.5831	0.00
39.7882	13.71	38.6934	12.51
29.3041	21.13	29.3017	17.73
23.1789	21.32	23.0317	20.74
19.3302	28.17	18.8789	22.96
16.4201	27.99	16.2718	25.02
14.3310	28.17	14.2473	26.68
11.8246	28.17	11.8642	27.87
10.6456	26.01	10.6891	28.90
9.6792	23.39	9.7239	29.37
8.8799	23.48	8.9182	29.69
8.2027	23.67	8.2361	30.16
7.6215	23.85	7.6515	30.88
7.1171	23.95	7.1442	31.51
6.6753	24.04	6.6997	31.99
6.2851	24.14	6.3074	32.54
5.9386	24.79	5.9584	33.01
5.6283	25.45	5.6458	33.25
4.9783	27.33	4.9915	34.36
4.4631	29.77	4.4734	35.86
3.6966	31.46	3.7041	38.32
3.1551	34.47	3.1605	40.38
2.7524	39.26	2.7562	43.31
2.4406	42.17	2.4438	47.03
2.1925	47.05	2.1951	51.22
1.9900	51.00	1.9922	55.02
1.8219	55.88	1.8238	59.62
1.2809	81.71	1.2818	79.73
0.9876	104.25	0.9880	95.72
0.6771	131.29	0.6773	117.89
0.5150	143.69	0.5152	132.53
0.4156	156.93	0.4156	141.96
0.3483	162.47	0.3483	146.15
0.2631	181.73	0.2631	159.45
0.2114	204.08	0.2114	170.22
0.1418	262.12	0.1417	194.76
0.1066	297.15	0.1066	215.82
0.0854	314.43	0.0854	246.86
0.0713	317.34	0.0713	263.33
0.0611	318.56	0.0611	273.78
0.0535	318.94	0.0535	281.06
0.0476	319.13	0.0476	285.65
0.0429	319.60	0.0429	288.42
0.0390	320.16	0.0390	289.85
0.0357	320.16	0.0357	290.56
0.0330	320.54	0.0330	290.80
0.0306	320.63	0.0306	291.04
0.0286	321.00	0.0286	291.67
0.0268	321.47	0.0268	291.91
0.0252	321.76	0.0252	291.59
0.0238	322.32	0.0238	291.99
0.0226	322.88	0.0226	291.59
0.0215	322.88	0.0215	291.12
0.0204	322.79	0.0204	290.96
0.0195	322.70	0.0195	291.91
0.0187	322.98	0.0187	291.99
0.0179	323.45	0.0179	291.99
0.0172	323.45	0.0172	291.99
0.0165	324.39	0.0165	291.83
0.0159	323.82	0.0159	292.38
0.0153	324.10	0.0153	292.38
0.0148	323.63	0.0148	292.70
0.0143	323.82	0.0143	292.70

Sample N15

PORE-ENTRANCE DIAMETER, MICRONS	CUMULATIVE PORE-VOLUME, CU MM/G
58.58	0
39.38	12.55
29.05	19.38
22.92	21.56
19.06	23.74
16.21	25.47
14.09	26.84
11.86	28.02
10.69	29.84
9.72	30.39
8.92	30.93
8.23	31.20
7.65	31.48
7.14	31.66
6.70	32.02
6.30	32.57
5.96	33.12
5.64	33.57
4.99	34.66
4.47	35.84
3.70	37.30
3.16	39.76
2.76	43.31
2.44	46.94
2.19	50.86
1.99	55.13
1.82	59.41
1.28	81.24
0.99	98.17
0.68	123.28
0.52	138.01
0.430	152.75
0.358	161.67
0.269	201.15
0.215	241.73
0.143	286.49
0.108	292.31
0.086	294.13
0.072	294.26
0.0614	294.77
0.0537	294.77
0.0478	295.04
0.0430	295.32
0.0391	295.68
0.0358	295.77
0.0331	296.04
0.0307	296.41
0.0287	296.23
0.0269	296.77
0.0253	297.41
0.0239	297.41
0.0226	297.68
0.0215	297.96
0.0204	297.86
0.0195	297.68
0.0186	297.59
0.0179	297.50
0.0172	297.86
0.0165	297.68
0.0159	298.41
0.0154	298.68
0.0148	298.87
0.0143	299.32

Sample N16

PORE-ENTRANCE DIAMETER, MICRONS	CUMULATIVE PORE-VOLUME, CU MM/G
58.5831	0.00
39.0653	8.72
28.8529	12.97
22.9621	14.82
19.0113	16.25
16.3489	17.09
14.1715	18.04
11.8235	18.76
10.6522	18.82
9.6913	18.70
8.8905	18.88
8.2116	18.94
7.6300	19.36
7.1246	19.48
6.6823	19.72
6.2919	20.08
5.9442	20.26
5.6330	20.43
4.9813	21.03
4.4649	21.87
3.6976	22.59
3.1557	24.14
2.7522	25.39
2.4402	26.65
2.1918	28.14
1.9893	29.64
1.8210	30.65
1.2797	36.51
0.9865	42.18
0.6763	49.00
0.5146	53.78
0.4152	57.96
0.3480	60.41
0.2629	68.47
0.2113	75.64
0.1417	85.44
0.1066	88.55
0.0854	91.00
0.0713	91.66
0.0611	92.38
0.0535	92.61
0.0476	93.27
0.0429	93.69
0.0390	94.23
0.0357	94.82
0.0330	95.78
0.0306	96.26
0.0286	96.74
0.0268	97.45
0.0252	98.05
0.0238	98.11
0.0226	98.77
0.0215	98.83
0.0204	99.37
0.0195	99.60
0.0187	99.72
0.0179	99.55
0.0172	100.14
0.0165	100.92
0.0159	100.92
0.0153	100.62
0.0148	100.86
0.0143	100.74

Sample 01

PORE-ENTRANCE DIAMETER, MICRONS	CUMULATIVE PORE-VOLUME. CU MM/G
58.58	
38.39	8.98
23.04	19.24
19.06	22.55
16.41	25.98
14.30	28.55
13.06	30.28
11.80	32.80
10.64	35.49
9.69	35.64
8.89	36.59
8.21	38.24
7.63	39.59
7.13	41.24
6.69	42.73
6.30	43.92
5.95	45.02
5.64	46.21
4.990	49.44
4.473	51.89
3.703	54.41
3.160	57.80
2.756	60.55
2.443	63.09
2.194	65.13
1.991	67.03
1.822	68.76
1.280	75.70
0.987	82.24
0.677	95.97
0.515	109.21
0.430	123.16
0.358	131.84
0.269	148.87
0.215	159.68
0.143	174.18
0.108	180.11
0.086	184.12
0.072	185.86
0.0537	187.91
0.0430	189.57
0.0358	190.75
0.0307	192.01
0.0269	192.72
0.0239	193.19
0.0215	193.67
0.0195	194.45
0.0179	195.16
0.0165	195.48
0.0154	195.79
0.0143	196.35

Sample 02

PORE-ENTRANCE DIAMETER, MICRONS	CUMULATIVE PORE-VOLUME, CU MM/G
58.58	
38.87	10.11
28.89	16.09
22.85	20.14
18.99	22.81
16.37	24.75
14 26	27.04
12.87	28.79
11.79	29.84
10.64	32.35
9.68	33.16
8.88	34.13
8.21	35.18
7.63	35.91
7.12	36.88
6.68	37.93
6.29	39.39
5.95	39.95
5.64	40.60
4.98	43.84
4.47	47.47
3.70	50.79
3.16	53.14
2.75	55.80
2.44	57.66
2.19	58.79
1.99	61.22
1.82	63.49
1.28	72.38
0.987	78.45
0.677	93.24
0.515	107.72
0.430	120.51
0.358	129.88
0.269	142.02
0.215	154.32
0.143	165.79
0.108	171.22
0.086	175.82
0.072	177.31
0.0537	178.35
0.0430	181.63
0.0358	183.87
0.0307	184.46
0.0269	185.65
0.0239	185.95
0.0215	186.10
0.0195	186.10
0.0179	186.50
0.0165	186.70
0.0154	187.74
0.0143	187.59

NATIONAL COAL BOARD

FINAL REPORT

JU[illegible] 1970 - JUNE 1971

REDUCTION OF ATMOSPHERIC POLLUTION

APPENDIX 9. METHODS FOR DETERMINATION OF NITROGEN OXIDES

PREPARED FOR

ENVIRONMENTAL PROTECTION AGENCY
OFFICE OF AIR PROGRAMS
411 WEST CHAPEL HILL STREET
DURHAM, NORTH CAROLINA 27701

REFERENCE NO. DHB 060971

SEPTEMBER 1971

FLUIDISED COMBUSTION
CONTROL GROUP

NATIONAL COAL BOARD
LONDON, ENGLAND

Research on reducing emission of sulphur oxides, nitrogen oxides and particulates by using fluidised bed combustion of coal

Appendix 9. Methods for determination of nitrogen oxides

Report prepared by: J.T. Shaw

Report approved by: A.D. Dainton and H.R. Hoy

Preceding page blank

Page No.

1. Introduction A9. 1

2. Sampling Trains A9. 1
   - 2.1 Probe used in 48 in x 24 in pressurised combustor A9. 1
   - 2.2 Probes used in atmospheric pressure combustors A9. 2
   - 2.3 Rate of flow of gas through the probes A9. 2
   - 2.4 Material of connecting tubes A9. 2
   - 2.5 Conditioning the probes and associated tubing A9. 3
   - 2.6 Rate of off-take of gas from the probes to the analytical train A9. 3
   - 2.7 Removal of SO_2, HCl and other soluble gases from the gas led to the analytical train A9. 3

3. Methods of Analysis A9. 4
   - 3.1 Determination of NO_x remaining in the gas A9. 4
     - 3.1.1 Use of BS 2069[3] grab-sample bottles containing Saltzman's reagent A9. 4
     - 3.1.2 Use of BS 2069 grab-sample bottles not containing any reagent A9. 6
     - 3.1.3 Use of BCURA NO_x Box A9. 7
   - 3.2 Determination of NO_x removed from the gas by water A9.10
     - 3.2.1 Analysis of the quenching water A9.11
     - 3.2.2 Analysis of the water from the Drechsel bottles A9.11
   - 3.3 A typical calculation A9.12
   - 3.4 Relevance of the 'Saltzman Factor' A9.13

4. References A9.14

Figures A9.1 - A9.4

(Note that when referring to Tables and Figures in the text the prefix A9 is omitted).

Preceding page blank

1. INTRODUCTION

Measurements of the NO_x content of the flue gases were made in Tasks I, II and III. The difficulties encountered in obtaining an accurate measurement of the concentration of oxides of nitrogen in flue gases are well-known and much more development work is necessary before a definitive method can be proposed. Accordingly, the procedures used in the present programme are described in detail in this Appendix.

Because of delays in delivery of equipment it was not possible to measure the NO_x concentrations by infra-red absorption, as had been intended.

2. SAMPLING TRAINS

The determination of reactive constituents of flue gas such as NO and NO_2 is complicated by their tendency to 'disappear' as they pass through the sampling system. Therefore, in addition to the importance of choosing a sampling position that permits a truly representative sample to be obtained is that of ensuring that as far as possible the sample so obtained is preserved without change in NO_x content until it enters the analytical system.

Halstead, Nation and Turner[1] in work confirmed and extended by Shaw and Gray[2], showed that hot stainless steel is amongst those materials capable of causing losses of NO_x in certain conditions, whereas silica appears to be inactive. These findings led to the following designs of sample probe.

2.1 Probe used in 48 in x 24 in pressurised combustor

The flue gases from this combustor were at 1450°F and 5 atm pressure. These conditions coupled with the general design of the combustor made it difficult to fit a silica probe. A stainless steel probe having water injection at the gas inlet was therefore set up. The flow of water was sufficient to cool the gas very quickly to below 200°F, thus it is believed quenching the reactions that might otherwise have led to undue loss of NO or of NO_2. An incidental advantage of using water is that it removed SO_2, HCl and other soluble compounds that if allowed to remain would have interfered with the chemical determinations of NO_x in the gas. The amount of NO_x removed from the gas phase by the water was determined by methods described in section 3.2.

Water injection was not always used. Tests were carried out to see what difference was made by turning the water on and off. No difference was found, indicating that the water was unnecessary in the conditions in which the combustor operated. The conditions in which the water might have been expected to be really necessary (low O_2, high CO in the gas) were never encountered during the present tests.

2.2 Probes used in atmospheric pressure combustors

A silica tube supported externally by a steel tube was used for sampling from the atmospheric combustors where the gas temperature was typically 600°F.

2.3 Rate of flow of gas through the probes

In order to minimise surface/volume effects the rate of flow of gas was kept as high as possible.

There was no difficulty in getting a high rate of flow from the pressurised combustor, about 45 litres/min, but from the 1 atmos. combustors the capacity of the pump used (a Dymax II) was a limitation and enabled only some hundreds of ml/min to be withdrawn.

2.4 Material of connecting tubes

At the pressurised combustor the main length of tube connecting the probe to the analytical train (about 20 metres) was made of stainless steel. The great preponderance of NO over NO_2 in the NO_x content of the flue gas made it practical to use flexible PVC tubing as opposed to PTFE to connect the glass apparatus in the analytical train, but the lengths were kept short, i.e. about 1 metre in all. The rate of flow through the PVC was 100 ml/min. At the atmospheric pressure combustors, NO again preponderated greatly over NO_2 in the flue gas making it again practical to use flexible PVC. The main length of tube connecting the silica probe to the glass apparatus was of this material, with some PTFE. Total length was about 5 metres.

3. METHODS OF ANALYSIS

This section describes the analysis of the gas and of the water used for injection and in the Drechsel bottles, and ends with a comment on the 'Saltzman Factor'.

3.1 Determination of NO_x remaining in the gas

Of the three methods that were used to determine the NO_x content remaining in the gas, two were chemical and one used an instrument, the BCURA NO_x Box. The three methods are described in detail below.

3.1.1. Use of BS 2069[3] grab-sample bottles containing Saltzman's reagent

This method has the advantage that absorption of NO_x in the reagent can begin as soon as the sample has been obtained. Grab-sample bottles made up in accordance with BS 2069 and having a volume of about 400 ml were used. They were cleaned initially, and later whenever necessary, with trichlorethylene which was then washed out with acetone. Before each test the bottles were cleaned by rinsing with nitrite-free hot water followed by acetone which was then evaporated off in a current of air. The taps were greased with the minimum of Apiezon N.

To carry out a test, Saltzman's reagent was made up in accordance with instructions.[4] The grab-sample bottles were partially evacuated to enable the required quantity of reagent to be sucked in; a convenient volume was found to be 40 ml of reagent in each bottle. Air was then removed from the bottles as far as possible by means of a filter pump. The taps were closed and checked for leakage, after which the bottles were ready for use. Before taking a sample into the first of a series of bottles, the flue gas was led at 100 ml/min through the Drechsel bottles described in section 2.7 for about 10 minutes to flush out all air as described in sections 2.5 and 2.7. The gas was then drawn slowly into the gas sample bottle by suction, keeping the flow through the Drechsel bottles at about 100 ml/min. The gas sample bottle was held upright with the gas inlet at the bottom so that the gas bubbled through the reagent. When no more gas would enter, the tap was closed. After disconnecting the bottle, the tap was carefully opened a little in order to bring the pressure back to that of the atmosphere (the flow control valves were always adjusted in such a way as to ensure that the pressure in that part of the line between the pump and the grab sample bottle slightly

2.5 Conditioning the probes and associated tubing

In order to reduce any effect of the probes and tubing on the samples, gas was drawn through at the normal rate for about an hour before analyses were begun. This occasionally produced condensation in the tube leading from the dry probes (i.e. those without water injection) but this was ignored on the grounds that the condensate would be in equilibrium with the NO in the gas and that, because the NO_2 concentration was low, losses of this gas could safely be ignored. The purging for 1 hour did not extend to the Drechsel bottles (section 2.7) where these were used; they were purged for 10 minutes only to prevent undue contamination of the water.

2.6 Rate of off-take of gas from the probes to the analytical train

From the probes the main gas flow was divided into a major portion, which went to waste, and a minor portion, 100 ml/min, which was led to the analytical train through short tubes.

2.7 Removal of SO_2, HCl and other soluble gases from the gas led to the analytical train

The gas flowing at 100 ml/min to the analytical train from the silica probe still contained SO_2, HCl and other soluble gases, as this probe had no water injection. These constituents were removed by leading the gas through two 250 ml glass Drechsel bottles in series, each containing about 200 ml of (initially) distilled water, which was changed regularly, usually after about 5 litres of gas had bubbled through. Chemical analysis showed that, although the water removed SO_2 very efficiently, it did not dissolve much of the NO_x in the gas passing through, the amount dissolved usually being under 5% of the amount of NO_x remaining in the gas. Purging the Drechsel bottles with flue gas was carried on for 10 minutes at 100 ml/min before the first grab-sample bottle of a series was attached. (See also section 2.5).

As mentioned in section 2.1 some of the tests at the pressurised combustor were carried out without water injection, and for these the system of Drechsel bottles was used to ensure the removal of SO_2. The visual indication of flow afforded by the Drechsel bottles was found to be useful and they were retained thereafter whether the injection water was on or not.

exceeded that of the atmosphere to preclude any possibility of inleakage of air). Because the NO_x content of the gas was preponderantly NO, any error involved through excess absorption in the reagent during the very brief period of slight excess pressure can be ignored.

The barometric pressure and the temperature of the sample bottle were measured and the next bottle was then applied to the gas flow.

A description of the technique of working up the solutions follows.

3.1.1.1 Working up the solution

(a) The gas bottle containing reagent was left for about 30 minutes. Then it was held vertically over a flask and the bottom tap was opened to let the coloured reagent run out, if the pressure in the bottle would permit this. If the reagent ran out freely (as when the laboratory was warmer than the sampling site) care had to be taken not to lose some gas also. If the reagent did not run out freely the top tap was opened to let in air, thus allowing the reagent to run out.

(b) When all the reagent had run out the taps were closed and the central portion of the bottle was cooled in solid CO_2. (A special box was made from expanded polystyrene for this purpose; the ends of the bottle carrying the taps protruded through holes at each end of the box).

(c) A vessel containing a fresh quantity of Saltzman's reagent was connected to the gas sample bottle. The tap of the bottle was opened to admit the reagent, which was drawn in by suction. As much reagent as possible was drawn in at this stage.

(d) The gas sample bottle was removed from the solid CO_2 and was allowed to warm up. After about 30 minutes, the bottle was again held vertically and the lower tap was opened to allow the (by now coloured) reagent to flow into a graduated flask. Although the pressure within the bottle was often more than sufficient to expel all the reagent, in which case particular care was taken to avoid loss of gas, it was often the case that not all the reagent would flow out. The upper tap was then opened to admit air and allow the rest of the reagent to flow into the flask. The solution was diluted at this stage with fresh reagent if the colour was very strong.

(e) The gas bottle was cooled again, and more reagent was sucked in, together with some air to encourage oxidation of the NO remaining in the bottle, if not enough air had been drawn in previously.

(f) The procedures (d) and (e) were repeated until the colour developed by the solution after 30 minutes was no longer appreciable with respect to that of the first extraction. The solutions were then pooled and made up to a known volume with fresh reagent. After dilution of an aliquot with fresh reagent, if necessary, the intensity of the colour was measured. This precluded error due to loss of colour intensity overnight in this solution.

(g) Procedure (e) was repeated and the bottle was left overnight.containing the reagent. The coloured solution was withdrawn the following morning, was made up to a known volume, and the intensity of colour was measured at 550 nm using a Unicam SP600 spectrophotometer.

3.1.2 Use of BS 2069 grab-sample bottles not containing any reagent

Provided that reagent was introduced within a few minutes of obtaining the sample, so as to minimise losses due to conversion of NO_2 to nitrate or other causes, this method was found to give results in good agreement with that described in section 3.1.1, but had the advantage that the volume of gas sample trapped in the bottle could be more accurately known.

The bottles were not evacuated after washing and drying, but were attached one at a time to the flow of gas emerging from the Drechsel bottles referred to in sections 2.5, 2.7 and 3.1.1 and gas was allowed to flow through at 100 ml/min (checked by a rotameter at the outlet end) for 20 minutes. The taps were closed, and after removing the bottle from the gas-line and bringing the contents down to atmospheric pressure by momentarily opening one tap, the bottle was cooled in dry ice as described in section 3.1.1 (b) for introduction of reagent. Subsequent procedure was as described in 3.1.1 (c) onwards.

3.1.3 Use of BCURA NO_x Box

The heart of the NO_x Box is an oxidant-sensing device, the basic principle of which was described by Hersch[5,6]. It was described again by Shaw[7] who gave a modified construction for it. Further improvements have since been made and the latest construction is shown in Fig. 1. The device is not specific but will determine NO_2 if this is the only species reaching the device that is oxidisable or reducible at the electrodes.

To determine NO_x or NO by means of this meter it is necessary to incorporate an oxidiser that will convert NO to NO_2. The one used in the BCURA NO_x Box, consisting of glass wool impregnated with chromium trioxide and sulphuric acid, was described by Bethell, Shaw and Thomas[8] and again by Shaw[7].

Other necessary constituents of the NO_x Box are a gas flowmeter and a microammeter. Optional adjuncts are a gas flow control valve and a constant-flow device, gas-washing bottle, a drying tube, a soda-lime tube, a gas pump, a range-change facility and a plug to connect the electrical output of the meter to a chart recorder. (The recorder does not form part of the meter). Except for the range-change facility and plug for electrical connection to a recorder, which are mounted in or on the casing of the NO_x Box, these optional adjuncts can be mounted inside the box or they can be kept separate if that is more convenient.

The flow chart for the NO_x Box is given in Fig. 3.

3.1.3.1 Galvanic principle of the NO_2 sensor

The NO_2 sensor is believed to work as follows:

At the moist platinum gauze electrode:

$$NO_2 + H_2O + 2e = NO + 2OH^-$$

Hydroxyl ions travel through the electrolyte to the active carbon electrode, at which:

$$2OH^- + \cdot\cdot\cdot C(s) = H_2O + \cdot\cdot\cdot CO + 2e$$

The hydroxyl ions are discharged, and the electrons flow through the external circuit where they actuate a galvanometer, and return to the platinum gauze. The oxygen combines with the active carbon to form a (presumably) solid product written as $\cdot\cdot\cdot CO$.

Not all the NO_2 reaching the sensor reacts thus. Some is dissolved non-galvanically.

$$H_2O + 3NO_2 = 2HNO_3 + NO$$

and the NO thus produced is swept out of the sensor with the rest of the gas, which normally also contains some NO_2 that has not reacted in any way. The rate of the non-galvanic reaction is temperature-dependent, as also is the efficiency with which NO_2 diffuses to the gauze. Accordingly, the efficiency with which NO_2 is trapped to react galvanically is also a function of temperature. For the best results therefore, the instrument should be kept at constant temperature.

3.1.3.2 Electrolyte

This consists of 3 moles KCl and 0.1 mole each of KH_2PO_4 and K_2HPO_4 per litre of water.

3.1.3.3. Electrical Circuits

For most purposes hitherto encountered by BCURA, a 100 μa fsd microammeter is sensitive enough to give useful indications of the output from the sensor, as at low concentrations of NO_2 the response is about 1 μa per p.p.m. v/v, when the flow rate of gas is 100 ml/min.

The response falls off at higher concentrations so that a current of 100 μa represents more than 100 p.p.m.

For concentrations that would otherwise overload the microammeter a shunt is fitted. (If this is not sufficient the gas must be diluted). For use with concentrations that would give too small a deflection on the microammeter there is a potential divider the potential difference across which can be recorded on a chart recorder if one is available. This is usually arranged to give sensitivities equal to x 10 and x 100 that of the microammeter.

The circuit diagram for a typical example of the meter is given in Fig. 4 and is discussed below.

The full sensitivity of the sensor/microammeter set-up is obtained by having no resistance in series with them. To obtain good sensitivity on a recorder, together with a range-change facility, and at the same time make the recorder indicate a number (e.g. 6.7 millivolts) corresponding to the number (e.g. 67, 6.7 or 0.67 microamperes) indicated by the pointer of the microammeter, a fairly high-resistance potential divider is connected in parallel with the sensor and microammeter. In the range-change facility the resistances across which the recorder can be connected are 100, 1000 or 10,000 ohms. The total resistance of the potential divider shown on Fig. 4 is 11,500 ohms, which is 10 times that of the microammeter that was fitted to the NO_x Box for which the circuit was prepared. For a microammeter having a different resistance obviously a different make-up resistance would be needed in order to obtain a potential divider having 10 times the resistance of the microammeter. Resistances of the exact values needed are not normally obtainable but can easily be made up by connecting resistances in series and/or in parallel.

The resistance of the potential divider as a whole is high enough to have little desensitising effect on the meter, i.e. it shunts off only 9.1% of the total sensor current output. This slight loss can easily be further reduced e.g. if the resistance of the potential divider were made 10 times as great, the current shunted off would become only 0.99% of the total sensor output.

A further shunt is shown on Fig. 4. This, a resistance of 760 ohms, is the amount found necessary by trial and error to divide the meter and recorder readings by 2, on the instrument for which the circuit was prepared.

An account of the way in which the NO_x Box responds to changes in the NO_x concentration, flow-rate of carrier gas, and temperature is given in Shaw[7].

3.1.3.4 Setting up the NO_x Box

The electrolyte level was checked. The Drechsel bottles (see sections 2.5, 2.7 and 3.1.1) were filled with fresh distilled water. About a dozen small lumps of blue silica gel were placed in the PVC tube leading from the Drechsel bottles to the oxidiser of the NO_x Box. This was enough to dry the gas sufficiently well to prevent undue moistening of the oxidiser, but not enough to cause undue delay in reaching equilibrium conditions as regards passage of NO over the drying agent, which absorbs NO to some extent.

3.1.3.5 Calibrating the NO_x Box

This was done by passing known concentrations of NO in N_2 through the Drechsel bottles, drying agent and NO_x Box at the standard flow rate of 100 ml/min and waiting till a steady electrical output was attained in each case. The known concentrations were obtained from cylinders supplied by British Oxygen Ltd., London.

A graph was plotted in order to relate the meter reading of the NO_x Box to the known NO concentration passing in.

3.1.3.6 Determination of the NO_x content of a flue gas

The gas was passed at 100 ml/min through the Drechsel bottles, drying agent and NO_x Box until a steady electrical output was obtained. The NO_x concentration was read from the calibration graph referred to in section 3.1.3.5.

3.2 Determination of NO_x removed from the gas by water

This section covers analysis of the quenching water used with the stainless steel probe, and of the water from the Drechsel bottles used with both probes.

3.2.1 Analysis of the quenching water

The rates of flow of water and gas were measured. The analysis was carried out by means of Saltzman's reagent. Probably because of the presence of dissolved sulphur dioxide, the colours obtained were not very stable. It was found, also, that if Saltzman's reagent was added to aliquots of a sample at different times after obtaining the sample, the strongest colour was obtained from the aliquot treated first. The experiments were therefore carried out without loss of time after each sample had been obtained.

In calculating the results, it was assumed that for each mole of NO_x dissolved from the gas, half a mole of nitrite ion appeared in the water.

The method was quick and was easy to use, and from that point of view had great advantages over the phenol disulphonic acid method. The validity of the method was tested by an experiment in which flue gas was drawn through a probe not fitted with water injection during combustion conditions such that loss of NO_x in a dry probe would not be expected. Good agreement was obtained between the NO_x values so obtained and those obtained through the "wet" probe after adding the concetration of NO_x removed by the water and determined as above.

3.2.2 Analysis of the water from the Drechsel bottles

This was carried out by two methods, namely the Saltzman method and the phenol disulphonic acid method.

3.2.2.1 Saltzman method

As with the quenching water, Saltzman's reagent was added to aliquots of the 'Drechsel water' and the colour intensity was measured. It was assumed that each mole of NO_x dissolved from the gas gave rise to half a mole of nitrite ion in the water.

3.2.2.2 Phenol sulphonic acid method

This was carried out in accordance with the provisions of NCB Report No. 26/95[9] but phenol disulphonic acid was used instead of phenol para sulphonic acid. The method is closely similar to that of ASTM D 1608-60.[10]

3.2.2.3 Results of analyses of the 'Drechsel water'

The two methods referred to above each indicated that the amount of NO_x dissolved from the gas sample by the water in the Drechsel bottles was small, although they varied in their indications of quite *how* small. On the whole the Saltzman method used with the assumptions mentioned gave the highest results, usually showing that the water had retained NO_x amounting to up to 5% of the quantity determined as remaining in the gas.

3.3 A typical calculation

Barometric pressure 765 mm Hg.

Temperature of gas bottle 23°C.

Volume of gas bottle 407 ml.

Coloured solutions were pooled and made up to 250 ml.

An aliquot of 10 ml was diluted to 50 ml.

Optical density of the diluted aliquot : 0.343 units.

Optical density of a solution containing 2.00 ml of $Na\ NO_2$ (0.0203 g/l) made up to 50 ml with Saltzman's reagent was 0.539 units. (1.00 ml of the nitrite ≡10.0 μ l of NO_2 at 25°C, 760 mm Hg.

Vapour pressure of water at 23°C : 21.13 mm Hg.

The Drechsel bottles were purged with gas for 45 minutes altogether, at 100 ml/min.

The equivalent of 20.4 μg of NO_2 was found in the first Drechsel bottle, by the phenol disulphonic acid method.

The equivalent of 6.9 μg of NO_2 was found by the same method in the second Drechsel bottle.

P.p.m. v/v (dry basis) of NO_x in the gas sample in the bottle:

$$20 \times \frac{250}{50} \times \frac{50}{10} \times \frac{0.343}{0.539} \times \frac{1000}{407} \times \frac{760}{765} \times \frac{296}{298} \times \frac{(\ \ 760\ \ )}{(760-21)} = 793.4$$

Volume of NO_x, per 407 ml of sample, dissolved by the Drechsel water:

$$\frac{(20.4 + 6.9)}{46} \times 0.0224 \times \frac{407}{45 \times 100} \text{ ml} = A$$

(Assuming constant rate of solution)

On a p.p.m. v/v basis the correction becomes $A \times \frac{10^6}{407}$

$$= \frac{(20.4 + 6.9)}{46} \times 0.0224 \times \frac{10^4}{45} = 3.0$$

Therefore,

Total NO_x in the original gas sample
(dry basis) = 796.4 p.p.m., say 800.

3.4 Relevance of the 'Saltzman Factor'

NO_x measurements quoted in the Main Report and the Appendices have been calculated on the basis that the 'Saltzman Factor' is 0.72. There is reason to believe that when grab sample bottles are used (as in the work reported here) as opposed to sintered bubblers a Saltzman Factor of 1.0 may be more appropriate. If this proves to be true it means that the NO_x concentrations quoted up to now are too high and should be multiplied by 0.72.

The NO_x Box was calibrated with NO/N_2 mixtures the concentration of which, certified by British Oxygen Company Ltd. London, is believed to have been measured on the basis of a 0.72 factor when possibly it should have been 1.0, as grab sample analysis was used by British Oxygen Company Ltd. London. If this is so, it means that the NO_x Box values are also too high and should be multiplied by 0.72. The good agreement between NO_x Box and Saltzman determinations at the fluidised bed combustors would remain unaffected if this were so.

4. REFERENCES

1. Halstead, C.J., Nation, G.H. and Turner, L. 1970, Private communication.

2. Shaw, J.T. and Gray, B.A. 1970, Private communication.

3. BS 2069 Design of grab-sample bottles. British Standards Intitute, London, 1954.

4. Saltzman, B.E. Analyt.Chem., 1954 26, 1949-1955.

5. Hersch, P. & Deuringer, R., Paper to Anachem. Conf., Detroit, October 1963.

6. Hersch, P. Galvanic analysis, Advances in Analytical Chemistry and Instrumentation, Ed. Reilly, C.N., Vol. 3, Interscience, New York, 1964. 230,233-234.

7. Shaw, J.T., 1968, Brit. J. Anaesth. 40, 299-303.

8. Bethell, F.V., Shaw, J.T. and Thomas, A., Chem. Ind. 1968 (3) 91.

9. NCB, East Midlands Division Scientific Dept. Rpt. No. 29/65, 1965.

10. D 1608-60. American Society for Testing Materials, 1960.

5. ACKNOWLEDGEMENT

Members of staff of BCURA who took part in the experimental work included B.A. Gray and M.P. Mendoza.

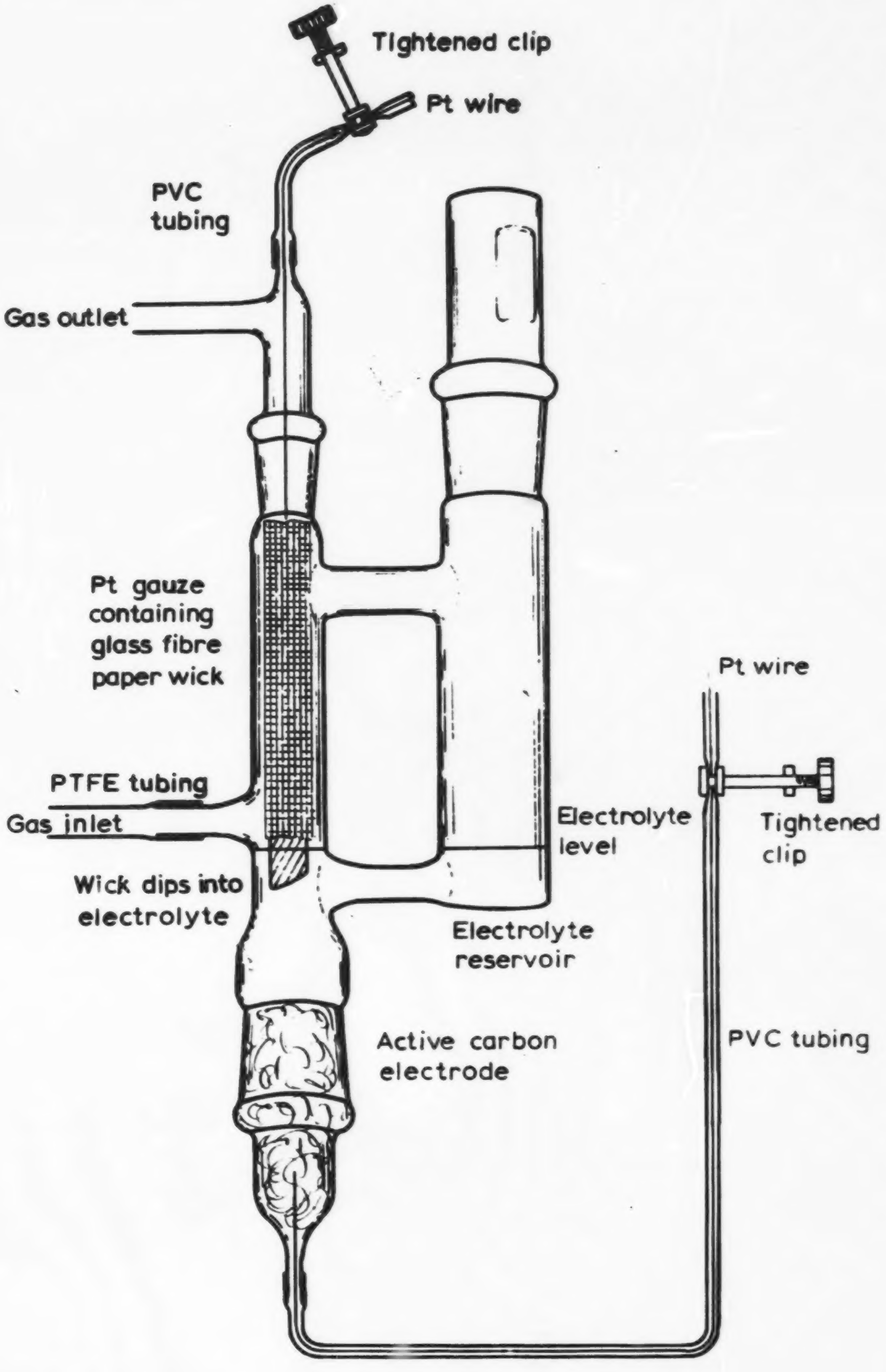
Tightened clip
Pt wire
PVC tubing
Gas outlet
Pt gauze containing glass fibre paper wick
PTFE tubing
Gas inlet
Wick dips into electrolyte
Electrolyte level
Electrolyte reservoir
Active carbon electrode
Pt wire
Tightened clip
PVC tubing

Fig. A9.1. The sensor : 1970 design

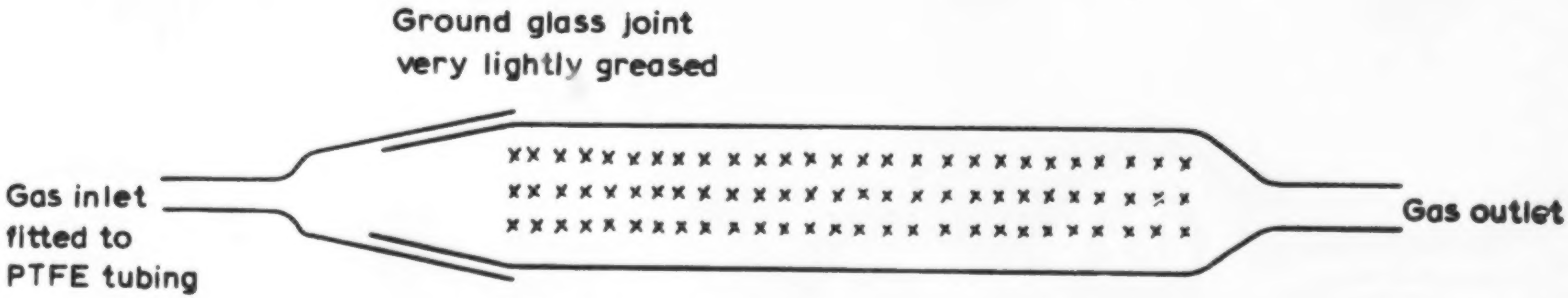
Ground glass joint
very lightly greased
Gas inlet
fitted to
PTFE tubing
Gas outlet

Fig. A9. 2 NO oxidiser unit, oxidising NO to NO_2. Also retains some SO_2

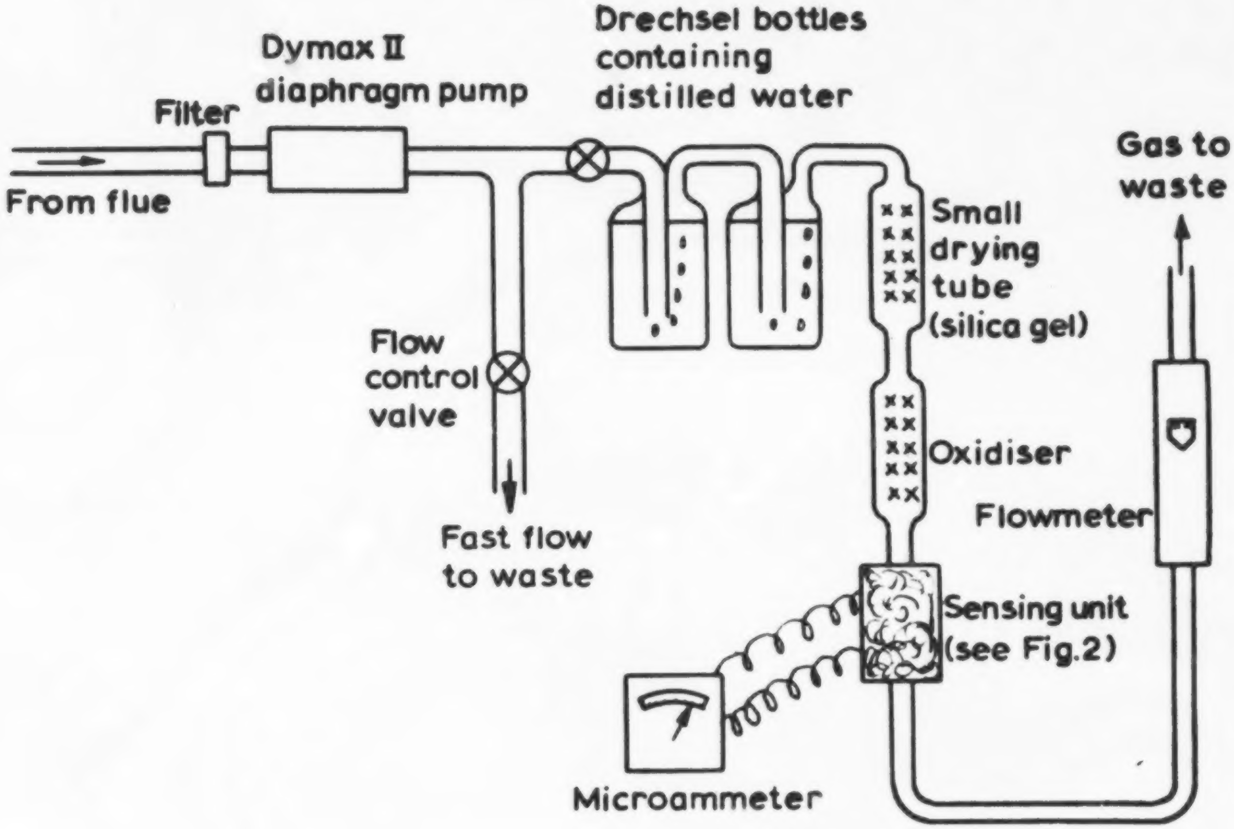
Drechsel bottles
containing
distilled water
Dymax II
diaphragm pump
Filter
From flue
Gas to
waste
Small
drying
tube
(silica gel)
Flow
control
valve
Oxidiser
Flowmeter
Fast flow
to waste
Sensing unit
(see Fig.2)
Microammeter

Fig. A9.3. Flow chart for use when determining NO_x in flue gas when sampling from a duct at atmospheric pressure. (The NO_x is presumed to be mainly NO)

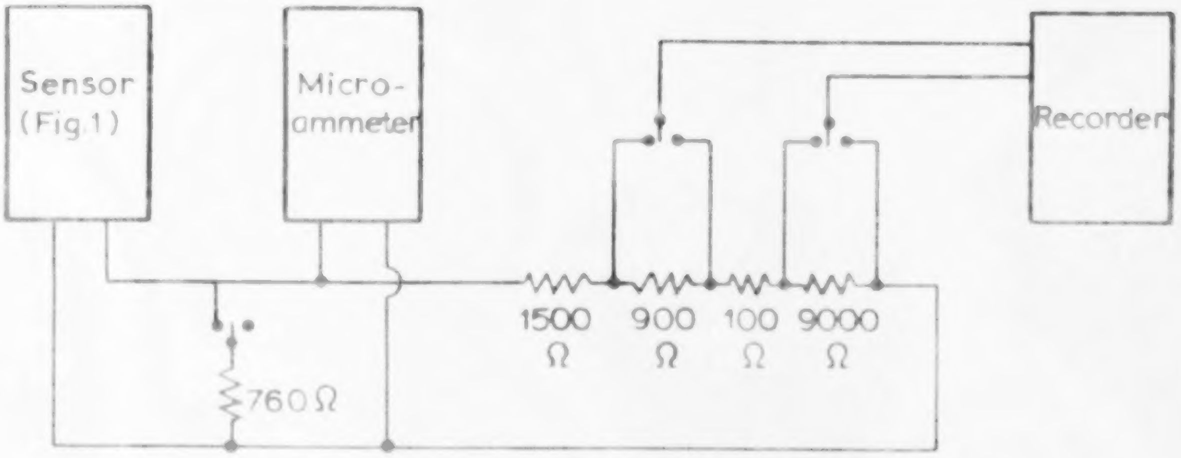
Sensor
(Fig.1)
Micro-
ammeter
Recorder
1500 Ω
900 Ω
100 Ω
9000 Ω
760 Ω

Fig. A9. 4. Circuit diagram with typical resistance values for BCURA NO_x meter

END
DATE
FILMED
8-4-72